# NOVEL RADIOPHARMACEUTICALS: CHARACTERIZATION, SUBSTITUTION KINETICS AND BIOLOGICAL EVALUATION OF TRICARBONYL COMPLEXES OF RHENIUM(I)

by

**MARIETJIE SCHUTTE**

A thesis submitted to meet the requirements for the degree of

**PHILOSOPHIAE DOCTOR**

In the

**DEPARTMENT OF CHEMISTRY**

**FACULTY OF SCIENCE**

at the

**UNIVERSITY OF THE FREE STATE**

**Supervisor: Prof. Hendrik G. Visser**

**Co-Supervisor: Prof. Andreas Roodt**

**November 2011**

***Actually it is easy – get what makes you happy and get the person that makes you life complete and you're set for success.***

I would like to thank my Heavenly Father for the strength, courage, perseverance and intelligence. Without Him in charge, I would have never been able to complete this work with the same enthusiasm.

I would like to thank my colleagues and the Inorganic Chemistry group at the University of the Free State for the training and all of the assistance, always with a smile on their faces. I would like to specifically mention Theuns Muller, Alice Brink, Carla Pretorius, Cyril Young and Anke Mouton. Without your help, encouragement, smiles, talks, jokes and never ending friendliness, this work would have been much less exciting.

Prof André Roodt, for your time, effort, input, patience, help and for always being the best role-model, not only professionally but also as a person. Thank you for all the opportunities you presented to me, for all the national and international conference contributions I were able to make as well as the exposure I got. Words cannot explain how much I appreciate you as a mentor.

A huge thank you to my supervisor, Prof Deon Visser, for your continuous assistance in my research, the encouragement, your time and the utmost patience you supported me with during the last few years. I could not ask for a better leader during my studies.

A special thanks to Prof Roger Alberto at the ACI in Zurich, Switzerland. Thank you for making the three month visit to your facility possible and for the opportunity to work in your group. Thank you for all the inputs, the continuous interest you show in my work and for the time you spent with me. I would also like to acknowledge Daniel Can, Dr Henrik Braband, Dr Fabio Zobi and Dr Bernard Spingler for your support, effort, time and friendliness during my visit. You really made my stay there something to remember. I also look forward to working with you in future on new projects and to keep up the collaborative efforts.

Without the support from my family, I don’t believe I would have made a success of this work. My mom and dad, thanks for the example you keep on setting for us children. The love, support, continuous interest and for always understanding the time I spent at work. Thanks for being the best parents anyone could wish for. For my brothers and sisters, Wilma, Marida, A.D., J.P.A. and Flippie, as well as my

brother in law Andries and sister in law Luré – thank you for your support, love and the example you set for me in all facets of life. Thank you for being my best friends. I'm proud to be part of this family.

To the love of my life, my fiancé, Charles. Thank you for being part of my life, for setting an example with your love for life, the ambition for every challenge, for your never ending support through the rough times, your interest in my work and for all your love. Thank you for teaching me that it is not important to hold all the good cards in life, but how well you play the cards you hold. I love you endlessly.

***Every success is built on the ability to do and to be better than just good enough.***

# TABLE OF CONTENTS


Abbreviations i

Abstract iii

Opsomming vi

1. *General Background and Aim*

1.1. Introduction 1

1.2. Diagnostic and therapeutic radiopharmaceuticals 1

1.3. Rhenium and Technetium in nuclear medicine 2

1.4. Aim of this study 5

2. *Literature Study*

2.1. Brief history of potential agents with $^{99m}$Tc and Re in the last 20 years 9

2.2. Different Rhenium and Technetium synthons in radiopharmacy 18

2.2.1. The application of the oxo core 19

2.2.2. Nitrido complexes 20

2.2.3. Nitrosyl complexes 21

2.2.4. *fac*-Tricarbonyl core 22

2.3. The design of Radiopharmaceuticals 23

2.3.1. Diagnostic and Therapeutic Radiopharmaceuticals 23

2.3.2. Different strategies 28

2.4. The *fac*-$[M(CO)_3(H_2O)_3]^+$ synthon 33

2.4.1. Synthesis of fac-$[M(CO)_3X_3]^{2-}$ from $[MO_4]^-$ 33

2.4.2. Hydrolytic behaviour of *fac*-$[M(CO)_3(H_2O)_3]^+$ 34

2.4.3. Application of the *fac*-$[M(CO)_3]^+$ moiety 35

2.5. Chelating systems and linkage 37

2.5.1. Introduction 37

2.5.2. Choice of radioactive core 38

2.5.3. Activation of the functional group/linking 40

2.5.4. *In vivo* behaviour 42

2.6. Recent highlights in radiopharmaceutical research 42

**Table of Contents**


2.6.1. Research towards the central nervous system 42
2.6.2. Using the luminescence properties of different ligands/conjugates 44
2.6.3. Melanoma targeting agents 46
2.6.4. Renal tracers 49
2.6.5. Tripodal/tridentate ligand type complexes 49
2.6.6. Pendant carbohydrates and the *fac*-$[M(CO)_3]^+$ core 52
2.6.7. $^{99m}$Tc/Re with oxime-type ligands 52
2.6.8. Research towards prostate cancer 53
2.7. Mechanistic studies of *fac*-$[Re(CO)_3(H_2O)_3]^+$ 56
2.7.1. Water substitution on *fac*-$[Re(CO)_3(H_2O)_3]^+$ 56
2.7.2. Ligand exchange rate of *fac*-$[Re(CO)_3(H_2O)_3]^+$ 60
2.7.3. Methanol substitution kinetics in complexes of the form *fac*-$[Re(L,L'\text{-bid})(CO)_3(MeOH)]^n$ 61
2.8. Conclusion 65
3. *Synthesis and Characterization of Ligands and Metal Compounds*
3.1. Introduction 67
3.2. Chemicals and apparatus used 68
3.3. Handling of radioactive isotopes 72
3.4. Synthesis of organic ligands 73
3.5. Synthesis of Rhenium compounds 77
3.6. In situ synthesis of $^{99m}$Tc compounds 93
3.7. Discussion 96
4. *Crystallographic study of Re(I) complexes*
4.1. Introduction 99
4.2. Experimental 101
4.3. Crystal structure of *fac*-$[NEt_4][Re(Trop)(CO)_3(Br)]$ (**1**) 107
4.4. Crystal structure of *fac*-$[NEt_4][Re(Trop)(CO)_3(H_2O)].NO_3.H_2O$ (**2**) 111
4.5. Crystal structure of *fac*-$[Re(Trop)(CO)_3(Py)]$ (**3**) 116
4.6. Crystal structure of *fac*-$[Re(Trop)(CO)_3(DMAP)]$ (**4**) 121
4.7. Crystal structure of *fac*-$[NEt_4][Re(2,5\text{-PicoH})(CO)_3(Br)].H_2O$ (**5**) 125
4.8. Crystal structure of *fac*-$[NEt_4][Re(2,5\text{-PicoMe})(CO)_3(Br)]$ (**6**) 130

**Table of Contents**


4.9. Crystal structure of *fac*-[$NEt_4$][Re(BHA)$(CO)_3$(Br)] (**7**) 134

4.10. Crystal structure of *fac*-[Re(Flav)$(CO)_3(H_2O)$].Flav (**8**) 139

4.11. Crystal structure of μ-(*fac*-[Re(BipyDC)$(CO)_3$])$_2$.4$H_2O$ (**9**) 145

4.12. Crystal structure of *fac*-[Re(PNP)$(CO)_3$(Br)] (**10**) 151

4.13. Discussion 155

5. *Kinetic Investigation of Methanol Substitution Reactions in Rhenium(I) Complexes*

5.1. Background information and previous research 160

5.2. Experimental 163

5.2.1. General Procedure 163

5.2.2. Treatment of data 164

5.3. Results and Discussion 165

5.4. Substitution reactions of *fac*-[Re(2,5-PicoH)$(CO)_3$(MeOH)] with monodentate ligands in methanol 168

5.4.1. *fac*-[Re(2,5-PicoH)$(CO)_3$(MeOH)] + bromide ions 169

5.4.2. *fac*-[Re(2,5-PicoH)$(CO)_3$(MeOH)] + iodide ions 171

5.4.3. *fac*-[Re(2,5-PicoH)$(CO)_3$(MeOH) + pyridine 173

5.4.4. *fac*-[Re(2,5-PicoH)$(CO)_3$(MeOH)] + imidazole 175

5.4.5. *fac*-[Re(2,5-PicoH)$(CO)_3$(MeOH)] + thiocyanate ions 177

5.4.6. *fac*-[Re(2,5-PicoH)$(CO)_3$(MeOH)] + thiourea 179

5.4.7. *fac*-[Re(2,5-PicoH)$(CO)_3$(MeOH)] + 1-methyl-2-thiourea 181

5.4.8. Summary of the results of the substitution reactions of *fac*-[Re(2,5-PicoH)$(CO)_3$(MeOH)] with the range of entering ligands 183

5.5. Substitution reactions of *fac*-[Re(Isa)$(CO)_3$(MeOH)] with monodentate ligands in methanol 185

5.5.1. *fac*-[Re(Isa)$(CO)_3$(MeOH)] + pyridine 186

5.5.2. *fac*-[Re(Isa)$(CO)_3$(MeOH)] + thiocyanate ions 189

5.5.3. *fac*-[Re(Isa)$(CO)_3$(MeOH)] + thiourea 190

5.5.4. *fac*-[Re(Isa)$(CO)_3$(MeOH)] + 1-methyl-2-thiourea 192

5.5.5. Summary of the results of the substitution reactions of *fac*-[Re(Isa)$(CO)_3$(MeOH)] with different entering ligands 194

**Table of Contents**


5.6. Reactions of *fac*-[Re(Trop)$(CO)_3$(MeOH)] with monodentate entering ligands 196

5.6.1. *fac*-[Re(Trop)$(CO)_3$(MeOH)] + bromide ions 197

5.6.2. *fac*-[Re(Trop)$(CO)_3$(MeOH)] + iodide ions 199

5.6.3. *fac*-[Re(Trop)$(CO)_3$(MeOH)] + pyridine 201

5.6.4. *fac*-[Re(Trop)$(CO)_3$(MeOH)] + imidazole 203

5.6.5. *fac*-[Re(Trop)$(CO)_{3(}$MeOH)] + thiocyanate ions 205

5.6.6. *fac*-[Re(Trop)$(CO)_3$(MeOH)] + 4-dimethylaminopyridine 207

5.6.7. *fac*-[Re(Trop)$(CO)_3$(MeOH)] + thiourea 209

5.6.8. *fac*-[Re(Trop)$(CO)_3$(MeOH)] + 1-methyl-2-thiourea 212

5.6.9. Summary of the results of the methanol substitution reactions of the *fac*-[Re(Trop)$(CO)_3$(MeOH)] complex 213

5.7. Discussion 216

6. *High Pressure Kinetic Investigation of the Methanol Substitution in fac-[Re(Trop)$(CO)_3$(MeOH]*

6.1. Introduction 223

6.2. Background theory 225

6.2.1. Activation volume and activation entropy 225

6.3. Materials and methods 227

6.4. Results and Discussion 228

7. *Substitution Kinetics of fac-[Re(Trop)$(CO)_3(H_2O)$] in Aqueous Medium*

7.1. Introduction 235

7.2. Experimental procedure 236

7.3. Results and Discussion 237

7.3.1. Influence of $H^+$ ions on *fac*-[Re(Trop)$(CO)_3(H_2O)$] 237

7.3.2. Substitution reactions of *fac*-[Re(Trop)$(CO)_3(H_2O)$] with $NCS^-$ ions 239

7.3.3. Discussion 247

8. *$^{99m}$Tc in Radiopharmacy and In Vitro Cancer Screening Report*

8.1. Background of $^{99m}$Tc radiopharmaceuticals 249

8.2. Future of $^{99m}$Tc-radiopharmaceuticals 250

8.2.1. Nitrido labelling 251

**Table of Contents**


8.2.2. HYNIC labelling 251
8.2.3. Tricarbonyl labelling 252
8.3. Rhenium as analogue for $^{99m}$Tc 252
8.4. *In vitro* cancer screening report for some Re(I) compounds 253
8.4.1. Assay background and method 253
8.4.2. Results 255
8.5. Conclusion 256
9. *Critical Evaluation of the Study*
9.1. Results obtained 258
9.2. Future research 260
Appendix A 263
Appendix B 318

# ABBREVIATIONS

| | |
|---|---|
| 2,5-Pico$H_2$ | Pyridine-2,5-dicarboxylic acid |
| Å | Angstrom |
| AMP | 2-Aminomethylpyridine |
| AMP-NA | N-(Pyridin-2-ylmethyl)nicotinamide |
| BenzIsa | N-Benzylindole-2,3-dione |
| BHAH | Benzohydroxamic acid |
| Bipy | 2,2'-Bipyridine |
| BipyDC | 2,2'-Bipyridine-3,3'-dicarboxylic acid |
| ChrysH | Chrysin |
| Cl-oxH | 5-Chloro-8-hydroxyquinoline |
| DMAP | 4-dimethylaminopyridine |
| DMe-oxH | 5,7-Dimethyl-8-hydroxyquinoline |
| DMS | Dimethylsulphide |
| *fac* | Facial |
| $F_3$COIsaH | 5-(Trifluoromethoxy)isatin |
| FlavH | 3-Hydroxyflavone |
| Gly | Glycine |
| His | Histamine |
| His-BHA | N'-(1-(1H-imidazol-4-yl)ethyl)benzohydrazide |
| His-Prol | N-(2-(1H-imidazol-4-yl)ethyl)pyrrolidine-2-carboxamide |
| Im | Imidazole |
| IR | Infra Red |
| Isa | Isatin |
| $k_{obs}$ | Observed *pseudo* first-order rate constant |
| $k_1$ | First-order constant for the forward reaction |
| $k_{-1}$ | Rate constant for the reverse reaction |
| $K_1$ | Equilibrium constant |
| L,L'-bid | Bidentate ligand |

## Abbreviations

| | |
|---|---|
| LET | High-linear energy transfer |
| mAb | Monoclonal antibody |
| MeTU | 1-Methyl-2-thiourea |
| MLCT | Metal to Ligand Charge Transfer |
| NA | Nicotinic acid |
| $NCS^-$ | Thiocyanate ions |
| $[NEt_4]^+$ | Tetraethylammonium cation |
| NMR | Nuclear Magnetic Resonance Spectroscopy |
| $NO_3$IsaH | 5-Nitroisatin |
| $NTAH_3$ | Nitrilotriacetic acid |
| oxH | 8-Hydroxyquinoline |
| PET | Positron Emission Tomography |
| PMABut | N,N'-Bis(2-pyridylmethyl)-2-aminobutanol |
| PMAEth | N,N'-Bis(2-pyridylmethyl)-2-aminoethanol |
| PMAProp | N,N'-Bis(2-pyridylmethyl)-2-aminopropanol |
| PMAProp-Gly | 2-(3-(Bis(pyridine-2-yl)methyl)amino)propylamino)acetic acid |
| PMAProp-His | N'-(2-(1H-imidazol-4-yl)-$N^3$,$N^3$-bis(pyridine-2-ylmethyl)propane-1,3-diamine |
| PNP | Bis(diphenylphosphino)-propylamine |
| Prol | Proline |
| Py | Pyridine |
| ReAA | $[NEt_4]_2[Re(CO)_3(Br)_3]$ |
| SPECT | Single Photon Emission Computed Tomography |
| $t_{1/2}$ | Half-life |
| TropH | Troplone |
| TU | Thiourea |
| UV/Vis | Ultraviolet/Visible Spectroscopy |
| $\Delta H^{\ddagger}_{(k1)}$ | Enthalpy activation energy |
| $\Delta S^{\ddagger}_{(k1)}$ | Entropy activation energy |
| ° | Degrees |
| $\nu_{CO}$ | C=O stretching frequency |

# ABSTRACT

Over the past few years, significant interest has been shown in Rhenium and Technetium tricarbonyl complexes of the form *fac*-$[M(L,L'\text{-bid})(CO)_3(X)]^n$ (M = Tc(I) and Re(I), (L,L'-bid) = different donor atom bidentate ligands, X = range of monodentate ligands), as potential diagnostic and therapeutic radiopharmaceuticals, respectively. This is mainly due to the discovery of the *fac*-$[M(CO)_3(H_2O)_3]^+$ synthon with the inert *fac*-$[M(CO)_3]^+$ core and the labile water molecules. These main characteristics make the synthons very attractive for application in nuclear medicine.

Overall, the idea of this study was to gain further insight into the chemistry, coordination and kinetic behaviour of complexes containing the *fac*-$[M(CO)_3]^+$ core. From this idea, it was decided to synthesize a few novel ligand systems. This include *N*-benzylindole-2,3-dione, N,N'-bis(2-pyridylmethyl)-2-aminoethanol, N,N'-bis(2-pyridylmethyl)-2-amino-propanol, N,N'-bis(2-pyridylmethyl)-2-aminobutanol, N'-(2-(1H-imidazol-4-yl)ethyl)-$N^3$,$N^3$-bis(pyridine-2-ylmethyl)-propane-1,3-diamine, 2-(3-(bis(pyridin-2-yl)methyl)-amino)propylamino)-acetic acid, *N*-(2-(1H-imidazol-4-yl)ethyl)pyrrolidine-2-carboxamide, N'-(2-(1H-imidazol-4-yl)ethyl)benzohydrazide and N-(pyridin-2-ylmethyl)nicotinamide. Some of these ligands were successfully coordinated to the *fac*-$[Re(CO)_3]^+$ core as well. The ligand systems, as well as these Rhenium(I) compounds, were sent for *in vitro* testing. The ligand systems synthesized were designed with the idea to be potentially biologically active by itself as well.

A range of tricarbonyl complexes, of the form *fac*-$[Re(L,L'\text{-bid})(CO)_3X]$, were synthesized by using a wide variety of bidentate ligands (L,L'-bid), with systematically chosen donor atoms. The bidentate ligands include 2,2'-bipyridine-3,3'-dicarboxylic acid, 2,5-pyridinedicarboxylic acid, 8-hydroxyquinoline, 5-chloro-8-hydroxyquinoline, 5,7-dimethyl-8-hydroxyquinoline, tropolone, isatin, 5-nitroisatin, 5-(trifluoromethoxy)-isatin, benzohydroxamic acid, 3-hydroxyflavone, chrysin and bis(diphenylphosphino)-propylamine, X = variety of monodentate ligands and n = 0, 1.

During the study, four $^{99m}$Tc complexes were successfully synthesized, including *fac*-$[^{99m}Tc(2,5\text{-PicoH})(CO)_3(H_2O)]$, *fac*-$[^{99m}Tc(Trop)(CO)_3(H_2O)]$, *fac*-$[^{99m}Tc(Cl-$

ox)$(CO)_3(H_2O)$] and *fac*-[$^{99m}$Tc(DMe-ox)$(CO)_3(H_2O)$]. We were unable to isolate the $^{99m}$Tc compounds of five different ligand systems, even though the Rhenium analogues were successfully synthesized. This once again proved the similarities in chemistry of Rhenium and Technetium, but that this cannot always be assumed.

The lability and mechanism of substitution of the methanol ligand by simple monodentate nuclephiles were evaluated. The methanol substitution reactions, between *fac*-[Re(2,5-PicoH)$(CO)_3$(MeOH)], *fac*-[Re(Isa)$(CO)_3$(MeOH)] and *fac*-[Re(Trop)$(CO)_3$(MeOH)] and the variety of incoming ligands (bromide ions, iodide ions, pyridine, 4-dimethylaminopyridine, imidazole, thiocyanate ions, thiourea and 1-methyl-2-thiourea), all pointed towards an interchange associative or associative type mechanism, predicted from the negative $\Delta S^{\ddagger}$ values calculated. High pressure studies were performed and from the results, an interchange dissociative type mechanism was assigned, with a definite decrease in the reaction rate with an increase in pressure. These results once again proved the only way to unambiguously determine a reaction mechanism, is by means of the high pressure studies.

For the first time ever, the water substitution reaction of a compound of the type *fac*-[Re(L,L'-bid)$(CO)_3(H_2O)$] was performed. The reaction between *fac*-[Re(Trop)$(CO)_3(H_2O)$] and thiocyanate ions were followed. Overall the water substitution reaction has larger $k_1$ and $K_1$ values compared to the corresponding methanol substitution reaction, therefore indicating a faster reaction and a more stable product. These are especially great results for the use in nuclear medicine.

From the kinetic studies performed, excellent results were obtained of which one is the definite increase in reaction rate from N,O- to O,O'-donor bidentate ligand compounds. This was expected due to the increase in electron density on the metal centre and therefore the weakening of the Re-MeOH bond. The O,O'-donor bidentate ligands activate the Re(I) metal centre to an even greater extent, as was reported before. The '3+1' concept was proven, from the synthesis of *fac*-[Re(PMAEth-An)$(CO)_3$][$NO_3$], *fac*-[Re(PMAProp-His)$(CO)_3$][$NO_3$] and *fac*-[$NEt_4$]/[Na][Re(NTA-An)$(CO)_3$], by linking a biologically active ligand to the backbone of a tridentate ligand that is coordinated to the *fac*-$[Re(CO)_3]^+$ core. This leaves huge scope for potential radiopharmaceutical agents of this type.

**Abstract**

Four of the ten crystal structure reports in this study are monodentate substituted complexes, which serves as further confirmation of the kinetic end products.

# OPSOMMING

Die laaste paar jaar het die belangstelling in Renium en Tegnesium trikarboniel komplekse, *fac*-$[M(CO)_3]^+$ (M = Tc(I) en Re(I)), beduidend toegeneem as potensiële diagnostiese en terapeutiese radiofarmaseutiese middels onderskeidelik. Dit is grotendeels agv die ontdekking van die *fac*-$[M(CO)_3(H_2O)_3]^+$ moïeteit. Verskeie belowende komplekse, wat die trikarboniel moïeteit bevat, is al gesintetiseer en twee van die hoof eienskappe wat die moïeteit so aantreklik maak vir die gebruik in kliniese medisyne, is die inerte *fac*-$[M(CO)_3]^+$ kern en die labiele water molekule.

Die algehele motief van die studie was om meer inligting en beter insig ten opsigte van die chemiese, koördinatiewe en kinetiese gedrag van die *fac*-$[M(CO)_3]^+$ tipe komplekse te verkry. Vanaf hierdie uitgangspunt, is daar besluit om `n reeks nuwe vry ligande te sintetiseer, om te gebruik as potensiële biologies-aktiewe verbindings self, en om te koordineer met *fac*-$[Re(CO)_3]^+$ om sodoende `n potensiële aktiewe kompleks te verkry. Die ligande sluit in *N*-bensielindol-2,3-dioon, N,N'-bis(2-piridielmetiel)-2-aminoetanol, N,N'-bis(2-piridielmetiel)-2-aminopropanol, N,N'-bis(2-piridielmetiel)-2-aminobutanol, N'-(2-(1H-imiedasool-4-iel)etiel)-$N^3$,$N^3$-bis(piridien-2-ielmetiel)-propaan-1,3-diamien, 2-(3-(bis(piridien-2-iel)metiel)amino)propielamino)-asynsuur, *N*-(2-(1H-imiedasool-4-iel)etiel)pirrolidien-2-karboksamied, N'-(2-(1H-imiedasool-4-iel)etiel)bensohidrasied en N-(pyridin-2-ielmetiel)nikotinamied. Sommige van die ligande is suksesvol gekoördineer met die *fac*-$[Re(CO)_3]^+$ moïeteit en die ligand sisteme sowel as die Rhenium(I) komplekse is gestuur vir *in vitro* toetse.

`n Reeks trikarboniel komplekse, *fac*-$[Re(L,L'\text{-bid})(CO)_3X]$, is gesintetiseer met `n wye reeks bidentate ligande (L,L'-bid) met sistematies gekose donor atome. Die bidentate ligande sluit in 2,2'-bipiridien-3,3'-dikarboksielsuur, 2,5-piridiendikarboksielsuur, 8-hidroksiequinolien, 5-chloro-8-hidroksiequinolien, 5,7-dimetiel-8-hidroksiequinolien, tropoloon, isatien, 5-nitroisatien, 5-(trifloorometoksie)isatien, bensohidroksaamsuur, 3-hidroksieflavoon, chrysien en bis(difenielfosfino)-propielamien, X = reeks monodentate ligande en n = 0, 1.

## Opsomming

Vier $^{99m}$Tc komplekse is ook suksesvol gesintetiseer, insluitend *fac*-[$^{99m}$Tc(2,5-PicoH)$(CO)_3(H_2O)$], *fac*-[$^{99m}$Tc(Trop)$(CO)_3(H_2O)$], *fac*-[$^{99m}$Tc(Cl-ox)$(CO)_3(H_2O)$] en *fac*-[$^{99m}$Tc(DMe-ox)$(CO)_3(H_2O)$]. Die isolasie van vyf $^{99m}$Tc komplekse, waarvan die Rhenium komplekse suksesvol gesintetiseer is, was egter onsuksesvol. Hierdie is net weereens `n bewys dat die ooreenkomste in the chemie van Rhenium en Technetium nie altyd aanvaar kan word nie.

Die labiliteit en meganisme van die methanol ligand se substitusie is evalueer deur eenvoudige monodentate nukleofiele. Die metanol substitusie reaksies tussen *fac*-[Re(2,5-PicoH)$(CO)_3$(MeOH)], *fac*-[Re(Isa)$(CO)_3$(MeOH)] en *fac*-[Re(Trop)$(CO)_3$(MeOH)] en ‘n reeks inkomende ligande (bromied ione, jodied ione, piridien, 4-dimetielaminopiridien, imiedasool, tiosianaat ione, tio-ureum en 1-metiel-2-tio-ureum), het almal `n uitruilings assosiatiewe tipe meganisme voorgestel vanuit die negatiewe aktiveringsentropie waardes and postiewe aktiveringsentalpie waardes. Hierna is hoë-druk studies bestudeer en vanuit die resultate is ‘n uitruilings dissosiatiewe meganisme voorgestel, met ‘n defnitiewe afname in die reaksietempo met ‘n toename in druk. Hierdie resultate het weereens bewys dat die enigste manier om sonder enige twyfel `n reaksie meganisme voor te stel, hoë-druk studies en die bepaling van die aktiveringsvolume is.

Vir die eerste keer is die water substitusie reaksie van `n kompleks van die vorm *fac*-[Re(L,L’-bid)$(CO)_3(H_2O)$] bestudeer. Die water substitusie reaksie tussen *fac*-[Re(Trop)$(CO)_3(H_2O)$] and tiosianaat ione is gevolg. In totaal het die water substitusie reaksie hoër $k_1$ en $K_1$ waardes as die ooreenstemmende metanol substitusie reaksies. Dit dui op ‘n vinniger en `n meer stabiele produk vir die water substitusie reaksie. Hierdie is uitsonderlike goeie resultate, veral vir die potensiële gebruik in kliniese medisyne.

Vanuit die kinetiese studies is uitstekende resultate verkry. `n Duidelike toename in die reaksietempo van die N,O- na die O,O‘-donor bidentate ligand komplekse is verkry wat egter verwag was agv die toename in the elektrondigtheid op die metaal senter en daarom die verswakking van die Re-MeOH binding. Die O,O’-donor bidentate ligande aktiveer die Re(I) metaal senter tot ‘n groter mate as wat vroeër gerapporteer is.

## Opsomming

Die ‘3+1’ konsep is bewys deur die sintese van *fac*-[Re(PMAEth-An)$(CO)_3$][$NO_3$], *fac*-[Re(PMAProp-His)$(CO)_3$][$NO_3$] en *fac*-[$NEt_4$]/[Na][Re(NTA-An)$(CO)_3$], deur ‘n biologiese aktiewe ligand te ‘link’ op die ruggraat van ‘n tridentate ligand wat reeds gekoordineer is met *fac*-[$Re(CO)_3]^+$. Hierdie resultate maak ‘n wye veld oop vir potensiële radiofarmaseutiese agente.

Vier van die tien kristalstrukture in hierdie studie is monodentaat gesubstitueerde komplekse wat verder as bewys dien van die kinetiese eindprodukte.

# 1 GENERAL BACKGROUND AND AIM

## 1.1 Introduction

It is estimated that 571 950 people would have died of cancer in 2011 in the USA alone. That equates to more than 1 500 people dying of cancer every day. Cancer is the second largest cause of death in the US, exceeded only by heart disease, and accounts for a quarter of the total number of deaths each year. In 2007, 7.6 million people died of cancer over the world and it is estimated that there were 12 million new cases of cancer during that year. Globally, lung cancer is by far the most fatal cancer in men (29%) and women (26%), followed by prostate (11%) and breast (15%) cancer respectively. These terrifying statistics are the main reason why the diagnosis of cancer is such a very high priority in medicine today. However the number of new radiopharmaceuticals have fallen to a historic low and adds to the strain on the success of the nuclear medicinal industry.

## 1.2 Diagnostic and therapeutic radiopharmaceuticals

Radiotherapy targets cancer cells for cell destruction and it is essential that the particle emission from the radionuclide have decay energy that is deposited over a short range in tissue (α, β & Auger-conversion). This is the case for $^{186}$Re and $^{188}$Re nuclides.

The two radioactive isotopes of Rhenium, $^{186}$Re and $^{188}$Re, are of interest in therapeutic application in nuclear medicine because of their β-radiation characteristics. The physical properties (availability, tissue range, half-life and energy) of these two nuclides are ideal for the effective transfer of energy to the cancerous tissue. β-emitting radionuclides are extensively applied in radiotherapy, because of their low ionisation densities and therefore low linear energy transfer radiation (LET). High energy β-particles are perfect for large tumor areas where, even if it is heterogeneously spaced in the tumour, the distribution of the dose will still be uniform. For smaller tumors or single

disseminated tumor cells, α-particles are popular for the treatment because it produces high densities of ionisation, which is depositied over short ranges.

Most radiopharmaceuticals available today are for diagnostic purposes. The imaging of the tracer biodistribution is possible with γ-ray energy. The drawback is that the γ-emission contribute little to the drug's tumor dose and extensively to the whole body radiation burden. The ideal properties for a nuclide to be used as in an imaging agent, for measurements, biodistribution studies, scintigraphy and dosimetric calculations, will be γ-rays of 100 – 200 keV with a 5-20% abundance.

Several radionuclides can be considered for PET imaging purposes. The most useful nuclides are $^{11}C$ ($t_{1/2}$ = 20.3 min),$^{13}N$ ($t_{1/2}$ = 9.97 min), $^{15}O$ ($t_{1/2}$ = 2.03 min), $^{18}F$ ($t_{1/2}$ = 109.7 min), $^{64}Cu$ ($t_{1/2}$ = 720 min) and $^{68}Ga$ ($t_{1/2}$ = 68 min). With PET as imaging modality, accurate and quantitative data on the distribution of the radionuclide in the desired target cells are provided. Another option is Auger electron emitters, but in this case the nuclide must be carried directly into the nucleus of every cancer cell since its range is very short. The preferred nuclide for imaging in nuclear medicine is $^{99m}Tc$, because of its availability, chemical versatility and physical properties.

## 1.3 Rhenium and Technetium in nuclear medicine

The $^{99m}Tc$ isotope, incorporated as radionuclide in radiopharmaceuticals, is used in more than 85% of diagnostic scans performed each year in hospitals and is the most widely used radiometal in diagnostic imaging. It is produced, for medical applications, by a $^{99}Mo/^{99m}Tc$ generator *via* the decay of $^{99}Mo$, with a half-life of 67 hours meaning that $^{99m}Tc$, with $t_{1/2}$ = 6h, is constantly produced.

Even though there is no stable isotope of Technetium, the chemistry thereof is relatively well explored. Ever since 1970 when the importance of this metal as diagnostic radionuclide ($^{99m}Tc$) became apparent, the research on Technetium was one of the focal points in many laboratories. The main reason for the popularity of $^{99m}Tc$ in diagnostic use, is the fact that the γ-rays emitted by this nuclide has virtually the same wavelength as that of soft X-rays utilized in modern medicine, ensuring adequate penetration and the minimal damage done. Furthermore, its other properties also add to the popularity

of the radionuclide: $t_{1/2}$ = 6 hours, γ-rays (140 keV, 89%) and availability from a $^{99}Mo/^{99m}Tc$ generator.

$^{99m}Tc$ is a 4$^{th}$ row congener of Rhenium, with the chemistry of $^{99m}Tc$ and $^{186/188}Re$ sometimes being almost identical. With the increasing popularity of Technetium in radiopharmacy, the interest in Rhenium also increased in the nuclear medicine field.

Rhenium, being the rarest of all natural occurring elements, occurs in nature as a mixture of two non-radioactive isotopes, $^{185}Re$ (37.4%) and $^{187}Re$ (62.6%). For the application in nuclear medicine, two isotopes $^{186}Re$ ($t_{1/2}$ = 89.2 h, ~ 10 % 137 keV γ-rays, 107 keV β-rays) and $^{188}Re$ ($t_{1/2}$ = 16.9 h, ~ 10 % 155 keV γ-rays, 201 keV β-rays) with their β-irradiation is of interest for therapeutic use.

$^{188}Re$ is produced by a $^{188}W/^{188}Re$ generator, while no-carrier-added $^{186}Re$ is available from a cyclotron by a (p, n) reaction on $^{186}W$, or it can be produced from reactors following a one neutron capture process[1]. The nuclear properties are of prime importance when a choice has to be made for a specific therapeutic application.[2] $^{186}Re$ and $^{188}Re$ are usually included as possible radionuclides in potential radiopharmaceuticals when considering predominant nuclides in therapeutic nuclear medicine. This is due to its similar chemistry to that of Technetium and because of its favourable properties for use in therapy.

One of the focus areas during the last ten years was the development of broadly applicable tracers for metabolism and receptor studies. This involved the incorporation of the radionuclide, $^{99m}Tc$, into the biologically active molecule by means of chelating the nuclide followed by linking the biomolecule to the chelate. For a chelating group to be considered, it should be highly stable, small in size, should have an adaptable lipophilicity and preferably should not have isomers.[2,3,4]

The radionuclides, $^{186/188}Re$ and $^{99m}Tc$, are basically applied in nuclear medicine in two different ways; as a highly stable metal complex with no biomolecule on the backbone that is completely resistant to metabolic processes or as metal complexes with

[1] Moustapha, M.E., Ehrhardt, G.J., Smith, C.J., Szajek, L.P., Eckelman, W.C., Jurisson, S.S. *Nucl. Med. Biol.* **2006**, *33*, 81-89.
[2] Dilworth, J.R., Parrott, S.J. *Chem. Soc. Rev*. **1998**, *27*, 43-45.
[3] Schubiger, P.A., Alberto, R., Smith, A. *Bioconjug. Chem*. **1996**, *7*, 165-179.
[4] Ham, R., Katzenellenbogen, J. *Nucl. Med. Biol*. **1997**, *24*, 485-498.

biomolecules attached to it. The second type of radiopharmaceuticals consisted primarily of iodinated biomolecules. $^{99m}$Tc and $^{188}$Re radiolabeled compounds have substituted these compounds because of convenience and availability and thereby a new generation of radiopharmaceuticals was introduced. A few limitations were expected with this change of radionuclide: Firstly the label will be much larger in size than the idodine atom, and this will interfere with the bioactivity and physico-chemical properties of the biomolecule. Therefore the metal core should be kept small and its physico-chemical properties should adopt those of the biomolecule. Furthermore, with regards to the design and application, the labeling should be a one-step reaction in a saline solution (0.9% NaCl in water/buffer) with very high purity (98% yield), a 1:1 radionuclide: molecule relationship and the time required for the labeling should be compatible with the half-life of the nuclide. The fact that the synthesis should be done in a saline solution made organometallic compounds until recently, quite unattractive.

Traditionally, when Technetium are used in nuclear medicine, it is complexed to isocyanide or tetradentate N- and S donating ligand systems, for example $[Tc(MIBI)_6]^+$ (MIBI = 2-methoxy-2-methylpropylisocyanide) with its isocyanide ligand.[5,6] Nevertheless, in literature it was proposed to use the organometallic Rhenium and Technetium carbonyl complexes for potential application in nuclear medicine.[7,8]

Much research have since gone towards utilizing the *fac*-$[M(CO)_3]^+$ (M = Re, Tc) core, especially after the breakthrough by Alberto *et al*. of synthesizing the complexes bearing the *fac*-$[M(CO)_3]^+$ moiety by avoiding the usual high pressure route.[9,10] The three labile aqua ligands allow a wide range of ligand systems to be coordinated to the *fac*-$[M(CO)_3]^+$ core under mild conditions.

[5] Abram, U., Beyer, R., Münze, R. *Inorg. Chim. Acta*. **1989**, *160*, 139-142.
[6] Abrams, J.M., Davison, A., Jones, A.G., Costello, C.E., Pang, H. *Inorg. Chem*. **1983**, *22,* 2798-2800.
[7] Salmain, M., Gunn, M., Gorfi, A., Top, S., Jaouen, G. *Bioconjug. Chem*. **1993**, *4*, 425-433.
[8] Top, S., Hafa, E.H., Vessières, A., Quivy, J., Vaissermann, J., Hughes, D.W., McGlinchey, M.J., Mornan, J.-P., Thoreau, E., Jaouen, G., *J. Am. Chem. Soc*. **1995**, *117*, 8372-8380.
[9] Spradau, T.W., Katzenellenbogen, J.A. *Organometallics* **1998**, *17*, 2009-2017.
[10] Alberto, R., Schibli, R., Egli, A. Patent no 97201232.2, 1997.

## 1.4 Aim of this study

Many metals with radioactive isotopes exist that emit radiation which is suitable for the radiation of tumors eg. $^{188}$Re, $^{67}$Cu, and $^{90}$Y. The challenge however has always been to synthesize a drug that can highly selectively deliver the radiation to the tumor cells, and is not as obvious as it is sometimes thought to be. Many factors need to be considered and taken into account. These considerations are discussed in detail in Chapter 2.

Regarding imaging in nuclear medicine, many coordination compounds of $^{99m}$Tc are well known and relatively effective. Also, some of the synthetic approaches used in Technetium chemistry can be used for Rhenium complexes.

*fac*-$[M(CO)_3(H_2O)_3]^+$ complexes (M = $^{186/188}$Re, $^{99m}$Tc) have been a focus point for some time due to, if labelled with proper director ligands, their potential use as diagnostic and therapeutic agents. The preferred starting synthon for these complexes containing the *fac*-$[Re(CO)_3]^+$ moiety is *fac*-$[NEt_4]_2[Re(CO)_3(Br)_3]$. In the past, it was prepared from perrhenate, $BH_3$.THF and $(NEt_4)Br$ under a 1 atm CO atmosphere. Nowadays it is prepared from the Rhenium dimer, $[Re_2(CO)_{10}]$, and $Br_2$, under strict Schlenck conditions for optimum yield.

One of the main reasons why the *fac*-$[NEt_4]_2[Re(CO)_3(Br)_3]$ synthon is so popular is its inert *fac*-$[M(CO)_3]^+$ core. Also, the three labile bromido ligands, due to the *trans* influence of the three facial carbonyl ligands, is another advantage. These bromido ligands can exchange under mild conditions with a wide variety of ligand systems, and provides significant scope for a systematic and wide variation of complexes with different sized ligand systems, different donor atom sets, functionalities and physical properties.

To ideally incorporate the $^{99m}$Tc and $^{188}$Re nuclides into biomolecules, it is imperative to fully study the reactivity of these complexes. It is important to understand, and even be able to sometimes predict, the complex formation and rates of reactions of these complexes. The thermodynamic and kinetic investigation of the aqua and methanol substitution reactions of *fac*-$[Re(L,L'\text{-bid})(CO)_3(H_2O)]^n$ and *fac*-$[Re(L,L'\text{-bid})(CO)_3(MeOH)]^n$ respectively (with (L,L'-bid = variety of bidentate ligands), are of

special interest in this study; thus the residence time of the coordinated water and methanol ligand on the metal complexes.

With the '2+1' approach, bidentate ligand systems are used to link the biological molecule to the *fac*-$[Re(CO)_3]^+$ core. This leaves the third position on the metal core available for substitution by electron rich monodentate ligands. *In vivo*, this imply that this third position is exposed to possible nucleophilic attack by ligands in the blood, eg. $NCS^-$ and halides. This exemplifies the importance to investigate the reactivity and kinetics of these systems to potential entering ligands.

After a detailed literature search, it was found that a large number of synthetic procedures of the Re(I) tricarbonyl core has been reported, with a wide variety of different ligand systems. However, there is almost no evidence available of reactivity studies for these types of complexes.

One of the main objectives of this study was therefore to focus on the kinetic behaviour of a range of model *fac*-$[Re(CO)_3]^+$ complexes. The stepwise aims of this study are summarized below:

- Synthesis of new ligands including *N*-benzylindole-2,3-dione (BenzIsa), N,N'-bis(2-pyridylmethyl)-2-aminoethanol (PMAEth), N,N'-bis(2-pyridylmethyl)-2-aminopropanol (PMAProp), N,N'-bis(2-pyridylmethyl)-2-aminobutanol (PMABut), N'-(2-(1H-imidazol-4-yl)ethyl)-$N^3$,$N^3$-bis(pyridine-2-ylmethyl)propane-1,3-diamine (PMAProp-His), 2-(3-(bis(pyridin-2-yl)methyl)amino)propylamino)acetic acid (PMAProp-Gly), *N*-(2-(1H-imidazol-4-yl)ethyl)pyrrolidine-2-carboxamide (His-Prol), N'-(2-(1H-imidazol-4-yl)ethyl)benzohydrazide (His-BHA) and N-(pyridin-2-ylmethyl)nicotinamide (AMP-NA).
- Synthesis of complexes of the type *fac*-$[Re(L,L'\text{-bid})(CO)_3X]^n$, with a wide range of selected bidentate ligands. L,L'-bid = different N,N'-, N,O'-, O,O'- and P,P'-donor bidentate ligands, X = $H_2O$, $Br^-$, $I^-$, Py (pyridine), DMAP (4-dimethylaminopyridine), Im (imidazole), $NCS^-$ (thiocyanate ions), TU (thiourea) and MeTU (1-methyl-2-thiourea) and n = 0, 1. As N,N'-donor bidentate ligands, 2,2'-bipyridine-3,3'-dicarboxylic acid (BipyDC) were used. The N,O-donor bidentate ligands used are 2,5-pyridinedicarboxylic acid (2,5-Pico$H_2$), 8-hydroxyquinoline (oxH), 5-chloro-8-hydroxyquinoline (Cl-oxH) and 5,7-dimethyl-

8-hydroxyquinoline (DMe-oxH). As O,O'-donor bidentate ligands, tropolone (TropH), isatin (IsaH), 5-nitroisatin ($NO_2$IsaH), 5-(trifluoromethoxy)isatin ($F_3$COIsaH), benzohydroxamic acid (BHAH), 3-hydroxyflavone (FlavH) and chrysin (ChrysH) were used. The P,P'-donor bidentate ligand used was bis(diphenylphosphino)-propylamine (PNP).

- Synthesis of complexes of the type *fac*-[Re(L,L'-tri)$(CO)_3]^n$, with L,L'-tri = different N,N,N- and O,N,O-donor tridentate ligand systems and n = 0, 1. N,N'-Bis(2-pyridylmethyl)-2-aminoethanol (PMAEth), N,N'-Bis(2-pyridylmethyl)-2-aminopropanol (PMAProp) and N,N'-Bis(2-pyridylmethyl)-2-aminobutanol (PMABut) were used as N,N,N-donor tridentate ligands and nitrilotriacetic acid ($NTAH_2$) as O,N,O-tridentate ligand.
- Synthesis of *fac*-[$^{99m}$Tc(L,L'-bid)$(CO)_3(H_2O)]^n$ and *fac*-[$^{99m}$Tc(L,L'-tri)$(CO)_3]^n$ type complexes with L,L'-bid = different bidentate ligands, L,L'-tri = different tridentate ligands and n = 0, 1. 2,5-Pyridinedicarboxylic acid (2,5-Pico$H_2$), tropolone (TropH), 5,7-dimethyl-8-hydroxyquinoline (DMe-oxH), 5-chloro-8-hydroxyquinoline (Cl-oxH), isatin (Isa), 2,2'-bipyridine-3,3'-dicarboxylic acid (BipyDC) and benzohydroxamic acid (BHAH) was used as bidentate ligand systems and bis(diphenylphosphino)-propylamine and N,N'-bis(2-pyridylmethyl)-2-aminoethanol (PMAEth) was used as tridentate ligand systems.
- Linking of biologically active molecules to the backbone of a ligand system that is coordinated to the *fac*-$[M(CO)_3]^+$ core. Also, to first link the biologically active molecule to the ligand system and then coordinating the moiety to the *fac*-$[M(CO)_3]^+$ core.
- Synthesis of water soluble *fac*-[Re(L,L'-bid)$(CO)_3(H_2O)$] type complexes, to be able to evaluate the kinetic reactivity in aqueous medium. There is no available kinetic data for complexes of this type, where aqua substitution reactions between *fac*-[Re(L,L'-bid)$(CO)_3(H_2O)$] type complexes and monodentate entering ligands are intensely studied. It is imperative to completely understand the reactivity and stability of these complexes in aqueous medium, since most labeling kits today are in saline, especially for the potential use in nuclear medicine.

- Characterize these complexes and ligands by single crystal X-ray crystallography, IR, $^{1}H$ NMR and $^{13}C$ NMR. In some cases the complexes were characterized by HPLC and MS as well. The $^{99m}Tc$ complexes were characterized only by HPLC (connected to a γ-detector).
- Determination of the mechanism of the aqua substitution reactions between *fac*-[Re(Trop)$(CO)_3(H_2O)$] and thiocyanate ions and the methanol substitution reactions between *fac*-[Re(Trop)$(CO)_3$(MeOH)], *fac*-[Re(2,5-PicoH)$(CO)_3$(MeOH)] and *fac*-[Re(Isa)$(CO)_3$(MeOH)] and different entering ligands (bromide and iodide ions, pyridine, imidazole, 4-dimethylaminopyridine, thiocyanate ions, thiourea and 1-methyl-2-thiourea) by means of a kinetic and temperature study, and isolation and characterization of the final products.
- Perform high pressure studies in order to unambiguously propose an intimate mechanism for the reaction between *fac*-[Re(Trop)$(CO)_3$(MeOH)] and pyridine, imidazole, thiourea and 1-methyl-2-thiourea as entering ligands. It has been found that the errors in the $\Delta V^{\ddagger}$ values are much less than those in the $\Delta S^{\ddagger}$ values, in experiments that have been repeated using both methods.[11]

[11] Newman, K.E., Meyer, F.K., Merbach, A.E. *J. Am. Chem. Soc* **1979**, *101*, 1470-1476.

# 2 LITERATURE STUDY

## 2.1 Brief history of potential agents with $^{99m}$Tc and Re in the last 20 years

Over the past few decades, a large amount of research has gone into the development of potential radiopharmaceuticals. With a wide range of promising metal cores, ligand systems and strategies/approaches, there is a significant number of possibilities to explore. One of the strategies on the oxo core, the '3+1' mixed ligand complex, is described as the $[^{99m}TcO]^{3+}$ core, coordinated by a tridentate ligand, and a monomeric complex. This approach has been exploited for the labeling of receptor-binding molecules. The general pathway is presented in Figure 2.1.

**Figure 2.1: Schematic representation for the preparation of '3+1' $^{99m}$Tc complexes.**

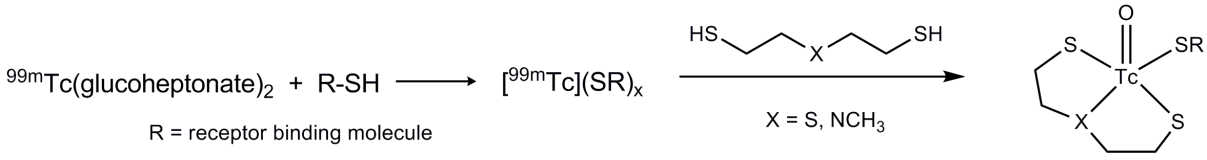


The approach in Figure 2.1 utilizes a biological molecule containing an available thiol, which is mixed with $^{99m}$Tc-glucoheptonate in the presence of a tridentate ligand. Some of these '3+1' complexes have shown instability[1], but generally the complexes from a tridentate aminedithiol are more stable than the thioetherdithiols.[2,3,4] Pietzsch and co-workers studied the basic chemistry of radiotracer design of these metal

[1] Syhre, R., Seifert, S., Spies, H., Gupta, A., Johannsen, B. *Eur. J. Nucl. Med*. **1998**, *25*, 793-796.
[2] Skaddan, M.B., Wust, F., Katzenellenbogen, J.A. *J. Org. Chem*. **1999**, *64*, 8108-8121.
[3] Wust, F., Carlson, K.E., Katzenellenbogen, J.A., Spies, H., Johannsen, B. *Steroids* **1998**, *63*, 665-671.
[4] Bergmann, R., Brust, P., Scheunemann, M., Pietzsch, H.-J., Seifert, S., Roux, F., Johannsen, B. *Nucl. Med. Biol*. **2000**, *27*, 135-141.

tricarbonyl thioether complexes with various thioether ligand systems designed to act as linkers to the biologically active molecules.[5]

It was previously reported that dithiocarbamates, as bidentate chelators, coordinate strongly to the *fac*-$[M(CO)_3]^+$ core and are very stable throughout a wide pH range.[6] The advantages of dithiocarbamates as bidentate ligands are their 'soft' Lewis base character, which implies a high affinity for the 'soft' acids – *fac*-$[M(CO)_3]^+$, and their potential to be modified so that there is a free carboxy group for potential coupling with biological molecules.

A typical '2+1' mixed ligand approach is based on two concepts; firstly where the radiolabelled biomolecule is present as the bidentate ligand or as part thereof ('$2_B$ + 1') and in the second instance where the monodentate ligand presents the labelled biomolecule ('2 + $1_B$').

The '2+1' strategy with the dithiocarbamate ligand has been explored with the *fac*-Re(I) tricarbonyl moiety with various monodentate ligands (phosphines, isocyanides etc.),[8,7] also by multi-step reactions and by the use of thiuram disulfides or thallium salts. In 2004, dithiocarbamate-isocyanide systems were studied for labeling amino acids and peptides with the *fac*-$[M(CO)_3]^+$ core and great results were obtained.[8]

Katzenellenbogen developed a 1-pot method and thereafter a double ligand-transfer method to prepare *fac*-$[Re(CO)_3(Cp)]$ complexes linked to biomolecules.[9,10,11,12] A schematic overview is given in Figure 2.2.

---

[5] Pietzch, H.J., Grupta, A., Reisgys, M., Drews, A., Seifert, S., Syhre, R., Spies, H., Alberto, R., Abram, U., Schubiger, A.P., Johannsen, B. *Bioconjug. Chem*. **2000**, *11*, 414-424.

[6] Gorschkov, N.I., Katzenellenbogen, J.A., Luyt, L.G., Lumpov, A.A., Miroslavov, A.E., Suglobov, D.N. *Technetium, Rhenium and Other Metals in Chemistry and Nuclear Medicine*, SG Editorial, Padova, **2002**, 127-130.

[7] Mattia Riondato, D.C., Martin, D., Suades, J., Alvarez-Larena, A., Mazzi, U. *Eur. J. Inorg. Chem*. **2005**, 4048-4055.

[8] Gorshkov, N.I., Schibli, R., Schubiger, A.P., Lumpov, A.A., Miroslovov, A.E., Suglobov, D.N. *J. Organomet. Chem*. **2004**, *689*, 4757-4763.

[9] Minutolo, F., Katzenellenbogen, J.A. *J. Am. Chem. Soc*. **1998**, *120*, 13264-13265.

[10] Minutolo, F., Katzenellenbogen, J.A. *J. Am. Chem. Soc*. **1998**, *120*, 4514-4515.

[11] Minutolo, F., Katzenellenbogen, J.A. *Organometallics* **1998**, *18*, 2519-2530.

[12] Spradau, T.W., Edwards, W.B., Anderson, C.J., Welch, M.J., Katzenellenbogen, J.A. *Nucl. Med. Biol*. **1999**, *26*, 1-7.

**Figure 2.2: Synthesis of *fac*-tricarbonyl metal complexes by the double ligand-transfer method, complex activation and conjugation to the biomolecule.**

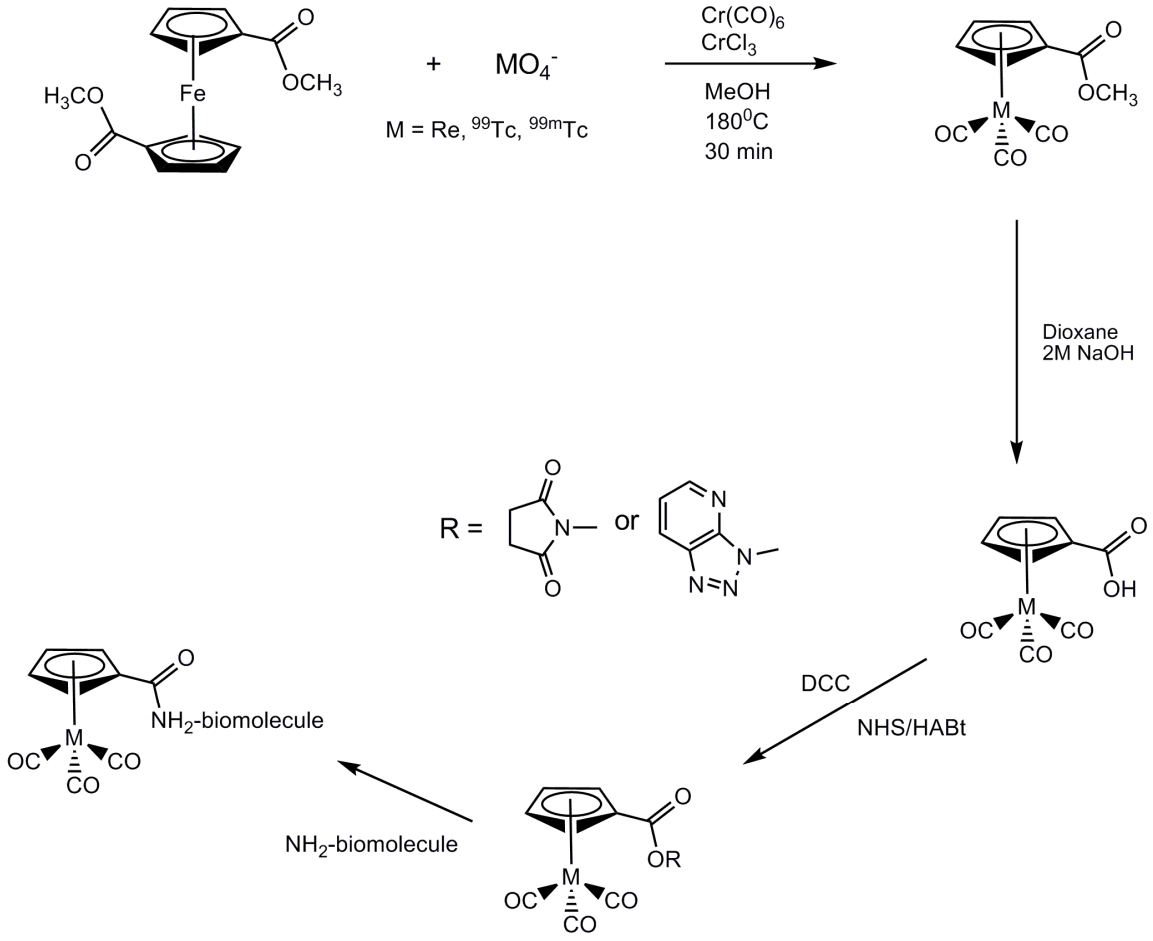


Integrated labeling methods, where chelating groups for Rhenium and Technetium are incorporated into a steroid-like carbon skeleton have been investigated, by mimicking the 3D configuration of a steroid. There are two methods that have been explored. Two bidentate aminethiol ligands have been used to mimic androgen and progesterone (**A**, **B**).[13,14,15]

[13] Chi, D.Y., O'Neil, J.P., Anderson, C.J., Welch, M.J., Katzenellenbogen, J.A. *J. Med. Chem*. **1994**, *37*, 928-937.
[14] Chi, D.Y., Katzenellenbogen, J.A. *J. Am. Chem. Soc*. **1993**, *115*, 7045-7046.
[15] Ham, R.K., Chi, D.Y., Katzenellenbogen, J.A. *J. Org. Chem*. **1996**, *61*, 2624-2631.

**Figure 2.3: Examples of Steroid-inclusion compounds.**

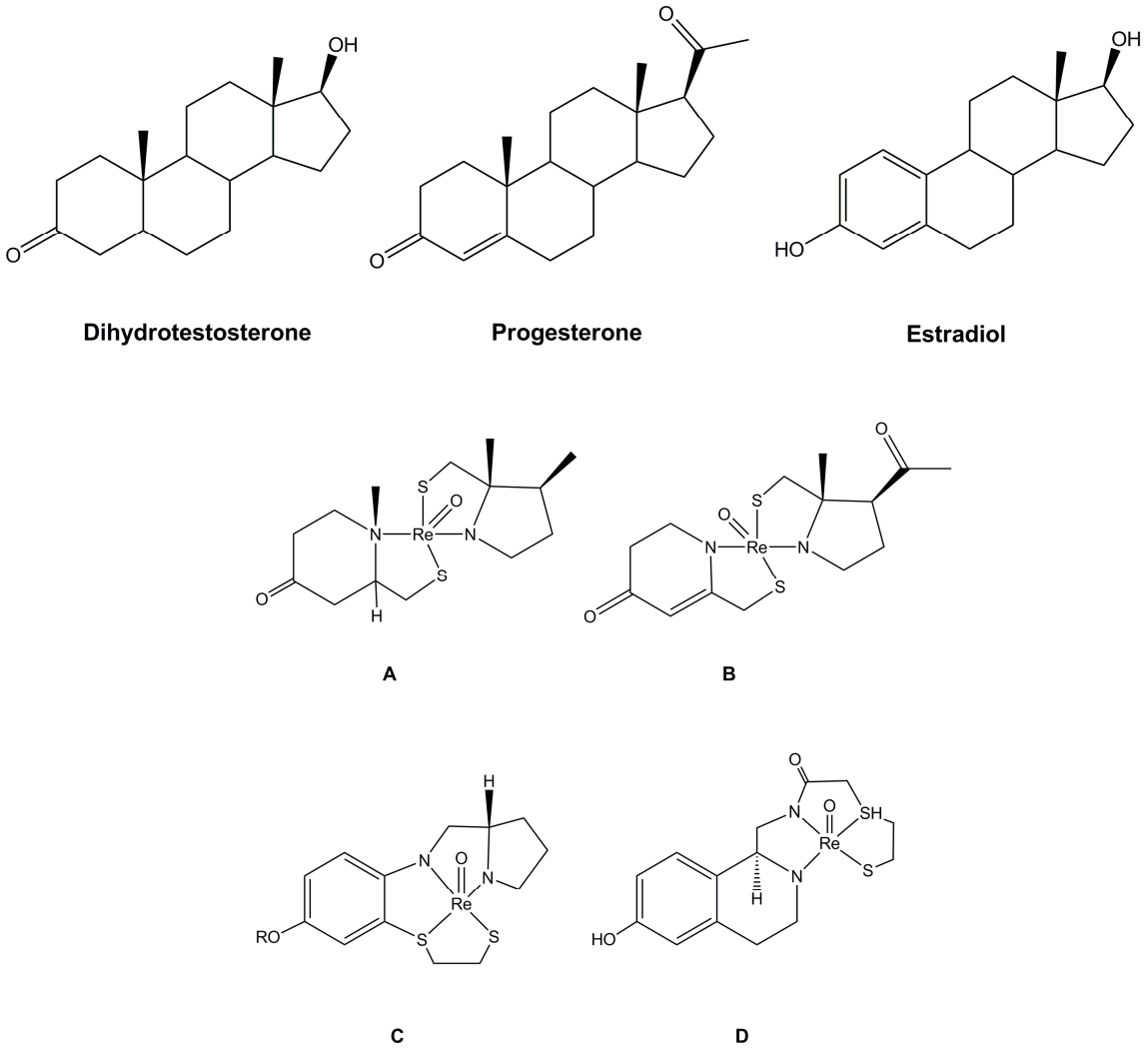


In the other method, four coordinating groups for Rhenium are built into the pseudosteroid precursor. The coordination of Rhenium then joins the B and C rings for compound C and rings C and D to form compound D, shown in Figure 2.3.[16]

There are several examples where amino acid sequences, that coordinate *via* N and S atoms, have been added to a peptide or incorporated into the peptide before radiolabeling[17] (Figure 2.4).

$^{99m}$Tc-MAG$_3$ is another example and it incorporated the amino acid sequence Gly-Gy-Gly as part of the multidentate ligand.

[16] Ham, R.K., Katzenellenbogen, J.A. *J. Org. Chem*. **1997**, *62*, 6290-6297.
[17] Liu, S., Edwards, D.S. *Chem. Rev*. **1999**, *99*, 2235-2268.

**Figure 2.4: Stable $^{99m}$Tc complexes with short amino acid sequences.**

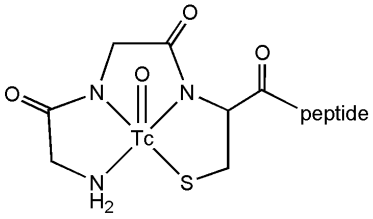


[TcO(Gly-Gly-Cys)]

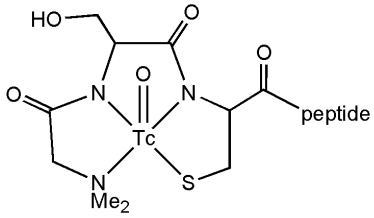


[TcO(Me$_2$Gly-Ser-Cys)]

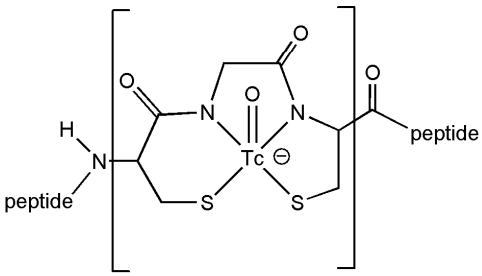


[TcO(Cys-Gly-Cys)]$^-$

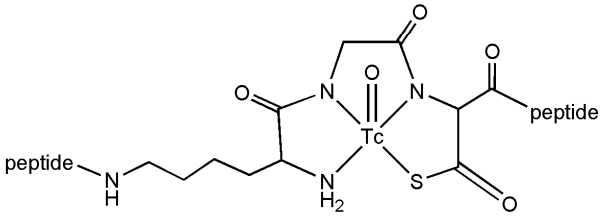


[TcO(Lys-Gly-Cys)]

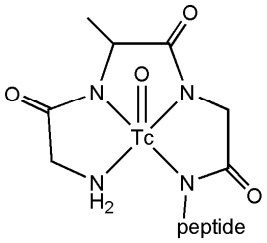


[TcO(Gly-Ala-Gly)]

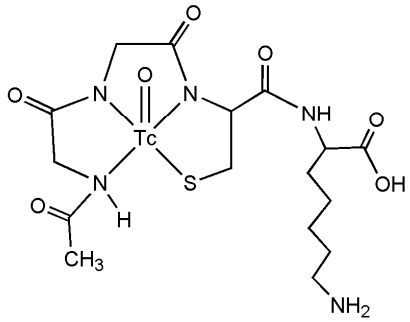


[TcO(Gly-Gly-Cys-Lys)]

Many of hydrazinonicotinamide (HYNIC) conjugates have been used to label proteins with $^{99m}$Tc.[17,18] A new and modified HYNIC method was developed and used to prepare a variety of potential agents, but is limited to robust proteins and peptides.[18,19]

If a biomolecule contains heteroatoms (N,S,O) available for coordination, one can always suggest the preformed complex approach (Figure 2.5). It involves the

[18] Edwards, D.S., Liu, S., Barrett, J.A., Harris, A.R., Looby, R.J., Ziegler, M.C., Heminway, S.J., Carroll, T.R. *Bioconjug. Chem*. **1997**, *8*, 146-154.
[19] Decristoforo, C., Mather, S.J. *Nucl. Med. Biol*. **1999**, *26*, 389-396.

formation of a stable Technetium complex which is then linked to the larger molecule by an activated ester that has been incorporated into a chelating ligand.

**Figure 2.5: General procedure for the labeling of biomolecules with a preformed $^{99m}$Tc complex.**

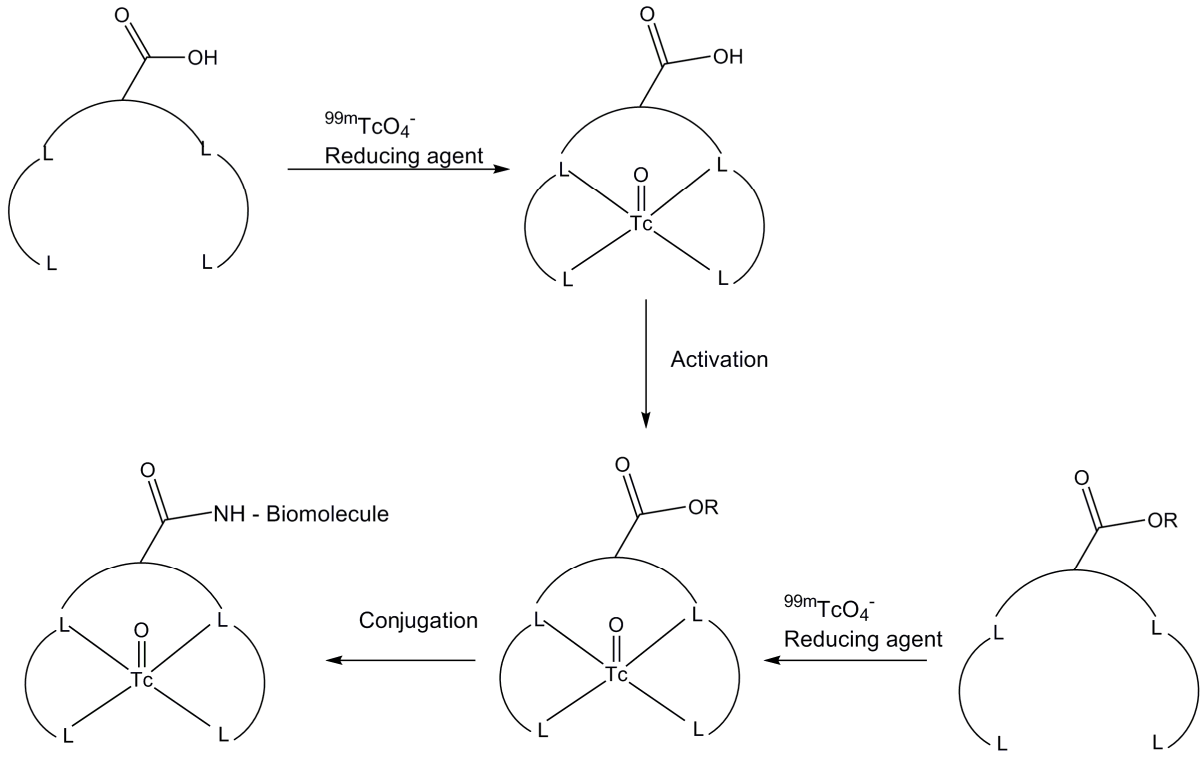


A prechelation kit procedure, for labeling antibodies, has been reported by Kasina *et al*.[20] A more simplified kit has been developed by the group since[21] and a few complexes have been prepared by this means.[22] To detect malignant tumors by imaging techniques, one can use the tumor cells' increased metabolic rates of glucose, lipids and amino acids. Cancer cells are known to have an intense uptake of amino acids.[23] As the cancer cells grow uncontrollably, its protein synthesis within the cells increases. That leads to a higher uptake of amino acids as a source.[24] A

[20] Kasina, S., Rao, T.N., Srinivasan, A., Sanderson, J.A., Fitzner, J.N., Reno, J.M., Beaumier, P.L., Fritzberg, A.R. *J. Nucl. Med*. **1991**, *32*, 1445-1451.
[21] Kasina, S., Sanderson, J.A., Fritzner, J.N., Srinivasan, A., Rao, T.N., Hobson, L.J., Reno, J.M., Axwarthy, D.B., Beaumier, P.L., Fritzberg, A.R. *Bioconjug. Chem.* **1998**, *9*, 108-117.
[22] Karra, S.R., Schibli, R., Gali, H., Katti, K.V., Hoffman, T.J., Higginbotham, C., Sieckman, G.L., Volkert, W.A. *Bioconjug. Chem*. **1999**, *10*, 254-260.
[23] Von Waarde, A., Elsinga, P.H. *Curr. Pharm. Des*. **2008**, *14*, 3326-3339.
[24] Ganopathy, V., Thangaraju, M., Prasad, P.D. *Pharmacol. Ther*. **2009**, *1*, 29-40.

few radiolabeled amino acids already play a huge role in especially brain tumor imaging.[25,26]

At the moment it is believed that amino acids could overcome the two limitations of FDG (2-$^{18}$[F] fluoro-2-deoxy-D-glucose) as imaging agent – high accumulation of the agent in inflammatory tissue and a high uptake in normal brain cells. Recently, another promising complex was prepared, with phenylalanine as amino acid and biological evaluations suggested it to be a potential imaging agent (Figure 2.6).[27]

**Figure 2.6: Synthesis of *p*-(2-[$^{18}$F]fluoroethyl)-L-phenylalanine.**

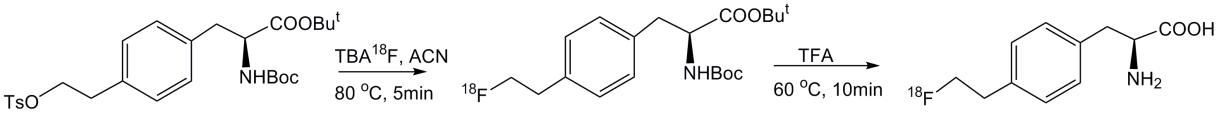


A few *in vivo* studies were reported where peptides and proteins, with an affinity for tumor cells, and labeled with *fac*-[$^{99m}$Tc(CO)$_3$]$^+$ and *fac*-[$^{188}$Re(CO)$_3$]$^+$ showed promising results.[28,29,30,31] For example, Müller *et al*. labeled folatate derivatives with $^{99m}$Tc/$^{188}$Re for potential targeted radionuclide therapy of folate receptor (FR) positive tumors, got good results and also proved that the pharmacokinetics of the $^{99m}$Tc- and $^{188}$Re-folate derivative compounds are almost identical which poses again that the concept of $^{99m}$Tc/$^{188}$Re as a potential 'double whammy' is not too farfetched.

Due to the relatively high chemical stability of the *fac*-[M(CO)$_3$]$^+$ (M = Re, Tc) precursor, radiolabeling under mild physiological conditions are feasible. Proteins that are temperature-sensitive, for example, can be labelled with this method.[32,33,34,35]

---

[25] McConathy, J., Goodman, M.M. *Cancer Metastasis Rev*. **2008**, *27*, 555-573.
[26] Jager, P.L., Vaalburg, W., Pruim, J., de Vries, E.G., Langen, K.J., Piers, D.A. *J. Nucl. Med*. **2001**, *42*, 432-445.
[27] Wang, L., Qu, W., Lieberman, B.P., Plössl, K., Kung, H.F. *Nucl. Med. Biol*. **2011**, *38*, 53-62.
[28] Plummer, R., Rees, C., Hughes, A., Beale, P., Highly, M., Trigo, J., Gokul, S., Judson, I., Calvert, H., Jackman, A., Mitchell, F., Smith, R., Douglass, E. *Clin. Cancer Res*. **2003**, *9*, 1313-1322.
[29] Moustapha, M.E., Ehrhardt, G.J., Smith, C.J., Szakjek, L.P., Eckelman, W.C., Jurisson, S.S. *Nucl. Med. Biol*. **2006**, *33*, 81-89.
[30] Murray, A., Simms, M.S., Scholfield, D.P., Vincent, R.M., Denton, G., Bishop, M.C., Price, M.R., Perkins, A.C. *J. Nucl. Med*. **2001**, *42*, 726-732.
[31] Muller, C., Schubiger, P.A., Schibli, R. *Nucl. Med. Biol*. **2007**, *34*, 595-601.
[32] Deyev, S.M., Waibel, R., Lebedenko, E.N., Schubiger, A.P., Plückthun, A. *Nat. Biotechnol*. **2003**, *21*, 1486-1492.
[33] Willuda, J., Kubetzko, S., Waibel, R., Schubiger, P.A., Zangemeister-Wittke, U., Plückthun, A. *J. Biol. Chem*. **2001**, *276*, 14385-14392.
[34] Chen, K.T., Lee, T.W., Lo, J.M. *Nucl. Med. Biol*. **2009**, *36*, 355-361.

To date, monoclonal antibodies (mAb) contributed a lot to the success of hematological tumor therapy. Freeze-dried kits for instant preparation of $^{188}$Re-labeled mAb's are in development and preliminary studies on the biokinetics of these type of labeled compounds in patients have been reported by Torres-García *et al*.[36,37] A murine mAb labeled with $^{131}$I have been used to successfully cure mice with xenografted human tumors, but still no success have been had with producing a monoclonal antibody that is truly tumor specific.[38,39,40] The pharmacokinetics of monoclonal antibodies can be modified by proteolytic degradation by proteolytic enzymes like pepsin and papain;[41,42] a lot of research have been done on the pharmacokinetic biodistribution, *in vivo* behaviour and fragmentation of these antibodies.[43,44,45,46,47]

In 1998 the FDA licensed Herceptin (Trastuzumab) as an anti cancer monoclonal antibody for the treatment of breast cancer.[48] Since trastuzumab has excelent binding affinity to HER2, it is an excellent choice to conjugate to various radionuclides for potential use as a RIT agent (radioimmunotherapy agent) for the treatment of breast cancer. Another example of the use of Tc and Re as a therapy/imaging pair is shown by the study done by Chen *et al*. They prepared $^{99m}$Tc-labeled trastuzumab from the *fac*-$[^{99m}Tc(CO)_3(H_2O)_3]^+$ moiety and developed a novel labeling method for its congener *fac*-$[^{188}Re(CO)_3(H_2O)_3]^+$ with trastuzumab, a

---

[35] Dias, C.R., Jeger, S., Osso, J.A. Jr., Müller, C., De Pasquale, C., Hohn, A., Waibel, R., Schibli, R. *Nucl. Med. Biol*. **2011**, *38*, 19-28.
[36] Ferro-Flores, G., Torres-García, E., García-Pedroza, L., Arteaga de Murphy, C., Pedraza-López, M., Garnica-Garza, H. *Nucl. Med. Comm*. **2005**, *26*, 793-799.
[37] Torres-Garciá, E., Ferro-Flores, G., Arteaga de Murphy, C., Correa-González, L., Pichardo-Romero, P.A. *Arch. Med. Res*. **2008**, *39*, 100-109.
[38] Cheung, N.-K.V., Landmeier, B ., Neeley, J., Nelson, A.D., Abramowsky, C., Ellery, S., Adams, R.B., Miraldi, F. *J. Natl. Cancer Inst*. **1986**, *77*, 739-745.
[39] Buchegger, F., Pelegrin, A., Delaloye, B., Bischof-Delaloye, A., Mach, J.P. *J. Nucl. Med*. **1990**, *31*, 1035-1044.
[40] Smith, A., Waibel, R., Stahel, R.A., *Br. J. Cancer* **1990**, *64*, 263-266.
[41] Milenic D.E., Esteban, J.M., Colcher, D. *J. Immunol. Methods* **1989**, *120*, 71-83.
[42] Buchegger, F., Haskell, C.M., Schryer, M., Scazziga, B.R., Randin, S., Carrel, S., Mach, J.-P. *J. Exp. Med*. **1983**, *158*, 413-427.
[43] Smith, A., Alberto, R., Blaeuenstein, P., Novak-Hofer, I., Maecke, H., Schubiger, P.A. *Cancer Res.* **1993**, *53*, 5727-5733.
[44] Smith, A., Zangemeister-Wittke, U., Waibel, R., Schenker, T., Schubiger, P.A., Stahel, R.A. *Int. J. Cancer* **1994**, *8*, 43-48.
[45] Press, O.W., De Santes, K., Anderson, S.K., Geissler, F. *Cancer Res*. **1990**, *50*, 1243-1250.
[46] Pochon, S., Buchegger, F., Pelegrin, A., Mach, J.-P., Offord, R.E., Ryser, J.E., Rose, K. *Int. J. Cancer* **1989**, *43*, 1188-1194.
[47] Bischof-Delaloye, A., Delaloye, B., Buchegger, F., Vogel, C.-A., Gillet, M., Mach, J.-P., Smith, A., Schubiger, P.A. *J. Nucl. Med*. **1997**, *38*, 847-853.
[48] Harris, M. *Lancet. Oncol*. **2004**, *5*, 292-302.

monoclonal antibody that interacts with the HER2/neu receptor. The Rhenium complex exhibited specific and high accumulation in HER2/neu-overexpressive BT-474 human breast cancer cells.[49,50]

One of the target enzymes of interest for tumor detection is thymidine kinase (TK). The accumulation of thymidine in tumor cells are mainly in proliferating tumor cells where the TK1 has elevated activity. Different substitution sites on thymidine have been explored with the N-3 position of the pyrimidine nucleus being the most promising site to date.[51,52,53,54] It is known that enzymes are well recognized as natural targets for metal complexes. Thus, the inorganic and organometallic drugs seem quite promising for potential use as diagnostic or therapeutic radiopharmaceuticals for tumors associated with abnormal enzymatic activity.[51,55,56]

A drawback to the $^{99m}$Tc/$^{188}$Re nuclide pair motive is the inhibition towards specific enzymes of Re-complexes in oxidation states (I) and (V). This present the opportunity to use its surrogate $^{99m}$Tc-complexes for probing enzyme levels *in vivo*.[51,57] Even though radiopharmaceuticals used as PET agents have strict prerequisites, the activity of several enzymes have been successfully probed *in vivo* with PET by means of either the radiolabeled inhibitor approach or the substrate approach.[58,59]

The enzyme nitric oxide synthase (NOS) is responsible for the endogenous production of nitric oxide (NO), which is a very important signalling mammalian mediator in processes like vasolidation, neurotransmission, host-defense and

---

[49] Chen, K.T., Lee, T.W., Lo, J.M. *Nucl. Med. Biol*. **2009**, *36*, 355-361.
[50] Chen, W.J., Yen, C.L., Lo, S.T., Chen, K.T., Lo, J.M. *Appl. Radiat. Isot*. **2008**, *66*, 340-345.
[51] Stichelberger, M., Desbouis, D., Spiwok, V., Scapozza, L., Schubiger, P.A., Schibli, R. *J. Organomet. Chem*. **2007**, *692*, 1255-1264.
[52] Al-Madhaun, A.S., Johnsamuel, J., Barth, R.F., Tjarks, W., Eriksson, S. *Cancer Res*. **2004**, *64*, 6280-6286.
[53] Bandyopadhyaya, A.K., Johnsamuel, J., Al-Madhaun, A.S., Eriksson, S., Tjarks, W. *Bioorg. Med. Chem*. **2005**, *13*, 1681-1689.
[54] Lunato, A.J., Wang, J., Woollard, J.E., Anisuzzaman, A.K.M., Ji, W., Rang, F.G., Ikeda, S., Soloway, A.H., Eriksson, S., Ives, D.H., Blue, T.E., Tjarks, W. *J. Med. Chem*. **1999**, *42*, 3378-3389.
[55] Schatzschneider, U., Metzler-Nolte, N. *Angew. Chem. Int. Ed*. **2006**, *45*, 1504-1507.
[56] Louie, A.Y., Meade, T.J. *Chem. Rev*. **1999**, *99*, 2711-2734.
[57] Schibli, R., Netter, M., Scapozza, L., Birringer, M., Schelling, P., Dumas, C., Schoch, J., Schubiger, P.A. *J. Organomet. Chem*. **2003**, *668*, 67-74.
[58] McCarthy, T.J., Sheriff, A.U., Graneto, M.J., Talley, J.J., Welch, M.J. *J. Nucl. Med*. **2002**, *43*, 117-124.
[59] Jensen, S.B., DiSanto, R., Olsen, A.K., Pedersen, K., Costi, R., Cirilli, R., Cumming, P. *J. Nucl. Med*. **2008**, *51*, 1617-1622.

platelet aggregation.[60,61,62,63] NOS endogenously produce NO by conversion of L-Arginine and L-Citrulline. If one can target the NOS expression *in vivo* by a non-invasive technique, insight into a variety of pathophysiologic processes will be provided. Previous research suggests that an enhanced expression of NOS (iNOS and eNOS) is observed in certain tumors (melanoma, breast and gastric cancers).[64,65]

## 2.2 Different Rhenium and Technetium synthons in radiopharmacy

Worldwide there has been a continuing interest in *fac*-Re(I) tricarbonyl systems, for more than one reason. Not only does it have potential biomedical properties[66,67,68,69], it also has promising photophysical behaviour derived from MLCT transitions[70]. This can be used in energy and electron transfer studies[71,72], display technology[73,74] and solar energy conversion and photocatalysis.[75,76]

The significant thrust towards Technetium and Rhenium as radionuclides for biomedical use can be explained by the ideal decay properties, for imaging and therapy respectively, as well as its on-site availability due to the generator systems. $^{99m}$Tc is perfect for diagnostics whereas $^{188}$Re is favoured for imaging. Also, Rhenium and Technetium reveal similar chemical properties. This propose an excellent possibility of developing a diagnostic and a therapeutic tracer at the same

---

[60] Mancada, S., Palmer, R.M.J., Higgs, E.A., *Pharmacol. Rev*. **1991**, *43*, 109-142.
[61] Kerwin, J.F., Lancaster, J.R. *J. Med. Chem*. **1995**, *38*, 4343-4356.
[62] Marletta, M.A. *J. Biol. Chem*. **1993**, *268*, 12231-12234.
[63] Alderton, W.K., Cooper, L.E., Knowles, R.G. *Biochem. J*. **2001**, *357*, 593-596.
[64] Lechner, M., Lirk, P., Rieder, J. *Semin. Cancer Biol*. **2005**, *15*, 277-289.
[65] Fukumura, D., Kashiwagi, S., Jain, R.K. *Nat. Rev. Cancer* **2006**, *6*, 521-534.
[66] Dilworth, J.R., Parrott, S.J. *Chem. Soc. Rev*. **1998**, *27*, 43-45.
[67] Oliveira, B.L., Correia, J.D.G., Raposhinho, P.D., Santos, I., Ferreira, A., Cordeiro, C., Freire, A.P. *Dalton Trans*. **2009**, 152-162.
[68] Maria, L., Cunha, S., Videira, M., Gano, L., Paulo, A., Santos, I.C., Santos, I. *Dalton Trans*. **2007**, 3010-3019.
[69] Alberto, R. *Top. Curr. Chem*. **2005**, *252*, 1-44.
[70] Kirgan, R.A., Sullivan, B.P., Rillema, D.P. *Top. Curr. Chem*. **2007**, *281*, 45-100.
[71] Walther, M.E., Wenger, O.S. *Dalton Trans*. **2008**, 6311-6318.
[72] Vlcek, G.A., Busby, M. *Coord. Chem. Rev*. **2005**, *250*, 1755-1762.
[73] Si, Z., Li, J., Li, B., Zhao, F., Liu, S., Li, W. *Inorg. Chem*. **2007**, *46*, 6155-6163.
[74] Lundin, N.J., Blackman, A.G., Gordon, K.C., Officer, D.L. *Angew. Chem. Int. Ed*. **2006**, *45*, 2582-2584.
[75] Meyer, G.J. *Inorg. Chem*. **2005**, *44*, 6852-6864.
[76] Kalyanasundoram, K., Gratzel, M. *Coord. Chem. Rev*. **1998**, *177*, 347-414.

time, with $^{99m}$Tc and $^{188}$Re as respective radionuclides. Possible identical chemical behaviour and presumably similar pharmacokinetic characteristics might be obtained.[77]

The chemistry of Technetium in water is very complex and adding to that, the radionuclide $^{99m}$Tc is only available at tracer levels. This complicates the characterisation methods, in fact no routine methods are possible. The next obvious option is to study the Rhenium complexes instead since the two metals have similar chemical characteristics. However, in most of the reports on Re and $^{99m}$Tc, the products that formed were different because of different reaction conditions as well as the hydrolization and polymerization of the Technetium compounds in water. Today, the only way to monitor Technetium and the chemistry thereof, is by HPLC methods and other γ-detection analytical methods.

Since Technetium has such diverse redox chemistry, it is difficult to control the oxidation state and the stability of the complexes, but on the contrary, it opens a lot of potential for modifications by chelating systems.

## 2.2.1 The application of the oxo core

During the last few years a couple of concepts for chelating ligands were developed of which the most successful ones contained the $[Tc=O]_3^+$ moiety. These complexes are readily accessible by the reduction of $[TcO_4]^-$ in the presence of whatever suitable chelators are used eg. tetradentate $N_2S_2$[13,78,79] ligands or ligand mixtures for the use in the '3+1' approach.[80,81,82,83] A disadvantage of this square-pyramidal oxo core with a free position *trans* to the oxo ligand, is its polarity. With the requirements for specific agents getting stricter, it is still unsure whether this is beneficial or not.

---

[77] Müller, C., Schubiger, P.A., Schibli, R. *Nucl. Med. Biol*. **2007**, *34*, 595-601.
[78] Zhuang, Z.P., Plössl, K., Kung, M.P., Mu, M., Kung, H.F. *Nucl. Med. Biol*. **1999**, *262*, 217-224.
[79] O'Neil, J.P., Carlson, K.E., Anderson, C.J., Welch, M.J., Katzenellenbogen, J.A. *Bioconjug. Chem*. **1994**, *5*, 182-193.
[80] Pietzch, H.-J., Spies, H., Hoffmann, S. *Inorg. Chim. Acta*. **1989**, *165*, 163-166.
[81] Spyriounis, D.M., Pelecanou, M., Stassinopoulou, C.I., Raptopaulou, C.P., Terzis, A., Chiotellis, E. *Inorg. Chem*. **1995**, *34*, 1077-1082.
[82] Seifert, S., Pietzsch, H.-J., Scheunemann, M., Spies, H., Syhre, R., Johannsen, B. *Appl. Rad. Isot*. **1998**, *49*, 5-11.
[83] Spies, H., Fietz, T., Pietzsch, H.-J., Johannsen, B., Leibnitz, P., Reck, G., Scheller, D., Klostermann, K. *J. Chem. Soc., Dalton Trans*. **1995**, 2277-2280.

At the end of last year, Dorbes and co-workers[84] synthesized, characterized and evaluated new oxorhenium and oxotechnetium complexes. They wanted to design new labeled complexes that might be suitable for the molecular imaging of the cholecystokinin-2 receptors (CCK2-R). These receptors are overexpressed in a few neuroendocrine tumors. The group designed several modified CCK derivatives and the ReO and TcO complexes formed, were stable, produced in high yield and one complex showed promising *in vitro* characteristics.

**Figure 2.7: Structure of Rhenium and Technetium complexes designed by Dorbes *et al*.[84]**

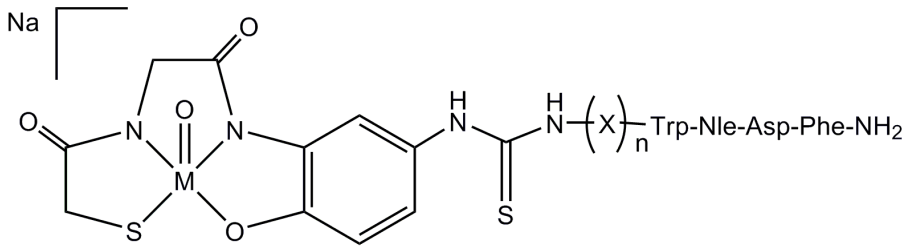


M = Tc, Re

## 2.2.2 Nitrido complexes

In the $[Tc{\equiv}N]^{2+}$ core, the nitrido ligand stabilizes Tc(V) to a great extent because of its powerful π-electron donating capability, and forms Tc(V) complexes with a wide variety of chelators. Earlier this year Thieme *et al.*[85] found that [$^{188}$Re(N)(PNP)]-based complexes (with PNP = diphosphinoamine) could be useful in the development of target-specific radiopharmaceuticals, but is limited by the low labeling efficiency.

[84] Dorbes, S., Mestre-Voegtlé, B., Coulais, Y., Picard, C., Silvente-Poirot, S., Poirot, M., Benoist, R. E. *J. Med. Chem*. **2010**, *45*, 423-429.
[85] Thieme, S., Agostini, S., Bergmann, R., Pietzsch, J., Pietzsch, H.-J., Carta, D., Salvarese, N., Refosco, F., Bolzati, C. *Nucl. Med. Biol*. **2011**, *38*, 399-415.

**Figure 2.8: Rhenium and Technetium complexes used in the study by Thieme and co-workers.[85]**

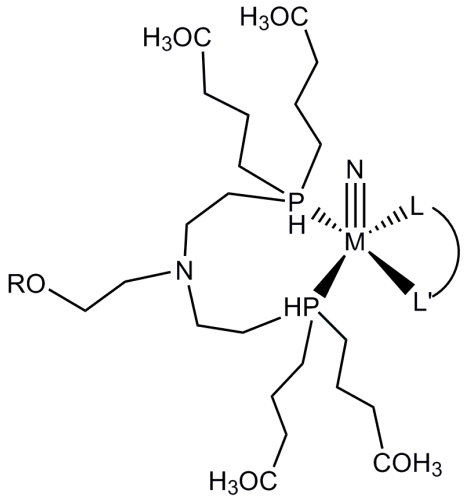


R = $CH_3$, $CH_2CH_3$
L,L' = cysteine derivative ligands
M = Tc, Re

## 2.2.3 Nitrosyl complexes

Rattat *et al*. studied the reaction of $[N(CH_2CH_3)_4][MX_3(CO)_2(NO)]$ (M = Re, Tc; X = Cl, Br) with picolinic acid in detail to exemplify the potential of the $[M(CO)_2(NO)]^{2+}$ moiety (Figure 2.9) . The results from this study indicate that it is feasible to directly label antibodies/peptides with $[M(CO)_2(NO)]^{2+}$ to produce a $[MX(Ab)(CO)_2(NO)]$ radioimmnoconjugate (Ab = antibody or peptide).

**Figure 2.9: Synthesis of *fac*-$[Re(CO)_2(NO)(Pic)X]$ with X = Br, Cl.**

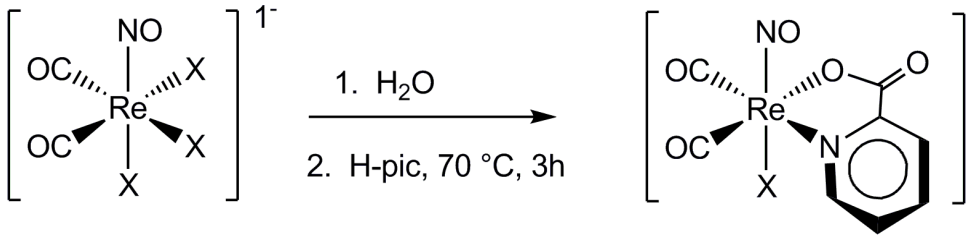


Like the *fac*-Re(I) and Tc(I) tricarbonyl complexes, the size of the $[M(CO)_2(NO)]^{2+}$ moiety does not interfere with the binding site of a biomolecule, indicating that it will retain its biological activity.[86]

[86] Schibli, R., Alberto, R., Schaffland, A.O., Schubiger, P.A., Abram, U., Pietzsch, H.-J., Johannsen, B. *J. Labelled Cpd. Radiopharm*. **1999**, *42* (suppl 1) 5147.

## 2.2.4 *fac*-Tricarbonyl core

Since (V) oxidation state metals are easily accessible by the reduction of the permetallate, $[MO_4]^-$ (M = Re, Tc), with $SnCl_2$, these complexes have been widely used. Compared to (V) complexes, (I) oxidation state complexes have not been investigated as much, especially for clinical purposes. Ever since the complex $[^{99m}Tc(CN\text{-}R)_6]^+$ became the successful scintigraphy agent, Re and Tc in low oxidation states have become of more interest.[87,88]

The *fac*-$[M(CO)_3]^+$ core especially have excellent potential because of the reasons mentioned before (coordination properties, $d^6$ low-spin electron configuration, very stable kinetically). Ever since Alberto synthesized the *fac*-$[^{99m}Tc(CO)_3(H_2O)_3]^+$ in aqueous medium and under mild conditions,[89] this *fac*-$[M(CO)_3]^+$ core became a huge focus point for researchers. More advantages include the water solubility and stability of *fac*-$[NEt_4]_2[M(CO)_3X_3]$ and the cationic form *fac*-$[M(CO)_3(H_2O)_3]^+$ respectively. It readily reacts with bidentate and tridentate ligand chelators to form stable complexes. The synthesis of this synthon is illustrated in Scheme 2.1. *fac*-$[M(CO)_3(H_2O)_3]^+$ can not only be prepared in THF but also in saline.[89] These synthons are ideal for radiopharmacy with properties like stability towards hydrolysis and redox decomposition, exchangeable ligands, well characterized composition and formation of robust complexes. An in-depth discussion on this *fac*-tricarbonyl core follows in Paragraph 2.4.

**Scheme 2.1: Synthetic pathway of *fac*-$[M(CO)_3(H_2O)_3]^+$ from $[MO_4]^-$, M = Re, $^{99m}$Tc.**

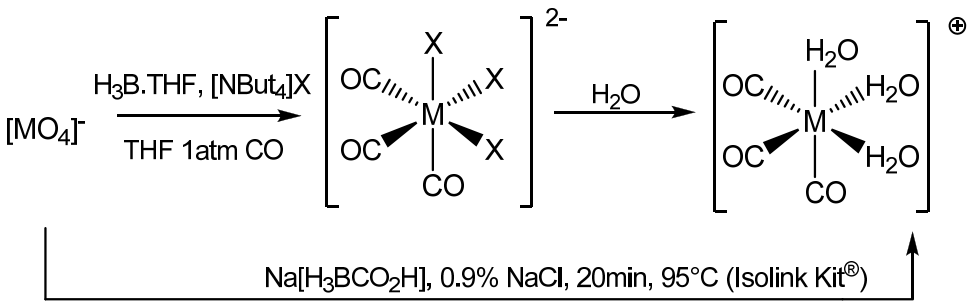


[87] Yoshihara, K., Omori, T. (Eds.) Technetium and Rhenium – their chemistry and its applications. *Topics in Current Chemistry*, **1995**, *176*, Springer-Verlag, Berlin.
[88] Nicolini, M., Bandoli, G., Mazzi, U. (Eds) *Technetium and Rhenium in Chemistry and Nuclear Medicine 3*. Raven Press, New York, **1990**.
[89] Alberto, R., Schibli, R., Waibel, R., Abram, U., Schubiger, A.P. *Coord. Chem. Rev*. **1999**, *190-192*, 901-919.

A few examples of complexes prepared by Schutte *et al*.[90] are shown in Figure 2.10. These complexes showed extremely interesting reactivity characteristics towards methanol substitution reactions. The kinetic study of these complexes is discussed in detail in Paragraph 2.7.3

**Figure 2.10: Structural representation of a few *fac*-Rhenium tricarbonyl complexes synthesized.**

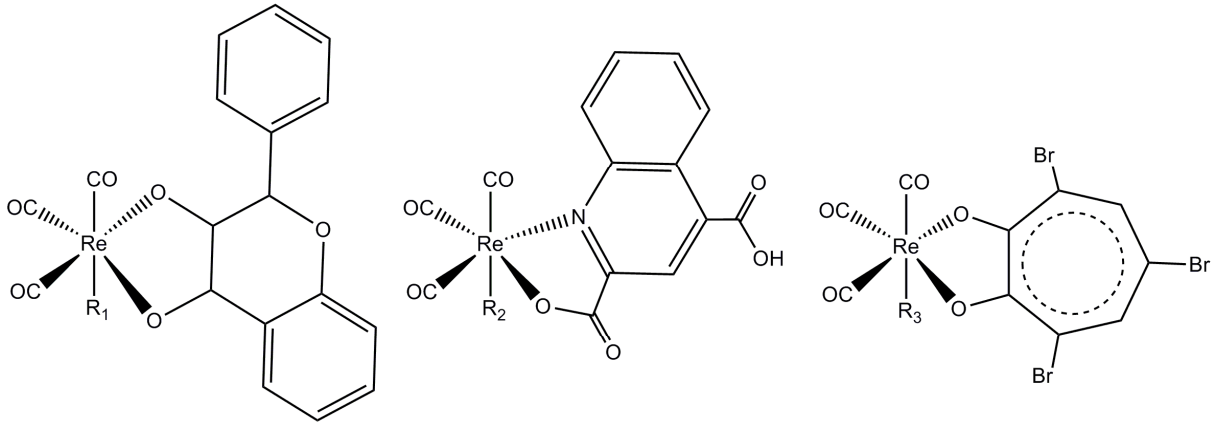


$\mathbf{R_1}$ = $H_2O$, Br, $CH_3OH$, $\mathbf{R_2}$ = $H_2O$, Br, $\mathbf{R_3}$ = $H_2O$, Br

# 2.3 The design of Radiopharmaceuticals

## 2.3.1 Diagnostic and Therapeutic Radiopharmaceuticals

The basic concept of molecular imaging with radionuclides is the site-specific targeting of receptors and genes that are overexpressed in tumors or neurodegenerative diseases. The imaging modalities available are PET (positron emission tomography) and SPECT (single photon emission computed tomography) radiopharmaceuticals, MRI contrast agents and photoactive fluorescent compounds. The latter two probes need a stimulus from outside like spectroscopic excitation or a magnetic field while the radiopharmaceuticals are active as is. For molecular imaging, the radiopharmaceutical has a target portion that binds to a receptor, for example. With the accumulation at the target cells, one can visualize the enhanced expression of receptors or metabolic processes. For the imaging of cancer cells, the

[90] Schutte, M., Kemp, G., Visser, H.G., Roodt, A. *Inorg. Chem*. **2011**, *50(24)*, 12486-12498.

targets are mostly cell bound peptide receptors, because they are often overexpressed in fast proliferating cells.[91]

A few examples of $^{99m}$Tc radiopharmaceuticals available for clinical use is the perfusion agent for the heart, $^{99m}$Tc-MIBI (Cardiolite®), the perfusion agents for the brain, $^{99m}$Tc-ECD (Neurolite®) and $^{99m}$Tc-HMPAO (Ceretec®) and the renal function agent, $^{99m}$Tc-MAG$_3$ (TechneScan MAG$_3$®).[92,93,94]

**Figure 2.11: Some of the $^{99m}$Tc Radiopharmaceuticals in clinical use today.**

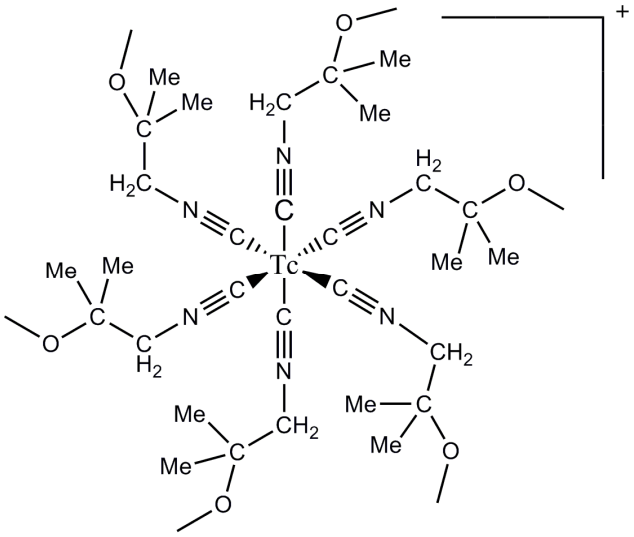

$^{99m}$Tc-MIBI

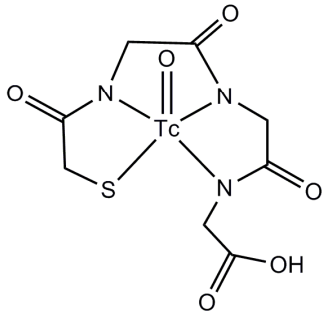

$^{99m}$Tc-MAG$_3$

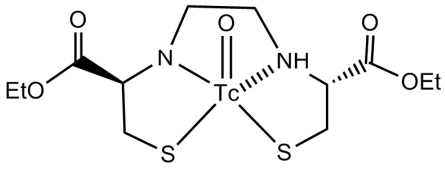

$^{99m}$Tc-((L,L)-ECD)

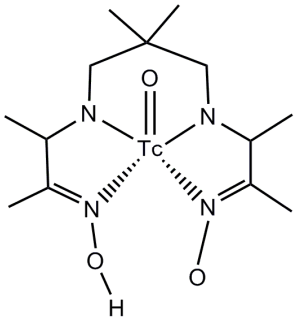

$^{99m}$Tc-((*d,l*)-HMPAO)

[91] Shields, A.F., Grierson, J.R., Dohmen, B.M., Machulla, H.-J., Stayanoff, J.C., Lawhorn-Crews, J.M., Obradovich, J.E., Muzik, O., Mangner, T.J. *Nat. Med*. **1998**, *4*, 1334-1336.
[92] Fritzberg, A.R., Kasina, S., Eshima, D., Johnson, D.L. *J. Nucl. Med*. **1986**, *27*, 111-116.
[93] Taylor, A. Jr., Eshima, D., Christian, P.E., Wooten, W.W., Hansen, L., McElvany, K. *J. Nucl. Med*. **1988**, *29*, 616-622.
[94] Taylor, A. Jr., Eshima, D., Fritzberg, A.R., Christian, P.E., Kasina, S. *J. Nucl. Med*. **1986**, *27*, 795-803.

The success of these compounds is in the design thereof. One or more physical property or metabolic characteristic is incorporated into the compounds that are required for tissue specificity. $^{99m}$Tc-MIBI is a cationic heart perfusion agent and it was designed as an analogue of the ions that localize in the heart, the large positively charged $K^+$, $Cs^+$ and $Tl^+$ ions. Also, the high lipophilicity of the compound made organ specificity possible.[95]

Ceretec® is a neutral compound and the result of optimal properties – neutral charge and lipophilic character to cross the blood-brain barrier and to be retained in neural tissue.[96] $^{99m}$Tc-ECD, Neurolite®, also have a neutral and lipophilic character, which is the reason for the uptake in the brain and thereafter the hydrolysis of one of the ester groups in the brain cells to prolong the retention of this anionic metabolite.[97]

Despite the approach where the radiopharmaceutical is synthesized by looking at the tissue-localizing properties, there is another method that is not yet much explored. This is where a small molecule (receptor) is labeled with $^{99m}$Tc to act as ligand systems for hormones, neurotransmitters or receptors. As these receptors are part of the regulation of vital functions in the body, this type of radiopharmaceuticals can be used to monitor abnormalities in the functioning of the receptors and also monitor the effect of therapy on the site. Most receptor-bound radiopharmaceuticals are labeled with $^{18}$F, $^{11}$C and $^{123}$I.

In RIT the radionuclide is transported to the cancer cells or target site by target-selective vehicles. The advantage of Radioimmunotherapy is the radiation-induces cytotoxicity of the drug combined with the ability to also kill tumor cells in close proximity of the binding site of the labeled antibody. It is therefore imperative to consider the optimal properties of the specific nuclide as well as the *in vivo* behaviour of the vehicle used.

One of the most promising radionuclides for use in radioimmunotherapy is $^{186}$Re. According to its decay properties, a high dose will be deposited at the tumor site with less exposure to the rest of the body. Opposed to $^{131}$I, that is frequently used and almost insignificantly contributes to the dose of the tumor but is heavily responsible

[95] McCarthy, T.J., Schwarz, S.W., Welch, M.J. *J. Chem. Ed*. **1994**, *71*, 830-836.
[96] Walovitch, R.C., Williams, S.J., Lafrance, N.D. *Nucl. Med. Biol*. **1990**, *17*, 77-83.
[97] Edwards, D.S., Cheesman, E.H., Watson, M.W., Maheu, L.J., Nguyen, S.A., Dimitre, L. *Technetium and Rhenium in Chemistry and Nuclear Medicine* **1990**, *3*, 433-444.

for the whole body radiation and dose-limiting toxicity to the bone marrow. The penetrating radiation of $^{131}$I accounts for 30-50% of the burden to the bone marrow. By comparing $^{67}$Cu (γ, ~60% abundance), $^{186}$Re (γ, 16% abundance) and $^{111}$Ag (γ, ~7% abundance) to $^{131}$I, the radiation burden to the bone marrow will significantly decrease, respectively. All in all, it is important to remember that there is no one ideal radionuclide for therapy application, just more suitable candidates than others. Basically the following characteristics should be taken into account when selecting a nuclide for a given target-specific vehicle:

### 2.3.1.1 The radiation

To obtain optimal tumor cell killing, radionuclides should emit relatively high high-linear energy transfer radiations and should deposit most of its ionising energy in the tumor itself. Because of the wide variety of vehicles and target sites available, the optimal range of these emissions differs quite significantly, and according to vehicle and site. Humm gave an intense explanation and discussion on the radiation dosimetry in radioimmunotherapy in 1986.[98]

### 2.3.1.2 The energy

After some time it was found that $^{131}$I (main γ = 360 keV, 82% abundance) is not ideal as radionuclide and that optimally, one will look at a radionuclide with a 5-20% γ-radiation in the 100 – 200 keV range, due to the whole body radiation burden of the highly penetrating γ-radiation.[99,100] This will allow easy measurement during the synthesis, biodistribution studies, scintigraphy and dosimetric calculations.
Regarding high-energy β-emitters like $^{90}$Y with a higher penetrance, the bone marrow is subjected to a more uniform irradiation. This means it might be more advantageous to use lower-energy β-emitters like $^{67}$Cu to lower the exposure to the bone marrow.[99]

[98] Humm, J.L. *J. Nucl. Med*. **1986**, *27*, 1490-1497.
[99] Langmuir, V.K. *Nucl. Med. Biol*. **1992**, *19*, 213-225.
[100] Buchegger, F., Chalandon, Y., Pelegrin, A., Hardman, N., Mach, J.P. *J. Nucl. Med*. **1991**, *32*, 1414-1421.

### 2.3.1.3 The half-life

The physical half-life of the radionuclide of choice should be long enough to irradiate all the target cells but not too long to expose the body and normal tissue to unnecessary radiation. Therefore the half-life of the nuclide should be similar to the biological half-life of the radioimmunoconjugate at the tumor cells. Basically the half-life should be long enough to allow for the synthesis, the transportation, the administration to the patient and then long enough to accumulate in the target tissue and be optimally cleared from the non-target organs. For example, a nuclide with a long half-life of hours to a few days will be used for targeting disseminated cells whereas a half-life of a few weeks will be necessary for a solid tumor mass, where high uptakes are usually needed.

### 2.3.1.4 The stability and reliability

The reason why only nuclides with stable or very long-lived daughter nuclides should be used in potential therapeutic agents is that the residual atom liberated after the binding of the drug to the target site, might have an *in vivo* distribution pattern very different from that of the original agent. If the daughter nuclide is unstable, the normal tissue may get exposed to uncontrollable and unwanted radiation. 'Sites of recognition' presented by the target cells for all biological vehicles, are limited, therefore limiting the number of molecules that can interact with the target cells. Thus, it is very important for the therapeutic nuclide to have a very high specific activity or must be at least produced in a carrier-free form, must be of good quality and need to be reproducible within a narrow range of reliability.

### 2.3.1.5 The availability

The specific activity of a radionuclide should be adequate and reproducible within a narrow range of reliability. It is very important since trace amounts of impurities can influence the labeling process and therefore the yields. A detailed review article by Volkert *et al*. gives methods for the production of therapeutic nuclides.[101]

[101] Volkert, W.A., Goeckeler, W.F., Ehrhardt, G.J., Ketring, A.R. *J. Nucl. Med*. **1991**, *32*, 174-185.

## 2.3.2 Different strategies

At first the concept of targeting cancerous cells seems simple and therefore attractive to researchers. By the use of a delivery system, that possesses a desired affinity for the target tumor, the cytotoxic agent is carried to the tumor where the cancer cells are killed and the normal tissue is spared. When considering immunotargeting, a variety of strategies are known based around the delivery of cytotoxic proteins, conventional chemotherapeutics and high-linear energy transfer radionuclides. Each strategy comes with its own problems and challenges. The two most frequently used strategies to design receptor-specific targeting molecules are the integrated approach and the bifunctional approach.

### 2.3.2.1 Integrated strategy

With the integrated approach, also known as an intrinsic receptor binding method, the structure of the metal compound mimics the binding site of a biomolecule. Part of a receptor ligand, with a high affinity, is replaced by the metal chelate, thus directly incorporated into the targeting moiety. This is done without notably altering the size, conformation and receptor binding affinity.

The advantage of this strategy is that it improves the stability, tumor uptake and retention of the radiopharmaceutical. The disadvantages are a decrease in the receptor binding affinity and an obvious bigger task to synthesize this challenging target molecule.

To mimic a biomolecule's binding site, the topology, dipole moment distribution and more physico-chemical characteristics of the original compound has to be incorporated into the metal compound, making it an enormous challenge. Examples of this are (A – B) that mimic dopamine and (C) a serotogenic receptor. (Figure 2.12)

**Figure 2.12: Technetium compounds for the imaging of dopamine and serotin.**

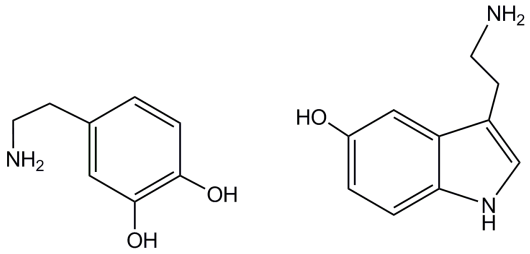


Dopamine




Serotonin

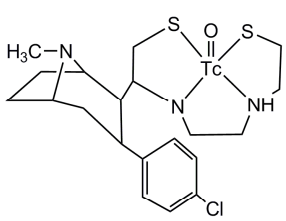


A

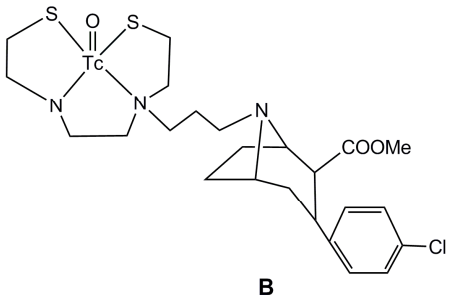


B

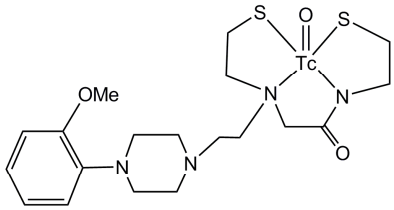


C

Overall it was found that complexes with a low molecular mass, a well-balanced lipophilicity and a high specificity and selectivity for the receptor yield potential successful molecules. Another observation was if one keeps the metal's coordination site and the targeting part of the molecule apart, better results overall will be obtained as well as simpler synthetic procedures.

### 2.3.2.2 Bifunctional approach

In the bifunctional approach to design a radiopharmaceutical, a receptor binding molecule is coupled to a metal chelate, sometimes *via* a linker. A receptor ligand, with a high binding affinity, is used as targeting molecules, like antibodies and proteins. A bifunctional chelating agent chelates the metal and provides a functional group for the attachment of the biomolecule. Sometimes a linker is used to attach the metal complex to the target molecule. The functionality for the connection of the metal to the biomolecule is usually an amine group or a carboxylate, which can be activated. The chelating agent should be able to coordinate strongly under low concentrations, yield one product with high yield, form stable complexes and should not influence the biological properties of the conjugate.

With the variety of metal cores in combination with a wide range of ligand system possibilities, this is sometimes called the mixed ligand approach. This is the most

ambitious approach in terms of flexibility. Different metal cores, like $[MO]^{3+}$, $[MN]^{2+}$, *fac*-$[M(CO)_3]^{+}$ or $M^{3+}$, can be used with a variety of combination ligand systems ('4+1', '3+1', '3+2' etc). These mixed ligand combinations give the opportunity for fine-tuning of the coordination site.

Good results were obtained by Pietzsch *et al*.[102] and Spies and co-workers[103,104] with ('4+1') mixed ligand complexes containing NSSS tetradentate ligands and isocyanides as monodentate ligands. The HYNIC approach, where biomolecules are linked to 6-hydrazinonicotinamide and co-ligands occupy the remaining coordination sites, has the advantage of a big potential variety in co-ligands, for tuning the biological properties.

A big interest is the '2+1' approach, illustrated in Scheme 2.2. It consists of a bidentate ligand of which the lipophilicity can be controlled and a monodentate bifunctional that can act as a potential linker to a biologically active molecule.[69,105,106] Some isocyanides and imidazole derivatives have been used as monodentate ligands because it can easily be made bifunctional. The '2+1' ligand approach became very well known since it is possible to link a biomolecule to either the bidentate ligand or the monodentate in the axial position.

This make the '2+1' approach a versatile synthetic pathway where one can optimize the properties of the radiopharmaceuticals eg. target tissue specificity, pharmacokinetics and the yield of labeling, by means of the linked biomolecule.[107,108]

---

[102] Pietzsch, H.J., Seifert, S., Syhre, R., Tisato, F., Refosco, F., Leibnitz, P., Spies, H. *Bioconjug. Chem*. **2003**, *14*, 136-143.
[103] Spies, H., Glaser, M., Pietzsch, H.J., Hahn, F.E., Kintzel, O., Luegger, T. *Angew. Chem*. **1994**, *106*, 1416-1419.
[104] Spies, H., Glaser, M. *Inorg. Chim. Acta*. **1995**, *240*, 465-478.
[105] Gorshkov, N.I., Schibli, R., Schubiger, A.P., Lumpov, A.A., Miroslavov, A.E., Suglobov, D.N. *J. Organomet. Chem*. **2004**, *689*, 4757-4763.
[106] Mundwiler, S., Kundig, M., Ortner, K., Alberto, R. *J. Chem. Soc., Dalton Trans*. **2004**, *9*, 1320-1328.
[107] Gorshkov, N.I., Schibli, R., Schubiger, A.P., Lumpov, A.A., Miroslavov, A.E., Suglobov, D.N. *J. Organomet. Chem*. **2004**, *689*, 4757-4763.
[108] Riondato, M., Camporese, D., Martin, D., Suades, J., Alvarez-Lorena, A., Mazzi, U. *Eur. J. Inorg. Chem*. **2005**, 4048-4055.

**Scheme 2.2: '2+1' Mixed ligand concept.**

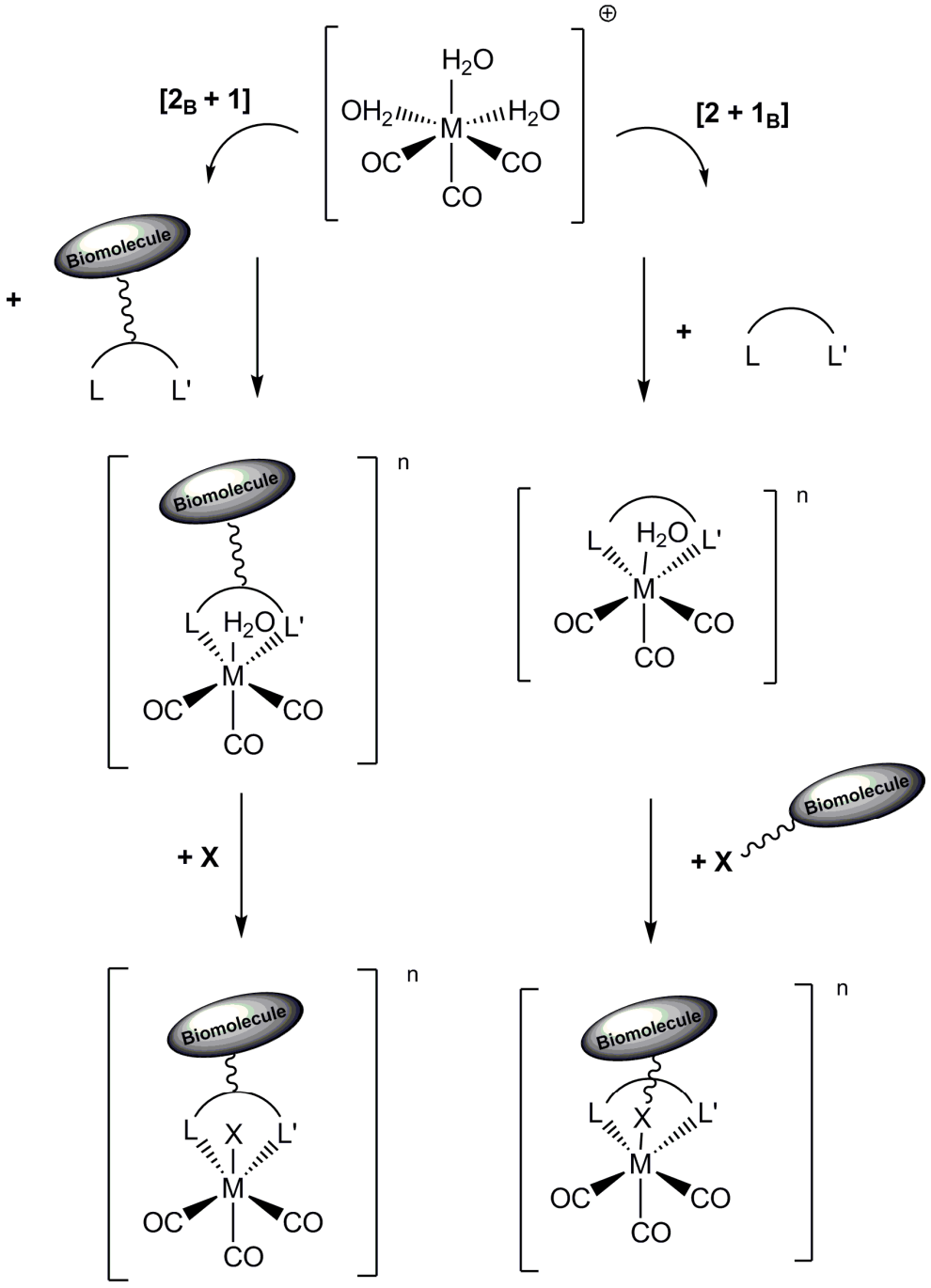


n = depending on the charge of the ligand systems

The '2+1' mixed-ligand approach has been adopted by several research groups. Mainly studies showed that isocyanide derivatives, as potential linkers, form stable '2+1' *fac*-tricarbonyl Technetium(I) complexes whereas imidazole moieties are often a fragment of biomolecules that are of interest for nuclear medicine. Fuks and co-workers investigated cationic *fac*-tricarbonyl Rhenium(I) and Technetium(I)

complexes with neutral bidentate ligands and $H_2O$ at the third position and found it to be much less stable compared to the complexes where imidazole and tert-butyl-3-isocyanopropionate substituted the labile $H_2O$ ligand.[109] Overall, the Rhenium complexes were found to be much more stable and more resistant to these ligand exchange studies.

Sagnou and his co-workers investigated the '2+1' approach with acetylacetone (acac) as bidentate ligand and isocyanide as monodentate ligand.[110] Acetylacetone is a well known bidentate ligand that coordinates to many transition metals. Also, a targeting biomolecule can be incorporated at $C_2$ or $C_4/C_5$ on the backbone.[111,112]

**Figure 2.13: Synthetic pathway for complexes prepared by Sagnou *et al.*[110]**

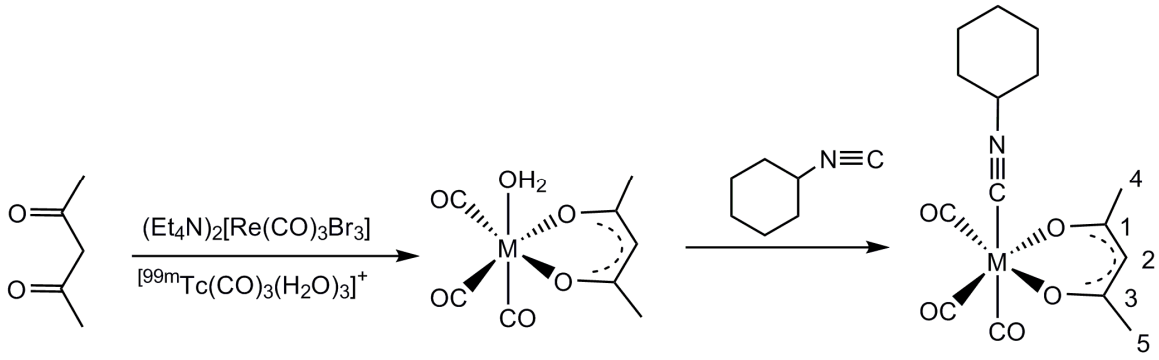


A synthetic pathway for their work is presented in Figure 2.13. Quite a few investigations towards acac and Re/$^{99m}$Tc complexes, in various oxidation states, have been reported. For example, *fac*-[$Re(CO)_3$(acac)(pyridine)] has been synthesized by the '2+1' approach *via* the *fac*-[$Re(CO)_3$(acac)($H_2O$)] intermediate.[113]

It is also known that isocyanide (isc) is a strong, functionalisable monodentate ligand and has been used in a few Rhenium and Technetium synthesized complexes.[107,114,115,116] $^{99m}$Tc-MIBI, the myocardial imaging agent, is one of the most

---

[109] Fuks, L., Gniazdowska, E., Kozminski, P., Lyczko, M., Mieczkowski, J., Narbutt, J. *Appl. Rad. Isotopes* **2010**, *68*, 90-95.
[110] Sagnou, M., Tsoukalas, C., Triantis, C., Raptopoulou, C.P., Terzis, A., Pirmettis, I., Pelecanou, M., Papadopoulos, M. *Inorg. Chim. Acta*. **2010**, *363*, 1649-1653.
[111] Aromí, G., Gamez, P., Reedijk, J. *Coord. Chem. Rev*. **2008**, *252*, 964-989.
[112] Morena-Mãnas, M., Marquet, J., Vallribera, A. *Tetrahedron* **1996**, *52*, 3377-3401.
[113] Benny, P.D., Fugate, G.A., Barden, A.O., Morley, J.E., Silva-Lopez, E., Twamley, B. *Inorg. Chem*. **2008**, *47*, 2240-2242.
[114] Abrams, J.M., Davison, A., Jones, A.G., Costello, C.E., Pang, H. *Inorg. Chem*. **1983**, *22*, 2798-2800.
[115] Agorastos, N., Borsig, L., Renard, A., Antoni, P., Viola, G., Spingler, B., Kruz, P., Alberto, R. *Chem. Eur. J*. **2007**, *13*, 3842-3852.

successful radiopharmaceuticals where an isocyanide derivative is incorporated into the $^{99m}$Tc core. They synthesized the *fac*-[Re(CO)$_3$(acac)(isc)] complex (isc = isocyanocyclohexane) with isc used as a derivative of the isocyanide ligand. They also managed to obtain the corresponding $^{99m}$Tc complex in high yield. The second step in the synthesis of these complexes - the replacement of the water molecule by the isocyanocyclohexane monodentate ligand - proceeds quickly at room temperature for both the Rhenium and the $^{99m}$Tc complex. An almost quantitative yield was reported, indicating the high affinity of the isocyanide ligands for the *fac*-[Re(CO)$_3$]$^+$ core. This is enough reason to further investigate the incorporation of suitable pharmacophoric ligands to produce target specific complexes.

# 2.4 The *fac*-[M(CO)$_3$(H$_2$O)$_3$]$^+$ synthon

## 2.4.1 Synthesis of *fac*-[M(CO)$_3$X$_3$]$^{2-}$ from [MO$_4$]$^-$

Traditionally, carbonyl complexes were synthesized in autoclaves like [Re$_2$(CO)$_{10}$] and [Tc$_2$(CO)$_{10}$].[117,118,119] In the past, [NEt$_4$]$_2$[ReBr$_3$(CO)$_3$] was prepared by the bromination of [Re$_2$(CO)$_{10}$] to [ReBr(CO)$_5$] and the substitution of two CO ligands by [NEt$_4$]Br.[120] The direct reduction of [MO$_4$]$^-$ from oxidation state (VII) to (I) was the biggest problem at the time. This problem was overcome and Tc(VII) and/or Re(VII) to Tc(I) and Re(I) and the coordination of three CO ligands could be achieved at low pressure by bubbling CO through a solution of the metal complex and Cl$^-$ in THF.[121,122] It is clear that this procedure is not possible for compounds used in nuclear medicine since the synthesis must be done in saline only. A one step reaction approach in saline solution within 30 minutes, by means of NaBH$_4$ from [$^{99m}$TcO$_4$]$^-$ was developed by Alberto *et al.* in 1999.[89]

---

[116] Gorshkov, N.I., Lumpov, A.A., Miroslavov, A.E., Suglobov, D.N. *Radiochemistry* **2005**, *47*, 45-49.
[117] Grimm, C.C., Clark, R.J. *Organometallics* **1990**, *9*, 1123-1127.
[118] Calderazza, F., Mazzi, U., Pampaloni, G., Poli, R., Tisato, F., Zanazzi, P.F. *Gazz. Chim. Ital*. **1989**, *119*, 241-247.
[119] Heinekey, D.M., Crocker, L.S., Gould, G.J. *J. Organomet. Chem*. **1988**, *342*, 243-244.
[120] Abel, E.W., Butler, I.S., Garnokar, M.C., Kenkins, C.R., Stiddard, M.H.B. *Inorg. Chem*. **1966**, *5*, 25-27.
[121] Alberto, R., Schibli, R., Schubiger, P.A., Abram, U., Kaden, T.A. *Polyhedron* **1996**, *15*, 1079-1089.
[122] Alberto, R., Schibli, R., Egli, A., Schubiger, A.P., Herrmann, W.A., Artus, G., Abram, U., Kaden, T.A. *J. Organomet. Chem*. **1995**, *493*, 119-127.

## 2.4.2 Hydrolytic behaviour of *fac*-$[M(CO)_3(H_2O)_3]^+$

Alberto *et al*. also studied the hydrolytic behaviour of *fac*-$[M(CO)_3X_3]^{2-}$ in water.[89] *fac*-$[Re(CO)_3(H_2O)_3]^+$ and *fac*-$[^{99m}Tc(CO)_3(H_2O)_3]^+$ both act as Brönstedt acids and it is expected that they will exhibit these characteristics as well.[89] However, it was found that mono-cationic species are in general not very acidic, with $pK_a$ values of more than 8.[123]

*fac*-$[Re(CO)_3(H_2O)_3]^+$ and *fac*-$[^{99m}Tc(CO)_3(H_2O)_3]^+$ were titrated with $OH^-$ and the nature of the intermediates were deduced and most of the postulated species have been isolated and characterized.[124,125] At and below physiological pH of 7.4, it was found that *fac*-$[Re(CO)_3(H_2O)_3]^+$ and *fac*-$[^{99m}Tc(CO)_3(H_2O)_3]^+$ were indeed the predominant species. As a base was added, deprotonation and oligomerization was observed and dinuclear and trinuclear complexes were essentially rationalized.[89] The hydrolytic oligomerization was slow and fully reversible for both the Technetium and Rhenium complexes. The $pK_a$ of *fac*-$[Re(CO)_3(H_2O)_3]^+$ is about 7.5 with the Technetium analogue at about 1 $pK_a$ unit lower, indicating the contrast in electronic properties between the elements.

Similar observations between Technetium and Rhenium have been mentioned before.[126] A quantitative analysis of the entire hydrolytic reaction scheme of *fac*-$[Re(CO)_3(H_2O)_3]^+$ are given in Scheme 2.3, with ● = *fac*-$[Re(CO)_3]^+$.

[123] Martell, A.E., Smith, R.M., Motekaitis, R.J. *Critically Selected Stability constants for Metal Complexes,* NIST Standard Reference Data Base 46, *Vers. 2.0*, NIST, Gaithersburg, MD, **1995**.
[124] Alberto, R., Egli, A., Abram, U., Hegetschweiler, K., Gramlich, V., Schubiger, P.A. *J. Chem. Soc., Dalton Trans*. **1994**, 2815-2820.
[125] Egli, A., Hegetschweiler, K., Alberto, R., Abram, U., Schibli, R., Hedinger, R., Gramlich, V., Kissner, R., Schubiger, P.A. *Organomet*. **1997**, *16*, 1833-1840
[126] Abou-Hamdan, A., Roodt, A., Merbach, A.E. *Inorg. Chem*. **1998**, *37*, 1278-1288.

**Scheme 2.3: The hydrolytic reaction scheme of *fac*-$[Re(CO)_3(H_2O)_3]^+$ as depicted by Egli *et al*.[125]**

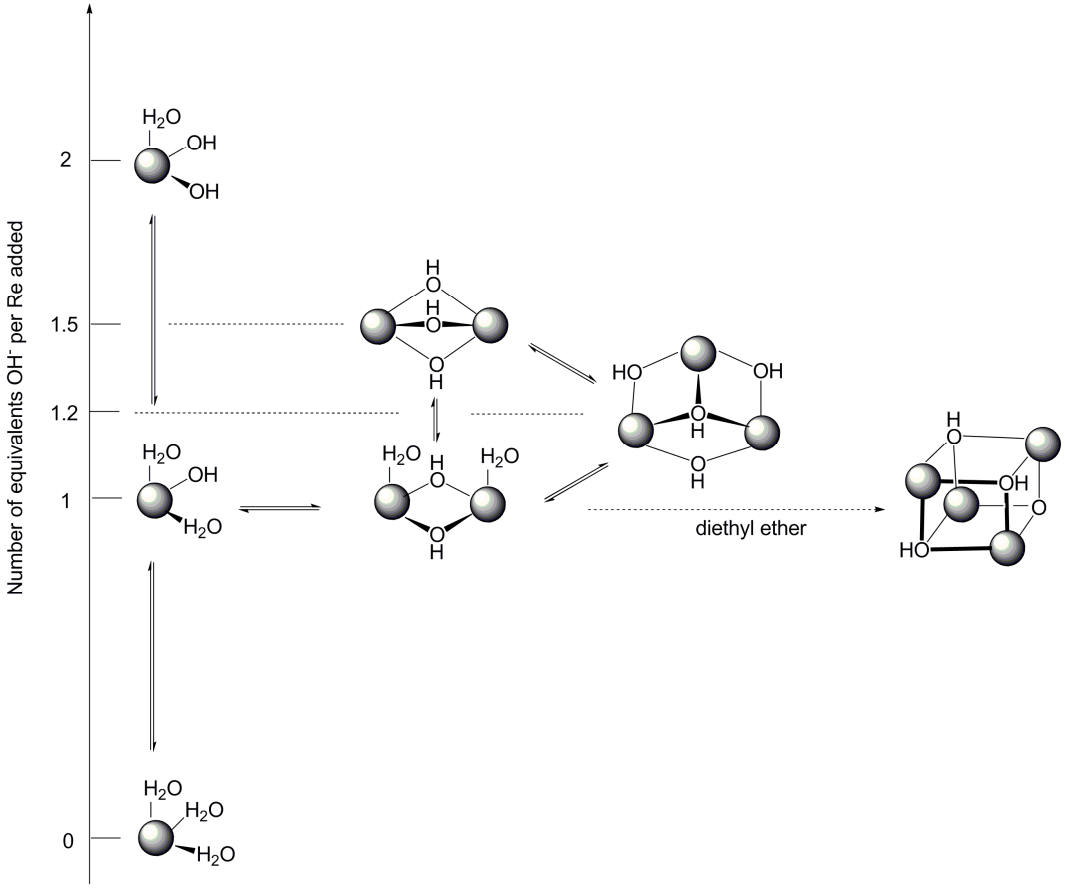


## 2.4.3 Application of the *fac*-$[M(CO)_3]^+$ moiety

The *fac*-$[M(CO)_3]^+$ core (M = $^{99m}$Tc, $^{188}$Re) is one of the main compounds used worldwide for the investigation of radiopharmaceuticals due to its relatively compact size, low positive charge (+1) and extreme stability. Because of its low-valent, kinetic inert organometallic core, it possesses high *in vivo* stability.[127] It is a versatile synthon for the labeling of different bioactive molecules, recombinant proteins and small molecules.[128] A one-step kit formulation is available for the preparation of *fac*-$[^{99m}Tc(CO)_3]^+$ [129,130] while a two-step kit is in development for the $^{188}$Re synthon.[127]

Ever since the production of *fac*-$[M(CO)_3(H_2O)_3]^+$ (M = $^{99m}$Tc, Re) in aqueous medium, the *fac*-$[M(CO)_3]^+$ core was established as an accessible synthon for the

[127] Schibli, R., Schwarzbach, R., Alberto, R., Ortner, K., Schmalle, H., Dumas, C. *Bioconjug. Chem*. **2002**, *13*, 750-756.
[128] Raposinho, P.D., Correia, J.D.G., Alves, S., Botelho, M.F., Santos, A.C., Santos, I. *Nucl. Med. Biol*. **2008**, *35*, 91-99.
[129] Isolink, Covidien, Petten, The Netherlands.
[130] Alberto, R., Ortner, K., Wheatley, N., Schibli, R., Schubiger, A.P. *J. Am. Chem. Soc*. **2001**, *123*, 3135-3136.

synthesis of radiopharmaceuticals.[122,124,125] This precursor is not only water-soluble but also stable from pH 2 to pH 12 for a few hours. By labeling with $^{99m}$Tc or $^{188}$Re, a diagnostic agent or therapeutic agent respectively, are produced. The main reason and advantage in the use of the *fac*-$[M(CO)_3(H_2O)_3]^+$ synthon is the stable *fac*-Rhenium tricarbonyl core with the other three facial sites occupied by water molecules that are labile and easily replaceable by different ligands and ligand combinations like amines, imines, thioethers, thiols, phosphines and oxygen donors like carboxylates, phosphonates and phosphates.[69,106,107,108,115,116] Considering the *fac*-$[Re(CO)_3(H_2O)_3]^+$ core compared to the $^{99m}Tc^{V}O$ core, amino acid analogues and polyaminocarboxylic acid ligands with acetate groups readily form stable complexes.[131,132]

Despite all the advantages of *fac*-$[M(CO)_3]^+$ (M = Re, Tc) as synthon to be used in potential therapeutic and imaging agents, one of the biggest challenges is to develop a chelating core with a strong complexation to *fac*-$[M(CO)_3]^+$ but with a minimal effect on the properties of the biomolecule.

The chelating units should meet the following requirements – have a high affinity to the metal ion core, must form thermodynamic and kinetic stable complexes and must have complete complexation to *fac*-$[^{99m}Tc(CO)_3]^+$ at a ligand concentration of $10^{-5}$ M – $10^{-4}$ M. The latter prerequisite is especially important when labeling receptor ligands like steroids and small peptides. At ligand concentrations higher than $10^{-4}$ M, the free receptor sites can get saturated with unlabeled biomolecules therefore a decrease in the selectivity of the radionuclide accumulation in the target tissue.

Keeping all of the above in mind, tridentate chelators seem to be a better choice since it meet all the requirement mentioned above, but the synthetic procedure of conjugating it with a biomolecule is more complex than the bidentate chelators that can be more readily derivatized.[5,89] However, previous studies have shown that *fac*-$[M(CO)_3]^+$ complexes with bidentate ligands, except species with diphosphine ligands, are unstable *in vivo* and *in vitro* because of the weak ligand that occupies the third coordination site.[5,133,134] Schibli *et al*. investigated *fac*-$[^{99m}Tc(CO)_3]^+$

[131] Adams, K.M., Marzilli, L.G. *Inorg. Chem.* **2007**, *46*, 4926-4936.
[132] Mundwiler, S., Waibel, R., Spingler, B., Kunze, S., Alberto, R. *Nucl. Med. Biol*. **2005**, *32*, 473-484.
[133] Schibli, R., Katti, K.V., Higginbotham, C., Volkert, W.A., Alberto, R. *Nucl. Med. Biol*. **1999**, *26*, 711-716.
[134] Schibli, R., La Bella, R., Alberto, R., Carcia-Garayoa, E., Ortner, K. *Bioconjug. Chem*. **2000**, *11*, 345-351.

complexes with a variety of bi- and tridentate ligands. The tridentate complexes showed a much better and faster clearance from the whole body than the bidentate complexes that had high retention of activity in the liver and kidneys. The reason for this are speculated to be a lower thermodynamic stability and the potential substitution site of the aqua ligand by the functional groups of proteins.[134]

$^{99m}$Tc could be used for targeted therapy and diagnosis at once with one compound. Lately, Reilly *et al*. demonstrated that it is indeed possible to use $^{99m}$Tc's Auger electrons for therapy with the VEGF-2 K peptide.[135] The aim of Zelenka *et al*. in their 2011 study was to synthesize a trifunctional imaging agent, that consists of a receptor specific peptide, a nucleus targeting luminescent part and then the $^{99m}$Tc part. The peptide bound to a monodentate ligand, to facilitate the release thereof, is called the inverted '2+1' approach. With Rhenium compounds, fluorescence allows for localization and the $^{99m}$Tc analogues can be used for *in vivo* imaging.

# 2.5 Chelating systems and linkage

## 2.5.1 Introduction

It was known from previous studies on the *fac*-$[Tc(CO)_3(H_2O)_3]^+$ moiety that the ideal chelating system for this precursor for application as potential radiopharmaceutical should contain at least one amine, preferably in an aromatic heterocycle and a carboxylic acid functionality. It was because of this that Schibli and co-workers studied the *in vivo* and *in vitro* behaviour of model *fac*-Re(I) and Tc(I) tricarbonyl complexes with bi- and tridentate ligand systems of this sort.[136]

The bidentate complexes were almost completely bound to proteins after 60 minutes while the complexes with tridentate ligand systems showed no reaction towards serum proteins. The biodistribution characteristics and the *in vivo* stability revealed fast clearance from all organs for the tridentate complexes while the complexes with bidentate ligands showed a higher retention and activity in the liver, kidneys and blood pool.

[135] Chan, C.R., Cai, Z.L., Su, R.F., Reilly, R.M. *Nucl. Med. Biol.* **2010**, *37*, 105-115.
[136] Schibli, R., La Bella, R., Alberto, R., Garcia-Garayoa, E., Ortner, K., Abram, U., Schubiger, P.A. *Bioconjug. Chem*. **2000**, *11*, 345-351.

All in all, these results initiated the assumption that tridentate chelating systems are better options than bidentate chelating systems for the functionalization of biomolecules, because of the more favourable pharmacokinetics.

Labeling strategies usually rely on the use of multidentate chelating ligands although a direct approach to label antibodies is known where the internal disulphide bonds are reduced and the nuclide directly react with the sulfhydryl groups that resulted from the reduction.[137] An ideal chelator will be one that forms a complex that allows the chelated nuclide to be rapidly excreted without intracellular retention and the conjugate selectively retained in the tumor cells. Lately, with quite alot of potential dugs, retention of the metal nuclides and sometimes still in the chelated form, are found.[138]

To predict the *in vivo* behaviour of a chelated nuclide is not easy, therefore the choice of what multidentate ligand to potentially use is directed/indicated by the general/accepted chelation chemistry. The multidentate ligand should have a bifunctional coordination site for metal complexation a well as a liking site for potential coupling to an available functional group within the protein. The demand for a bifunctional coordination site specifically, decrease the number of potential ligands dramatically since it isn't always synthetically easy to introduce a linking group without changing the coordination ability and properties of the ligand. An example is polyamino-polycarboxylic ligands since no derivatization is necessary because it has a coordination site and a group for linkage as is.[139,140,141,142]

## 2.5.2 Choice of radioactive core

With Rhenium (in several oxidation states), tetradentate N,S systems give the best results (as with $^{99m}$Tc), with the $MAG_3$ type of ligands being the most prominent. An example is the kidney imaging agent $^{99m}$TcO-mercaptoacetyltriglycine presented in Figure 2.14.

---

[137] Griffiths, G.L., Goldenberg, D.M., Knapp, F.F., Callahan, A.P., Cheng, C.H., Hansen, H.J. *Cancer Res*. **1991**, *51*, 4594-4602.
[138] Anderson, C.J., Rogers, B.E., Connett, J.M., Guo, L.W., Schwarz, S.W., Zim, K.R., Welch, M.J. *Tenth International Symposium on Radiopharmacy Chemistry Abstracts*, p. 313, **1993**.
[139] Kosmas, C., Maraveyas, A., Gooden, C.S., Snook, D., Epenetos, A.A. *J. Nucl. Med*. **1995**, *36*, 746-753.
[140] Stewart, J.S.W., Hird, V., Snook, D. *J. Clin. Oncol*. **1990**, *8*, 1941-1950.
[141] Vriesendrop, H.M., Herpst, J.M., Germack, M.A., Klein, J.L., Leichner, P.K., Loudenslager, D.M., Order, S.E. *J. Clin. Oncol*. **1991**, *9*, 918-928.
[142] Quadri, S.M., Vriesendrop, M., Leichner, P.K., Williams, J.R. *J. Nucl. Med*. **1993**, *34*, 938-945.

**Figure 2.14: Structure of [$^{99m}$TcO(MAG$_3$)]$^-$.**

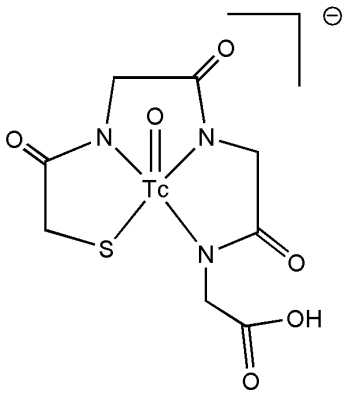

Intense investigations into a variety of these ligand types have been reported.[143,144,145,146]

Another approach is the use of hexadentate $N_2S_4$ ligands where one of the thiol groups are used for linking to thiol groups in proteins, which are generated by the reduction of the disulphide bridges. The coordination to the Re=O core is assumed to be the same as for the $MAG_3$ ligands.[147] A newer approach was to link molecules like propionic acid to the *fac*-$[Re(CO)_3]^+$ core.[148] It was proven to have a high *in vivo* stability when bound to the antibody. At that stage it was only prepared with the inactive complex because the radioactive complex $[Re_2(CO)_{10}]$ had to be prepared *via* high pressure synthesis.

In 1995, Alberto *et al*. described a low pressure synthesis method for the *fac*-$[Re(CO)_3(H_2O)_3]^+$, with $^{188}$Re, complex.[122] From then onwards, it was a much easier job to synthesize organometallic Re(I) compounds. It has been proven that *fac*-$[Re(CO)_3(H_2O)_3]^+$ is very stable, even in aerobic conditions, in water and at elevated temperatures. In the same study they showed the inertness at various chemical

[143] Goldrosen, M.H., Biddle, W.C., Pancook, J., Bakshi, S., Vanderheyden, J.-L., Fritzberg, A.R., Morgan, A.C., Foon, K.A. *Cancer Res*. **1990**, *50*, 7973-7978.
[144] Beaumier, P.L., Venkatesan, P., Vanderheyden, J.-L., Burgua, W.D., Kunz, L.L., Fritzberg, A.R., Abrams, P.G., Morgan, A.C. *Cancer Res*. **1991**, *51*, 676-681.
[145] Breitz, H.B., Weiden, P.L., Vanderheyden, J.L., Appelbaum, J.W., Bjorn, M.J., Fer, M.F., Wolf, S.B., Ratliff, B.A., Seiler, C.A., Foisie, D.C., Fischer, D.R., Schroff, R.W., Fritzberg, A.R., Abrams, P.G. *J. Nucl. Med*. **1992**, *33*, 1099-1112.
[146] Visser, G.W.M., Gerretson, M., Herscheid, J.D.M., Snow, G.B., van Dangen, G. *J. Nucl. Med*. **1993**, *34*, 1953-1963.
[147] Najafi, A., Alauddin, M.M., Sosa, A., Ma, G.Q., Chen, D.C.P., Epstein, A.L., Siegel, M.E. *Nucl. Med. Biol*. **1992**, *19*, 205-212.
[148] Salmain, M., Gunn, M., Gorfi, A., Top, S., Jaouen, G. *Bioconjug. Chem*. **1993**, *4*, 425-433.

conditions and therefore expected high *in vivo* stability from the compounds of *fac*-$[Re(CO)_3]^+$ with various tridentate thiomacrocycles.

Another advantage of *fac*-$[Re(CO)_3(H_2O)_3]^+$ is the fact that it can be seen as an aquo-ion and it is therefore possible to consider postlabeling with for instance the macrocyclic thioethers compared to the conventional prelabeling used with $MAG_3$ ligands. The above mentioned results show the wide variety of properties to take into account when considering a nuclide with more than one oxidation state. It is therefore very difficult to decide if a ligand is worthy of investigation if it is not very stable but highly inert.

## 2.5.3 Activation of the functional group/linking

Once the difficult and very important decision on what bifunctional ligand will be used have been made, the next step will possibly be the activation of the functional group to enable the ligand to be bound to the carrier molecule. A schematic representation of this procedure is given in Figure 2.15.

**Figure 2.15: Activation, coupling and radiolabeling of bifunctional ligands.**

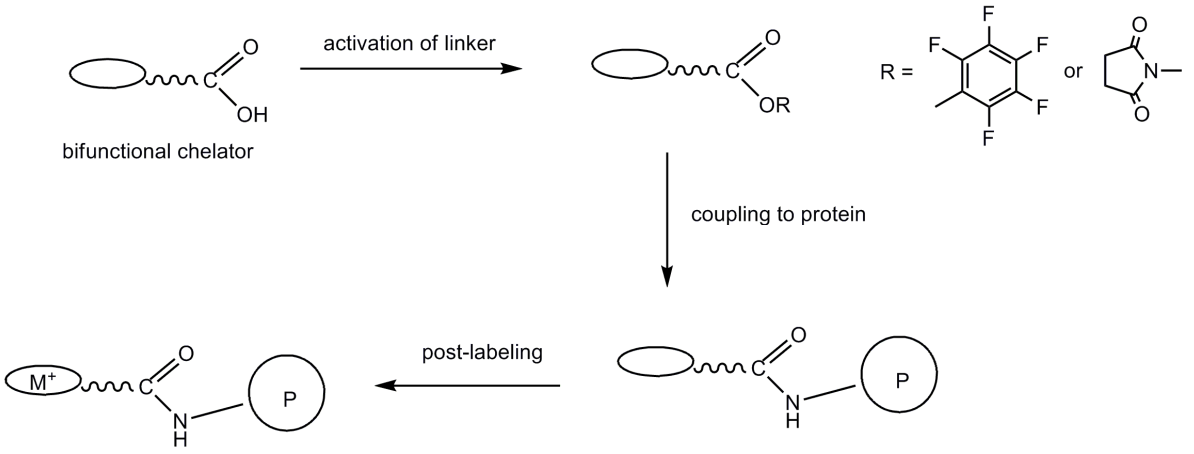


This is then reacted with an accessible primary amino group in the antibody, in aqueous solution, where hydrolysis will now be a strong competitor to aminolysis. Usually to achieve a reasonable yield, one needs to apply up to a 100 fold excess of the activated ligand to the antibody. This literature search showed that the functional group used is mostly a carboxylic acid.

Bodansky *et al*. described almost all of the possible functionalities, with its activation reagents and protocols in 1984.[149] One special linking method is the so-called anhydride method. It is specifically for polyamino-polycarboxylic acid type ligands and it is necessary to have two carboxylic acids in the system that can form a 6-membered cyclic anhydride. The primary amine group of lysine will then follow with amide formation, with one carboxylic acid available again for coordination to the metal centre. This approach has been used with a lot of the typical hard metal centres like Y(III) and In(III).

Another example of labeling a potential radioimmunoconjugate is by means of intraconversion in organic solvents of primary amines into isothiocyanato groups by thiophosgene. It is a basic procedure since the isothiocyanato group reacts with the primary amine residues of lysine selectively in water and forms stable thiourea bridges. If the bifunctional chelator have a thiol group incorporated, it can be used to reduce the disulphide bridges in the carrier antibody itself. As these disulphide bridges are cleaved, disulphide bridges are formed to the ligand. Najafi *et al*. did an intensive study on how the biological activity of the antibody can be hindered/lost with the reduction of too many disulphide bridges.[147]

To bind ligands covalently to proteins, the proteins have to be derivatized by various chemical procedures. One has already been mentioned, where the disulphide bridges are reduced to reactive thiol groups. Another way to introduce thiol groups to the protein is by the reaction of the α-amino groups of the lysines with a variety of organic molecules. The thiol group that is introduced in this way then selectively reacts with functional groups on the bifunctional ligand.

McCall *et al*. studied this type of approach and found that in this method, hydrolysis does not compete with the linking as much as with the activation of the carboxylic acid method.[150] Therefore increasing the yield and lowering the amount of ligand necessary to be added. The disadvantage is that one needs to work under anaerobic conditions because the free thiols have a tendency to crosslink in the presence of air to form disulphide bridges.

---

[149] Bodansky, M., Bodansky, A. *Practice of peptide synthesis* **1984**, ISBN 3-540-13471, Springer-Verlag, Berlin.

[150] McCall M.J., Diril, H., Meares, C.F. *Bioconjug. Chem*. **1990**, *1*, 222-226.

Very thorough investigations and discussions on techniques and methods for labeling and the practical application of protein conjugation can be found in literature.[149,151,152,153]

### 2.5.4 *In vivo* behaviour

When considering the *in vivo* behaviour of the above mentioned type of radionuclide labeled antibodies, it's found that it accumulates in unwanted areas/cells as well. From previous studies it is clear that one should then look at the linker between the carrier molecule and the chelator, since this can significantly change the properties and therefore the biodistribution of the compound.[154,155,156] Another study by Weber and co-workers tested a compound with a $N_3S$ chelator and a linker with an ester group functionality.[157] Tests showed the compound with this linker had reduced non-specific radionuclide accumulation compared to the compound with a linker without an ester group.

## 2.6 Recent highlights in radiopharmaceutical research

### 2.6.1 Research towards the central nervous system

New ligand systems to use as diagnostic tools and to quantify neuroreceptors in the central nervous system became of big interest in the last decade. Most neurological diseases are related to the change in density of specific receptors. This could only be detected by post mortem studies in the past.[158]

---

[151] Rose, K., Vilaseca, L.A., Werlen, R., Meunier, A., Fisch, I., Jones, R.M.L., Offord, R.E. *Bioconjug. Chem.* **1991**, *2*, 154-159.
[152] Fisch, I., Künzi, G., Rose, K., Offord, R.E. *Bioconjug. Chem*. **1992**, *3*, 147-153.
[153] Wang, S.S. Chemsitry of protein conjugation and cross-linking **1993**, ISBN 0-8493-5886-8, CRC Press Inc., Boca Raton, Florida.
[154] Meares, C.F., McCall, M.J., Deshpande, S.V., DeNardo, S.J., Goodwin, D.A. *Int. J. Cancer* **1958**, *2* (Suppl.), 99-102.
[155] Deshpande, S.V., DeNardo, S.J., Meares, C.F., McCall, M.J., Adams, G.P., DeNardo, G.L. *Nucl. Med. Biol*. **1989**, *16*, 587-597.
[156] Paik, C.H., Yokoyama, K., Reynolds, J.C., Quadri, S.M., Min, C.Y., Shin, S.Y., Maloney, P.J., Larson, S.M., Reba, R. *J. Nucl. Med*. **1989**, *30*, 1693-1701.
[157] Weber, R.W., Boutin, R.H., Nedelman, M.A., Lister-James, J., Deon, R.T. *Bioconjug. Chem*. **1990**, *1*, 431-437.
[158] Halldin, C., Gulyás, B., Langer, O., Farde, L. *Q. J. Nucl. Med.* **2001**, *45*, 139-152.

An important subtype of receptors, involved in processes in the brain, is the 5-$HT_{1A}$ subtype for serotonin. A change in the number of these receptors is associated with diseases like Alzeimer's, Schizophrenia and depression.[159] Even with successful compounds like [Carbonyl-$^{11}$C] WAY-100635 (WAY) and *p*-[$^{18}$F] MPPF, there is still a need for the development of Tc labelled 5-$HT_{1A}$ ligands for potential use in SPECT imaging (Figure 2.16) .[158,159]

**Figure 2.16: Radiosynthesis of [$^{11}$C]WAY 100635 in A and [$^{18}$F]*p*-MPPF in B.**

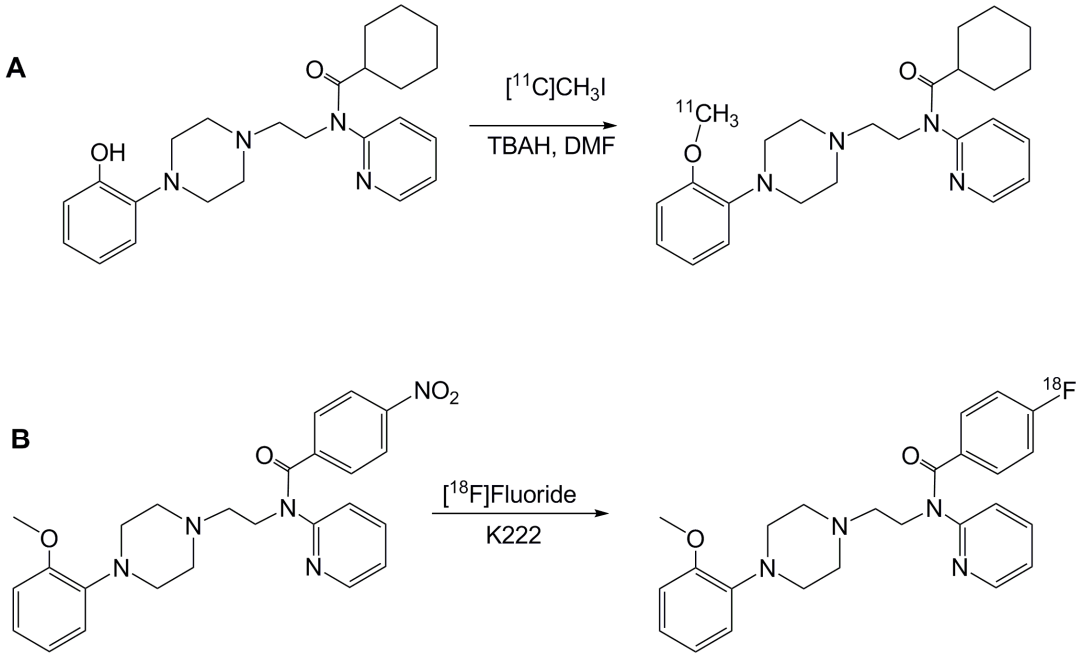


The only agent for central nervous system receptors up to date that successfully targets CNS receptors, is [$^{99m}$Tc] TRODAT-1, shown in Figure 2.17.[160]

**Figure 2.17: Structure of [$^{99m}$Tc] TRODAT-1.**

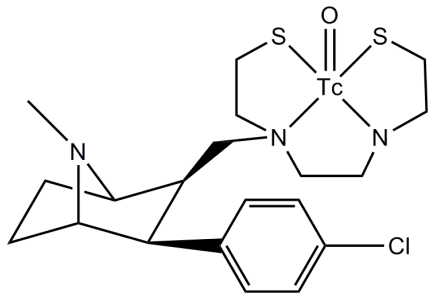


[159] Passchier, J., Waarde, A.V. *Eur. J. Nucl. Med*. **2001**, *28*,113-129.
[160] Johannsen, B., Pietzsch, H.-J. *Eur. J. Nucl. Med*. **2002**, *29*, 263-266.

Since the development of *fac*-[$^{99m}$Tc(CO)$_3$(H$_2$O)$_3$]$^+$ and its wide use in the labeling of biomolecules, quite a few complexes where peptides and CNS receptor ligands were labeled by using a variety of bifunctional chelating agents.[130,161] In spite of all the new compounds and development regarding a CNS receptor imaging agent, the problem is still *in vivo* and *in vitro* stability and behaviour.

Correia and his co-workers synthesized a wide variety of heterofunctionalized phosphines that stabilizes the Rhenium and Technetium metal core.[162,163,164] The first *fac*-Rhenium tricarbonyl compounds that are anchored by phosphines with PN$_2$ and PNO donor atoms were published by Correia *et al*. The preliminary studies showed good yields for the labeling of H$_2$PNO, HPN$_2$ and the 5-HT$_{1A}$ (N-[4-(3-aminopropyl)-1-(2-methoxyphenyl)piperazine]-2-(diphenylphosphonyl)-benzamide) ligands with *fac*-[$^{99m}$Tc(CO)$_3$]$^+$.

In 2004, the group derivatized the pharmacophore (2-mehoxyphenyl)piperazine (a part of the successful WAY-100635 structure) with phosphinoarylbenzylamide - with PO donor atoms – and phosphinoarylbenzylamine - with PN donor groups – as chelator systems. They varied the length of the spacer between the chelator unit and the receptor binding domain.[165] The results confirmed the importance of the relationship between the structure and the activity.

## 2.6.2 Using the luminescence properties of different ligands/conjugates

Mononuclear *fac*-Re(I) tricarbonyl complexes, because of their ground- and excited state properties, draw continuing investigation. The bipyridine and phenanthroline *fac*-Re(I) tricarbonyl complexes emit from their triplet excited states. At room temperature, the excitation into metal-to-ligand charge-transfer absorptions gives

---

[161] Alberto, R., Schibli, R., Schubiger, A.P., Abram, U., Pietzsch, H.J., Johannsen, B. *J. Am. Chem. Soc*. **1999**, *121*, 6076-6077.
[162] Correia, J.D.G., Domingos, Ã., Santos, I., Alberto, R., Ortner, K. *Inorg. Chem*. **2001**, *40*, 5147-5151.
[163] Correia, J.D.G., Santos, I., Alberto, R., Ortner, K., Spies, H., Drews, A. *J. Label. Compd. Radiopharm*. **2001**, *44*, S507.
[164] Fernandes, C., Kniess, T., Gano, L., Seifert, S., Spies, H., Santos, I. *Nucl. Med. Biol*. **2004**, *31*, 785-793.
[165] Palma, E., Correia, J.D.G., Domingos, Ã., Santos, I., Alberto, R., Spies, H. *J. Organomet. Chem.* **2004**, *689*, 4811-4819.

sub-microsecond luminescence for these complexes. At lower temperatures it has longer lifetimes.[166,167,168]

Zubieta and co-workers[169] introduced chelating ligands bearing quinoline, tryptophan and benzimidazole donors, when bound to the Re(I) core, they act as Luminescence probes and when *fac*-$[^{99m}Tc(CO)_3]^+$ is incorporated, it acts as potential radioimaging agents. The diimine carbonyl Re(I) systems, prepared by various groups, have limited visible absorption and restricts their photochemical uses.[170,171] The azadipyrromethenes are a broad set of ligands with an excellent red-light absorbing capability.[172,173,174]

Recently Partyka *et al*. synthesized a few *fac*-Rhenium(I) tricarbonyl azadipyrromethene complexes by reacting the chromophore with *fac*-$[Re(CO)_3(H_2O)_3]^+$. The azadipyrromethenes and their boron chelates keep their absorption features when bound to the Re(I) core. The lability of *fac*-$[Re(CO)_3]^+$ promote the attachment to Lewis bases in a variety of conditions/environments. The Rhenium(I) azadipyrromethene complexes and the free ligands undergo reductive electrochemistry. There is a second reduction step that is reversible for the ligand but irreversible for the complex. This might indicate the participation of the *fac*-$[Re(CO)_3]^+$ moiety. The conclusion of this study indicate the potential for further investigation into the optical and electrochemical properties of these Re(I) azadipyrromethenes and their use in light capture.[175] Recently, work done on boron adducts has produced efficient fluorophores and possible drug candidates for photodynamic therapy in humans.[176] Figure 2.18 illustrates the synthetic procedure for these complexes with X = pyridine, tetrahydrothiophene, *N*-benzylimidazole and *t*-butylisonitrile. The azadipyrromethene ligands are chelating N-donor ligands with good resemblance to the phenanthrolines and bipyridines. This characteristic

[166] Giordano, P.J., Wrighton, M.S. *J. Am. Chem. Soc*. **1979**, *101*, 2888-2897.
[167] Dattelbaum, D.M., Martin, R.L., Scoonover, J.R., Meyer, T.J. *J. Phys. Chem. A* **2004**, *108*, 3518-3526.
[168] Lees, A.J. *Chem. Rev*. **1987**, *87*, 711-743.
[169] Wie, L., Babich, J.W., Ouellette, W., Zubieta, J. *Inorg. Chem*. **2006**, *4*, 3057-3066.
[170] Reece, S.Y., Nocera, D.G. *J. Am. Chem. Soc*. **2005**, *127*, 9448-9458.
[171] Yam, V.W.-W., Lo, K.K.-W., Cheung, K.-K., Kang, R.Y.-C. *J. Chem. Soc., Chem. Commun.* **1995**, 1191-1193.
[172] Rogers, M.A.T. *J. Chem. Soc*. **1943**, 596-597.
[173] Zhao, W., Carreira, E.M. *Angew. Chem., Int. Ed*. **2005**, *44*, 1677-1679.
[174] Teets, T.S., Partyka, D.V., Updegraff, J.B. III, Gray, T.G. *Inorg. Chem*. **2008**, *47*, 2338-2346.
[175] Partyka, D.V., Deligonul, N., Washington, M.P., Gray, T.G. *Organometallics* **2009**, *28*, 5837-5840.
[176] Gorman, A., Killoran, J., O'Shea, C., Kenna, T., Gallagher, W.M., O'Shea, D.F. *J. Am. Chem. Soc.* **2004**, *126*, 10619-10631.

together with the favourable excited state properties of the studied Re(I) diimine complexes, initiated the investigation of (azadipyrromethene) Re(I) chromophores.

**Figure 2.18: General preparation method for the complexes synthesized by Gorman *et al*.[176]**

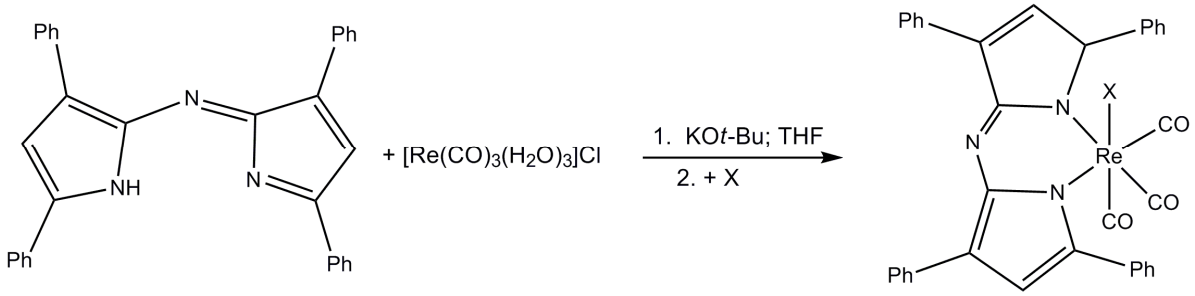


Organic light-emitting diodes (OLED's) have huge potential due to their application in flat panel displays and lighting sources. Research efforts have gained a lot of interest to develop efficient phosphorescent materials.[177] Very little complexes with Re(I) as the phosphorescent emitter, have been investigated, even with its advantageous characteristics.[178,179,180] Li *et al*. designed and synthesized a novel fluorinated *fac*-Re(I) tricarbonyl complex with excellent results.[181] It suggests that the fluorine introduction brings about highly efficient electrophosphorescent complexes, something to remember when designing these compounds.

## 2.6.3 Melanoma targeting agents

Melanoma, skin tumor, is known for its aggressiveness, its extensive spreading/distribution to other organs early on and its poor prognosis once it metastasized. At an early stage, melanoma can be cured by surgical treatment, whereas patients with distant metastases don't have many options other than surgical removal of the original tumor and all the metastases.[182]

---

[177] Reineke, S., Lindner, F., Schwartz, G., Seidler, N., Walzer, K., Lüssem, B., Leo, K. *Nature* **2009**, *459*, 234-238.
[178] Liu, C.B., Li, J., Li, B., Hang, Z.R., Zhao, F.F., Liu, S.Y., Li, W.L. *Appl. Phys. Lett*. **2006**, *89*, 243511.
[179] Si, Z., Li, J., Li, B., Hang, Z., Lu, S., Liu, S., Li, W. *Appl. Phys. A* **2007**, *88*, 643-646.
[180] Si, Z.J., Li, J., Li, B., Zhao, F.F., Liu, S.Y., Li, W.L. *Inorg. Chem*. **2007**, *46*, 6155-6163.
[181] Li, X., Wu, S., Zhang, D., Su, Z., Lei, P., Zhang, Z., Hu, Z., Li, W. *Synthetic Metals*. **2010**, *160*, 390-393.
[182] Camacho, L.H., Antonia, S., Sosman, J., Kirkwood, J.M., Gajewski, T.F., Redman, B., Pavlov, D., Bulanhagui, C., Bozon, V.A., Gomez-Navarro, J., Ribas, A. *J. Clin. Oncol.* **2009**, *27*, 1075-1081.

The development of a melanoma targeting radioimmunopharmaceutical is therefore quite important for early diagnosis and follow-up imaging of the patient. A very important characteristic of melanoma tumors is the extensive pigmentation. Therefore the tumor cells have an excess of melanin present which scientists recognized as an attractive target. Many agents with melanin affinity have been evaluated, but with limited success. These included monoclonal antibodies,[183,184] nucleic acids[185,186] and small radioiodinated amino acids.[187,188]

Another class of radiopharmaceuticals that detect melanoma, is radioiodinated benzamides. $^{123}$I-*N*-(2-diethylaminoethyl)-4-iodobenzamide ($^{123}$I-BZA) and (*N*-benzylpiperidine-4-yl)-2-iodobenzamide (2-IBP) are two examples of this type that showed good tumor uptake.[189,190] Only a few $^{99m}$Tc labelled benzamide derivatives are known. One example is the work by Eisenhut *et al*. where $[^{99m}Tc=O]^{3+}$ complexes with $N_2S_2$ chelates were conjugated to N-dialkylaminoalkyl groups, and obtained high tumor uptake.[191]

To obtain an agent with a high target/non target ratio in a short period of time is of great essence for precise diagnosis. The problem is the size of the complex and the chelator functionalities that can govern the biological behaviour of the vector.[192] The ideal ligand, to optimise these parameters, is cyclopentadienyl (Cp). It is small in size, binds stable to the *fac*-$[M(CO)_3]^+$ core and it mimics arene rings in pharmaceuticals and biomolecules. It has also been shown that amino acids derivatised with ferrocene or *fac*-$[Re(CO)_3(Cp)]$ are surrogates for natural amino acids. Since Cp is very sensitive, it is a challenge to use in an aqueous synthetic pathway – clinical agents are prepared in water.

---

[183] Buraggi, G.L., Callegaro, L., Marioni, G., Turrin, A., Cascinelli, N., Attili, A., Bombardieri, E., Terno, G., Plassio, G., Dovis, M., Mazzuca, N., Natali, P.G., Scassellati, G.A., Rosa, U., Ferrone, S. *Cancer Res.* **1985**, *45*, 3378-3387.
[184] Larson, S.M. *J. Nucl. Med.* **1991**, *32*, 287-291.
[185] Larsson, B., Olander, K., Dencker, L., Holmqvist, L. *Br. J. Cancer* **1982**, *46*, 538-550.
[186] Van Langevelde, A., Bakker, C.N., Broxterman, H.J., Journée-De Korver, J.G., Kaspersen, F.M., Oosterhuis, J.A., Pauwels, E.K. *Eur. J. Nucl. Med*. **1983**, *8*, 45-51.
[187] Kloss, G., Leven, M. *Eur. J. Nucl. Med*. **1979**, *4*, 179-186.
[188] Bubeck, B., Eisenhut, M., Heimke, U., Zum Winkel, K. *Eur. J. Nucl. Med*. **1981**, *6*, 227-233.
[189] Michelot, J.M., Moreau, M.F., Labarre, P.G., Mademont, J.C., Veyre, A.J., Papon, J.M., Parry, D.F., Bonafous, J.F., Boire, J.Y., Desplanches, G.G *J. Nucl. Med*. **1991**, *32*, 1573-1580.
[190] John, C.S., Gulden, M.E., Li, J., Bowen, W.D., Mcafee, J.G., Thakur, M.L. *Nucl. Med. Biol*. **1998**, *25*, 189-194.
[191] Eisenhut, M., Mohammed, A., Mier, W., Schönsiegel, F., Friebe, M., Mahmood, S., Jones, A.G., Haberkorn, U. *J. Med. Chem*. **2002**, *45*, 5802-5805.
[192] Liu, S. *Chem. Soc. Rev*. **2004**, *33*, 443-461.

Previous studies have shown that the piano-stool complex [(Cp-R)M(CO)$_3$] is able to substitute a phenyl ring in biomolecules, eg. steroid hormones and antibodies.[148,193] The synthesis of [$^{99m}$Tc(CO)$_3$(Cp-R)] in organic solvents, prepared in autoclaves have been reported.[194] The group of Peindy N'Dongo introduced a synthetic pathway from water, but an even better preparation with a high yield was reported in 2008 by the same group by reacting *fac*-[$^{99m}$Tc(CO)$_3$(H$_2$O)$_3$]$^+$ with Thiele's acid in water to produce the complex *fac*-[$^{99m}$Tc(CO)$_3$(Cp-COOH)].[195]

These results initiated the approach to prepare bioactive complexes like *fac*-[$^{99m}$Tc(CO)$_3$(Cp-R)] with R = amino acids or a benzamide group to potentially apply these half-sandwich complexes as mimics of phenyl groups in biomolecules.[196] The study reported in 2010 showed that the phenyl rings in radioiodinated benzamides, for use in melanoma imaging, can be replaced by complexes of the type *fac*-[$^{99m}$Tc(CO)$_3$(Cp-R)] under retention of tumor uptake and clearance from the body.[197]

**Figure 2.19: Structures of the organic compounds BZA and IBP and its corresponding *fac*-[$^{99m}$Tc(CO)$_3$Cp] mimics.**

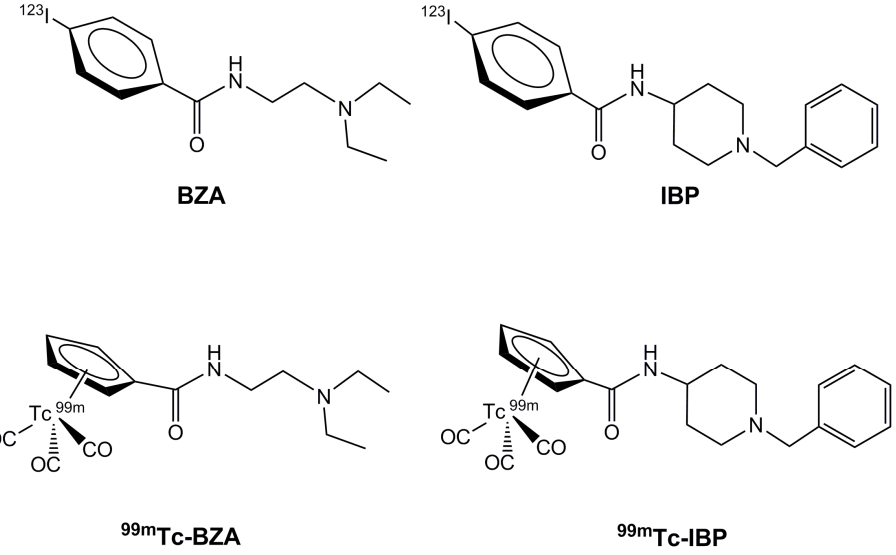


[193] Top, S., Hafa, E.H., Vessières, A., Quivy, J., Vaissermann, J., Hughes, D.W., McGlinchey, M.J., Mornan, J.-P., Thoreau, E., Jaouen, G. *J. Am. Chem. Soc*. **1995**, *117*, 8372-8380.
[194] Spradau, T.W., Katzenellenbogen, J.A. *Organometallics* **1998**, *17*, 2009-2017.
[195] Liu, Y., Spingler, B., Schmutz, P., Alberto, R. *J. Am. Chem. Soc*. **2008**, *130*, 1554-1555.
[196] Peindy, N'Dongo, H.W., Liu, Y., Con, D., Schmutz, P., Spingler, B., Alberto, R. *J. Organomet. Chem*. **2009**, *694*, 981-987.
[197] Peindy, N'Dongo, H.W., Raposinho, P.D., Fernandes, C., Santos, I., Con, D., Schmutz, P., Spingler, B., Alberto, R. *Nucl. Med. Biol*. **2010**, *37*, 255-264.

$^{99m}$Tc complexes that surrogate iodobenzamide were described (Figure 2.19). It has a high affinity for melanoma tumor cells and one of the prepared complexes showed good *in vitro* stability and good retention in the tumor.

## 2.6.4 Renal tracers

Lipowska and co-workers investigated $^{99m}$Tc agents, specifically radiopharmaceuticals with a rapid renal clearance.[198] This led the group to use ligands with an uncoordinated carboxyl group.[199] This is important because the renal receptor's interaction with this dangling carboxyl group is important for clearance of small peptides.[200] They used polyaminocarboxylate ligands and robust anionic complexes were formed with a free carboxyl group useful for renal targeting. Unfortunately a mixture of two major anionic agents was sometimes formed in a ratio differing with the conditions of the preparation method.

The Rhenium analogue was then used to investigate how temperature and pH affect the formation and properties of the analogues formed. At low pH, for the compound with one carboxylate oxygen bound to the Rhenium core and one dangling, protonated potential amine is often favored, kinetically and thermodynamically. At higher pH, the Rhenium core has a higher affinity for the amine group. For renal tracers, the labeling can therefore be performed at high temperature and low pH.

At room temperature it can be converted to the N coordination mode by lowering the pH. Many robust $^{99m}Tc^{V}O$ anionic compounds have been investigated where the ligands have one or two dangling carboxylic groups.[201] Under some conditions, the carboxylic groups can coordinate, which poses problems.

## 2.6.5 Tripodal/tridentate ligand type complexes

As noted before, tridentate chelators are the best ligands to stabilize the *fac*-$[M(CO)_3]^+$ cores due to its high *in vivo* and *in vitro* stability.[69,134] Pyrazole-type tripods, like the tris(azolyl)hydroborate and tris(pyrazolyl) methane types, are the obvious choice amongst tridentate ligands due to their topology, denticity and donor

[198] Lipowska, M., He, H., Xu, X., Taylor, A.T., Marzilli, P.A., Marzilli, L.G. *Inorg. Chem*. **2010**, *49*, 3141-3151.
[199] Lipowska, M., Marzilli, L.G., Taylor, A.T. *J. Nucl. Med*. **2009**, *50*, 454-460.
[200] Shikano, N., Kanai, Y., Kawai, K., Ishikawa, N., Endou, H. *J. Nucl. Med*. **2004**, *45*, 80-85.
[201] Taylor, A., Lipowska, H., Hansen, L., Malveaux, E., Marzilli, L.G. *J. Nucl. Med*. **2004**, *45*, 885-891.

atom sets.[202,203] Maria *et al*. synthesized and evaluated cationic *fac*-$^{99m}$Tc tricarbonyl complexes in aqueous medium, that are anchored by ether containing tris(pyrazolyl)methane or bis(pyrazolyl)ethanamine ligands.[68] Great results were obtained. The ether functionalities introduced do not have an effect on the coordination and no transchelation occurs. The lipophilicity, pharmacokinetics and metabolic stability of the complexes are significantly influenced/altered by the introduction of an ether group in the central carbon atom or primary amine of the tripod, or the replacement of an azolyl ring by a primary amine. Two potential tridentate ligands with a peptide nucleic acid monomer containing thymidine as nucleobase has been synthesized by Xavier *et al*.[204] It has also been reacted with *fac*-$[Re(CO)_3]^+$ and *fac*-$[^{99m}Tc(CO)_3]^+$ to produce the metal complexes in high yield. This results confirmed that it is possible to attach these 2 ligand systems to peptide nucleic acid sequences of a target mRNA.

A while back, Kinuta and co-workers focussed their study on 3-(S-carboxymethylthio)-3-(1H-imidazol-4-yl)propanoic acid, which is a natural metabolite of L-histidine.[205] The advantages of this ligand include the N,S,O donor atom system and the free carboxylic group that can act as linker/anchor for conjugation to amine containing biomolecules. In 2010, they synthesized the facially substituted *fac*-Re and Tc tricarbonyl complexes in high yield, with 3-(carboxymethylthio)-3-(1H-imidazol-4-yl) propanoic acid coordinated in a tridentate fashion and the free carboxylic acid open for potential linking.[206]

Banerjee *et al*. produced a series of conjugates with a tridentate donor group linked to a sugar moiety.[207] They synthesized the tridentate ligands by linking glucosamine and its analogues to N,N-bis(quindinoyl)amino valeric acid. It formed stable complexes with the *fac*-Rhenium and Technetium tricarbonyl moieties and in high yield.

---

[202] Paulo, A., Correia, J.D.G., Campello, M.P.C., Santos, I. *Polyhedron* **2004**, *23*, 331-369.
[203] Bigmore, H.R., Lawrence, S.C., Mountford, P., Tredget, C.S. *Dalton Trans*. **2005**, 635-651.
[204] Xavier, C., Pak, J.-K., Santos, I., Alberto, R. *J. Organomet. Chem*. **2007**, *692*, 1332-1339.
[205] Kinuta, M., Yao, K., Masuoka, N., Ohta, J., Teraoka, T., Ubuka, T. *Biochem. J*. **1991**, *275*, 617-621.
[206] Papagiannopoulou, D., Makris, G., Tsoukalas, C., Raptopoulou, C.P., Terzis, A., Pelecanou, M., Pirmettis, I., Papadopoulos, M.S. *Polyhedron* **2010**, *29*, 876-880.
[207] Banerjee, S.R., Babich, J.W., Zubieta, J. *Inorg. Chim. Acta*. **2006**, *359*, 1603-1612.

Previously, S-substituted derivatives of homocysteine or cysteine was reacted with *fac*-$[Re(CO)_3Br_3]^+$ to form stable complexes in high yield.[208] Karagiorgou *et al*. continued this type of investigation by synthesizing two new N-acetyl cysteine derivatized ligands and managed to synthesize the corresponding Re and Tc complexes as well.[209] The primary amine of the cysteine moiety was acetylated to allow the ligand to bind tridentately *via* the N (pyridine), the S (thioether) and the O (carboxylate). The conclusion was made that the N-acetyl group in cysteine can in principle be replaced by a variety of pharmacophore groups by the formation of an amide bond.

In the study by Griffiths *et al.* in 2009, where several N-substituted tris(pyridin-2-yl)methylamine ligands were reacted with $[Re(CO)_5Br]$, it was found that the substituent have an important impact on the nature and the stability of the complex formed.[210]

**Figure 2.20: N-substituted tris(pyridine-2-yl)methylamine ligands used by Griffiths *et al*.[210]**

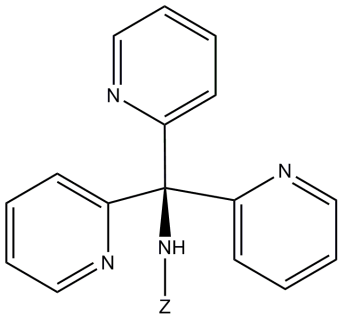


**1a** Z = H
**1b** Z = COPh
**1c** Z = COMe
**1d** Z = $CH_2Ph$

Ligands 1b and 1c (Figure 2.20) reacted with $Re(CO)_5Br$ to form the cationic complexes where the 3 pyridine rings are coordinated to the metal. The complex with 1b underwent loss of HBr to form a neutral octahedral complex where the coordination occurs *via* two of the pyridine rings and *via* the deprotonated amide nitrogen. 1a and 1d formed cationic complexes with 2 pyridine rings and the NH of the benzylamine portion of the ligand coordinated. Their work following this will be

[208] Karagiorgou, O., Patsis, G., Pelecanou, M., Raptopoulou, C.P., Terzis, A., Siatra-Papastaikoudi, T., Alberto, R., Pirmettis, I., Papadopoulos, M.S. *Inorg. Chem.* **2005**, *44*, 4118-4120.
[209] Karagiorgou, O., Papagiannopoulou, D., Kyprianidou, P., Patsis, G., Panagiotopoulou, A., Tsoukalas, C., Raptopoulou, C.P., Pelecanou, M., Pirmettis, I., Papadopoulos, M.S. *Polyhedron* **2009**, *28*, 3317-2231.
[210] Griffiths, D.V., Al-Jeboori, M.J., Arnold, P.J., Cheang, Y.-K., Duncanson, P., Motevalli, M. *Inorg. Chim. Acta*. **2010**, *363*, 1186-1194.

published at a later stage. Essentially one would like to determine how to derivatise the amine group to gain the required biodistribution.

## 2.6.6 Pendant carbohydrates and the *fac*-$[M(CO)_3]^+$ core

It is no secret that carbohydrates play an important role in the development of new radiopharmaceuticals. They have a low toxicity and high hydrophilicity and are therefore used to improve renal clearance and reduce liver accumulation. Several complexes with a peptide, incorporating a carbohydrate, have been reported and have improved its pharmacokinetic properties.[211,212] Some of the first $^{99m}$Tc complexes of carbohydrates, bound directly to the metal centre, negatively influenced the stability and other biological properties of the complex.[213] After some improvements on the ligand design, high stability complexes with pendant carbohydrates were reported.[214] Some of these complexes even showed promising biodistribution and tumor uptake in mice.[215] Very stable and robust complexes form when the *fac*-$[Re(CO)_3]^+$ moiety reacts with derivatives of dipicolylamine. These types of bifunctional chelates have also shown to be able to attach biomolecules to its core.[216,217] *fac*-$[Re(CO)_3]^+$ complexes with dipicolylamine chelators, with pending carbohydrates, have also been documented. The publication by Ferreira *et al*. in 2010,[218] focussed on the expansion of the study of dipicolylamine chelators with pendant carbohydrates. They wanted to evaluate these ligands as potential imaging agents for glucose metabolism.

## 2.6.7 $^{99m}$Tc/Re with oxime-type ligands

Several studies on thiosemicarbazane complexes of Re(I) have been done. Costa *et al*. explored the fundamental chemistry of dioxime and pyridine-2-aldoxime *fac*-

---

[211] Bapst, J.-P., Calome, M., Tanner, H., Eberle, A.N. *Bioconjug. Chem.* **2009**, *20*, 984-993.
[212] Scheinsberg, C., Maes, V., Brans, L., Blauenstein, P., Taurwe, D.A., Schubiger, P.A., Schibli, R., Garayoa, E.G. *Bioconjug. Chem*. **2008**, *19*, 2432-2439.
[213] Bayly, S.R., Fisher, C.L., Storr, T., Adam, M.J., Orvig, C. *Bioconjug. Chem*. **2004**, *15*, 923-926.
[214] Bowem, M.L., Lim, N.C., Ewart, C.B., Misri, R., Ferreira, C.L., Hafel, U., Adam, M.J., Orvig, C. *Dalton Trans*. **2009**, 9216-9227.
[215] Chen, Y., Huang, Z.W., He, L., Zheng, S.L., Li, J.L., Qin, D.L. *Appl. Radiat. Isot*. **2006**, *64*, 342-347.
[216] Banerjee, S.R., Schaffer, P., Babich, J., Valliant, J., Zubieta, J. *Dalton Trans*. **2005**, 3886-3897.
[217] Stephenson, K.A., Zubieta, J., Banerjee, S.R., Levadala, M.K., Taggart, L., Ryan, L., McFarlane, N., Boreham, D.R., Maresca, K.P., Babich, J., Valliant, *J. Bioconjug. Chem*. **2004**, *15*, 128-136.
[218] Ferreira, C.L., Marques, F.L.N., Okamoto, M.R.Y., Otake, A.H., Sugai, Y., Mikata, Y., Storr, T., Bowen, M., Yano, S., Adam, M.J., Chammas, R., Orvig, C. *Appl. Rad. Isot*. **2010**, *68*, 1087-1093.

Rhenium(I) tricarbonyl complexes for the potential use as targets for bifunctional chelating agents.[219] Once again the possibility arises where a targeting moiety can be attached *via* a monodentate ligand like isonitrile, pyridine or imidazole in the sixth position by substitution of the halide.[127]

Benzamidoxime is a bidentate ligand, thiol free and gives stable complexes with $^{99m}$Tc in high yield and at low bidentate ligand concentration.[220] This is enough to make this ligand an attractive bidentate ligand for potential molecular imaging. Thipyapang and co-workers further investigated these types of ligands by synthesizing three N-alkyl derivatives of benzamidoxime and forming the $^{99m}$Tc complexes.[221] Good results were obtained.

## 2.6.8 Research towards prostate cancer

In the US, prostate cancer is the second biggest in the total number of cancer patients.[222] The three methods available today to screen for prostate cancer involve the digital rectal exam, a prostate specific antigen and/or prostate core biopsies.[223,224] All three methods have limitations of its own.

Today, it is impossible to noninvasively image and spatially resolve cancerous cells amongst the normal cells without altering the function of the prostate, one of the major limitations to diagnostic methods. It has been found that prostate cancer cells overexpress the androgen receptor during the development of the cancer, giving an excellent way of discriminating between normal and cancerous cells.[225,226]

The first treatment for a patient diagnosed with prostate cancer will be hormone therapy which will control the size of the prostate and tumor growth. Hormone therapy involves the targeting of the androgen receptor. For several years now nonsteroidal antiandrogens like nilutamide, bicalutamide, flutamide and

---

[219] Costa, R., Barone, N., Gorczycka, C., Powers, E.F., Cupelo, W., Lopez, J., Herrick, R.S., Ziegler, C.J. *J. Organomet. Chem*. **2009**, *694*, 2163-2170.
[220] Nakayama, M., Xu, L.C., Koga, Y., Harada, K., Sugii, A., Nakayama, H., Tomiguchi, S., Kojima, A., Ohyama, Y., Takahashi, M., Okabayashi, I. *Appl. Radiat. Isot*. **1997**, *48*, 571-577.
[221] Thipyapang, K., Uehara, T., Tooyama, Y., Braband, H., Alberto, R., Arano, Y. *Inorg. Chem*. **2011**, *50*, 992-998.
[222] Jemal, A., Siegel, R., Ward, E., Murray, T., Xu, J.Q., Thun, M.J. *CA Cancer J. Clin*. **2007**, *57*, 43-66.
[223] http://www.cancer.gov/cancertopics/pdq/treatment/prostatic/patient
[224] http://www.prostate_cancer.com/
[225] De Marzo, A.M., Nelson, W.G., Isaacs, W.B., Epstein, J.I. *Lancet*. **2003**, *361*, 955-964.
[226] Culig, Z.R., Klocker, H., Bartsch, G., Steiner, H., Hobisch, A. *J. Uro*l. **2003**, *170*, 1363-1369.

hydroxyflutamide have been used.[227,228,229,230,231] The structures of these molecules are reported in Figure 2.21.

A big disadvantage of hormone therapy, is the possibility of the re-occurrence of recurrent or hormone refractory prostate cancers after 1 to 3 years. It occurs as an advanced form of metastatic cancer, being resistant to chemotherapy and is androgen-independent because of mutation of the androgen receptor.[232] The presence or absence of the androgen receptor can be useful as indicator in early screening or to indicate the progress of the disease. A few PET androgen targeting analogues have been reported but it is believed the half-life of the positron emitting isotopes, necessary for PET, and the production as well as the instrumentation needed for PET imaging may have restricted the clinical applications thereof.[233,234,235]

[227] Singh, S.M., Gauthier, S., Labrie, F. *Curr. Med. Chem*. **2000***, 7*, 211-247.
[228] Gao, W.Q., Kearbey, J.D., Nair, V.A., Chung, K.W., Parlow, A.F., Miller, D.D., Dalton, J.T. *Endocrinology* **2004**, *145*, 5420-5428.
[229] Urushibara, M., Ishioka, J., Hyochi, N., Kihara, K., Hara, S., Singh, P., Isaacs, J.T., Kageyama, Y. *Prostate* **2007**, *67*, 799-807.
[230] Yin, D.H., He, Y.L., Perera, M.A., Hang, S.S., Marhefka, C., Stourman, N., Krikovsky, L., Miller, D.D., Dalton, J.T. *Mol. Pharmacol*. **2003**, *63*, 211-223.
[231] Bohl, C.E., Chang, C., Mohler, M.L., Chen, J.Y., Miller, D.D., Swaan, P.W., Dalton, J.T. *J. Med. Chem*. **2004**, *47*, 3765-3776.
[232] Isaacs, J.T., Isaacs, W.B*. Nat. Med*. **2004**, *10*, 26-27.
[233] Parent, E.E., Dance, C.S., Jenks, C., Sharp, T.L., Welch, M.J., Katzellenbogen, J.A. *J. Med. Chem.* **2007**, *50*, 1028-1040.
[234] Payen, O., Top, S., Vessieres, A., Brule, E., Plamant, M.A., McGlinchey, M.J., Muller-Bunz, H., Jaouen, G. *J. Med. Chem*. **2008**, *51*, 1791-1799.
[235] Nair, V.A., Mustafa, S.M., Mohler, M.L., Yang, J., Kirkovsky, L.I., Dalton, J.T., Miller, D.D*. Tetrahedron Lett*. **2005**, *4*6, 4821-4823.

**Figure 2.21: Nonsteriodal antiandrogens used in hormone therapy for prostate cancer.**

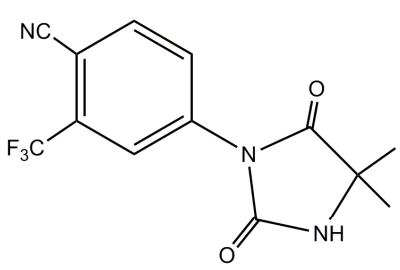


Nilutamide

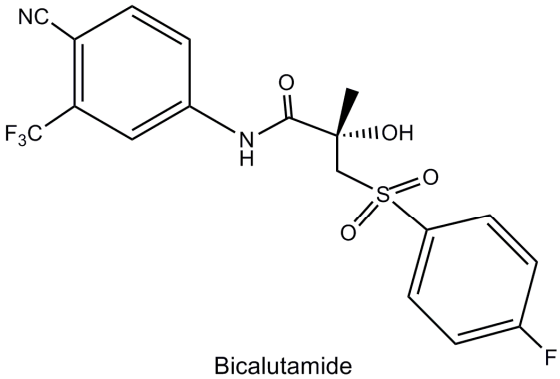


Bicalutamide

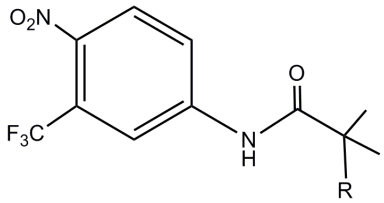


Flutamide (R = H)
Hydroxyflutamide (R = OH)

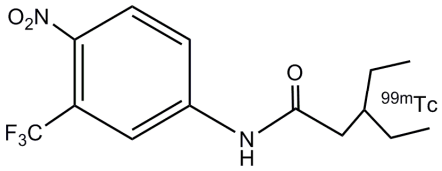


$^{99m}$Tc-Flutamide

The use of a SPECT imaging agent will be more feasible. It will provide an alternative method for hospitals that already have a SPECT camera, even if it has decreased resolution.

A few $^{99m}$Tc(V) oxo complexes with steroids have been reported for prostate imaging.[236,237] The development of *fac*-[$^{99m}$Tc(CO)$_3$(H$_2$O)$_3$]$^+$ have a few advantages over the use of the oxo core for biological targeting.[161,238,239] An Isolink kit is also available for the aqueous production of *fac*-[$^{99m}$Tc(CO)$_3$(H$_2$O)$_3$]$^+$ by Tyco.[130] Some of the advantages of the use of *fac*-[$^{99m}$Tc(CO)$_3$]$^+$ over Tc(V) (oxo) is a decrease in molecular weight, volume, polarity and ligand size. The stability of the CO ligands also increases the lipophilicity which can help with hepatic clearance rather than clearance *via* the renal tract. The structural and chemical differences of complexes

[236] Jurisson, S.S., Lydon, J.D. *Chem. Rev*. **1999**, *99*, 2205-2218.
[237] Das, T., Banerjee, S., Samuel, G., Bapat, K., Subramanian, S., Pillai, M.R.A., Venkatesh, M. *Bioorg. Med. Chem. Lett*. **2006**, *16*, 5788-5792.
[238] Aebischer, N., Schibli, R., Alberto, R., Merbach, A.E. *Angew. Chem. Int. Ed*. **2000**, *39*, 254-256.
[239] Alberto, R., Pak, J.K., van Staveren, D., Mundwiler, S., Benny, P. *Biopolymers* **2004**, *76*, 324-333.

of *fac*-[$^{99m}$Tc(CO)$_3$]$^+$ *vs* [$^{99m}$Tc=O]$^{3+}$ have large implications in the biological interactions of the complexes.

He *et al*. investigated a range of flutamide and derivatives of the *fac*-[$^{99m}$Tc(CO)$_3$(H$_2$O)$_3$]$^+$ precursor; also, alkylation methods to link a number of ligand systems to the flutamide derivatives. These flutamide-linked ligands were coordinated to both the Rhenium and analogous $^{99m}$Tc synthons to determine the stability and the effective labeling.[240] It was found that the amide bond of the flutamide is unstable due to hydrolytic cleavage. Nevertheless, they found conditions to produce the compounds in high yield. Tridentate ligand systems on *fac*-[$^{99m}$Tc(CO)$_3$(H$_2$O)$_3$]$^+$ gave higher labeling yields and a higher stability compared to the '2+1' approach where an imidazole analogue was used. The tridentate ligands showed excellent radiochemical stability at 37 ° C, at physiological pH and in mouse serum. The *in vitro* studies indicated limited uptake in the prostate cancer cells. More follow-up studies on the metabolic activations of *fac*-[$^{99m}$Tc(CO)$_3$]$^+$-linked flutamide complexes to the hydroxyflutamide analogue and *in vivo* studies are underway.

# 2.7 Mechanistic studies of *fac*-[Re(CO)$_3$(H$_2$O)$_3$]$^+$

## 2.7.1 Water substitution on *fac*-[Re(CO)$_3$(H$_2$O)$_3$]$^+$

The water exchange rate of *fac*-[Re(CO)$_3$(H$_2$O)$_3$]$^+$ calculated by Salignac *et al*.[241], revealed a relatively low rate constant of $k_{ex}$ = 6.3 x $10^{-3}$ $s^{-1}$. A variety of ligands were used to estimate the response of *fac*-[Re(CO)$_3$(H$_2$O)$_3$]$^+$ to the nucleophilicity of the entering ligand. A small increase in the rate constant from the harder trifluoroacetate anion (TFA) – 2.9 x $10^{-3}$ – to the softer thiourea (TU) – 41.5 x $10^{-3}$ – is in contrast with the wide variation typical for associative reactions.[242] The positive activation entropy $\Delta S^{\ddagger}_{ex}$ for the water exchange on *fac*-[Re(CO)$_3$(H$_2$O)$_3$]$^+$ (+14 ±10 $JK^{-1}mol^{-1}$) is indicative of a dissociative activation.

---

[240] He, H., Marely, J.E., Silva-Lopez, E., Bottenus, B., Montajano, M., Fugate, G.A., Twamley, B., Benny, P.D. *Bioconjug. Chem*. **2009**, *20*, 78-86.

[241] Salignac, B., Grundler, P.V., Cayemittes, S., Frey, U., Scopelliti, R., Merbach, A.E., Hedinger, R., Hegetschweiler, K., Alberto, R., Prinz, U., Raabe, G., Kölle, U., Hall, S. *Inorg. Chem*. **2003**, *42*, 3516-3526.

[242] Tobe, M.L., Burgess, J. *Inorganic Reaction Mechanisms*, Addision-Wesley Longman Ltd, Reading MA, **1999**.

However, it is also known that large experimental errors can be made in the extrapolation to estimate the $\Delta S^{\ddagger}$ values from the intercepts. It is therefore imperative to calculate $\Delta V^{\ddagger}$ to unambiguously determine the mechanism for the complex formation.

Grundler *et al*.[243] reported variable pressure kinetic studies on the *fac*-$[Re(CO)_3(H_2O)_3]^+$ complex with hard N-donor and soft S-donor ligands (pyrazine [Pz], tetrahydrothiophene [THT] and dimethylsulphide [DMS]) to determine the complex formation mechanism.[243]

The results obtained for these complexes' formation are consistent with the variety of ligands reported by Salignac. Table 2.1 gives a summary of the data collected by Salignac and Grundler.[241,243]

**Table 2.1: Rate and equilibrium constants for the complex formation of *fac*-$[Re(CO)_3(H_2O)_3]^+$ with various ligands (L). I = 1 M, T = 298 K.**

| L | TFA[a] | $Br^-$ [a] | $CH_3CN$[a] | Pyz[b] | THT[b] | DMS[b] | TU[a] |
|---|---|---|---|---|---|---|---|
| $10^3\ k_{f,1}\ (M^{-1}s^{-1})$ | 0.81(1) | 1.6(3) | 0.76(4) | 1.06(5) | 1.28(7) | 1.18(6) | 2.49(9) |
| $10^5\ k_{r,1}\ (s^{-1})$ | 99(2) | 230(100) | 16(2) | 0.45(4) | 3.05(9) | 14.2(8) | 1.6(2) |
| $10^3\ k_{f,2}\ (M^{-1}s^{-1})$ | | | | | | 0.76(2) | 5(2) |
| $10^5\ k_{r,2}\ (s^{-1})$ | | | | | | 1.62(5) | |
| $10^3\ k_{f,3}\ (M^{-1}s^{-1})$ | | | | | | 0.106(4) | 6(1) |
| $10^5\ k_{r,3}\ (s^{-1})$ | | | | | | 0.20(2) | |

[a] – from Reference *241*, [b] – from Reference *243*

Along the whole range of ligands, only a factor of 3 increase can be seen in the formation rate constant, $k_{f,1}$. To compare charged and uncharged ligands and the water exchange rate, $k_{ex}$, interchange rate constants, $k_i$, were calculated – $k_f$ values divided by the outer-sphere association constants, $K_{os}$, and corrected to give rate constants $k_{i,1}$.[244]

The interchange rate constant $k_{i,1}$ for the two ligands of Grundler as well as the range investigated by Salignac are reported in Table 2.2. Incoming ligands' nucleophilic reactivity is often compared in terms of basicity or the polarizability.[245] Here, the reactivity of the incoming ligand does not correlate with the basicity toward the proton because Re(I) is a soft acid and $H^+$ a hard acid, according to Pearson

[243] Grundler, P.V., Salignac, B., Cayemittes, S., Alberto, R., Merbach, A.E. *Inorg. Chem*. **2004**, *43*, 865-873.
[244] Aebischer, N., Merbach, A.E. *Inorg. React. Mech*. **1999**, *1*, 233-245.
[245] Edwards, J.O. *J. Am. Chem. Soc*. **1954**, *76*, 1540-1547.

HSAB classification. The reaction of *fac*-$[Re(CO)_3(H_2O)_3]^+$ with $Hpyz^+$ has a 26 fold lower rate constant $k_{i,1}$ ($0.68 \times 10^{-3}$ $s^{-1}$) than the neutral Pyz ligand ($17.7 \times 10^{-3}$ $s^{-1}$) because of its strongly reduced nucleophilic character (calculated with the $K_{os}$ value adequate for charged ligands). But, considering $Hpyz^+$, with an opposite charge to the nucleophilic site, one can state that it acts more like a neutral ligand, therefore it only leads to a 6 fold lower rate constant, $k_{i,1}$.

**Table 2.2: Interchange rate constants ($k_i^1$) for the water substitution by various ligands (L) on *fac*-$[Re(CO)_3(H_2O)_3]^+$. ($NaCF_3SO_3$) = 1 M, T = 298 K.**[241,243]

| L | $10^3$ $k_{f,1}^{298}$ ($M^{-1}s^{-1}$) | $10^3$ $k_{i,1}$ [a] ($s^{-1}$) |
|---|---|---|
| $H_2O$[b] | 6.3 | 6.3 |
| TFA | 0.81 | 2.9 |
| Br- | 1.6 | 5.8 |
| $CH_3CN$ | 0.76 | 12.7 |
| Pyz | 1.06 | 17.7 |
| THT | 1.28 | 21.3 |
| DMS | 1.52 | 22 |
| TU | 2.49 | 41.5 |

[a] – $k_i^1 = (k_{f,1}f)/(K_{os}n_c)$, 1/f = probability factor (= 1/12); $n_c$ = coordination number (= 3); $K_{os}$ = 1.1 $M^{-1}$ for charged ligands and $K_{os}$ = 0.24 $M^{-1}$ for neutral ligands.
[b] – $k_{ex}$ = rate constant for the exchange of a particular water molecule.

Also important to note is that NMR experiments showed that the complex, *fac*-$[Re(CO)_3(H_2O)(Pyz)]$, is insensitive to variable acidity, therefore the $pK_a$ of pyrazine is decreased when it is bound to the *fac*-Rhenium(I) tricarbonyl moiety. The pyrazine mainly acts as an σ-donor ligand and therefore causes an increase of its acidity.

Another interesting trend when looking at these results, is the big increase of 3 orders of magnitude in $k_{r,1}$, the rate constant for the reverse reaction, from Pyz to $Br^-$. This indicates the changing nucleofugal ability of all the species, which is inversely related to the basic character of each of the complexes. Bromide ($pK_a$ (HBr) = -4.7) is the fastest leaving group and Pyz ($pK_{a2}$ ($Hpyz^+$) = 0.6) is the slowest leaving group. Since the forward rate constants change to a lesser extent than the reverse rate constants, the equilibrium constants $K_1$ strongly increases form $Br^-$ to Pyz.

A plot of $k_{r,1}$ *vs* $pK_1$ gives a slope of 0.93(7). This agrees with the general principle of a linear free energy relationship. Similar correlations were observed for Co(III) and Ir(III) pentaamines.[246,247]

Since Langford stated that a slope with a value of 1 for the straight line indicates the nature of the leaving group in the transition state is almost the same as in the product (in the solvated species), Grundler *et al*. concluded to a dissociatively activated mechanism. The only problem in applying Langford's theory to this study is that the free energy relationship (slope = 1) means that the rates of formation is the same for the whole series of ligands, which is obviously not the case. Although, the free energy theory seems to be prevalent since the $k_{f,1}$ varies only by a factor of 3 from TFA to TU, but is not totally insensitive to the entering ligand. This is also supported by the 14 factor change in the intrinsic rate constants $k_i^1$. It was therefore more appropriate for the group to examine the inversed logarithmic dependence of $k_{r,1}$ *vs* $K_i$ ($K_1/K_{os}$) therefore log $k_{r,1}$ *versus* log ($K_{os}/K_1$) that gives a slope of 0.73(6). This is then much less indicative of a dissociative character.

The interchange rate constants $k_i^1$ were all found to be very close to the water exchange rate, $k_{ex}$ which revealed that the rate of the complex formation might be limited by the Re-$OH_2$ bond-breaking, through an $I_d$ mechanism. But the discrimination between nucleophiles exists ($k_i^1$) and indicates that it might be bound to the Rhenium in an $I_a$ transition state.

According to the original Langford-Gray nomenclature,[248] an $I_d$ mechanism is defined, with great influence, from the leaving group and the $I_a$ mechanism with the highest sensitivity toward the nature of the entering group. To make a sensible decision regarding mechanism type, it was necessary to confront the activation volumes that will give a better indication towards the complex formation mechanism.

The high pressure investigations with DMS, THT and Pyz done by Grundler and his group suggests an $I_d$ or $I_a$ mechanism as the sign changes from positive for Pyz ($\Delta V^{\ddagger}_{f,1}$ = +5(2) and $\Delta V^{\ddagger}_{r,1}$ = +8(1) $cm^3\ mol^{-1}$) to negative for DMS ($\Delta V^{\ddagger}_{f,1}$ = -10(2) and $\Delta V^{\ddagger}_{r,1}$ = -6(2) $cm^3\ mol^{-1}$). Hence it is safe to say that the mechanism is dual, changing to $I_a$ with better nucleophiles.

---

[246] Langford, C.H. *Inorg. Chem*. **1965**, *4*, 265-266.
[247] Lamb, A.B., Fairhall, L.T. *J. Am. Chem. Soc*. **1923**, *45*, 378-395.
[248] Langford, C.H., Gray, H.B. *Ligand Substitution Processes*, WA Benjamin Inc.: New York, **1965**.

The Eigen-Wilkins mechanism states that the observed activation volume, $\Delta V^{\ddagger}_{obs}$ consists of an intrinsic activation volume, $\Delta V^{\ddagger}_{I}$ and a solvation activation volume $\Delta V^{\ddagger}_{solv}$.

$$\Delta V^{\ddagger}_{obs} = \Delta V^{\ddagger}_{solv} + \Delta V^{\ddagger}_{I} \qquad \textbf{Equation 2.1}$$

DMS ($pK_{ow}$ = 0.8(3)) and THT ($pK_{ow}$ = 1.2(4)) are hydrophobic molecules and Pyz is hydrophilic ($pK_{ow}$ = 0.26).[249,250] It was therefore an obvious question as to how the difference in solvation will affect the $\Delta V^{\ddagger}_{solv}$ and finally $\Delta V^{\ddagger}_{obs}$ for the different ligands. But looking at the negative values for the reaction volumes $\Delta V^{0}$, it has no trend from Pyz ($\Delta V_1^{0}$ = -3(1) to THT ($\Delta V_1^{0}$ = -0.4(5)) to DMS ($\Delta V_1^{0}$ = -10(2) $cm^3\ mol^{-1}$) indicating that solvation is only a minor contribution to $\Delta V^{\ddagger}_{obs}$.

It was therefore clear that the reaction mechanisms, from the volume profiles, indicated an $I_d$ for Pyz and an $I_a$ mechanism for THT and DMS.

Lastly, they also highlighted the results of the three successive reactions with DMS and TU, forming the mono-, bis- and tris ligand complexes. As the substitution increase for the DMS reaction, the formation rates decrease. This is due to the steric hindrance on the metal centre. These results were then a further indication for an $I_a$ substitution mechanism. For TU, which is less bulky, the inverse is applicable and this might be because the metal centre is softened by the already coordinated ligand(s). This trend was also observed by Good *et al.* on $Nb^{5+}$ and $Ta^{5+}$ ions.[251]

## 2.7.2 Ligand exchange rate of *fac*-$[Re(CO)_3(H_2O)_3]^+$

In 2006, Grundler *et al*. kinetically investigated the water exchange process on *fac*-$Mn(CO)_3(H_2O)_3]^+$ and *fac*-$[Tc(CO)_3(H_2O)_3]^+$ with $^{17}O$ NMR as a function of the acidity, temperature and pressure.[252] Up to pH 6.3 and 4.4 respectively, the exchange rate in the complexes is not affected. This indicates that the mono-hydroxo species *fac*-$[M(CO)_3(H_2O)_2(OH)]^-$ is not that significant. This correlates with the higher $pK_a$ for these complexes compared to the Rhenium homologue. The water exchange rate

[249] Calculated using Advanced Chemistry Developpement (ACD) Software Solaris V4.67; ACD, 1994-2003.
[250] Hansch, C., Leo, A., Hoekman, D., Heller, S.R. Hydrophobic, Electronic and Steric constants, American Chemical Society, Washington, DC, **1995**.
[251] Good, R., Merbach, A.E. *Inorg. Chem*. **1974**, *14*, 1030-1034.
[252] Grundler, P.V., Helm, L., Alberto, R., Merbach, A.E. *Inorg. Chem*. **2006**, *45*, 10378-10390.

decreases from Mn to Re down group 7 indicating the decrease in reactivity – Mn ($k_{ex}$ = 23 $s^{-1}$) > Tc ($k_{ex}$ = 0.49 $s^{-1}$) > Re ($k_{ex}$ = 0.0054 $s^{-1}$) – indicating an $I_d$ mechanism. This is also an important trend to remember since one can now estimate an approximate time scale for a labeling process to go to completion. In the case of Rhenium, it was decided to be a $I_d/I_a$ changeover mechanism with a maximum volume for pyrazine and a minimum for DMS as entering ligands. It was speculated that the mechanism for the harder N donor ligands were affected by the fact that it is more difficult for the N donors to discriminate between water and the entering ligand than for the S donors that are better nucleophiles.

## 2.7.3 Methanol substitution kinetics in complexes of the form *fac*-[Re(L,L'-bid)(CO)$_3$(MeOH)]$^n$

There is potential to activate complexes of the form *fac*-[Re(L,L'-bid)(CO)$_3$(MeOH)]$^n$ (with L,L'-bid = bidentate ligands with a range of donor atoms and n = 0, +1) and it can therefore be considered as potential radiopharmaceuticals specifically bearing in mind the '2+1' approach mentioned before.[106]

Earlier this year[90] our group reported the effect of bidentate ligands on the reactivity of the *fac*-[Re(CO)$_3$]$^+$ core compared to the typically inert *fac*-Re(I) tricarbonyl, low-spin $d^6$ complexes. A range of complexes with a variety of bidentate ligands were chosen and the lability and the mechanism of the aqua substitution by monodentate nucleophiles were evaluated.

In this study, it was assumed that the aqua complexes exchange the $H_2O$ ligand, when dissolved in methanol, with a MeOH ligand. This was because of the rates and the concentration dependences obtained as well as the isolation and characterization of a crystal that was grown from methanol as solvent, with the aqua site occupied by methanol.[90,253]

The complexes used in the substitution kinetics were *fac*-[Re(Phen)(CO)$_3$(MeOH)]$^+$ (Phen = 1,10-phenanthroline), *fac*-[Re(Bipy)(CO)$_3$(MeOH)]$^+$ (Bipy = 2,2'-bipyridine), *fac*-[Re(2,4-dPicoH)(CO)$_3$(MeOH)] (2,4-dPicoH = 2,4-dipicolinate), *fac*-[Re(2,4-dQuinH)(CO)$_3$(MeOH)] (2,4-dQuinH = 2,4-diquinolinate), *fac*-[Re(Pico)(CO)$_3$(MeOH)] (Pico = 2-picolinate), *fac*-[Re(Quin)(CO)$_3$(MeOH)] (Quin = 2-quinolinate), *fac*-

[253] Brink, A., Visser, H.G., Roodt, A. *J. Coord. Chem*. **2011**, *64*, 122-133.

[Re(TropBr$_3$)(CO)$_3$(MeOH)] (TropBr$_3$ = tribromotropolonate) and *fac*-[Re(Flav)(CO)$_3$(MeOH)] (Flav = hydroxyflavonate). The kinetic data obtained for all 8 complexes are reported in Table 2.3 below and the structures of the ligands are reported in Figure 2.22.

**Figure 2.22: Schematic representation of the ligands used in the study by our group.**

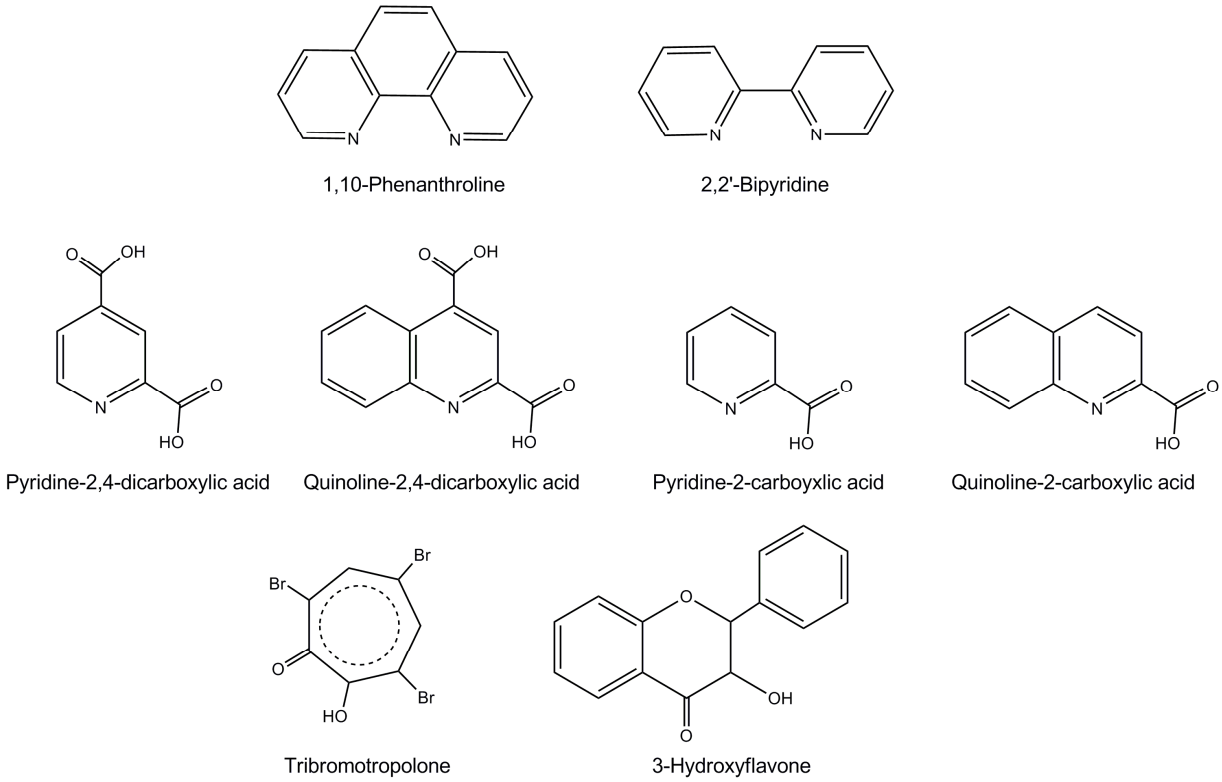


The substitution kinetics on the methanol complexes were divided into three groups. First of all, the complexes with the N,N'-bidentate ligands, *fac*-[Re(Phen)(CO)$_3$(MeOH)]$^+$ and *fac*-[Re(Bipy)(CO)$_3$(MeOH)]$^+$ yielded similar rates of formation, $k_1$, for reactions with the incoming ligands. The values for the halides as entering ligands are generally 300 to 400 times larger than the $k_1$ values for the neutral pyridine type ligands; ~4 times faster than the values for PTA (1,3,5-triaza-7-phosphadamantane) and ~2 times faster than the formation constants calculated for MeTU (1-methyl-2-thiourea) as entering ligand.

Initially the high affinity of the cationic metal complexes for the negatively charged halides points towards an associative mode of activation. The rate for the reactions with *m*Mepy (*meta*-methylpyridine) compared to pyridine is 4 to 6 times slower and could be explained by the sterical hindrance of *m*Mepy compared to pyridine that has

no steric demand. A decrease in rate for *p*Mepy is also observed although it has no sterics when compared to pyridine.

**Table 2.3: Rate constants and equilibrium constants for the reactions of the complexes with different entering ligands.**

| | ***fac*-[Re(Bipy)(CO)$_3$(MeOH)]$^+$** | | | ***fac*-[Re(Phen)(CO)$_3$(MeOH)]$^+$** | | |
|---|---|---|---|---|---|---|
| | $10^3$ $k_1$ ($M^{-1}s^{-1}$) | $10^3$ $k_{-1}$ ($s^{-1}$) | $K_1$ [b] ($M^{-1}$) | $10^3$ $k_1$ ($M^{-1}s^{-1}$) | $10^3$ $k_{-1}$ ($s^{-1}$) | $K_1$ [b] ($M^{-1}$) |
| $Cl^-$ | 17(2) | 0.16(1) | 100(11) | 36(4) | 0.41(3) | 87(11) |
| $Br^-$ | 42(7) | 0.65(2) | 60(8) | 50(3) | 0.59(3) | 84(7) |
| $I^-$ | 49(3) | 0.68(1) | 70(5) | 53(1) | 0.7(1) | 76(11) |
| Py | 0.096(1) | 0.0012(1) | 8.0(7) | 0.064(3) | 0.0058(4) | 11(1) |
| *m*-Mepy | 0.025(1) | 0.008(1) | 3.0(4) | 0.012(1) | 0.005(2) | 2.4(9) |
| *p*-Mepy | 0.028(1) | 0.0047(1) | 5.0(2) | 0.014(1) | 0.0035(1) | 4.0(3) |
| PTA | 12.3(1) | 0.12(2) | 100(20) | 7.9(1) | 0.11(1) | 70(9) |
| Metu | 17.3(1) | 0.011(1) | 157(14) | 13.7(1) | 0.11(1) | 120(11) |
| | ***fac*-[Re(2,4-dPicoH)(CO)$_3$(MeOH)]** | | | ***fac*-[Re(2,4-dQuinH)(CO)$_3$(MeOH)]** | | |
| $Br^-$ | 15.7(2) | 0.63(8) | 25(3) | -- | -- | -- |
| Py | 1.641(8) | 0.030(2) | 21(1) | 3.31(2) | 0.051(7) | 65(9) [c] |
| DIMAP | 3.21(4) | 0.11(1) | 29(3) | 6.52(9) | 0.025(3) | 260(30) [d] |
| Pz | 2.336(9) | 0.016(3) | 146(27) | -- | -- | -- |
| Im | 1.44(4) | 0.070(5) | 21(2) | -- | -- | -- |
| | ***fac*-[Re(Pico)(CO)$_3$(MeOH)]** | | | ***fac*-[Re(Quin)(CO)$_3$(MeOH)]** | | |
| $Br^-$ | 11.8(1) | 0.8(1) | 15(2) | 29.6(3) | 0.7(1) | 42(6) |
| $I^-$ | 14(1) | 0.64(1) | 22(2) | 28.0(1) | 0.9(1) | 31(4) |
| Py | 1.6(1) | 0.0084(1) | 190(10) | 3.9(1) | 0.02(1) | 195(97) |
| | ***fac*-[Re(TropBr$_3$)(CO)$_3$(MeOH)]** | | | ***fac*-[Re(Flav)(CO)$_3$(MeOH)]** | | |
| $Br^-$ | 70.6(4) | 4(1) | 18(4) | 7.2(3)x$10^3$ | 3.17(9)x$10^3$ | 2.5(2) |
| Py | 20.3(7) | 1.6(2) | 12(2) [e] | 1.38(8)x$10^3$ | 0.3(1) | 4.6(1)x$10^3$ |
| DMAP | 34.5(7) | 0.26(2) | 133(11) [f] | 5.1(2)x$10^3$ | 0.16(4) | 3.2(8)x$10^4$ |

It is clear from Table 2.3 that a large variation in $k_1$ values with the type of entering ligand was obtained. This is not the case for the substitution reactions of *fac*-[Re(CO)$_3$(H$_2$O)$_3$]$^+$ found and confirmed by high-pressure studies, where an $I_d$ type mechanism was proposed.[243] As discussed in Paragraph 2.7.1, Salignac *et al*.[241] obtained a $k_1$ value of 1.6(3) x $10^{-3}$ $M^{-1}$ $s^{-1}$ for the formation of *fac*-[Re(CO)$_3$(H$_2$O)$_2$Br]. This is 20 to 30 times slower than the corresponding reactions of the Bipy and Phen complexes with $Br^-$. This indicates that Bipy and Phen as bidentate ligands activate the metal complex to a small extent.

**Table 2.4: Activation parameters for the reactions performed by Schutte *et al*.[90]**

| | | $\Delta H^{\ddagger}_{(k1)}$ (kJ mol$^{-1}$) | $\Delta S^{\ddagger}_{(k1)}$ (J K$^{-1}$ mol$^{-1}$) | $\Delta G^{\ddagger}_{298}$ (kJ mol$^{-1}$) |
|---|---|---|---|---|
| ***fac*-[Re(Phen)(CO)$_3$(MeOH)]$^+$** | $I^-$ | 70(1) | -35(3) | 80(2) |
| | MeTU | 80(1) | -9(3) | 83(2) |
| ***fac*-[Re(2,4-dPicoH)(CO)$_3$(MeOH)]** | $Br^-$ | 80.8(6) | -8(2) | 82(1) |
| | Py | 84(2) | -19(4) | 90(3) |
| | Pz | 83(1) | -18(3) | 88(2) |
| | Im | 85.2(7) | -13(2) | 89(1) |
| | DMAP | 84.3(3) | -10(1) | 87(1) |
| ***fac*-[Re(Pico)(CO)$_3$(MeOH)]** | $I^-$ | 77(1) | -19(3) | 83(2) |
| | Py | 84(1) | -16(4) | 89(2) |
| ***fac*-[Re(TropBr$_3$)(CO)$_3$(MeOH)]** | $Br^-$ | 63(6) | -54(19) | 79(6) |
| | Py | 53(5) | -102(17) | 83(6) |
| | DMAP | 69(4) | -42(12) | 82(5) |
| ***fac*-[Re(Flav)(CO)$_3$(MeOH)]** | $Br^-$ | 52(5) | -52(15) | 67(6) |
| | Py | 54(6) | -60(21) | 72(6) |
| | DMAP | 84(4) | 51(14) | 69(5) |

When looking at the data for the *fac*-[Re(2,4-dPico)(CO)$_3$(MeOH)] complex, the reaction with $Br^-$ is 5 to 7 times faster than the reactions with the neutral ligands. The p$K_a$ values of DMAP, imidazole, pyridine and pyrazole are 9.8, 6.99, 5.25 and 2.49 respectively. The $k_1$ values decrease for $Br^-$ > DMAP > Py, Pz, Im, and is generally consistent with their nucleophilicities, shown by the p$K_a$ values of the entering ligands and points towards an associative activated mechanism. Also, the negative $\Delta S^{\ddagger}$ values for the reactions of *fac*-[Re(2,4-dPico)(CO)$_3$(MeOH)] suggests an $I_a$ type mechanism. Overall, the $k_1$ values for the reactions of *fac*-[Re(2,4-dPico)(CO)$_3$(MeOH)] is comparable to that of *fac*-[Re(2,4-dQuin)(CO)$_3$(MeOH)] as was expected. By comparing the cationic N,N'-bidentate complexes with the neutral N,O-bidentate complexes a definite increase in the forward rate constant is found for the $Br^-$ entering ligand in the N,N'-bidentate complexes. For the rest of the entering ligands, the opposite is seen with higher $k_1$ values for the N,O-bidentate complexes. This is interesting since one would expect the cationic complexes to be more reactive in associative activated reactions, but this observation then point towards an $I_d$ mechanism for the neutral complexes.

In the O,O'-bidentate complexes a huge increase is seen when moving from the reaction with $Br^-$ with *fac*-[Re(TropBr$_3$)(CO)$_3$(MeOH)] to *fac*-[Re(Flav)(CO)$_3$(MeOH)]. This was explained by the electronwithdrawing effects of the bromide atoms on the tribromotropolone ligand. The Flav ligand labilize the Re-MeOH bond to a big extent

and is reflected in the rate constants for the reactions of *fac*-[Re(Flav)$(CO)_3$(MeOH)] which is the largest for all the entering ligands used.

All in all, it was found that an increase in electron density on the Rhenium metal centre will increase the rate of the substitution reactions. No definite conclusion could be made regarding the mechanism, with the uncertainties in the $\Delta S^{\ddagger}$ values making the O,O'-bidentate complexes comparable to the N,N'- and N,O-bidentate systems. Overall it seemed that the cationic N,N'-complexes lean towards an $I_a$ mechanism while the data for the neutral N,O- and O,O'-bidentate complexes tend to suggest an $I_d$ mechanism. From the results obtained it was clear that the O,O'-bidentate complexes activate the Rhenium centre significantly more than the N,O- and N,N'-bidentate systems.

The fascinating results for the *fac*-[Re(Flav)$(CO)_3$(MeOH)] complex fuelled new interest towards biologically active ligand systems since it seem to have even better activation properties towards the metal centre. The study highlighted the fact that high pressure studies needed to be performed to try to clarify the mechanism of these reactions. Also, a wider range of complexes and entering ligands will have to be explored.

## 2.8 Conclusion

In order to label a biomolecule with *fac*-$[Re(CO)_3(H_2O)_3]^+$ or *fac*-$[^{99m}Tc(CO)_3(H_2O)_3]^+$, at least one water ligand have to be substituted. Therefore the upper limit is the water self exchange rate of the complex itself. The water exchange rate of *fac*-$[Re(CO)_3(H_2O)_3]^+$, calculated by Salignac *et al*.[254], is $k_{ex}$ = 6.3 x $10^{-3}$ $s^{-1}$. The exchange rate is a crucial factor since it makes it possible to predict the rate and the convenience of the reaction in practice. The results obtained by Salignac *et al*. also illustrated a strong pH dependence of the water exchange reactions. This suggests that the water exchange at physiological pH must be fast. This rationalizes the application of the *fac*-$[M(CO)_3(H_2O)_3]^+$ core for the labeling of biomolecules, at least from the evidence for the water self exchange.

[254] Salignac, B., Grundler, P.V., Cayemittes, S., Frey, U., Scopelliti, R., Merbach, A.E., Hedinger, R., Hegetschweiler, K., Alberto, R., Prinz, U., Raabe, G., Kölle, U., Hall, S. *Inorg. Chem*. **2003**, *42*, 3516-3526.

From the preceding paragraphs it is clear that there is significant uncertainty concerning the mechanism of the aqua substitution reactions of *fac*-Rhenium(I) tricarbonyl complexes.

Taking all of the above and the fact that *fac*-Rhenium(I) tricarbonyl complexes easily form polymers in aqueous solution and also that most labeling kits on the market is in saline (aqueous solution), it seems imperative that the aqueous substitution kinetics of these type of complexes should be studied. Most of the work reported on the *fac*-[Re(L,L'-bid)$(CO)_3$(MeOH)] type complexes stated that the complex or the product is insoluble in water, therefore the kinetics in water was not performed.

# 3 SYNTHESIS AND CHARACTERIZATION OF LIGANDS AND METAL COMPOUNDS

## 3.1 Introduction

$^{99m}$Technetium is the most widely used radionuclide in diagnostic nuclear medicine in the world today, with an estimated 85% of all 25 million diagnostic studies per year carried out with $^{99m}$Tc radiopharmaceuticals. One of the major reasons for $^{99m}$Tc that has supported the international use of it in nuclear medicine today, is the availability of this short lived isotope ($t_{1/2}$ = 6 hours), as the daughter isotope of the long lived $^{99}$Mo ($t_{1/2}$ = 66 hours), from a $^{99}$Mo/$^{99m}$Tc generator.

Rhenium is a good model for Technetium for two reasons: possessing similar chemistry as well as being non-radioactive. In addition to this, the two beta emitting isotopes, $^{186}$Re and $^{188}$Re are good potential radionuclides for therapeutic radiopharmaceuticals which might be expected to be analogous to the diagnostic $^{99m}$Tc radiopharmaceuticals. This is however not very often the case and therefore the development of $^{186/188}$Rhenium radiopharmaceuticals cannot always be predicted from the known chemistry and biological behavior of $^{99m}$Tc radiopharmaceuticals. The chemical differences are basically explained by the greater stability of the higher oxidation states of Rhenium compared to Technetium, as well as the increased inertness towards substitution of the reduced Rhenium compounds. Despite these chemical differences, the similarity between Rhenium and Technetium has been a useful guide in the development of potential radiopharmaceuticals.

Recently the drive towards developing radiopharmaceuticals with positron emitters for the use as SPECT (single photon emission computed tomography) and PET (Positron Emission Tomography) tracers increased which in turn raises the importance of the role of $^{99m}$Tc in imaging agents and the future thereof in nuclear medicine. Even with the considerable improvements in the $^{99m}$Tc labeling methods,

there has been a limited number of new products commercially developed in the last ten years.

Nowadays, the $^{99m}$Tc labeling methods is extremely efficient and sophisticated, with the high specific activities that are needed for low concentration targets easily achievable by employing the novel [$^{99m}$Tc(CO)$_3$]$^+$, $^{99m}$Tc nitrido and $^{99m}$Tc(III) cores. It is mentioned in a report by the IAEA that there is no other labeling method known that have achieved the same high level of chemical development than that of $^{99m}$Tc.[1]

A large amount of synthetic work has been undertaken on the *fac*-Rhenium(I) and Technetium(I) tricarbonyl cores although these are two of the most recent synthons to be explored. Since the aqueous synthesis of *fac*-[M(CO)$_3$(H$_2$O)$_3$]$^+$ (M = $^{99m}$Tc/Re) was developed,[2] the field gained significant interest. In Chapter 2, paragraphs on the history as well as novel reported work are presented (Paragraph 2.1, 2.4 and 2.6).

A literature search for promising ligand systems, for this study, to coordinate to the *fac*-[M(CO)$_3$]$^+$ core (M = $^{99m}$Tc/Re) revealed that N,O-bidentate ligands are not that much explored and the number of O,O'-bidentate ligands utilized are almost nonexistent. Indicated in Chapter 1, the aim of this study therefore was to explore the ability of the *fac*-[M(CO)$_3$]$^+$ core to interact and coordinate to N,N'-, N,O- and O,O'-bidentate systems, as well as O,N,O- and N,N,N-tridentate ligands. Also, the possibility to 'link' an organic molecule to a ligand system coordinated to the metal centre was explored.

## 3.2 Chemicals and apparatus used

Unless otherwise stated, all the reagents used in the preparation and characterization were of analytical grade and were purchased from Sigma-Aldrich or Merck, South Africa. All the reagents were used as is, without any further purification. All organic solvents were dried and distilled before it was used. Rhenium pentacarbonyl bromide was purchased from Strem Chemicals, Newburyport, USA. Some of the *fac*-[NEt$_4$]$_2$[Re(CO)$_3$Br$_3$] used in the synthesis of the Rhenium compounds was donated by Prof. R. Alberto, Zurich, Switzerland. If the pH of a reaction mixture was adjusted, it was done with HNO$_3$ or NaOH solutions. The

[1] IAEA Radioisotopes and Radiopharmaceuticals Series No.1, Vienna, 2009.
[2] Alberto, R., Schibli, R., Waibel, R., Abram, U., Schubiger, A.P. *Coord. Chem. Rev*. **1999**, *190-192*, 901-919.

experiments were performed aerobically, unless otherwise stated, using double distilled water and dry solvents.

The following bidentate ligands were used in this study:

- Tropolone (TropH), isatin (IsaH), 5-nitroisatin ($NO_2$IsaH), 5-(trifluoromethoxy)-isatin ($F_3$COIsaH), benzohydroxamic acid (BHAH), 3-hydroxyflavone (FlavH) and chrysin (ChrysH) as O,O'-donor bidentate ligands,
- 2,5-pyridinedicarboxylic acid (2,5-Pico$H_2$), 8-hydroxyquinoline (oxH), 5-chloro-8-hydroxyquinoline (Cl-oxH), 5,7-dimethyl-8-hydoxyquinoline (DMe-oxH) as N,O-donor bidentate ligands,
- 2,2'-bipyridine-3,3'-dicarboxylic acid (BipyDC) as N,N'-donor bidentate ligand and
- bis(diphenylphosphino)-propylamine (PNP) as P,P'-donor bidentate ligand.

The tridentate ligand systems used in this study was:

- N,N'-Bis(2-pyridylmethyl)-2-aminoethanol (PMAEth), N,N'-Bis(2-pyridyl-methyl)-2-aminopropanol (PMAProp), N,N'-Bis(2-pyridylmethyl)-2-amino-butanol (PMABut) and nitrilotriacetic acid (NTA$H_2$).

Nine novel free ligands were synthesized. That include:

- *N*-Benzylindole-2,3-dione (BenzIsa),
- N,N'-Bis(2-pyridylmethyl)-2-aminoethanol (PMAEth),
- N,N'-Bis(2-pyridylmethyl)-2-aminopropanol (PMAProp),
- N,N'-Bis(2-pyridylmethyl)-2-aminobutanol (PMABut),
- N'-(2-(1H-imidazol-4-yl)ethyl)-$N^3$,$N^3$-bis(pyridine-2-ylmethyl)propane-1,3-diamine (PMAProp-His),
- 2-(3-(Bis(pyridin-2-yl)methyl)amino)propylamino)acetic acid (PMAProp-Gly),
- *N*-(2-(1H-imidazol-4-yl)ethyl)pyrrolidine-2-carboxamide (His-Prol),
- N'-(2-(1H-imidazol-4-yl)ethyl)benzohydrazide (His-BHA) and
- N-(Pyridin-2-ylmethyl)nicotinamide (AMP-NA).

A schematic representation of the bidentate and tridentate ligand systems used in this study are reported in Scheme 3.1.

**Scheme 3.1: Schematic representation of the bidentate and tridentate ligand systems used.**

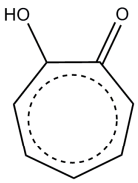


Tropolone

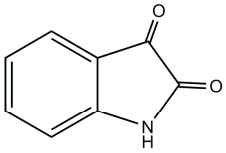


Isatin

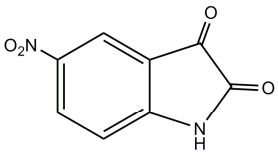


5-Nitroisatin

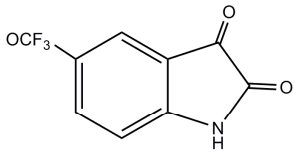


5-(Trifluoromethoxy)isatin

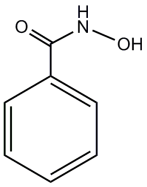


Benzohydroxamic acid

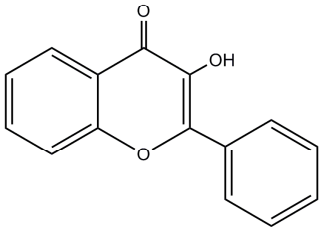


3-Hydroxyflavone

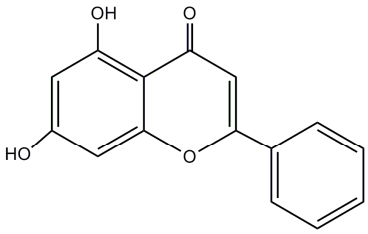


Chrysin

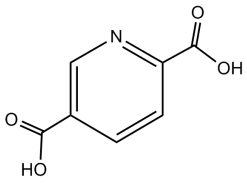


2,5-Pyridinedicarboxylic acid

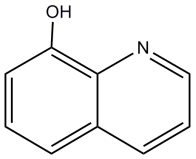


8-Hydroxyquinoline

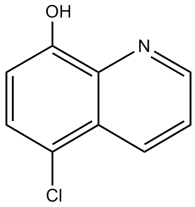


5-Chloro-8-hydroxyquinoline

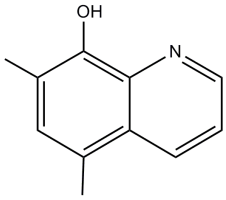


5,7-Dimethyl-8-hydroxyquinoline

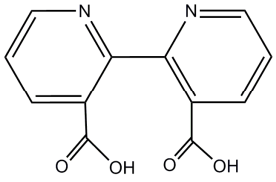


2,2'-Bipyridine-3,3'-dicarboxylic acid

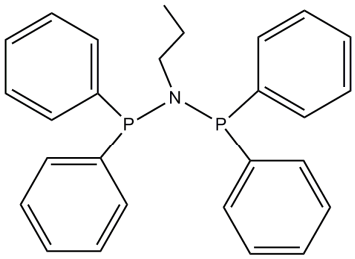


bis(diphenylphosphino)-propylamine

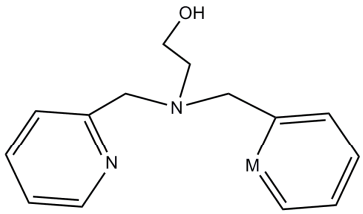


N,N'-Bis(2-Pyridylmethyl)-2-aminoethanol

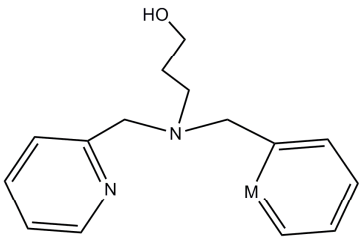


N,N'-Bis(2-pyridylmethyl)-2-aminopropanol

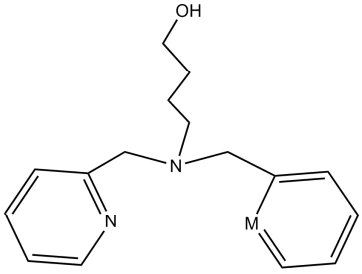


N,N'-Bis(2-pyridylmethyl)-2-aminobutanol

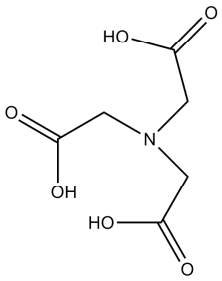


Nitrilotriacetic acid

The ligand benzylisatin (BenzIsa) was synthesized for two reasons. Firstly to prove the concept that the nitrogen atom in isatin and isatin derivatives, can be functionalized and that the possibility to link a biomolecule at that position is feasible. Secondly, to prove that isatin undergoes keto-enol tautomerism by the movement of the hydrogen atom from the nitrogen to the ketone, to be able to coordinate in a bidentate formation to the Re(I) metal core. With the position on the nitrogen 'blocked' by a benzyl functionality, coordination to Rhenium(I) tricarbonyl was proven to be impossible. This is also confirmed in the synthesis of all the Re(I) compounds with Isa, $(NO_2)$Isa and $(F_3CO)$Isa, where NaOH is repeatedly added to get and maintain the pH at 6.5, in order for the ligand to coordinate.

The infrared spectra of the complexes and organic molecules were recorded at room temperature, on a Bruker Tensor 27 Standard System or a Perkin Elmer BX II IR spectrometer with a laser range of 4000 – 370 $cm^{-1}$ that is coupled to a computer. The IR spectrometers were equipped with a temperature cell regulator, accurate within 0.3 °C. Solid samples were analyzed as KBr pellets. The UV/Vis spectra were collected on a Varian Cary 50 Conc UV-Visible Spectrophotometer. The spectrometer is equipped with a Julabo F12-mV temperature cell regulator, accurate within 0.1 °C, in 1.000 ± 0.001 cm quartz cuvette cells.

The HPLC analysis was performed on a Merck-Hitachi L-700 apparatus with a Macherey-Nagel C-18ec reversed-phase column with 5 µm particle size, 100 Å pore size and 250 x 3 mm. The solvents used were a 0.1% trifluoroacetic acid solution in water (solvent A) and HPLC-grade methanol (solvent B). The mobile phase used was a variable TFA (trifluoroacetic acid) gradient: 0 - 3 min, 100% A; 3 - 3.1 min, 0 - 25% B; 3.1 - 9 min, 75% A, 25% B; 9 - 9.1 min, 25 - 34% B, 75 - 66% A; 9.1 - 20 min, 34 - 100% B; 20 - 25 min, 100% B; 25 - 25.1 min, 100% B to 100% A; 25.1 - 30min, 100% A. The flow rate was 0.5 ml/min at 250 nm. Unless otherwise stated, the TFA gradient was used.

The $^{1}H$ and $^{13}C$ NMR spectra were recorded on Bruker 300 MHz, Bruker 600 MHz and a Bruker Advance 400 MHz nuclear magnetic resonance spectrometers (s = singulet, d = doublet, m = multiplet, t = triplet, dd = doublet of doublets, td = triplet of doublets, dt = doublet of triplets). Different deuterated solvents were used and are indicated in each case. Chemical shifts δ in ppm are relative to tetramethylsilane (TMS) and coupling constants *J* are reported in Hz, using the $CD_3OD$ (3.31 ppm,

49.05 ppm), $CD_3COCD_3$ (2.05 ppm, 30.83 ppm), $CD_3SOCD_3$ (2.50 ppm, 39.43 ppm), $D_2O$ (4.80 ppm) and $CDCl_3$ (7.26 ppm, 77.0 ppm) peak for $^{1}H$ and $^{13}C$ respectively.
The electrospray ionisation mass spectra (ESI-MS), were recorded on a Merck Hitachi M-8000 spectrometer, obtained during a visit to the University of Zurich.
It was assumed that the methanol complexes, *fac*-[Re(L,L'-bid)$(CO)_3$(MeOH)], are formed immediately after the aqua complexes, *fac*-[Re(L,L'-bid)$(CO)_3(H_2O)$] are dissolved in methanol.[5]

## 3.3 Handling of radioactive isotopes

To be able to use Rhenium and Technetium in diagnostic and therapeutic nuclear medicine, respectively, the availability of the unstable, radioactive forms of certain metals are necessary. Therefore, certain safety precautions are imperative when handling it in research of its basic chemistry.
The two natural occurring isotopes of Rhenium is $^{185}Re$ (37.4%), which is stable, and $^{187}Re$ (62.6%) which is unstable with a very long half-life of $4.12 \times 10^{10}$ years and $\beta^-$ decay energy of 2.6 keV. It can therefore be handled without any safety precautions and are used in many laboratories for basic 'cold' chemistry.
Technetium on the other hand, does not occur in nature in any stable form. Normal radiation safety procedures have to be complied with when working with this metal. $^{99m}Tc$ emits γ-rays of low energy, 0.143 MeV and specific activity of $5.3 \times 10^7$ Ci/g ($1.95 \times 10^{17}$ Bq/g), with a physical half-life of 6 hours. All the $^{99m}Tc$ chemicals were stored behind a 0.6 cm thick lead-tower shield; it was handled with tools and was never directly in contact with the body. The labeling with $^{99m}Tc$ in this study was performed in a certified radiation laboratory at the Inorganic Institute of Chemistry in Zurich. The radioactive samples were handled when wearing protective clothing, gloves and safety glasses at all times. The radioactive waste was disposed of in special, equipped containers.

# 3.4 Synthesis of organic ligands

## 3.4.1 *N*-Benzylindole-2,3-dione (BenzIsa)

The preparation was performed under strict Schlenk conditions. Isatin (0.2 g, 1.36 mmol) was dissolved in dry dimethylformamide (3 ml). Powdered calcium hydride (0.191g, 4.54 mmol) was added to the mixture and stirred at 45 °C for 30 minutes. Benzylchloride (0.258 ml, 2.04 mmol) was added to the mixture and stirred at room temperature for 16 hours. The reaction mixture was dried, dissolved in ethylacetate and washed three times with water. The combined ethylacetate layers were dried with $Na_2SO_4$. The product was purified with column chromatography with DCM:Hex 1:1 as eluent and monitored with TLC. The resulting orange product was dried under vacuum. Orange crystals were grown from a methanol solution of the product.

Yield: 0.218 g, 68%. IR (KBr, $cm^{-1}$): 1614 (s), 1732 (s). $^1$H NMR ($CDCl_3$): δ = 4.91 (s, 2H), 6.76 (d, 1H, *J* = 3.6 Hz), 7.07 (t, 1H, *J* = 7.2 Hz), 7.32 (m, 5H), 7.46 (dt, 1H, *J* = 1.2, 7.2 Hz), 7.59 (d, 1H, *J* = 7.2 Hz). $^{13}$C NMR ($CDCl_3$): δ = 44.3, 111.2, 117.9, 124.1, 125.6, 127.6, 128.4, 129.3, 134.7, 138.5, 150.9, 158.5, 183.4.

## 3.4.2 N,N'-Bis(2-pyridylmethyl)-2-aminoethanol (PMAEth)

This ligand was prepared as described by Botha *et al*.[3] 2-(Chloromethyl)pyridine hydrochloride (1 g, 6.1 mmol), sodium hydroxide (0.244 g, 6.1 mmol) and 2-amino-ethanol (0.186 g, 3.05 mmol) was dissolved in 5 ml water and stirred for 48 hours at room temperature. A 1 ml aqueous solution of sodium hydroxide (0.244 g, 6.1 mmol) was added to the reaction mixture and stirred for another 48 hours at room temperature. The reaction mixture was extracted with chloroform (3 x 20 ml). The organic layer was washed with water (50 ml), combined and dried with sodium sulphate. The chloroform was evaporated from the resulting product and yielded an orange oil.

Yield: 0.639 g, 86%. $^1$H NMR ($CD_3OD$): δ = 2.73 (t, 2H, *J* = 6 Hz), 3.66 (t, 2H, *J* = 6 Hz), 3.83 (s, 4H), 7.25 (t, 2H, *J* = 6.4 Hz), 7.59 (d, 2H, *J* = 7.6 Hz), 7.76 (dt, 2H,

[3] Botha, J.M., Umakoshi, K., Sasaki, Y., Lamprecht, G.J. *Inorg. Chem*. **1998**, *37*, 1609-1615.

*J* = 1.6 Hz, 7.6 Hz), 8.43 (d, 2H, *J* = 4.8 Hz). $^{13}$C NMR ($CD_3OD$): δ = 58.1, 60.6, 61.3, 123.8, 125.1, 138.7, 149.5, 160.6.

### 3.4.3 N,N'-Bis(2-pyridylmethyl)-2-aminopropanol (PMAProp)

2-(Chloromethyl)pyridine hydrochloride (1 g, 6.1 mmol), sodium hydroxide (0.244 g, 6.1 mmol) and 3-aminopropanol (0.228 g, 3.05 mmol) was added to 10 ml of water and stirred for 48 hours at room temperature. A solution of sodium hydroxide (0.224 g, 6.1 mmol) in 1 ml water was added to the reaction mixture and stirred for 48 hours at room temperature. The reaction mixture was extracted with chloroform (3 x 20 ml). The combined chloroform layers was washed with water (50 ml). The organic layer was dried with sodium sulphate and chloroform was evaporated to yield a dark orange oil.

Yield: 0.725 g, 91%. $^{1}$H NMR ($CDCl_3$): δ = 1.870 (t, 2H, *J* = 5.4 Hz), 2.93 (t, 2H, *J* = 6 Hz), 3.74 (t, 2H, *J* = 5.4 Hz), 4.00 (s, 4H), 7.20 (dt, 2H, *J* = 1.2 Hz, 6 Hz), 7.49 (d, 2H, *J* = 7.8 Hz), 7.67 (dt, 2H, *J* = 1.8 Hz, 7.5 Hz), 8.56 (dd, 2H, *J* = 1.2 Hz, 4.8 Hz). $^{13}$C NMR ($CD_3OD$): δ = 29.6, 53.8, 60.1, 61.2, 124.4, 125.0, 138.9, 149.9, 157.3.

### 3.4.4 N,N'-Bis(2-pyridylmethyl)-2-aminobutanol (PMABut)

To 10 ml of water, 2-(chloromethyl)pyridine hydrochloride (1 g, 6.1 mmol), sodium hydroxide (0.244 g, 6.1 mmol) and 4-aminobutanol (0.27 g, 3.05 mmol) was added. The mixture was stirred at room temperature for 48 hours. A 1 ml solution of sodium hydroxide (0.224 g, 6.1 mmol) was added to the mixture and stirred for a further 48 hours at room temperature. The mixture was extracted with chloroform (3 x 20 ml) and the combined organic layers were washed with water (50 ml). Sodium sulphate was used to dry the organic layer and the chloroform was then evaporated to yield an orange oil.

Yield: 0.681 g, 82%. $^{1}$H NMR ($CDCl_3$): δ = 1.60 (t, 2H, *J* = 6 Hz), 1.74 (t, 2H, *J* = 6.6 Hz), 2.65 (t, 2H, *J* = 6.6 Hz), 3.61 (t, 2H, *J* = 6 Hz), 3.87 (s, 4H), 7.16 (dt, 2H, *J* = 1.2 Hz, 6 Hz), 7.49 (d, 2H, *J* = 7.8 Hz), 7.67 (dt, 2H, *J* = 1.8 Hz, 7.8 Hz), 8.55 (td, 2H, *J* = 0.9 Hz, 4.8 Hz). $^{13}$C NMR ($CD_3OD$): δ = 23.9, 24.1, 55.2, 61.80, 62.9, 120.1, 124.6, 140.9, 149.2, 158.0.

## 3.4.5 N'-(2-(1H-imidazol-4-yl)ethyl)-$N^3$,$N^3$-bis(pyridine-2-ylmethyl)propane-1,3-diamine (PMAProp-His)

N,N'-Bis(2-pyridylmethyl)-2-aminopropanol (0.051 g, 0.198 mmol) was dissolved in 15 ml water (pH 7). Histamine (0.022 g, 0.198 mmol) and two drops sulphuric acid was added to the solution and stirred for 24 hours at 60 °C. The reaction mixture was dried *in vacuo* and purified by column chromatography with MeOH:EtOAc 9:1 as eluent and monitored with TLC. The resulting brown product was dried under vacuum.

Yield: 0.057 g, 82%. $^1$H NMR ($D_2O$): δ = 1.70 (t, 2H, *J* = 7.2 Hz), 2.73 (t, 2H, *J* = 7.2 Hz), 3.11 (t, 2H, *J* = 7.2 Hz), 3.29 (t, 2H, *J* = 7.2 Hz), 3.50 (t, 2H, *J* = 6 Hz), 4.27 (s, 4H), 7.33 (s, 1H), 7.89 (t, 2H, *J* = 6.6 Hz), 7.97 (d, 2H, *J* = 8.1 Hz), 8.44 (t, 2H, *J* = 7.8 Hz), 8.61 (s, 1H), 8.71 (d, 2H, *J* = 5.4 Hz). $^{13}$C NMR ($D_2O$): δ = 27.0, 29.8, 48.1, 48.9, 54.2, 64.8, 117.1, 120.9, 124.8, 133.0, 136.9, 139.4, 148.6, 158.0.

## 3.4.6 2-(3-(Bis(pyridin-2-yl)methyl)amino)propylamino)acetic acid (PMAProp-Gly)

N,N'-Bis(2-pyridylmethyl)-2-aminopropanol (0.051 g, 0.198 mmol) was dissolved in 15 ml water (pH 7). Glycine ( 0.0149 g, 0.198 mmol) and two drops of sulphuric acid was added to the solution and stirred at 60 °C for 1 day. It was dried *in vacuo* and purified by means of column chromatography. The mobile phase used was MeOH:EtOAc 9:1 and it was monitored with TLC. The brown product was dried under vacuum.

Yield: 0.054 g, 86 %. $^1$H NMR ($D_2O$): δ = 1.78 (t, 2H, *J* = 6 Hz), 2.79 (t, 2H, *J* = 6.6 Hz), 3.59 (t, 2H, *J* = 6 Hz), 3.90 (s, 2H), 4.35 (s, 4H), 8.00 (t, 2H, *J* = 6.3 Hz), 8.08 (d, 2H, *J* = 8.1 Hz), 8.56 (t, 2H, *J* = 7.8 Hz), 8.81 (d, 2H, *J* = 5.4 Hz). $^{13}$C NMR ($D_2O$): δ = 27.4, 46.8, 53.4, 53.6, 63.9, 121.0, 124.8, 140.0, 148.5, 157.4, 181.0.

## 3.4.7 *N*-(2-(1H-imidazol-4-yl)ethyl)pyrrolidine-2-carboxamide (His-Prol)

Proline (0.2 g, 1.7 mmol) was dissolved in 20 ml water (pH 7). Histamine (0.19 g, 1.7 mmol) was added to the solution. Three drops sulphuric acid was added to the

mixture and stirred for 48 hours at 80 °C. Afterwards, the reaction mixture was cooled to room temperature and dried *in vacuo* and yielded the orange oily product.
Yield: 0.28 g, 79%. IR (KBr, $cm^{-1}$): 618, 777, 839, 970, 1124, 1409, 1624. $^{1}H$ NMR ($D_2O$): δ = 2.03 (m, 2H), 2.37 (m, 2H), 3.15 (t, 2H, *J* = 7.2 Hz), 3.37 (t, 2H, *J* = 6.6 Hz), 3.46 (m, 2H), 4.16 (t, 1H, *J* = 7.2 Hz), 7.33 (s, 1H), 8.42 (s, 1H). $^{13}C$ NMR ($D_2O$): δ = 22.4, 23.5, 28.8, 38.1, 45.8, 60.9, 116.6, 129.3, 134.2, 174.5.

## 3.4.8 N'-(2-(1H-imidazol-4-yl)ethyl)benzohydrazide (His-BHA)

Benzohydroxamic acid (0.2 g, 1.46 mmol) was dissolved in 20 ml water (pH 7). Histamine (0.16 g, 1.46 mmol) and three drops sulphuric acid was added and the reaction mixture was stirred for 2 days at 80 °C. The mixture was cooled down and dried *in vacuo* to yield the product as an orange oil.
Yield: 0.322 g, 96%. IR (KBr, $cm^{-1}$): 617, 691, 798, 972, 1124, 1465, 1564, 1625, 3022, 3297, 3535. $^{1}H$ NMR ($D_2O$): δ = 3.19 (t, 2H, *J* = 7.2 Hz), 3.38 (t, 2H, *J* = 7.2 Hz), 7.41 (s, 1H), 7.56 (t, 2H, *J* = 7.5 Hz), 7.66 (d, 1H, *J* = 7.2 Hz), 7.74 (d, 2H, *J* = 7.8 Hz), 8.64 (s, 1H). $^{13}C$ NMR ($D_2O$): δ = 22.6, 54.7, 115.0, 126.9, 128.8, 131.0, 132.3, 134.4, 174.9.

## 3.4.9 N-(Pyridin-2-ylmethyl)nicotinamide (AMP-NA)

2-Aminomethyl pyridine (0.1 g, 0.925 mmol) was dissolved in 20 ml water (pH 7). Nicotinic acid (0.114 g, 0.925 mmol) and three drops sulphuric acid was added to the solution and stirred for 2 days at 80 °C. It was cooled down, filtered and dried *in vacuo* to yield the light pink product.
Yield: 0.118 g, 95%. IR (KBr, $cm^{-1}$): 619, 768, 1125, 1301, 1387, 1626, 3451. $^{1}H$ NMR ($D_2O$): δ = 4.47 (s, 2H), 7.70 (m, 2H), 8.16 (m, 2H), 8.69 (d, 1H, *J* = 4.8 Hz), 8.90 (d, 1H, *J* = 5.7 Hz), 8.98 (d, 1H, *J* = 8.1 Hz), 9.19 (s, 1H). $^{13}C$ NMR ($D_2O$): δ = 49.9, 120.4, 124.8, 125.2, 130.2, 135.0, 139.1, 148.1, 148.6, 152.0, 156.2, 169.1.

## 3.4.10 Unsuccessful attempts to functionalize 2,2-bipyridine-3,3'-dicarboxylic acid

Various attempts to functionalize both the carboxylic acid groups on the bipyridine backbone of 2,2'-bipyridine-3,3'-dicarboxylic acid (BipyDC) was unsuccessful. The

reason for the attempts were born from the crystal structure obtained, μ-(*fac*-[Re(BipyDC)$(CO)_3$])$_2$.4$H_2O$ (Paragraph 4.11). The idea was to block the two possible linking sites, at the two carboxylic substituents on the backbone, in order to prevent linking between Rhenium units *via* the sixth position, initially occupied by $H_2O$ or Br. Acetylation in pyridine with acetic anhydride and stirring for six days at high temperatures was unsuccessful. Methylation was attempted with methyliodide and potassium carbonate. After stirring the mixture in methanol for five days at 80 °C, only one carboxylic acid was methylated. The same procedure was attempted but only in THF, but that was unsuccessful as well. Acid catalyzed methylation was tried next. The procedure was performed in methanol with $H_2SO_4$ but once again only one carboxylic acid was methylated. The obvious next step was to first reduce the carboxylic acid to an alcohol, by means of $NaBH_4$ and $I_2$ in THF and after that adding $CH_3I$ and $K_2CO_3$. Once again only one carboxylic acid was methylated. The last attempt was sulphonation, using two different methods. It was tried with tosylchloride in pyridine as well as with triflic anhydride in DCM with pyridine. Both methods were unsuccessful. In these two cases, not even one of the groups was functionalized.

# 3.5 Synthesis of Rhenium compounds

The synthesis of the starting synthon, *fac*-[$NEt_4$]$_2$[Re$(CO)_3Br_3$], referred to from now onwards as ReAA, was performed under strict Schlenk conditions, for optimal yields.

## 3.5.1 Synthesis of [Re$(CO)_5$(Br)]

The preparation of ReAA is a two step synthesis by firstly preparing the pentacarbonyl and then the tricarbonyl Rhenium compound.

$[Re_2(CO)_{10}] + Br_2 \longrightarrow 2[Re(CO)_5(Br)]$

$Re_2(CO)_{10}$ (5 g, 7.65 mmol) was dissolved in 125 ml of distilled dichloromethane and cooled in an ice bath. $Br_2$ (0.432 ml, 8.425 mmol), in 25 ml cooled distilled dichloromethane was slowly added to the Rhenium solution while stirring on an ice bath. The product precipitates out of the dichloromethane solution as a white solid. After filtering the reaction mixture, the precipitate was washed with cold dichloromethane and dried under vacuum. The volume of the filtrate was reduced on a rotary evaporator and left in a freezer overnight. The rest of the product was

retrieved from the filtrate, washed with dichloromethane, dried and weighed. Yield: 5.5 g, 89%. IR (KBr, $cm^{-1}$): $\nu_{CO}$ = 1963, 2034, 2059.

## 3.5.2 Synthesis of $[NEt_4]_2[Re(CO)_3(Br)_3]$ (ReAA)

$[Re(CO)_5(Br)] + 2(NEt_4)Br \longrightarrow [NEt_4]_2[Re(CO)_3(Br)_3] + 2CO$

The $(NEt_4)Br$ (5.25 g, 0.025 mol) was grounded to a powder and dried. 2,5,8-Trioxanone diglyme (150 ml) was added to the $(NEt_4)Br$ under dry nitrogen and slurried on an oil bath at 180 °C for 30 minutes. During this time, the system was evacuated and purged with $N_2$ several times. The solid $Re(CO)_5Br$ (5 g, 0.0123 mol) was added to the mixture and stirred for 15 hours at 115 °C. The whole system needs good stirring and ventilation because of the continuous evolution of CO gas. The reaction mixture was cooled to room temperature, filtered and dried. The colourless solid was stirred in a small amount of cold ethanol for 5 minutes, filtered, washed with cold DCM and dried.

Yield: 8.646 g, 91%. IR (KBr, $cm^{-1}$): $\nu_{CO}$ = 1864, 1998. EA: calculated: C: 29.62%, H: 5.23%, N: 3.64%; found: C: 29.59%, H: 5.19%, N: 3.65%. HPLC: $R_t$ = 4.18 min. MS (ESI): m/z $[M]^+$ 393.24 (m/z calculated for *fac*-$[Re(CO)_3(NCMe)_3]^+$ = 393.85).

## 3.5.3 *fac*-$[NEt_4][Re(Trop)(CO)_3(Br)]$

Synthesized according to Schutte *et al*.[4]

## 3.5.4 *fac*-$[NEt_4][Re(Trop)(CO)_3(H_2O)].NO_3.H_2O$

ReAA (0.1 g, 0.130 mmol) was dissolved in $H_2O$ at pH 2.2 (adjusted with $HNO_3$). Silver nitrate (0.066 g, 0.389 mmol) was added to the solution and stirred for 24 hours at room temperature. After the AgBr was filtered off, tropolone (0.016 g, 0.131 mmol) was added to the solution and stirred under $N_2$ for 48 hours. The reaction mixture was filtered and the filtrate (pH = 2.5) was dried *in vacuo*. The product was found to be soluble in water when diluted. The crystal structure of *fac*-$[NEt_4][Re(Trop)(CO)_3(H_2O)].NO_3.H_2O$ is reported in Paragraph 4.4.

Yield: 0.0737 g, 92%. IR (KBr, $cm^{-1}$): $\nu_{CO}$ = 1879, 2006. $^1H$ NMR ($CD_3COCD_3$): **δ =** 2.05 (s, 12H), 2.85 (s, 8H), 7.23 (q, 1H, *J* = 10 Hz, 21.2 Hz), 7.40 (dd, 2H,

[4] Schutte, M., Visser, H.G., Roodt, A. *Acta Cryst*. **2010**, *E66*, m859-m860.

*J* = 4.8 Hz, 11.2 Hz), 7.62 (t, 2H, *J* = 10 Hz). $^{13}$C NMR ($CD_3COCD_3$): δ = 11.5, 52.1, 127.5, 128.0, 128.5, 139.0, 139.2, 185.3. HPLC: 18.79 min.

## 3.5.5 *fac*-[$NEt_4$][Re(Trop)$(CO)_3$(I)]

Sodium iodide (1 ml of a 1.95 x $10^{-3}$ M methanol solution) and *fac*-[Re(Trop)$(CO)_3(H_2O)$] (10 ml of a 1.95 x $10^{-4}$ M methanol solution) were stirred for 1 hour at room temperature. The reaction mixture was dried *in vacuo* to yield the yellow product.

Yield: 0.0011 g, 89 %. IR (KBr, $cm^{-1}$): $\nu_{CO}$ = 1885, 2015. $^1$H NMR ($CD_3COCD_3$): δ = 1.29 (s, 12H), 2.82 (s, 8H), 6.90 (t, 1H, *J* = 9.6 Hz), 7.04 (d, 2H, *J* = 10.8 Hz), 7.32 (t, 2H, *J* = 10.8 Hz). $^{13}$C NMR ($CD_3COCD_3$): δ = 10.8, 51.7, 125.7, 127.4, 138.3, 187.2.

## 3.5.6 *fac*-[Re(Trop)$(CO)_3$(Py)]

Pyridine (1 ml of a 1.95 x $10^{-3}$ M methanol solution) and *fac*-[Re(Trop)$(CO)_3(H_2O)$] (10 ml of a 1.95 x $10^{-4}$ M methanol solution) were stirred for 1 hour at room temperature. The reaction mixture was dried *in vacuo* to yield the yellow product. The crystals reported in Paragraph 4.5 were grown from a methanol solution of the product.

Yield: 0.0009 g, 98 %. IR (KBr, $cm^{-1}$): $\nu_{CO}$ = 1889, 2011. $^1$H NMR ($CD_3COCD_3$): δ = 7.11 (t, 1H, *J* = 9.6 Hz), 7.33 (d, 2H, *J* = 10.8 Hz), 7.51 (d, 2H, *J* = 10.8 Hz), 7.56 (q, 2H, *J* = 5.4 Hz), 8.00 (tt, 1H, *J* = 1.8 Hz, 7.8 Hz), 8.58 (dd, 2H, *J* = 1.8 Hz, 6.6 Hz). $^{13}$C NMR ($CD_3COCD_3$): δ = 120.9, 122.6, 124.1, 128.3, 135.9, 136.1, 137.9, 149.1, 172.6.

## 3.5.7 *fac*-[Re(Trop)$(CO)_3$(Im)]

Imidazole (1 ml of a 1.95 x $10^{-3}$ M methanol solution) and *fac*-[Re(Trop)$(CO)_3(H_2O)$] (10 ml of a 1.95 x $10^{-4}$ M methanol solution) were stirred at room temperature for 1 hour. The yellow product was dried *in vacuo*.

Yield: 0.00087 g, 97 %. IR (KBr, $cm^{-1}$): $\nu_{CO}$ = 1877, 2014. $^1$H NMR ($CD_3COCD_3$): δ = 7.02 (s, 1H), 7.11 (t, 1H, *J* = 9.6 Hz), 7.23 (s, 1H), 7.30 (d, 2H, *J* = 10.8 Hz), 7.53 (t, 2H, *J* = 10.8 Hz), 7.92 (s, 1H). $^{13}$C NMR ($CD_3COCD_3$): δ = 123.4, 127.8, 128.0, 129.2, 138.9, 185.2.

## 3.5.8 *fac*-[$NEt_4$][$Re(Trop)(CO)_3(NCS)$]

Sodium thiocyanate (1 ml of a 1.95 x $10^{-3}$ M methanol solution) was added to *fac*-[$Re(Trop)(CO)_3(H_2O)$] (10 ml of a 1.95 x $10^{-4}$ M methanol solution) and stirred at room temperature for 1 hour. The yellow product was dried *in vacuo*.

Yield: 0.0010 g, 92 %. IR (KBr, $cm^{-1}$): $\nu_{CO}$ = 1900, 2020. $^1$H NMR ($CD_3COCD_3$): δ = 1.29 (s, 12H), 2.82 (s, 8H), 6.98 (t, 1H, *J* = 9.6 Hz), 7.18 (d, 2H, *J* = 10.8 Hz), 7.45 (t, 2H, *J* = 10.8 Hz). $^{13}$C NMR: ($CD_3COCD_3$): δ = 11.2, 31.5, 50. 8, 127.4, 129.0, 138.7, 184.4.

## 3.5.9 *fac*-[$Re(Trop)(CO)_3(DMAP)$]

4-Dimethylaminopyridine (1 ml of a 1.95 x $10^{-3}$ M methanol solution) was added to *fac*-[$Re(Trop)(CO)_3(H_2O)$] (10 ml of a 1.95 x $10^{-4}$ M methanol solution) and stirred at room temperature for 1 hour. The yellow product was dried *in vacuo*. The crystals reported in Paragraph 4.6 were grown from a methanol solution of the product.

Yield: 0.0009 g, 93 %. IR (KBr, $cm^{-1}$): $\nu_{CO}$ = 1886, 2007. $^1$H NMR ($CD_3COCD_3$): δ = 3.04 (s, 6H), 6.61 (dd, 2H, *J* = 1.8 Hz, 6 Hz), 7.10 (t, 1H, *J* = 9.6 Hz), 7.31 (d, 2H, *J* = 10.8 Hz), 7.52 (t, 2H, *J* = 10.8 Hz), 7.98 (dd, 2H, *J* = 1.8 Hz, 6 Hz). $^{13}$C NMR ($CD_3COCD_3$): δ = 39.8, 108.8, 128.4, 129.0, 139.3, 151.8, 156.3, 185.5.

## 3.5.10 *fac*-[$Re(Trop)(CO)_3(TU)$]

Thiourea (1 ml of a 1.95 x $10^{-3}$ M methanol solution) and *fac*-[$Re(Trop)(CO)_3(H_2O)$] (10 ml of a 1.95 x $10^{-4}$ M methanol solution) were stirred for 1 hour at room temperature. The resulting product was dried *in vacuo* to yield the yellow product.

Yield: 0.00088 g, 97 %. IR (KBr, $cm^{-1}$): $\nu_{CO}$ = 1888, 2015. $^1$H NMR ($CD_3COCD_3$): δ = 7.17 (t, 1H, *J* = 9.6 Hz), 7.33 (d, 2H, *J* = 10.8 Hz), 7.55 (s, 2H), 7.70 (t, 2H, *J* = 10.8 Hz), 7.80 (s, 2H). $^{13}$C NMR ($CD_3COCD_3$): δ = 127.5, 128.7, 139.0, 185.1, 186.7.

## 3.5.11 *fac*-[$Re(Trop)(CO)_3(MeTU)$]

1-Methyl-2-thiourea (1 ml of a 1.95 x $10^{-3}$ M methanol solution) and *fac*-[$Re(Trop)(CO)_3(H_2O)$] (10 ml of a 1.95 x $10^{-4}$ M methanol solution) were stirred together at room temperature for 1 hour. The yellow product was dried *in vacuo*.

Yield: 0.00092 g, 98 %. IR (KBr, $cm^{-1}$): $\nu_{CO}$ = 1884, 2013. $^{1}H$ NMR ($CD_3COCD_3$): δ = 3.23 (s, 3H), 7.17 (t, 1H, *J* = 9.6 Hz), 7.33 (d, 2H, *J* = 10.8 Hz), 7.57 (t, 2H, *J* = 10.8 Hz). $^{13}C$ NMR: ($CD_3COCD_3$): δ = 32.5, 128.9, 129.1, 139.3, 183.0, 185.3, 186.8.

## 3.5.12 *fac*-[$NEt_4$][Re(2,5-PicoH)$(CO)_3$(Br)].$H_2O$

ReAA (0.1 g, 0.130 mmol) was dissolved in water at pH 6. 2,5-Pyridine dicarboxylic acid (0.023 g, 0.138 mmol) was added to the mixture and stirred for 24 hours at room temperature. The reaction mixture was filtered and the product was found to be precipitating from the water mixture when it is too concentrated. The pH of the filtrate was recorded as 2.5. The yellow cuboid crystal reported in Paragraph 4.7 was obtained from the filtrate of the reaction mixture over time.

Yield: 0.0554 g, 94 %. IR (KBr, $cm^{-1}$): $\nu_{CO}$ = 1900, 2018, 2040. $^{1}H$ NMR ($CD_3OD$): δ = 1.31 (t, 12H, *J* = 2.4 Hz), 3.12 (q, 8H, *J* = 2.4 Hz), 8.23 (d, 1H, *J* = 8.4 Hz), 8.70 (dd, 1H, *J* = 2 Hz, 8 Hz), 9.22 (s, 1H). $^{13}C$ NMR ($CD_3OD$): δ = 10.2, 58.1, 128.4, 133.2, 143.2, 153.8, 154.5, 165.6, 174.5. HPLC: 17.91 min.

## 3.5.13 *fac*-[Re(2,5-PicoH)$(CO)_3$($H_2O$)]

ReAA (0.1 g, 0.130 mmol) was dissolved in water, adjusted to pH 2.2 by nitric acid. Silver nitrate (0.066 g, 0.389 mmol) was added to the solution and stirred for 24 hours at room temperature. After the reaction mixture was filtered (AgBr), 2,5-pyridine dicarboxylic acid (0.022 g, 0.133 mmol) was added to the solution and stirred under $N_2$ at room temperature for 48 hours. The product was found to be water soluble when dilute. The mixture was filtered and the filtrate (pH 2.5) was dried *in vacuo*. Attempts to grow crystals from the filtrate or from various solvent solutions were unsuccessfull.

Yield: 0.0791 g, 92 %. IR (KBr, $cm^{-1}$): $\nu_{CO}$ = 1899, 2017, 2043. $^{1}H$ NMR ($CD_3COCD_3$): δ = 7.93 (d, 1H, *J* = 8.1 Hz), 8.58 (dd, 1H, *J* = 1.8 Hz, 8.1 Hz), 9.47 (s, 1H). $^{13}C$ NMR ($CD_3COCD_3$): δ = 128.7, 132.9, 142.7, 151.6, 154.5, 164.5, 178.0, 195.0, 197.6, 198.1. HPLC: 17.84 min.

## 3.5.14 *fac*-[$NEt_4$][Re(2,5-PicoH)$(CO)_3$(I)]

Sodium iodide (1 ml of a 2 x $10^{-3}$ M methanol solution) and *fac*-[Re(2,5-PicoH)$(CO)_3(H_2O)$] (10 ml of a 2 x $10^{-4}$ M methanol solution) were stirred for 1 hour at room temperature. The resulting light yellow product was dried *in vacuo*.

Yield: 0.0012 g, 89 %. IR (KBr, $cm^{-1}$): $\nu_{CO}$ = 1883, 2023. $^1$H NMR ($CD_3COCD_3$): δ = 1.18 (t, 12H, *J* = 6.8 Hz), 2.21 (q, 8H, *J* = 6.8 Hz), 8.05 (d, 1H, *J* = 9.0 Hz), 8.64 (dd, 1H, *J* = 1.4 Hz, 9.0 Hz), 9.36 (s, 1H). $^{13}$C NMR ($CD_3COCD_3$): δ = 11.0, 51.0, 127.2, 131.9, 143.2, 150.6, 154.0, 165.1, 178.5.

## 3.5.15 *fac*-[Re(2,5-PicoH)$(CO)_3$(Py)]

Pyridine (1 ml of a 2 x $10^{-3}$ M methanol solution) and *fac*-[Re(2,5-PicoH)$(CO)_3(H_2O)$] (10 ml of a 2 x $10^{-4}$ M methanol solution) were stirred for at room temperature for 1 hour. The resulting light yellow product was dried *in vacuo*.

Yield: 0.00093 g, 90 %. IR (KBr, $cm^{-1}$): $\nu_{CO}$ = 1888, 2027. $^1$H NMR ($CD_3COCD_3$): δ = 7.23 (t, 2H, *J* = 5.8 Hz), 7.76 (d, 1H, *J* = 7.8 Hz), 7.98 (dt, 1H, *J* = 1.2 Hz, 5.8 Hz), 8.33 (dd, 1H, *J* = 1.4 Hz, 7.8 Hz), 8.70 (d, 2H, *J* = 6.0 Hz), 9.11 (s, 1H). $^{13}$C NMR ($CD_3COCD_3$): δ = 123.1, 130.6, 134.0, 138.5, 141.0, 150.9, 151.0, 154.1, 168.6, 177.1.

## 3.5.16 *fac*-[Re(2,5-PicoH)$(CO)_3$(Im)]

Imidazole (1 ml of a 2 x $10^{-3}$ M methanol solution) and *fac*-[Re(2,5-PicoH)$(CO)_3(H_2O)$] (10 ml of a 2 x $10^{-4}$ M methanol solution) were stirred for 1 hour at room temperature. The resulting light yellow product was dried *in vacuo*.

Yield: 0.00093 g, 92 %. IR (KBr, $cm^{-1}$): $\nu_{CO}$ = 1888, 2023. $^1$H NMR ($CD_3COCD_3$): δ = 7.04 (s, 1H), 7.43 (d, 1H, *J* = 7.4 Hz), 7.58 (s, 1H), 8.37 (dd, 1H, *J* = 1.8 Hz, 7.4 Hz), 9.48 (s, 1H). $^{13}$C NMR ($CD_3COCD_3$): δ = 120.0, 126.9, 131.3, 139.5, 141.8, 151.0, 152.4, 163.0, 180.6.

## 3.5.17 *fac*-[$NEt_4$][Re(2,5-PicoH)$(CO)_3$(NCS)]

Sodium thiocyanate (1 ml of a 2 x $10^{-3}$ M methanol solution) and *fac*-[Re(2,5-PicoH)$(CO)_3(H_2O)$] (10 ml of a 2 x $10^{-4}$ M methanol solution) were stirred for 1 hour at room temperature. The resulting light yellow product was dried *in vacuo*.

Yield: 0.0011 g, 91 %. IR (KBr, $cm^{-1}$): $\nu_{CO}$ = 1906, 2024. $^{1}H$ NMR ($CD_3COCD_3$): δ = 1.15 (t, 12H, *J* = 4.2 Hz), 2.45 (q, 8H, *J* = 4.2 Hz), 7.65 (d, 1H, *J* = 8.4 Hz), 8.45 (d, 1H, *J* = 8.4 Hz), 9.52 (s, 1H). $^{13}C$ NMR ($CD_3COCD_3$): δ = 10.5, 31.8, 50.3, 127.0, 131.5, 142.0, 150.9, 153.3, 164.1, 179.6.

## 3.5.18 *fac*-[Re(2,5-PicoH)(CO)$_3$(TU)]

Thiourea (1 ml of a 2 x $10^{-3}$ M methanol solution) and *fac*-[Re(2,5-PicoH)(CO)$_3$($H_2O$)] (10 ml of a 2 x $10^{-4}$ M methanol solution) were stirred for 1 hour at room temperature. The resulting light yellow product was dried *in vacuo*.

Yield: 0.001 g, 97 %. IR (KBr, $cm^{-1}$): $\nu_{CO}$ = 1897, 2025. $^{1}H$ NMR ($CD_3COCD_3$): δ = 7.45 (s, 2H), 7.98 (s, 2H), 8.07 (d, 1H, *J* = 7.2 Hz), 8.43 (dd, 1H, *J* = 1.2 Hz, 7.2 Hz), 9.62 (s, 1H). $^{13}C$ NMR ($CD_3COCD_3$): δ = 126.5, 130.9, 142.9, 151.9, 153.0, 163.9, 180.8, 189.2.

## 3.5.19 *fac*-[Re(2,5-PicoH)(CO)$_3$(MeTU)]

1-Methyl-2-thiourea (1 ml of a 2 x $10^{-3}$ M methanol solution) and *fac*-[Re(2,5-PicoH)(CO)$_3$($H_2O$)] (10 ml of a 2 x $10^{-4}$ M methanol solution) were stirred for 1 hour at room temperature. The resulting light yellow product was dried *in vacuo*.

Yield: 0.001 g, 98 %. IR (KBr, $cm^{-1}$): $\nu_{CO}$ = 1894, 2024. $^{1}H$ NMR ($CD_3COCD_3$): δ = 2.41 (s, 3H), 7.77 (d, 1H, *J* = 8.0 Hz), 8.41 (dd, 1H, *J* = 1.6 Hz, 8.0 Hz), 8.79 (s, 2H), 9.31 (s, 1H). $^{13}C$ NMR ($CD_3COCD_3$): δ = 31.8, 129.5, 132.0, 142.0, 150.4, 153.9, 166.6, 180.1, 187.8.

## 3.5.20 *fac*-[NEt$_4$][Re(2,5-PicoMe)(CO)$_3$(Br)]

ReAA (0.03 g, 0.039 mmol) was dissolved in 20 ml MeOH. 2,5-Pyridinedicarboxylic acid (0.0065g, 0.039 mmol) was added as a solid and the mixture was stirred at 50 °C for 24 hours. Sodium hydroxide (0.002 g, 0.050 mmol) and methyl iodide (0.05 ml, 0.070 mmol) was added to the solution and stirred for 48 hours at 60 °C. The reaction mixture was cooled to room temperature, filtered and the filtrate was dried *in vacuo*. Yellow cuboidal crystals, reported in Paragraph 4.8, were grown from a methanol solution of the product.

Yield: 0.0205 g, 79%. IR (KBr, $cm^{-1}$): $\nu_{CO}$ = 1910, 2021. $^{1}H$ NMR ($CD_3OD$): δ = 1.28 (t, 12H, *J* = 2.4 Hz), 2.41 (q, 8H, *J* = 2.4 Hz), 4.01 (s, 3H), 8.12 (d, 1H,

*J* = 8.1 Hz), 8.65 (d, 1H, *J* = 8 Hz), 9.14 (s, 1H). $^{13}$C NMR ($CD_3OD$): δ = 11.2, 60.5, 124.8, 131.9, 145.3, 154.4, 156.9, 164.1, 173.2.

## 3.5.21 *fac*-[$NEt_4$][Re(Isa)$(CO)_3$(Br)]

ReAA (0.5 g, 0.650 mmol) was dissolved in 20 ml water (pH 5). Isatin (0.1 g, 0.680 mmol) was added to the solution and stirred for 10 minutes. The pH was increased from 5 to 7 with a NaOH solution. After stirring the solution for 30 minutes at room temperature, the pH dropped to 6 and was adjusted with NaOH to pH 7. This was repeated 5 times until the pH stabilized at 7. The reaction mixture was stirred overnight. After filtration, the water soluble product was dried *in vacuo* to yield the orange precipitate. Attempts to grow crystals from a methanol solution, as well as the aqueous reaction mixture were unsuccessful and the crystals obtained were not of good enough quality.

Yield: 0.338 g, 83 %. IR (KBr, $cm^{-1}$): $\nu_{CO}$ = 1872, 2009. $^1$H NMR ($CD_3SOCD_3$): δ = 1.14 (t, 12H, *J* = 3.6 Hz), 2.50 (q, 8H, *J* = 3.6 Hz), 6.93 (d, 1H, *J* = 8.1 Hz), 7.05 (t, 1H, *J* = 7.5 Hz), 7.49 (d, 1H, *J* = 7.5 Hz), 7.58 (dt, 1H, *J* = 1.5 Hz, 6 Hz) $^{13}$C NMR ($CD_3SOCD_3$): δ = 11.4, 50.9, 112.9, 117.1, 130.5, 131.0, 136.7, 151.8, 160.5, 185.9.

## 3.5.22 *fac*-[Re(Isa)$(CO)_3(H_2O)$]

ReAA (0.15 g, 0.195 mmol) was dissolved in 20 ml water at pH 2.2, adjusted with $HNO_3$. Silver nitrate (0.099 g, 0.585 mmol) was added and the mixture stirred for 24 hours at room temperature. Isatin (0.0288 g, 0.197 mmol) was added to the filtrate and stirred for 10 hours at 70 °C at pH 6. The pH constantly decreased and needed to be increased to pH 6 with NaOH for about an hour, after which it stabilized. The reaction mixture was cooled, filtered and the filtrate was dried *in vacuo*.

Yield: 0.0743 g, 83 %. IR (KBr, $cm^{-1}$): $\nu_{CO}$ = 1903, 2019. $^1$H NMR ($CD_3SOCD_3$): δ = 6.47 (d, 1H, *J* = 8.1 Hz), 6.67 (d, 1H, *J* = 7.5 Hz), 7.16 (t, 1H, *J* = 7.5 Hz), 7.49 (d, 1H, *J* = 7.2 Hz). $^{13}$C NMR ($CD_3SOCD_3$): δ = 113.0, 117.0, 131.1, 131.9, 136.1, 152.0, 162.1, 186.1.

## 3.5.23 *fac*-[Re(Isa)(CO)$_3$(Py)]

Pyridine (1 ml of a 3.68 x $10^{-3}$ M methanol solution) and *fac*-[Re(Isa)(CO)$_3$(H$_2$O)] (10 ml of a 3.68 x $10^{-4}$ M methanol solution) were stirred for 1 hour at room temperature. The resulting orange product was dried *in vacuo*.

Yield: 0.0016 g, 91 %. IR (KBr, cm$^{-1}$): $\nu_{CO}$ = 1900, 2018. $^1$H NMR ($CD_3SOCD_3$): δ = 6.44 (d, 1H, *J* = 9.0 Hz), 6.58 (d, 1H, *J* = 8.2 Hz), 7.10 (t, 1H, *J* = 8.2 Hz), 7.29 (t, 2H, *J* = 4.8 Hz), 7.59 (d, 1H, *J* = 8.0 Hz), 7.8 (dt, 1H, *J* = 1.4 Hz, 8.0 Hz), 8.72 (d, 2H, *J* = 7.6 Hz). $^{13}$C NMR ($CD_3SOCD_3$): δ = 113.9, 119.0, 122.2, 130.8, 131.0, 134.9, 135.1, 150.6, 151.5, 160.6, 187.0.

## 3.5.24 *fac*-[NEt$_4$][Re(Isa)(CO)$_3$(NCS)]

Thiocyanate ions (1 ml of a 3.68 x $10^{-3}$ M sodium thiocyanate solution in methanol) and *fac*-[Re(Isa)(CO)$_3$(H$_2$O)] (10 ml of a 3.68 x $10^{-4}$ M methanol solution) were stirred for 1 hour at room temperature. The resulting orange product was dried *in vacuo*.

Yield: 0.0021 g, 93 %. IR (KBr, cm$^{-1}$): $\nu_{CO}$ = 1903, 2017. $^1$H NMR ($CD_3SOCD_3$): δ = 1.45 (t, 12H, *J* = 3.8 Hz), 2.63 (q, 8H, *J* = 3.8 Hz), 6.38 (d, 1H, *J* = 8.0 Hz), 6.84 (d, 1H, *J* = 7.2 Hz), 7.23 (t, 1H, *J* = 7.2 Hz), 7.52 (d, 1H, *J* = 7.0 Hz). $^{13}$C NMR ($CD_3SOCD_3$): δ = 10.5, 52.0, 111.9, 115.1, 130.5, 134.0, 134.1, 137.6, 152.8, 163.9, 189.0.

## 3.5.25 *fac*-[Re(Isa)(CO)$_3$(TU)]

Thiourea (1 ml of a 3.68 x $10^{-3}$ M methanol solution) and *fac*-[Re(Isa)(CO)$_3$(H$_2$O)] (10 ml of a 3.68 x $10^{-4}$ M methanol solution) were stirred for 1 hour at room temperature. The resulting orange product was dried *in vacuo*.

Yield: 0.0017 g, 92 %. IR (KBr, cm$^{-1}$): $\nu_{CO}$ = 1905, 2019. $^1$H NMR ($CD_3SOCD_3$): δ = 6.87 (d, 1H, *J* = 8.6 Hz), 6.97 (d, 1H, *J* = 8.0 Hz), 7.34 (t, 1H, *J* = 8.0 Hz), 7.59 (d, 1H, *J* = 7.8 Hz), 8.78 (s, 4H). $^{13}$C NMR ($CD_3SOCD_3$): δ = 112.7, 115.2, 130.1, 131.7, 135.6, 152.1, 161.1, 185.0, 186.9.

## 3.5.26 *fac*-[Re(Isa)(CO)$_3$(MeTU)]

1-Methyl-2-thiourea (1 ml of a 3.68 x $10^{-3}$ M methanol solution) and *fac*-[Re(Isa)(CO)$_3$(H$_2$O)] (10 ml of a 3.68 x $10^{-4}$ M methanol solution) were stirred for 1 hour at room temperature. The resulting orange product was dried *in vacuo*.

Yield: 0.0017 g, 94 %. IR (KBr, $cm^{-1}$): $\nu_{CO}$ = 1905, 2020. $^{1}H$ NMR ($CD_3SOCD_3$): δ = 2.12 (s, 3H), 6.37 (d, 1H, *J* = 8.4 Hz), 6.78 (d, 1H, *J* = 8.0 Hz), 7.11 (t, 1H, *J* = 8.0 Hz), 7.39 (d, 1H, *J* = 7.8 Hz), 8.45 (s, 2H). $^{13}C$ NMR ($CD_3SOCD_3$): δ = 30.1, 111.9, 114.3, 130.9, 132.0, 135.9, 152.5, 160.5, 180.9, 183.5.

## 3.5.27 *fac*-[$NEt_4$][Re(BHA)$(CO)_3$(Br)]

Benzohydroxamic acid (0.019 g, 0.140 mmol) was added to 3 ml of water at pH 7.5 (adjusted with NaOH) and stirred until dissolved. ReAA (0.09 g, 0.116 mmol) was added to the solution and stirred for 3 hours after which the solution was freeze-dried. Colourless block crystals were collected by dissolving the product in acetonitrile and by vapour diffusion with ether. The crystal structure is reported in Paragraph 4.9.

Yield: 0.0623 g, 89 %. IR (KBr, $cm^{-1}$): $\nu_{CO}$ = 1881, 2004. $^{1}H$ NMR ($CD_3COCD_3$): δ = 1.13 (t, 12H, *J* = 4.8 Hz), 2.48 (q, 8H, *J* = 4.8 Hz), 7.60 (d, 1H, *J* = 10.8 Hz), 7.84 (dd, 2H, *J* = 4.8, 10.8 Hz), 8.14 (d, 2H, *J* = 4.8 Hz). $^{13}C$ NMR ($CD_3COCD_3$): δ = 10.5, 51.5, 127.1, 128.5, 132.4, 135.2, 170.0.

## 3.5.28 *fac*-[Re(BHA)$(CO)_3(H_2O)$]

ReAA (0.5 g, 0.650 mmol) was dissolved in 20 ml water at pH 2.2. Silver nitrate (0.331 g, 1.948 mmol) was added to the solution and stirred for 24 hours at room temperature. Benzohydroxamic acid (0.0889 g, 0.650 mmol) was added to the filtrate, at pH 7 (adjusted with NaOH), and stirred for 20 hours at 80 °C. The reaction mixture was cooled to room temperature, filtered and the filtrate was freeze-dried.

Yield: 0.230 g, 86 %. IR (KBr, $cm^{-1}$): $\nu_{CO}$ = 1859, 2008. $^{1}H$ NMR ($CD_3COCD_3$): δ = 7.50 (d, 1H, *J* = 10.4 Hz), 7.78 (dd, 2H, *J* = 4.0 Hz, 10.4 Hz), 8.20 (d, 2H, *J* = 4.0 Hz). $^{13}C$ NMR ($CD_3COCD_3$): δ = 126.8, 128.1, 133.0, 135.1, 170. 5.

## 3.5.29 *fac*-[Re(Flav)$(CO)_3(H_2O)$].Flav

Synthesized according to Schutte *et al*.[5]

[5] Schutte, M., Kemp, G., Visser, H.G., Roodt, A. *Inorg. Chem*. **2011**, *50(24)*, 12486-12498.

## 3.5.30 μ-(*fac*-[Re(BipyDC)(CO)$_3$])$_2$.4H$_2$O

ReAA (0.1 g, 0.130 mmol) was dissolved in 20 ml water, adjusted to pH 2.2 with $HNO_3$. Silver nitrate (0.066 g, 0.389 mmol) was added to the solution and it was stirred for 24 hours at room temperature. The precipitate, AgBr, was filtered off and 2,2'-bipyridine-3,3'-dicarboxylic acid (0.032 g, 0.131 mmol) was added the filtrate and stirred for 3 hours at room temperature. The product was found in the yellow filtrate as well as the bright yellow precipitate. The crystal structure of μ-(*fac*-[Re(BipyDC)(CO)$_3$])$_2$.4H$_2$O is reported in Paragraph 4.11.

Yield: 0.127 g, 90 %. IR (KBr, cm$^{-1}$): $\nu_{CO}$ = 1900, 2025. $^1$H NMR ($CD_3COCD_3$): δ = 7.39 (dd, 1H, *J* = 5.2 Hz, 8 Hz), 7.70 (dd, 1H, *J* = 5.2 Hz, 8 Hz), 7.95 (dd, 1H, *J* = 1.6 Hz, 8 Hz), 8.45 (dd, 1H, *J* = 1.6 Hz, 8 Hz), 8.72 (dd, 1H, *J* = 1.6 Hz, 5.2 Hz), 8.87 (dd, 1H, *J* = 1.6 Hz, 5.2 Hz). $^{13}$C NMR ($CD_3COCD_3$): δ = 119.4, 120.3, 139.1, 149.2, 152.4, 167.5, 174.1. HPLC: 19.69 min.

## 3.5.31 *fac*-[Re(PNP)(CO)$_3$(Br)]

Synthesized according to Schutte *et al*.[6]

## 3.5.32 *fac*-[NEt$_4$][Re(NO$_2$Isa)(CO)$_3$(Br)]

ReAA (0.1 g, 0.130 mmol) was dissolved in 20 ml water. 5-Nitroisatin (0.025 g, 0.130 mmol) was added to the solution and the pH was increased with NaOH and stabilized at pH 6 after a few minutes. The mixture was stirred at 80 °C for 20 hours. The reaction mixture was cooled to room temperature, filtered and the filtrate was dried *in vacuo*.

Yield: 0.0692 g, 79 %. IR (KBr, cm$^{-1}$): $\nu_{CO}$ = 1901, 2019. $^1$H NMR ($CD_3COCD_3$): δ = 1.38 (dt, 12H, *J* = 1.8 Hz, 7.2 Hz), 3.52 (q, 8H, *J* = 7.2 Hz), 7.68 (d, 1H, *J* = 8.7 Hz), 8.27 (d, 1H, *J* = 2.4 Hz), 8.49 (dd, 1H, *J* = 2.4 Hz, 8.7 Hz). $^{13}$C NMR ($CD_3COCD_3$): δ = 8.8, 54.0, 115.1, 119.5, 121.3, 134.6, 158.0, 160.5, 184.9, 199.1.

## 3.5.33 *fac*-[Re(NO$_2$Isa)(CO)$_3$(H$_2$O)]

ReAA (0.3 g, 0.389 mmol) was dissolved in 20 ml water, at pH 2.2 (adjusted with $HNO_3$), and silver nitrate (0.198 g, 1.166 mmol) was added to the solution. It was

[6] Schutte, M., Visser, H.G., Brink, A. *Acta Cryst*. **2009**, *E65*, m1575-m1576.

stirred at room temperature for 24 hours. The grey precipitate, AgBr, was filtered off and 5-nitroisatin (0.075 g, 0.390 mmol) was added to the solution. The pH of the solution was increased to 6 with NaOH, and monitored for an hour to ensure that the pH of the solution is stable. The temperature was increased to 80 °C, and the mixture stirred for 24 hours. The mixture was left to cool down, filtered and the filtrate was freeze dried.

Yield: 0.163 g, 87%. IR (KBr, $cm^{-1}$): $\nu_{CO}$ = 1905, 2020. $^{1}H$ NMR ($CD_3COCD_3$): δ = 6.99 (d, 1H, *J* = 8 Hz), 8.02 (d, 1H, *J* = 8 Hz), 8.87 (s, 1H). $^{13}C$ NMR ($CD_3COCD_3$): δ = 119.8, 121.3, 121.6, 130.5, 149.6, 154.9, 160.8, 182.4.

## 3.5.34 *fac*-[$NEt_4$][$Re(F_3COIsa)(CO)_3(Br)$]

ReAA (0.1 g, 0.130 mmol) was dissolved in 20 ml water at pH 5. 5-(Trifluoro-methoxy)-isatin (0.03 g, 0.130 mmol) was added to the solution and in order to keep the pH at 6, NaOH was constantly added since the pH kept on decreasing. After the pH stabilized at 6, the mixture was stirred overnight at 70 °C. After cooling to room temperature, the mixture was filtered and the orange filtrate dried *in vacuo*.

Yield: 0.0739 g, 80 %. IR (KBr, $cm^{-1}$): $\nu_{CO}$ = 1904, 2019. $^{1}H$ NMR ($CD_3COCD_3$): δ = 1.45 (t, 12H, *J* = 7.0 Hz), 2.58 (q, 8H, *J* = 7.0 Hz), 6.89 (d, 1H, *J* = 8.2 Hz), 7.22 (d, 1H, *J* = 10.2 Hz), 7.80 (s, 1H). $^{13}C$ NMR ($CD_3COCD_3$): δ = 10.2, 50.5, 111.0, 119.2, 127.6, 128.9, 133.1, 142.0, 155.9, 158.5, 185.2.

## 3.5.35 *fac*-[$Re(F_3COIsa)(CO)_3(H_2O)$]

ReAA (0.3 g, 0.389 mmol) was dissolved in 20 ml water, at pH 2.2 (adjusted with $HNO_3$), and silver nitrate (0.198 g, 1.166 mmol) was added to the solution. It was stirred at room temperature for 24 hours. The grey precipitate, AgBr, was filtered off and 5-(trifluoromethoxy)isatin (0.09 g, 0.391 mmol) was added to the solution. The pH of the reaction mixture was adjusted to pH 6 and monitored in order to keep it stable at pH 6. The mixture was stirred at 80 °C for 24 hours at pH 6. It was cooled and the filtrate was freeze dried.

Yield: 0.165 g, 82%. IR (KBr, $cm^{-1}$): $\nu_{CO}$ = 1898, 2017. $^{1}H$ NMR ($CD_3COCD_3$): δ = 6.91 (d, 1H, *J* = 8.8 Hz), 7.20 (d, 1H, *J* = 9.6 Hz), 7.75 (s, 1H). $^{13}C$ NMR ($CD_3COCD_3$): δ = 110.8, 118.9, 127.2, 128.8, 132.0, 142.3, 156.1, 158.6, 186.1.

## 3.5.36 *fac*-[Re(PMAEth)(CO)$_3$][NO$_3$]

ReAA (0.3 g, 0.389 mmol) was dissolved in 20 ml water. 2-(Bis-(2-pyridylmethyl)-amino)-ethanol (0.095 g, 0.390 mmol) was added to the solution and stirred for 8 hours at room temperature. The light orange mixture was filtered and the filtrate freeze-dried. The product precipitates from the water solution at high concentrations.

Yield: 0.180 g, 90 %. IR (KBr, cm$^{-1}$): $\nu_{CO}$ = 1879, 2002, 2031. $^1$H NMR ($CD_3OD$): δ = 4.01 (t, 2H, *J* = 4.8 Hz), 4.10 (t, 2H, *J* = 4.8 Hz), 4.97 (s, 4H), 7.37 (t, 2H, *J* = 6.4 Hz), 7.55 (d, 2H, *J* = 8 Hz), 7.94 (dt, 2H, *J* = 1.6 Hz, 8 Hz), 8.87 (d, 2H, *J* = 4.8 Hz). $^{13}$C NMR ($CD_3OD$): δ = 60.1, 69.7, 72.9, 124.9, 127.0, 141.8, 153.2, 162.5.

## 3.5.37 *fac*-[Re(PMAEth-An)(CO)$_3$][NO$_3$]

*fac*-[Re(PMAEth)(CO)$_3$] (0.009 g, 0.0175 mmol) was dissolved in 3 ml DCM. *p*-toluene-sulphonyl chloride (0.0035 g, 0.0184 mmol) and triethylamine (0.0019 g, 0.0175 mmol) was added to the solution and stirred at 60 °C for 24 hours. Afterwards, the reaction mixture was dried *in vacuo*. Aniline (0.003 g, 0.035 mmol) was added to the product, dissolved in THF, and stirred for 24 hours at 60 °C. The mixture was dried *in vacuo*. The product, dissolved in methanol (20 ml), was washed with hexane (3 x 10 ml). The combined methanol layers were washed with water (3 x 10 ml) to yield the product.

Yield: 0.003 g, 29 %. IR (KBr, cm$^{-1}$): $\nu_{CO}$ = 1895, 2009. $^1$H NMR ($CD_3OD$): δ = 2.94 (s, 2H), 3.12 (s, 2H), 3.25 (s, 4H), 7.28 (m, 5H), 7.37 (dt, 2H, *J* = 3.6 Hz, 7.2 Hz), 7.43 (d, 2H, *J* = 8.4 Hz), 7.54 (d, 2H, *J* = 8.4 Hz), 7.64 (dd, 2H, *J* = 7.6 Hz, 16 Hz). $^{13}$C NMR ($CD_3OD$): δ = 34.2, 55.2, 63.9, 120.9, 124.6, 125.5, 127.8, 128.7, 138.9, 138.9, 149.3, 156.9.

## 3.5.38 *fac*-[Re(PMAProp)(CO)$_3$][NO$_3$]

ReAA (0.3 g, 0.389 mmol) was dissolved in 20 ml water. 2-(Bis-(2-pyridylmethyl)-amino)-propanol (0.1 g, 0.390 mmol) was added and the reaction mixture was stirred at room temperature for 8 hours. The brown mixture was dried, dissolved in methanol and washed with hexane (3 x 10 ml). The oily product was dried *in vacuo*.

Yield: 0.180 g, 88 %. IR (KBr, cm$^{-1}$): $\nu_{CO}$ = 1918, 1991, 2027. $^1$H NMR ($CD_3SOCD_3$): δ = 1.58 (t, 2H, *J* = 6 Hz), 2.91 (t, 2H, *J* = 6.9 Hz), 3.81 (t, 2H,

*J* = 6 Hz), 4.38 (s, 4H), 7.38 (t, 2H, *J* = 6 Hz), 7.55 (d, 2H, *J* = 7.8 Hz), 7.84 (dt, 2H, *J* = 1.5 Hz, 6 Hz), 8.57 (d, 2H, *J* = 4.8 Hz). $^{13}$C NMR ($CD_3OD$): δ = 28.2, 52.5, 59.2, 68.0, 123.9, 126.2, 140.9, 152.5, 161.4.

## 3.5.39 *fac*-[Re(PMAProp-His)(CO)$_3$][NO$_3$]

ReAA (0.075 g, 0.0974 mmol) was dissolved in water (pH 6.5). 2-(Bis-(2-pyridylmethyl)-amino)-propanol (0.025 g, 0.0974 mmol) was added and stirred at 70 °C for 6 hours. Histamine (0.011 g, 0.099 mmol) and one drop sulphuric acid was added and the mixture was stirred at 80 °C for 24 hours. It was left to cool to room temperature. The oily product was dissolved in methanol and washed with hexane (3 x 10 ml). The product was dried *in vacuo*.

Yield: 0.0381 g, 63 %. IR (KBr, cm$^{-1}$): $\nu_{CO}$ = 1914, 2030. $^1$H NMR ($CD_3OD$): δ = 1.68 (s, 2H), 2.20 (t, 2H, *J* = 5.1 Hz), 3.18 (d, 4H, *J* = 7.5 Hz), 3.76 (t, 2H, *J* = 6Hz), 4.00 (s, 2H), 4.19 (t, *J* = 6 Hz), 7.39 (t, 2H, *J* = 6.6 Hz), 7.52 (s, 2H), 7.59 (d, 2H, *J* = 7.8 Hz), 7.96 (t, 2H, *J* = 7.8 Hz), 8.90 (d, 2H, *J* = 7.5 Hz). $^{13}$C NMR ($CD_3OD$): δ = 27.9, 29.0, 45.9, 48.8, 55.4, 62.7, 118.3, 120.8, 124.3, 132.7, 138.9, 139.4, 147.9, 158.0.

## 3.5.40 *fac*-[Re(PMABut)(CO)$_3$][NO$_3$]

ReAA (0.3 g, 0.389 mmol) was dissolved in 20 ml water. 2-(Bis-(2-pyridylmethyl)-amino)-butanol (0.107 g, 0.393 mmol) was added and the reaction mixture was stirred at room temperature for 8 hours. The brown mixture was dried, dissolved in methanol and washed with hexane (3 x 10 ml). The oily product was dried *in vacuo*.

Yield: 0.175 g, 83 %. IR (KBr, cm$^{-1}$): $\nu_{CO}$ = 1908, 2029. $^1$H NMR ($CD_3OD$): δ = 1.38 (t, 2H, *J* = 4.0 Hz), 1.50 (t, 2H, *J* = 5.2 Hz), 2.42 (t, 2H, *J* = 4.0 Hz), 3.48 (t, 2H, *J* = 5.2 Hz), 3.68 (s, 4H), 7.20 (m, 4H), 7.84 (dt, 2H, *J* = 1.4 Hz, 7.0 Hz), 8.51 (d, 2H, *J* = 7.0 Hz). $^{13}$C NMR ($CD_3OD$): δ = 24.0, 24.4, 54.8, 63.1, 63.2, 119.9, 125.1, 139.4, 148.6, 156.9.

## 3.5.41 *fac*-[NEt$_4$][Re(Chrys)(CO)$_3$(Br)]

ReAA (0.05 g, 0.0650 mmol) was dissolved in 20 ml water at pH 6. Chrysin (0.017 g, 0.0670 mmol) was added to the solution. The pH was adjusted until

stabilized at pH 6. The mixture was stirred for 24 hours at 80 °C. It was left to cool down and the mixture was filtered and the filtrate was freeze-dried.

Yield: 0.0392 g, 92 %. IR (KBr, $cm^{-1}$): $\nu_{CO}$ = 1898, 2018. $^{1}H$ NMR ($CD_3SOCD_3$): δ = 1.16 (t, 12H, *J* = 2.4 Hz), 3.21 (q, 8H, *J* = 2.4 Hz), 6.23 (s, 1H), 6.54 (s, 1H), 6.98 (s, 1H), 7.59 (m, 3H), 8.07 (d, 2H, *J* = 5.4 Hz). $^{13}C$ NMR ($CD_3SOCD_3$): δ = 9.0, 51.3, 94.1, 98.9, 103.9, 105.1, 126.3, 129.1, 130.6, 131.9, 157.4, 161.4, 163.1, 164.4, 181.8.

## 3.5.42 *fac*-[Re(Chrys)(CO)$_3$(H$_2$O)]

ReAA (0.3 g, 0.389 mmol) was dissolved in 20 ml water, adjusted to pH 2.2 with $HNO_3$. Silver nitrate (0.198 g, 1.166 mmol) was added to the solution and it was stirred for 24 hours at room temperature. The AgBr precipitate was filtered off and chrysin (0.11 g, 0.433 mmol) was added to the filtrate. The pH was increased to pH 6 with NaOH and the reaction mixture was stirred at 60 °C for 5 hours. The reaction mixture was filtered and the filtrate was freeze-dried.

Yield: 0.165 g, 78%. IR (KBr, $cm^{-1}$): $\nu_{CO}$ = 1900, 2018. $^{1}H$ NMR ($CD_3SOCD_3$): δ = 6.42 (s, 1H), 6.65 (s, 1H), 7.01 (s, 1H), 7.50 (m, 3H), 8.22 (d, 2H, *J* = 6.2 Hz). $^{13}C$ NMR ($CD_3SOCD_3$): δ = 95.1, 98.8, 104.1, 105.0, 126.5, 129.9, 129.4, 131.7, 157.6, 162.0, 163.1, 164.9, 181.7.

## 3.5.43 *fac*-[NEt$_4$][Re(ox)(CO)$_3$(Br)]

ReAA (0.03 g, 0.0389 mmol) was dissolved in methanol. 8-Hydroxyquinoline (0.0057 g, 0.0393 mmol) was added and the mixture was stirred at 60 °C for 24 hours. It was left to cool down, filtered and the filtrate was dried *in vacuo*.

Yield: 0.0213 g, 88 %. IR (KBr, $cm^{-1}$): $\nu_{CO}$ = 1875, 2016. $^{1}H$ NMR ($CD_3SOCD_3$): δ = 1.42 (t, 12H, *J* = 4.2 Hz), 2.31 (q, 8H, *J* = 4.2 Hz), 7.23 (dd, 1H, *J* = 1.0 Hz, 4.2 Hz), 7.68 (m, 3H), 8.58 (d, 1H, *J* = 4.8 Hz), 8.94 (dd, 1H, *J* = 1.4 Hz, 6.2 Hz). $^{13}C$ NMR ($CD_3SOCD_3$): δ = 111.8, 118.9, 122.8, 127.9, 129.4, 136.0, 139.9, 150.9, 156.9.

## 3.5.44 *fac*-[Re(ox)(CO)$_3$(H$_2$O)]

ReAA (0.15 g, 0.195 mmol) was dissolved in $H_2O$, at pH 2.2 (adjusted with $HNO_3$), and silver nitrate (0.1 g, 0.585 mmol) was added. The mixture was stirred at room temperature for 24 hours and the precipitate was filtered off. 8-Hydroxyquinoline

(0.028 g, 0.195 mmol) was added and the mixture stirred at room temperature for 8 hours. The reaction mixture was filtered and the filtrate dried *in vacuo*.

Yield: 0.0783 g, 93 %. IR (KBr, $cm^{-1}$): $\nu_{CO}$ = 1880, 2018. $^{1}H$ NMR ($CD_3SOCD_3$): δ = 7.32 (dd, 1H, *J* = 1.4 Hz, 4.8 Hz), 7.75 (m, 3H), 8.42 (d, 1H, *J* = 4.8 Hz), 9.10 (dd, 1H, *J* = 1.8 Hz, 7.0 Hz). $^{13}C$ NMR ($CD_3SOCD_3$): δ = 112.2, 119.1, 124.8, 126.5, 129.8, 135.5, 139.2, 151.4, 155.8.

## 3.5.45 *fac*-[Re(Cl-ox)(CO)$_3$(H$_2$O)]

ReAA (0.3 g, 0.389 mmol) was dissolved in 20 ml water at pH 2.2. Silver nitrate (0.198 g, 1.166 mmol) was added and the mixture was stirred at room temperature for 24 hours. The precipitate was filtered off, 5-chloro-8-hydroxyquinoline (0.07 g, 0.390 mmol) was added to the filtrate and the reaction mixture was stirred overnight. The mixture was filtered and the filtrate was freeze-dried.

Yield: 0.169 g, 93%. IR (KBr, $cm^{-1}$): $\nu_{CO}$ = 1878, 2019. $^{1}H$ NMR ($CD_3SOCD_3$): δ = 6.99 (d, 1H, *J* = 8.4 Hz), 7.54 (d, 1H, *J* = 8.4 Hz), 7.67 (t, 1H, *J* = 7.5 Hz), 8.71 (d, 1H, *J* = 7.5 Hz), 9.06 (d, 1H, *J* = 2.1 Hz). $^{13}C$ NMR ($CD_3SOCD_3$): δ = 110.0, 117.7, 122.1, 126.5, 128.2, 134.1, 139.9, 152.9, 155.1.

## 3.5.46 *fac*-[Re(DMe-ox)(CO)$_3$(H$_2$O)]

ReAA (0.3 g, 0.389 mmol) was dissolved in 20 ml water at pH 2.2. Silver nitrate (0.198 g, 1.166 mmol) was added and the mixture was stirred at room temperature for 24 hours. After the mixture was filtered, 5,7-dimethyl-8-hydroxyquinoline (0.0675 g, 0.390 mmol) was added and then it was stirred at room termperature for 24 hours. It was found that the product precipitates from the filtrate at high concentrations. The filtrate was freeze-dried.

Yield: 0.157 g, 88 %. IR (KBr, $cm^{-1}$): $\nu_{CO}$ = 1903, 1930, 2021. $^{1}H$ NMR ($CD_3SOCD_3$): δ = 2.31 (s, 3H), 3.20 (s, 3H), 7.28 (s, 1H), 7.54 (t, 1H, *J* = 4.2 Hz), 8.55 (td, 1H, *J* = 1.2 Hz, 8.4 Hz), 8.93 (d, 1H, *J* = 1.2 Hz). $^{13}C$ NMR ($CD_3SOCD_3$): δ = 14.0, 18.2, 120.4, 122.8, 126.4, 128.3, 129.0, 130.2, 138.9, 148.9, 150.9.

### 3.5.47 *fac*-[$NEt_4$]/[Na][Re(NTA-An)$(CO)_3$]

*fac*-[$NEt_4$]/[Na][Re(NTA)$(CO)_3$] (0.14 g, 0.238 mmol), as prepared by Marti *et al*.[7], was dissolved in 5 ml DCM. Oxalyl chloride (0.03 g, 0.250 mmol) was added. After stirring for 5 minutes a 40 °C, 1 drop DMF was added to the reaction mixture and stirred for 4 hours. The reaction mixture was dried *in vacuo*, dissolved in 5 ml THF and Aniline (0.044 g, mmol) was added to the solution. This was stirred at 60 °C for 6 hours. It was cooled to room temperature and filtered. The filtrate was dried *in vacuo*, dissolved in ethylacetate and washed with water (3 x 10 ml). The ethylacetate solution was dried *in vacuo*.

Yield: 0.109 g, 0.165 mmol. IR (KBr, $cm^{-1}$): $\nu_{CO}$ = 1921, 2026. $^1$H NMR ($CDCl_3$): δ = 1.08 (t, 12H, *J* = 2.4 Hz), 2.32 (q, 8H, *J* = 2.4 Hz), 2.07 (s, 4H), 2.07 (s, 2H), 6.69 (d, 2H, *J* = 7.6 Hz), 6.76 (t, 1H, *J* = 7.2 Hz), 7.14 (t, 2H, *J* = 8 Hz). $^{13}$C NMR ($CDCl_3$): δ = 14.3, 30.2, 60.6, 115.6, 119.1, 129.5, 146.1, 171.7, 178.6.

## 3.6 *In situ* synthesis of $^{99m}$Tc compounds

Most of the labeling efforts were unsuccessful. The preparation of *fac*-[$^{99m}$Tc(Isa)$(CO)_3(H_2O)$] was unsuccessful as expected. The synthesis of the Rhenium analogue, *fac*-[Re(Isa)$(CO)_3(H_2O)$], is very dependent on the pH. During the synthesis of $^{99m}$Technetium compounds, HPLC with the gamma detector is the only characterization method. The pH of the HPLC column decrease up to pH 2, meaning the *fac*-[$^{99m}$Tc(Isa)$(CO)_3(H_2O)$] that could possibly have formed, will decompose when coming into contact with the column. A small peak at 20.12 min can be seen, but even after 6 hours it doesn't increase and stay at about 10 % yield. For the same reasons, the Rhenium analogue can not be used for a co-injection.

It was also attempted to synthesize *fac*-[$^{99m}$Tc(BipyDC)$(CO)_3(H_2O)]^+$, but two products were formed. This might be the *fac*-[$^{99m}$Tc(BipyDC)$(H_2O)]^+$ compound and the other product might be the dimer, where one of the free carboxylic acids on the Bipy rings coordinates to the next Re(I) centre in the sixth position, substituting the water ligand. This is seen for the Rhenium analogue where the crystal μ-(*fac*-[Re(BipyDC)$(CO)_3]$)$_2$.$4H_2O$ was isolated (Paragraph 4.11). The characterization was

[7] Marti, N., Spingler, B., Breher, F., Schibli, R. *Inorg. Chem*. **2005**, *44*, 6082-6091.

not investigated any further since the application is useless with two products forming.

During the attempted labeling process of benzohydroxamic acid (BHA), the amount of *fac*-[$^{99m}$Tc(CO)$_3$(H$_2$O)]$^+$ decreased from 100% to 60% in 30 minutes after adding the ligand and after a total of 90 minutes, there was 100% pertechnetate in the vial. From this it is clear that benzohydroxamic acid acts as an oxidizing agent during this process. At no stage was there any sign of a product forming. Interestingly, the synthesis of the Rhenium analogue, *fac*-[NEt$_4$][Re(BHA)(CO)$_3$(Br)] was successful and it was possible to isolate the crystal structure as well.

The labeling of *fac*-[$^{99m}$Tc(CO)$_3$(H$_2$O)$_3$]$^+$ with bis(diphenylphosphino)-propylamine (PNP) was unsuccessful as well, even though the Rhenium analogue was synthesized. The crystal structure of *fac*-[Re(PNP)(CO)$_3$] is reported in Paragraph 4.12.

The last unsuccessful labeling attempt was with the tridentate ligand, N,N'-bis(2-pyridylmethyl)-2-aminoethanol (PMAEth). Two distinct products were formed with $R_t$ = 16.35 min and 18.75 min. Once again, the Rhenium analogue, *fac*-[Re(PMAEth)(CO)$_3$][NO$_3$] was synthesized successfully as reported in Paragraph 3.6.36.

## 3.6.1 *fac*-[$^{99m}$Tc(2,5-PicoH)(CO)$_3$(H$_2$O)]

Sodium boranocarbonate (4.4 mg, 0.054 mol), disodium tartrate dihydrate (8.1 mg, 0.035 mmol), disodium tetraborate pentahydrate (7.6 mg, 0.02 mmol) and $^{99m}$Technetium pertechnetate (eluted from the $^{99}$Mo/$^{99m}$Tc generator) was added to a vial, flushed with N$_2$ and heated at 85 °C for 30 minutes. HPLC analysis confirmed 100% reduction of [$^{99m}$TcO$_4$]$^-$ to *fac*-[$^{99m}$Tc(CO)$_3$(H$_2$O)$_3$]$^+$. In a separate vial, 2,5-pyridinedicarboxylic acid (20 mg, 0.120 mmol) was added and flushed with N$_2$. 1 ml of the prepared *fac*-[$^{99m}$Tc(CO)$_3$(H$_2$O)$_3$]$^+$, was added to the ligand and heated for 30 minutes at 85 °C. Only one product was formed. A co-injection with the Rhenium analogue, *fac*-[Re(2,5-PicoH)(CO)$_3$(H$_2$O)] confirmed this ($R_t$ = 17.95 min).

HPLC: $R_t$ = 18.22 min.

## 3.6.2 *fac*-[$^{99m}$Tc(Trop)(CO)$_3$(H$_2$O)]

In a vial flushed with $N_2$, sodium boranocarbonate (3.4 mg, 0.042 mmol), disodium tartrate dihydrate (6.3 mg, 0.027 mmol), disodium tetraborate pentahydrate (6.3 mg, 0.017 mmol) and 1ml pertechnetate (eluted from the $^{99}$Mo/$^{99m}$Tc generator) was heated at 85 °C for 30 minutes. By HPLC it was confirmed that all the pertechnetate was reduced to *fac*-[$^{99m}$Tc(CO)$_3$(H$_2$O)$_3$]$^+$. In a separate vial, tropolone (20 mg, 0.164 mmol) was added and flushed with $N_2$. 1 ml of the prepared *fac*-[$^{99m}$Tc(CO)$_3$(H$_2$O)$_3$]$^+$ was added to the vial and heated at 85 °C for 30 minutes. One product was formed and a co-injection with *fac*-[Re(Trop)(CO)$_3$(H$_2$O)] ($R_t$ = 18.79 min) confirmed this.

HPLC: $R_t$ = 19.32 min

## 3.6.3 *fac*-[$^{99m}$Tc(DMe-ox)(CO)$_3$(H$_2$O)]

Sodium boranocarbonate (3.7 mg, 0.045 mmol), disodium tartrate dehydrate (6.6 mg, 0.029 mmol) and disodium tetraborate pentahydrate (6.9 mg, 0.018 mmol) was added to a vial and flushed with $N_2$. 1 ml Pertechnetate (eluted from the $^{99}$Mo/$^{99m}$Tc generator) was added to the vial and heated for 30 min at 85 °C. It was confirmed by HPLC that 100 % *fac*-[$^{99m}$Tc(CO)$_3$(H$_2$O)$_3$]$^+$ was formed. 5-Chloro-8-hydroxyquinoline (25 mg, 0.139 mmol) was added to a second vial, flushed with $N_2$ and 0.4 ml *fac*-[$^{99m}$Tc(CO)$_3$(H$_2$O)]$^+$ and 0.6 ml saline was added to it. The vial was heated for 30 minutes at 85 °C and a 100% yield of the product was formed.

HPLC: $R_t$ = 20.88 min.

## 3.6.4 *fac*-[$^{99m}$Tc(Cl-ox)(CO)$_3$(H$_2$O)]

Sodium boranocarbonate (3.7 mg, 0.045 mmol), disodium tartrate dehydrate (6.6 mg, 0.029 mmol) and disodium tetraborate pentahydrate (6.9 mg, 0.018 mmol) was added to a vial flushed with $N_2$. 1 ml Pertechnetate (eluted from the $^{99}$Mo/$^{99m}$Tc generator) was added and the vial was heated for 30 min at 85 °C. It was confirmed by HPLC that 100 % *fac*-[$^{99m}$Tc(CO)$_3$(H$_2$O)$_3$]$^+$ was formed. 5,7-Dimethyl-8-hydroxyquinoline (25 mg, 0.144 mmol) was added to a separate vial, flushed with $N_2$ and 0.4 ml *fac*-[$^{99m}$Tc(CO)$_3$(H$_2$O)$_3$]$^+$ and 0.6 ml saline was added. The vial was heated for 30 minutes at 85 °C. Only one product was formed in 100% yield.

HPLC: $R_t$ = 20.57 min.

# 3.7 Discussion

In this chapter, the synthesis of 9 free ligand systems, 4 *fac*-[$^{99m}$Tc(CO)$_3$]$^+$ type compounds and 45 *fac*-[Re(CO)$_3$]$^+$ type compounds are reported.

One of the aims of the study was to synthesize water soluble compounds and to study the kinetic behaviour of the complexes in aqueous medium. Eight water soluble compounds were successfully synthesized. These are *fac*-[Re(Trop)(CO)$_3$(H$_2$O)], *fac*-[Re(Chrys)(CO)$_3$(H$_2$O)], *fac*-[Re(Isa)(CO)$_3$(H$_2$O)], *fac*-[Re(NO$_2$Isa)(CO)$_3$(H$_2$O)], *fac*-[Re(F$_3$COIsa)(CO)$_3$(H$_2$O)], *fac*-[Re(ox)(CO)$_3$(H$_2$O)], *fac*-[Re(Cl-ox)(CO)$_3$(H$_2$O)] and *fac*-[Re(DMe-ox)(CO)$_3$(H$_2$O)]. An aqua substitution kinetic study is reported in Chapter 7 between *fac*-[Re(Trop)(CO)$_3$(H$_2$O)] and NCS$^-$ ions.

Nine novel ligand systems were successfully synthesized. The initial idea was to link biologically active molecules to bidentate ligands to investigate the '2+1' approach and to potentially synthesize ligand systems that are biologically active itself. Also, some novel bidentate ligands were synthesized from monodentate ligand systems. Some of these ligands were also successfully coordinated to the *fac*-[Re(CO)$_3$]$^+$ core. The ligands were sent for clinical *in vitro* tests and some of the results obtained are reported in Chapter 8. The rest of the results were not yet known at the time of this report.

The tricarbonyl carbon atom peaks in most of the Rhenium complexes were not observed on the $^{13}$C NMR spectra. This is due to the long relaxation time of these carbons. Considering the time and financial implications this will have *vs* the little information gained from these tricarbonyl peaks, the other characterization methods were considered to be sufficient.

A trend was observed for the IR stretching frequencies of the metal complexes, although there are some exceptions. It is expected that the compounds with better electron donor ligands, will increase the electron density on the Re(I) metal core as well as the backbonding from the carbonyl ligands and therefore will have lower IR stretching frequencies.

The synthesis of the bromido complexes, [Re(L,L'-bid)(CO)$_3$Br]$^-$, were quite straight forward and generally, high yields were obtained. With the synthesis of the aqua complexes, *fac*-[Re(L,L'-bid)(CO)$_3$(H$_2$O)], special care needs to be taken to ensure that the tri-aqua species is formed before addition of the bidentate ligand. This was

done by subjecting ReAA to 3 equivalents of $AgNO_3$ and stirring it for 24 hours. After several experiments by Kemp[8], it was found that 24 hours is necessary to remove all three the bromido ligands. For all the aqua complexes, the AgBr was dried and weighed for every synthesis to ensure all three bromido ligands were hydrolyzed. Also, the pH of these solutions were adjusted to 2.2 in order to avoid the formation of polymeric hydroxy-bridged species in the solution. The pH of the aqueous solutions was carefully monitored to ensure the protonated form of the bidentate ligands, especially the 2,5-pyridinedicarboxylic acid ligand.

The compound *fac*-[Re(PMAProp-His)$(CO)_3$][$NO_3$] has been synthesized firstly by coordinating the tridentate ligand to the Re(I) core and then linking the histamine on the backbone and secondly by linking histamine to PMAProp and then coordinating the ligand system to the Re(I) core. This illustrates the possibilities available for linking biologically active molecules to backbones on the metal core.

The following Rhenium complexes were successfully synthesized, *fac*-[Re(Isa)$(CO)_3(H_2O)$], *fac*-[Re(BHA)$(CO)_3(H_2O)$], *fac*-[Re(PMAEth)$(CO)_3$][$NO_3$] and μ-(*fac*-[Re(BipyDC)$(CO)_3(H_2O)$])$_2$.$4H_2O$. To prove that the chemistry of Rhenium and Technetium is not always similar as sometimes presumed, the attempts to synthesize the analogous $^{99m}$Technetium complexes were unsuccessful. The pH might be the limiting factor in the synthesis of *fac*-[$^{99m}$Tc(Isa)$(CO)_3(H_2O)$] since the Rhenium analogue exhibit great pH dependency. For the BipyDC ligand system, two products were formed when reacted with *fac*-[$^{99m}$Tc$(CO)_3(H_2O)_3]^+$. This might be due to the same coordinating effect of one of the free carboxylic acids to the next Technetium unit. These results show that it is not always safe to assume that these two metals react in the same way, but that there is still very much to learn.

The crystal structure of μ-(*fac*-[Re(BipyDC)$(CO)_3$])$_2$.$4H_2O$ was obtained from the aqua complex, *fac*-[Re(BipyDC)$(CO)_3(H_2O)]^+$. It was decided to prepare the bromido complex as well to see of the dimer formation is still observed. The crystal structure of *fac*-[Re(BipyDC)$(CO)_3$(Br)] yielded the same coordination of one of the carboxylic acids to the neighbouring Rhenium unit's 6$^{th}$ position.

Linking histamine to the free carboxylic acid in *fac*-[$NEt_4$][Re(2,4-PicoH)$(CO)_3$(Br)] was unsuccessful. Even with various methods and reaction conditions, three products were formed. It was suggested that the histamine can also attack at the

[8] Kemp, G. PhD Thesis, University of Johannesburg, 2006.

bromido site which then interferes with the mole ratios of metal to histamine and therefore opens the possibility for by-products. It was decided to use tridentate ligand complexes for linking histamine, where the problem at the $6^{th}$ position is eliminated.

One challenge observed during this study is the problem to separate the charged Rhenium compounds by column chromatography. This is a huge problem since many of the compounds cannot be separated completely by extraction. In the cases where the products are water soluble or does not precipitate from the reaction mixture, column chromatography would be the next step in separation.

# 4 CRYSTALLOGRAPHIC STUDY OF RE(I) COMPLEXES

## 4.1 Introduction

There are many crystal structure reports of Rhenium(I) tricarbonyl complexes in literature, but very few on O,O'-donor bidentate ligands as part of the coordination sphere around Rhenium. In fact, a literature search revealed only twelve structures with O,O'-donor bidentate ligands for the *fac*-Re(I) tricarbonyl core.[1]

In this chapter, ten new Rhenium(I) tricarbonyl crystal structures of the form, *fac*-$[Re(L,L'\text{-bid})(CO)_3X]^n$, are reported with L,L'-bid = O,O'-, N,O-, N,N'- and P,P'-donor bidentate ligands. The bidentate ligand systems used are:

- tropolone (TropH), 3-hydroxyflavone (FlavH) and benzohydroxamic acid (BHAH) as O,O-bidentate ligands,
- 2,5-pyridinedicarboxylic acid (2,5-Pico$H_2$) as N,O-bidentate ligand,
- 2,2'-bipyridine-3,3'-dicarboxylic acid (BipyDC) as N,N'- bidentate ligand and
- bis(diphenylphosphino)propylamine (PNP) as P,P'-bidentate ligand.

A schematic representation of the 10 crystal structures reported in this chapter is illustrated in Scheme 4.1. The crystallographic data of the crystal structures of (**1**) – (**10**) are summarized in Table 4.1 to Table 4.4. The structures of *fac*-$[NEt_4][Re(Trop)(CO)_3(Br)]$ (**1**), *fac*-$[Re(Trop)(CO)_3(Py)]$ (**3**), *fac*-$[Re(Trop)(CO)_3(DMAP)]$ (**4**) and *fac*-$[NEt_4][Re(2,5\text{-PicoH})(CO)_3(Br)]$ (**5**) were isolated from the reaction mixtures of the kinetic studies between *fac*-$[Re(Trop)(CO)_3(H_2O)]$ and $Br^-$, Py and DMAP, for **1**, **3** and **4** respectively and between *fac*-$[Re(2,5\text{-PicoH})(CO)_3(H_2O)]$ and $Br^-$ ions for **5**.

[1] *Cambridge Structural Database* (CSD), Version 5.32, Feb 2011 update. F.H. Allen, *Acta Cryst*. **2002**, *B58*, 380.

# Chapter 4

**Scheme 4.1: Illustration of the crystal structures reported in this chapter, (1) – (10).**

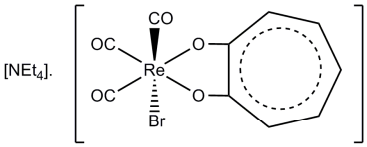


*fac*-[$NEt_4$][Re(Trop)$(CO)_3$(Br)] **(1)**

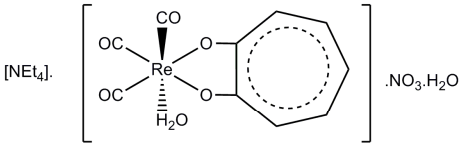


*fac*-[$NEt_4$][Re(Trop)$(CO)_3(H_2O)$].$NO_3$.$H_2O$ **(2)**

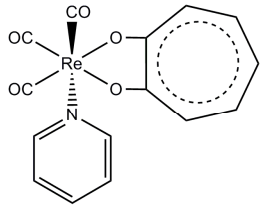


*fac*-[Re(Trop)$(CO)_3$(Py)] **(3)**

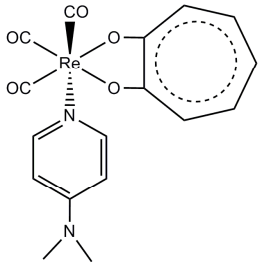


*fac*-[Re(Trop)$(CO)_3$(DMAP)] **(4)**

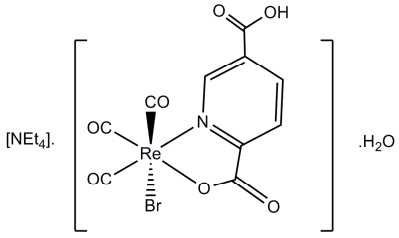


*fac*-[$NEt_4$][Re(2,5-PicoH)$(CO)_3$(Br)].$H_2O$ **(5)**

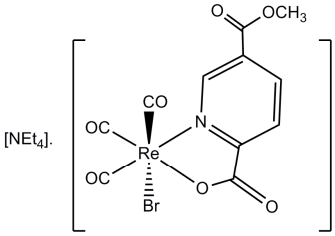


*fac*-[$NEt_4$][Re(2,5-PicoMe)$(CO)_3$(Br)] **(6)**

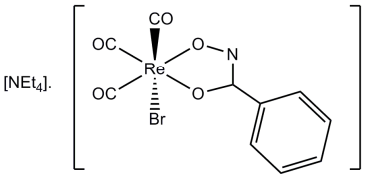


*fac*-[$NEt_4$][Re(BHA)$(CO)_3$(Br)] **(7)**

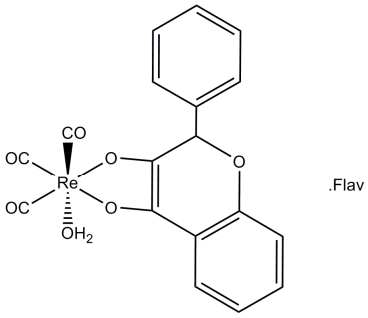


*fac*-[Re(Flav)$(CO)_3(H_2O)$].Flav **(8)**

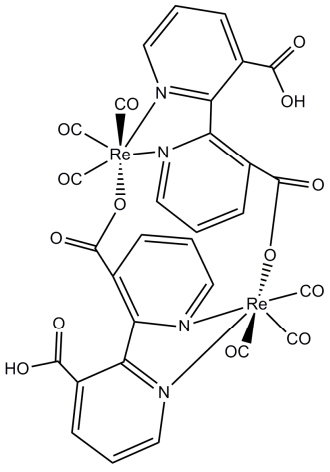


μ-(*fac*-[Re(BipyDC)$(CO)_3$])$_2$.$4H_2O$ **(9)**

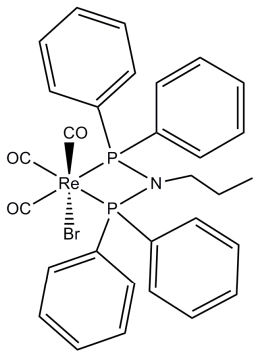


*fac*-[Re(PNP)$(CO)_3$(Br)] **(10)**

A schematic illustration of the general synthetic pathway for these type of complexes is presented in Scheme 4.2.

For the sake of brevity and uniformity, the plane formed by the two carbonyl ligands *trans* to the bidentate ligand and the ligand itself, will be referred to as the equatorial plane throughout.

**Scheme 4.2: General synthetic procedure of compounds reported.**

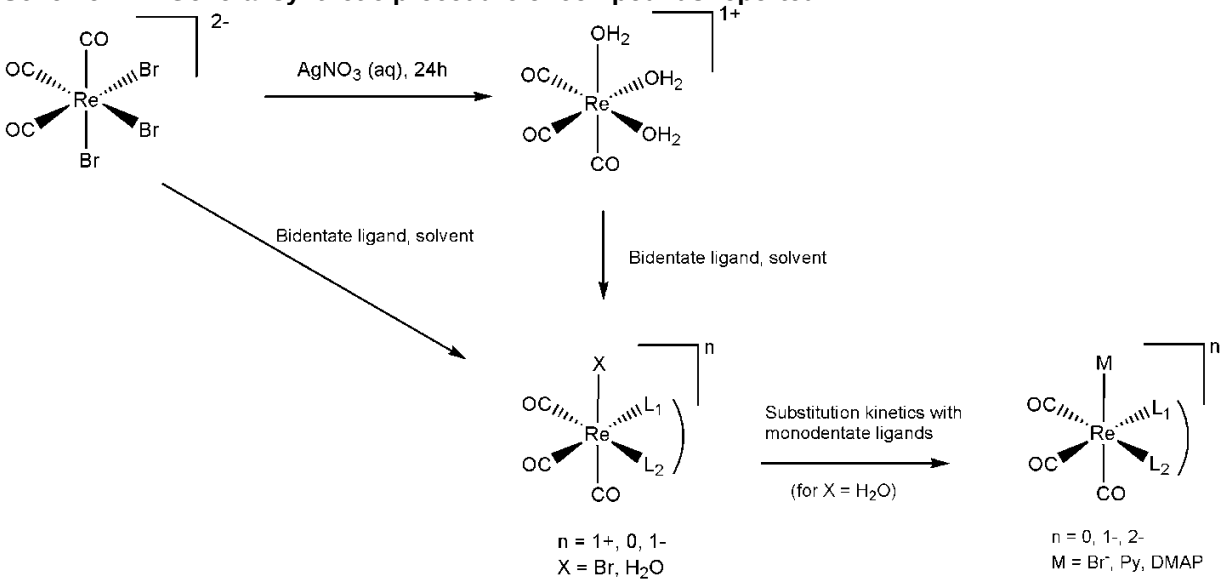


# 4.2 Experimental

The reflection data for the structure determinations for **2** were collected on an Oxford Diffraction Xcalibur system while the rest of the structure determinations were collected on a Bruker X8 Apex Π 4K diffractometer. The Bruker apparatus is equipped with graphite monochromated Mo *K*α radiation, with a wavelength of 0.71073 Å, and with ω- and φ-scans at 100 K. The Oxford Xcalibur system is equipped with a Ruby detector using Mo $K_\alpha$ radiation (λ = 0.71070 Å) that was graphite-monochromated, at 100 K.

All the cell refinements were performed with SAINT-Plus[2] and CALC-OH[3] while the data reduction was done with SAINT-Plus, XPREP[2] and CrysAlis$^{Pro}$[4]. The absorption corrections were obtained by the use of the multi-scan technique and the SADABS[5] software package. All the structures were solved with the use of the SIR-97[6] package, refinement was done with SHELXL-97[7] and WinGX[8] and the molecular graphics were completed with DIAMOND[9].

Unless otherwise stated, all the structures are shown with thermal ellipsoids drawn at a 50% probability level and all non-hydrogen atoms were anisotropically refined. Methyl and aromatic hydrogen atoms were placed in geometrically idealized positions, C-H = 0.95 to 0.98 Å, and constrained to ride on their parent atoms, $U_{iso}$(H) = 1.5 $U_{eq}$(C) and 1.2 $U_{eq}$(C) respectively. All the atomic coordinates, anisotropic displacement parameters, bond distances, angles, torsion angles and hydrogen coordinates, of all the crystal reported in this chapter, are given in the supplementary data (Appendix A).

[2] Bruker, *SAINT-Plus*, Version 7.12 (including XPREP), Bruker AXS Inc., Madison, Wisconsin, USA, **2004**.
[3] Nardelli, M. *J. Appl. Cryst*. **1999**, *32*, 563-571.
[4] *CrysAlis$^{Pro}$ Software system*; Oxford Diffraction Ltd., Version 171.32 Oxford, UK, **2007**.
[5] Bruker, *SADABS*, Version 2004/1, Bruker AXS Inc., Madison, Wisconsin, USA, **1998**.
[6] Altomare, A., Burla, M.C., Camalli, M., Cascarano, G.L., Giacovazzo, C., Guagliardi, A., Moliterni, A.G.G., Polidori, G., Spagna, R. *J. Appl. Cryst*. **1999**, *32*, 837-838.
[7] Sheldrick, G.M., *SHELXL97*, Program for the refinement of crystal structures, University of Göttingen, Germany, **1997**.
[8] Farrugia, L.J. *J. Appl. Cryst*. **1999**, *32*, 837-838.
[9] Brandenburg, K., Putz, H., *DIAMOND*, Release 3.0c, Crystal Impact GbR, Bonn, Germany, **2006**.

**Table 4.1: Crystallographic data of *fac*-[$NEt_4$][Re(Trop)$(CO)_3$(Br)] (1), *fac*-[$NEt_4$][Re(Trop)$(CO)_3(H_2O)$].$NO_3$.$H_2O$ (2) and *fac*-[Re(Trop)$(CO)_3$(Py)] (3).**

| Crystallographic data | 1 | 2 | 3 |
|---|---|---|---|
| Emperical formula | $C_{18}H_{25}BrNO_5Re$ | $C_{28}H_{34}N_2O_{17}Re_2$ | $C_{15}H_{10}NO_5Re$ |
| Formula weight (g $mol^{-1}$) | 601.5 | 1042.99 | 470.45 |
| Crystal system | Monoclinic | Monoclinic | Monoclinic |
| Space group | $P2_1/n$ | P21/c | $P2_1/c$ |
| a (Å) | 12.334(5) | 14.5451(7) | 16.349(5) |
| b (Å) | 10.754(5) | 10.3208(4) | 6.890(5) |
| c (Å) | 16.053(5) | 11.6301(4) | 14.239(5) |
| α (°) | 90.000(5) | 90.00 | 90.000(5) |
| β (°) | 101.983(5) | 90.372(4) | 114.390(5) |
| γ (°) | 90.000(5) | 90.00 | 90.000(50 |
| Volume ($A^3$) | 2082.9(14) | 1744.34(12) | 1460.8(13) |
| Z | 4 | 2 | 4 |
| $\rho_{calc}$ (g $cm^{-3}$) | 1.918 | 1.986 | 2.139 |
| Crystal colour | Orange | Yellow | Yellow |
| Crystal morphology | Cuboid | Cuboid | Needle |
| Crystal size (mm) | 0.58x0.18x0.17 | 0.11x0.08x0.05 | 0.18x0.06x0.03 |
| μ ($mm^{-1}$) | 7.779 | 7.010 | 8.341 |
| F(000) | 1160 | 1004.0 | 888.0 |
| θ range (°) | 1.9 – 28.31 | 2.6268 – 30.8164 | 3.26 – 28.20 |
| Index ranges | -16 ≤ h ≤ 16<br>-14 ≤ k ≤ 12<br>-21 ≤ l ≤ 21 | -19 ≤ h ≤ 14<br>-9 ≤ k ≤ 13<br>-15 ≤ l ≤ 11 | -21 ≤ h ≤ 19<br>-9 ≤ k ≤ 9<br>-14 ≤ l ≤ 18 |
| Reflections collected | 16808 | 9950 | 20542 |
| Unique reflections | 5183 | 4500 | 3635 |
| Reflections with I > 2σ(I) | 4700 | 3316 | 2983 |
| $R_{int}$ | 0.0465 | 0.0505 | 0.0437 |
| Completeness to 2 theta (°, %) | 28.31, 99.5 | 28.70, 99.6 | 28.31, 99.3 |
| Data / restraints / parameters | 5183/3/251 | 4500/5/280 | 3635/0/199 |
| GooF | 1.13 | 1.063 | 1.189 |
| R [I > 2σ(I)] | $R_1$ = 0.0343<br>$wR_2$ = 0.0843 | $R_1$ = 0.0534<br>$wR_2$ = 0.1001 | $R_1$ = 0.0228<br>$wR_2$ = 0.0577 |
| R (all data) | $R_1$ = 0.0387<br>$wR_2$ = 0.0862 | $R_1$ = 0.0866<br>$wR_2$ = 0.1086 | $R_1$ = 0.0347<br>$wR_2$ = 0.0858 |
| $\rho_{max}$, $\rho_{min}$ (e $A^{-3}$) | 3.159, -1.413 | 2.593, -2.761 | 1.074, -1.325 |

Trop = tropolonato

**Table 4.2: Crystallographic data *fac*-[Re(Trop)(CO)$_3$(DMAP)] (4), *fac*-[NEt$_4$][Re(2,5-PicoH)(CO)$_3$(Br)] (5) and *fac*-[NEt$_4$][Re(2,5-PicoMe)(CO)$_3$(Br)] (6).**

| Crystallographic data | 4 | 5 | 6 |
|---|---|---|---|
| Emperical formula | $C_{17}H_{15}N_2O_5Re$ | $C_{18}H_{26}BrN_2O_8Re$ | $C_{19}H_{26}BrN_2O_7Re$ |
| Formula weight (g mol$^{-1}$) | 513.51 | 664.52 | 660.53 |
| Crystal system | Monoclinic | Monoclinic | Monoclinic |
| Space group | $P2_1/n$ | $Cc$ | $C2/c$ |
| a (Å) | 8.041(5) | 12.085(5) | 13.118(5) |
| b (Å) | 14.996(5) | 30.613(5) | 12.641(5) |
| c (Å) | 14.385(5) | 7.005(5) | 27.956(5) |
| α (°) | 90.000(5) | 90.000(5) | 90.000(5) |
| β (°) | 98.333(5) | 120.922(5) | 99.995(5) |
| γ (°) | 90.000(5) | 90.000(5) | 90.000(5) |
| Volume (A$^3$) | 1716.3(13) | 2223.2(19) | 4565(3) |
| Z | 4 | 4 | 8 |
| $\rho_{calc}$ (g cm$^{-3}$) | 1.987 | 1.985 | 1.922 |
| Crystal colour | Yellow | Yellow | Yellow |
| Crystal morphology | Cuboid | Cuboid | Cuboid |
| Crystal size (mm) | 0.33x0.24x0.12 | 0.35 x 0.33 x 0.20 | 0.50 x 0.33 x 0.30 |
| μ (mm$^{-1}$) | 7.110 | 7.309 | 7.115 |
| F(000) | 984 | 1288.0 | 2560 |
| θ range (°) | 2.72 – 28.33 | 2.80 – 28.37 | 2.25 – 28.31 |
| Index ranges | -10 ≤ h ≤ 10<br>-19 ≤ k ≤ 19<br>-19 ≤ l ≤ 19 | -15 ≤ h ≤ 16<br>-40 ≤ k ≤ 40<br>-9 ≤ l ≤ 9 | -12 ≤ h ≤ 17<br>-14 ≤ k ≤ 16<br>-37 ≤ l ≤ 28 |
| Reflections collected | 26990 | 19342 | 23787 |
| Unique reflections | 4267 | 5375 | 5519 |
| Reflections with I > 2σ(I) | 3620 | 5137 | 4846 |
| $R_{int}$ | 0.0324 | 0.0502 | 0.0446 |
| Completeness to 2 theta (°, %) | 28.28, 99.4 | 28.38, 99.8 | 28.33, 96.9 |
| Data / restraints / parameters | 4267/0/196 | 5375/5/274 | 5519/0/271 |
| GooF | 1.049 | 1.163 | 1.163 |
| R [I > 2σ(I)] | $R_1$ = 0.0339<br>$wR_2$ = 0.0713 | $R_1$ = 0.0266<br>$wR_2$ = 0.0675 | $R_1$ = 0.0320<br>$wR_2$ = 0.0618 |
| R (all data) | $R_1$ = 0.0435<br>$wR_2$ = 0.0784 | $R_1$ = 0.0301<br>$wR_2$ = 0.0844 | $R_1$ = 0.0400<br>$wR_2$ = 0.0675 |
| $\rho_{max}$, $\rho_{min}$ (e A$^{-3}$) | 2.396, -2.258 | 1.123, -1.299 | 1.086, -0.891 |

2,5-PicoH = pyridine-2-carboxylato-5-carboxylic acid, 2,5-PicoMe = pyridine-2-carboxylato-5-carboxylic acid 5-methyl ester

**Table 4.3: Crystallographic data of *fac*-[$NEt_4$][Re(BHA)$(CO)_3$(Br)] (7) and *fac*-[Re(Flav)$(CO)_3(H_2O)$].Flav (8).**

| Crystallographic data | 7 | 8 |
|---|---|---|
| Emperical formula | $C_{18}H_{26}BrN_2O_5Re$ | $C_{33}H_{21}O_{10}Re$ |
| Formula weight (g $mol^{-1}$) | 616.52 | 763.71 |
| Crystal system | Triclinic | Triclinic |
| Space group | $P\bar{1}$ | $P\bar{1}$ |
| a (Å) | 9.6321(13) | 10.521(5) |
| b (Å) | 9.8793(11) | 11.936(5) |
| c (Å) | 12.826(2) | 12.446(5) |
| α (°) | 95.806(10) | 108.277(5) |
| β (°) | 108.520(11) | 102.745(5) |
| γ (°) | 112.895(7) | 104.252(5) |
| Volume ($A^3$) | 1030.2(3) | 1361.0(10) |
| Z | 2 | 2 |
| $\rho_{calc}$ (g $cm^{-3}$) | 1.987 | 1.864 |
| Crystal colour | Colourless | Yellow |
| Crystal morphology | Cuboid | Plate |
| Crystal size (mm) | 0.38 x 0.25 x 0.11 | 0.55 x 0.17 x 0.08 |
| μ ($mm^{-1}$) | 7.867 | 4.529 |
| F(000) | 596 | 748.0 |
| θ range (°) | 2.53 – 28.29 | 2.91 – 28.57 |
| Index ranges | -12 ≤ h ≤ 12<br>-12 ≤ k ≤ 12<br>-16 ≤ l ≤ 16 | -13 ≤ h ≤ 13<br>-15 ≤ k ≤ 15<br>-16 ≤ l ≤ 16 |
| Reflections collected | 17119 | 22724 |
| Unique reflections | 4493 | 6577 |
| Reflections with I > 2σ(I) | 4299 | 5821 |
| $R_{int}$ | 0.0376 | 0.0373 |
| Completeness to 2 theta (°, %) | 27.00, 99.8 | 28.00, 97.2 |
| Data / restraints / parameters | 4493/3/247 | 6577/3/409 |
| GooF | 1.047 | 1.140 |
| R [I > 2σ(I)] | $R_1$ = 0.0203<br>$wR_2$ = 0.0484 | $R_1$ = 0.0267<br>$wR_2$ = 0.0696 |
| R (all data) | $R_1$ = 0.0215<br>$wR_2$ = 0.0489 | $R_1$ = 0.0317<br>$wR_2$ = 0.0723 |
| $\rho_{max}$, $\rho_{min}$ (e $A^{-3}$) | 1.644, -1.824 | 1.193, -2.078 |

BHA = benzohydroxamato, Flav = 3-hydroxyflavonato

**Table 4.4: Crystallographic data of μ-(*fac*-[Re(BipyDC)(CO)$_3$])$_2$.4H$_2$O (9) and *fac*-[Re(PNP)(CO)$_3$(Br)] (10).**

| Crystallographic data | 9 | 10 |
|---|---|---|
| Emperical formula | $C_{30}H_{22}N_4O_{18}Re_2$ | $C_{30}H_{27}BrNO_3P_2Re$ |
| Formula weight (g mol$^{-1}$) | 1098.94 | 777.58 |
| Crystal system | Monoclinic | Monoclinic |
| Space group | $P2_1/c$ | $P2_1/n$ |
| a (Å) | 10.149(5) | 11.0120(2) |
| b (Å) | 17.518(5) | 17.1620(3) |
| c (Å) | 19.942(5) | 15.2090(2) |
| α (°) | 90.000(5) | 90.00 |
| β (°) | 98.773(5) | 96.735(2) |
| γ (°) | 90.000(5) | 90.00 |
| Volume (A$^3$) | 3504(2) | 2854.48(7) |
| Z | 4 | 4 |
| $\rho_{calc}$ (g cm$^{-3}$) | 2.083 | 1.809 |
| Crystal colour | Yellow | Colourless |
| Crystal morphology | Plate | Cuboid |
| Crystal size (mm) | 0.16 x 0.13 x 0.09 | 0.10 x 0.08 x 0.05 |
| μ (mm$^{-1}$) | 6.989 | 5.801 |
| F(000) | 2096 | 1512 |
| θ range (°) | 2.54 – 28.00 | 2.2035 – 33.1450 |
| Index ranges | -13 ≤ h ≤ 13<br>-23 ≤ k ≤ 23<br>-26 ≤ l ≤ 26 | -11 ≤ h ≤ 14<br>-22 ≤ k ≤ 21<br>-20 ≤ l ≤ 16 |
| Reflections collected | 81066 | 22483 |
| Unique reflections | 8476 | 6863 |
| Reflections with I > 2σ(I) | 7037 | 5197 |
| $R_{int}$ | 0.0485 | 0.0457 |
| Completeness to 2 theta (°, %) | 28.00, 99.7 | 28.00, 99.5 |
| Data / restraints / parameters | 8476/6/525 | 22483/387/0 |
| GooF | 1.059 | 1.025 |
| R [I > 2σ(I)] | $R_1$ = 0.0269<br>$wR_2$ = 0.0563 | $R_1$ = 0.0334<br>$wR_2$ = 0.0766 |
| R (all data) | $R_1$ = 0.0385<br>$wR_2$ = 0.0604 | $R_1$ = 0.0536<br>$wR_2$ = 0.0883 |
| $\rho_{max}$, $\rho_{min}$ (e A$^{-3}$) | 1.151, -0.849 | 1.947, -1.110 |

PNP = bis(diphenylphosphino)propylamine, BipyDC = 2,2'-bipyridine-3-carboxylato-3'-carboxylic acid

# 4.3 Crystal structure of *fac*-[$NEt_4$][$Re(Trop)(CO)_3(Br)$] (1)

The complex, *fac*-[$NEt_4$][$Re(Trop)(CO)_3(Br)$], have been synthesized as described in Paragraph 3.5.3 according to Schutte *et al*.[10] The orange cuboidal crystals were obtained from a methanol solution of the product.

This complex crystallizes in the monoclinic $P2_1/n$ space group with the two ionic fragments independent of the other in the asymmetric unit, an anionic Re(I) compound and a tetraethylammonium cation. The bromido ligand and the axial carbonyl ligand are substitutionally disordered over two positions in a 0.922(3):0.078(3) ratio, as illustrated in Figure 4.1. In the structure of *fac*-[$NEt_4$][$Re(Trop)(CO)_3(Br)$], the Re atom is octahedrally surrounded by three facially orientated carbonyl ligands, one bidendate tropolonato ligand and a bromido ligand.

**Figure 4.1: Molecular representation of the crystal structure of *fac*-[$NEt_4$][$Re(Trop)(CO)_3(Br)$] (1).**

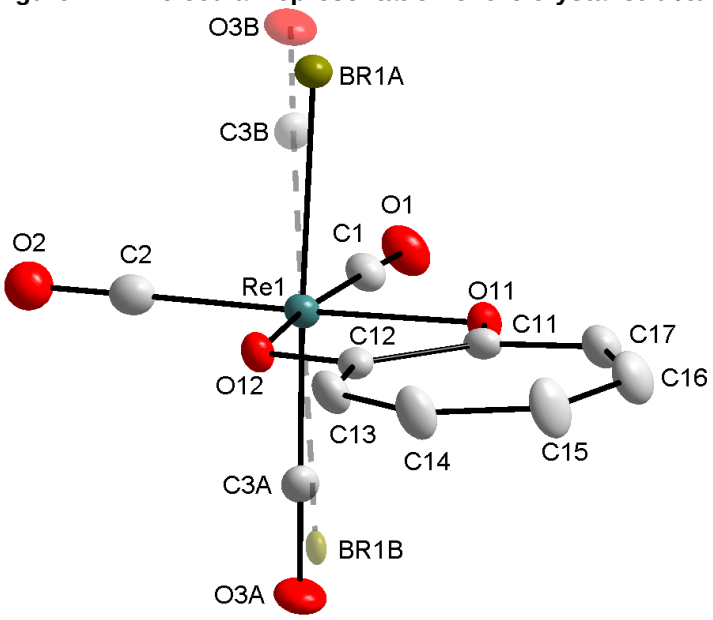


A summary of the general crystal data is given in Table 4.1 while the numbering scheme of the anion is shown in Figure 4.1. The hydrogen atoms and the cation are

[10] Schutte, M., Visser, H.G., Roodt, R. *Acta Cryst* **2010**, *E66*, m859-m860.

omitted for clarity. Some of the important bond distances and angles were selected and are summarized in Table 4.5.

**Table 4.5: Selected bond lengths and angles for the crystal structure of *fac*-[$NEt_4$][Re(Trop)$(CO)_3$(Br)] (1).**

| Selected bond lengths (Å) | | Selected bond angles (°) | | Selected torsion angles (°) | |
|---|---|---|---|---|---|
| **Re1-C1** | 1.906(5) | **O11-Re1-O12** | 74.88(12) | **O11-C11-C12-O12** | -2.7(6) |
| **Re1-C2** | 1.903(5) | **C1-Re1-C2** | 87.6(2) | | |
| **Re1-C3A** | 1.861(7) | **Br1A-Re1-O11** | 82.07(9) | | |
| **Re1-C3B** | 1.923(18) | **C3A-Re1-O11** | 94.4(2) | | |
| **Re1-O11** | 2.126(3) | **Br1B-Re1-O11** | 86.3(3) | | |
| **Re1-O12** | 2.135(3) | **C3B-Re1-O11** | 89(2) | | |
| **Re1-Br1A** | 2.6334(9) | **O11-Re1-C1** | 97.33(17) | | |
| **Re1-Br1B** | 2.467(16) | **O12-Re1-C2** | 100.19(16) | | |
| | | **C3A-Re1-Br1A** | 175.61(19) | | |
| | | **C3B-Re1-Br1B** | 171.5(19) | | |

The bond distances from Re1 to the three carbonyl carbons (C1, C2 and C3) are all within range of similar structures.[11,12,13,14,15,16] The metal to bromido distances of 2.467(16) Å and 2.6334(9) Å for this disordered structure are also comparable to other bromido complexes.[10,11,13] The Rhenium to oxygen bond distances, O11 and O12 of the tropolonato ligand, correspond well to the 2.141(2) Å and 2.132(2) Å found in the tribromotropolonato analogue of the complex.[13]

The small bite angle, O11-Re-O12, of 74.88(12) ° leads to a distortion of the octahedral coordination sphere. This is clear from the angle of 82.07(9) ° for Br1A-Re1-O11, 97.33(17) ° for O11-Re1-C1 and 171.5(19) ° for C3B-Re1-Br1B.

The planarity of the ring system, O11-C11-C12-C13-C14-C15-C16-C17-O12, of the tropolonato ring is illustrated by the very small deviations of all the atoms from the plane (largest deviation from the plane is 0.054(4) Å for C17) in Figure 4.2. A dihedral angle of 2.1(2) ° is calculated between the plane through the tropolonato ligand system and the equatorial plane. This is also illustrated in Figure 4.2. From this it is clear that the tropolonato ligand 'bends' out of the equatorial plane to some extent.

[11] Schutte, M., Visser, H.G., Brink, A. *Acta Cryst*. **2009**, *E65*, m1757-m1576.
[12] Schutte, M., Visser, H.G. *Acta Cryst*. **2008**, *E64*, m1226-m1227.
[13] Schutte, M., Visser, H.G., Steyl, G. *Acta Cryst*. **2007**, *E63*, m3195-m3196.
[14] Schutte, M., Visser, H.G., Roodt, A. *Acta Cryst*. **2008**, *E64*, m1610-m1611.
[15] Alberto, R., Herrmann, W.A., Kiprof, P., Baumgartner, F. *Inorg. Chem*. **1992**, *31*, 895-899.
[16] Brasey, T., Buryak, A., Scopelliti, R., Severin, K. *Eur. J. Inorg. Chem*. **2004**, 964-967.

The tropolonato ligand system 'twist' to a certain extent with a torsion angle of -2.7(6) ° reported for O11-C11-C12-O12.

**Figure 4.2: Illustration of the equatorial plane and the plane through the tropolonato ligand, indicating the dihedral angle between these planes in *fac*-[$NEt_4$][Re(Trop)$(CO)_3$(Br)] (1).**

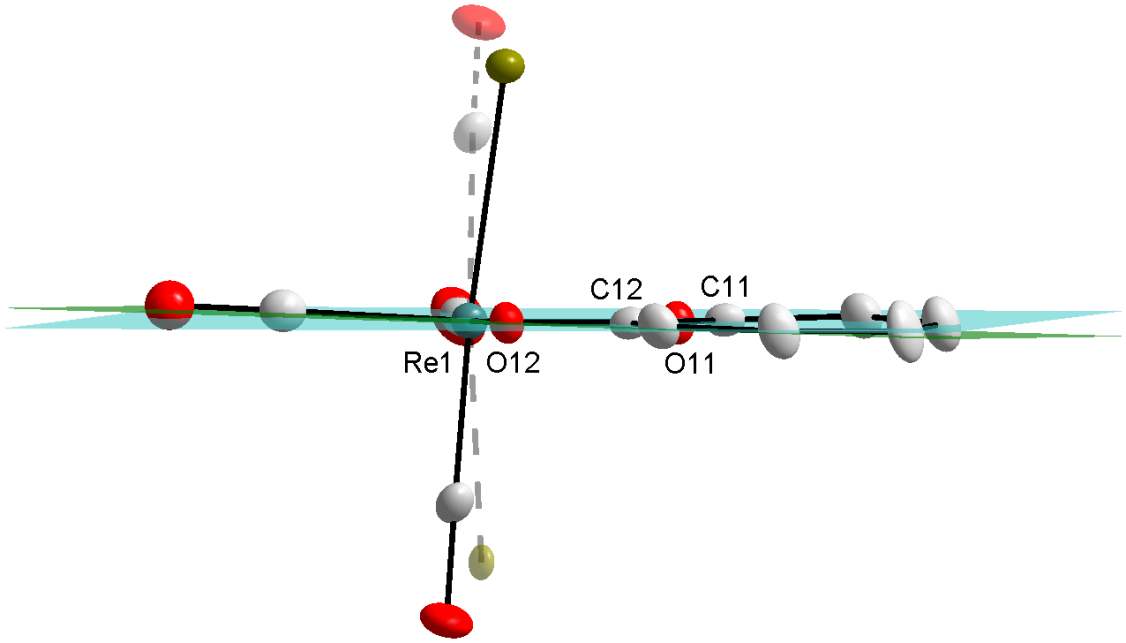


An array of C-H…O and C-H…Br hydrogen-bonding interactions between the cations and neighbouring Rhenate anions stabilize the crystal packing. The hydrogen bonds observed in *fac*-[$NEt_4$][Re(Trop)$(CO)_3$(Br)] are illustrated in Figure 4.3 with the distances, angles and symmetry operators summarized in Table 4.6.

**Figure 4.3: Hydrogen bonds observed in *fac*-[$NEt_4$][Re(Trop)$(CO)_3$(Br)] (1), viewed along the c-axis. Hydrogen atoms, not taking part in the hydrogen bonds, are omitted for clarity.**

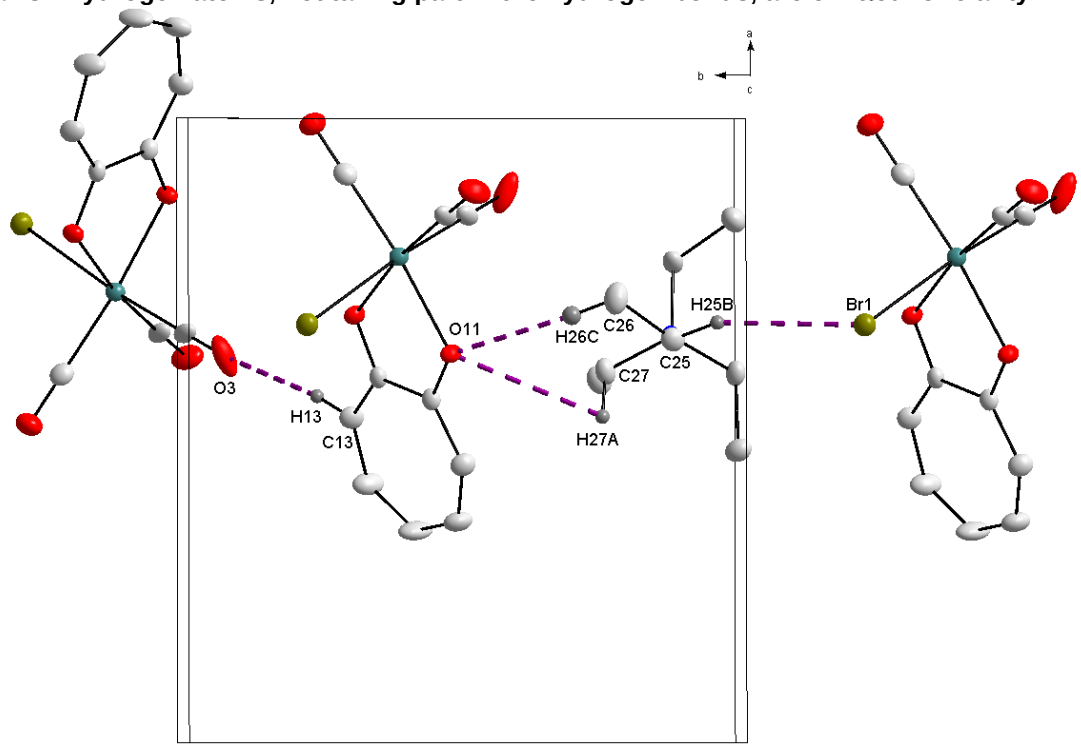


**Table 4.6: Summary of the hydrogen bond distances (Å) and angles (°) observed in *fac*-[$NEt_4$][Re(Trop)$(CO)_3$(Br)] (1).**

| D-H…A | d (D-H) | d (H…A) | d (D…A) | D-H…A angle |
|---|---|---|---|---|
| C13-H13…O3A[a] | 0.93 | 2.43 | 3.344(7) | 169 |
| C25-H25A…Br1A[b] | 0.97 | 2.89 | 3.809(5) | 157.7 |
| C26-H26C…O11 | 0.96 | 2.58 | 3.542(7) | 176.2 |
| C27-H27B…O11 | 0.97 | 2.57 | 3.401(6) | 143.4 |

Symmetry codes, transformations used to generate equivalent atoms:
[a] -x + 3/2, y + 1/2, -z + ½; [b] x, y - 1, z

The metal complex packs in a head-to-head fashion along the a,b-plane, as illustrated in Figure 4.4. The hydrogen atoms as well as the tetraethylammonium cations are omitted for clarity.

**Figure 4.4: Packing of *fac*-[$NEt_4$][Re(Trop)$(CO)_3$(Br)] (1) complex in the unit cell, viewed along the c-axis. Hydrogen atoms and cations are omitted for clarity.**

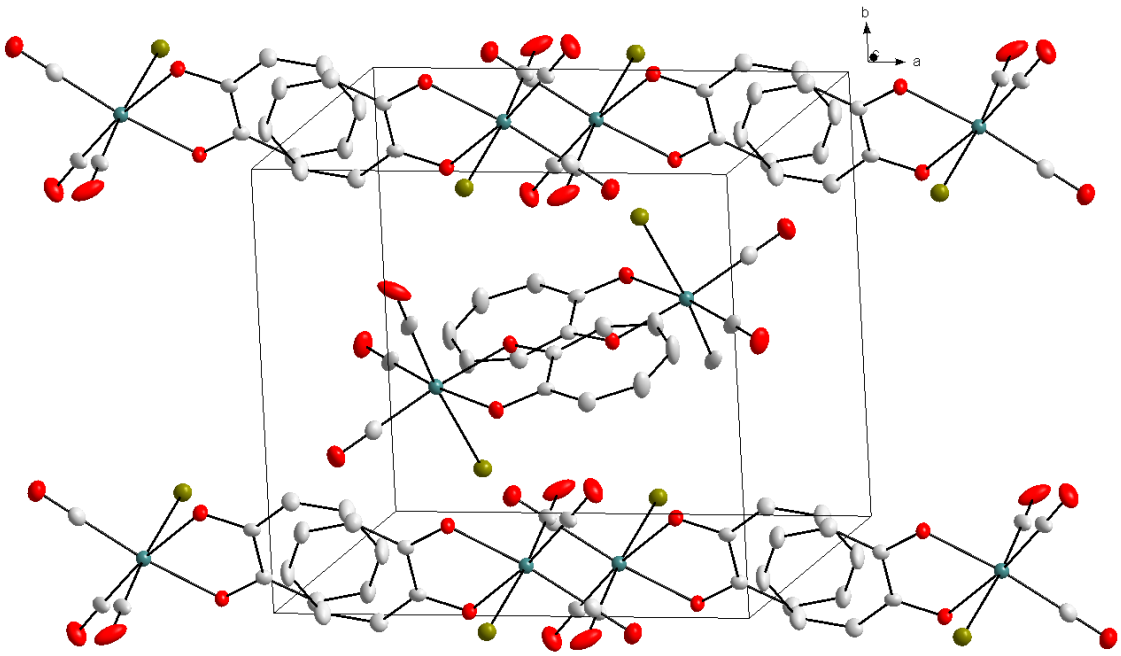


## 4.4 Crystal structure of *fac*-[$NEt_4$][Re(Trop)$(CO)_3(H_2O)$].$NO_3$.$H_2O$ (2)

The title compound was synthesized as described in Paragraph 3.5.4. *fac*-[$NEt_4$][Re(Trop)$(CO)_3(H_2O)$].$NO_3$.$H_2O$ crystallized in the monoclinic $P2_1/c$ space group with a neutral Rhenium(I) compound, a tetraethylammonium cation, a nitrate anion and a solvate water molecule in the asymmetric unit. The diffraction images of *fac*-[$NEt_4$][Re(Trop)$(CO)_3(H_2O)$].$NO_3$.$H_2O$ were integrated as a non-merohedral twin (ratio 89:11).[17] The two components are related by a 20.92 ° rotation around the hkl: 0.9980 0.0624 -0.0081. In the refinement, only the major component was considered.

The N1 and N2 atoms, of the nitrate and the tetraethylammonium ions respectively, are located on inversion centres. This causes the nitrate and the tetraethylammonium ions to exhibit a positional disorder in a 0.5:0.5 ratio. In the structure of *fac*-

[17] Herbst-Irmer, R., Sheldrick, G.M. *Acta Cryst*. **1998**, *B54*, 443-449.

$[NEt_4][Re(Trop)(CO)_3(H_2O)].NO_3.H_2O$, the Re(I) centre is surrounded by three facially orientated carbonyl ligands, a tropolonato bidentate ligand and an aqua ligand.

A molecular diagram with the numbering scheme for *fac*-$[NEt_4][Re(Trop)(CO)_3(H_2O)].NO_3.H_2O$ is illustrated in Figure 4.5 and some selected bond distances and angles are reported in Table 4.7. The hydrogen atoms, cation, anion and solvate water molecule are omitted for clarity (Figure 4.5).

**Figure 4.5: Molecular diagram of *fac*-$[NEt_4[Re(Trop)(CO)_3(H_2O)].NO_3.H_2O$ (2). Hydrogen atoms, cation, anion and solvate molecules omitted for clarity.**

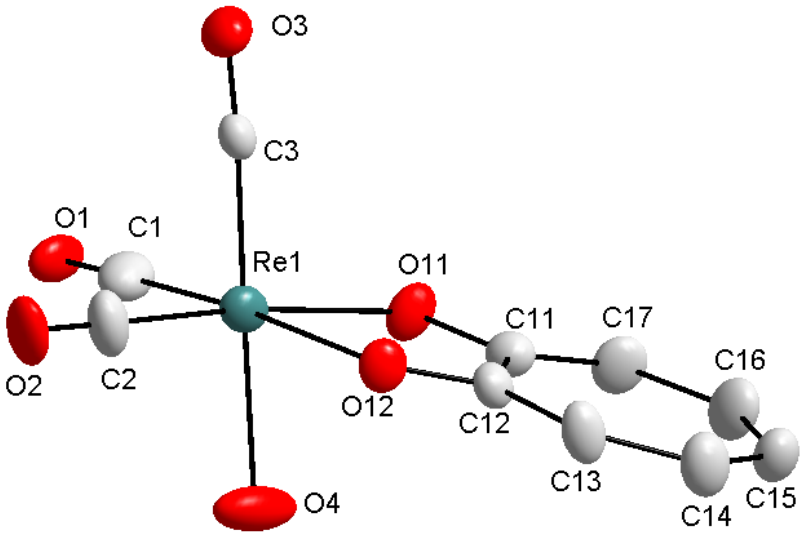


**Table 4.7: Selected bond distances and angles for *fac*-$[NEt_4][Re(Trop)(CO)_3(H_2O)].NO_3.H_2O$ (2).**

| Selected bond lengths (Å) | | Selected bond angles (°) | | Selected torsion angles (°) | |
|---|---|---|---|---|---|
| **Re1-C1** | 1.894(8) | **O11-Re1-O12** | 74.82(17) | **O11-C11-C12-O12** | -0.6(9) |
| **Re1-C2** | 1.886(8) | **C1-Re1-C2** | 87.3(4) | | |
| **Re1-C3** | 1.890(7) | **O4-Re1-O11** | 79.5(2) | | |
| **Re1-O11** | 2.121(5) | **O4-Re1-O12** | 80.38(19) | | |
| **Re1-O12** | 2.108(4) | **O11-Re1-C1** | 100.7(3) | | |
| **Re1-O4** | 2.213(5) | **O12-Re1-C2** | 96.8(3) | | |
| | | **O4-Re1-C3** | 176.8(2) | | |

The Rhenium tricarbonyl distances vary between 1.886 Å to 1.894(8) Å and are well within the normal range.[11-16] The Rhenium to oxygen distances (O11 and O12) of the tropolonato ligand, of 2.121(5) Å and 2.108(4) Å, compare well with similar structures[10,12,13] as well as three other structures reported in this chapter (Paragraph 4.3, 4.5 and 4.6). The Re1-O4 distance of 2.213(5) Å compare well to the tribromotropolonato complex, *fac*-[Re(TropBr$_3$)(CO)$_3$(H$_2$O)].CH$_3$OH with a Rhenium aqua distance of 2.170(5) Å.[14]

The octahedral geometry around the Rhenium(I) core are slightly distorted and can be seen in the angles around the Re(I) core. The angle, O4-Re1-O11, is reported as 79.5(2) °, O11-Re1-C1 as 100.7(3) ° and O4-Re1-C3 as 176.8(2) °. This might be due to the small bite angle of 74.82(18) ° for the tropolonato ligand. This compare well to the bite angle for the tribromotropolonato complex, *fac*-[Re(TropBr$_3$)(CO)$_3$(H$_2$O)].CH$_3$OH, of 74.07(16) ° and also to the other tropolonato compounds reported in this chapter (Paragraph 4.3, 4.5 and 4.6).

The planarity of the tropolonato ring system, O11-O12-C11-C12-C13-C14-C15-C16-C17, is illustrated by the small deviations from the plane through these atoms with the largest deviation being 0.021(6) Å for C17. A dihedral angle of 9.1(2) ° is reported for the angle between the equatorial plane and the plane through the tropolonato ligand, as defined previously. This illustrates the significant twist of the tropolonato ligand from the equatorial plane. The two planes and the planarity of the ligand are illustrated in Figure 4.6, with the hydrogen atoms, anions and solvent molecules omitted for clarity.

The torsion angle, O11-C11-C12-O12, of the tropolonato ligand is almost zero (0.6(9) °), indicating the flexible nature of the ligand, compared to the twist observed in *fac*-[NEt$_4$][Re(Trop)(CO)$_3$(Br)].

**Figure 4.6: Illustration of the equatorial plane and the plane through O11-O12-C11-C12-C13-C14-C15-C16-C17, indicating the planarity of the tropolonato ligand as well as the dihedral angle between these planes in *fac*-[$NEt_4$][$Re(Trop)(CO)_3(H_2O)$].$NO_3$.$H_2O$ (2).**

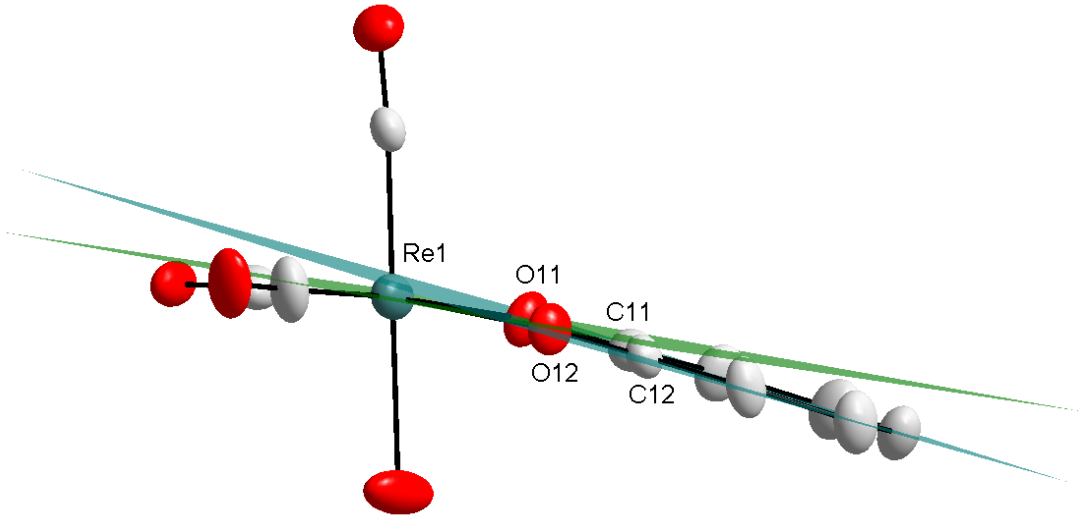


An array of hydrogen bonds are observed in *fac*-[$NEt_4$][$Re(Trop)(CO)_3(H_2O)$].$NO_3$.$H_2O$, two intramolecular (O-H…O) and six intermolecular hydrogen bonds (C-H…O and O-H…O). Figure 4.7 illustrate the hydrogen bonds observed and a summary of the hydrogen bond distances and angles are reported in Table 4.8. Hydrogen atoms not taking part in such interactions are omitted for clarity.

**Figure 4.7: Hydrogen bonds observed in *fac*-[$NEt_4$][Re(Trop)$(CO)_3(H_2O)$].$NO_3$.$H_2O$ (2).**

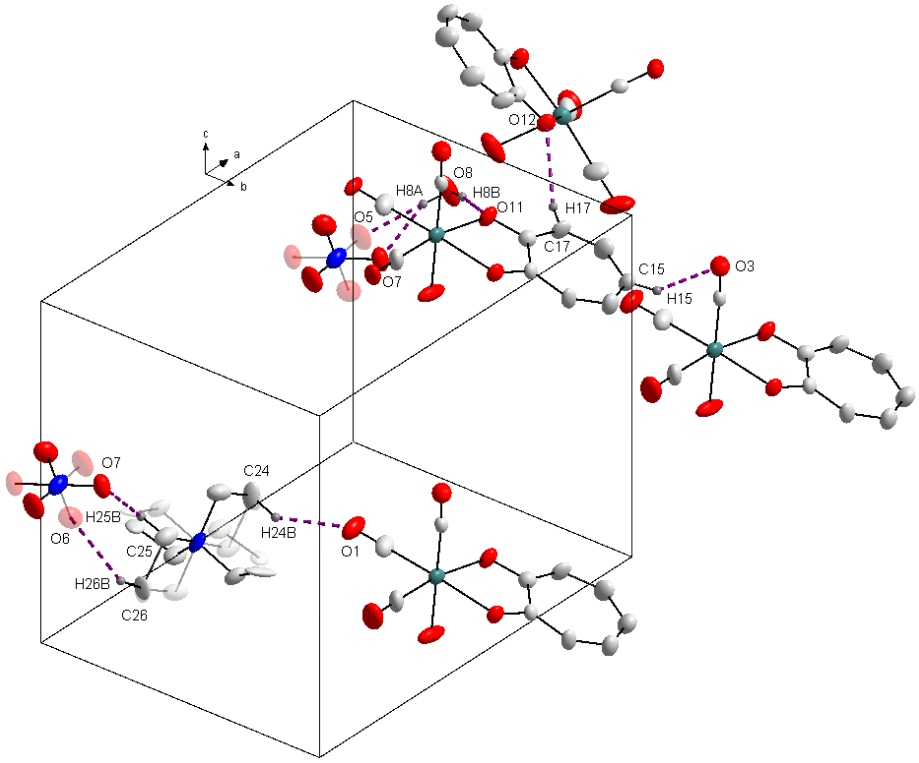


**Table 4.8: Summary of the hydrogen bond distances (Å) and angles (°) observed in *fac*-[$NEt_4$][Re(Trop)$(CO)_3(H_2O)$].$NO_3$.$H_2O$ (2).**

| D-H…A | d (D-H) | d (H…A) | d (D…A) | D-H…A angle |
|---|---|---|---|---|
| O8-H8A…O7 | 0.85(2) | 2.08(5) | 2.847(11) | 151(7) |
| O8-H8A…O5[a] | 0.85(2) | 2.05(2) | 2.898(14) | 178(9) |
| O8-H8B…O11 | 0.85(2) | 1.90(2) | 2.738(7) | 173(7) |
| C15-H15…O3[b] | 0.95 | 2.58 | 3.376(10) | 141.1 |
| C17-H17…O12[c] | 0.95 | 2.50 | 3.346(8) | 147.9 |
| C24-H24B…O1[d] | 0.98 | 2.33 | 3.19(5) | 146.5 |
| C25-H25B…O7[e] | 0.99 | 2.46 | 2.91(2) | 107.6 |
| C26-H26B…O6[f] | 0.98 | 2.60 | 3.45(5) | 145.7 |

[a] 1 - x, 1 - y, 2 - z; [b] x, 1 + y, z; [c] x, 1.5 - y, 0.5 + z; [d] x, y, -1 + z; [e] x, -1 + y, -1 + z; [f] 1 - x, -y, 1 - z

The packing in the unit cell is illustrated in Figure 4.8. The Rhenium(I) units pack in alternating orientations along the a,b-plane, in a head-to-head fashion. The hydrogen atoms, tetraethylammonium cations, nitrate anions and solvent water molecules are omitted for clarity.

**Figure 4.8: Packing of *fac*-[$NEt_4$][Re(Trop)$(CO)_3(H_2O)$].$NO_3$.$H_2O$ (2) in the unit cell, viewed along the b-axis. Hydrogen atoms, anions and solvent molecules are omitted for clarity.**

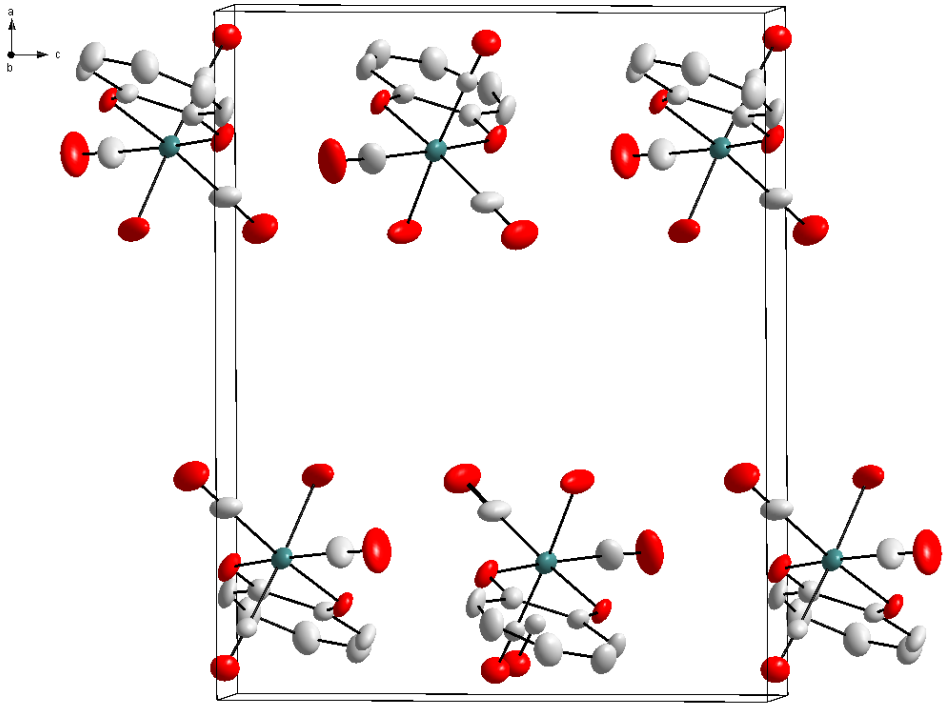


## 4.5 Crystal structure of *fac*-[Re(Trop)$(CO)_3$(Py)] (3)

The neutral complex, *fac*-[Re(Trop)$(CO)_3$(Py)], was synthesized as described in Paragraph 3.5.6 and the yellow crystals were grown from a methanol solution of the product.

*fac*-[Re(Trop)$(CO)_3$(Py)] crystallized in the monoclinic $P2_1/c$ space group, with four molecules in the asymmetric unit. The Re(I) centre is surrounded by three facially coordinated carbonyl ligands, a tropolonato bidentate ligand and a pyridine ligand in the sixth position. A summary of the general crystal data of *fac*-[Re(Trop)$(CO)_3$(Py)] is given in Table 4.1. A molecular diagram with the numbering scheme is given in Figure 4.9, with the hydrogen atoms omitted for clarity. Some of the bond distances and angles were selected and are reported in Table 4.9.

**Figure 4.9: Molecular representation of the crystal structure of *fac*-[Re(Trop)(CO)$_3$(Py)] (3), hydrogen atoms omitted for clarity.**

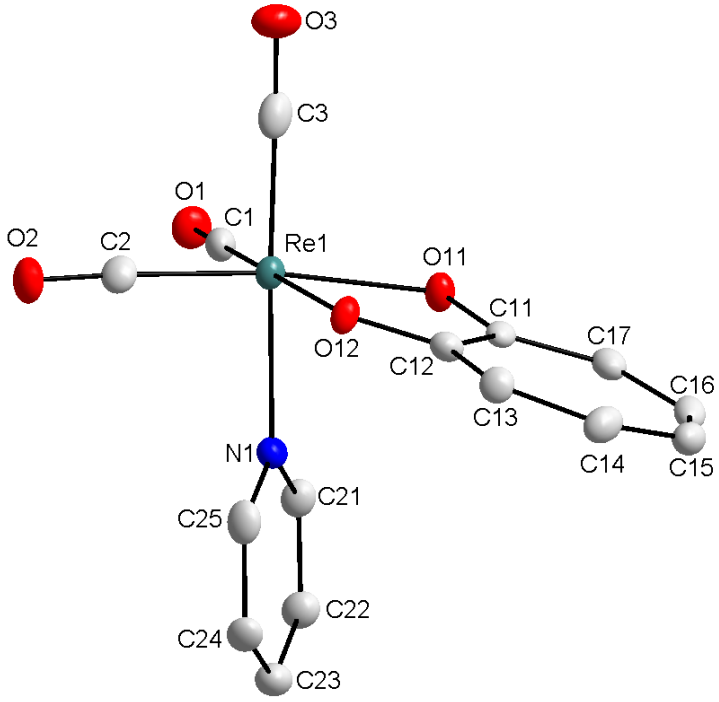


**Table 4.9: Selected bond lengths and angles for the crystal structure of *fac*-[Re(Trop)(CO)$_3$(Py)] (3).**

| Selected bond lengths (Å) | | Selected bond angles (°) | | Selected torsion angles (°) | |
|---|---|---|---|---|---|
| **Re1-C1** | 1.898(5) | **O11-Re1-O12** | 74.68(14) | **O11-C11-C12-O12** | 0.6(7) |
| **Re1-C2** | 1.909(6) | **C1-Re1-C2** | 87.3(2) | | |
| **Re1-C3** | 1.930(6) | **N1-Re1-O11** | 81.66(15) | | |
| **Re1-O11** | 2.121(4) | **N1-Re1-O12** | 82.03(15) | | |
| **Re1-O12** | 2.136(3) | **C3-Re1-O11** | 95.96(19) | | |
| **Re1-N1** | 2.208(4) | **O11-Re1-C1** | 98.01(18) | | |
| | | **O12-Re1-C2** | 99.7(2) | | |
| | | **C3-Re1-N1** | 177.55(18) | | |

The Rhenium to carbonyl ligand distances are within normal range.[11-16] The 'axial' Re1-N1 distance of 2.208(4) Å compare well with other Rhenium(I) – pyridine distances. Some examples include a distance of 2.209(2) Å reported by Benny *et al.*[18], 2.220(5) Å by Casanova *et al*.[19] and 2.216(4) Å by Franklin *et al*.[20] The Rhenium to tropolonato

[18] Benny, P.D., Fugate, G.A., Barden, A.O., Morley, J.E., Silva-Lopez, E., Twamley, B. *Inorg. Chem*. **2008**, *47*, 2240-2242.
[19] Casanova, M., Zangrondo, E., Munini, F., Iengo, E., Alessio, E. *Dalton Trans*. **2006**, 5033-5045.

distances of 2.121(4) Å and 2.136(3) Å correspond well with that of the *fac*-[$NEt_4$][Re(Trop)$(CO)_3$Br] structure described in Paragraph 4.3, i.e. 2.126(3) Å *vs* 2.135(3) Å. The octahedral geometry around the Re(I) centre is slightly distorted due to the small bite angle, O11-Re1-O12, of 74.68(14) °. This is seen in the angles around the Re(I) core of 81.66(15) ° (N1-Re1-O11), 98.01(18) ° (O11-Re1-C1) and 99.7(2) ° (O12-Re1-C2).

The planarity of the tropolonato ring, O11-C11-C12-C13-C14-C15-C16-C17-O12, is illustrated by the very small deviations of all the atoms from the plane. The largest deviation from the plane is 0.042(4) Å for C16. A dihedral angle of 12.9(2) ° is reported between the equatorial plane and the plane through the tropolonato ligand, as defined previously. From this it is clear that the ligand system is significantly 'bent' away from the equatorial plane. In Figure 4.10 this dihedral angle is illustrated as well as the planarity of the ligand system.

The tropolonato ligand coordinates to the Re(I) core with a torsion angle, O11-C11-C12-O12, of 0.6(7) °.

[20] Franklin, B.R., Herrick, R.S., Ziegler, C.J., Cetin, A., Barone, N., London, L.R. *Inorg. Chem*. **2008**, *47*, 5902-5909.

**Figure 4.10: Illustration of the plane through the tropolonato ligand system in *fac*-[Re(Trop)(CO)$_3$(Py)] (3).**

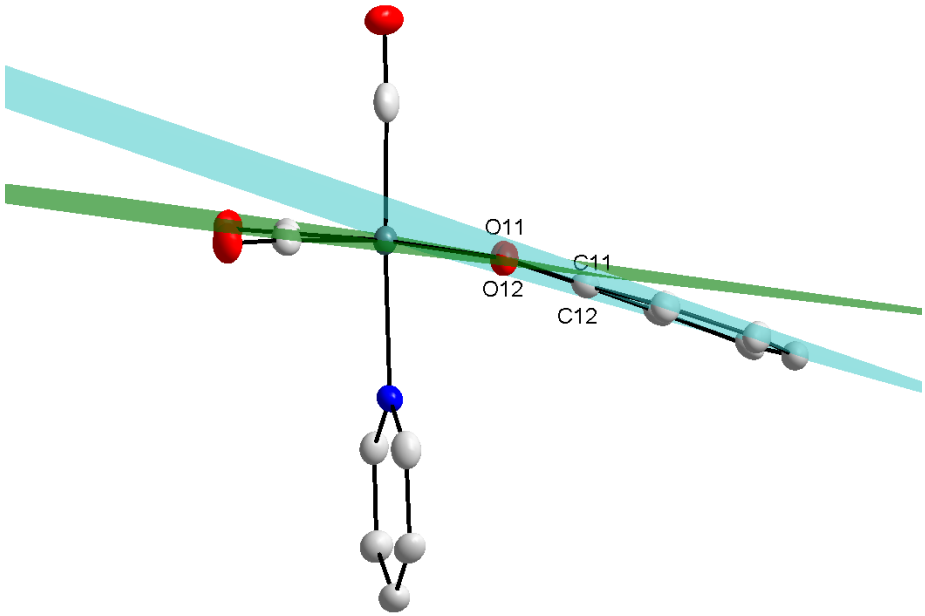


Three C-H…O hydrogen bonds are observed in the crystal structure of *fac*-[Re(Trop)(CO)$_3$(Py)]. All three of these hydrogen bonds are intermolecular bonds from the coordinated pyridine ring. Two of the hydrogen bonds observed bond toward an equatorial carbonyl oxygen of the next molecule and the other one to an oxygen atom of a coordinated tropolonato ligand from another molecule. To illustrate this, Figure 4.11 presents the hydrogen bonds present in this structure while Table 4.10 contains a summary of the angles and distances of the hydrogen bonds.

**Figure 4.11: Hydrogen bonds observed in *fac*-[Re(Trop)(CO)$_3$(Py)] (3). Hydrogen atoms, not taking part in the hydrogen bonds, are omitted for clarity.**

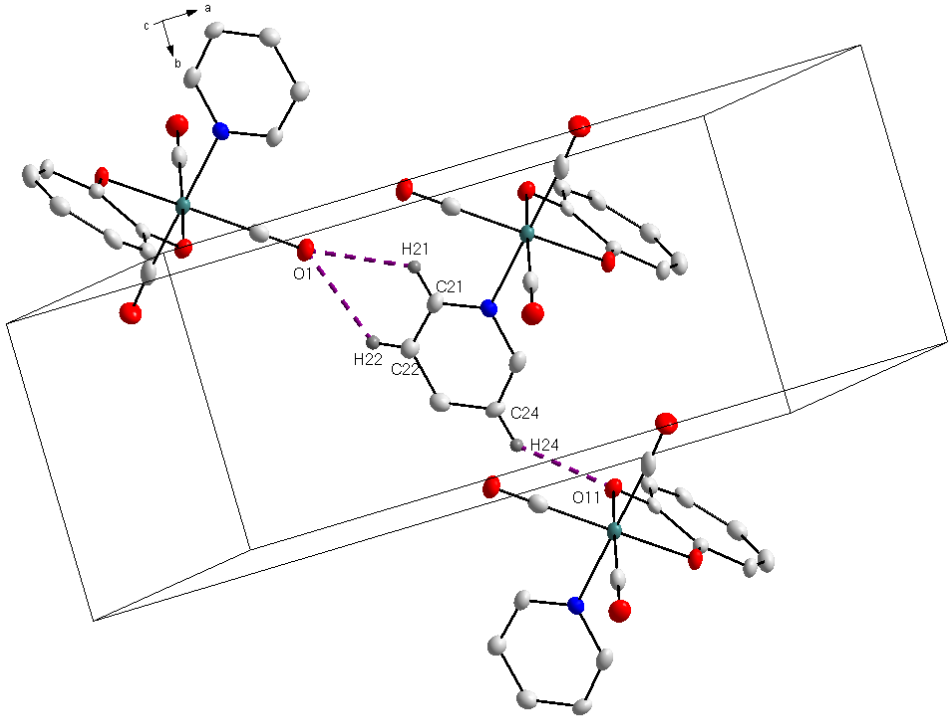


**Table 4.10: Hydrogen bond angles and distances (°, Å) for *fac*-[Re(Trop)(CO)$_3$(Py)] (3).**

| D-H…A | d (D-H) | d (H…A) | d (D…A) | D-H…A angle |
|---|---|---|---|---|
| C21-H21…O1[a] | 0.93 | 2.58 | 3.198(7) | 124.3 |
| C22-H22…O1[a] | 0.93 | 2.58 | 3.187(7) | 123.1 |
| C24-H24…O11[b] | 0.93 | 2.40 | 3.178(7) | 141.6 |

Symmetry codes, transformations used to generate equivalent atoms:
[a] 1 - x, -y, 2 - z; [b] x, 1 + y, z

The molecules pack in a head-to-head fashion, in alternating ‘columns’, along the a-axis. This is illustrated in Figure 4.12 where the hydrogen atoms are omitted for clarity.

**Figure 4.12: Packing of *fac*-[Re(Trop)(CO)$_3$(Py)] (3) in the unit cell, viewed along the b-axis.**

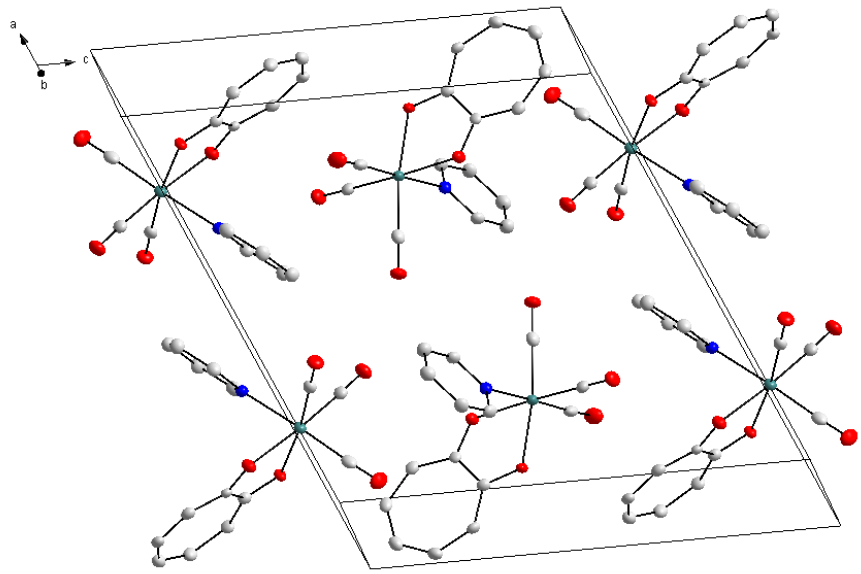


# 4.6 Crystal structure of *fac*-[Re(Trop)(CO)$_3$(DMAP)] (4)

The neutral Rhenium(I) compound, *fac*-[Re(Trop)(CO)$_3$(DMAP)], was synthesized as reported in Paragraph 3.5.9. The yellow crystals were grown from the a methanol solution of the product.

*fac*-[Re(Trop)(CO)$_3$(DMAP)] crystallizes in the monoclinic $P2_1/n$ space group with 4 molecules in the asymmetric unit. The Rhenium(I) centre is surrounded by three facial carbonyl ligands, a tropolonato ligand and a 4-dimethylaminopyridine ligand in the axial position. In Table 4.2, a summary of the general crystal data of *fac*-[Re(Trop)(CO)$_3$(DMAP)] is given. A molecular diagram with the numbering scheme is reported in Figure 4.13 with the hydrogen atoms omitted for clarity. Some of the selected bond distances and bond angles are reported in Table 4.11.

**Figure 4.13: Molecular representation of the crystal structure of *fac*-[Re(Trop)(CO)$_3$(DMAP)] (4), hydrogen atoms omitted for clarity.**

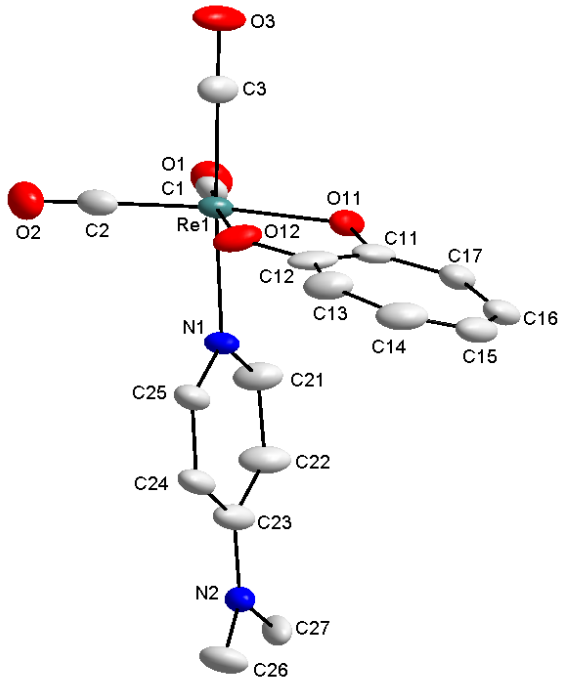


**Table 4.11: Selected bond distances and bond angles of *fac*-[Re(Trop)(CO)$_3$(DMAP)] (4).**

| Selected bond distances (Å) | | Selected bond angles (°) | | Selected torsion angles (°) | |
|---|---|---|---|---|---|
| **Re1-C1** | 1.893(6) | **O11-Re1-O12** | 74.90(18) | **O11-C11-C12-O12** | -3.2(8) |
| **Re1-C2** | 1.915(7) | **C1-Re1-C2** | 87.4(2) | | |
| **Re1-C3** | 1.916(6) | **N1-Re1-O11** | 81.20(17) | | |
| **Re1-O11** | 2.129(4) | **N1-Re1-O12** | 82.01(16) | | |
| **Re1-O12** | 2.121(4) | **C3-Re1-O11** | 95.5(2) | | |
| **Re1-N1** | 2.205(4) | **O11-Re1-C1** | 97.3(2) | | |
| | | **O12-Re1-C2** | 100.1(2) | | |
| | | **C3-Re1-N1** | 176.6(2) | | |

The Rhenium to carbonyl ligand distances, varying from 1.893(6) Å to 1.916(6) Å, are well within the normal range.[11-16] The Rhenium to bidentate oxygen distances, O11 and O12, of 2.129(4) Å and 2.121(4) Å compare well with other Re(I) structures with O,O-bidentate ligands[10,12,13] as well as the two analogous structures reported in Paragraph 4.3, 4.4 and 4.5. The Rhenium(I) to N1 (DMAP) distance of 2.205(4) Å match well with a similar Rhenium(I) tricarbonyl structure reported by Garcia *et al*.[21]

[21] Garcia, R., Domingos, A., Paulo, A., Santos, I., Alberto, R. *Inorg. Chem*. **2002**, *41*, 2422-2428.

The octahedral geometry around the Rhenium(I) centre is slightly distorted which might be due to the small bite angle of 74.90(18) ° for O11-Re1-O12. This is clear from the angles N1-Re1-O11 of 81.20(17) °, O12-Re1-C2 of 100.1(2) ° and O11-Re1-C1 of 97.3(2) °.

The planarity of the tropolonato ligand system, O11-C11-C12-C13-C14-C15-C16-C17-O12, is illustrated by the very small deviations of all the atoms from the plane (largest deviation from the plane is 0.071(4) Å for O12). A dihedral angle of 11.7(2) ° is reported between the equatorial plane and the plane through the ligand system, as previously defined. From this dihedral angle, it is seen that the tropolonato ligand is significantly 'bent' out of the equatorial plane. This is illustrated in Figure 4.14.

The tropolonato ligand coordinates to the Re(I) core with a torsion angle, O11-C11-C12-O12, reported as -3.2(8) °.

**Figure 4.14: Illustration of the equatorial plane and the plane through the tropolonato ligand system in *fac*-[Re(Trop)(CO)$_3$(DMAP)] (4).**

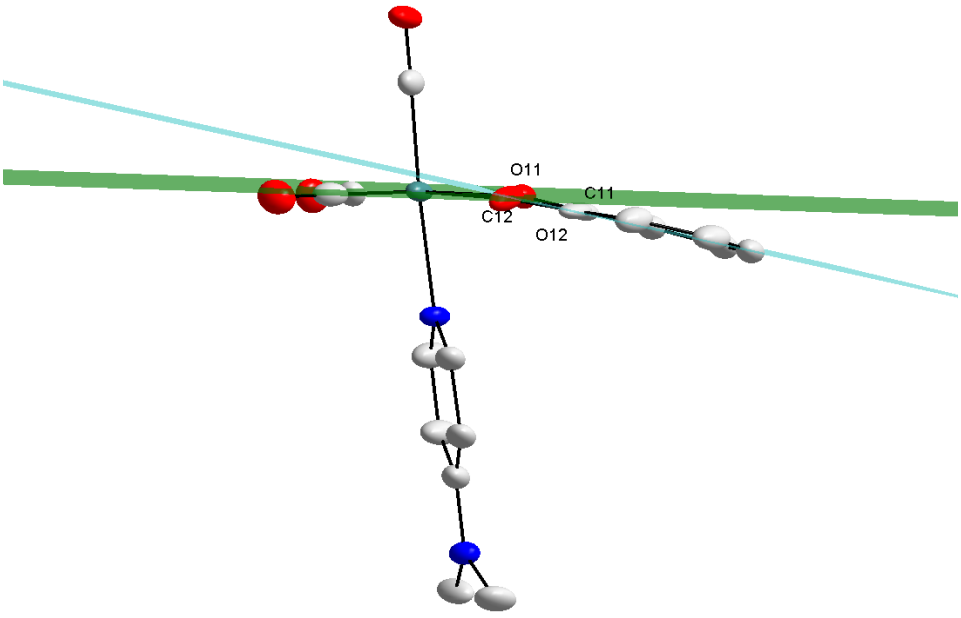


There are four C-H…O hydrogen-bonding interactions present in the crystal structure of *fac*-[Re(Trop)(CO)$_3$(DMAP)], three intermolecular hydrogen bonds to three separate

Rhenium units and one intramolecular hydrogen bond. This is illustrated in Figure 4.15 with the hydrogen bond distances and angles summarized in Table 4.12

**Figure 4.15: Hydrogen bonds in *fac*-[Re(Trop)(CO)$_3$(DMAP)] (4). Hydrogen atoms, not taking part in the hydrogen bonds, are omitted for clarity.**

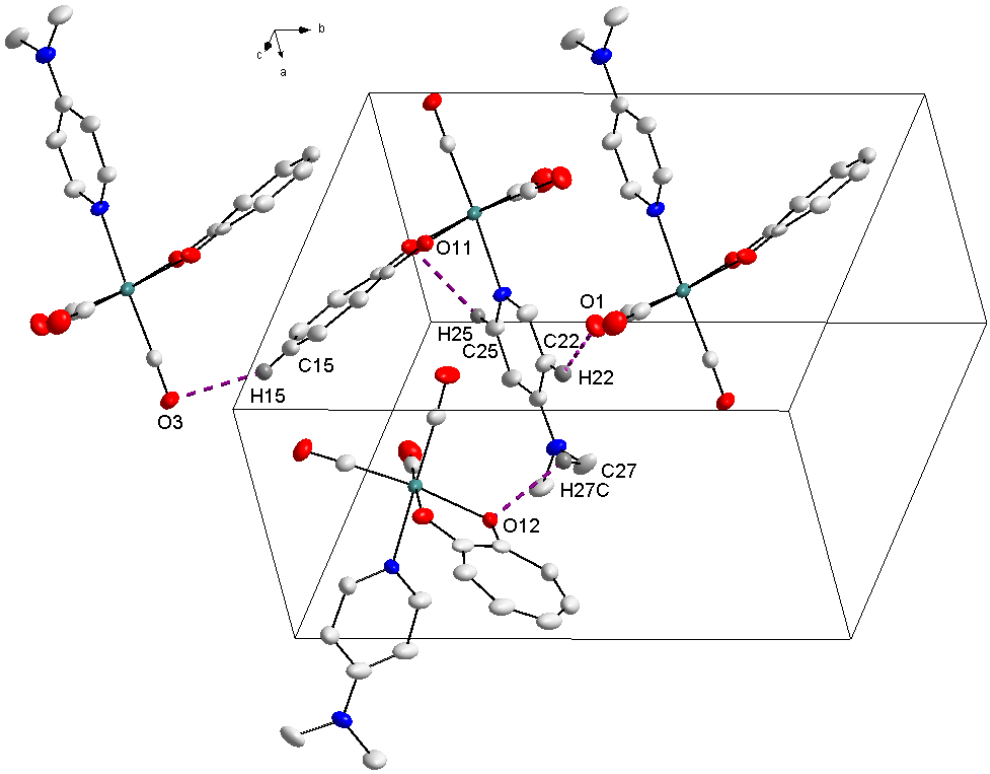


**Table 4.12: Hydrogen bond distances and angles (Å, °) for *fac*-[Re(Trop)(CO)$_3$(DMAP)] (4).**

| D-H…A | d (D-H) | d (H…A) | d (D…A) | D-H…A angle |
|---|---|---|---|---|
| C15-H15…O3[a] | 0.93 | 2.58 | 3.449(8) | 155.4 |
| C22-H22…O1[b] | 0.93 | 2.58 | 3.297(9) | 134.1 |
| C25-H25…O12 | 0.93 | 2.57 | 2.994(7) | 108.4 |
| C27-H27C…O12[c] | 0.96 | 2.55 | 3.229(8) | 128.0 |

Symmetry codes, transformations used to generate equivalent atoms:
[a] -x, -y, 1 - z; [b] -x, 1 - y, 1 - z; [c] 0.5 + x, 0.5 - y, 0.5 + z

The Rhenium units pack in an alternating head-to-head fashion along the b,c-plane. This is illustrated in Figure 4.16, where the hydrogen atoms are omitted for clarity.

**Figure 4.16: Packing of *fac*-[Re(Trop)(CO)$_3$(DMAP)] (4) in the unit cell, viewed along the a-axis. Hydrogen atoms omitted for clarity.**

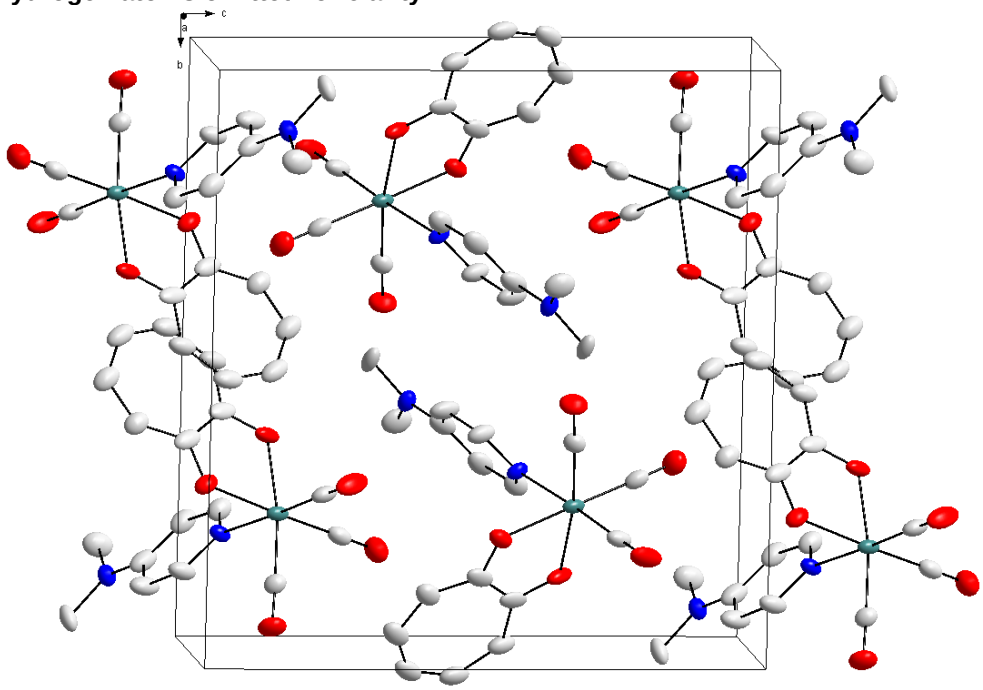


## 4.7 Crystal structure of *fac*-[NEt$_4$][Re(2,5-PicoH)(CO)$_3$(Br)].H$_2$O (5)

The title compound was synthesized as described in 3.5.12. The yellow cuboid crystals were obtained from a methanol solution of the product.

*fac*-[NEt$_4$][Re(2,5-PicoH)(CO)$_3$(Br)] crystallizes in the monoclinic *Cc* space group with an anionic *fac*-[Re(2,5-PicoH)(CO)$_3$(Br)]$^-$ metal unit, a [NEt$_4$]$^+$ counterion and a water solvent molecule in the asymmetric unit. The Rhenium(I) metal centre is octahedrally surrounded by three facially orientated carbonyl ligands, a pyridine-2-carboxylato-5-carboxylic acid bidentate ligand and a bromido ligand. A summary of the crystal data of this crystal is reported in Table 4.2.

**Figure 4.17: Molecular diagram and numbering scheme of *fac*-[$NEt_4$][Re(2,5-PicoH)$(CO)_3$(Br)].$H_2O$ (5). Hydrogen atoms, cation and solvate molecule are omitted for clarity.**

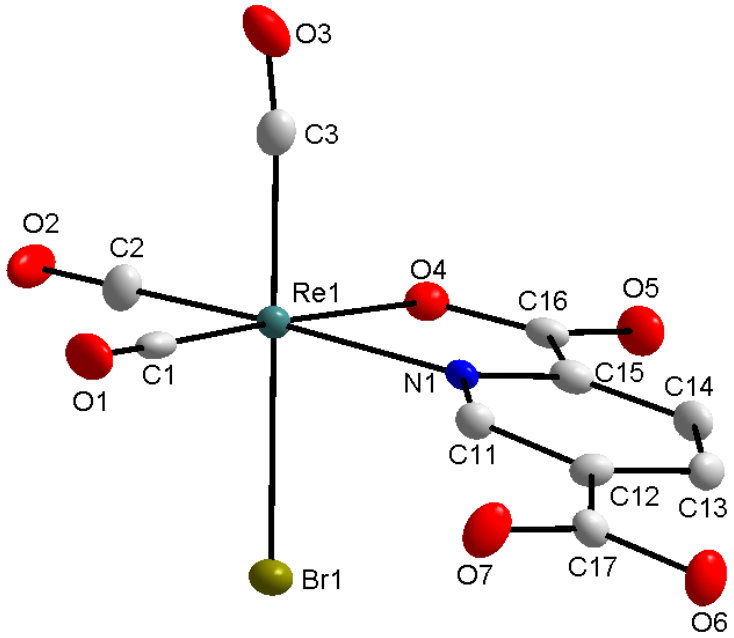


The molecular diagram and the numbering scheme is illustrated in Figure 4.17, for *fac*-[$NEt_4$][Re(2,5-PicoH)$(CO)_3$(Br)].$H_2O$, with the cation and solvent molecule omitted for clarity. Some of the selected bond distances and bond angles are reported in Table 4.13 below.

**Table 4.13: Selected bond distances and bond angles of *fac*-[$NEt_4$][Re(2,5-PicoH)$(CO)_3$(Br)].$H_2O$ (5).**

| Selected bond distances (Å) | | Selected bond angles (°) | | Selected torsion angles (°) | |
|---|---|---|---|---|---|
| **Re1-C1** | 1.906(7) | **O4-Re1-N1** | 74.38(18) | **N1-C15-C16-O4** | 0.8(9) |
| **Re1-C2** | 1.904(7) | **C1-Re1-C2** | 89.3(3) | | |
| **Re1-C3** | 1.963(8) | **Br1-Re1-N1** | 82.99(14) | | |
| **Re1-O4** | 2.152(15) | **Br1-Re1-O4** | 86.60(13) | | |
| **Re1-N1** | 2.182(5) | **C3-Re1-O4** | 94.6(2) | | |
| **Re1-Br1** | 2.6188(13) | **N1-Re1-C1** | 98.4(2) | | |
| | | **O4-Re1-C2** | 97.9(2) | | |
| | | **C3-Re1-Br1** | 178.1(2) | | |

The three Rhenium to carbonyl bond distances of 1.906(7) Å, 1.904(7) Å and 1.963(8) Å (for C1, C2 and C3) are well within the normal range.[11-16] The Re1-Br1 bond distance of 2.6188(13) Å compare well with that of similar structures[10,11,13] and (**1**) described in Paragraph 4.3. The Re1 to O4 and N1 distances, 2.152(15) Å and 2.182(5) Å

respectively, compare well with the values of the similar structure of *fac*-[Re(2,4-PicoH)$(CO)_3(H_2O)$] (2,4-PicoH = pyridine-2-carboxylato-4-carboxylic acid) of 2.153(3)/2.148(3) Å and 2.180(4)/2.166(4) Å for the Re-O and Re-N distances, respectively[12].

The small bite angle of 74.38(18) °, O4-Re1-N1, might be the reason for the slight distortion of the octahedral geometry around the Rhenium(I) centre. The distortion is seen in the angles around the Re(I) core, like 82.99(14) ° for Br1-Re1-N1, 98.4(2) ° for N1-Re1-C1 and 97.9(2) ° for O4-Re1-C2.

The planarity of the system, C11-C12-C13-C14-C15-C16-O4-N1, is illustrated by the small deviations of all the atoms from this plane (largest deviation is 0.057(4) Å for O4). The dihedral angle between the equatorial plane and the plane through the ligand system, defined before, is calculated as 7.7(3) °. The two planes identified in *fac*-$[NEt_4][Re(2,5\text{-PicoH})(CO)_3(Br)].H_2O$ as well as the dihedral angle is illustrated in Figure 4.18. The significant 'bending' of the tropolonato ligand system from the equatorial plane is also illustrated.

The torsion angle, N1-C15-C16-O4, of the tropolonato ligand system is reported as 0.8(9) °.

**Figure 4.18: Illustration of the planes identified in *fac*-[NEt4][Re(2,5-PicoH)(CO)$_3$(Br)].H$_2$O (5).**

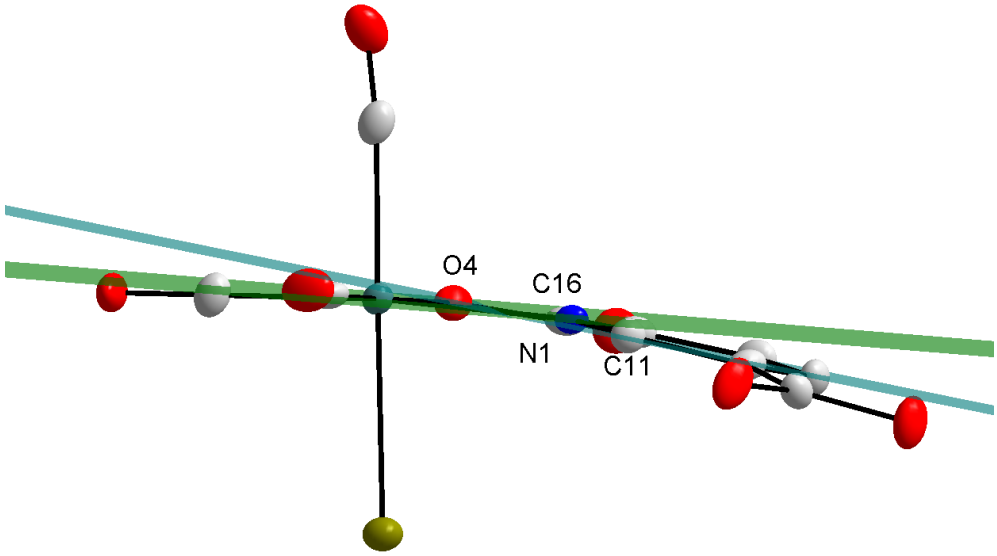


There are six hydrogen bonds observed in *fac*-[NEt$_4$][Re(2,5-PicoH)(CO)$_3$(Br)].H$_2$O, illustrated in Figure 4.19. There are two O-H…O and one C-H…O intramolecular hydrogen bonds observed in the structure. Three intermolecular hydrogen bonds are observed – one C-H…Br, one C-H…O and one O-H…O hydrogen bond. An array of hydrogen bonds between the Rhenate anions, water solvent molecule, cations and the neighbouring Rhenate anions seem to stabilize the crystal packing. The hydrogen bond distances and angles for *fac*-[NEt$_4$][Re(2,5-PicoH)(CO)$_3$(Br)].H$_2$O are reported in Table 4.14.

**Figure 4.19: Hydrogen bonds observed for *fac*-[$NEt_4$][Re(2,5-PicoH)$(CO)_3$(Br)].$H_2O$ (5).**

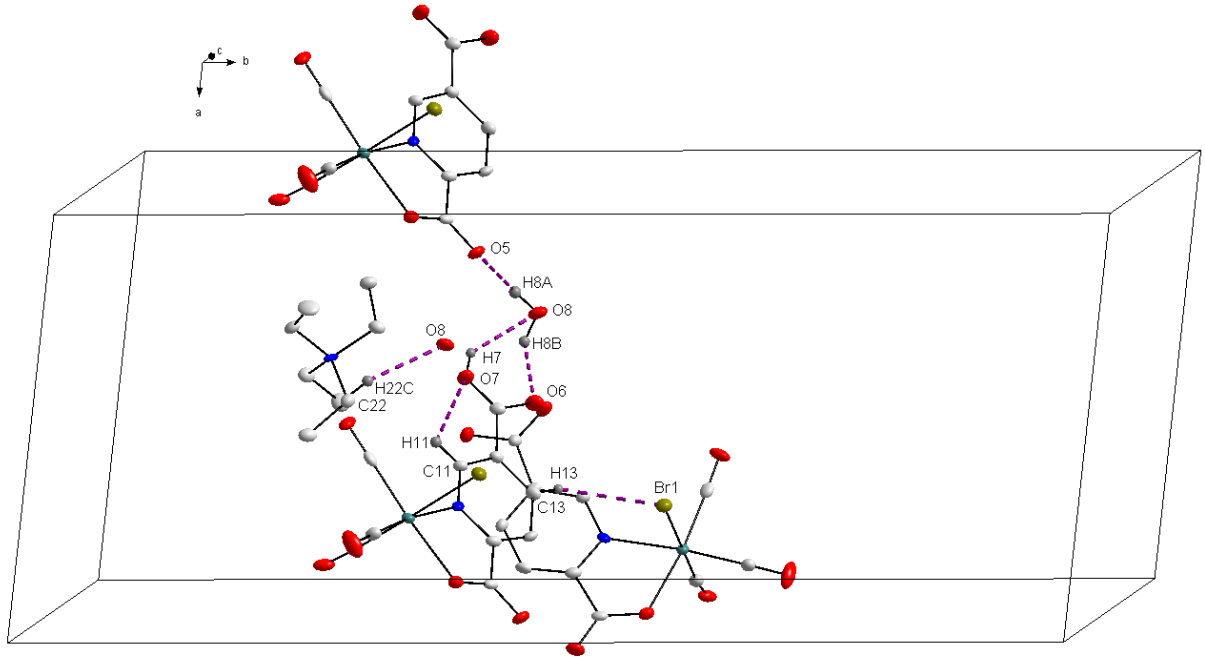


**Table 4.14: Hydrogen bond distances and angles (Å, °) of *fac*-[$NEt_4$][Re(2,5-PicoH)$(CO)_3$(Br)].$H_2O$ (5).**

| D-H…A | d (D-H) | d (H…A) | d (D…A) | D-H…A angle |
|---|---|---|---|---|
| O7-H7…O8 | 0.82 | 2.51 | 3.192(7) | 141.0 |
| O8-H8B…O6 | 0.852(5) | 1.87(6) | 2.550(7) | 135(8) |
| C11-H11…O7 | 0.93 | 2.43 | 2.766(8) | 100.9 |
| C13-H13…Br1[a] | 0.93 | 2.88 | 3.613(7) | 136(4) |
| C22-H22C…O8[a] | 0.96 | 2.50 | 3.436(10) | 165.6 |
| O8-H8A…O5[b] | 0.851(5) | 2.08(5) | 2.830(8) | 148(8) |

Symmetry codes, transformations used to generate equivalent atoms:
[a] x, 1 - y, -0.5 + z; [b] -1 + x, y, -1 + z

The Rhenium(I) units pack in a head-to-head fashion in ‘column-like’ structures along the c-axis, as illustrated in Figure 4.20, with hydrogen atoms, the cations and water molecules omitted for clarity. The tetraethylammonium counter ion and the water solvent molecule pack in between the Rhenium(I) units, almost surrounding the metal units. It forms ‘links’ between the Rhenium(I) units, *via* hydrogen bonding (explained above).

**Figure 4.20: Packing in the unit cell of *fac*-[NEt$_4$][Re(2,5-PicoH)(CO)$_3$(Br)].H$_2$O (5), viewed along the c-axis.**

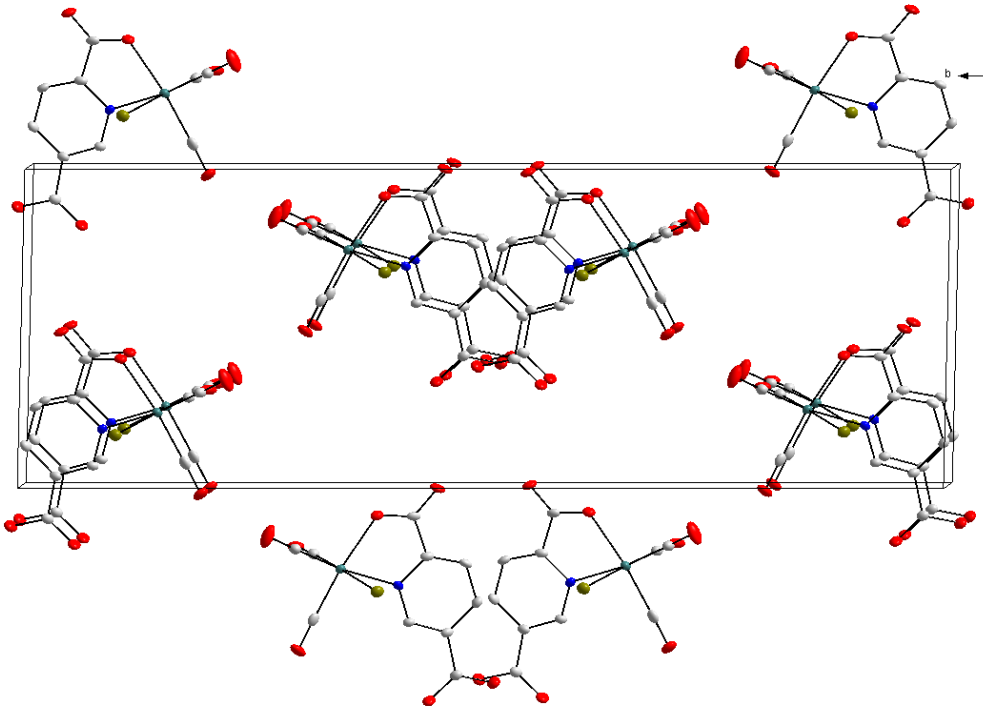

# 4.8 Crystal structure of *fac*-[NEt$_4$][Re(2,5-PicoMe)(CO)$_3$(Br)] (6)

*fac*-[NEt$_4$][Re(2,5-PicoMe)(CO)$_3$(Br)] was synthesized as described in Paragraph 3.5.20 and the yellow crystals were grown from the reaction mixture in methanol.

The compound crystallizes in the monoclinic *C*2/c space group with two ionic fragments independent of the other in the asymmetric unit, an anionic Rhenium compound and a tetraethylammonium cation. The Rhenium(I) metal centre is coordinated to three facial carbonyl ligands, a pyridine-2-carboxylato-5-carboxylic acid 5-methylester bidentate ligand as well as a bromido ligand. A summary of the general crystal data for *fac*-[NEt$_4$][Re(2,5-PicoMe)(CO)$_3$(Br)] is reported in Table 4.2. A molecular diagram, indicating the numbering scheme is illustrated in Figure 4.21 with the hydrogen atoms and cation omitted for clarity. Some selected bond distances and angles are reported in Table 4.15 below.

**Figure 4.21: Molecular diagram and numbering scheme of *fac*-[$NEt_4$][Re(2,5-PicoMe)$(CO)_3$(Br)] (6), with the hydrogen atoms and cation omitted for clarity.**

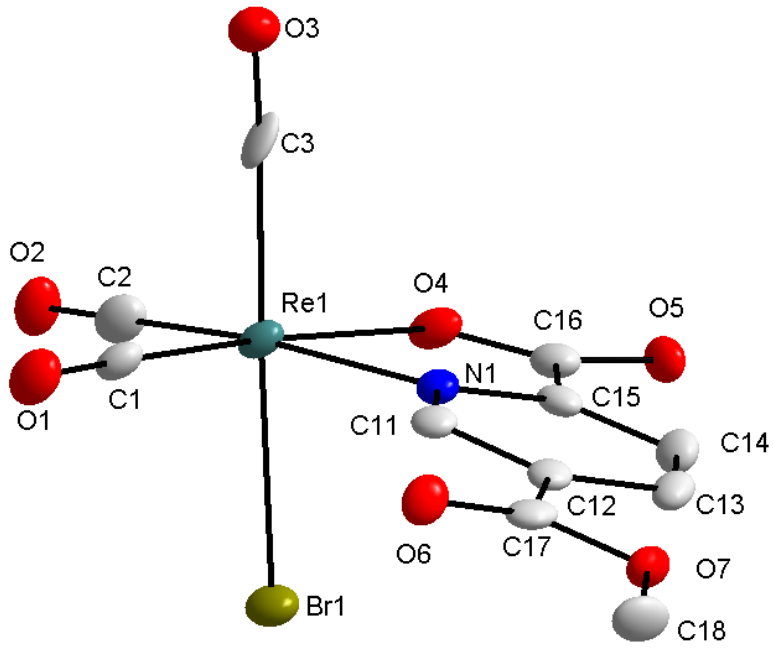


**Table 4.15: Selected bond distances and angles of *fac*-[$NEt_4$][Re(2,5-PicoMe)$(CO)_3$(Br)] (6).**

| Selected bond distances (Å) | | Selected bond angles (°) | | Selected torsion angles (°) | |
|---|---|---|---|---|---|
| **Re1-C1** | 1.910(4) | **O4-Re1-N1** | 75.67(13) | **N1-C15-C16-O4** | 4.9(6) |
| **Re1-C2** | 1.918(5) | **C1-Re1-C2** | 89.47(19) | | |
| **Re1-C3** | 1.943(5) | **Br1-Re1-O4** | 84.44(8) | | |
| **Re1-O4** | 2.136(3) | **Br1-Re1-N1** | 82.00(10) | | |
| **Re1-N1** | 2.178(4) | **C3-Re1-O4** | 92.63(15) | | |
| **Re1-Br1** | 2.6129(8) | **N1-Re1-C1** | 97.68(17) | | |
| | | **O4-Re1-C2** | 96.90(16) | | |
| | | **C3-Re1-Br1** | 177.47(13) | | |

The three Rhenium to carbonyl distances of 1.910(4) Å, 1.918(5) Å and 1.943(5) Å, for C1, C2 and C3, are all within normal range.[11-16] The Re1 to the bidentate donor oxygen and nitrogen distances, O4 and N1, of 2.136(3) Å and 2.178(4) Å respectively compare well to similar structures[12] as well as *fac*-[$NEt_4$][Re(2,5-Pico)$(CO)_3$(Br)].$H_2O$ reported in Paragraph 4.7. The Re1-Br1 distance of 2.6129(8) Å are well within range of the reported distances of 2.617(3)/2.619(2) Å[11], 2.6270(3) Å[13] and 2.467(16)/2.6334(9) Å.[10]

The octahedral geometry around the metal centre is slightly distorted and could possibly be due to the small bite angle (O4-Re1-N1) of 75.67(13) °. The distortion can be seen from the angles of 89.47(1) ° for C1-Re1-C2, 82.00(10) ° for Br1-Re1-N1 and 97.68(17) ° for N1-Re1-C1.

The planarity of the system, C11-C12-C13-C14-C15-C16-O4-N1, is illustrated by relatively small deviations of all the atoms from this plane (largest deviation from the plane is 0.07(9) Å for O4). The dihedral angle between these two planes is calculated as 12.0(8) °. The 'bending' of the ligand system from the equatorial plane can be seen in the illustration. The two planes identified in the crystal structure of *fac*-[$NEt_4$][Re(2,5-PicoMe)$(CO)_3$(Br)], as well as the dihedral angle, is illustrated in Figure 4.22 below.

The bidentate ligand coordinate to the Re(I) core with a torsion angle, N1-C15-C16-O4, of 5.9(6) °.

**Figure 4.22: Illustration of the planes defined in *fac*-[$NEt_4$][Re(2,5-PicoMe)$(CO)_3$(Br)] (6).**

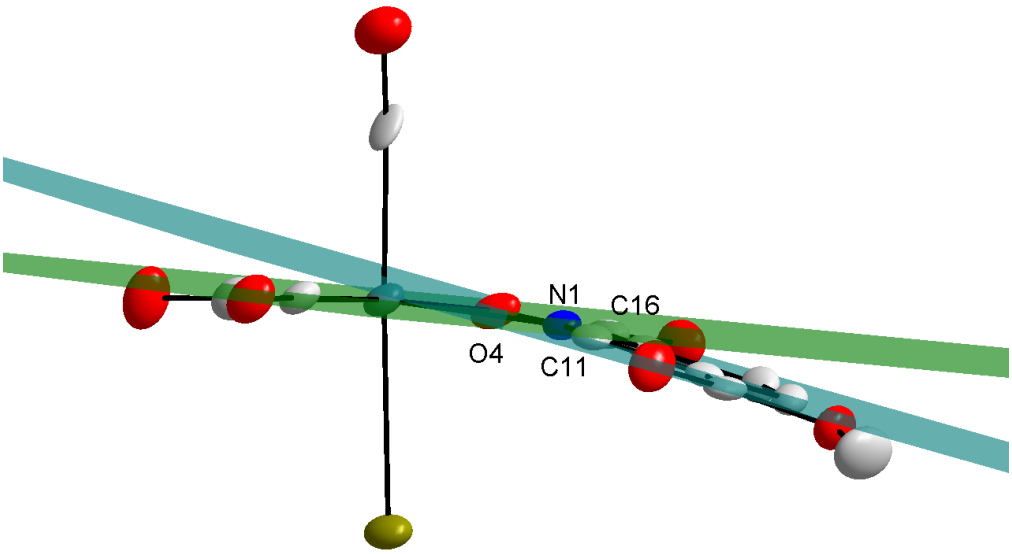


There are three hydrogen bonds observed in the structure of *fac*-[$NEt_4$][Re(2,5-PicoMe)$(CO)_3$(Br)], as illustrated in Figure 4.23. One intramolecular, C11-H11…O6, hydrogen bond is observed, and two C-H…O intermolecular hydrogen bonds, between the cationic counter ion and the next Rhenium(I) unit. The hydrogen bond distances and angles for *fac*-[NEt4][Re(2,5-PicoMe)$(CO)_3$(Br)] is reported in Table 4.16.

**Figure 4.23: Hydrogen bonds observed of *fac*-[$NEt_4$][Re(2,5-PicoMe)$(CO)_3$(Br)] (6).**

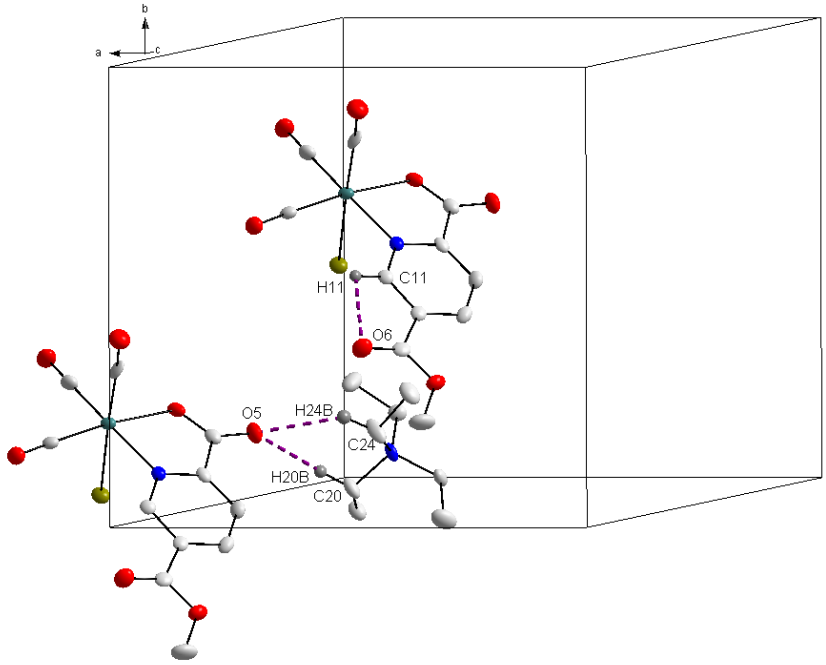


**Table 4.16: Hydrogen bond distances and angles (Å, °) observed for *fac*-[$NEt_4$][Re(2,5-PicoMe)$(CO)_3$(Br)] (6).**

| D-H…A | d (D-H) | d (H…A) | d (D…A) | D-H…A angle |
|---|---|---|---|---|
| C11-H11…O6 | 0.93 | 2.49 | 2.808(5) | 100.0 |
| C20-H20B…O5[a] | 0.97 | 2.39 | 3.289(6) | 153.1 |
| C24-H24B…O5[a] | 0.97 | 2.54 | 3.384(6) | 146.0 |

Symmetry codes, transformations used to generate equivalent atoms:
[a] 0.5 + x, -0.5 + y, z

The packing of the ionic units in the unit cell is illustrated in Figure 4.24, viewed along the a-axis, with the hydrogen atoms and cations omitted for clarity. The Rhenium units pack in a head-to-head fashion, with the ligand systems overlapping. The cationic tetraethylammonium cation fits in between the Rhenium units, basically surrounding the Re(I) units.

**Figure 4.24: Packing in the unit cell of *fac*-[NEt$_4$][Re(2,5-PicoMe)(CO)$_3$(Br)] (6), viewed along the a-axis.**

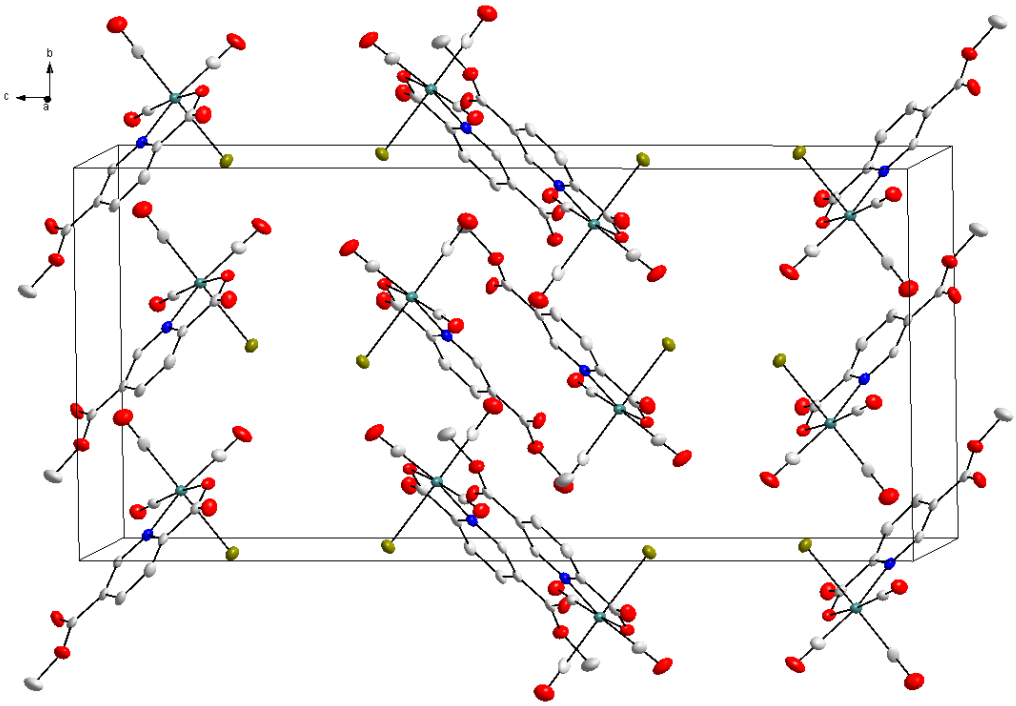

## 4.9 Crystal structure of *fac*-[NEt$_4$][Re(BHA)(CO)$_3$(Br)] (7)

The title complex was synthesized as described in Paragraph 3.5.27. It crystallizes in the triclinic $P\bar{1}$ space group with the two ionic fragments, independent of the other in the asymmetric unit. The Rhenium(I) metal core is facially surrounded by three carbonyl ligands. The rest of the octrahedral geometry is occupied by a benzohydroxamato bidentate ligand and a bromido ligand in the sixth position.

The general crystal data of *fac*-[NEt$_4$][Re(BHA)(CO)$_3$(Br)] is summarized in Table 4.3. The molecular diagram and numbering scheme of *fac*-[NEt$_4$][Re(BHA)(CO)$_3$(Br)] are illustrated in Figure 4.25, with the hydrogen atoms and cation omitted for clarity. Selected bond distances and bond angles are summarized in Table 4.17.

**Figure 4.25: Molecular diagram and numbering scheme of *fac*-[$NEt_4$][Re(BHA)$(CO)_3$(Br)] (7), with the hydrogen atoms and cation omitted for clarity.**

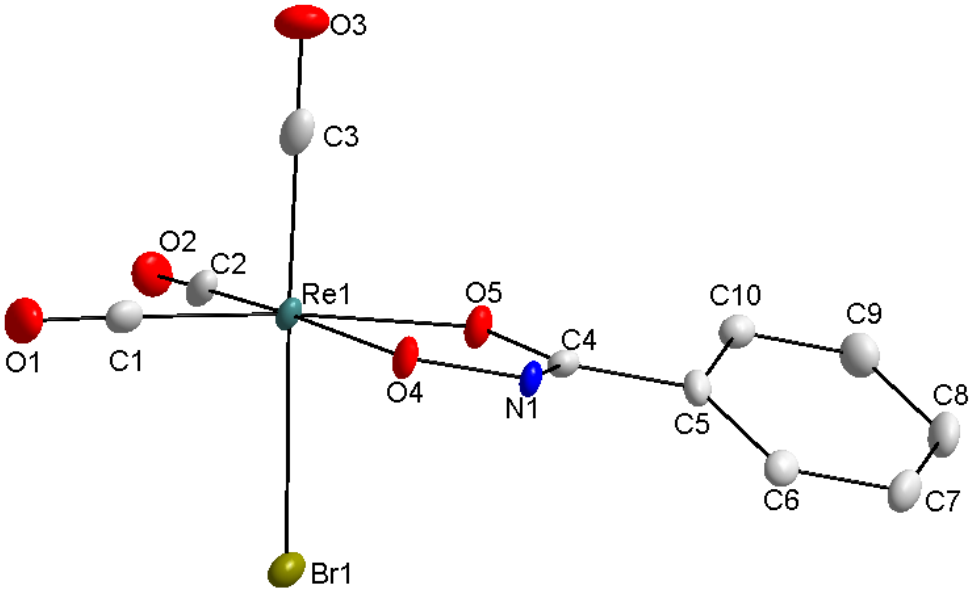


**Table 4.17: Selected bond distances and angles of *fac*-[$NEt_4$][Re(BHA)$(CO)_3$(Br)] (7).**

| Selected bond distances (Å) | | Selected bond angles (°) | | Selected torsion angles (°) | |
|---|---|---|---|---|---|
| **Re1-C1** | 1.899(3) | **O4-Re1-O5** | 76.80(7) | **O5-C4-N1-O4** | -1.1(4) |
| **Re1-C2** | 1.910(3) | **C1-Re1-C2** | 87.98(12) | **N1-C4-C5-C6** | -23.2(5) |
| **Re1-C3** | 1.897(3) | **Br1-Re1-O4** | 83.49(6) | | |
| **Re1-O4** | 2.1201(19) | **Br1-Re1-O5** | 84.24(6) | | |
| **Re1-O5** | 2.128(2) | **C2-Re1-O5** | 96.08(10) | | |
| **Re1-Br1** | 2.6690(5) | **O4-Re1-C1** | 98.84(10) | | |
| | | **C3-Re1-Br1** | 177.86(9) | | |

The three Rhenium to carbonyl carbon bond distances of 1.899(3) Å, 1.910(3) Å and 1.897(3) Å, for C1-C3, are well within normal range.[11-16] The Rhenium-bromido distance of 2.6690(5) Å compare well with similar structures with Re-Br distances that vary from 2.467(16) Å to 2.6334(9) Å.[10,11,13] The distances from the Rhenium(I) metal core to the bidentate ligand, Re1-O4 and Re-O5, compare well with similar structures with O,O'-bidentate ligand systems.[10,13,14]

The octahedral geometry around the metal core is slightly distorted, possibly due to the small bite angle of 76.80(7) ° that the metal forms with the bidentate ligand, O4-Re1-O5.

This is also seen in the angles 83.49(6) ° for Br1-Re1-O4, 96.08(10) ° for C2-Re1-O5 and 98.84(10) ° for O4-Re1-Br1.

The planarity of the system O4-N1-C4-O5 clear from the very small deviations of all the atoms from this plane, with the largest deviation from the plane being 0.005(2) Å for C4. The dihedral angle between the equatorial plane and this defined plane is calculated as 7.8(2) °. The two planes and the dihedral angle between them are illustrated in Figure 4.26.

A torsion angle of -1.1(4) ° is observed for the angle the benzohydroxamic acid ligand forms when coordinated to the Rhenium(I) core, O5-C4-N1-O4. The phenyl ring of the ligand system 'twists' from the equatorial plane, with a torsion angle of -23.2(5) ° observed for N1-C4-C5-C6.

**Figure 4.26: Illustration of the two planes defined in *fac*-[NEt$_4$][Re(BHA)(CO)$_3$(Br)] (7).**

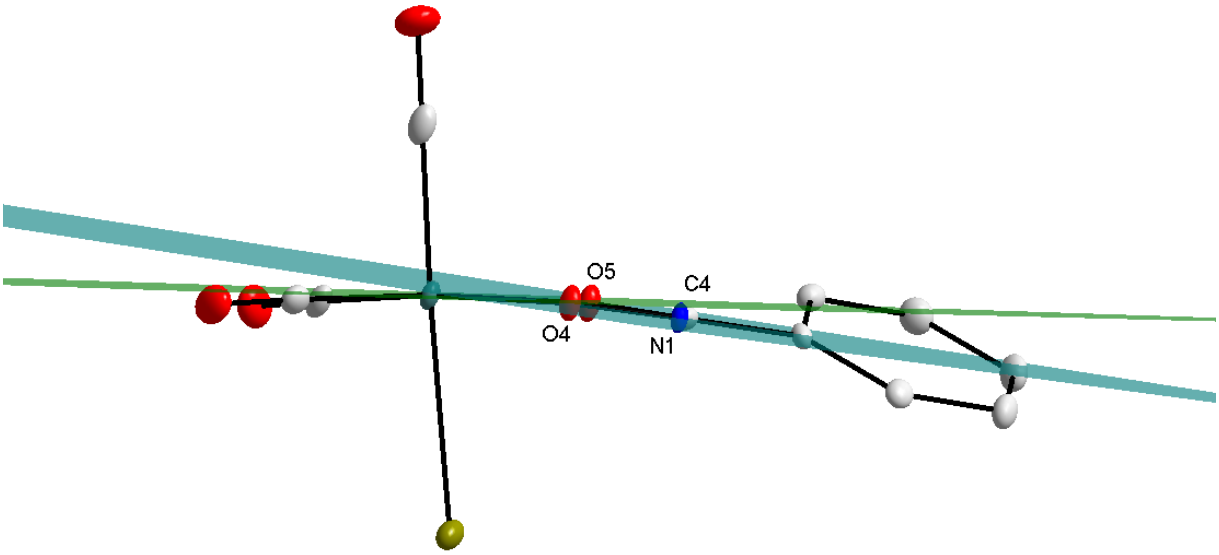


There are five hydrogen bonds observed in the crystal structure of *fac*-[NEt$_4$][Re(BHA)(CO)$_3$(Br)], illustrated in Figure 4.27, including N-H…Br and C-H…O bonds. Hydrogen atoms and tetraethylammonium cations, not part of the hydrogen bonds, are omitted for clarity. Four hydrogen bonds are observed between the tetraethylammonium cation and the four surrounding Rhenium units. One hydrogen bond is observed between the nitrogen atom of the benzohydroxamato ligand system to

the next Rhenium unit's bromido ligand. The hydrogen bond distances and angles are reported in Table 4.18.

**Figure 4.27: Hydrogen bonds observed in the crystal structure of *fac*-[$NEt_4$][Re(BHA)$(CO)_3$(Br)] (7).**

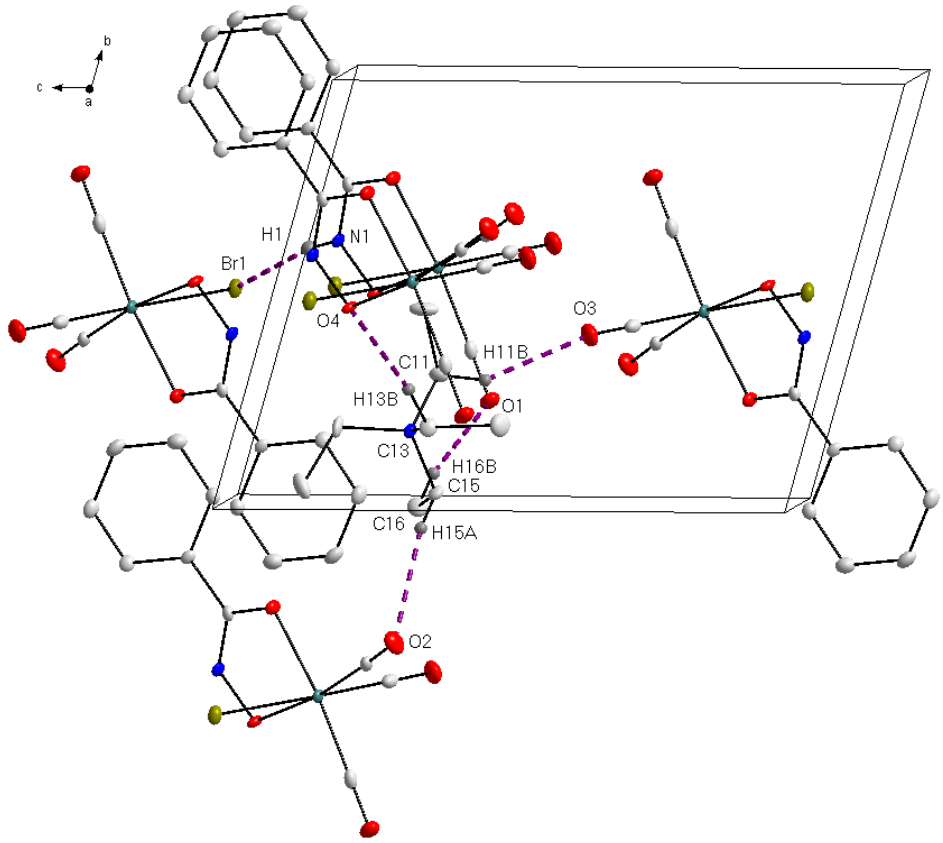


**Table 4.18: Hydrogen bond distances and angles (Å, °) for *fac*-[$NEt_4$][Re(BHA)$(CO)_3$(Br)] (7).**

| D-H…A | d (D-H) | d (H…A) | d (D…A) | D-H…A angle |
|---|---|---|---|---|
| N1-H1…Br1[a] | 0.90(4) | 2.53(4) | 3.421(2) | 170(3) |
| C15-H15A…O2[b] | 0.97 | 2.59 | 3.520(4) | 161.6 |
| C13-H13B…O4[c] | 0.97 | 2.43 | 3.387(3) | 170.1 |
| C11-H11B…O3[d] | 0.97 | 2.42 | 3.285(4) | 148.7 |
| C16-H16B…O1 | 0.96 | 2.58 | 3.521(4) | 168.6 |

Symmetry codes, transformations used to generate equivalent atoms:
[a] 1 - x, 1 - y, 2 - z; [b] x, -1 + y, z; [c] 1 + x, y, z; [d] 1 - x, 1 - y, 1 – z

Some π-stacking is observed between the ring systems of the benzohydroxamato ligands of neighbouring Rhenium units. This is illustrated in Figure 4.28, where hydrogen atoms and the cations are omitted for clarity. The centroid-to-centroid distance between these ring systems is 3.839(2) Å.

**Figure 4.28: Some π-stacking observed for *fac*-[$NEt_4$][Re(BHA)$(CO)_3$(Br)] (7).**

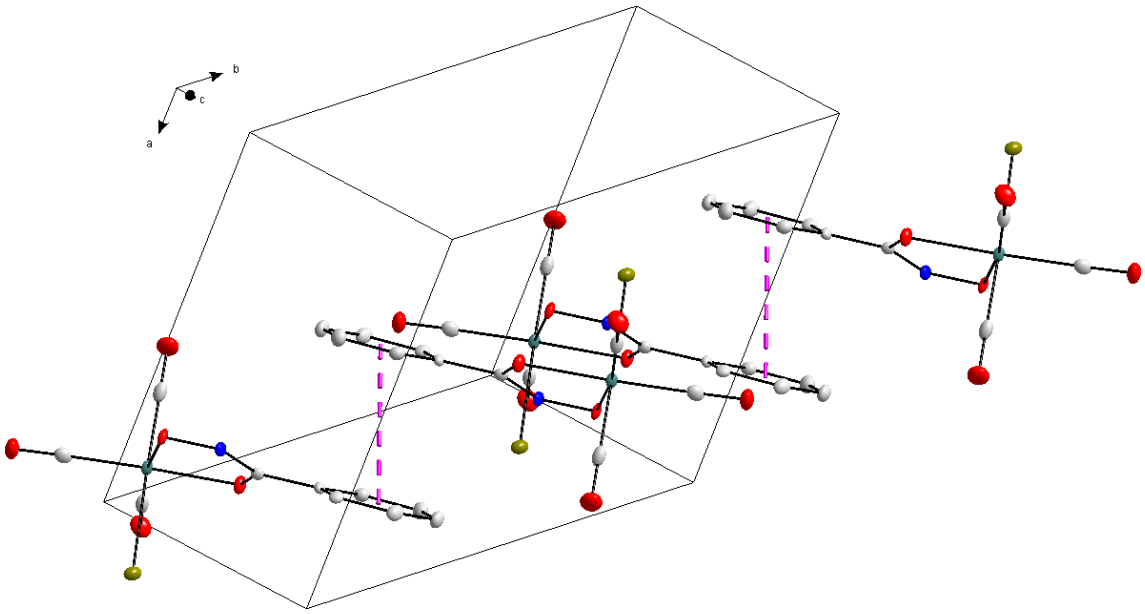


The Rhenium units pack in layers in a head-to-head fashion, each surrounded by four tetraethylammonium cations. Figure 4.29 illustrates the packing of *fac*-[$NEt_4$][Re(BHA)$(CO)_3$(Br)], with hydrogen atoms and cations omitted for clarity.

**Figure 4.29: Packing of *fac*-[$NEt_4$][Re(BHA)$(CO)_3$(Br)] (7) in the unit cell, viewed along the b-axis.**

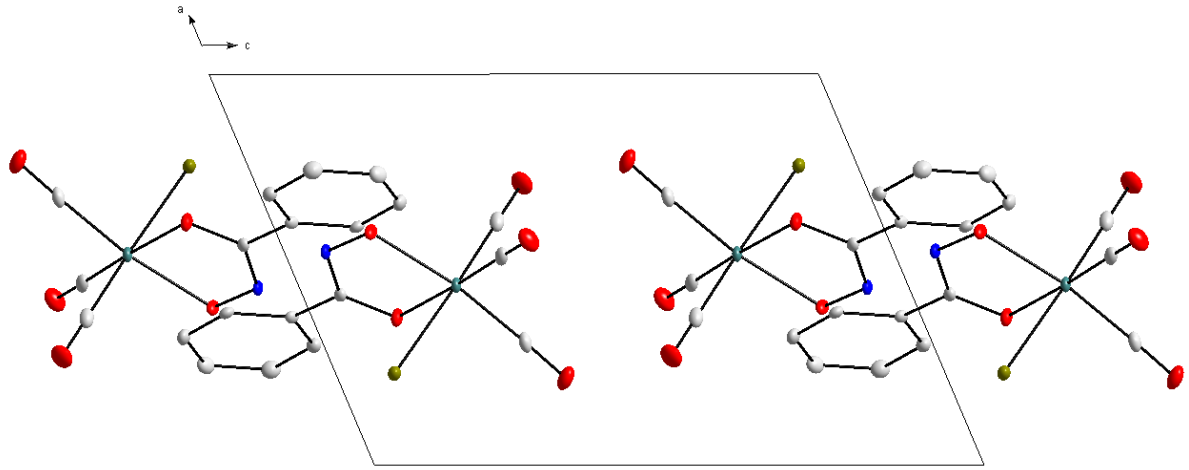


## 4.10 Crystal structure of *fac*-[Re(Flav)$(CO)_3(H_2O)$].Flav (8)

The compound, *fac*-[Re(Flav)$(CO)_3(H_2O)$].Flav was synthesized as described by Schutte *et al*.[22] The yellow cuboid crystals were collected from the filtrate of the reaction mixture in water. *fac*-[Re(Flav)$(CO)_3(H_2O)$].Flav crystallizes in the Triclinic $P\bar{1}$ space group with a neutral Re(I) unit and a free ligand in the unit cell. The Re(I) core is surrounded by three facial carbonyl ligands, a 3-hydroxyflavonato ligand and a water ligand.

The general crystal data for *fac*-[Re(Flav)$(CO)_3(H_2O)$].Flav is reported in Table 4.3. For clarity, the normal ring-numbering system for flavonoid-type ligands was used, and is illustrated in Figure 4.30. A molecular diagram with the numbering scheme of *fac*-[Re(Flav)$(CO)_3(H_2O)$].Flav, where the hydrogen atoms and free flavone ligand are omitted for clarity (Figure 4.31), as well as some selected bond distances and angles (Table 4.19) are reported.

[22] Schutte, M., Kemp, G., Visser, H.G., Roodt, A. *Inorg Chem*. **2011**, *50(24)*, 12486-12498.

**Figure 4.30: Flavonoid ring system numbering scheme.**

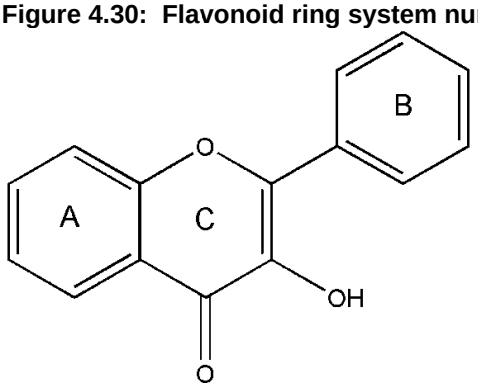


**Figure 4.31: Molecular diagram and numbering scheme of *fac*-[Re(Flav)(CO)$_3$(H$_2$O).Flav (8). Hydrogen atoms and free flavone ligand omitted for clarity.**

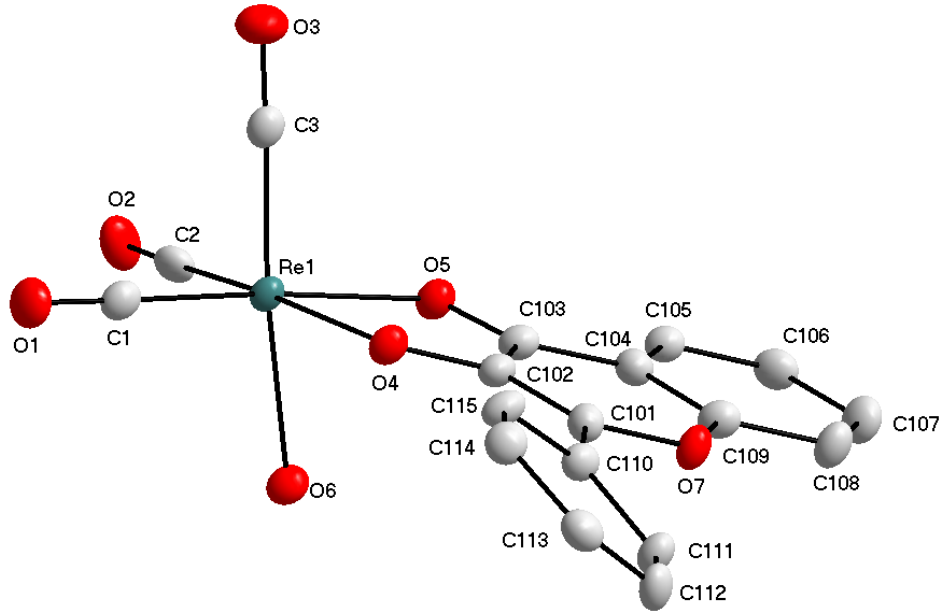


The crystal structure of *fac*-[Re(Flav)(CO)$_3$(MeOH)].MeOH has been reported recently[22], where the aqua ligand was substituted by a methanol molecule. The Rhenium carbonyl distances, varying from 1.895(4) Å to 1.903(4) Å, are well within the normal range.[11-16] The Rhenium to oxygen atom distances, of the bidentate ligand, of 2.151(3) Å and 2.130(3) Å compare well with that of *fac*-[Re(Flav)(CO)$_3$(MeOH)].MeOH, 2.141(3) Å and 2.147(3) Å reported earlier.[22] The distance from the Re(I) core to the aqua ligand of 2.188(3) Å are well within range of other similar aqua structures, with Rhenium aqua distances of 2.170(5) Å[14], 2.153(3)/2.170(3) Å[12] and 2.182(4) Å[22].

**Table 4.19: Selected bond distances and angles of *fac*-[Re(Flav)(CO)$_3$(H$_2$O)].Flav (8).**

| Selected bond distances (Å) | | Selected bond angles (°) | | Selected torsion angles (°) | |
|---|---|---|---|---|---|
| **Re1-C1** | 1.903(4) | **O4-Re1-O5** | 76.61(11) | **O4-C102-C103-O5** | -2.0(6) |
| **Re1-C2** | 1.897(4) | **C1-Re1-C2** | 87.13(17) | **O7-C101-C110-C111** | -24.1(6) |
| **Re1-C3** | 1.895(4) | **O6-Re1-O4** | 78.13(11) | | |
| **Re1-O4** | 2.151(3) | **O6-Re1-O5** | 78.49(11) | | |
| **Re1-O5** | 2.130(3) | **C2-Re1-O5** | 96.36(14) | | |
| **Re1-O6** | 2.188(3) | **O4-Re1-C1** | 99.58(14) | | |
| | | **C3-Re1-O6** | 174.38(14) | | |

The octahedral geometry around the Rhenium(I) core is slightly distorted, possibly due to the small bite angle (O4-Re1-O5) of 76.61(11) °. The distortion is seen in the angles of 78.13(11) ° for O6-Re1-O4, 78.49(11) ° for O6-Re1-O5 and 99.58(14) ° for O4-Re1-C1. A very similar bite angle of 76.24(11) ° are reported for the analogues *fac*-[Re(Flav)(CO)$_3$(MeOH)].MeOH structure.

Considering the coordinated ligand system, the planarity of the A- and C ring, C101-C102-C103-C104-C105-C106-C107-C108-C109-O7, is clear from the small deviations of all these atoms from the plane, the largest deviation from the plane being 0.023(3) Å for O7. Very small deviations is also found for all the atoms from the plane in the B ring, C110-C111-C112-C113-C114-C115, with the largest deviation 0.012(3) Å for C113. Both these ring systems can be considered planar with a calculated dihedral angle of 26.6(1) °.

In the free ligand, the same two corresponding planes were defined. The planarity of the A- and C ring, C201-C202-C203-C204-C205-C206-C207-C208-C209-O17, as well as the B ring, C210-C211-C212-C213-C214-C215, is clear from small deviations of these atoms from the respective planes with the largest deviations from the plane 0.020(3) Å for C202 and 0.013(3) Å for C210 in the two planes respectively. The dihedral angle between these two planes is 11.9(1) °.

From this it is clear that there is a much bigger twist of the B-ring relative to the A, C rings in the coordinated ligand system than in the free ligand. This is also seen in the torsion angles discussed earlier.

The dihedral angle between the equatorial plane and the plane through O4-C102-C103-O5 is reported as 12.0(1) °; indicating the significant 'twisting' of the ligand from the equatorial plane. The planarity of the plane through O4-C102-C103-O5 is illustrated by

the small deviations of these atoms from the plane. The largest deviation from the plane is 0.008(2) Å for C103. This is illustrated in Figure 4.32.

The torsion angle, O4-C102-C103-O5 (ligand to metal core) is -2.0(6) ° while the B-ring of the coordinated ligand system (O7-C101-C110-C111) bends out of the A and C ring's 'plane' with a torsion angle of -24.1(6) °. Compared to the analogous complex *fac*-[Re(Flav)$(CO)_3$(MeOH)].MeOH which are 6.4(6) ° and -6.1(6) ° respectively.

By comparing the coordinated 3-hydroxyflavonato ligand system to the free ligand in *fac*-[Re(Flav)$(CO)_3(H_2O)$].Flav, the B-ring of the coordinated ligand twists away from the A and C ring's plane to a much bigger extend, O7-C101-C110-C111 of -24.1(6) °, than in the free ligand system, O17-C201-C210-C211 of 9.7(6).

**Figure 4.32: Illustration of the equatorial plane and the plane through O4-C102-C103-O5 in *fac*-[Re(Flav)$(CO)_3(H_2O)$].Flav (8).**

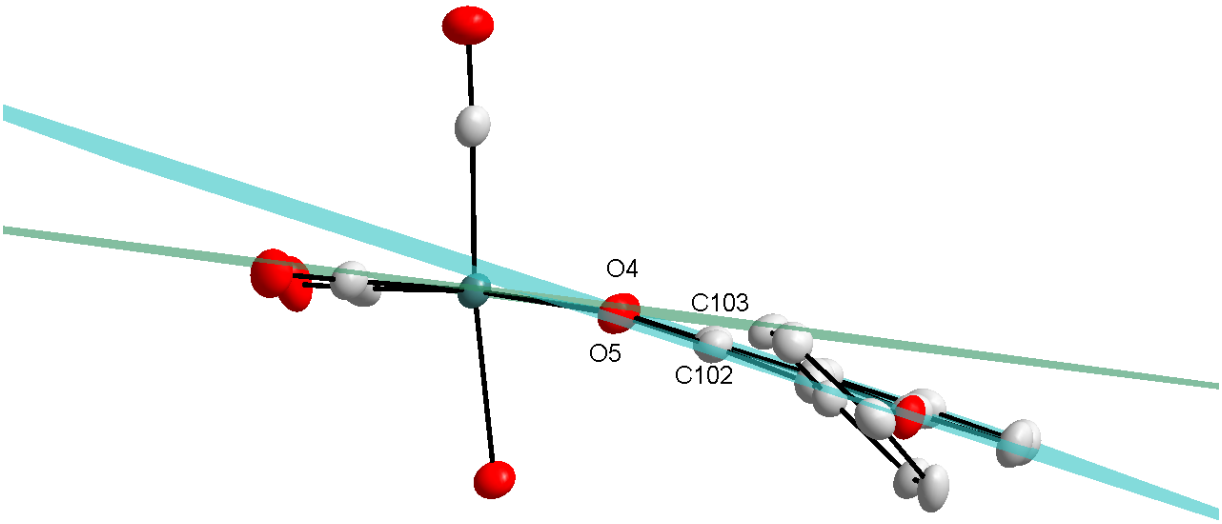


In total, seven hydrogen bonds (O-H…O and C-H…O) are observed for *fac*-[Re(Flav)$(CO)_3(H_2O)$].Flav, of which four are intramolecular and three are intermolecular hydrogen bonds (Figure 4.33). It is clear that this array of hydrogen bonds stabilize the packing of the Rhenium units and ligand molecules in the crystal.

**Figure 4.33: Hydrogen bonds observed in the crystal structure of *fac*-[Re(Flav)(CO)$_3$(H$_2$O)].Flav (8).**

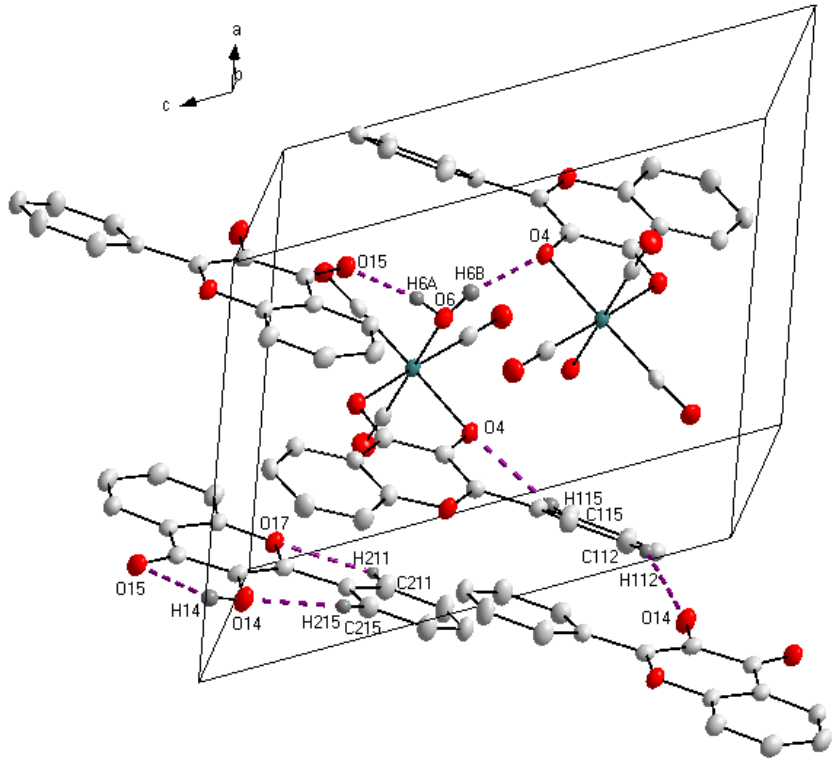


**Table 4.20: Hydrogen bond distances and angles (Å, °) observed in *fac*-[Re(Flav)(CO)$_3$(H$_2$O)].Flav (8).**

| D-H…A | d (D-H) | d (H…A) | d (D…A) | D-H…A angle |
|---|---|---|---|---|
| O6-H6A…O15[a] | 0.842(19) | 1.81(2) | 2.636(4) | 166(5) |
| O6-H6B…O4[b] | 0.853(19) | 1.86(3) | 2.663(4) | 157(5) |
| O14-H14…O15 | 0.85(2) | 2.07(5) | 2.596(4) | 119(5) |
| C112-H112…O14[c] | 0.93 | 2.48 | 3.335(5) | 153.0 |
| C115-H115…O4 | 0.93 | 2.42 | 2.985(5) | 119.0 |
| C211-H211…O17 | 0.93 | 2.35 | 2.696(5) | 101.5 |
| C215-H215…O14 | 0.93 | 2.22 | 2.863(5) | 125.2 |

Symmetry codes, transformations used to generate equivalent atoms:
[a] 1 - x, 1 - y, 2 - z; [b] 1 - x, 1 - y, 1 - z; [c] -x, -y, 1 - z

In Table 4.20, the hydrogen bond distances and angles observed in the crystal structure *fac*-[Re(Flav)(CO)$_3$(H$_2$O)].Flav are summarized.

**Figure 4.34: Some π-stacking in the unit cell of *fac*-[Re(Flav)(CO)$_3$(H$_2$O)].Flav (8).**

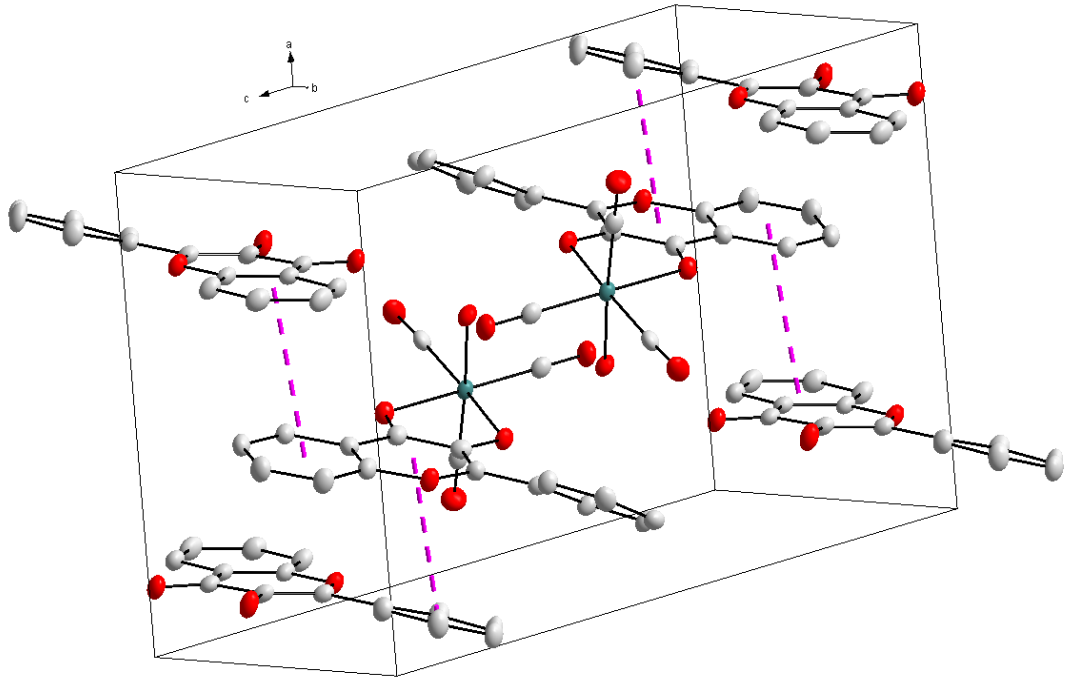


Some π-stacking is observed in *fac*-[Re(Flav)(CO)$_3$(H$_2$O)].Flav. From the Rhenium(I) unit, one interaction from the C-ring to the next free ligand's B-ring is observed as well as from the A-ring to another free ligand's A-ring, with centroid-to-centroid distances of 3.684(3) Å and 3.658(3) Å respectively. This is illustrated in Figure 4.34.

**Figure 4.35: Packing in the unit cell of *fac*-[Re(Flav)(CO)$_3$(H$_2$O)].Flav (8), viewed along the b-axis.**

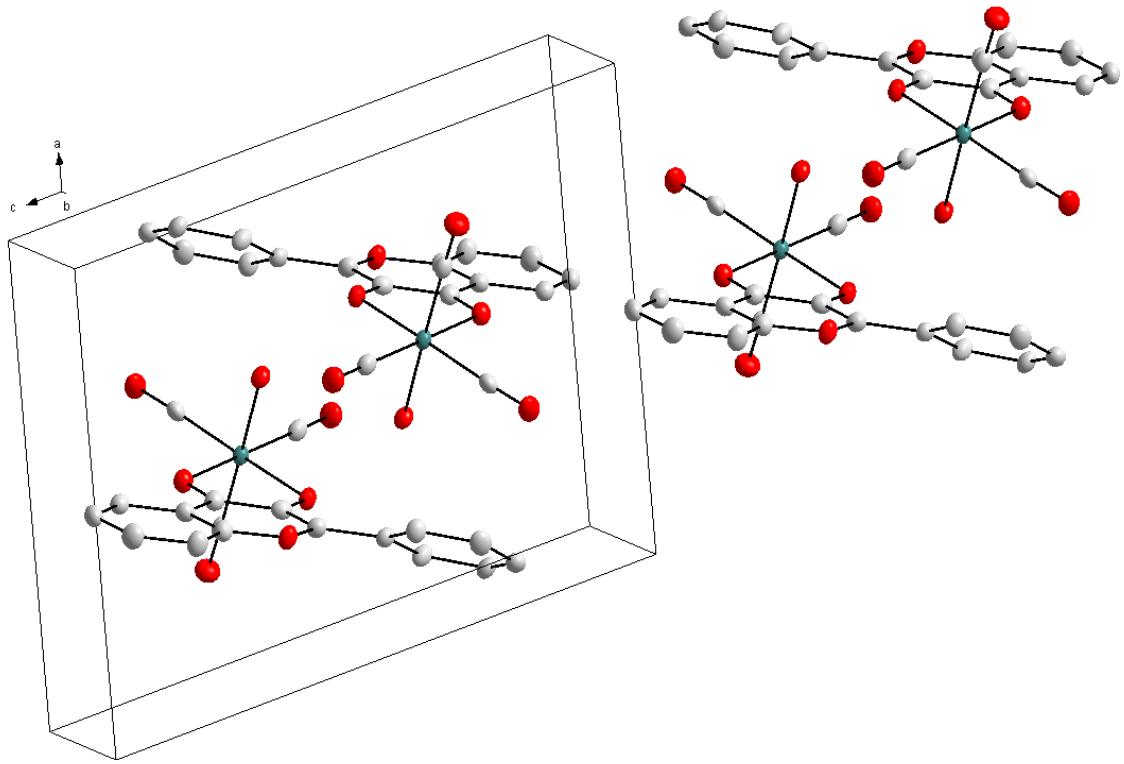


The Rhenium units pack in a head-to-head fashion, with each two units 'enclosed' by four free 3-hydroxyflavone ligands. In Figure 4.35 the packing is viewed along the b-axis. Hydrogen atoms and free 3-hydroxyflavone molecules are omitted for clarity.

## 4.11 Crystal structure of μ-(*fac*-[Re(BipyDC)(CO)$_3$])$_2$.4H$_2$O (9)

The compound, *fac*-[Re(BipyDC)(CO)$_3$(H$_2$O)], was prepared as described in Paragraph 3.5.30. μ-(*fac*-[Re(BipyDC)(CO)$_3$])$_2$.4H$_2$O was obtained as yellow cuboidal single crystals from the product in a methanol solution. The neutral μ-(*fac*-[Re(BipyDC)(CO)$_3$])$_2$.4H$_2$O crystallized in the monoclinic $P2_1/c$ space group with two Rhenium(I) units and four water solvent molecules in the asymmetric unit. One of the carboxylate groups, on the 2,2'-bipyridine backbone, is coordinated to the next Rhenium unit, substituting the aqua ligand in the sixth position, while the second carboxylic acid is

uncoordinated, thus forming a Rhenium dimer. The Rhenium(I) metal cores are surrounded by three facial carbonyl ligands and a bidentate 2,2-bipyridine-3,3'-dicarboxylic acid ligand. The sixth position is occupied by the carbonyl oxygen of the carboxylic acid on the bidentate ligand of the next Rhenium unit. The four water solvent molecules were positioned using CALC-OH[3] and both coordinates and $U_{iso}$ values were freely refined.

The hydroxyl and carbonyl oxygen atoms, O5A/B and O6A/B, are substitutionally disordered over two positions in a 0.722(15):0.278(15) ratio. Two of the solvent water molecules also exhibit substitution disorders over two positions, O09 and O10 as well as O11 and O12, with 0.456(12):0.544(12) and 0.794(10):0.206(10) ratios respectively.

The molecular diagram indicating the numbering scheme is illustrated in Figure 4.36, with the hydrogen atoms and water molecules omitted for clarity, and some selected bond distances and angles are reported in Table 4.21.

**Figure 4.36: Molecular diagram and numbering scheme of μ-(*fac*-[Re(BipyDC)(CO)$_3$])$_2$.4H$_2$O (9), with the hydrogen atoms and water molecules omitted for clarity.**

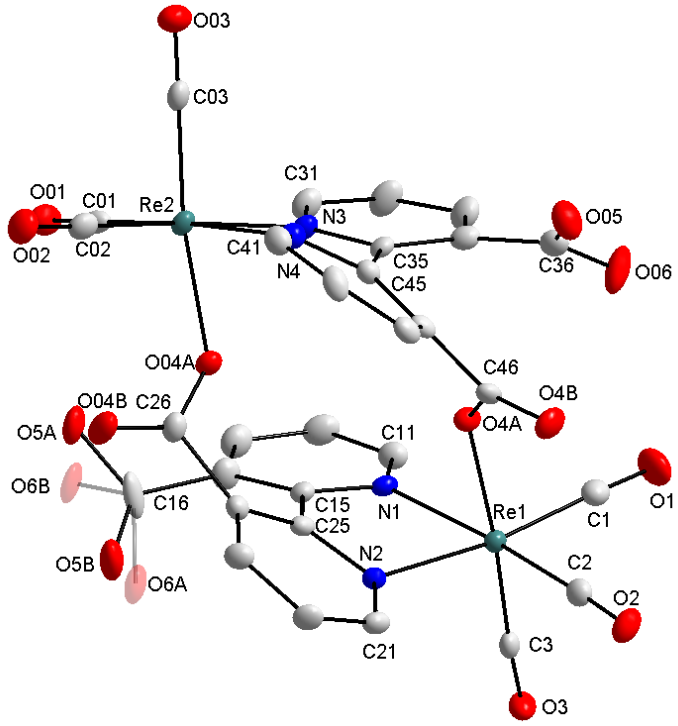

**Table 4.21: Selected bond distances and angles of μ-(*fac*-[Re(BipyDC)(CO)$_3$])$_2$.4H$_2$O (9).**

| Selected bond distances (Å) | | Selected bond angles (°) | | Selected torsion angles (°) | |
|---|---|---|---|---|---|
| **Re1-C1** | 1.924(5) | **N1-Re1-N2** | 74.60(12) | **N1-C15-C25-N2** | -26.3(5) |
| **Re2-C01** | 1.912(4) | **C1-Re1-C2** | 88.31(18) | **C14-C15-C25-C24** | -30.8(6) |
| **Re1-C2** | 1.922(4) | **O4A-Re1-N1** | 77.59(11) | **N3-C35-C45-N4** | -25.5(5) |
| **Re2-C02** | 1.922(5) | **O4A-Re1-N2** | 78.92(12) | **C34-C35-C45-C44** | -31.0(6) |
| **Re1-C3** | 1.895(4) | **C1-Re1-N1** | 100.38(16) | | |
| **Re2-C03** | 1.902(5) | **C2-Re1-N2** | 96.41(15) | | |
| **Re1-N1** | 2.172(3) | **C3-Re1-O4A** | 173.12(14) | | |
| **Re2-N3** | 2.164(4) | **N3-Re2-N4** | 74.31(13) | | |
| **Re1-N2** | 2.186(3) | **C01-Re2-C02** | 86.76(17) | | |
| **Re2-N4** | 2.185(3) | **O04A-Re2-N3** | 79.06(12) | | |
| **Re1-O4A** | 2.138(3) | **O04A-Re2-N4** | 77.84(12) | | |
| **Re2-O04A** | 2.128(3) | **C02-Re2-N4** | 99.34(15) | | |
| | | **C01-Re2-N3** | 99.34(15) | | |
| | | **C03-Re2-O04A** | 171.56(14) | | |

The Rhenium carbonyl distances are all within normal range, varying from 1.895(4) Å to 1.924(5) Å. The distances from the Rhenium metal core to the bidentate's nitrogen atoms of 2.164(4) Å – 2.186(3) Å compare well with the structures of Kemp[23], of 2.178(8) Å for *fac*-[Re(Bipy)(CO)$_3$Br] and 2.172(5) Å and 2.168(5) Å for *fac*-[Re(Bipy)(CO)$_3$(H$_2$O)].NO$_3$.H$_2$O. The distances from the metal to the carbonyl oxygen atom (2.138(3) Å and 2.128(3) Å) are comparable to that of the Rhenium aqua distance of 2.188(3) Å in *fac*-[Re(Flav)(CO)$_3$(H$_2$O)].Flav.

The octahedral geometry around the Re(I) metal core is slightly distorted, which might be due to the small bite angles of 74.60(12) ° and 74.31 (13) ° for N1-Re1-N2 and N3-Re2-N4 respectively. These correspond well with the bite angles of the similar structures, *fac*-[Re(Bipy)(CO)$_3$Br] and *fac*-[Re(Bipy)(CO)$_3$(H$_2$O)].NO$_3$.H$_2$O (Bipy = 2,2'-bipyridine), by Kemp[23] of 74.7(4) ° and 74.92(18) ° respectively. In this structure, the distortion can be seen from the angles around the Re(I) core – 77.59(11) ° for O4A-Re1-N1, 100.38(16) ° for C1-Re1-N1 and 77.84(12) ° for O04A-Re2-N4.

The torsion angles that the bidentate ligands form with the Re(I) centre (N1-C15-C25-N2 and N3-C35-C45-N4) of -26.3(5) ° and -25.5(5) ° indicate the twist of the ligands. Also, at the other end of the coordinated ligands (C14-C15-C25-C24 and C34-C35-C45-C44), the torsion angles of -30.8(6) ° and -31.0(6) ° again shows the twisting of the

[23] Kemp, G. PhD Dissertation, University of Johannesburg, 2006.

ligand, possibly to facilitate the coordination of the one carboxyl oxygen to the next Rhenium(I) unit. Overall, the bond distances and bond angles of the two Rhenium units in the asymmetric unit are very similar.

**Figure 4.37: Illustration of the two planes defined in μ-(*fac*-[Re(BipyDC)(CO)$_3$])$_2$.4H$_2$O (9).**

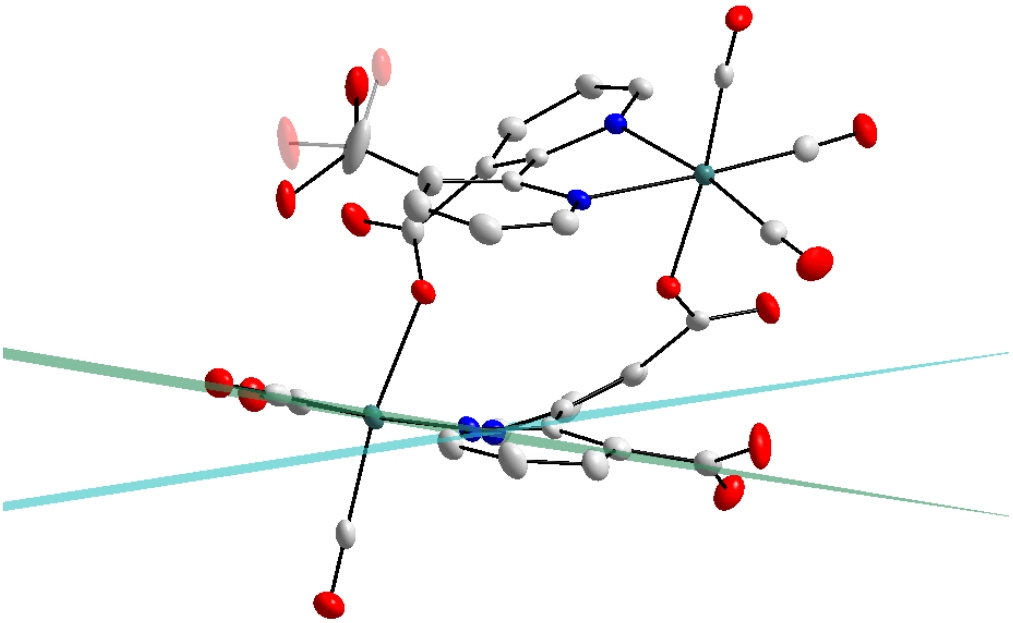

To illustrate the 'twist' of the bidentate ligand, the planes through N1-C15-C25-N2 and N3-C35-C45-N4 were defined. The planarity of the two planes is illustrated in the deviations of all the atoms from the defined planes. The largest deviation is 0.123(2) Å for C15 and 0.120(2) Å for C35 for the two planes respectively. The dihedral angle between the equatorial plane and the plane through N1-C15-C25-N2 is calculated as 17.0(2) ° and the dihedral angle between the equatorial plane and the plane through N3-C35-C45-N4 is 18.3(2) °. In Figure 4.37 the defined planes for the one Rhenium unit is illustrated. The torsion angles can also be observed. The solvent water molecules and the hydrogen atoms are omitted for clarity.

**Figure 4.38: Hydrogen bonds observed in the structure of μ-(*fac*-[Re(BipyDC)(CO)$_3$])$_2$.4H$_2$O (9). For the sake of clarity, the rest of the Re(I) units from the O02, O3, O03 and O4B atoms are omitted.**

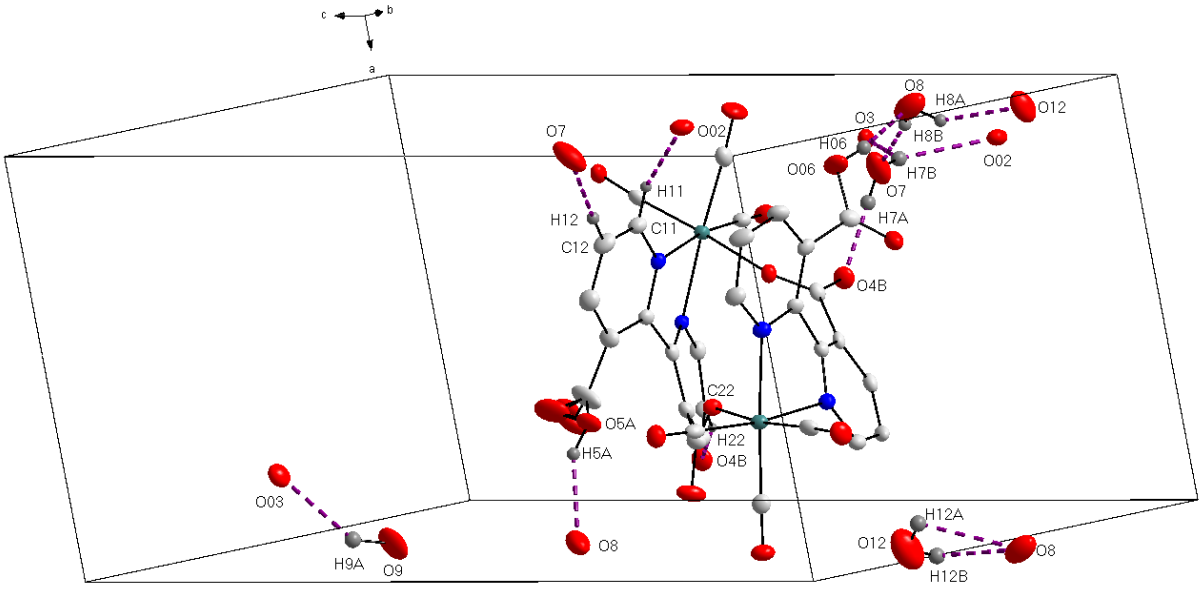


In total, there are thirteen hydrogen bonds observed in the crystal structure of μ-(*fac*-[Re(BipyDC)(CO)$_3$])$_2$.4H$_2$O (O-H…O and C-H…O) of which three are intramolecular hydrogen bonds. It is observed between neighbouring Rhenium units, between water solvent molecules and also between Rhenium units and water molecules. The array of hydrogen bonds observed seems to enhance the solid state ordering of the compound. In Figure 4.38, the hydrogen bonds observed are illustrated. For clarity, the hydrogen atoms and solvent water molecules not participating in hydrogen bonding are omitted. Also, three of the hydrogen bonds are to the neighbouring Rhenium(I) units. For clarity and the sake of space, these Rhenium(I) units are omitted with only the carbonyl oxygen atoms illustrated (O7-H7B…O02, C11-H11…O02 and O9-H9…O03). The hydrogen bond distances and angles are reported in Table 4.22.

.

**Table 4.22: Hydrogen bond distances and angles (Å, °) of μ-(*fac*-[Re(BipyDC)(CO)$_3$])$_2$.4H$_2$O (9).**

| D-H…A | d (D-H) | d (H…A) | d (D…A) | D-H…A angle |
|---|---|---|---|---|
| O06-H06…O8 | 0.82 | 1.83 | 2.620(5) | 160.5 |
| O5A-H5A…O8[a] | 0.82 | 2.17 | 2.886(7) | 145.6 |
| O7-H7A…O4B | 0.856(4) | 1.972(3) | 2.751(5) | 150.8(3) |
| O7-H7B…O02[b] | 0.853(4) | 2.530(3) | 3.288(5) | 148.5(3) |
| O7-H7B…O3[c] | 0.853(4) | 2.394(3) | 2.983(5) | 126.6(3) |
| O8-H8A…O12[d] | 0.84(2) | 2.06(6) | 2.808(9) | 148(11) |
| O8-H8B…O7 | 0.83(2) | 1.88(2) | 2.702(7) | 169(8) |
| C9-H9A…O03[e] | 0.98(3) | 2.468(3) | 3.33(3) | 145.3(18) |
| C12-H12A…O8[d] | 0.864(7) | 2.425(6) | 2.808(10) | 107.5(5) |
| C12-H12B…O8[d] | 0.864(7) | 2.425(6) | 2.808(10) | 107.5(5) |
| C11-H11…O02[f] | 0.93 | 2.53 | 3.137(5) | 123.4 |
| C12-H12…O7[e] | 0.93 | 2.53 | 3.453(6) | 172.5 |
| C22-H22…O4B[g] | 0.93 | 2.38 | 3.269(5) | 160.6 |

Symmetry codes, transformations used to generate equivalent atoms:
[a] 1 + x, 0.5 - y, 0.5 + z; [b] -1 + x, 0.5 - y, -0.5 + z; [c] - x, -y, -z; [d] 1 - x, 1 - y, -z; [e] x, 0.5 - y, 0.5 + z; [f] -1 + x, y, z; [g] 1 - x, -y, -z.

Viewed along the a-axis, the Rhenium(I) units pack in a head-to-head fashion in 'columns' along the c-axis with a slight angle to the neighbouring two units. This is illustrated in Figure 4.39, with the hydrogen atoms as well as the water solvent molecules omitted for clarity.

**Figure 4.39: Packing in the unit cell of μ-(*fac*-[Re(BipyDC)(CO)$_3$])$_2$.4H$_2$O (9), viewed along the a-axis.**

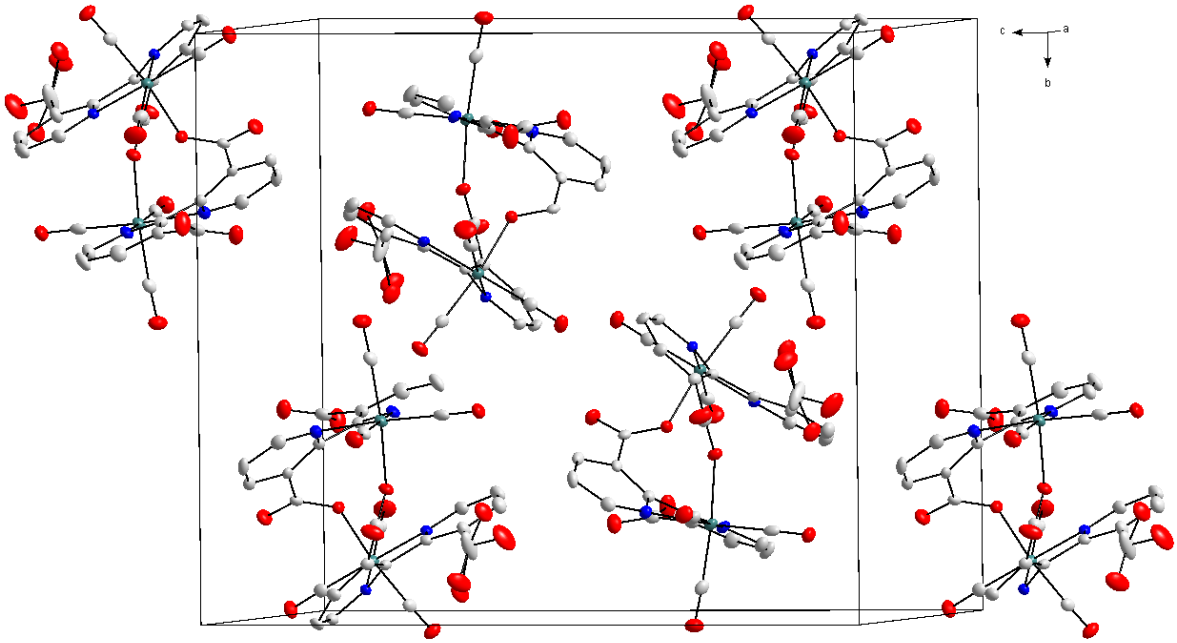


## 4.12 Crystal structure of *fac*-[Re(PNP)(CO)$_3$(Br)] (10)

The title complex was synthesized as described by Schutte *et al*.[11] It crystallizes in the triclinic $P2_1/n$ space group with one neutral Rheniun compound in the asymmetric unit. The Rhenium(I) metal core is facially surrounded by three carbonyl ligands. The rest of the octrahedral geometry is occupied by a bis(diphenylphosphino)-propylamine bidentate ligand and a bromido ligand in the sixth position.

The compound exhibits substitutional disorder of the bromido ligand and the axial carbonyl ligand, with almost 50% occupancy for both the bromido and the carbonyl ligand; 0.54(1) and 0.46(1), respectively. In addition, the propyl chain on the N atom of the bidentate ligand exhibits a 0.65(1):0.35(1) disorder.

The general crystal data of *fac*-[Re(PNP)(CO)$_3$(Br)] is summarized in Table 4.4. The molecular diagram and numbering scheme of *fac*-[Re(PNP)(CO)$_3$(Br)] are illustrated in Figure 4.40, with the disordered atoms faded out. The hydrogen atoms are omitted for clarity. Selected bond distances and bond angles are summarized in Table 4.23.

**Figure 4.40: Molecular diagram of *fac*-[Re(PNP)(CO)$_3$(Br)] (10), illustrating the two disorders. Hydrogen atoms are omitted for clarity.**

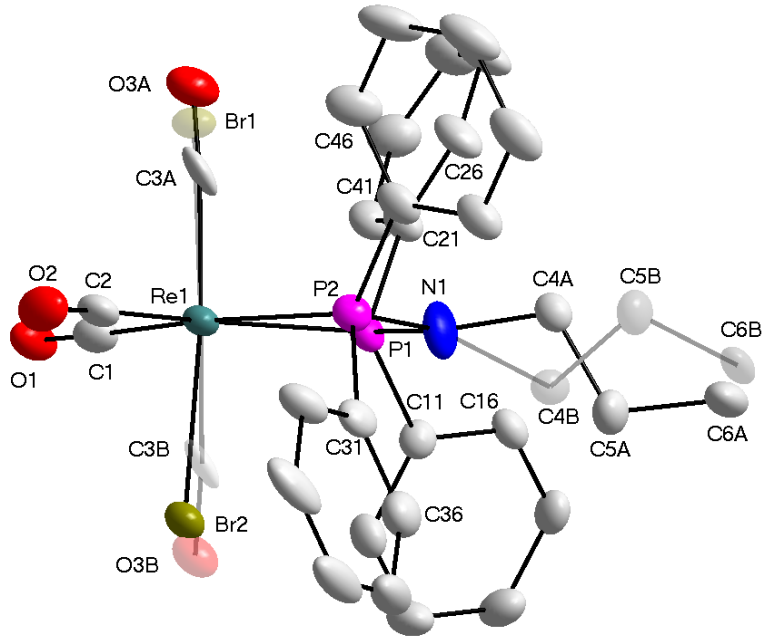


**Table 4.23: Selected bond distances (Å) and angles (°) of *fac*-[Re(PNP)(CO)$_3$(Br)] (10).**

| Selected bond distances (Å) | | Selected bond angles (°) | |
|---|---|---|---|
| **Re1-C1** | 1.962(6) | **P1-Re1-P2** | 66.65(4) |
| **Re1-C2** | 1.952(5) | **C1-Re1-C2** | 93.7(2) |
| **Re1-C3A** | 1.968(18) | **Br1-Re1-P1** | 88.92(7) |
| **Re1-C3B** | 1.866(15) | **Br1-Re1-P2** | 96.64(7) |
| **Re1-Br1** | 2.619(2) | **C2-Re1-P2** | 95.62(16) |
| **Re1-Br2** | 2.617(3) | **C1-Re1-P1** | 104.00(16) |
| **Re1-P1** | 2.4586(15) | **Br1-Re1-C3B** | 175.4(3) |
| **Re1-P2** | 2.4375(14) | **Br2-Re1-C3A** | 174.5(4) |

The bond distances and angles are well within normal range and compare well to that of a Platinum complex synthesized by Cloete *et al*.[24] The Rhenium carbonyl distances of 1.962(6) Å, 1.952(5) Å and 1.968(18) Å/1.866(15) Å are within range of the expected Re-CO distances[11-16]. The Rhenium bromido distances of 2.619(2) Å and 2.617(3) Å compare well with that of similar structures[10,11,13] and also to the structures reported in Paragraph 4.3, 4.7 and 4.8. It's clear that the Rhenium phosphorous bond distances in this structure is slightly longer than usual, 2.4586(15) Å and 2.4375(14) Å. In the

[24] Cloete, N., Visser, H.G., Roodt, A. *Acta Cryst*. **2010**, E66, m51-52.

square planar Pt(II) complex reported by Cloete *et al*.[24], the Pt-P distances are reported as 2.1932(7) Å and 2.2121(7) Å.

The octahedral geometry around the Rhenium(I) core is slightly distorted with the P1-Re1-P2 bite angle of 66.65(4) °, compared to 72.4(1) ° for the structure by Cloete *et al*.[24] The P-N-P angle is reported as 100.11(12) ° for the Pt(II) complex compared to 103.9(2) ° for this structure.

The planarity of the four phenyl rings is illustrated by the very small deviations of the atoms from the planes. For C11-C12-C13-C14-C15-C16, the largest deviation from the plane through these atoms is 0.0024(35) Å for C16. For the plane through C21-C22-C23-C24-C25-C26, C23 has the largest deviation from the plane, 0.018(5) Å. For C31-C32-C33-C34-C35-C36 and C41-C42-C43-C44-C45-C46, the largest deviation from the plane through these atoms are 0.0016(0.004) Å for C33 and 0.007(4) Å for C44 respectively.

The dihedral angle between the equatorial plane and the plane through P1-N1-P2 is calculated as 6.0(4) °. The 'bending' of the ligand is not that significant in this instance and is illustrated in Figure 4.41.

**Figure 4.41: Illustration of the equatorial plane and the plane through P1-N1-P2 in *fac*-[Re(PNP)(CO)$_3$(Br)] (10).**

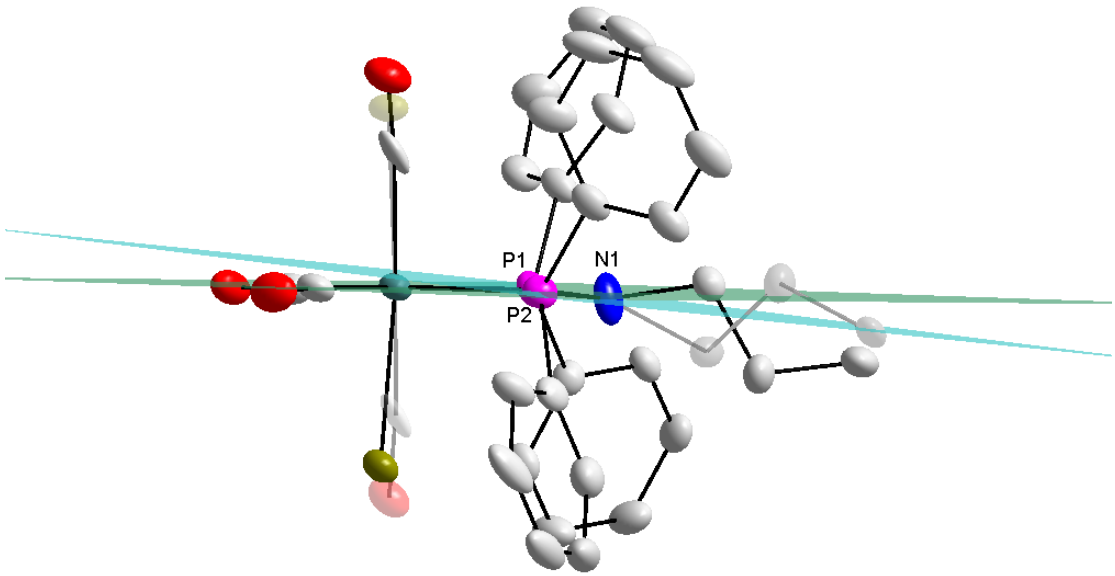

Three hydrogen bonds are observed in the structure of *fac*-[Re(PNP)(CO)$_3$(Br)], two intramolecular and one intermolecular hydrogen bond. This is illustrated in Figure 4.42 while the hydrogen bond distances and angles are reported in Table 4.24.

**Figure 4.42: Hydrogen bonds observed in the crystal structure of *fac*-[Re(PNP)(CO)$_3$(Br)] (10).**

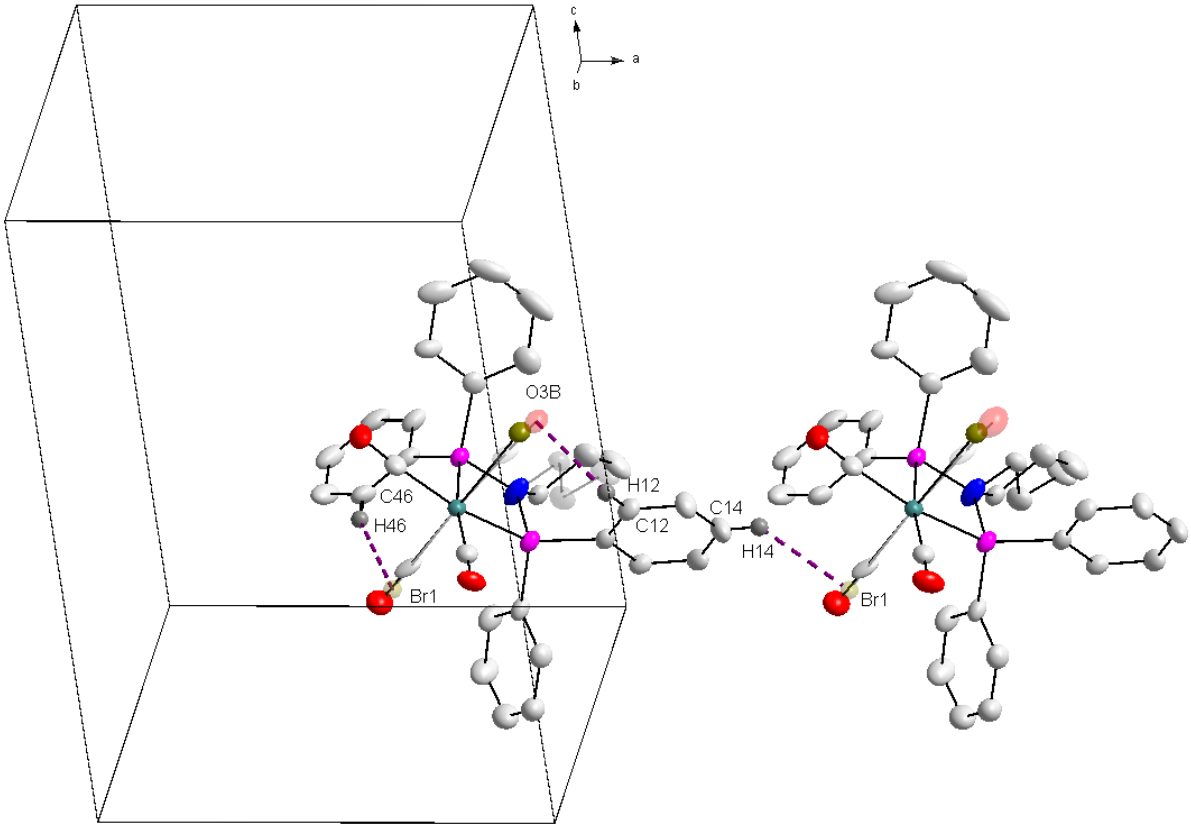


**Table 4.24: Hydrogen bond distances and angles (Å, °) observed in *fac*-[Re(PNP)(CO)$_3$(Br)] (10).**

| D-H…A | d (D-H) | d (H…A) | d (D…A) | D-H…A angle |
|---|---|---|---|---|
| C12-H12…O3B | 0.95 | 2.51 | 3.39(2) | 155.1 |
| C14-H14…Br1[a] | 0.95 | 2.81 | 3.524(6) | 133 |
| C46-H46…Br1 | 0.95 | 2.63 | 3.519(6) | 156.8 |

[a] 1 + x, y, z

The Rhenium units pack in a head-to-toe fashion when viewed along the c-axis. This is illustrated in Figure 4.43.

**Figure 4.43: Packing of *fac*-[Re(PNP)(CO)$_3$(Br)] (10) in the unit cell, viewed along the a-axis.**

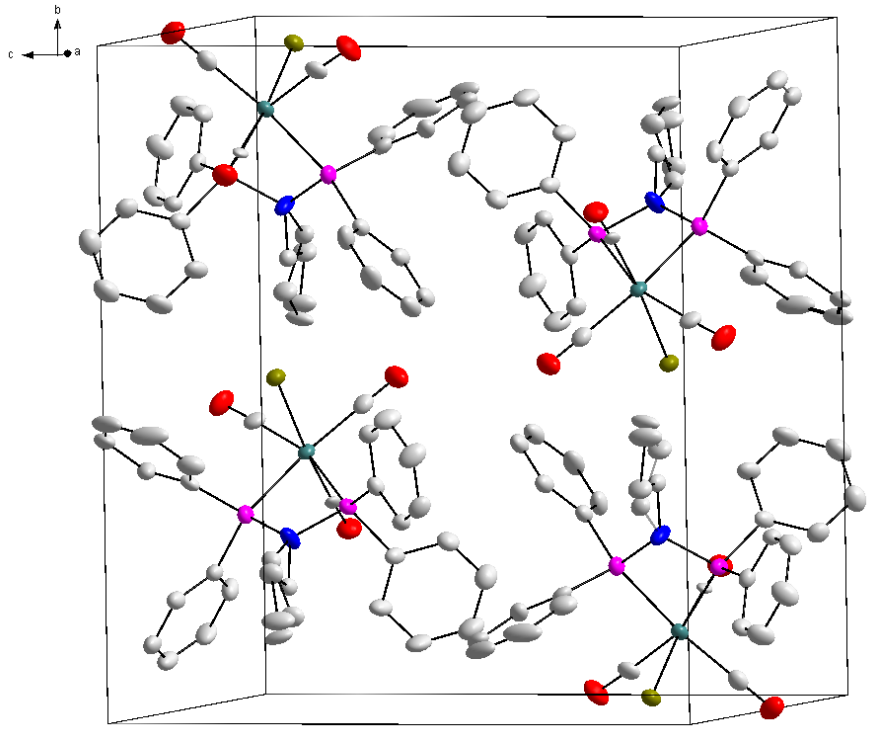


# 4.13 Discussion

In this chapter, ten new Rhenium(I) tricarbonyl structures which contained a pre-selected range of three and four membered bidentate ligands, are reported.

Reported complexes with O,O'-donor bidentate ligands are:

- *fac*-[NEt$_4$][Re(Trop)(CO)$_3$Br] (**1**),
- *fac*-[NEt$_4$][Re(Trop)(CO)$_3$(H$_2$O)].NO$_3$.H$_2$O (**2**),
- *fac*-[Re(Trop)(CO)$_3$Py] (**3**),
- *fac*-[Re(Trop)(CO)$_3$(DMAP)] (**4**),
- *fac*-[NEt$_4$][Re(BHA)(CO)$_3$Br] (**7**) and
- *fac*-[Re(Flav)(CO)$_3$(H$_2$O)].Flav (**8**).

Two complexes with N,O-donor bidentate ligands are reported,

- *fac*-[$NEt_4$][Re(2,5-PicoH)$(CO)_3$Br].$H_2O$ (**5**) and
- *fac*-[$NEt_4$][Re(2,5-PicoMe)$(CO)_3$Br] (**6**).

One complex with a N,N'-donor bidentate ligand is reported,

- μ-(*fac*- [Re(BipyDC)$(CO)_3$])$_2$.$4H_2O$ (**9**) and

one complex with a P,P'-donor bidentate ligand is reported,

- *fac*-[Re(PNP)$(CO)_3$(Br)] (**10**).

In Table 4.25, selected bond distances and angles of the ten structures are summarized for comparative reasons. Overall, the three Rhenium tricarbonyl distances are all within normal range. No definite differences can be seen in the equatorial and axial carbonyl distances. The Re-$L_1$ and Re-$L_2$ distances refer to the Rhenium-bidentate ligand distances. The X in the Re-X distances represent the different monodentate ligands in the sixth axial position. The bite angle ($L_1$-Re-$L_2$) and the $C_3$-Re-X angle is also included in the summary in Table 4.25.

The Rhenium oxygen distances, to the bidentate ligands, are all about the same ranging from 2.108(4) Å to 2.152(15) Å. The Rhenium to bidentate nitrogen distances, for three of these complexes are also well within range, varying from 2.164(4) Å to 2.186(3) Å. The two Re-P distances of 2.4586(15) Å and 2.4375(14) Å compare well with one another. Overall, the Rhenium to bidentate ligand distances increase from Re-O > Re-N > Re-P.

The Re-X distances, representing the Rhenium to axial monodentate ligand distances, vary significantly with the range of ligands. The Rhenium bromido distances are by far the largest as expected, ranging from 2.467(16) Å to 2.6690(5) Å. The Rhenium nitrogen and Rhenium oxygen distances are almost the same with Re-O distances between 2.128(3) Å and 2.213(5) Å and Re-N distances between 2.205(4) Å and 2.208(4) Å. A trend, Re-N ~ Re-O < Re-Br, in the Re-X distances can be made.

**Table 4.25: Summary of selected bond distances and angles for complexes 1 – 10.**

| Re-C1, C2, C3 (Å) | Re-$L_1$ (Å) | Re-$L_2$ (Å) | Re-X (Å) | $L_1$-Re-$L_2$ (°) | C3-Re-X (°) |
|---|---|---|---|---|---|
| ***fac*-[$NEt_4$][Re(Trop)$(CO)_3$Br] (1)** | | | | | |
| 1.906(5), 1.903(5), 1.861(7)/1.923(18) | 2.126(3) - **O** | 2.135(3) - **O** | 2.6334(9)/ 2.467(16) - **Br** | 74.88(2) | 175.61(19)/ 171.5(19) - **Br** |
| ***fac*-[$NEt_4$][Re(Trop)$(CO)_3(H_2O)$].$NO_3$.$H_2O$ (2)** | | | | | |
| 1.894(8), 1.886(8), 1.890(7) | 2.121(5) - **O** | 2.108(4) - **O** | 2.213(5) - **O** | 74.82(17) | 176.8(2) - **O** |
| ***fac*-[Re(Trop)$(CO)_3$Py] (3)** | | | | | |
| 1.898(5), 1,909(6), 1.930(6) | 2.121(4) - **O** | 2.136(3) - **O** | 2.208(4) - **N** | 74.68(14) | 177.55(18) - **N** |
| ***fac*-[Re(Trop)$(CO)_3$(DMAP)] (4)** | | | | | |
| 1.893(6), 1.915(7), 1.916(6) | 2.129(4) - **O** | 2.121(4) - **O** | 2.205(4) - **N** | 74.90(18) | 176.6(2) - **N** |
| ***fac*-[$NEt_4$][Re(2,5-PicoH)$(CO)_3$Br].$H_2O$ (5)** | | | | | |
| 1.906(7), 1.904(7), 1.963(8) | 2.152(15) - **O** | 2.182(5) - **N** | 2.6188(13) - **Br** | 74.38(18) | 178.1(2) - **Br** |
| ***fac*-[$NEt_4$][Re(2,5-PicoMe)$(CO)_3$Br] (6)** | | | | | |
| 1.910(4), 1.918(5), 1.943(5) | 2.136(3) - **O** | 2.178(4) - **N** | 2.6129(8) - **Br** | 75.67(13) | 177.47(13) - **Br** |
| ***fac*-[$NEt_4$][Re(BHA)$(CO)_3$Br] (7)** | | | | | |
| 1.899(3), 1.910(3), 1.897(3) | 2.1201(19) - **O** | 2.128(2) - **O** | 2.6690(5) - **Br** | 76.80(7) | 177.86(9) - **Br** |
| ***fac*-[Re(Flav)$(CO)_3(H_2O)$].Flav (8)** | | | | | |
| 1.903(4), 1.897(4), 1.895(4) | 2.151(3) - **O** | 2.130(3) - **O** | 2.188(3) - **O** | 76.61(11) | 174.38(14) - **O** |
| **μ-(*fac*-[Re(BipyDC)$(CO)_3$])$_2$.$4H_2O$ (9)** | | | | | |
| 1.924(5)/1.912(5), 1.922(4)/1.922(5), 1.895(4)/1.902(5) | 2.172(3)/ 2.164(4) - **N** | 2.186(3)/ 2.185(3) - **N** | 2.138(3)/ 2.128(3) - **O** | 74.60(12) 74.31(13) | 173.12(14) - **O** 171.56(14) - **O** |
| ***fac*-[Re(PNP)$(CO)_3$(Br)] (10)** | | | | | |
| 1.962(6), 1.952(5), 1.968(18)/1.866(15) | 2.4586(15) - **P** | 2.4375(14) - **P** | 2.619(2)/ 2.617(3) - **Br** | 66.65(4) | 175.4(3)/ 174.5(3) - **Br** |

The bite angles in the metallocycles, $L_1$-Re-$L_2$, of all the structures are within range, varying from 74.31(13) ° to 76.80(7) °, except that of the *fac*-[Re(PNP)$(CO)_3$(Br)] complex with a bite angle of 66.65(4). This might be due to the four-membered ring

formed between the metal and the ligand for this complex, compared to the five-membered rings for all the other structures.

Most of the structures exhibit a slight 'bending' of the axial monodentate ligand towards the bidentate ligand, which is clear from the C3-Re-X angle.

The crystal structures of *fac*-[$NEt_4$][Re(Trop)$(CO)_3$(Br)] (**1**), *fac*-[$NEt_4$][Re($TropBr_3$)$(CO)_3$(Br)] and *fac*-[Re($TropBr_3$)$(CO)_3(H_2O)$].MeOH, with $TropBr_3$ = 3,5,7-tribromotropolone, have already been published.[10,13,14] The Rhenium bromido distances for **1** and *fac*-[$NEt_4$][Re($TropBr_3$)$(CO)_3$(Br)] are 2.6334(9)/2.467(16) Å and 2.6270(3) Å respectively. For **2** and *fac*-[Re($TropBr_3$)$(CO)_3(H_2O)$].MeOH, the Rhenium aqua oxygen distances are 2.213(5) Å and 2.170(5) Å respectively. Even though one would expect a lengthening in the axial bond distance for the 3,5,7-tribromotropolonato complexes because of the electronwithdrawing effects of the bromide ligands, this is not found when comparing the data for the bromido and aqua complexes of the tribromotropolonato and the tropolonato ligand systems.

Overall, the bond angles and distances of complexes **1** - **4** compare well with the only significant difference being the axial monodentate ligand distance from the Rhenium(I) core.

The crystal structure of *fac*-[Re(2,4-PicoH)$(CO)_3(H_2O)$], with 2,4-PicoH = pyridine-2,4-dicarboxylato, has been reported before.[12] The bond distances and angles of *fac*-[$NEt_4$][Re(2,5-PicoH)$(CO)_3$(Br)].$H_2O$ (**5**) and *fac*-[$NEt_4$][Re(2,5-PicoMe)$(CO)_3$(Br)] (**6**), reported in this chapter, compare well with this complex. It does not seem that the position of the 'free' carboxylic acid on the ring has a significant influence on the bond distances and angles. Also, by comparing the data of **5** and **6**, it is clear that the methylated carboxylic acid in **6** does not influence the octahedral geometry or the distances from the Re(I) core.

The structure of *fac*-[$NEt_4$][Re(BHA)$(CO)_3$(Br)] (**7**) is the first of its kind, with the *fac*-Re(I) tricarbonyl core coordinated to this hydroxamic acid. The data of this structure compare well to other O,O'-donor bidentate ligands.

Earlier this year[22], the crystal data of *fac*-[Re(Flav)$(CO)_3$(MeOH)].MeOH was reported. By comparing the data of **8** with this complex, it is clear that the data are all within range

and compare quite well with Re-O distances of 2.141(3) Å and 2.147(3) Å and a bite angle of 76.24(11) ° reported for *fac*-[Re(Flav)$(CO)_3$(MeOH)].MeOH.

In the substituted bipyridine complex, μ-(*fac*-[Re(BipyDC)$(CO)_3$])$_2$.4$H_2O$ (**9**), very similar bond distances and angles are found when comparing it to the unsubstituted bipyridine complex reported by Kemp[23], *fac*-[Re(Bipy)$(CO)_3(H_2O)$].$NO_3$.$H_2O$ and *fac*-[Re(Bipy)$(CO)_3$(Br)].

Considering the four structures with the tropolonato bidentate ligand, **1** – **4**, the torsion angles of the ligand system and the dihedral angle between the equatorial plane and the plane through the ligand systems can be compared. A summary of this data is presented in Table 4.26.

**Table 4.26: Summary of the torsion and dihedral angles for 1 – 4.**

| Compound | Torsion angle (°) | Dihedral angle (°) |
|---|---|---|
| ***fac*-[$NEt_4$][Re(Trop)$(CO)_3$Br] (1)** | 2.7(6) | 2.1(2) |
| ***fac*-[$NEt_4$][Re(Trop)$(CO)_3(H_2O)$].$NO_3$.$H_2O$ (2)** | 0.6(9) | 9.1(2) |
| ***fac*-[Re(Trop)$(CO)_3$Py] (3)** | 0.6(7) | 12.9(2) |
| ***fac*-[Re(Trop)$(CO)_3$(DMAP)] (4)** | 3.2(8) | 11.7(2) |

From the data reported, no trend is found in the torsion angles of these tropolonato compounds. **4** exhibits the largest torsion angle while **2** and **3** have the smallest. Compound **3** and **4** have the largest dihedral angles, 12.9(2) and 11.7(2) respectively. The much smaller dihedral angle of **1** could be due to the disorder of the bromido and carbonyl ligand.

Overall, for all ten of the structures, a definite bending of the ligand system from the equatorial plane is observed. These dihedral angles vary from 2.1(2) ° for *fac*-[$NEt_4$][Re(Trop)$(CO)_3$(Br)] to 17.0(2) ° for μ-(*fac*-[Re(BipyDC)$(CO)_3$])$_2$.4$H_2O$.

The ten crystal structure reports in this chapter contributes significantly to the available data base for *fac*-Re(I) tricarbonyl complexes. Moreover, it unequivocally confirmed the coordination of the set of bidentate ligands to the Re(I) metal centre, it illustrated distortions and established the substitution products. These results are paramount for the derivation of the rate laws in the kinetic studies as reported in the next three chapters.

# 5 KINETIC INVESTIGATION OF METHANOL SUBSTITUTION REACTIONS IN RHENIUM(I) COMPLEXES

## 5.1 Background information and previous research

All potential radiopharmaceutical agents must be characterized completely by various means, including kinetic investigative studies,[1,2] since one gains significant information with regards to the biodistribution, *in vivo* stability, the rate of uptake as well as clearance from the body. Only a few reactivity studies have been reported for the *fac*-Rhenium(I) tricarbonyl core, some of which have been discussed in Chapter 2.[3,4,5,6,7,8,9]

Salignac and co-workers[4] kinetically investigated the water exchange process on *fac*-$[Re(CO)_3(H_2O)_3]^+$ as well as the water substitution reactions between *fac*-$[Re(CO)_3(H_2O)_3]^+$ and a variety of incoming ligands with various nucleophilicities. A more detailed description of this study can be found in Paragraph 2.7.

A year later, Grundler *et al*.[6] reported results similar to the values found in the study by Salignac, as well as activation volumes that revealed the ambivalent character of this Rhenium(I) moiety toward water substitution. These results were confirmed in 2006 by the same team[7].

Later on, Kemp studied the substitution reactions of Rhenium(I) complexes with coordinated bidentate ligands (N,N'- and N,O- donors) on *fac*-$[Re(CO)_3(H_2O)_3]^+$ and one

---

[1] Capellos, C., Bielski, B.H.J. *Kinetic Systems*, Wiley-Interscience, New York, **1972**.
[2] Frost, A.F., Pearson, R.G. *Kinetics and Mechanisms*, John Wiley and Sons, New York, **1953**.
[3] Alberto, R., Egli, A., Abram, U., Hegetschweiler, K., Gramlich, V., Schubiger, P.A. *J. Chem. Soc*., *Dalton Trans*. **1994**, 2815-2820.
[4] Salignac, B., Grundler, P.V., Cayemittes, S., Frey, U., Scopelliti, R., Merbach, A. *Inorg. Chem*. **2003**, *42*, 3516-3526.
[5] Helm, L. *Coord. Chem. Rev.* **2008**, *252*, 2346-2361.
[6] Grundler, P.V., Salignac, B., Cayemittes, S., Alberto, R., Merbach, A.E. *Inorg. Chem*. **2004**, *43*, 865-873.
[7] Grundler, P.V., Helm, L., Alberto, R., Merbach, A.E. *Inorg. Chem*. **2006**, *45*, 10378-10390.
[8] Kemp, G. PhD Thesis, University of Johannesburg, South Africa, **2006**.
[9] Schutte, M. MSc Dissertation, University of the Free State, South Africa, **2008**.

of the aims was to evaluate the reactivity of these complexes towards water substitution in the axial position. Kemp also explored the '2+1' approach with a range of incoming monodentate ligands.[8] It was clear that the substitution rates were dependent on the chemical nature of the entering ligand and it was concluded that the aqua substitution follow an interchange associative pathway.

The work of Kemp was expanded in our laboratory to include more N,O-bidentate ligand systems, and to introduce O,O'-bidentate ligands like tribromotropolone, 3-hydroxyflavone, tropolone and a range of isatins and flavanols[9].

One very important aspect of Kemp's and our previously reported work, is that all the reactions were performed in methanol solution due to the low solubility of the metal complexes in water. This of course raised the serious question whether water-substitution, and not methanol-substitution, due to solvation, is occurring here. After many test experiments involving different ratios of water and methanol as solvation systems and also including other solvents, it was concluded that it is more probable that solvation first occurs after which methanol substitution followed. These results were reported in a recent publication.[10]

The most important results from the previous work is that the O,O'-bidentate ligands utilized, activate the metal centre much more than the N,O-bidentate ligands. The excellent results with a biologically active ligand, close to the metal centre (3-hydroxyflavone), initiated further investigations into this type of ligand systems in this study. The results from these studies highlighted the need for a wider and more intense investigation of the various bidentate and monodentate ligand systems to clarify the mechanism of subsititution and the influences of the various ligand systems on the metal core. Also, the substitution kinetics of *fac*-[Re(Trop)$(CO)_3(H_2O)$] in aqueous medium was attempted for the first time (Chapter 7) to solve and obtain a comparison with the data obtained in methanol as solvent. Since high pressure studies are one way of proposing a mechanistic pathway of a chemical reaction with more certainty, it was decided to include and evaluate the pressure dependence of the substitution reactions between *fac*-[Re(Trop)$(CO)_3$(MeOH)] and various entering ligands.

[10] Schutte, M., Kemp, G., Visser, H.G., Roodt, A. *Inorg. Chem*. **2011**, *50(24)*, 12486-12498.

## Chapter 5

The complexes reported in this chapter are *fac*-[Re(2,5-PicoH)$(CO)_3$(MeOH)] (2,5-PicoH = pyridine-2-carboxylato-5-carboxylic acid), *fac*-[Re(Isa)$(CO)_3$(MeOH)] (Isa = isatin) and *fac*-[Re(Trop)$(CO)_3$(MeOH)] (Trop = tropolone), and are illustrated in Figure 5.1. The reported $pK_a$ value for tropolone is 6.7.[11] The two values speculated for 2,5-pyridine dicarboxylic are $pK_{a1}$ = 5.25 and $pK_{a2}$ = 4.4.[12]

**Figure 5.1: Schematic representation of the three complexes used in the methanol substitution kinetic study.**

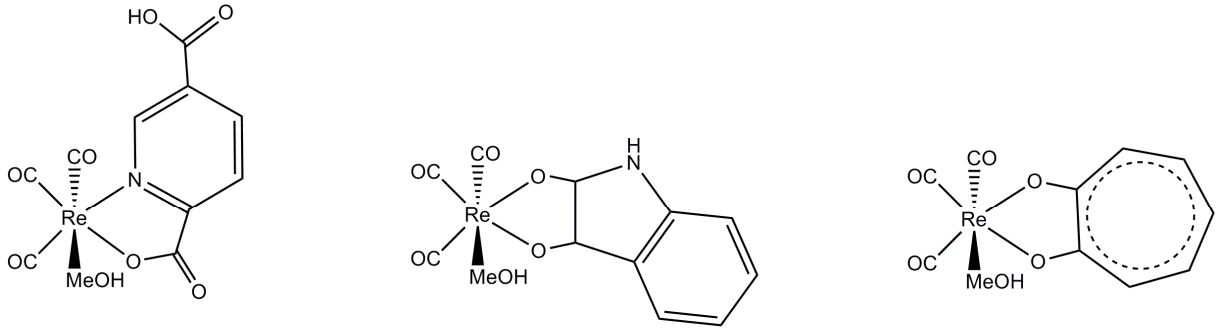


*fac*-[Re(2,5-PicoH)$(CO)_3$(MeOH)] *fac*-[Re(Isa)$(CO)_3$(MeOH)] *fac*-[Re(Trop)$(CO)_3$(MeOH)]

The methanol substitution reactions between the three complexes as shown in Figure 5.1, and various entering ligands were studied. As entering ligands, bromide ions ($Br^-$), iodide ions ($I^-$), imidazole (Im), pyridine (Py), thiocyanate ions ($NCS^-$), 4-dimethylaminopyridine (DMAP), thiourea (TU) and 1-methyl-2-thiourea (MeTU) was used. For this study, it was assumed that the thiocyanate ligand coordinate with the nitrogen atom, therefore it is written as $NCS^-$. A schematic representation of the substitution reactions is given in Figure 5.2.

The kinetic study was performed in methanol as solvent. The *fac*-[Re(Trop)$(CO)_3(H_2O)$] complex is moderately soluble in water and the aqueous kinetics of it could also be studied and is reported in Chapter 7.

It is assumed that the aqua complexes form the corresponding methanol substituted complexes as soon as it is dissolved in methanol for the kinetic study.[10]

[11] Bordwell, *ACR*, **1988**, *21*, 456.
[12] Vd Westhuizen, H.J., Meijboom, R., Schutte, M., Roodt, A. *Inorg. Chem*. **2010**, *49*, 9599-9608.

**Figure 5.2: Schematic representation of the methanol substitution reactions on the *fac*-[Re(L,L'-bid)$(CO)_3$(MeOH)] complexes by a wide range of entering ligands exhibiting a suitable range of ligand donor atoms.**

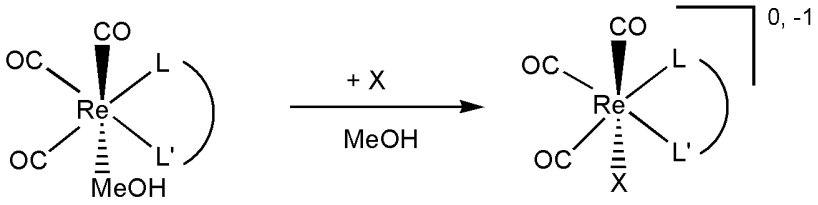


X = $Br^-$, $I^-$, Im, Py, $NCS^-$, DMAP, TU, MeTU

# 5.2 Experimental

## 5.2.1 General Procedure

All the chemicals and reagents used were of analytical grade, purchased from Sigma-Aldrich, South Africa. The kinetic measurements were performed on a Varian Cary 50 Conc UV-Visible spectrophotometer. The temperature in the system was controlled and maintained at ± 0.1 °C by a circulating water bath system. The Scientist Micromath, Version 2.01[13] program and Microsoft Office Excel 2007[14] were used to fit the data to the specific functions. All the kinetic runs were performed under *pseudo* first-order conditions with the ligand in excess in all the cases. In the figures presented, the solid lines represent the computer least-squares fits of the data and the single points respresent the experimental values, denoted by selected symbols. It was assumed that all the aqua complexes are converted to the corresponding methanol complexes upon dissolution in methanol for the kinetic studies.[10] The stability of all the complexes in methanol was established by monitoring solutions over several days on a UV/Vis spectrophotometer. All the experimental data, not included in this chapter, are reported in the supplementary material.

[13] MicroMath Scientist for Windows, Version 2.01, Copyright © 1986-1995, MicorMath, Inc.
[14] Microsoft Office 2007 Copyright © 2011 Microsoft Corporation.

## 5.2.2 Treatment of data

The Beer-Lambert law, with incorporation to the well-known first-order exponential, yields the following equation for the evaluation of the absorbance change *vs* time data in simple first-order reactions. Equation 5.1 was used in this study to treat all the data obtained.

$A_t = A_\infty - (A_\infty - A_0)e^{k_{obst}}$ **Equation 5.1**

The *pseudo* first-order rate constant ($k_{obs}$) is then determined by a least-squares fit of the absorbance *vs* time data for the reaction. This equation was used in all the kinetic runs that were followed in this study. All the observed rate constants that were calculated for the chemical reactions are reported in the supplementary material, if not documented in the text.

The activation parameters were calculated for a selection of the reactions to obtain more evidence of the type of mechanism for these reactions. Values for the standard activation enthalpy change ($\Delta H^{\ddagger}_{(k1)}$) and the standard activation entropy change ($\Delta S^{\ddagger}_{(k1)}$) were determined by using the logarithmic form of the Eyring equation (Equation 5.2).

$$\ln\left(\frac{k}{T}\right) = \ln\left(\frac{k_B}{h}\right) - \frac{\Delta H^{\neq}}{RT} + \frac{\Delta S^{\neq}}{R} \qquad \textbf{Equation 5.2}$$

By plotting $\ln\left(\frac{k}{T}\right)$ *vs*. $\frac{1}{T}$, a straight line with slope $(-\frac{\Delta H^{\neq}}{R})$ and intercept $(\ln\left(\frac{k_B}{h}\right) + \frac{\Delta S^{\neq}}{R})$ is obtained from which $\Delta H^{\ddagger}_{(k1)}$ and $\Delta S^{\ddagger}_{(k1)}$ could be obtained. In Equation 5.2 $K_B$ is the Boltzmann constant and h is Planck's constant.

## 5.3 Results and Discussion

Methanol substitution kinetics between *fac*-[Re(Isa)$(CO)_3$(MeOH)] (with Isa = isatin), *fac*-[Re(Trop)$(CO)_3$(MeOH)] (with Trop = tropolonato) and the *fac*-[Re(2,5-PicoH)$(CO)_3$(MeOH)] (with 2,5-PicoH = pyridine-2-carboxylato-5-carboxylic acid) complexes and various entering ligands were investigated and evaluated. The ligand systems were selected to compare and investigate the possible influence of different bidentate donor atoms on the rate.

The 2,5-pyridinedicarboxylic acid ligand was selected to compare the influence of the position of the free carboxylic acid group on the ligand backbone with the substitution kinetics data obtained previously for *fac*-[Re(2,4-PicoH)$(CO)_3$(MeOH)] (with 2,4-PicoH = pyridine-2-carboxylato-4-carboxylic acid). This ligand was also chosen because it has N,O-donor atoms as opposed to the O,O'-donor atoms of tropolone and isatin.

It is found from literature that isatin has a wide variety of biological applications on the central nervous system; it is used for instance as an anticonvulsant, anxiogenic and antiviral agent.[15,16,17,18,19,20,21] It is therefore a starting point for the design and synthesis of complexes directed at these targets. Moreover, very little is known of the coordination chemistry of isatin. The fact that a biological ligand is directly introduced onto a metal centre, opens interesting propositions for this ligand in radiopharmacy. Our previous studies have shown that 3-hydroxyflavone, as O,O'-bidentate ligand, is able to activate the normally inert Rhenium(I) metal centre quite substantially.[10] With the kinetic study of isatin as bidentatate ligand on the Rhenium(I) tricarbonyl core, we hoped to broaden the available knowledge base of the O,O'-donor ligands.

---

[15] Bhattacharya, S.K. *Biog. Amines* **1988**, *14*, 131-141.
[16] Bhattacharya, S.K., Chakraborti, A. *Indian. J. Exp. Biol*. **1998**, *36*, 118-121.
[17] Chen, L.R., Wang, Y.C., Lin, Y.W., Chou, S.Y., Chen, S.F., Liu, L.T., Wu, Y.T., Kuo, C.J., Chen, T.S.S., Juang, S.H. *Bioorg. Med. Chem. Lett*. **2005**, *15*, 3058-3062.
[18] Glover, V., Halket, J.M., Watkins, P.J., Clow, A., Goddwin, B.L., Sandler, M. *Neurochemistry* **1988**, *51*, 656-659.
[19] Medvedev, A.E., Goodwin, A., Clow, A., Halket, J., Glover, V., Sandler, M. *Biochem. Pharmacol*. **1992**, *44*, 590-592.
[20] Palit, G., Kumar, R., Patnaik, G.K., Bhattacharya, S.K. *Biogenic Amines* **1997**, *13*, 131-142.
[21] Webber, S.E., Tikhe, J., Worland, S.T., Fuhrman, S.A., Hendrickson, T.F., Matthews, D.A., Love, R.A., Patick, A.K., Weador, J.W., Ferre, R.A., Brown, E.L., Delisle, D.M., Ford, C.E., Binford, S.L. *J. Med. Chem*. **1996**, *39*, 5072-5082.

Tropolone, with its antibacterial properties, was chosen as the second O,O'-bidentate ligand.[22] This would enable us to compare the data to that obtained for the tribromotropolone complex, already studied by our group.

Preliminary stability and kinetic studies of *fac*-[Re(DMe-ox)$(CO)_3(H_2O)$] and *fac*-[Re(Cl-ox)$(CO)_3(H_2O)$] (with DMe-ox = 3,5-dimethyl-8-hydroxyquinolinato and Cl-ox = 5-chloro-8-hydroxyquinolinato) were performed in acetone and DMSO and it was found to be stable. Both these complexes were reacted with pyridine, imidazole and thiocyanate ions and all three reactions were found to be too fast for normal UV/Vis spectroscopy. The reactions can only be followed with a Stopped-flow apparatus, but since acetone and DMSO is not permitted as solvent on this apparatus, the kinetic studies of these two complexes are not possible at this stage.

Pyridine (Py), imidazole (Im), thiocyanate anions ($NCS^-$) and 4-dimethylaminopyridine (DMAP) as N-donor ligands, thiourea (TU) and 1-methyl-2-thiourea (MeTU) as S-donor ligands and the halides, iodide ($I^-$) and bromide ($Br^-$) ions, were selected as entering ligands for this study.

All of the methanol substitution reactions of *fac*-[Re(Isa)$(CO)_3$(MeOH)], *fac*-[Re(2,5-PicoH)$(CO)_3$(MeOH)] and *fac*-[Re(Trop)$(CO)_3$(MeOH)] with the above mentioned entering ligands were performed in methanol. Due to poor solubility in water, the first two mentioned complexes could only be studied in methanol. The aqueous kinetics of *fac*-[Re(Trop)$(CO)_3(H_2O)$] will be discussed in Chapter 7.

The synthesis of these three Rhenium complexes are reported in Chapter 3. The final UV/Vis spectra of the reaction solutions of each of the reactions reported here are in good agreement with the synthesized complexes (Paragraph 3.5.12, 3.5.14. 3.5.15, 3.5.16, 3.5.17, 3.5.18, 3.5.19 for the *fac*-[Re(2,5-PicoH)$(CO)_3(X)]^n$ complexes with X = $Br^-$, $I^-$, Py, Im, $NCS^-$, TU and MeTU; Paragraph 3.5.23, 3.5.24, 3.5.25, 3.5.26 for the *fac*-[Re(Isa)$(CO)_3(X)]^n$ complexes with X = Py, $NCS^-$, TU and MeTU; Paragraph 3.5.3, 3.5.5, 3.5.6, 3.5.7, 3.5.8, 3.5.9, 3.5.10, 3.5.11 for the *fac*-[Re(Trop)$(CO)_3(X)]^n$ complexes with X = $Br^-$, $I^-$, Py, Im, $NCS^-$, DMAP, TU and MeTU; n = 0, -1).

Under *pseudo* first-order conditions, with [X] >> *fac*-[Re(L,L'-bid)$(CO)_3$(X)] (L,L'-bid = bidentate ligand system, X = monodentate entering ligand), only one reaction was

[22] Trust, T.J. *Antimicrob. Agents Chemother*. **1975**, *7(5)*, 500-506.

observed for all of the reactions studied and the rates of these reactions increased systematically as the entering ligand's concentration was increased. It was established from all kinetics experiments that only one reaction (i.e. methanol substitution) took place for all the metal complexes and with all the relative entering ligands used (as illustrated by the formation of isosbestic points observed with successive absorbance *vs* wavelength scans). Spectrophotometrically, only one reaction was observed under these conditions. According to this, the following general mechanism can be predicted (Scheme 5.1):

**Scheme 5.1: The predicted mechanism for the methanol substitution reactions of complexes of the type *fac*-[Re(L,L'-bid)(CO)$_3$(MeOH)]$^n$.**

$$[Re(L,L'\text{-bid})(CO)_3(MeOH)] + X^{0,-1} \underset{k_{-1}}{\overset{k_1}{\rightleftharpoons}} [Re(L,L'\text{-bid})(CO)_3(X)]^{0,-1} + MeOH$$

L,L'-bid = N,O- or O,O'-donor bidentate ligands
X = $Br^-$, $I^-$, Py, Im, DMAP, $NCS^-$, TU, MeTU

The rate of the reaction is given in Equation 5.3 below.

$$\text{Rate} = k_1[Re(L,L'\text{-bid})(CO)_3(H_2O)][X] - k_{-1}[Re(L,L'\text{-bid})(CO)_3(X)] \qquad \textbf{Equation 5.3}$$

where $k_1$ and $k_{-1}$ represents the forward and reverse reactions respectively. *fac*-[Re(L,L'-bid)(CO)$_3$(MeOH)] is the methanol complex, *fac*-[Re(L,L'-bid)(CO)$_3$X] the substituted product and [X] is the entering ligand concentration. By employing *pseudo* first-order conditions, the concentration of the entering ligand is in excess ([X] >> *fac*-[Re(L,L'-bid)(CO)$_3$(MeOH)], *fac*-[Re(L,L'-bid)(CO)$_3$X]), and Equation 5.3 is reduced to:

$$k_{obs} = k_1[X] + k_{-1} \qquad \textbf{Equation 5.4}$$

with $k_{obs}$ the *pseudo* first-order rate constant. This expression enables one to determine the second order rate constant by first obtaining $k_{obs}$ at different ligand concentrations.

Equation 5.4 also holds for equilibrium reactions and the equilibrium constant $K_1$ is given by:

$$K_1 = \frac{k_1}{k_{-1}}$$ **Equation 5.5**

$k_1$ and $k_{-1}$ are calculated from a graph of $k_{obs}$ *vs* [X], that yields a straight line with $k_{-1}$ as the intercept and $k_1$ as the slope. The equilibrium constant, $K_1$, were determined throughout this study by means of Equation 5.5. The equilibrium constant, for one reaction per metal complex, was alternatively obtained by a non-linear least-squares fit to Equation 5.6, based on the UV/Vis data to confirm that the kinetically (Equation 5.5) and thermodynamically (Equation 5.6) equilibrium constants are the same.

$$A_{obs} = (A_M + A_{ML}K_1[L])/(1 + K_1[L])$$ **Equation 5.6**

In Equation 5.6, $A_M$ and $A_{ML}$ are the observed absorbance of *fac*-[Re(L,L'-bid)$(CO)_3$(MeOH)] and *fac*-[Re(L,L'-bid)$(CO)_3(X)]^n$ (X = monodentate entering ligand, n = 0, -1), $A_{obs}$ is the observerd absorbance and [L] is the concentration of the entering ligands.

## 5.4 Substitution reactions of *fac*-[Re(2,5-PicoH)$(CO)_3$(MeOH)] with monodentate ligands in methanol

The synthesis of the methanol complex, *fac*-[Re(2,5-PicoH)$(CO)_3$)(MeOH)], from the pentacarbonyl starting synthon, has been described in Chapter 3. The stabilities of the complex as well as the entering ligands were tested in methanol by monitoring the solutions on a UV/Vis spectrophotometer and were found to be stable for several hours. A range of entering ligands were used: as halides, bromide ($Br^-$) and iodide ions ($I^-$) were chosen, as nitrogen donors, pyridine (Py), imidazole (Im) and thiocyanate ($NCS^-$) and as sulphur donating ligands, thiourea (TU) and 1-methyl-2-thiourea (MeTU). The reactions were monitored at four temperatures, ranging from 15.0 °C to 45.0 °C and the

standard enthalpy change of activation ($\Delta H^{\ddagger}_{(k1)}$) and the standard entropy change of activation ($\Delta S^{\ddagger}_{(k1)}$) were determined for all the reactions from Eyring plots.

As a typical example of a UV/Vis spectral change, the spectrum for the substitution reaction between *fac*-[Re(2,5-PicoH)$(CO)_3$(MeOH)] and iodide ions is illustrated in Figure 5.3.

**Figure 5.3: Typical UV/Vis spectral change for the methanol substitution reaction between *fac*-[Re(2,5-PicoH)$(CO)_3$(MeOH)] and $I^-$ ions. [Re] = 1.0 x $10^{-4}$ M, [$I^-$] = 5.0 x $10^{-2}$ M, 25.0 °C, 275 nm, Δt = 120 s, MeOH. The insert indicate the Absorbance change *vs* time at 275 nm. The line shows the least-squares fit to Equation 5.1 ($k_{obs}$ = 0.00101(6) $s^{-1}$).**

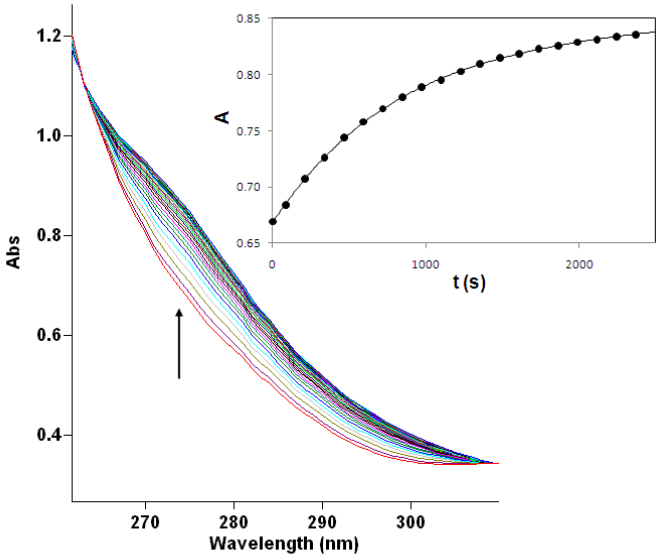


## 5.4.1 *fac*-[Re(2,5-PicoH)$(CO)_3$(MeOH)] + bromide ions

For the reaction between *fac*-[Re$(CO)_3$(2,5-PicoH)(MeOH)] and bromide ions ($Br^-$), performed in methanol and at four temperatures, the $k_{obs}$ *vs* $Br^-$ concentration data were obtained and fitted to Equation 5.4. The crystal structure of the substitution product, *fac*-[$NEt_4$][Re(2,5-PicoH)$(CO)_3$Br].$H_2O$ is reported in Paragraph 4.7. A plot of the temperature study, of $k_{obs}$ *vs* [$Br^-$], is given in Figure 5.4.

**Figure 5.4: Plot of $k_{obs}$ *vs* $[Br^-]$ for the reaction between *fac*-[Re(2,5-PicoH)(CO)$_3$(MeOH)] and bromide ions at different temperatures. [Re] = 1.0 x $10^{-4}$ M, $[Br^-]$ = 5.0 x $10^{-3}$ M – 5.0 x $10^{-2}$ M, 250 nm, MeOH.**

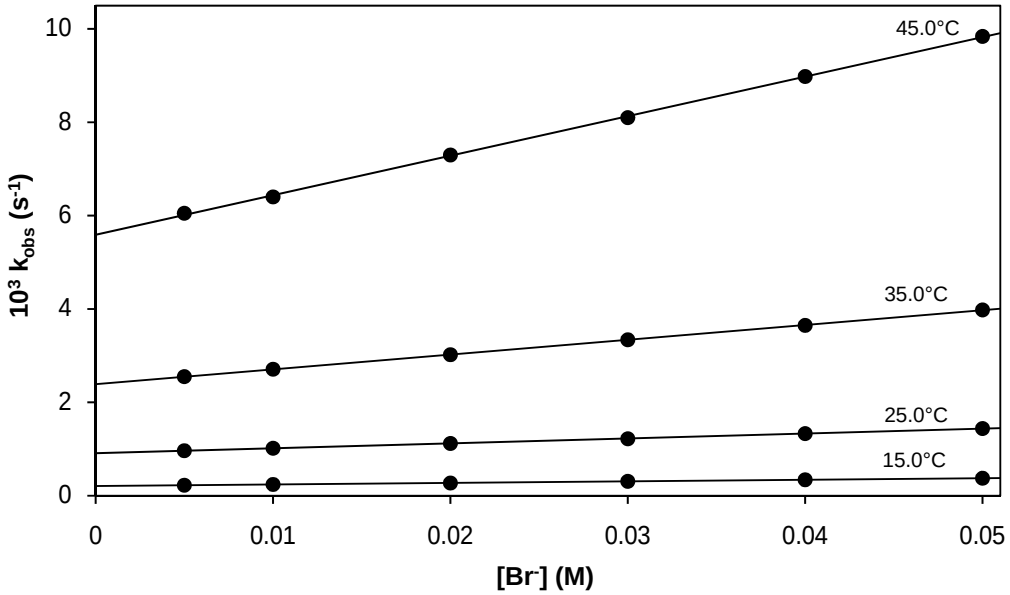


Fits of the $k_{obs}$ *vs* $[Br^-]$ data (Figure 5.4) to Equation 5.4 are presented in Table 5.1. From these results as well as the graphs obtained, it is clear that the experimental data fits well to the rate law. The UV/Vis spectrum for the synthesized *fac*-[Re(2,5-PicoH)(CO)$_3$Br]$^-$ complex in solution also corresponds to the final spectrum of this reaction mixture. It is therefore concluded that the mechanism proposed in Scheme 5.1, is a fair representation of these methanol substitution reactions of *fac*-[Re(2,5-PicoH)(CO)$_3$(MeOH)] and bromide ions.

**Table 5.1: Summary of the rate constants and activation parameters of the reaction between *fac*-[Re(2,5-PicoH)(CO)$_3$(MeOH)] and bromide ions at different temperatures (data in Figure 5.4).**

| | 15.0 °C | 25.0 °C | 35.0 °C | 45.0 °C |
|---|---|---|---|---|
| $10^3$ $k_1$ ($M^{-1}s^{-1}$) | 3.35(1) | 10.52(9) | 31.7(1) | 84.7(8) |
| $10^3$ $k_{-1}$ ($s^{-1}$) | 0.2067(4) | 0.910(3) | 2.390(4) | 5.59(3) |
| $K_1$ ($M^{-1}$) | 16.21(6) | 11.6(1) | 13.26(5) | 15.2(2) |
| $\Delta H^{\ddagger}_{(k1)}$ (kJ $mol^{-1}$) | | 79.7(5) | | |
| $\Delta S^{\ddagger}_{(k1)}$ (J $K^{-1}$ $mol^{-1}$) | | -15(2) | | |

The activation parameters of this reaction were determined by fitting the data to Equation 5.2. It is represented in Figure 5.5 and reported in Table 5.1. The values obtained for the paramaters were $\Delta H^{\ddagger}_{(k1)} = 79.7(5)$ kJ mol$^{-1}$ and $\Delta S^{\ddagger}_{(k1)} = -15(2)$ J K$^{-1}$ mol$^{-1}$.

**Figure 5.5: Eyring plot of ln($k_1$/T) *vs* 1/T for the reaction between *fac*-[Re(2,5-PicoH)(CO)$_3$(MeOH)] and bromide ions for a temperature range of 15.0 °C to 45.0 °C.**

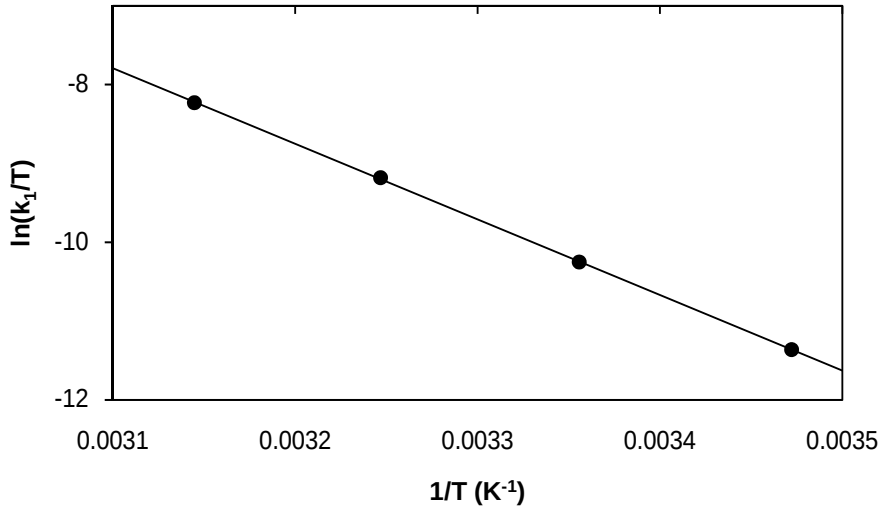


## 5.4.2 *fac*-[Re(2,5-PicoH)(CO)$_3$(MeOH)] + iodide ions

The methanol substitution reaction of *fac*-[Re(2,5-PicoH)(CO)$_3$(MeOH)] with iodide ions ($I^-$) was investigated under similar conditions to the reaction with bromide ions ($Br^-$) described before. The concentration of the iodide ions were varied from 5.0 x 10$^{-3}$ M and 5.0 x 10$^{-2}$ M. The reaction was followed at 275 nm in methanol and at four temperatures, 15.0 °C, 25.0 °C, 35.0 °C and 45.0 °C. The graph of $k_{obs}$ *vs* [$I^-$] at different temperatures are presented in Figure 5.6. The equilibrium constants are also determined thermodynamically and the $A_{obs}$ *vs* [$I^-$] data, for the reaction at 25.0 °C, is presented in Figure 5.7. The rate constants for the reactions are given in Table 5.2 and the Eyring plot are illustrated in Figure 5.8.

**Figure 5.6: Plot of $k_{obs}$ *vs* $[I^-]$ for the reaction of *fac*-[Re(2,5-PicoH)(CO)$_3$(MeOH)] with $I^-$ ions at different temperatures. [Re] = 1.0 x $10^{-4}$ M, $[I^-]$ = 5.0 x $10^{-3}$ – 5.0 x $10^{-2}$ M, 275 nm, MeOH.**

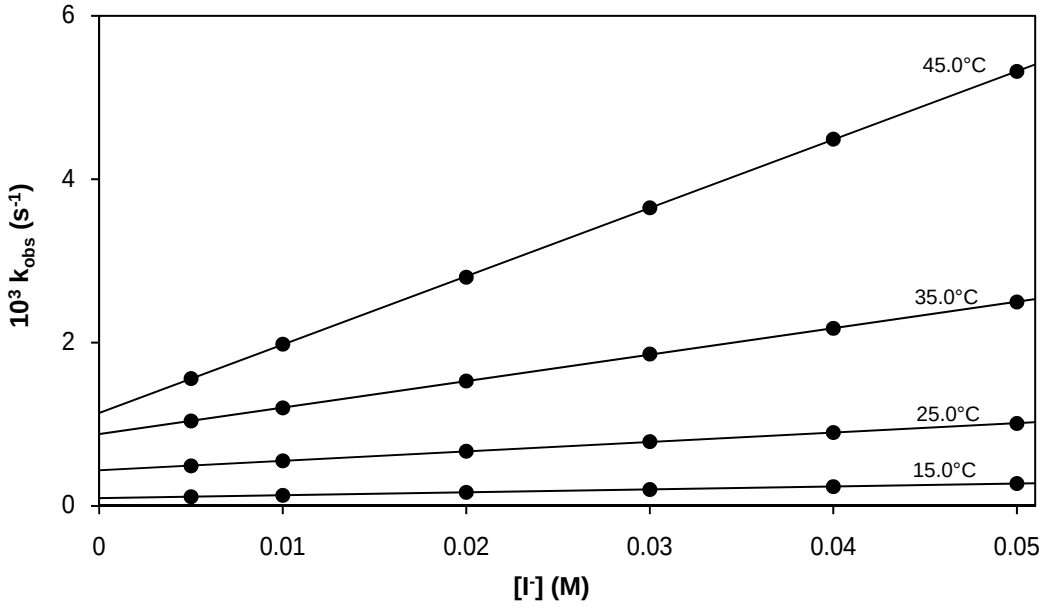


**Figure 5.7: Plot of $A_{obs}$ *vs* $[I^-]$ for the reaction of *fac*-[Re(2,5-PicoH)(CO)$_3$(MeOH)] with $I^-$ ions. [Re] = 1.0 x $10^{-4}$ M, 25.0 °C, 275 nm.**

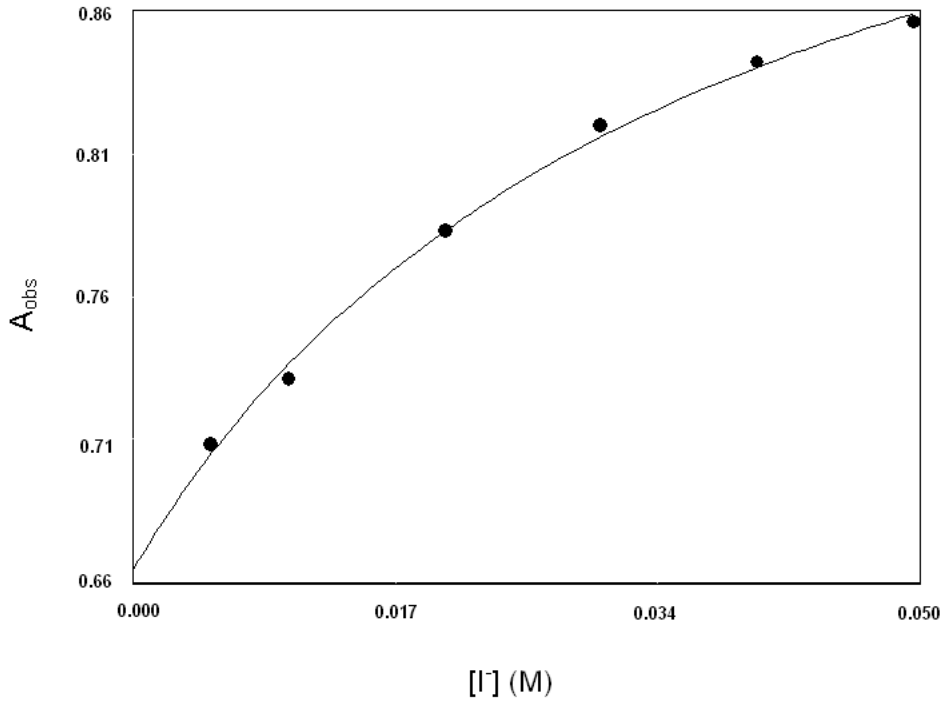

**Table 5.2: Summary of the rate constants and activation parameters of the reaction between *fac*-[Re(2,5-PicoH)(CO)$_3$(MeOH)] and $I^-$ ions at different temperatures (Data in Figure 5.6).**

| | 15.0 °C | 25.0 °C | 35.0 °C | 45.0 °C |
|---|---|---|---|---|
| $10^3$ $k_1$ ($M^{-1}s^{-1}$) | 3.57(2) | 11.53(9) | 32.4(1) | 83.6(2) |
| $10^3$ $k_{-1}$ ($s^{-1}$) | 0.0947(7) | 0.437(3) | 0.880(4) | 1.439(6) |
| $K_1$ ($M^{-1}$) | 37.7(3) | 26.4(3) | 36.8(2) | 73.4(4) |
| $K_1$ ($M^{-1}$)[a] | 31(4) | 27(8) | 29(3) | 66(9) |
| $\Delta H^{\ddagger}_{(k1)}$ (kJ $mol^{-1}$) | | 77(1) | | |
| $\Delta S^{\ddagger}_{(k1)}$ (J $K^{-1}$ $mol^{-1}$) | | -22(4) | | |

[a] Thermodynamically determined.

Equation 5.2 was applied to fit the $k_{obs}$ *vs* [$I^-$] data in order to determine the activation parameters for this reaction. It was determined as $\Delta H^{\ddagger}_{(k1)}$ = 77(1) kJ $mol^{-1}$ and $\Delta S^{\ddagger}_{(k1)}$ = -22(4) J $K^{-1}$ $mol^{-1}$.

**Figure 5.8: Eyring plot of ln($k_1$/T) *vs* 1/T for the reaction between *fac*-[Re(2,5-PicoH)(CO)$_3$(MeOH)] and $I^-$ for a temperature range of 15.0 °C to 45.0 °C.**

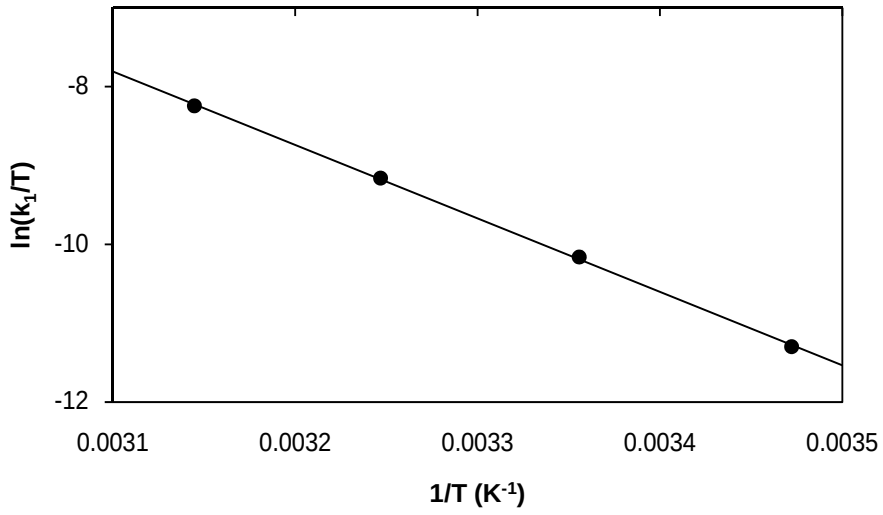


## 5.4.3 *fac*-[Re(2,5-PicoH)(CO)$_3$(MeOH) + pyridine

The methanol substitution reaction between *fac*-[Re(2,5-PicoH)(CO)$_3$(MeOH)] and pyridine (Py) were followed at 15.0 °C, 25.0 °C, 35.0 °C and 45.0 °C at 300 nm and in methanol as solvent. Pyridine concentrations varied between 5.0 x $10^{-2}$ M and

5.0 x $10^{-1}$ M and the Rhenium(I) complex concentration was 1.0 x $10^{-4}$ M. The data was fitted to Equation 5.4 and is illustrated in Figure 5.9.

**Figure 5.9: Plot of $k_{obs}$ *vs* [Py] for the reaction between *fac*-[Re(2,5-PicoH)(CO)$_3$(MeOH)] and pyridine at different temperatures. [Re] = 1.0 x $10^{-4}$ M, [Py] = 5.0 x $10^{-2}$ – 5.0 x $10^{-1}$ M, 300 nm, MeOH.**

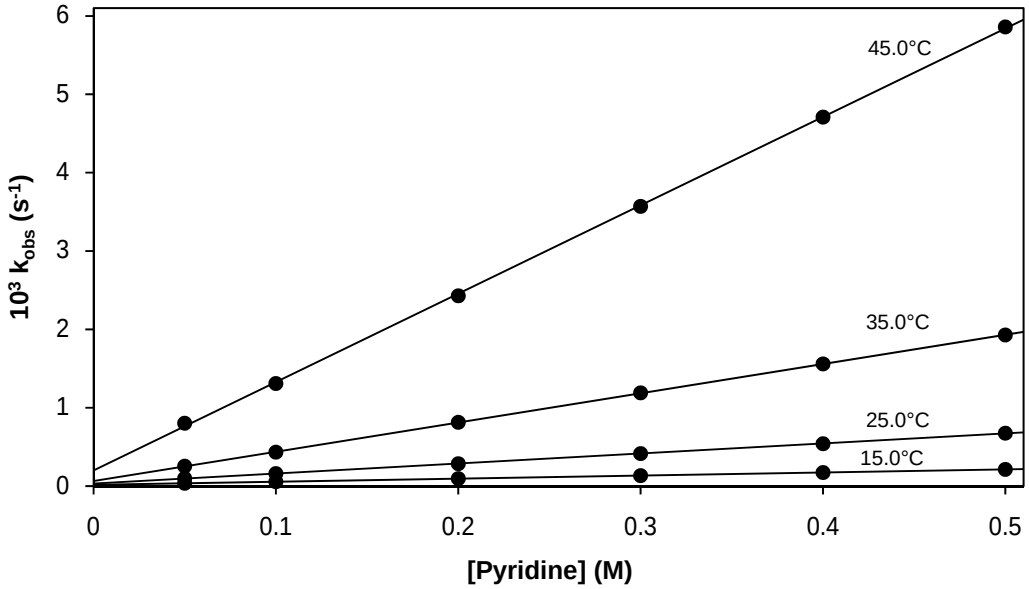


The rate constants were obtained from least-squares fits of the $k_{obs}$ *vs* [Py] data and are listed in Table 5.3. A plot of ln($k_1$/T) *vs* 1/T is presented in Figure 5.10 and the activation parameters were calculated as: $\Delta H^{\ddagger}_{(k1)}$ = 82(1) kJ mol$^{-1}$ and $\Delta S^{\ddagger}_{(k1)}$ = -25(4) J K$^{-1}$ mol$^{-1}$.

**Table 5.3: Summary of the rate constants and activation parameters of the reaction between *fac*-[Re(2,5-PicoH)(CO)$_3$(MeOH)] and pyridine at different temperatures.**

| | **15.0 °C** | **25.0 °C** | **35.0 °C** | **45.0 °C** |
|---|---|---|---|---|
| **$10^3$ $k_1$ ($M^{-1}s^{-1}$)** | 0.3966(3) | 1.281(7) | 3.73(1) | 11.28(7) |
| **$10^3$ $k_{-1}$ ($s^{-1}$)** | 0.0161(1) | 0.032(2) | 0.066(3) | 0.20(2) |
| **$K_1$ ($M^{-1}$)** | 24.7(2) | 40(3) | 57(3) | 56(6) |
| **$\Delta H^{\ddagger}_{(k1)}$ (kJ mol$^{-1}$)** | | 82(1) | | |
| **$\Delta S^{\ddagger}_{(k1)}$ (J K$^{-1}$ mol$^{-1}$)** | | -25(4) | | |

**Figure 5.10: Eyring plot of ln($k_1$/T) *vs* 1/T for the reaction between *fac*-[Re(2,5-PicoH)(CO)$_3$(MeOH)] and pyridine for a temperature range of 15.0 °C to 45.0 °C.**

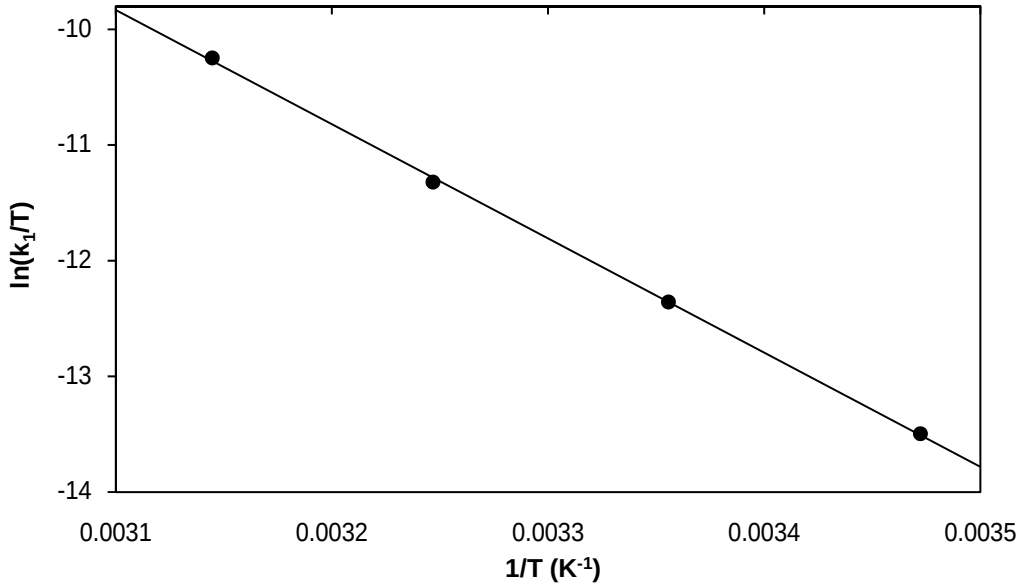


## 5.4.4 *fac*-[Re(2,5-PicoH)(CO)$_3$(MeOH)] + imidazole

The reaction between *fac*-[Re(2,5-PicoH)(CO)$_3$(MeOH)] and imidazole (Im) were followed at four temperatures, 15.0 °C to 45.0 °C, in methanol and at 264 nm. A plot of the obtained $k_{obs}$ values *vs* [Im] is provided in Figure 5.11. Table 5.4 gives a summary of the rate constants obtained for these reactions while a plot of ln($k_1$/T) *vs* 1/T is provided in Figure 5.12. From the Eyring equation (Equation 5.2), the activation parameters of 84(2) kJ mol$^{-1}$ and -19(6) J K$^{-1}$ mol$^{-1}$ for $\Delta H^{\ddagger}_{(k1)}$ and $\Delta S^{\ddagger}_{(k1)}$ respectively, were determined.

**Figure 5.11: Plot of $k_{obs}$ *vs* [Im] for the reaction between *fac*-[Re(2,5-PicoH)(CO)$_3$(MeOH)] and imidazole at different temperatures. [Re] = 1.0 x $10^{-4}$ M, [Im] = 5.0 x $10^{-2}$ M – 5.0 x $10^{-1}$ M, 264 nm, MeOH.**

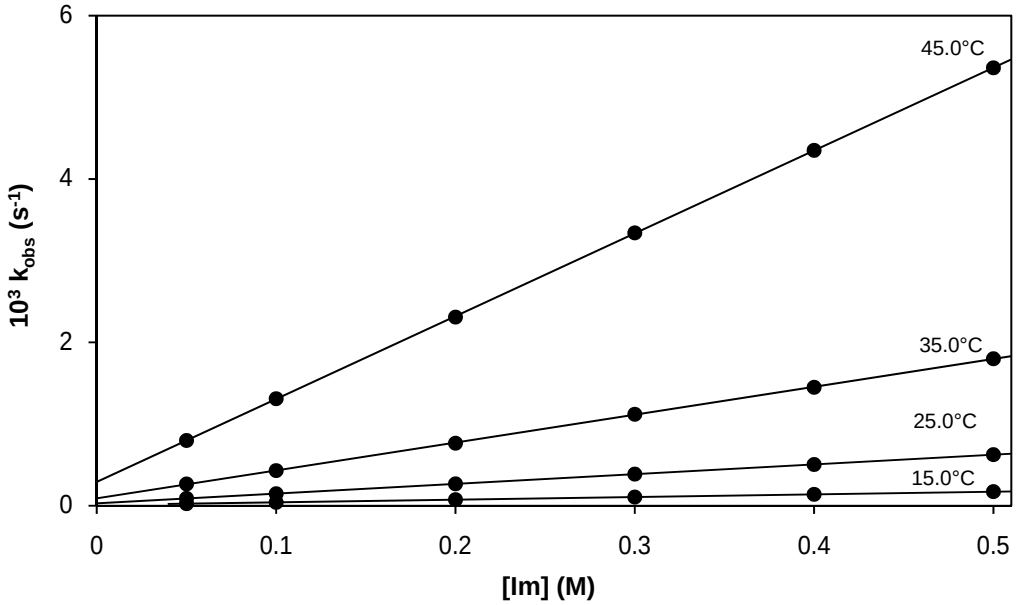


**Table 5.4: Summary of the rate constants and activation parameters of the reaction between *fac*-[Re(2,5-PicoH)(CO)$_3$(MeOH)] and imidazole at different temperatures.**

| | 15.0 °C | 25.0 °C | 35.0 °C | 45.0 °C |
|---|---|---|---|---|
| $10^3$ $k_1$ ($M^{-1}s^{-1}$) | 0.325(1) | 1.192(2) | 3.41(2) | 10.14(2) |
| $10^3$ $k_{-1}$ ($s^{-1}$) | 0.0089(3) | 0.0293(6) | 0.091(5) | 0.291(5) |
| $K_1$ ($M^{-1}$) | 37(1) | 40.7(8) | 37(2) | 34.8(6) |
| $\Delta H^{\ddagger}_{(k1)}$ (kJ $mol^{-1}$) | | 84(2) | | |
| $\Delta S^{\ddagger}_{(k1)}$ (J $K^{-1}$ $mol^{-1}$) | | -19(6) | | |

**Figure 5.12: Eyring plot of ln($k_1$/T) *vs* 1/T for the reaction between *fac*-[Re(2,5-PicoH)$(CO)_3$(MeOH)] and imidazole for a temperature range of 15.0 °C to 45.0 °C.**

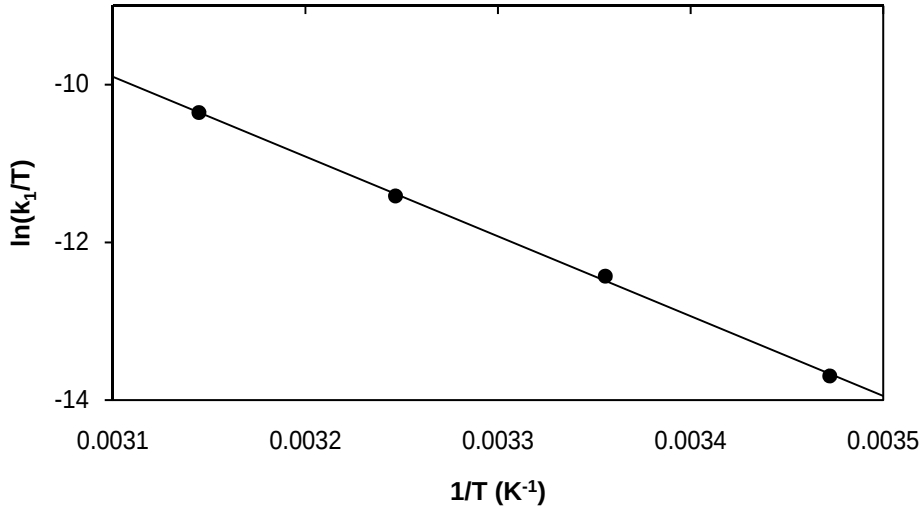


## 5.4.5 *fac*-[Re(2,5-PicoH)$(CO)_3$(MeOH)] + thiocyanate ions

The reaction of the third N-donating entering ligand, thiocyanate ($NCS^-$), with *fac*-[Re(2,5-PicoH)$(CO)_3$(MeOH)] were followed at 15.0 °C, 25.0 °C, 35.0 °C and 45.0 °C. The solutions were prepared in methanol and the reactions were followed at 270 nm. Figure 5.13 gives a representation of the $k_{obs}$ *vs* [$NCS^-$] data. The rate constants are given in Table 5.5 and the Eyring plot, with 1/T *vs* ln($k_1$/T) data, is illustrated in Figure 5.14.

**Figure 5.13: Plot of $k_{obs}$ *vs* [$NCS^-$] for the reaction between *fac*-[Re(2,5-PicoH)$(CO)_3$(MeOH)] and $NCS^-$ ions at different temperatures. [Re] = 1.0 x $10^{-4}$ M, [$NCS^-$] = 2.0 x $10^{-2}$ – 2.0 x $10^{-1}$ M, 270 nm, MeOH.**

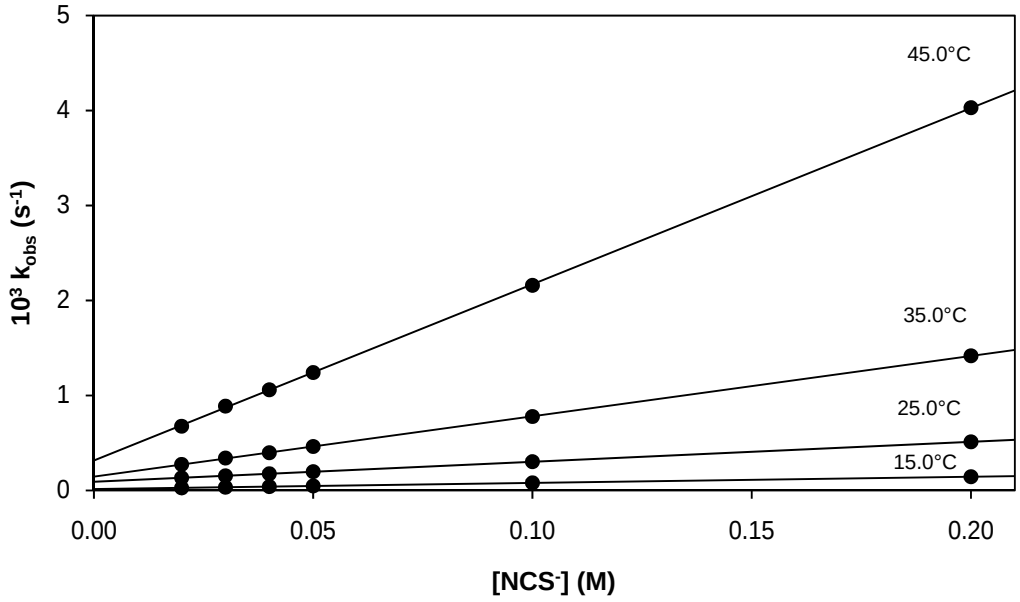


**Table 5.5: Summary of the rate constants and activation parameters of the reaction between *fac*-[Re(2,5-PicoH)$(CO)_3$(MeOH)] and $NCS^-$ ions at different temperatures.**

| | 15.0 °C | 25.0 °C | 35.0 °C | 45.0 °C |
|---|---|---|---|---|
| $10^3$ $k_1$ ($M^{-1}s^{-1}$) | 0.648(2) | 2.104(3) | 6.35(2) | 18.55(7) |
| $10^3$ $k_{-1}$ ($s^{-1}$) | 0.0153(2) | 0.0921(3) | 0.146(2) | 0.316(7) |
| $K_1$ ($M^{-1}$) | 42.4(6) | 22.84(8) | 43.5(6) | 59(1) |
| $\Delta H^{\ddagger}_{(k1)}$ (kJ $mol^{-1}$) | | 82.5(5) | | |
| $\Delta S^{\ddagger}_{(k1)}$ (J $K^{-1}$ $mol^{-1}$) | | -19(2) | | |

From the Eyring plot presented below (Figure 5.14), the activation parameters were determined. The activation enthalpy ($\Delta H^{\ddagger}_{(k1)}$) was calculated as 82.5(5) kJ $mol^{-1}$ and the activation entropy ($\Delta S^{\ddagger}_{(k1)}$) as -19(2) J $K^{-1}$ $mol^{-1}$.

**Figure 5.14: Eyring plot of ln($k_1$/T) *vs* 1/T for the reaction between *fac*-[Re(2,5-PicoH)$(CO)_3$(MeOH)] and $NCS^-$ ions for a temperature range of 15.0 °C to 45.0 °C.**

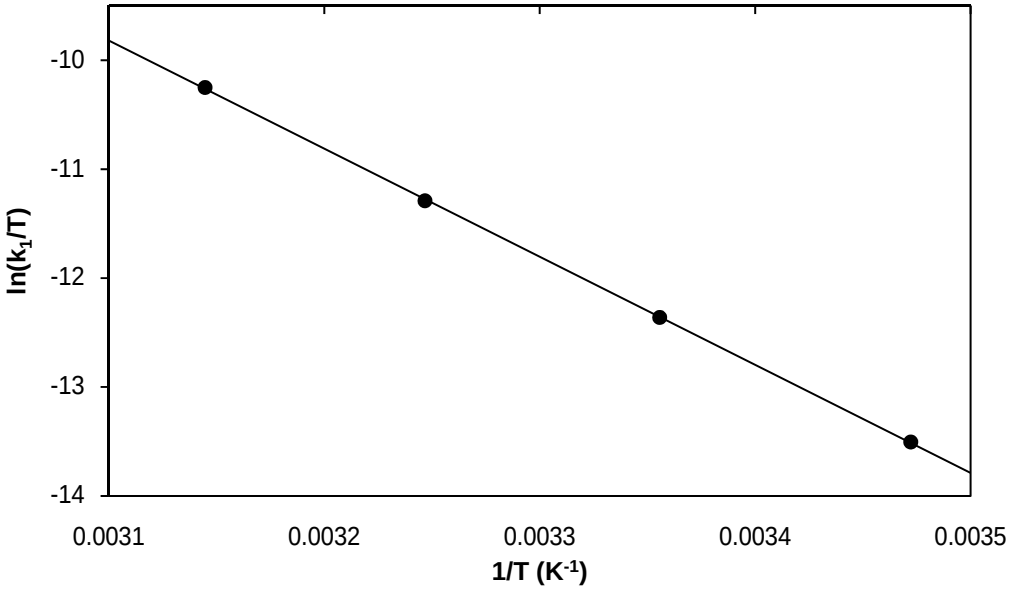


## 5.4.6 *fac*-[Re(2,5-PicoH)$(CO)_3$(MeOH)] + thiourea

A temperature study of the substitution reaction between *fac*-[Re(2,5-PicoH)$(CO)_3$(MeOH)] and thiourea (TU) as S-donating entering ligand was performed. The reactions were followed in methanol, at 326 nm and with ligand concentrations varying from 5.0 x $10^{-3}$ M to 5.0 x $10^{-2}$ M. Equation 5.4 was used to fit the data (Figure 5.14) and Table 5.6 summarizes the kinetic data for this reaction.

**Figure 5.15: Plot of $k_{obs}$ *vs* [TU] for the reaction between *fac*-[Re(2,5-PicoH)(CO)$_3$(MeOH)] and thiourea at different temperatures. [Re] = 1.0 x $10^{-4}$ M, [TU] = 5.0 x $10^{-3}$ – 5.0 x $10^{-2}$ M, 326 nm, MeOH.**

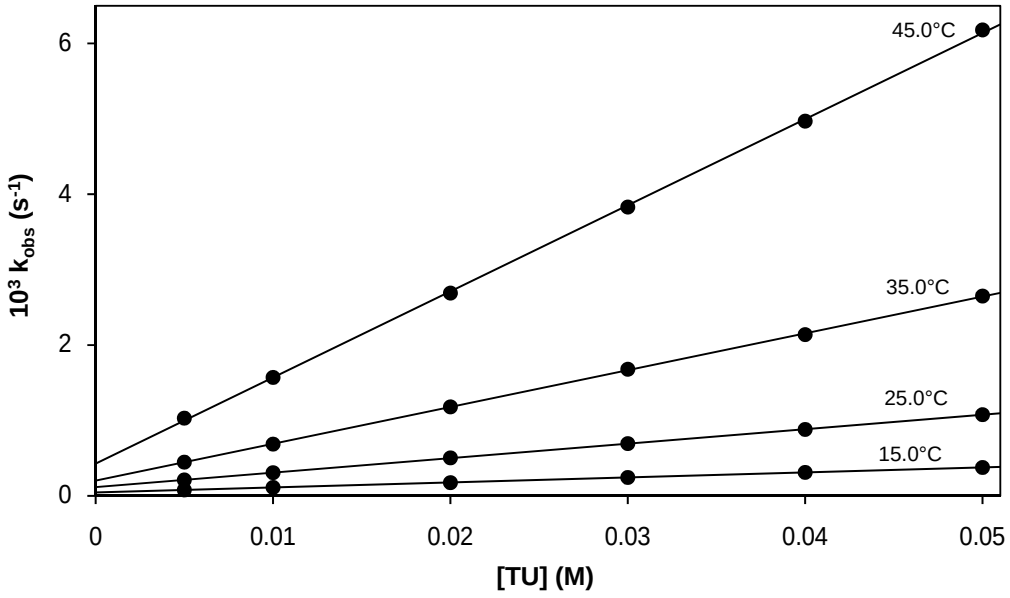


**Table 5.6: Summary of the rate constants and activation parameters of the reaction between *fac*-[Re(2,5-PicoH)(CO)$_3$(MeOH)] and thiourea at different temperatures.**

| | 15.0 °C | 25.0 °C | 35.0 °C | 45.0 °C |
|---|---|---|---|---|
| $10^3$ $k_1$ ($M^{-1}s^{-1}$) | 6.64(4) | 19.19(7) | 48.8(3) | 114.2(9) |
| $10^3$ $k_{-1}$ ($s^{-1}$) | 0.045(1) | 0.116(2) | 0.202(9) | 0.43(3) |
| $K_1$ ($M^{-1}$) | 148(3) | 165(3) | 242(11) | 266(19) |
| $\Delta H^{\ddagger}_{(k1)}$ (kJ $mol^{-1}$) | | 70(1) | | |
| $\Delta S^{\ddagger}_{(k1)}$ (J $K^{-1}$ $mol^{-1}$) | | -44(4) | | |

From the Eyring plot below (Figure 5.16) the activation parameters were calculated using Equation 5.2; $\Delta H^{\ddagger}_{(k1)}$ = 70(1) kJ $mol^{-1}$ and $\Delta S^{\ddagger}_{(k1)}$ = -44(4) J $K^{-1}$ $mol^{-1}$.

**Figure 5.16: Eyring plot of ln($k_1$/T) *vs* 1/T for the reaction between *fac*-[Re(2,5-PicoH)$(CO)_3$(MeOH)] and thiourea for a temperature range of 15.0 °C to 45.0 °C.**

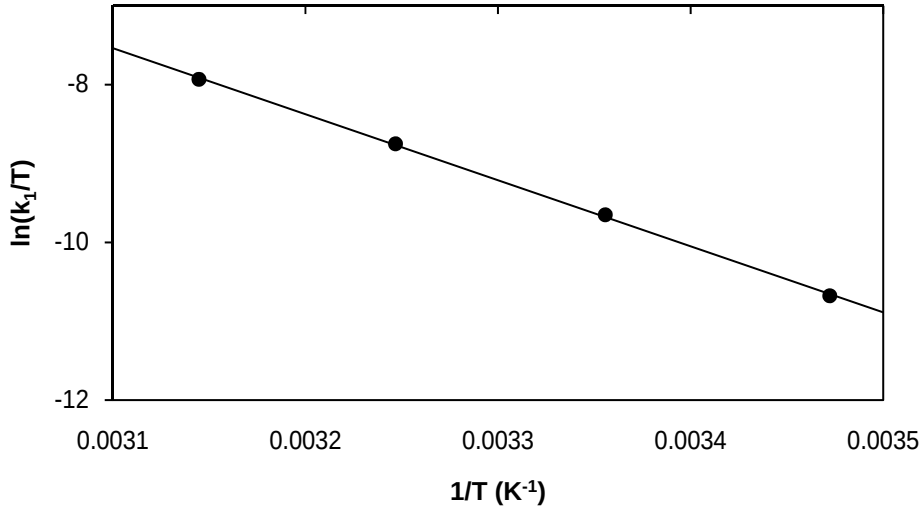


## 5.4.7 *fac*-[Re(2,5-PicoH)$(CO)_3$(MeOH)] + 1-methyl-2-thiourea

The methanol substitution reaction between *fac*-[Re(2,5-PicoH)$(CO)_3$(MeOH)] and 1-methyl-2-thiourea (MeTU) was followed. It was performed at four temperatures at 380 nm and the activation parameters, $\Delta H^{\ddagger}_{(k1)}$ and $\Delta S^{\ddagger}_{(k1)}$, were calculated. The kinetic data, $k_{obs}$ *vs* [MeTU], presented in Figure 5.17 were fitted to Equation 5.4 and the rate constants for this reaction was obtained and given in Table 5.7.

**Figure 5.17: Plot of $k_{obs}$ *vs* [MeTU] for the reaction between *fac*-[Re(2,5-PicoH)(CO)$_3$(MeOH)] and MeTU at different temperatures. [Re] = 1.0 x $10^{-4}$ M, [MeTU] = 5.0 x $10^{-3}$ – 5.0 x $10^{-2}$ M, 380 nm, MeOH.**

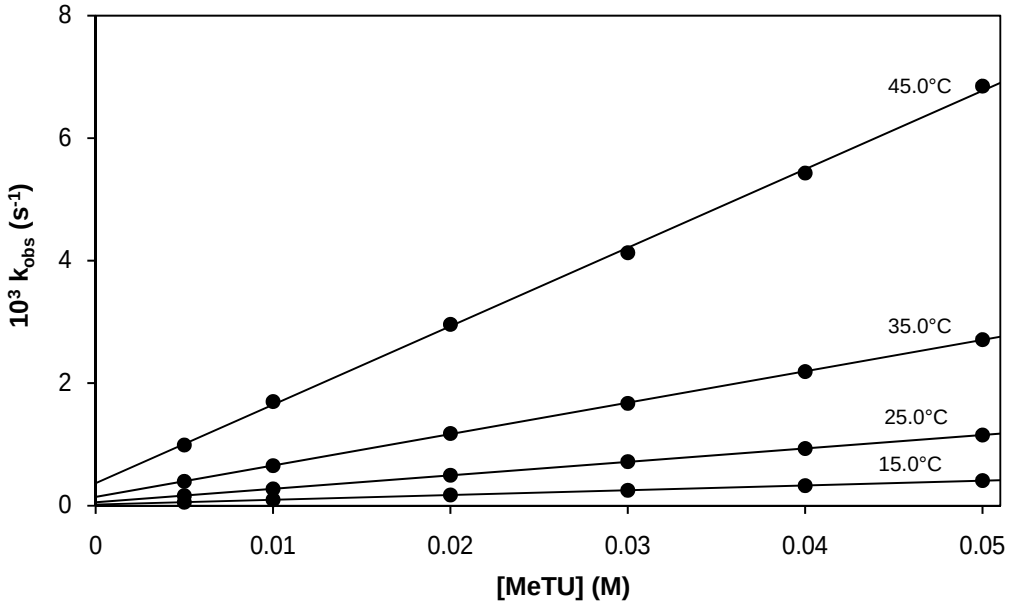


**Table 5.7: Summary of the rate constants and activation parameters of the reaction between *fac*-[Re(2,5-PicoH)(CO)$_3$(MeOH)] and MeTU at different temperatures.**

| | 15.0 °C | 25.0 °C | 35.0 °C | 45.0 °C |
|---|---|---|---|---|
| $10^3$ $k_1$ ($M^{-1}s^{-1}$) | 7.79(4) | 21.93(7) | 51.2(2) | 128(2) |
| $10^3$ $k_{-1}$ ($s^{-1}$) | 0.019(1) | 0.056(2) | 0.143(7) | 0.37(6) |
| $K_1$ ($M^{-1}$) | 410(22) | 392(14) | 358(18) | 346(56) |
| $\Delta H^{\ddagger}_{(k1)}$ (kJ $mol^{-1}$) | | 68(1) | | |
| $\Delta S^{\ddagger}_{(k1)}$ (J $K^{-1}$ $mol^{-1}$) | | -49(4) | | |

The activation parameters $\Delta H^{\ddagger}_{(k1)}$ and $\Delta S^{\ddagger}_{(k1)}$, calculated by means of Equation 5.2, were determined to be 68(1) kJ $mol^{-1}$ and -49(4) J $K^{-1}$ $mol^{-1}$ respectively (Figure 5.18).

**Figure 5.18: Eyring plot of ln($k_1$/T) *vs* 1/T for the reaction between *fac*-[Re(2,5-PicoH)(CO)$_3$(MeOH)] and MeTU for a temperature range of 15.0 °C to 45.0 °C.**

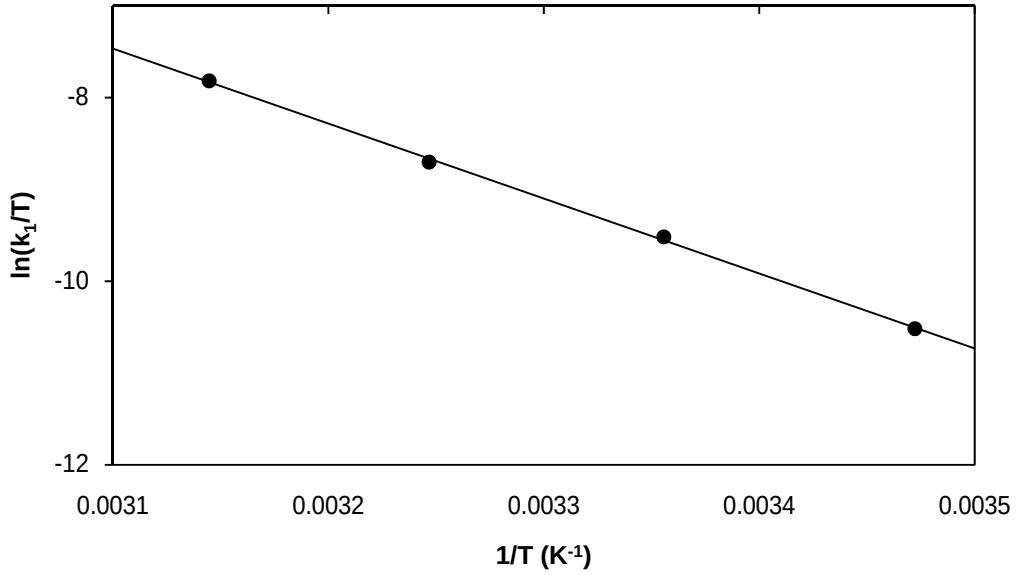


## 5.4.8 Summary of the results of the substitution reactions of *fac*-[Re(2,5-PicoH)(CO)$_3$(MeOH)] with the range of entering ligands

The substitution reactions between *fac*-[Re(2,5-PicoH)(CO)$_3$(MeOH)] and different monodentate entering ligands, at four temperatures, are summarized and presented in Figure 5.19 and Table 5.8 below. From the previous paragraphs, it is clear that all the reactions occur *via* the same mechanism. The $k_1$ values for the reactions with halides ($Br^-$ and $I^-$) are comparable and ~10 times faster than the reactions with the N-donor ligands (Py, Im and $NCS^-$). By comparing the N-donor ligands, an almost two times increase in rate for $NCS^-$ is observed compared to Py and Im and this could possibly be because of the negative charge of $NCS^-$ since the same trend is found between the negatively charged halides compared to the neutral N-donor ligands. The rate constants of thiourea and 1-methyl-2-thiourea are ~ 20 times faster than that of the N-donor ligands for the same Rhenium complex, indicating the seemingly higher affinity for the sulphur donating ligands.

**Figure 5.19: Illustrative comparison of the rates of reaction between *fac*-[Re(2,5-PicoH)(CO)$_3$(MeOH)] and different entering ligands at varying concentrations, at 25.0 °C.**

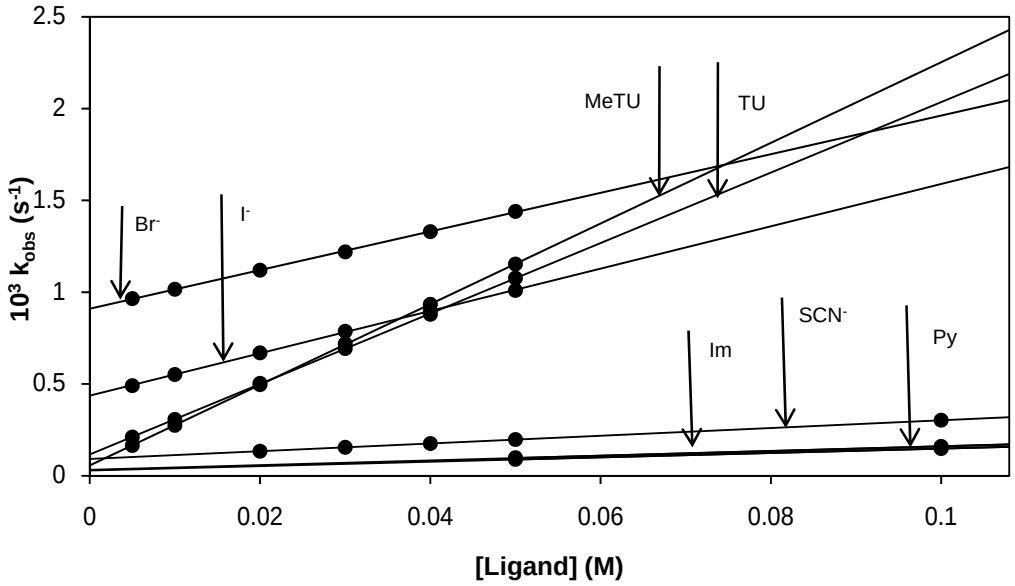


**Table 5.8: Summary of the rate constants and activation parameters of the *fac*-[Re(2,5-PicoH)(CO)$_3$(MeOH)] complex with entering ligands at 25.0 °C.**

| | $10^3 k_1$ ($M^{-1} s^{-1}$) | $10^3 k_{-1}$ ($s^{-1}$) | $K_1$ ($M^{-1}$) | $\Delta H^{\ddagger}_{(k1)}$ (kJ $mol^{-1}$) | $\Delta S^{\ddagger}_{(k1)}$ (J $K^{-1}$ $mol^{-1}$) |
|---|---|---|---|---|---|
| **$Br^-$** | 10.52(9) | 0.910(3) | 11.6(1) | 79.7(5) | -15(2) |
| **$I^-$** | 11.53(9) | 0.437(3) | 26.4(3) | 77(1) | -22(4) |
| **Py** | 1.281(7) | 0.032(2) | 40(3) | 82(1) | -25(4) |
| **Im** | 1.192(2) | 0.0293(6) | 40.7(8) | 84(2) | -19(6) |
| **$NCS^-$** | 2.104(3) | 0.0921(3) | 22.84(8) | 82.5(5) | -19(2) |
| **TU** | 19.19(7) | 0.116(2) | 165(3) | 70(1) | -44(4) |
| **MeTU** | 21.93(7) | 0.056(2) | 392(14) | 68(1) | -49(4) |

The second order rate constant observed for MeTU *vs* TU, shows a comparable rate constant but a larger stability constant. This might be due to the electrondonating methyl group on MeTU. Nevertheless, MeTU clearly has a larger affinity, based on the stability, for the Re(I) core compared to TU. The stability constants for *fac*-[Re(2,5-PicoH)(CO)$_3$(I)]$^-$ and *fac*-[Re(2,5-PicoH)(CO)$_3$(NCS)]$^-$ are of the same order while that of *fac*-[Re(2,5-PicoH)(CO)$_3$(Br)]$^-$ is less than half the value for these two complexes. The

$K_1$ values for *fac*-[Re(2,5-PicoH)$(CO)_3$(Im)] and *fac*-[Re(2,5-PicoH)$(CO)_3$(Py)] are almost identical, but twice that of the coordinated iodide and thiocyanate complexes, with a 4 times increase for *fac*-[Re(2,5-PicoH)$(CO)_3$(TU)] about 8 times increase for *fac*-[Re(2,5-PicoH)$(CO)_3$(MeTU)]. The affinity of the Re(I) core for the sulphur donating ligands are clearly illustrated in these values. The affinity of the metal complex for S-donating entering ligands can clearly be seen by the high stability constants for the TU and MeTU reactions.

A weak determination of the gradient of the $k_{obs}$ *vs* [L] graphs can have a significant influence on the $k_{-1}$ values and essentially big uncertainty/deviation in this data. The negative values for the standard entropy change of activation point towards an $I_a$ type mechanism. However, there is a larger deviation on the $k_{-1}$ values than the $k_1$ values which indicate less dependence on the entering ligand and therefore points towards a dissociative type mechanism.

## 5.5 Substitution reactions of *fac*-[Re(Isa)$(CO)_3$(MeOH)] with monodentate ligands in methanol

The synthesis of the neutral complex, *fac*-[Re(Isa)$(CO)_3$(MeOH)], from *fac*-$[NEt_4]_2[Re(CO)_3Br_3]$ is described in detail in Chapter 3. The stabilities of the complex as well as the entering ligands were tested in methanol and were found to be stable for several hours by monitoring the solutions on a UV/Vis spectrophotometer.

The monodentate entering ligands chosen for the substitution reactions were pyridine (Py), thiocyanate ($NCS^-$), thiourea (TU) and 1-methyl-2-thiourea (MeTU). The reactions were followed at a range of concentrations for each ligand at four temperatures, ranging from 15.0 °C to 45.0 °C. The concentration of the Rhenium complex, for all of the following reactions, was $1.25 \times 10^{-3}$ M. The activation parameters, standard enthalpy change of activation ($\Delta H^{\ddagger}_{(k1)}$) and the standard entropy change of activation ($\Delta S^{\ddagger}_{(k1)}$) for every reaction with entering ligand were obtained from Eyring plots.

Figure 5.20 represents a typical UV/Vis spectrum shift for the reaction between *fac*-[Re(Isa)$(CO)_3$(MeOH)] and in this case pyridine.

**Figure 5.20: Typical UV/Vis spectral change for the methanol substitution reactions of *fac*-[Re(Isa)(CO)$_3$(MeOH)] with pyridine. [Re] = 1.25 x 10$^{-3}$ M, [Py] = 4.0 x 10$^{-1}$ M, 25.0 °C, 370 nm, Δt = 24 s, MeOH. The insert indicate the Absorbance change *vs* time at 370 nm. The line shows the least-squares fit to Equation 5.1 (k$_{obs}$ = 0.00956(4) s$^{-1}$).**

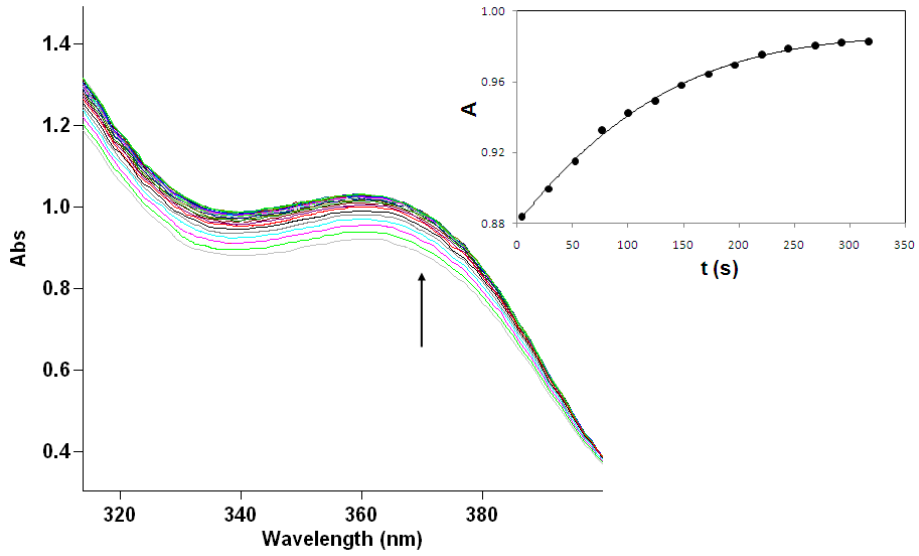


## 5.5.1 *fac*-[Re(Isa)(CO)$_3$(MeOH)] + pyridine

The methanol substitution reaction between *fac*-[Re(Isa)(CO)$_3$(MeOH)] and pyridine as entering ligand were followed. The reactions were monitored at 370 nm in methanol and were performed at four temperatures, 15.0 °C, 25.0 °C, 35.0 °C and 45.0 °C. A k$_{obs}$ *vs* [Py] plot for the reaction at four temperatures is given in Figure 5.21. The equilibrium constants are also determined thermodynamically and the A$_{obs}$ *vs* [Py] data, for the reaction at 25.0 °C, is presented in Figure 5.22.

**Figure 5.21: Plot of $k_{obs}$ *vs* [Py] for the reaction between *fac*-[Re(Isa)(CO)$_3$(MeOH)] and pyridine at different temperatures. [Re] = 1.25 x $10^{-3}$ M, [Py] = 5.0 x $10^{-2}$ M – 5.0 x $10^{-1}$ M, 370 nm, MeOH.**

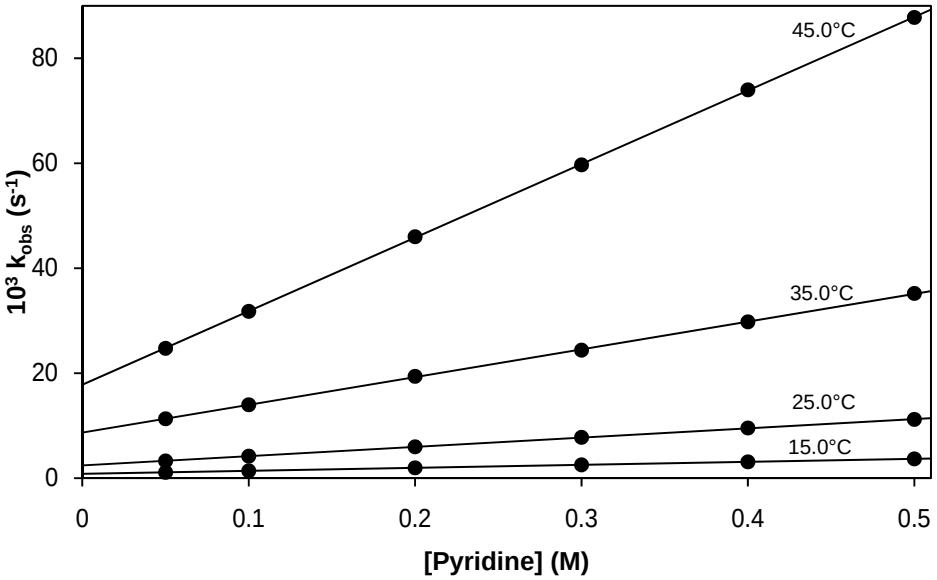


**Figure 5.22: Plot of $A_{obs}$ *vs* [Py] for the reaction of *fac*-[Re(Isa)(CO)$_3$(MeOH)] with pyridine. [Re] = 1.25 x $10^{-4}$ M, 25.0 °C, 370 nm.**

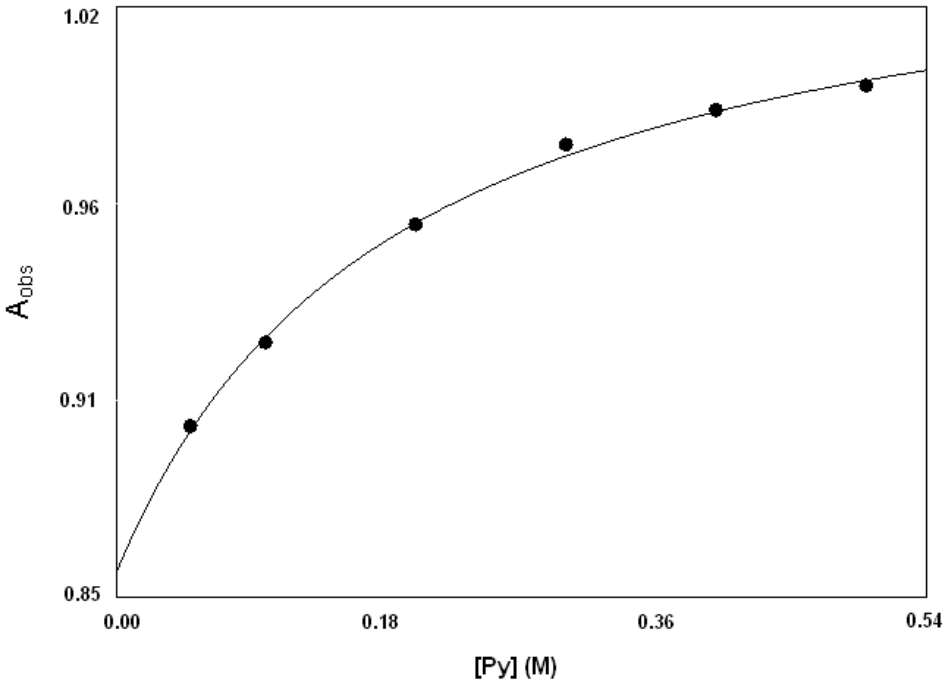

The kinetic data, for the reactions presented above, between *fac*-[Re(Isa)(CO)$_3$(MeOH)] and pyridine are summarized in Table 5.9 below for all four temperatures.

**Table 5.9: Summary of the rate constants and activation parameters of the reactions between *fac*-[Re(Isa)(CO)$_3$(MeOH)] and pyridine at different temperatures.**

| | **15.0 °C** | **25.0 °C** | **35.0 °C** | **45.0 °C** |
|---|---|---|---|---|
| **$10^3$ $k_1$ ($M^{-1}s^{-1}$)** | 5.69(2) | 17.7(2) | 52.8(3) | 140.1(4) |
| **$10^3$ $k_{-1}$ ($s^{-1}$)** | 0.837(7) | 2.44(5) | 8.70(9) | 17.8(1) |
| **$K_1$ ($M^{-1}$)** | 6.80(6) | 7.3(2) | 6.07(7) | 7.87(5) |
| **$K_1$ ($M^{-1}$)[a]** | 6(1) | 5(1) | 9.3(1) | 7.1(7) |
| **$\Delta H^{\ddagger}_{(k1)}$ (kJ $mol^{-1}$)** | | 79.0(5) | | |
| **$\Delta S^{\ddagger}_{(k1)}$ (J $K^{-1}$ $mol^{-1}$)** | | -13(2) | | |

[a] Thermodynamically determined.

From the Eyring plot, given in Figure 5.23, the activation parameters were calculated. The enthalpy of activation, $\Delta H^{\ddagger}_{(k1)}$, was determined as 79.0(5) kJ $mol^{-1}$ and the entropy of activation, $\Delta S^{\ddagger}_{(k1)}$, as -13(2) J $K^{-1}$ $mol^{-1}$.

**Figure 5.23: Eyring plot of $\ln(k_1/T)$ *vs* 1/T for the reaction between *fac*-[Re(Isa)(CO)$_3$(MeOH)] and pyridine for a temperature range of 15.0 °C to 45.0 °C.**

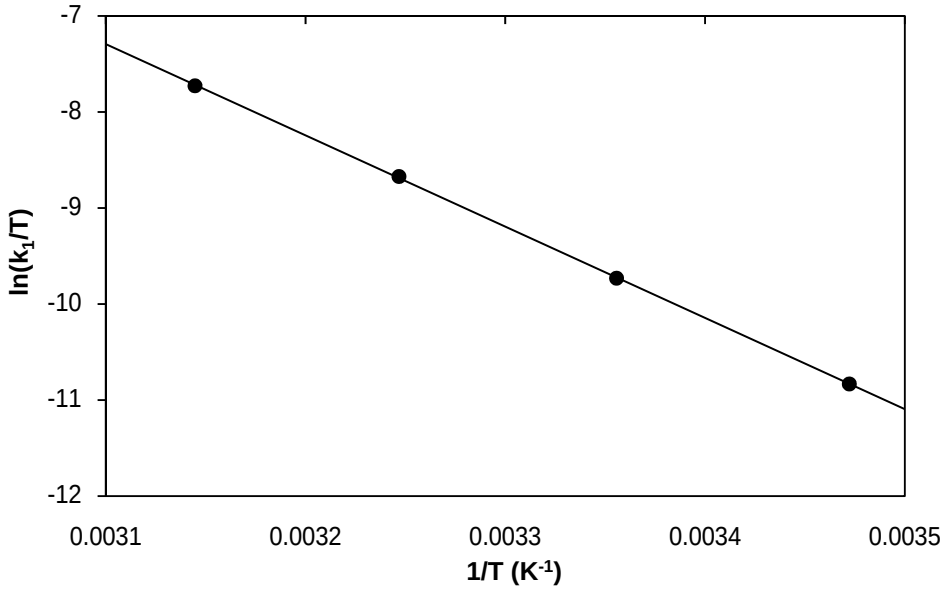

## 5.5.2 *fac*-[Re(Isa)(CO)$_3$(MeOH)] + thiocyanate ions

The substitution reaction between *fac*-[Re(Isa)(CO)$_3$(MeOH)] and thiocyanate ions were followed. The reaction was performed in methanol, at temperatures ranging from 15.0 °C to 45.0 °C. It was monitored at 378 nm with thiocyanate concentrations between 5.0 x $10^{-2}$ M and 5.0 x $10^{-1}$ M. The $k_{obs}$ *vs* [$NCS^-$] data was obtained (Figure 5.24) and fitted to Equation 5.4. The rate constants obtained from the fits are summarized in Table 5.10.

**Figure 5.24: Plot of $k_{obs}$ *vs* [$NCS^-$] for the reaction between *fac*-[Re(Isa)(CO)$_3$(MeOH)] and $NCS^-$ ions at different temperatures. [Re] = 1.25 x $10^{-3}$ M, [$NCS^-$] = 5.0 x $10^{-2}$ – 5.0 x $10^{-1}$ M, 378 nm, MeOH.**

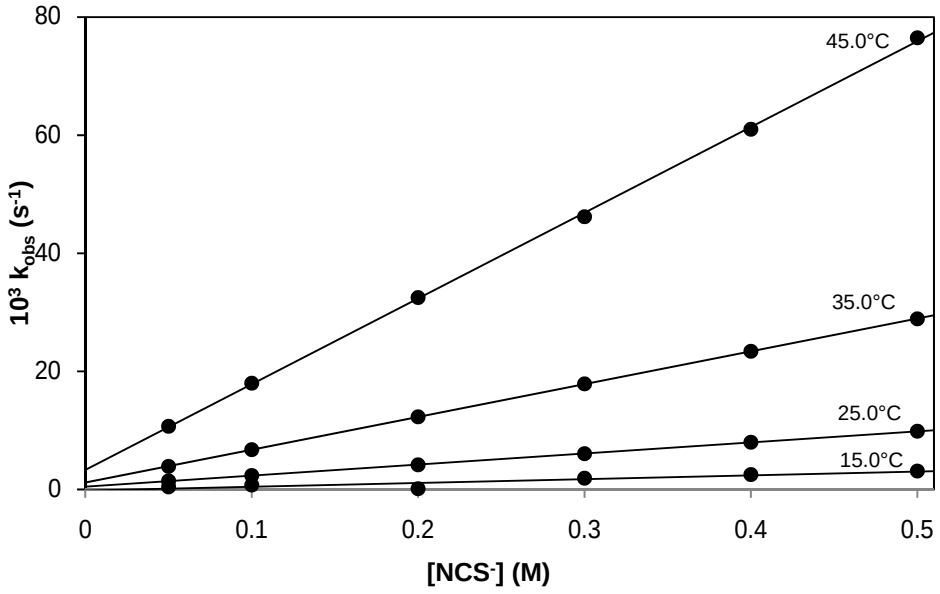


**Table 5.10: Summary of the rate constants and activation parameters of the reaction between *fac*-[Re(Isa)(CO)$_3$(MeOH)] and $NCS^-$ ions at different temperatures.**

| | 15.0 °C | 25.0 °C | 35.0 °C | 45.0 °C |
|---|---|---|---|---|
| $10^3$ $k_1$ ($M^{-1}s^{-1}$) | 5.96(2) | 18.7(1) | 55.5(1) | 145(1) |
| $10^3$ $k_{-1}$ ($s^{-1}$) | 0.139(6) | 0.48(4) | 1.18(4) | 3.3(4) |
| $K_1$ ($M^{-1}$) | 43(2) | 39(3) | 47(2) | 44(5) |
| $\Delta H^{\ddagger}_{(k1)}$ (kJ $mol^{-1}$) | | 78.7(7) | | |
| $\Delta S^{\ddagger}_{(k1)}$ (J $K^{-1}$ $mol^{-1}$) | | -14(2) | | |

The activation parameters for these reactions were determined by fitting the data in Table 5.10 to Equation 5.2 (Figure 5.25). The values obtained are as follows: $\Delta H^{\ddagger}_{(k1)}$ = 78.7(7) kJ $mol^{-1}$ and $\Delta S^{\ddagger}_{(k1)}$ = -14(2) J $K^{-1}$ $mol^{-1}$ for the standard enthalpy change of activation and the standard entropy change of activation respectively.

**Figure 5.25: Eyring plot of $\ln(k_1/T)$ *vs* 1/T for the reaction between *fac*-[Re(Isa)(CO)$_3$(MeOH)] and $NCS^-$ for a temperature range of 15.0 °C to 45.0 °C.**

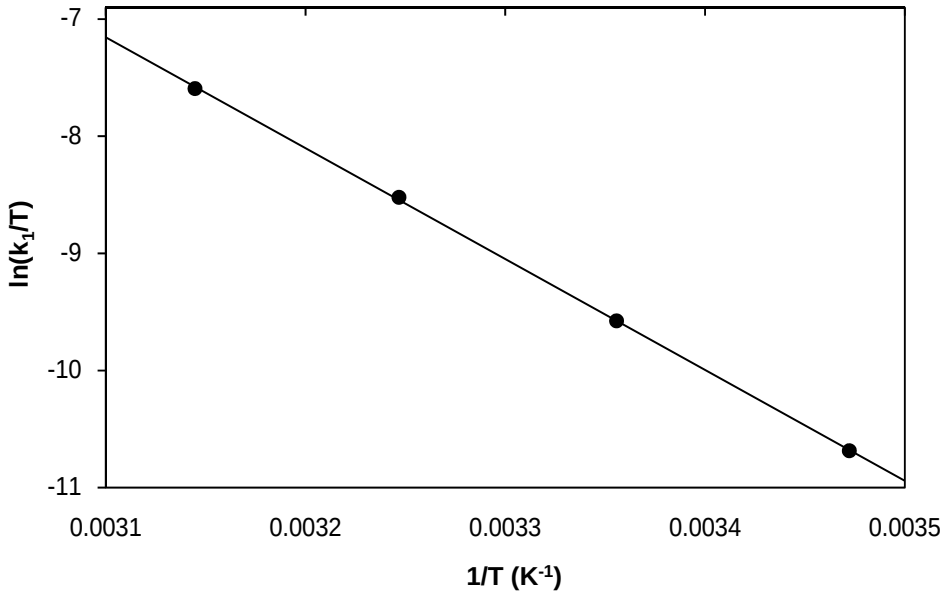


## 5.5.3 *fac*-[Re(Isa)(CO)$_3$(MeOH)] + thiourea

The methanol substitution reaction between *fac*-[Re(Isa)(CO)$_3$(MeOH)] and thiourea, as S-donating entering ligand, was investigated. The reaction was monitored at 320 nm, in methanol with the concentration of the complex at 1.25 x $10^{-3}$ M and the thiourea concentration varying between 5.0 x $10^{-3}$ M and 5.0 x $10^{-2}$ M. A plot of $k_{obs}$ *vs* [TU] data are presented in Figure 5.26. From this data, the rate constant values were obtained by fitting the $k_{obs}$ *vs* [TU] data to Equation 5.4. The kinetic data are presented in Table 5.11.

**Figure 5.26: A plot of $k_{obs}$ *vs* [TU] for the reaction between *fac*-[Re(Isa)(CO)$_3$(MeOH)] and thiourea at different temperatures. [Re] = 1.25 x $10^{-3}$ M, [TU] = 5.0 x $10^{-3}$ M to 5.0 x $10^{-2}$ M, 320 nm, MeOH.**

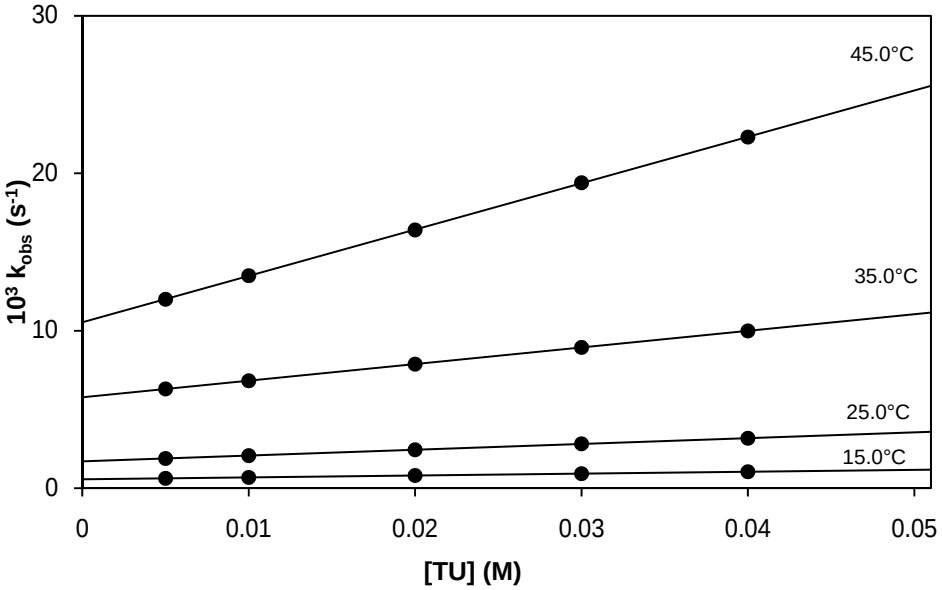


The standard enthalpy of activation ($\Delta H^{\ddagger}_{(k1)}$) and the standard entropy of activation ($\Delta S^{\ddagger}_{(k1)}$) were determined by fitting the data in Table 5.11 to Equation 5.2. The Eyring plot is given in Figure 5.27 and the values obtained are as follows: $\Delta H^{\ddagger}_{(k1)}$ = 78.9(5) kJ mol$^{-1}$ and $\Delta S^{\ddagger}_{(k1)}$ = -8(2) J K$^{-1}$ mol$^{-1}$ .

**Table 5.11: Summary of the rate constants and activation parameters of the reaction between *fac*-[Re(Isa)(CO)$_3$(MeOH)] and thiourea at different temperatures.**

| | **15.0 °C** | **25.0 °C** | **35.0 °C** | **45.0 °C** |
|---|---|---|---|---|
| **$10^3$ $k_1$ ($M^{-1}s^{-1}$)** | 11.85(6) | 36.5(2) | 105.4(1) | 293.5(8) |
| **$10^3$ $k_{-1}$ ($s^{-1}$)** | 0.570(2) | 1.709(6) | 5.772(4) | 10.55(2) |
| **$K_1$ ($M^{-1}$)** | 20.8(1) | 21.4(1) | 18.3(1) | 27.8(1) |
| **$\Delta H^{\ddagger}_{(k1)}$ (kJ mol$^{-1}$)** | | 78.9(5) | | |
| **$\Delta S^{\ddagger}_{(k1)}$ (J K$^{-1}$ mol$^{-1}$)** | | -8(2) | | |

**Figure 5.27: Eyring plot of ln($k_1$/T) *vs* 1/T for the reaction between *fac*-[Re(Isa)(CO)$_3$(MeOH)] and thiourea for a temperature range of 15.0 °C to 45.0 °C.**

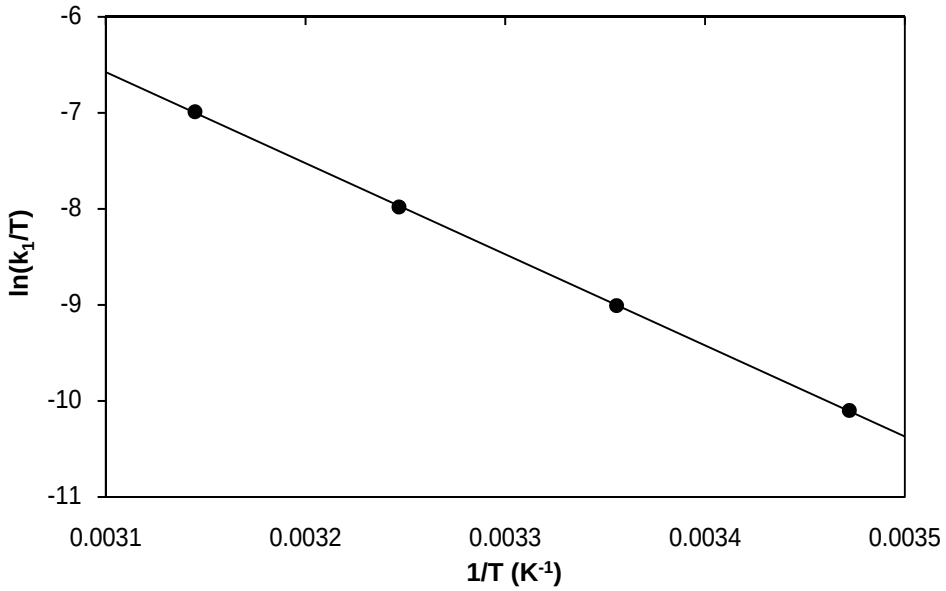


## 5.5.4 *fac*-[Re(Isa)(CO)$_3$(MeOH)] + 1-methyl-2-thiourea

The reaction of *fac*-[Re(Isa)(CO)$_3$(MeOH)] with MeTU as entering ligand was followed. From the tabulated data and figures below, it is clear that the experimental data fits well into the rate law. The reaction was monitored at 360 nm in methanol. The $k_{obs}$ *vs* [MeTU] data are given in Figure 5.28 and from this, by fitting it to Equation 5.4, the rate constants presented in Table 5.12 was obtained.

**Figure 5.28: Plot of $k_{obs}$ *vs* [MeTU] for the reaction between *fac*-[Re(Isa)(CO)$_3$(MeOH)] and MeTU at different temperatures. [Re] = 1.25 x $10^{-3}$ M, [MeTU] = 5.0 x $10^{-3}$ M to 5.0 x $10^{-2}$ M, 360 nm, MeOH.**

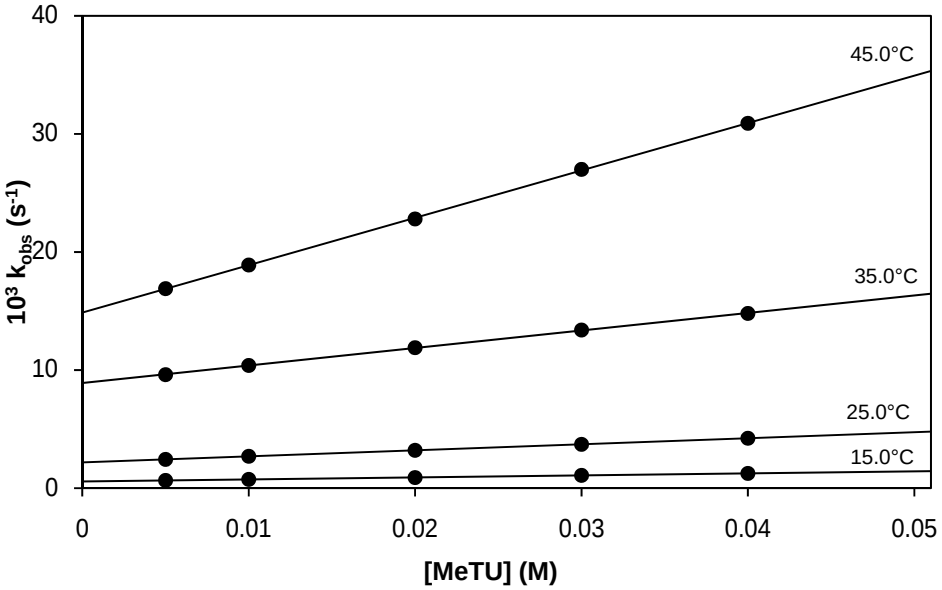


**Table 5.12: Summary of the rate constants and activation parameters of the reaction between *fac*-[Re(Isa)(CO)$_3$(MeOH)] and MeTU at different temperatures.**

| | **15.0 °C** | **25.0 °C** | **35.0 °C** | **45.0 °C** |
|---|---|---|---|---|
| **$10^3$ $k_1$ ($M^{-1}s^{-1}$)** | 17.1(1) | 50.9(1) | 146(1) | 402(2) |
| **$10^3$ $k_{-1}$ ($s^{-1}$)** | 0.572(4) | 2.190(3) | 8.94(4) | 14.86(6) |
| **$K_1$ ($M^{-1}$)** | 29.9(3) | 23.2(1) | 16.3(1) | 27.1(2) |
| **$\Delta H^{\ddagger}_{(k1)}$ (kJ $mol^{-1}$)** | | 77.6(7) | | |
| **$\Delta S^{\ddagger}_{(k1)}$ (J $K^{-1}$ $mol^{-1}$)** | | -9(2) | | |

The data in Table 5.12 was fitted to Equation 5.2 and the values for the activation parameters were determined. The standard enthalpy change of activation ($\Delta H^{\ddagger}_{(k1)}$) was calculated as 77.6(7) kJ $mol^{-1}$ and the standard entropy change of activation ($\Delta S^{\ddagger}_{(k1)}$) as -9(2) J $K^{-1}$ $mol^{-1}$. Figure 5.29 represents the Eyring plot for this reaction.

**Figure 5.29: Eyring plot of ln($k_1$/T) *vs* 1/T for the reaction between *fac*-[Re(Isa)(CO)$_3$(MeOH)] and MeTU for a temperature range of 15.0 °C to 45.0 °C.**

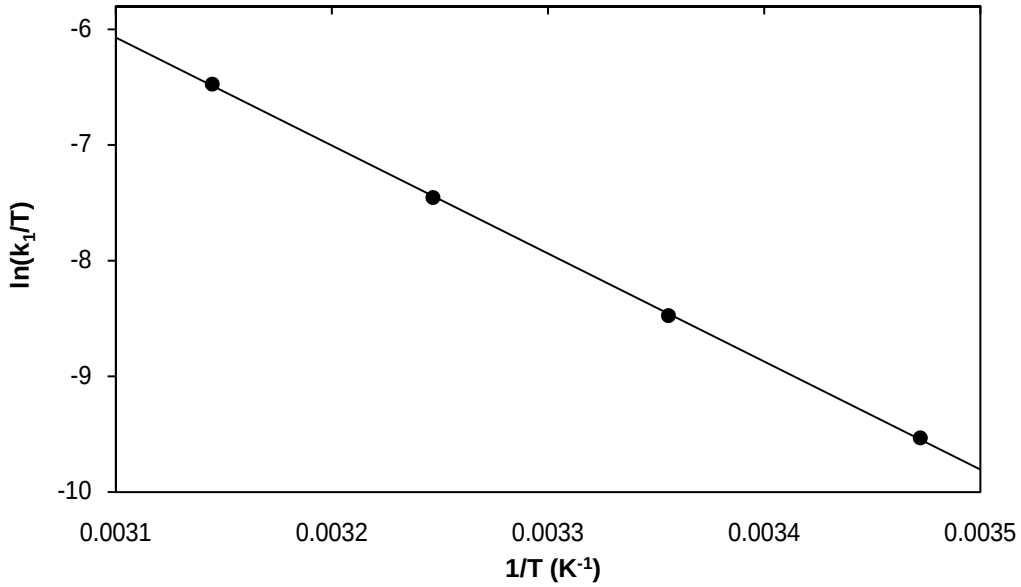


## 5.5.5 Summary of the results of the substitution reactions of *fac*-[Re(Isa)(CO)$_3$(MeOH)] with different entering ligands

The substitution reactions between *fac*-[Re(Isa)(CO)$_3$(MeOH)] and pyridine, thiocyanate, thiourea and 1-methyl-2-thiourea as entering ligands, were studied. This was performed in methanol and at temperatures ranging from 15.0 °C to 45.0 °C. The kinetic data are summarized in Table 5.13 and presented in Figure 5.30.

From the previous paragraphs, it is clear that all the reactions occur *via* the same mechanism. The second order rate constants for the reactions with the N-donor ligands, Py and $NCS^-$, are similar while the reactions with the sulphur donating ligands once again have larger $k_1$ values. The second order rate constant obtained for MeTU as entering ligand are larger than that for TU. Once again it is indicative of the high affinity of these type of complexes for the sulphur donating ligands.

**Figure 5.30: Illustrative comparison of $k_{obs}$ *vs* [ligand] for the reaction between *fac*-[Re(Isa)(CO)$_3$(MeOH)] and Py, $NCS^-$, TU and MeTU at 25.0 °C.**

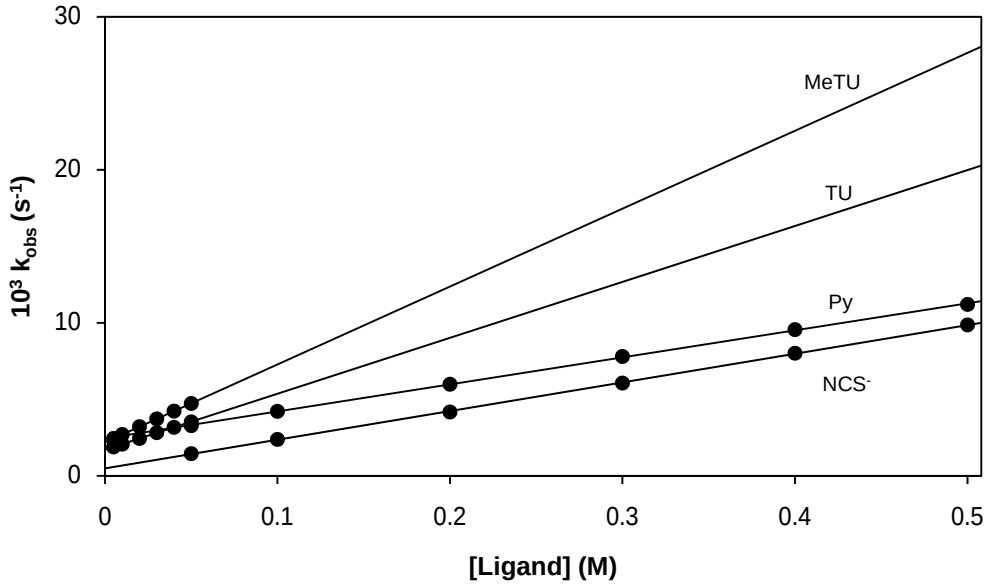


**Table 5.13: Summary of the rate constants and activation parameters for the reaction between *fac*-[Re(Isa)(CO)$_3$(MeOH)] and different entering ligands at 25.0 °C.**

| | $10^3$ $k_1$ ($M^{-1}$ $s^{-1}$) | $10^3$ $k_{-1}$ ($s^{-1}$) | $K_1$ ($M^{-1}$) | $\Delta H^{\ddagger}_{(k1)}$ (kJ $mol^{-1}$) | $\Delta S^{\ddagger}_{(k1)}$ (J $K^{-1}$ $mol^{-1}$) |
|---|---|---|---|---|---|
| **Py** | 17.7(2) | 2.44(5) | 7.3(2) | 79.0(5) | -13(2) |
| **$NCS^-$** | 18.7(1) | 0.48(4) | 39(3) | 78.7(7) | -14(2) |
| **TU** | 36.5(2) | 1.709(6) | 21.4(1) | 78.9(5) | -8(2) |
| **MeTU** | 50.9(1) | 2.190(3) | 23.24(6) | 77.6(7) | -9(2) |

If the stability constant, $K_1$, for the substitution reactions between *fac*-[Re(Isa)(CO)$_3$(MeOH)] and various entering ligands are compared, it is clear that the value for $K_1$ for *fac*-[Re(Isa)(CO)$_3$(Py)] is about a third of the value for *fac*-[Re(Isa)(CO)$_3$(TU)] and *fac*-[Re(Isa)(CO)$_3$(MeTU)] while the data for *fac*-[Re(Isa)(CO)$_3$(NCS)]$^-$ is almost twice that, being the most stable product. The $k_1$ values for the reaction with pyridine and thiocyanate as entering ligands are similar, while the reaction with thiourea is about two times larger and the reaction with MeTU about 3 times larger than that. The reverse reaction rate for the reactions between *fac*-[Re(Isa)(CO)$_3$(MeOH)] and the entering ligands increase from $NCS^-$ < TU < MeTU < Py.

This might indicate a more stable complex since the same trend is also found in the stability constant for that reaction, $K_1$ = 39(3) $M^{-1}$. The negative $\Delta S^{\ddagger}_{(k1)}$ values is indicative of an $I_a$ type mechanism, but this can only be confirmed by high pressure studies.

## 5.6 Reactions of *fac*-[Re(Trop)(CO)$_3$(MeOH)] with monodentate entering ligands

The Rhenium tricarbonyl complex *fac*-[Re(Trop)(CO)$_3$(MeOH)] has been prepared as described in Chapter 3. The stabilities of the complex as well as the entering ligands were tested in methanol and were found to be stable for several hours by monitoring the solutions on a UV/Vis spectrophotometer.

The range of entering ligands that were used are the following: as halides, bromide ($Br^-$) and iodide ions ($I^-$), as N-donating ligands, pyridine (Py), imidazole (Im) and thiocyanate ions ($NCS^-$) and as S-donating ligands, thiourea (TU) and 1-methyl-2-thiourea (MeTU). The reactions were followed at four temperatures and at different wavelengths for each reaction. The standard enthalpy change of activation ($\Delta H^{\ddagger}_{(k1)}$) and the standard entropy change of activation ($\Delta S^{\ddagger}_{(k1)}$) were determined for all of these substitution reactions.

**Figure 5.31: Typical UV/Vis spectral change for the reaction between *fac*-[Re(Trop)(CO)$_3$(MeOH)] and DMAP. [Re] = 1.0 x 10$^{-4}$ M, [DMAP] = 5.0 x 10$^{-3}$ M, 25 °C, 318 nm, $\Delta$t = 60 s, MeOH. The insert indicate the Absorbance change *vs* time at 318 nm. The line shows the least-squares fit to Equation 5.1 ($k_{obs}$ = 0.00331(4) s$^{-1}$).**

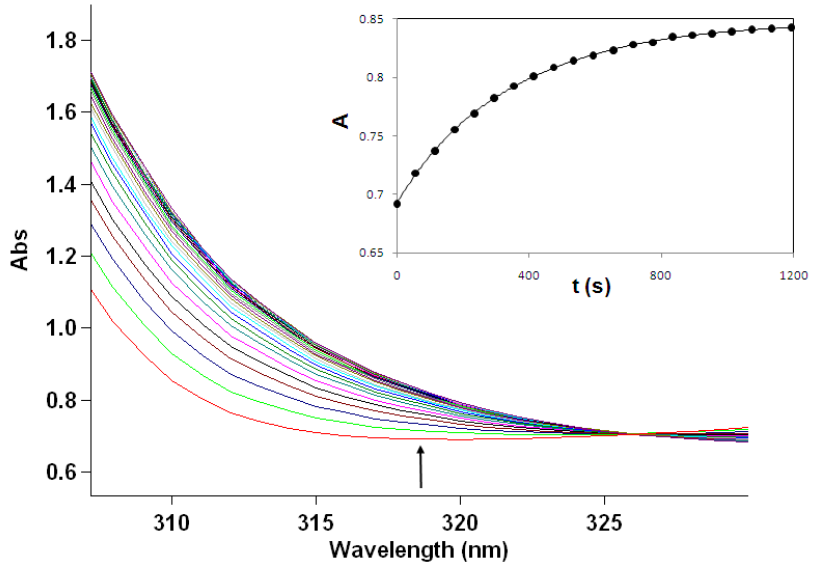


To represent a typical UV/Vis spectral change of the substitution reaction between *fac*-[Re(Trop)(CO)$_3$(MeOH)] and an entering ligand, Figure 5.31 is included.

## 5.6.1 *fac*-[Re(Trop)(CO)$_3$(MeOH)] + bromide ions

The reaction between *fac*-[Re(Trop)(CO)$_3$(MeOH)] and bromide ions were followed in methanol at temperatures ranging from 15.7 °C to 44.9 °C in order to also calculate the activation parameters, the activation enthalpy ($\Delta H^{\ddagger}_{(k1)}$) and the activation entropy ($\Delta S^{\ddagger}_{(k1)}$). The reaction was followed on a Stopped-flow apparatus at 430 nm and the concentration of bromide ions were varied between 2.0 x 10$^{-2}$ and 5.0 x 10$^{-1}$ M.

A wider range of ligand concentration was not possible for this reaction. The highest possible concentration of NaBr in methanol is a 1 M NaBr solution and for NaBr concentrations lower than 4.0 x 10$^{-1}$ M, the change in absorption over time is nearly insignificant. The final product of this reaction, the bromido-substituted complex, *fac*-

$[NEt_4][Re(Trop)(CO)_3(Br)]$[23], was isolated and single crystals of good quality was obtained.

**Figure 5.32: Plot of $k_{obs}$ *vs* $[Br^-]$ for the reaction between *fac*-$[Re(Trop)(CO)_3(MeOH)]$ and bromide ions at different temperatures. [Re] = 1.0 x $10^{-4}$ M, $[Br^-]$ = 2.0 x $10^{-1}$ M – 5.0 x $10^{-1}$ M, 430 nm, MeOH.**

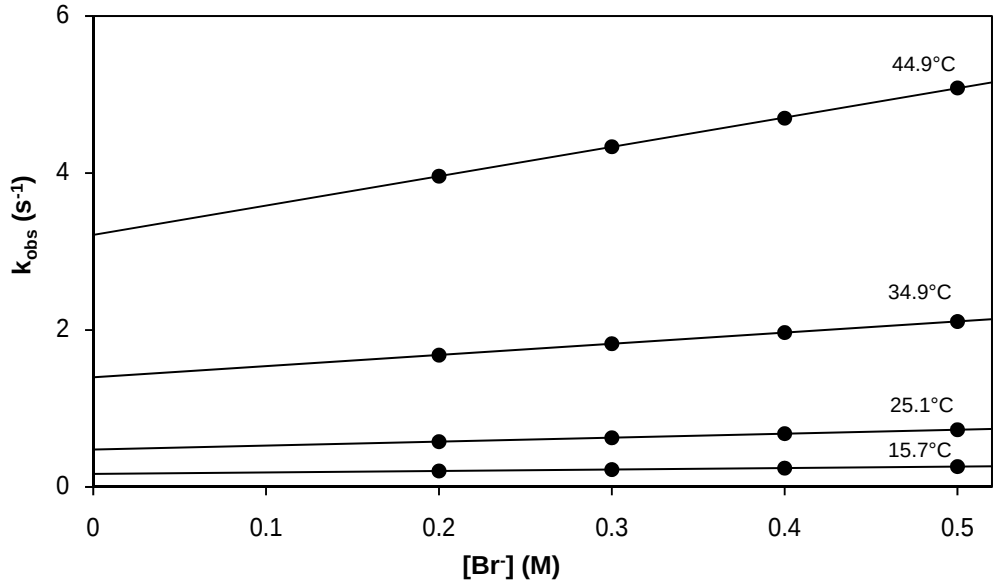


In Figure 5.32 the plots of $k_{obs}$ *vs* $[Br^-]$ values at different temperatures are given. From these values, the kinetic data (Table 5.14) were obtained by fitting the data in Figure 5.32 to Equation 5.4.

**Table 5.14: Summary of the rate constants and activation parameters of the reaction between *fac*-$[Re(Trop)(CO)_3(MeOH)]$ and bromide ions at different temperatures.**

| | **15.7 °C** | **25.1 °C** | **34.9 °C** | **44.9 °C** |
|---|---|---|---|---|
| **$k_1$ ($M^{-1}s^{-1}$)** | 0.186(1) | 0.505(4) | 1.424(7) | 3.74(3) |
| **$k_{-1}$ ($s^{-1}$)** | 0.1668(5) | 0.477(1) | 1.397(3) | 3.21(1) |
| **$K_1$ ($M^{-1}$)** | 1.115(7) | 1.059(9) | 1.019(5) | 1.16(1) |
| **$\Delta H^{\ddagger}_{(k1)}$ (kJ $mol^{-1}$)** | | 76.1(6) | | |
| **$\Delta S^{\ddagger}_{(k1)}$ (J $K^{-1}$ $mol^{-1}$)** | | 5(2) | | |

[23] Schutte, M., Visser, H.G., Roodt, A. *Acta. Cryst*. **2010**, *E66*, m859-m860.

The Eyring plot of this reaction is presented in Figure 5.33. The activation parameters were calculated, by using Equation 5.2, as 76.1(6) kJ $mol^{-1}$ for $\Delta H^{\ddagger}_{(k1)}$ and 5(2) J $K^{-1}$ $mol^{-1}$ for $\Delta S^{\ddagger}_{(k1)}$.

**Figure 5.33: Eyring plot of $\ln(k_1/T)$ *vs* 1/T for the reactions between *fac*-[Re(Trop)$(CO)_3$(MeOH)] and bromide ions for a temperature range of 15.7 °C to 44.9 °C.**

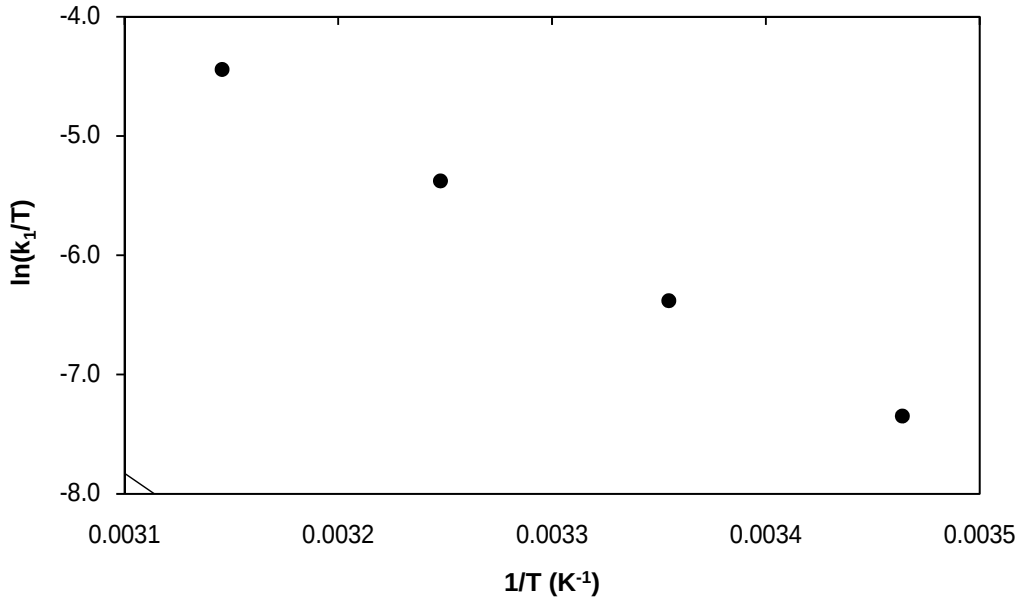


## 5.6.2 *fac*-[Re(Trop)$(CO)_3$(MeOH)] + iodide ions

The methanol substitution reaction between *fac*-[Re(Trop)$(CO)_3$(MeOH)] and iodide ions ($I^-$) was followed with a Stopped-flow apparatus. The reaction was performed in methanol and monitored at 430 nm. The iodide ion concentration was varied between 2.0 x $10^{-1}$ M and 7.0 x $10^{-1}$ M. At concentrations lower than 1.0 x $10^{-4}$ M, the change in absorbance of the reaction is very low, while the highest concentration possible for NaI in methanol is 1.4 M. The temperatures at which the reactions were performed are 15.8 °C, 24.3 °C, 34.4 °C and 44.2 °C.

**Figure 5.34: Plot of $k_{obs}$ *vs* $[I^-]$ for the reaction between *fac*-[Re(Trop)(CO)$_3$(MeOH)] and iodide ions at different temperatures. [Re] = 1.0 x $10^{-4}$ M, $[I^-]$ = 2.0 x $10^{-1}$ M – 7.0 x $10^{-1}$ M, 430 nm, MeOH.**

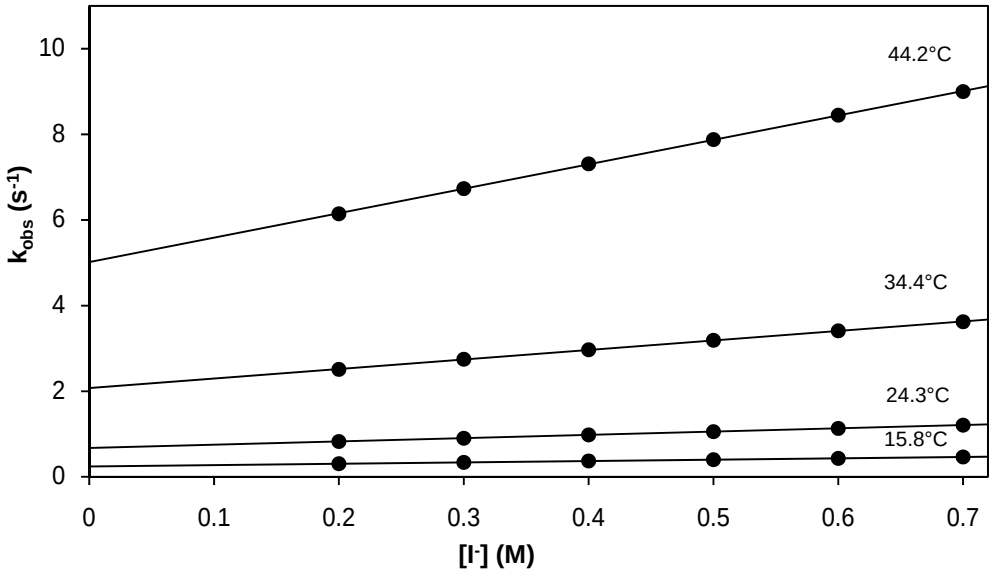


After the reactions between *fac*-[Re(Trop)(CO)$_3$(MeOH)] and iodide ions were followed at the different temperatures and ligand concentrations, Figure 5.34, a plot of $k_{obs}$ *vs* $[I^-]$, was produced. From that plot, the kinetic data given in Table 5.15 were determined from fits to Equation 5.4. The activation parameters, $\Delta H^{\ddagger}_{(k1)}$ and $\Delta S^{\ddagger}_{(k1)}$, the standard activation enthalpy and standard activation entropy respectively, were determined by fitting the data in Table 5.15 to Equation 5.2. The Eyring plot is presented in Figure 5.35.

**Table 5.15: Summary of the rate constants and activation parameters of the reaction between *fac*-[Re(Trop)(CO)$_3$(MeOH)] and iodide ions at different temperatures.**

| | **15.8 °C** | **24.3 °C** | **34.4 °C** | **44.2 °C** |
|---|---|---|---|---|
| **$k_1$ ($M^{-1}s^{-1}$)** | 0.3174(8) | 0.765(2) | 2.22(2) | 5.71(3) |
| **$k_{-1}$ ($s^{-1}$)** | 0.2428(4) | 0.674(1) | 2.075(9) | 5.02(1) |
| **$K_1$ ($M^{-1}$)** | 1.307(4) | 1.136(3) | 1.07(1) | 1.137(6) |
| **$\Delta H^{\ddagger}_{(k1)}$ (kJ $mol^{-1}$)** | | 75.3(9) | | |
| **$\Delta S^{\ddagger}_{(k1)}$ (J $K^{-1}$ $mol^{-1}$)** | | 6(3) | | |

**Figure 5.35: Eyring plot of $\ln(k_1/T)$ *vs* 1/T for the reaction between *fac*-[Re(Trop)(CO)$_3$(MeOH)] and iodide ions for a temperature range of 15.8 °C to 44.2 °C.**

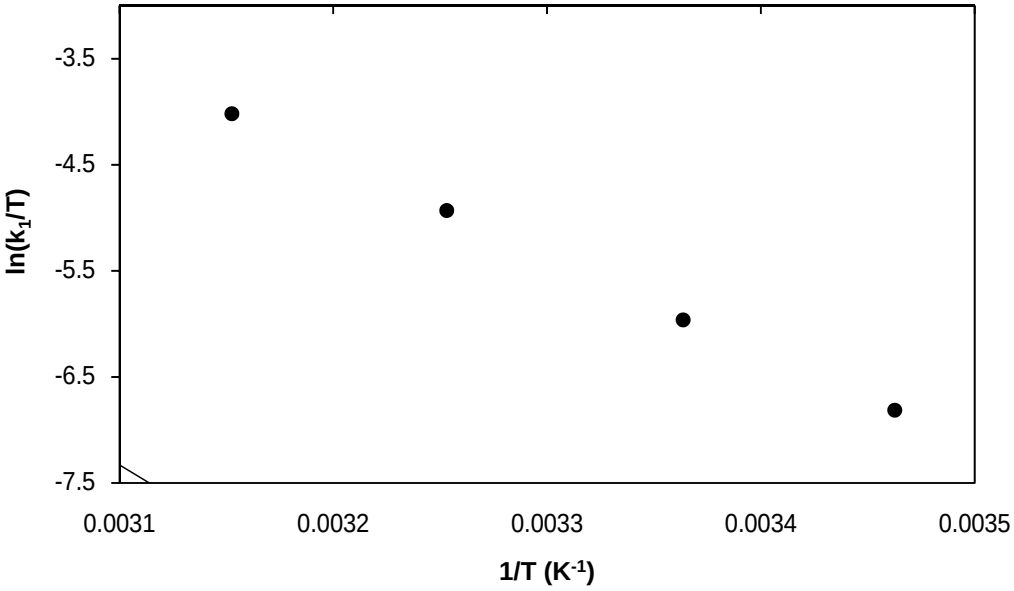


The activation parameters were determined as 75.3(9) kJ mol$^{-1}$ and 6(3) J K$^{-1}$ mol$^{-1}$ for $\Delta H^{\ddagger}_{(k1)}$ and $\Delta S^{\ddagger}_{(k1)}$ respectively.

## 5.6.3 *fac*-[Re(Trop)(CO)$_3$(MeOH)] + pyridine

The methanol substitution reaction between *fac*-[Re(Trop)(CO)$_3$(MeOH)] and pyridine was performed on a UV/Vis spectrophotometer. It was monitored at 312 nm, at four temperatures and in methanol. The Rhenium concentration was kept constant at 1.0 x 10$^{-4}$ M and the pyridine concentration was varied from 2.0 x 10$^{-2}$ M to 2.0 x 10$^{-1}$ M.

**Figure 5.36: Plot of $k_{obs}$ *vs* [Py] for the reaction between *fac*-[Re(Trop)(CO)$_3$(MeOH)] and pyridine at different temperatures. [Re] = 1.0 x 10$^{-4}$ M, [Py] = 2.0 x 10$^{-2}$ M – 2.0 x 10$^{-1}$ M, 312 nm, MeOH.**

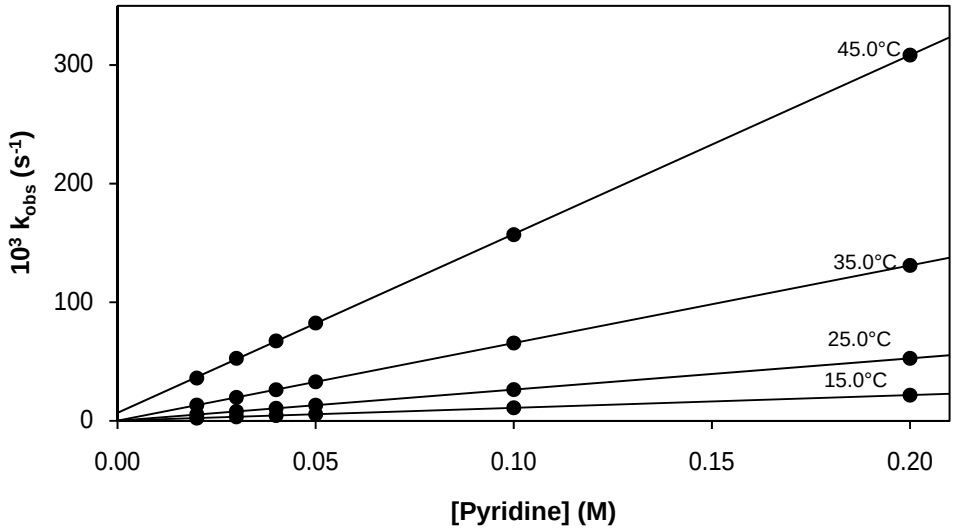


A plot of $k_{obs}$ *vs* [Py] for the reaction between *fac*-[Re(Trop)(CO)$_3$(MeOH)] and pyridine at different temperatures, is presented in Figure 5.36. This data was fitted to Equation 5.4 and the rate constants were obtained (tabulated in Table 5.16).

**Table 5.16: Summary of the rate constants and activation parameters of the reaction between *fac*-[Re(Trop)(CO)$_3$(MeOH)] and pyridine at different temperatures.**

| | **15.0 °C** | **25.0 °C** | **35.0 °C** | **45.0 °C** |
|---|---|---|---|---|
| **$k_1$ ($M^{-1}s^{-1}$)** | 0.1077(2) | 0.2632(1) | 0.6546(6) | 1.508(4) |
| **$10^3k_{-1}$ ($s^{-1}$)** | 0.18(2) | 0.07(1) | 0.16(6) | 6.8(4) |
| **$K_1$ ($M^{-1}$)** | 598(66) | 3760(537) | 4091(1534) | 222(13) |
| **$\Delta H^{\ddagger}_{(k1)}$ (kJ mol$^{-1}$)** | | 64.7(9) | | |
| **$\Delta S^{\ddagger}_{(k1)}$ (J K$^{-1}$ mol$^{-1}$)** | | -39(3) | | |

The activation parameters for this reaction were determined by a least-squares fit of the temperature dependent data of $k_1$ to the Eyring equation (Equation 5.2) and a value of 64.7(9) kJ mol$^{-1}$ and -39(3) J K$^{-1}$ mol$^{-1}$were calculated for $\Delta H^{\ddagger}_{(k1)}$ and $\Delta S^{\ddagger}_{(k1)}$ respectively (Figure 5.37).

**Figure 5.37: Eyring plot of $\ln(k_1/T)$ *vs* 1/T for the reaction between *fac*-[Re(Trop)(CO)$_3$(MeOH)] and pyridine for a temperature range of 15.0 °C to 45.0 °C.**

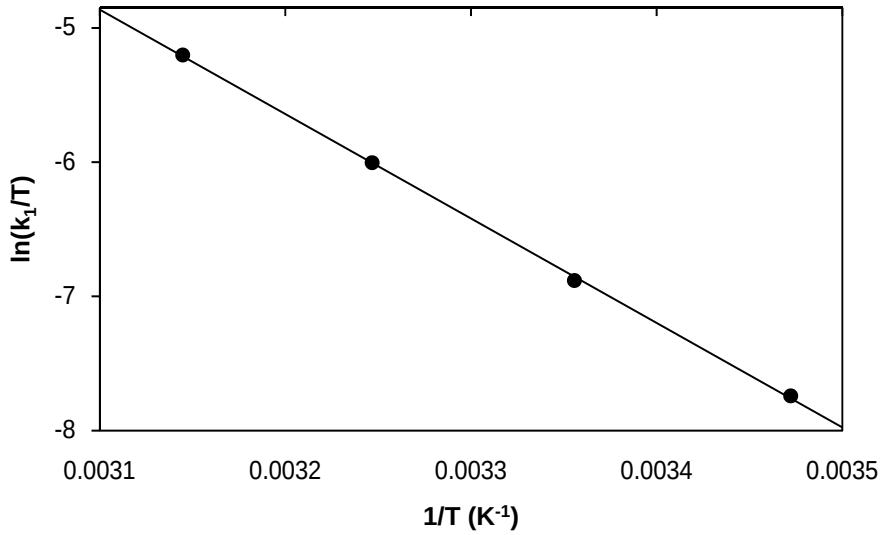


## 5.6.4 *fac*-[Re(Trop)(CO)$_3$(MeOH)] + imidazole

The substitution reaction between *fac*-[Re(Trop)(CO)$_3$(MeOH)] and imidazole were followed in methanol. The reaction was monitored at 255 nm and at four temperatures, in order to calculate the activation parameters $\Delta H^{\ddagger}_{(k1)}$ and $\Delta S^{\ddagger}_{(k1)}$. The Rhenium concentration was 1.0 x $10^{-4}$ M while the imidazole concentration was varied between 5.0 x $10^{-3}$ and 5.0 x $10^{-2}$ M. A plot of $k_{obs}$ *vs* [Im] for the reaction between *fac*-[Re(Trop)(CO)$_3$(MeOH)] and imidazole is illustrated in Figure 5.38.

**Figure 5.38: Plot of $k_{obs}$ *vs* [Im] for the reaction between *fac*-[Re(Trop)(CO)$_3$(MeOH)] and imidazole at different temperatures. [Re] = 1.0 x 10$^{-4}$ M, [Im] = 5.0 x 10$^{-3}$ – 5.0 x 10$^{-2}$ M, 255 nm, MeOH.**

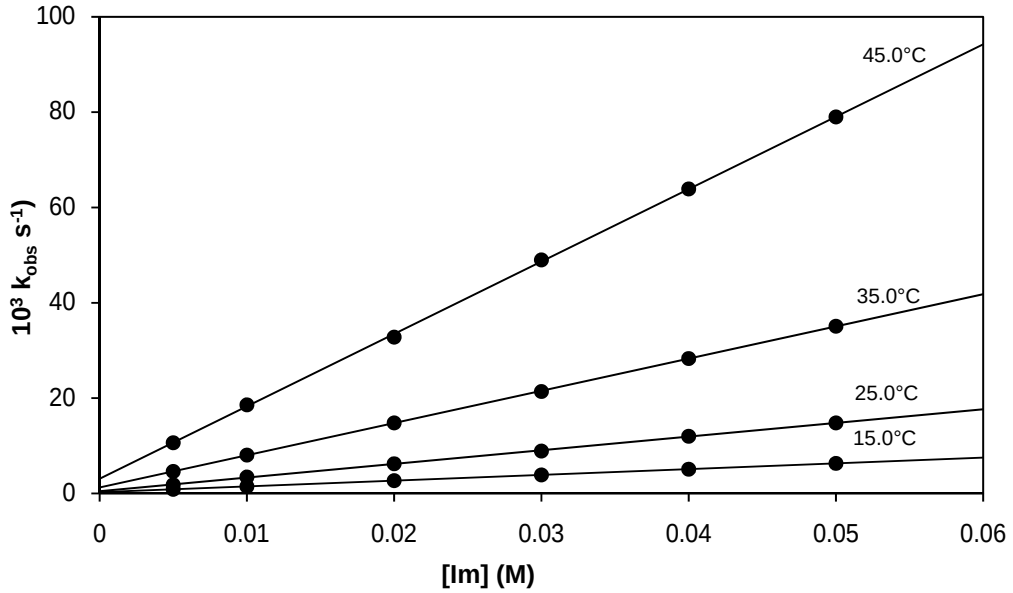


**Table 5.17: Summary of the rate constants and activation parameters of the reaction between *fac*-[Re(Trop)(CO)$_3$(MeOH)] and imidazole at different temperatures.**

| | 15.0 °C | 25.0 °C | 35.0 °C | 45.0 °C |
|---|---|---|---|---|
| $k_1$ ($M^{-1}s^{-1}$) | 0.1209(1) | 0.287(3) | 0.676(2) | 1.52(1) |
| $10^3k_{-1}$ ($s^{-1}$) | 0.266(4) | 0.46(9) | 1.25(6) | 3.1(3) |
| $K_1$ ($M^{-1}$) | 455(7) | 624(122) | 541(26) | 490(48) |
| $\Delta H^{\ddagger}_{(k1)}$ (kJ $mol^{-1}$) | | 61.8(7) | | |
| $\Delta S^{\ddagger}_{(k1)}$ (J $K^{-1}$ $mol^{-1}$) | | -48(2) | | |

The $k_{obs}$ *vs* [Im] data was fitted to Equation 5.4 in order to obtain the rate constants, provided in Table 5.17. From a least-squares fit of the data in Table 5.17 to Equation 5.2, the activation parameters were obtained. The standard enthalpy change of activation was calculated as 61.8(7) kJ $mol^{-1}$ and the standard entropy change of activation as -48(2) J $K^{-1}$ $mol^{-1}$. The Eyring plot is reported in Figure 5.39.

**Figure 5.39: Eyring plot of ln($k_1$/T) *vs* 1/T for the reaction between *fac*-[Re(Trop)(CO)$_3$(MeOH)] and imidazole for a temperature range of 15.0 °C to 45.0 °C.**

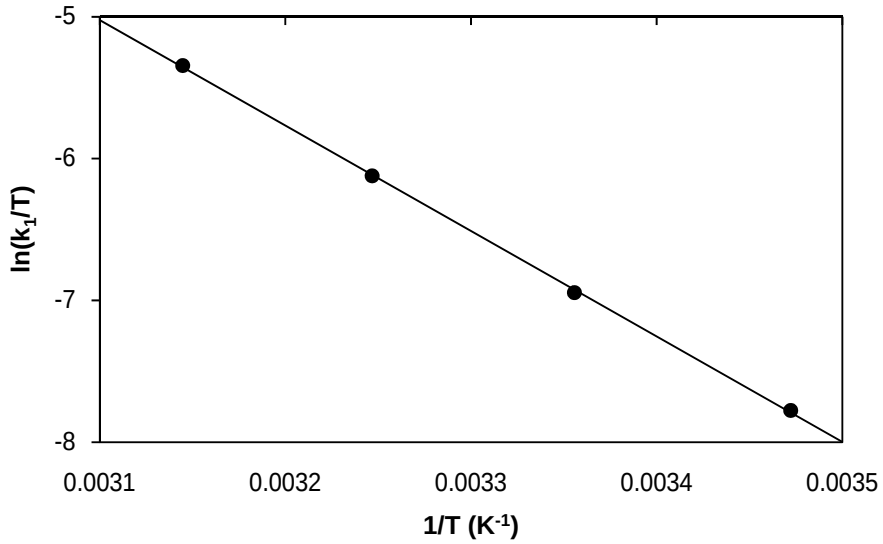


## 5.6.5 *fac*-[Re(Trop)(CO)$_3$(MeOH)] + thiocyanate ions

The methanol substitution reaction between *fac*-[Re(Trop)(CO)$_3$(MeOH)] and thiocyanate ions were performed in methanol. The reaction was monitored at 265 nm with the thiocyanate ion concentration varying between 2.0 x $10^{-2}$ to 2.0 x $10^{-1}$ M. A plot of $k_{obs}$ *vs* [$NCS^-$] for the reaction at four different temperatures is provided in Figure 5.40. After fitting the $k_{obs}$ *vs* [$NCS^-$] data to Equation 5.4, the rate constants were obtained and are summarized in Table 5.18.

**Figure 5.40: Plot of $k_{obs}$ *vs* [$NCS^-$] for the reaction between *fac*-[Re(Trop)$(CO)_3$(MeOH)] and $NCS^-$ ions at different temperatures. [Re] = 1.0 x $10^{-4}$ M, [$NCS^-$] = 2.0 x $10^{-2}$ – 2.0 x $10^{-1}$ M, 265 nm, MeOH.**

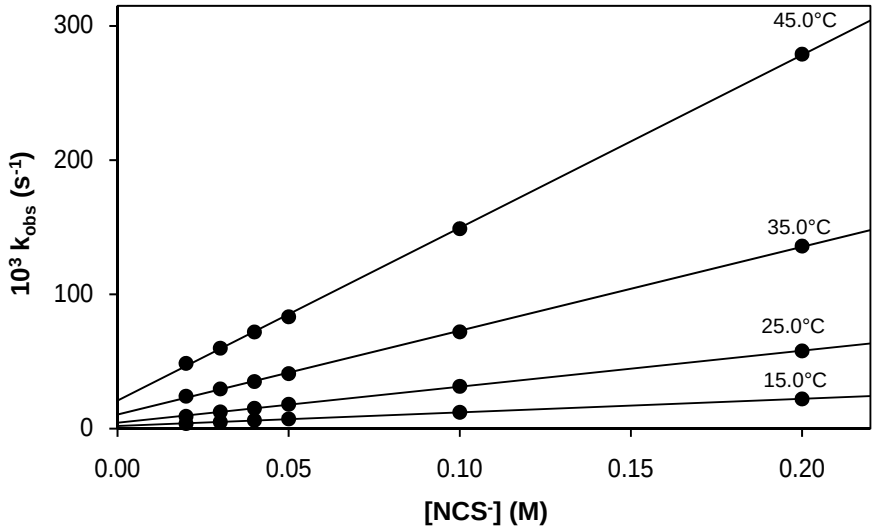


**Table 5.18: Summary of the rate constants and activation parameters of the reaction between *fac*-[Re(Trop)$(CO)_3$(MeOH)] and $NCS^-$ ions at different temperatures.**

| | 15.0 °C | 25.0 °C | 35.0 °C | 45.0 °C |
|---|---|---|---|---|
| $k_1$ ($M^{-1}s^{-1}$) | 0.101(1) | 0.268(2) | 0.625(6) | 1.29(1) |
| $10^3k_{-1}$ ($s^{-1}$) | 2.0(1) | 4.4(2) | 10.5(6) | 20.9(9) |
| $K_1$ ($M^{-1}$) | 51(3) | 61(3) | 60(3) | 62(3) |
| $\Delta H^{\ddagger}_{(k1)}$ (kJ $mol^{-1}$) | | 62(2) | | |
| $\Delta S^{\ddagger}_{(k1)}$ (J $K^{-1}$ $mol^{-1}$) | | -48(6) | | |

From a least-squares fit of the data in Table 5.18 to Equation 5.2, the activation parameters were calculated. The standard enthalpy change of activation, $\Delta H^{\ddagger}_{(k1)}$, was calculated as 62(2) kJ $mol^{-1}$ and the standard entropy change of activation, $\Delta S^{\ddagger}_{(k1)}$, as -48(6) J $K^{-1}$ $mol^{-1}$. The Eyring plot is reported in Figure 5.41.

**Figure 5.41: Eyring plot of ln($k_1$/T) *vs* 1/T for the reaction between *fac*-[Re(Trop)(CO)$_3$(MeOH)] and $NCS^-$ ions for a temperature range of 15.0 °C to 45.0 °C.**

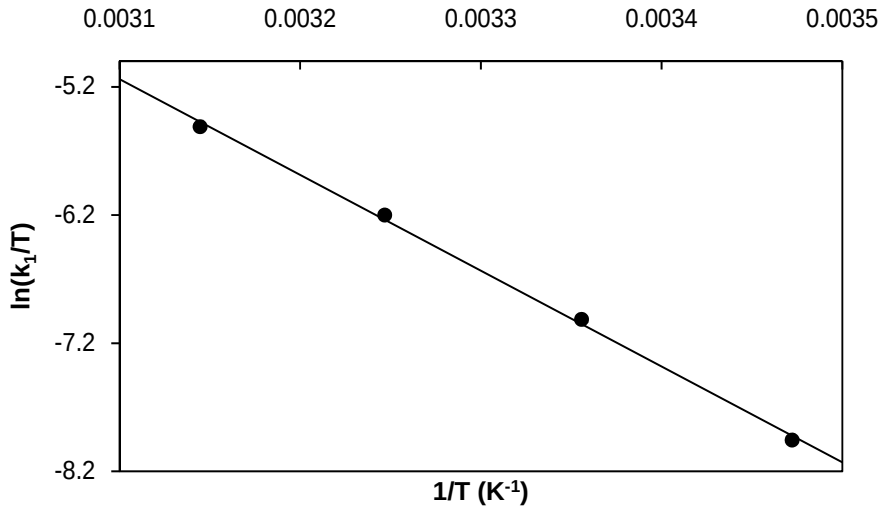


## 5.6.6 *fac*-[Re(Trop)(CO)$_3$(MeOH)] + 4-dimethylaminopyridine

The reaction between *fac*-[Re(Trop)(CO)$_3$(MeOH)] and DMAP (4-dimethyl-aminopyridine) was followed at 318 nm and in methanol as solvent. It was performed under *pseudo* first-order conditions with a metal concentration of 1.0 x $10^{-4}$ M and the ligand concentration between 5.0 x $10^{-3}$ to 5.0 x $10^{-2}$ M. The substitution reaction was repeated at four temperatures and the $k_{obs}$ *vs* [DMAP] data is presented in Figure 5.42.

**Figure 5.42: Plot of $k_{obs}$ *vs* [DMAP] for the reaction between *fac*-[Re(Trop)(CO)$_3$(MeOH)] and DMAP at different temperatures. [Re] = 1.0 x 10$^{-4}$ M, [DMAP] = 5.0 x 10$^{-3}$ – 5.0 x 10$^{-2}$ M, 318 nm, MeOH.**

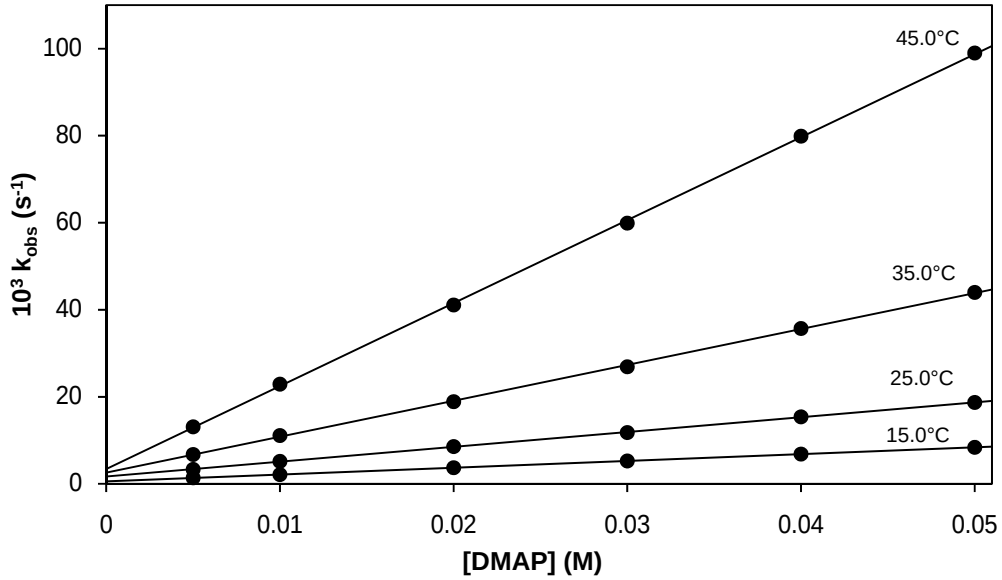


The data in Figure 5.42 was fitted to Equation 5.4 and the rate constants presented in Table 5.19 were obtained. The activation parameters, $\Delta H^{\ddagger}_{(k1)}$ and $\Delta S^{\ddagger}_{(k1)}$, were obtained by the use of Equation 5.2, and were calculated as 61(2) kJ mol$^{-1}$ and -47(7) J K$^{-1}$ mol$^{-1}$ respectively. The Eyring plot is reported in Figure 5.43.

**Table 5.19: Summary of the rate constants and activation parameters of the reaction between *fac*-[Re(Trop)(CO)$_3$(MeOH)] and DMAP at different temperatures.**

| | **15.0 °C** | **25.0 °C** | **35.0 °C** | **45.0 °C** |
|---|---|---|---|---|
| **$k_1$ ($M^{-1}s^{-1}$)** | 0.1563(2) | 0.341(2) | 0.825(7) | 1.91(1) |
| **$10^3k_{-1}$ ($s^{-1}$)** | 0.581(5) | 1.68(7) | 2.6(2) | 3.4(4) |
| **$K_1$ ($M^{-1}$)** | 269(2) | 203(9) | 317(25) | 562(66) |
| **$\Delta H^{\ddagger}_{(k1)}$ (kJ mol$^{-1}$)** | | 61(2) | | |
| **$\Delta S^{\ddagger}_{(k1)}$ (J K$^{-1}$ mol$^{-1}$)** | | -47(7) | | |

**Figure 5.43: Eyring plot of ln($k_1$/T) *vs* 1/T for the reaction between *fac*-[Re(Trop)(CO)$_3$(MeOH)] and DMAP for a temperature range of 15.0 °C to 45.0 °C.**

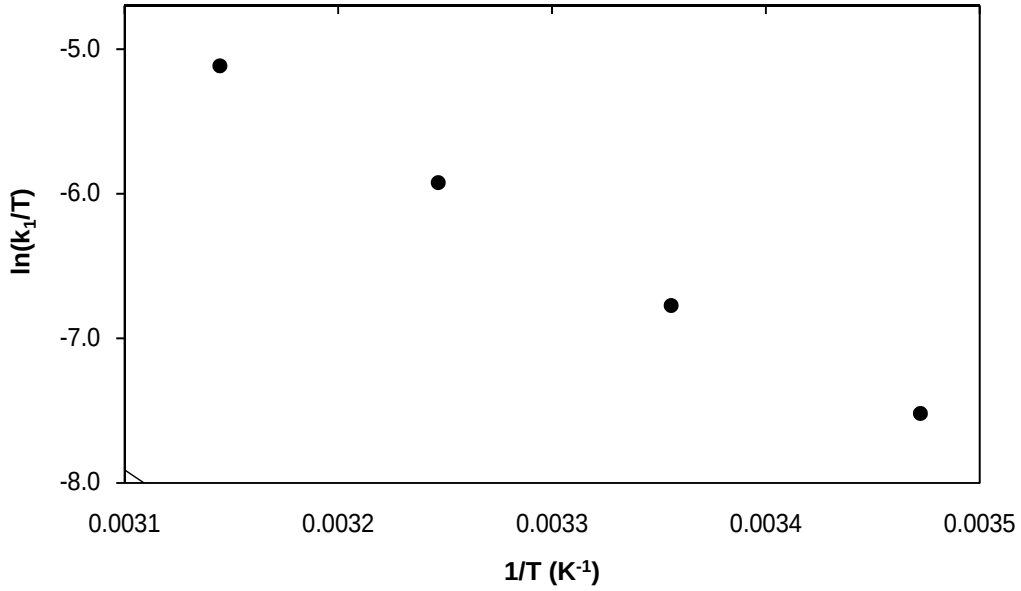


## 5.6.7 *fac*-[Re(Trop)(CO)$_3$(MeOH)] + thiourea

The methanol substitution reaction between *fac*-[Re(Trop)(CO)$_3$(MeOH)] and the S-donor ligand, thiourea, was followed. The reaction was performed in methanol and monitored at 440 nm. The $k_{obs}$ *vs* [TU] data obtained for the substitution reaction between *fac*-[Re(Trop)(CO)$_3$(MeOH)] and thiourea, at different temperatures, are presented in Figure 5.44 and Table 5.20. The equilibrium constants are also determined thermodynamically and the $A_{obs}$ *vs* [TU] data, for the reaction at 25.0 °C, is presented in Figure 5.45.

**Figure 5.44: Plot of $k_{obs}$ *vs* [TU] for the reaction between *fac*-[Re(Trop)(CO)$_3$(MeOH)] and thiourea at different temperatures. [Re] = 1.0 x 10$^{-4}$ M, [TU] = 5.0 x 10$^{-3}$ – 5.0 x 10$^{-2}$ M, 440 nm, MeOH.**

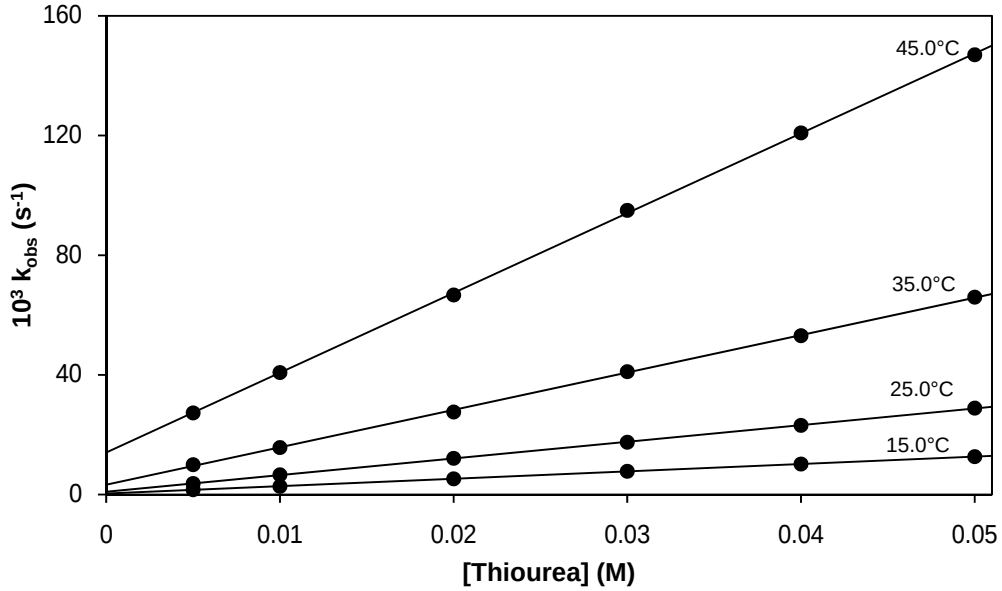


**Figure 5.45: Plot of $A_{obs}$ *vs* [TU] for the reaction of *fac*-[Re(Trop)(CO)$_3$(MeOH)] with thiourea. [Re] = 1.0 x 10$^{-4}$ M, 25.0 °C, 440 nm.**

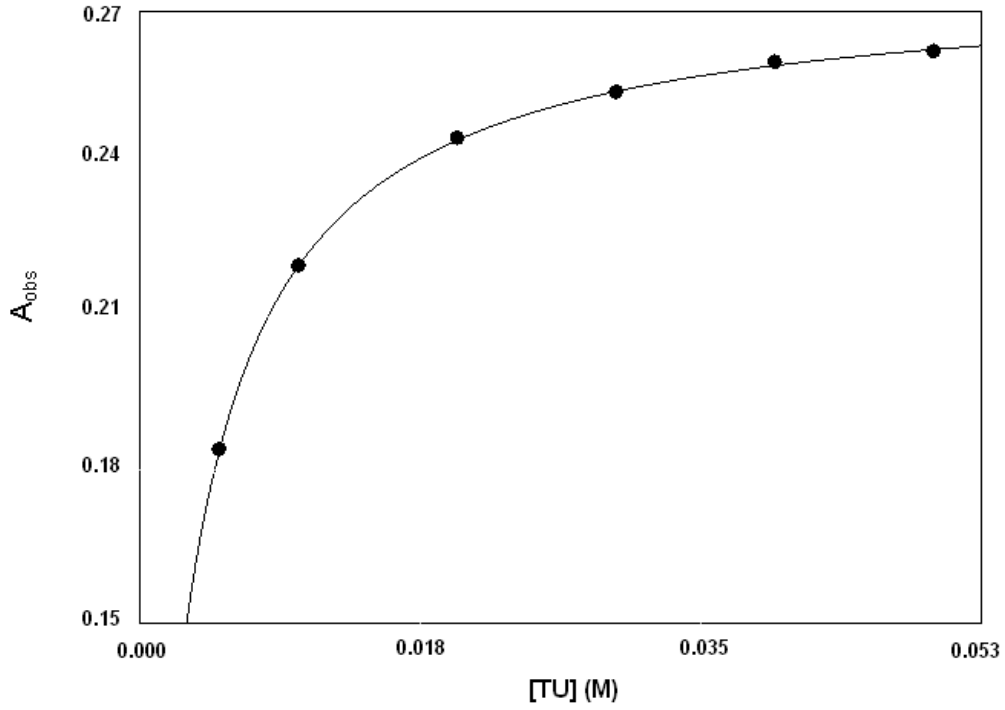

**Table 5.20: Summary of the rate constants and activation parameters of the reaction between *fac*-[Re(Trop)(CO)$_3$(MeOH)] and thiourea at different temperatures.**

| | 15.0 °C | 25.0 °C | 35.0 °C | 45.0 °C |
|---|---|---|---|---|
| $k_1$ ($M^{-1}s^{-1}$) | 0.247(1) | 0.556(3) | 1.25(1) | 2.67(2) |
| $10^3k_{-1}$ ($s^{-1}$) | 0.33(3) | 0.95(10) | 3.3(4) | 14.0(5) |
| $K_1$ ($M^{-1}$) | 748(68) | 585(62) | 379(46) | 191(7) |
| $K_1$ ($M^{-1}$)[a] | 808(74) | 373(35) | 355(48) | 344(33) |
| $\Delta H^{\ddagger}_{(k1)}$ (kJ $mol^{-1}$) | | 58.0(7) | | |
| $\Delta S^{\ddagger}_{(k1)}$ (J $K^{-1}$ $mol^{-1}$) | | -55(2) | | |

[a] Thermodynamically determined.

The activation parameters of the overall reaction between *fac*-[Re(Trop)(CO)$_3$(MeOH)] and thiourea as entering ligand were determined by a least-squares fit of the data in Table 5.20 to Equation 5.2. The activation parameters were calculated to be $\Delta H^{\ddagger}$ = 58.0(7) kJ $mol^{-1}$ and $\Delta S^{\ddagger}$ = -55(2) J $K^{-1}$ $mol^{-1}$ (Figure 5.46).

**Figure 5.46: Eyring plot of ln($k_1$/T) *vs* 1/T for the reaction between *fac*-[Re(Trop)(CO)$_3$(MeOH)] and thiourea for a temperature range of 15.0 °C to 45.0 °C.**

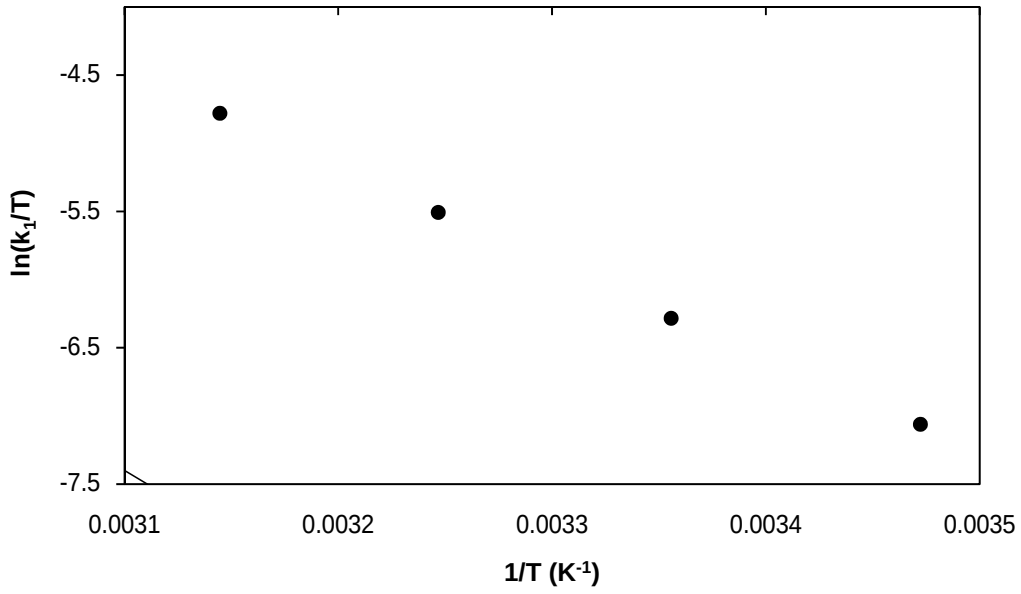

## 5.6.8 *fac*-[Re(Trop)(CO)$_3$(MeOH)] + 1-methyl-2-thiourea

The substitution reaction between *fac*-[Re(Trop)(CO)$_3$(MeOH)] and MeTU (1-methyl-2-thiourea) was followed on a Stopped-flow apparatus, at different temperatures, in methanol and was monitored at 435 nm. A plot of $k_{obs}$ *vs* [MeTU] is presented in Figure 5.47. This data was fitted to Equation 5.4 and the rate constants obtained are summarized in Table 5.21.

**Figure 5.47: Plot of $k_{obs}$ *vs* [MeTU] for the reaction between *fac*-[Re(Trop)(CO)$_3$(MeOH)] and MeTU at different temperatures. [Re] = 1.0 x 10$^{-4}$ M, [MeTU] = 5.0 x 10$^{-3}$ – 5.0 x 10$^{-2}$ M, 435 nm, MeOH.**

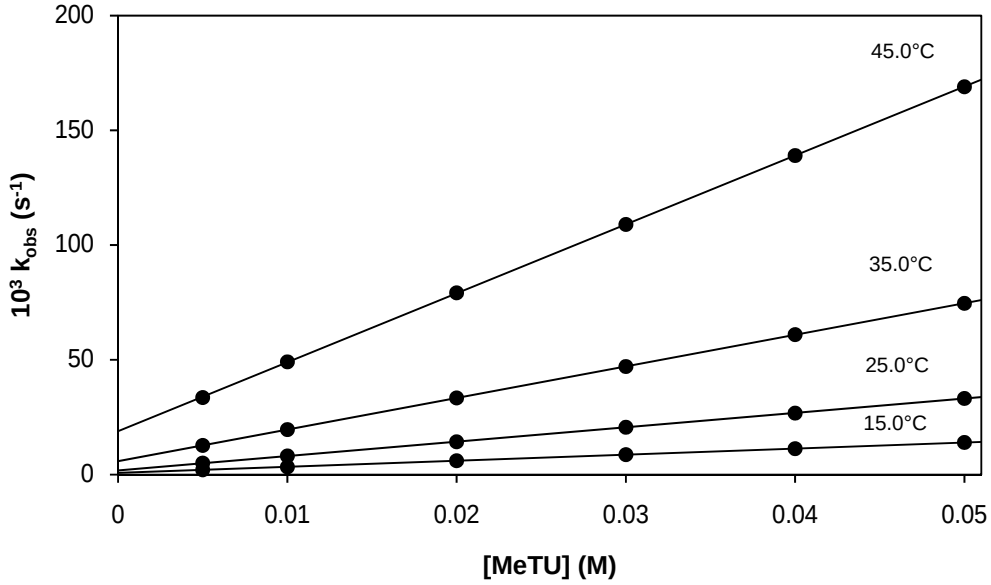


**Table 5.21: Summary of the rate constants and activation parameters of the reaction between *fac*-[Re(Trop)(CO)$_3$(MeOH)] and MeTU at different temperatures.**

| | 15.0 °C | 25.0 °C | 35.0 °C | 45.0 °C |
|---|---|---|---|---|
| $k_1$ ($M^{-1}s^{-1}$) | 0.265(1) | 0.626(2) | 1.377(2) | 3.004(6) |
| $10^3k_{-1}$ ($s^{-1}$) | 0.73(4) | 1.84(5) | 5.84(5) | 18.9(2) |
| $K_1$ ($M^{-1}$) | 363(20) | 340(9) | 236(2) | 159(2) |
| $\Delta H^{\ddagger}_{(k1)}$ (kJ mol$^{-1}$) | | 59.0(4) | | |
| $\Delta S^{\ddagger}_{(k1)}$ (J K$^{-1}$ mol$^{-1}$) | | -51(1) | | |

The activation parameters were calculated from the given data; $\Delta H^{\ddagger}_{(k1)}$ = 59.0(4) kJ mol$^{-1}$ and $\Delta S^{\ddagger}_{(k1)}$ = -51(1) J K$^{-1}$ mol$^{-1}$. The Eyring plot is reported in Figure 5.48.

**Figure 5.48: Eyring plot of ln($k_1$/T) *vs* 1/T for the reaction between *fac*-[Re(Trop)(CO)$_3$(MeOH)] and MeTU for a temperature range of 15.0 °C to 45.0 °C.**

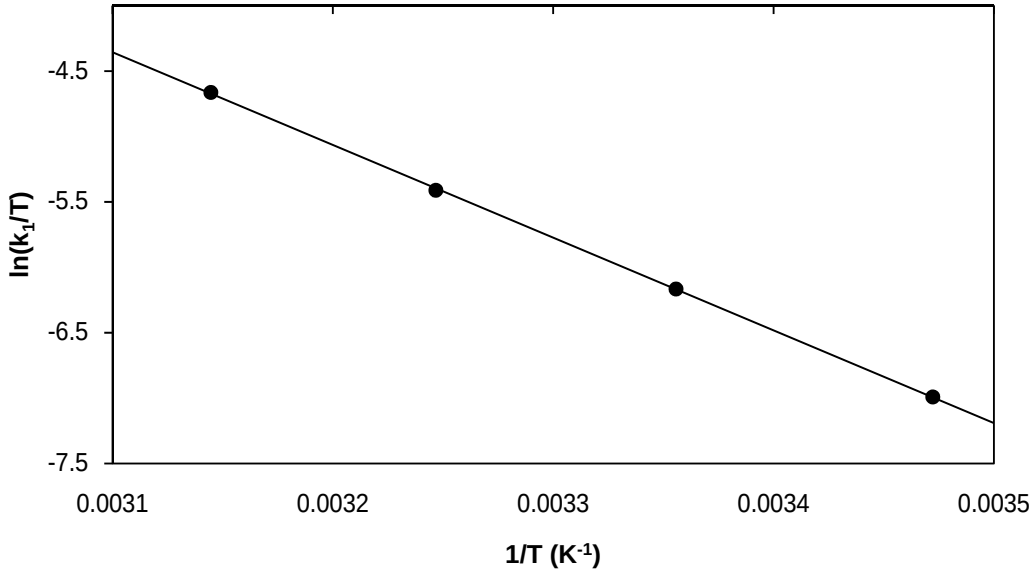


## 5.6.9 Summary of the results of the methanol substitution reactions of the *fac*-[Re(Trop)(CO)$_3$(MeOH)] complex

The substitution reactions between *fac*-[Re(Trop)(CO)$_3$(MeOH)] and a range of monodentate ligands have been studied (Paragraph 5.6.1 to 5.6.8 Bromide and idodide ions were chosen as halides; pyridine (Py), imidazole (Im), thiocyanate ions ($NCS^-$) and 4-dimethylaminopyridine (DMAP) as N-donating ligands and thiourea (TU) and 1-methyl-2-thiourea (MeTU) as S-donating ligands.

The crystal structures of three of the substitution products, *fac*-[Re(Trop)(CO)$_3$Br]$^-$, *fac*-[Re(Trop)(CO)$_3$(Py)] and *fac*-[Re(Trop)(CO)$_3$(DMAP)] are reported in Chapter 4. This serves as confirmation of the substitution products formed and therefore lends support to the proposed mechanism.

A comparison of the observed second order rate constants, $k_1$ (Table 5.22), revealed the following:

- the second order rate constant, $k_1$, for the reactions with halides are comparable, with $k_1$ (iodide ions) slightly larger than that of bromide ions;

- the second order rate constant for the reactions between *fac*-[Re(Trop)(CO)$_3$(MeOH)] and the nitrogen donating ligands are about 2 to 3 times slower than $k_1$ (halides), but are all comparable to $k_1$ (DMAP), the fastest entering ligand;
- the $k_1$ values for the substitution reactions with the S-donating ligands are comparable to each other, with $k_1$ (MeTU) > $k_1$ (TU). It is also comparable to the second order rate constants of the reactions with the halides.

No systematic variation in the $k_1$ value is observed between the reactions with the neutral ligands *vs* the charged ligands. A graph to illustrate the effect of the entering ligand on the rate of the reaction is reported in Figure 5.49.

The variation in $k_1$ for the reactions between *fac*-[Re(Trop)(CO)$_3$(MeOH)] and different entering ligands is at most a factor of 3, whereas $k_{-1}$ varies about 4 orders-of-magnitude. This clearly indicates that the reaction is less dependent on the type of entering ligand for the anation reactions, pointing towards a dissociative type of activation.

**Table 5.22: Rate constants of the different reactons between *fac*-[Re(Trop)(CO)$_3$(MeOH)] and different entering ligands at 25.0 °C.***

| | $k_1$ ($M^{-1}$ $s^{-1}$) | $10^3k_{-1}$ ($s^{-1}$) | $K_1$ ($M^{-1}$) | $\Delta H^{\ddagger}_{(k1)}$ (kJ $mol^{-1}$) | $\Delta S^{\ddagger}_{(k1)}$ (J $K^{-1}$ $mol^{-1}$) |
|---|---|---|---|---|---|
| **$Br^-$** [a] | 0.505(4) | 477(1) | 1.059(9) | 76.1(6) | 5(2) |
| **$I^-$** [b] | 0.765(2) | 674(1) | 1.136(3) | 75.3(9) | 6(3) |
| **Py** | 0.2632(1) | 0.07(1) | 3760(537) | 64.7(9) | -39(3) |
| **Im** | 0.287(3) | 0.46(9) | 624(122) | 61.8(7) | -48(2) |
| **$NCS^-$** | 0.268(2) | 4.4(2) | 61(3) | 62(2) | -48(6) |
| **DMAP** | 0.341(2) | 1.68(7) | 203(9) | 61(2) | -47(7) |
| **TU** | 0.556(3) | 0.95(10) | 585(62) | 58.0(7) | -55(2) |
| **MeTU** | 0.626(2) | 1.84(5) | 340(9) | 59.0(4) | -51(1) |

* except for $Br^-$ and $I^-$, see a and b

[a] 25.1 °C; [b] 24.3 °C

Regarding the stability of the products formed, it is clear that the reactions with the negatively charged entering ligands are less stable that the reactions with the neutral

ligands, as illustrated by the lower $K_1$ values, which are two to three orders-of-magnitude smaller than the neutral ligands (see Table 5.22)

The enthalpy of activation for all eight reactions compare well with each other. However, the entropy of activation differs significantly, with the values for the reactions with TU and MeTU indicating the highest order in the transition state and $Br^-$ ions and $I^-$ ions having the least ordered transition state. The negative values for $\Delta S^{\ddagger}_{(k1)}$ for the reactions with Py, Im, $NCS^-$, DMAP, TU and MeTU all suggest a more associative pathway whereas the positive values for the halides points towards a dissociatively activated mechanism. From this seemingly contradictory data it is clear that high pressure studies are required to more unambiguously determine the reaction mechanism.

**Figure 5.49: Schematic representation of the $k_{obs}$ *vs* [ligand] of the reactions between *fac*-[Re(Trop)(CO)$_3$(MeOH)] and various entering ligands at ~25 °C.**

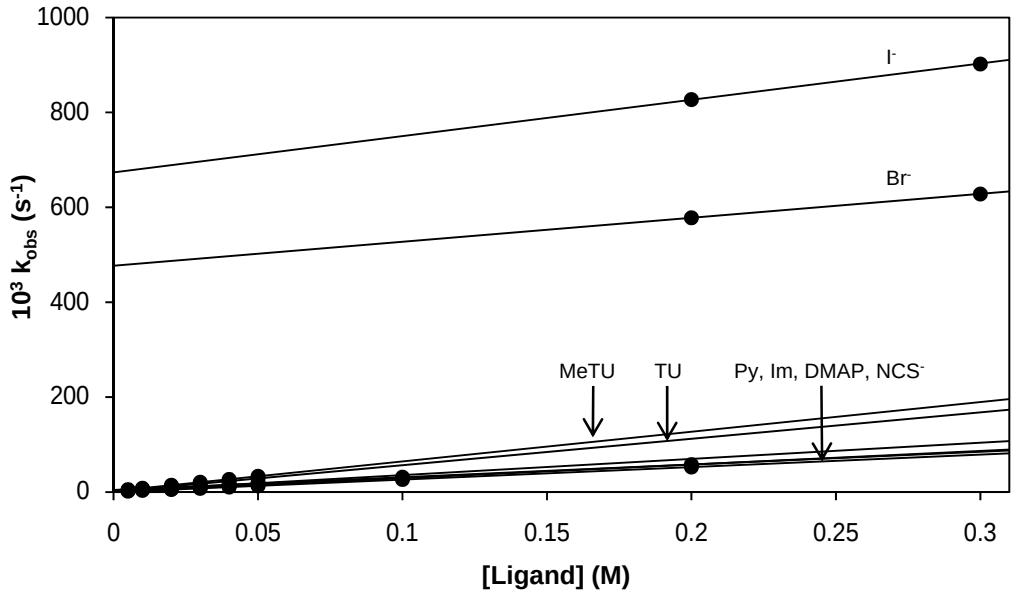

## 5.7 Discussion

The three neutral Re(I) tricarbonyl complexes selected for this methanol substitution study were *fac*-[Re(2,5-PicoH)$(CO)_3$(MeOH)], representing a complex with a N,O-bidentate ligand, and two complexes with an O,O'-bidentate ligand – *fac*-[Re(Isa)$(CO)_3$(MeOH)] and *fac*-[Re(Trop)$(CO)_3$(MeOH)]. A methanol ligand is available for substitution by monodentate ligands on these complexes. The rate constant data for these methanol substitution reactions, discussed in detail in Paragraph 5.4, 5.5 and 5.6 are summarized in Table 5.23.

- It is clear from Table 5.23, that there is an increase in $k_1$ for the substitution reactions from *fac*-[Re(2,5-PicoH)$(CO)_3$(MeOH)] to *fac*-[Re(Isa)$(CO)_3$(MeOH)] and to *fac*-[Re(Trop)$(CO)_3$(MeOH)], for every entering ligand. This represent approximately a one order of magnitude increase for the N-donor entering ligands from *fac*-[Re(2,5-PicoH)$(CO)_3$(MeOH)] to *fac*-[Re(Isa)$(CO)_3$(MeOH)] and to *fac*-[Re(Trop)$(CO)_3$(MeOH)]. This correspond to the reported $pK_a$ value for tropolone is 6.7[11] and the two speculated values for 2,5-pyridine dicarboxylic are $pK_{a1}$ = 5.25 and $pK_{a2}$ = 4.4.[12]
- The substitution reactions with the halides as entering ligands are generally ~ 50 times faster for the O,O'-bidentate complexes than for the N,O-bidentate complex.

**Table 5.23: Summary of the rate constants of methanol substitution reactions between three *fac*-Re(I) tricarbonyl complexes and various entering ligands at 25.0 °C.**

| | Constant | [Re(2,5-PicoH)] | [Re(Trop)] | [Re(Isa)] |
|---|---|---|---|---|
| **$Br^-$** | $10^3$ $k_1$ ($M^{-1}$ $s^{-1}$) | 10.52(9) | 505(4)[a] | - |
| | $10^3$ $k_{-1}$ ($s^{-1}$) | 0.910(3) | 477(1)[a] | - |
| | $K_1$ ($M^{-1}$) | 11.6(1) | 1.059(9) | - |
| | $\Delta H^{\ddagger}_{(k1)}$ (kJ $mol^{-1}$) | 79.7(5) | 76.1(6) | - |
| | $\Delta S^{\ddagger}_{(k1)}$ (J $K^{-1}$ $mol^{-1}$) | -15(2) | 5(2) | - |
| **$I^-$** | $10^3$ $k_1$ ($M^{-1}$ $s^{-1}$) | 11.53(9) | 765(2)[b] | - |
| | $10^3$ $k_{-1}$ ($s^{-1}$) | 0.437(3) | 674(1)[b] | - |
| | $K_1$ ($M^{-1}$) | 26.4(3) | 1.136(3) | - |
| | $\Delta H^{\ddagger}_{(k1)}$ (kJ $mol^{-1}$) | 77(1) | 75.3(9) | - |
| | $\Delta S^{\ddagger}_{(k1)}$ (J $K^{-1}$ $mol^{-1}$) | -22(4) | 6(3) | - |
| **Py** | $10^3$ $k_1$ ($M^{-1}$ $s^{-1}$) | 1.281(7) | 263.2(1) | 17.7(2) |
| | $10^3$ $k_{-1}$ ($s^{-1}$) | 0.032(2) | 0.07(1) | 2.44(5) |
| | $K_1$ ($M^{-1}$) | 40(3) | 3760(537) | 7.3(2) |
| | $\Delta H^{\ddagger}_{(k1)}$ (kJ $mol^{-1}$) | 82(1) | 64.7(9) | 79.0(5) |
| | $\Delta S^{\ddagger}_{(k1)}$ (J $K^{-1}$ $mol^{-1}$) | -25(4) | -39(3) | -13(2) |
| **Im** | $10^3$ $k_1$ ($M^{-1}$ $s^{-1}$) | 1.192(2) | 287(3) | - |
| | $10^3$ $k_{-1}$ ($s^{-1}$) | 0.0293(6) | 0.46(9) | - |
| | $K_1$ ($M^{-1}$) | 40.7(8) | 624(122) | - |
| | $\Delta H^{\ddagger}_{(k1)}$ (kJ $mol^{-1}$) | 84(2) | 61.8(7) | - |
| | $\Delta S^{\ddagger}_{(k1)}$ (J $K^{-1}$ $mol^{-1}$) | -19(6) | -48(2) | - |
| **$NCS^-$** | $10^3$ $k_1$ ($M^{-1}$ $s^{-1}$) | 2.104(3) | 268(2) | 18.7(1) |
| | $10^3$ $k_{-1}$ ($s^{-1}$) | 0.0921(3) | 4.4(2) | 0.48(4) |
| | $K_1$ ($M^{-1}$) | 22.84(8) | 61(3) | 39(3) |
| | $\Delta H^{\ddagger}_{(k1)}$ (kJ $mol^{-1}$) | 82.5(5) | 62(2) | 78.7(7) |
| | $\Delta S^{\ddagger}_{(k1)}$ (J $K^{-1}$ $mol^{-1}$) | -19(2) | -48(6) | -14(2) |
| **TU** | $10^3$ $k_1$ ($M^{-1}$ $s^{-1}$) | 19.19(7) | 556(3) | 36.5(2) |
| | $10^3$ $k_{-1}$ ($s^{-1}$) | 0.116(2) | 0.95(10) | 1.709(6) |
| | $K_1$ ($M^{-1}$) | 165(3) | 585(62) | 21.4(1) |
| | $\Delta H^{\ddagger}_{(k1)}$ (kJ $mol^{-1}$) | 70(1) | 58.0(7) | 78.9(5) |
| | $\Delta S^{\ddagger}_{(k1)}$ (J $K^{-1}$ $mol^{-1}$) | -44(4) | -55(2) | -8(2) |
| **MeTU** | $10^3$ $k_1$ ($M^{-1}$ $s^{-1}$) | 21.93(7) | 626(2) | 50.9(1) |
| | $10^3$ $k_{-1}$ ($s^{-1}$) | 0.056(2) | 1.84(5) | 2.190(3) |
| | $K_1$ ($M^{-1}$) | 392(14) | 340(9) | 23.24(6) |
| | $\Delta H^{\ddagger}_{(k1)}$ (kJ $mol^{-1}$) | 68(1) | 59.0(4) | 77.6(7) |
| | $\Delta S^{\ddagger}_{(k1)}$ (J $K^{-1}$ $mol^{-1}$) | -49(4) | -51(1) | -9(2) |

[a] 25.1 °C; [b] 24.3 °C
[Re(2,5-PicoH)] = *fac*-[Re(2,5-PicoH)$(CO)_3$(MeOH)]; [Re(Trop)] = *fac*-[Re(Trop)$(CO)_3$(MeOH)]; [Re(Isa)] = *fac*-[Re(Isa)$(CO)_3$(MeOH)].

- The fact that the complexes with the O,O'-bidentate ligands have larger forward rate constants than the corresponding reactions of complexes with N,O-bidentate ligands, have been reported before.[9,10]
- When considering the reactions with pyridine as entering ligand, the rate constant is ~13 and ~200 times larger for [Re(Isa)] (*fac*-[Re(Isa)$(CO)_3$(MeOH)]) and [Re(Trop)] (*fac*-[Re(Trop)$(CO)_3$(MeOH)]) respectively compared to that of [Re(2,5-PicoH)] (*fac*-[Re(2,5-PicoH)$(CO)_3$(MeOH)]). For $NCS^-$ as entering ligand, the rate constant is ~9 and ~130 times faster for [Re(Isa)] and [Re(Trop)] respectively compared to [Re(2,5-PicoH)]. By comparison of the rate constants for the S-donating ligands, it is clear that [Re(Isa)] and [Re(Trop)] both have larger rate constants for both TU and MeTU compared to the reactions of [Re(2,5-PicoH)].
- If the stability constants are compared, the [Re(Isa)] complexes are by far the least stable. The negatively charged entering ligands ($Br^-$, $I^-$ and $NCS^-$) form the least stable complexes for both [Re(Isa)] and [Re(Trop)] compared to the neutral entering ligands.
- It is clear from Figure 5.50 (Eyring plots of $\ln(k_1/T)$ *vs* 1/T), that the substitution reactions between [Re(2,5-PicoH)] (a), with a N,O-bidentate ligand, and the entering ligands have rate constants much slower than that of [Re(Isa)] (b), and [Re(Trop)] (c), with O,O'-bidentate ligands. An overall increase in the rate constants can be seen from [Re(2,5-PicoH)] < [Re(Isa)] < [Re(Trop)].
- The substitution reactions between [Re(Trop)] and the halides as entering ligands, are the fastest reactions, followed by the S-donor ligands, TU and MeTU. This trend is reversed for the reactions with [Re(2,5-PicoH)] as metal complex, indicating the higher affinity of the S-donors for [Re(2,5-PicoH)] compared to [Re(Trop)]. In all three metal centres, MeTU as entering ligand yields faster reactions than TU, and the rates of the S-donors were overall faster than the N-donors.
- The substitution kinetic data available for complexes of the type *fac*-[Re(O,O'-bid)$(CO)_3X]^n$ (X = monodentate entering ligand, n = -1, 0, 1) is very limited and the data reported in this study contributes to the available pool of data. When

isatin as O,O'-bidentate ligand was chosen, it was thought that *fac*-[Re(Isa)$(CO)_3$(MeOH)] will exhibit rate constants in the same order as that of *fac*-[Re(Trop)$(CO)_3$(MeOH)], however this was not found. The reactions with pyridine and TU are ~15 times slower for [Re(Isa)] compared to [Re(Trop)], but still ~10 and ~2 times faster than [Re(2,5-PicoH)] for pyridine and TU as entering ligands respectively.

- An overall view of the rates of the reactions between [Re(2,5-PicoH)], [Re(Isa)] and [Re(Trop)] and the various entering ligands, reveals a variation in $k_{-1}$ of 4 orders of magnitude, while the $k_1$ value varies by only a factor of *ca*. 600. This indicates less dependence on entering ligand for the anation reactions and might point towards a dissociative type of mechanism. However, the $\Delta S^{\ddagger}$ values for all of the reactions, except for the reactions between [Re(Trop)] an $Br^-$ and $I^-$, are small negative. Again it is clear that high pressure studies are required in order to determine the mode of activation for these reactions.

**Figure 5.50: Eyring plots of the reactions between (a) *fac*-[Re(2,5-PicoH)$(CO)_3$(MeOH)], (b) *fac*-[Re(Isa)$(CO)_3$(MeOH)] and (c) *fac*-[Re(Trop)$(CO)_3$(MeOH)] and different entering ligands.**

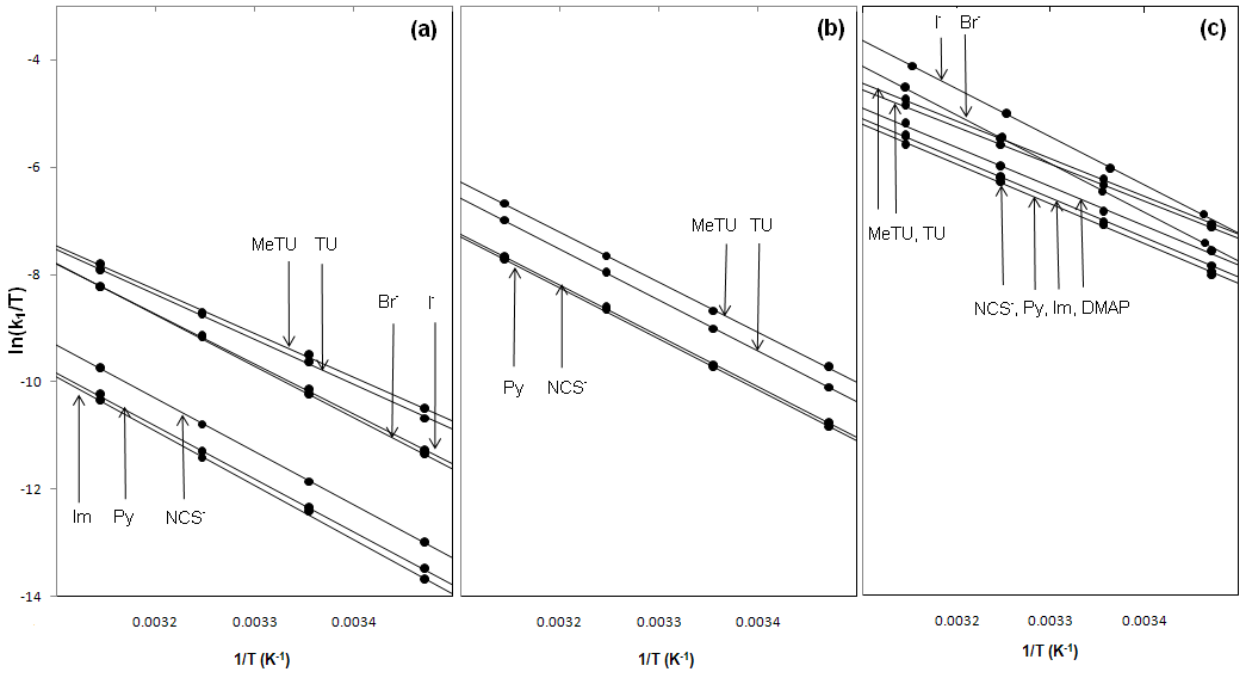

To compare these type of substitution reactions with each other and with the results reported by Salignac[4] on the *fac*-$[Re(CO)_3(H_2O)_3]^+$ complex, Table 5.24 was compiled.

**Table 5.24: Selected kinetic data for substitution reactions between different Re(I) tricarbonyl complexes and a selection of monodentate ligands at ~25.0 °C. In white – triaqua complex, shaded in blue – neutral N,O-donor bidentate complexes, shaded in beige – neutral O,O'-donor bidentate complexes and shaded in green – cationic N,N'-donor bidentate complexes.**

| | $10^3 k_1$ ($M^{-1} s^{-1}$) | $10^3 k_{-1}$ ($s^{-1}$) | K ($M^{-1}$) | $10^3 k_1$ ($M^{-1} s^{-1}$) | $10^3 k_{-1}$ ($s^{-1}$) | K ($M^{-1}$) |
|---|---|---|---|---|---|---|
| | ***fac*-$[Re(CO)_3(H_2O)_3]^+$ [a]** | | | ***fac*-$[Re(2,5\text{-}PicoH)(CO)_3(MeOH)]$ [b]** | | |
| **$Br^-$** | 1.6(3) | 2(1) | 0.7(3) | 10.52(9) | 0.910(3) | 11.6(1) |
| **Pyz** | 1.06(5) | 0.0045(4) | 237(15) | 1.281(7)[e] | 0.032(2)[e] | 40(3)[e] |
| **TU** | 2.49(9) | 0.016(2) | 160(8) | 19.19(7) | 0.116(2) | 165(3) |
| | ***fac*-$[Re(2,4PicoH)(CO)_3(MeOH)]$ [c]** | | | ***fac*-$[Re(2,4\text{-}QuinH)(CO)_3(MeOH)]$ [c]** | | |
| **$Br^-$** | 15.7(2) | 0.63(8) | 25(3) | - | - | - |
| **Py** | 1.641(8) | 0.030(2) | 21(1) | 3.31(2) | 0.051(7) | 65(9) |
| | ***fac*-$[Re(Pico)(CO)_3(MeOH)]$ [d]** | | | ***fac*-$[Re(Quin)(CO)_3(MeOH)]$ [d]** | | |
| **$Br^-$** | 11.8(1) | 0.8(1) | 15(2) | 29.6(3) | 0.7(1) | 42(6) |
| **Py** | 1.6(1) | 0.0084(1) | 190(10) | 3.9(1) | 0.02(1) | 195(97) |
| **MeTU** | 25.8(2) | 0.006(1) | 4300(700) | 46(1) | 0.003(2) | $1.5(10)\times10^4$ |
| | ***fac*-$[Re(Isa)(CO)_3(MeOH)]$ [b]** | | | ***fac*-$[Re(Trop)(CO)_3(MeOH)]$ [b]** | | |
| **$Br^-$** | - | - | - | 505(4) | 477(1) | 1.059(9) |
| **Py** | 17.7(2) | 2.44(5) | 7.3(2) | 263.2(1) | 0.07(1) | 3760(537) |
| **TU** | 36.5(2) | 1.709(6) | 21.4(1) | 556(3) | 0.95(10) | 585(62) |
| | ***fac*-$[Re(TropBr_3)(CO)_3(MeOH)]$ [c]** | | | ***fac*-$[Re(Flav)(CO)_3(MeOH)]$ [c]** | | |
| **$Br^-$** | 70.6(4) | 4(1) | 18(4) | $7.2(3)\times10^3$ | $3.17(9)\times10^3$ | 2.5(2) |
| **Py** | 20.3(7) | 1.6(2) | 12(2) | $1.38(8)\times10^3$ | 0.3(1) | $4.6(1)\times10^3$ |
| | ***fac*-$[Re(Bipy)(CO)_3(MeOH)]^+$ [d]** | | | ***fac*-$[Re(Phen)(CO)_3(MeOH)]^+$ [d]** | | |
| **$Br^-$** | 42(7) | 0.65(2) | 60(8) | 50(3) | 0.59(3) | 84(7) |
| **Py** | 0.096(1) | 0.0012(1) | 8.0(7) | 0.064(3) | 0.0058(4) | 11(1) |
| **MeTU** | 17.3(1) | 0.011(1) | 157(14) | 13.7(1) | 0.11(1) | 120(11) |

[a] Grundler *et al* [6], [b] This study, [c] Schutte *et al*[10] and Schutte[9], [d] Kemp[8], [e] Pyridine as entering ligand
Pyz = pyrazine, TFA = trifluoroacetate, $CH_3CN$ = acetonitrile, THT = tetrahydrothiophene, DMS = dimethylsulfide.

- It is clear that the *fac*-$[Re(CO)_3(H_2O)_3]^+$ complex exhibit the slowest reaction rates, compared to the other nine complexes, for the halides, pyridine type and thiourea type entering ligands. This means that the bidentate ligands activate the metal centre, to a different extent, as to be expected, depending on the strength of the Re-O,O'-bid bonds and the amount of electrondensity provided to the metal centre.
- The negatively charged bromide ions definitely have a larger relative affinity for the positively charged complexes, *fac*-$[Re(Bipy)(CO)_3(MeOH)]^+$ and *fac*-$[Re(Phen)(CO)_3(MeOH)]^+$. For the neutral N,O-bidentate complexes a ~10 times increase in the rate constant is seen from pyridine as entering ligand to $Br^-$. For the O,O'-bidentate complexes, an increase of between 2 to 5 is found. However, for the cationic N,N'-bidentate complexes a ~400 to ~800 times increase is seen for *fac*-$[Re(Bipy)(CO)_3(MeOH)]^+$ and *fac*-$[Re(Phen)(CO)_3(MeOH)]^+$ respectively.
- The rate constant values for the reactions with bromide ions as entering ligand for the N,O-bidentate ligand complexes are all of the same order. From there a definite increase is seen when moving to the O,O'-bidentate ligand complexes. A ~10 times increase for the *fac*-$[Re(TropBr_3)(CO)_3(MeOH)]$ complex, a ~100 times increase for *fac*-$[Re(Trop)(CO)_3(MeOH)]$ and a significant ~1 000 times increase for *fac*-$[Re(Flav)(CO)_3(MeOH)]$. The same trend is found for pyridine as entering ligand, only in this case the N,N'-bidentate complexes are ~100 times slower than the average N,O-bidentate ligand complexes.
- By comparison of the overall kinetic data of *fac*-$[Re(2,5\text{-}PicoH)(CO)_3(MeOH)]$ and *fac*-$[Re(2,4\text{-}PicoH)(CO)_3(MeOH)]$, it is clear that the *meta* substituted ligand (2,4-PicoH), coordinated to the Rhenium core, has larger $k_1$ values than the corresponding complex with the *para* substituted ligand (2,5-PicoH).
- One of the reasons why tropolone was chosen as bidentate ligand for this study was to compare the kinetic data of *fac*-$[Re(Trop)(CO)_3(MeOH)]$ with that of *fac*-$[Re(TropBr_3)(CO)_3(MeOH)]$. The *fac*-$[Re(Trop)(CO)_3(MeOH)]$ complex reacted ~10 times faster with bromide ions and ~7 times faster with pyridine as entering ligand, compared to the *fac*-$[Re(TropBr_3)(CO)_3(MeOH)]$ complex. This is assumed to be due to the electronwithdrawing groups on the tribromotropolone

ligand that donates less electrondensity from the O,O'-bid to the metal centre and thereby decreasing the Re-MeOH bond distance. The methanol substituted structures are not reported here but the effect of the bidentate ligand on the axial ligand can be confirmed by the solid state data of the *fac*-$[Re(TropBr_3)(CO)_3(H_2O)].CH_3OH$ complex with a Re-$H_2O$ bond distance of 2.170(5) Å[24] and a Re-$H_2O$ distance of 2.213(5) Å for the *fac*-$[NEt_4][Re(Trop)(CO)_3(H_2O)].NO_3.H_2O$ complex (Paragraph 4.4). The aqueous substitution kinetics of $[Re(Trop)(CO)_3(H_2O)]$ is discussed in Chapter 7.

- Finally the activation entropy values are negative, but not as large as usual for pure associative processes. Based on these (see Table 5.23) an Interchange intimate mechanism is proposed. Additional information, based on high pressure studies are discussed in following chapters.

[24] Schutte, M., Visser, H.G., Roodt, A. *Acta. Cryst*. **2008**, *E64*, m1610-m1611.

# 6 HIGH PRESSURE KINETIC INVESTIGATION OF THE METHANOL SUBSTITUTION IN *fac*-[RE(TROP)(CO)$_3$(MEOH]

## 6.1 Introduction

The effect of pressure on the rate of a reaction is a recognizable way to help interpret the mechanism of a reaction nowadays. There are many variable-pressure kinetic investigations reported, which includes solvent exchange and complex formation studies.[1] To gain the most direct information on the intimate reaction mechanism, the activation volume of the solvent exchange reactions should be considered. From the available data on a specific metal ion, the simple complex formation reaction take place *via* the same mechanism as the water exchange reaction in aqueous solution.[2]

Since the middle 1900's, papers have been published on high pressure NMR, but much less are reported where kinetic studies were used for the determination of the activation volume in inorganic compounds.[2,3,4,5] Especially for the *fac*-Rhenium(I) tricarbonyl core, the amount of research is very limited.[6]

Some of the reports on Rhenium(V) include a high pressure mechanistic investigation of the water substitution in the $[ReO(H_2O)(CN)_4]^-$ and $TcO(H_2O)(CN)_4]^-$ complexes, by Botha and Roodt[5], with $NCS^-$ (thiocyanate ions), TU (thiourea) and NNDMTU (N,N'-dimethylthiourea) as entering ligands. The negative activation volumes obtained, pointed towards an interchange associative mechanism for the $NCS^-$ ligand (Re(V) = 1.7(3) $cm^3\ mol^{-1}$, Tc(V) = -3.5(3) $cm^3\ mol^{-1}$) and an almost pure associative mechanism

---

[1] *Inorganic High Pressure Chemistry: Kinetics and Mechanisms* **1986**, van Eldik, R. (Ed.), Elsevier, Amsterdam.
[2] Laurenczy, G., DuCommun, Y., Merbach, A.E. *Inorg. Chem*. **1989**, *28*, 3024-3028.
[3] Maciejowska, I., van Eldik, R., Stochel, G., Stasicka, Z. *Inorg. Chem*. **1997**, *36*, 5409-5412.
[4] Leipoldt, J.G., Basson, S.S., Potgieter, I.M., Roodt, A. *Inorg. Chem*. **1987**, *26*, 57-59.
[5] Botha, J.M., Roodt, A. *Metal-Based Drugs* **2008**, ID 745989.
[6] Grundler, P.V., Salignac, B., Cayemittes, S., Alberto, R., Merbach, A.E. *Inorg. Chem*. **2004**, *43*, 865-873.

for the rest (Re(V) = -22.1(9) $cm^3$ $mol^{-1}$ (TU), Tc(V) = -14(1) $cm^3$ $mol^{-1}$ (NNDMTU), Tc(V) = -6.0(5) $cm^3$ $mol^{-1}$ (TU). These kinetic measurements were performed in a high pressure vessel on a spectrophotometer and in a stopped-flow high pressure vessel.

Two high pressure NMR studies have been reported by Grundler *et al*.[7,8] utilizing the *fac*-$[Re(CO)_3(H_2O)_3]^+$ complex. In their first study in 2004, the complex formation in water between the *fac*-$[Re(CO)_3(H_2O)_3]^+$ and Pyz (pyrazine), THT (tetrahydrothiophene) and DMS (dimethyl sulphide) were studied by high pressure $^1H$ NMR. The results were interpreted as a gradual changeover of the reaction mechanism. This is because the harder N-donor, pyrazine, gave a small positive $\Delta V^{\ddagger}$ value of 5.4(1.5) and 7.9(1.2) $cm^3$ $mol^{-1}$ for the forward and reverse reactions respectively, suggesting an $I_d$ type mechanism. However, the softer S-donors gave the following results: $\Delta V^{\ddagger}$ (THT) -7(1) and -6(1) $cm^3$ $mol^{-1}$; $\Delta V^{\ddagger}$ (DMS) -12(1) and -10(2) $cm^3$ $mol^{-1}$ for the forward and reverse reactions respectively, indicative of an associatively activated mechanism. The study revealed the ambivalent character of *fac*-$[Re(CO)_3(H_2O)_3]^+$ towards water substitution.

The second study by Grundler was focussed on the water exchange and substitution processes on the *fac*-$[Re(CO)_3(H_2O)_3]^+$ and *fac*-$[Tc(CO)_3(H_2O)_3]^+$ cores. It was kinetically investigated by $^{17}O$ NMR as a function of acidity, temperature and pressure. The overall conclusion was that for the substitution reactions of *fac*-$[Re(CO)_3(H_2O)_3]^+$, an $I_d/I_a$ changeover can be assigned since different volume profiles are found for the different entering ligands.

Other than these high pressure studies on Rhenium, no other work have been published at the time of this thesis. Therefore, in this chapter the high pressure kinetic study of *fac*-[Re(Trop)$(CO)_3$(MeOH)] is reported with four different entering ligands in an attempt to obtain additional information about the intimate reaction mechanism as discussed in Chapter 5.

[7] Grundler, P.V., Salignac, B., Cayemittes, S., Alberto, R., Merbach, A.E. *Inorg. Chem*. **2004**, *43*, 865-873.
[8] Grundler, P.V., Helm, L., Alberto, R., Merbach, A.E. *Inorg. Chem*. **2006**, *45*, 10378-10390.

# 6.2 Background theory

The clarification of the mechanism of a substitution reaction usually involves the dependence study of the reaction rate on the concentration of the reactants, the pH, ionic strength, temperature and solvent composition. The derived rate law, electronic and steric effects and all the available experimental and theoretical information are used to propose a mechanism for the reaction investigated. The electronic and steric effects are induced by variations of the leaving, entering or the non-reacting ligands on the rate constant. However, it is sometimes necessary to perform additional experiments to confirm the proposed mechanism or to differentiate between different options.

One of the primary physical variables that can influence the rate of a substitution reaction, in solution, is pressure. It is used to help with the assignment of mechanisms. The first high pressure kinetic study, in coordination chemistry, was done in 1958 by Hunt and Taube[9] but it only really started to develop in the 1980's.

## 6.2.1 Activation volume and activation entropy

The volume of activation ($\Delta V^{\ddagger}$), which is the difference between the partial molar volumes of the reactants and the transition state, is related to the pressure derivative of lnk as indicated in Equation 6.1.

$$(\delta \ln k/\delta P)_T = - \Delta V^{\ddagger}/RT \qquad \textbf{Equation 6.1}$$

The value of $\Delta V^{\ddagger}$ can be either positive or negative, depending on whether the reaction was slowed down or accelerated with the increase in pressure, respectively. The most popular equation used to account for the dependence of $\Delta V^{\ddagger}$ on the pressure is given by the quadratic equation represented as Equation 6.2.

$$\ln k = \ln k_0 - (\Delta V^{\ddagger} P/RT) + (\Delta \beta^{\ddagger} P^2/2RT) \qquad \textbf{Equation 6.2}$$

[9] Hunt, H.R., Taube, H. *J. Am. Chem. Soc.* **1958**, *80*, 2642-2646.

where $\Delta V^{\ddagger}$ is measured at zero pressure and $\Delta\beta^{\ddagger}$ is the compressibility coefficient of activation, which is dependent on the pressure effect on the $\Delta V^{\ddagger}$ value.

In a simple dissociative step of a reaction, the bond stretching will give rise to an increase in volume which means a lowering in the rate as the pressure increase, therefore a positive $\Delta V^{\ddagger}$ value. On the contrarily, the bond formation in an associative step will increase the rate constant if the pressure is increased, giving a negative value for $\Delta V^{\ddagger}$.

Another important contribution to the $\Delta V^{\ddagger}$ value is the changes in solvent electrostriction. This might occur when ions or dipoles are formed or neutralized in the transition state. This is the reason why the volume of activation that is measured ($\Delta V^{\ddagger}$) is always considered as a combination of this electrostrictive contribution ($\Delta V^{\ddagger}_{elec}$) and an intrinsic contribution ($\Delta V^{\ddagger}_{int}$), due to changes in the internuclear distances during the formation of the transition state. In an extreme case, where the substitution reactions may include a charged species, the observed $\Delta V^{\ddagger}$ can be dominated by the $\Delta V^{\ddagger}_{int}$ value to such an extent that the sign of $\Delta V^{\ddagger}$ might differ from that of $\Delta V^{\ddagger}_{int}$. However, with solvent/ligand exchange it is much simpler, since the electrostrictive changes can be excluded and therefore the sign of $\Delta V^{\ddagger}$ is directly indicative of the activation; a positive value for bond stretching and a negative value for bond formation.[1]

There is an ongoing argument about the best and most accurate way to determine the mechanism of a reaction. It mainly started when researchers repeated kinetic studies and obtained about the same experimental kinetic data but on many occasions, the activation parameters differed to a great extent[10].

The pressure dependence of a reaction rate can be discussed according to the transition state theory, through the activation volume, $\Delta V^{\ddagger}$. According to Swaddle, DuCommun and Stranks, the entropy of activation should in principle have a bigger tendency to error than $\Delta V^{\ddagger}$, the volume of activation since for $\Delta V^{\ddagger}$, an increase in rate with an increase in pressure implies a negative value and *vice versa*. According to Equation 6.1, this is the definition of the volume of activation.

On the other hand, for $\Delta S^{\ddagger}$ it is not so simple. One of the simplest relations for $\Delta S^{\ddagger}$ that is mostly used is given in Equation 6.3.

[10] Merbach, A.E. *Pure & Appl. Chem*. **1987**, *59*, 161-172.

$$\Delta S^{\ddagger}/R = \ln(k/T) - \ln(k_B/h) - (1/T)\delta\ln(k/T)\delta(1/T) \qquad \textbf{Equation 6.3}$$

with $\{\ln(k/T) - \ln(k_B/h)\} = -\Delta G^{\ddagger}/RT$ and $\{(1/T)\delta\ln(k/T)\delta(1/T)\} = +\Delta H^{\ddagger}/RT$. In the first term it is clear to see that errors in k will only introduce very small errors in $\Delta G^{\ddagger}$ because of the logarithmic relationship. The second term is usually large and never changes sign. Therefore, to calculate $\Delta S^{\ddagger}$, which is a small term and can be either negative or positive, the difference of the two terms, that is similar in magnitude is the reason for the error problems when determining $\Delta S^{\ddagger}$.

Furthermore to the error problem of the $\Delta S^{\ddagger}$ value, the right hand side of Equation 6.3 represent the extrapolation of the tangent to the ln(k/T) *vs* (1/T) curve to 1/T = 0. This extrapolation is in general very long and has a big tendency for errors.

Experimentally is has been found that the errors in $\Delta V^{\ddagger}$ are much less than those in $\Delta S^{\ddagger}$, in experiments that have been repeated using both methods.[11]

## 6.3 Materials and methods

All the reagents and chemicals used in this study were of analytical reagent grade, purchased from Sigma-Aldrich, South Africa. *fac*-[Re(Trop)$(CO)_3$(MeOH)] was prepared as described in Chapter 3, dissolving the product in methanol. The high pressure studies were performed on a HPSF-56 Stopped-flow system, supplied by TgK Scientific. The system can operate over a temperature range of -40 to 100 °C and up to 200 MPa. The dead time is less than 2 ms at 298 K and is pressure independent up to 200 MPa. The temperature within the system was controlled and maintained at ± 0.1 °C by means of a circulating water bath system. All the kinetic runs were performed under *pseudo* first-order conditions with the ligand in excess every time. The Scientist Micromath, Version 2.01 program[12], Microsoft Office Excel 2007[13] and Kinetic Studio, Version 1.0.8.32278[14] were used to fit the data to the specific functions. In all the figures, the solid lines represent the least-squares fits of the data and the experimental values are given as individual points.

[11] Newman, K.E., Meyer, F.K., Merbach, A.E. *J. Am. Chem. Soc* **1979**, *101*, 1470-1476.
[12] MicroMath Scientist for Windows, Version 2.01, Copyright © 1986-1995, MicroMath, Inc.
[13] Microsoft Office 2007 Copyright © 2011 Microsoft Corporation.
[14] Kinetic Studio, Version 1.0.8.32278, Copyright © 2008, TgK Scientific.

# 6.4 Results and Discussion

In order to compare the mechanism for the methanol substitution in the *fac*-[Re(Trop)(CO)$_3$(MeOH)] complex, a high pressure study with Im (imidazole), Py (pyridine), TU (thiourea) and MeTU (1-methyl-2-thiourea) was performed in methanol as solvent. A schematic representation is provided in Figure 6.1.

**Figure 6.1: Schematic representation of the methanol substitution reactions on the *fac*-[Re(Trop)(CO)$_3$(MeOH)] complex.**

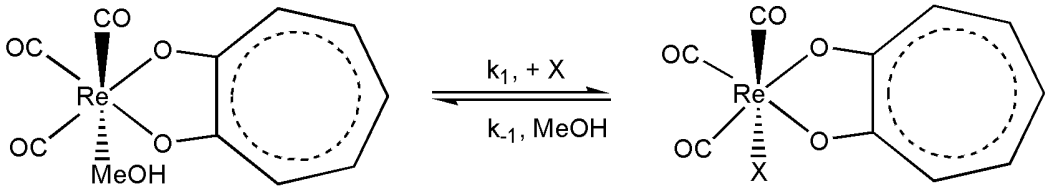


X = Imidazole, pyridine, thiourea, 1-methyl-2-thiourea

The reactions were performed at temperatures ~ 25.0 °C and at six different pressures, ranging from 0.6 to 100 MPa. The reactions were repeated at two different concentrations of the entering ligand for all four the ligands used. The pressure dependence for the substitution reactions studied, at the different pressure values, is given by Equation 6.4 (derived from Equation 6.1).

$$\ln(k_a/k_b) = -\Delta V^{\ddagger}_{expt}(P_a-P_b)/RT \qquad \textbf{Equation 6.4}$$

In Equation 6.4, a and b denotes the different pressures the reactions were performed under.

According to the data obtained in Chapter 5, for the same reactions performed under no pressure, it was found that the reverse reaction is negligible, with the y intercept very close to zero for these four reactions. Since the contribution by the reverse step is negligible in all four these cases, $k_{obs} = k_1[L] + k_{-1} \approx k_1[L]$ with L = imidazole ($5 \times 10^{-2}$ M), pyridine ($4 \times 10^{-2}$ M), thiourea ($5 \times 10^{-2}$ M) and 1-methyl-2-thiourea ($5 \times 10^{-2}$ M).

Therefore, the pressure dependence on $k_1$ was studied at the respective entering ligand concentrations.

The first reaction studied was that between *fac*-[Re(Trop)$(CO)_3$(MeOH)] and imidazole. The results are presented in Figure 6.2 and the data was fitted to Equation 6.4 to obtain the volume of activation of 9.0(2) $cm^3$ $mol^{-1}$. This physical value, as well as the fact that the reaction rate slowed down with an increase in pressure is indicative of either a dissociative or interchange dissociative mode of activation.

**Figure 6.2: High pressure depencence study for the reaction between *fac*-[Re(Trop)$(CO)_3$(MeOH)] and imidazole. [Re] = 1 x $10^{-4}$ M, [Im] = 5 x $10^{-2}$ M, 25.8 °C, 450 nm, methanol.**

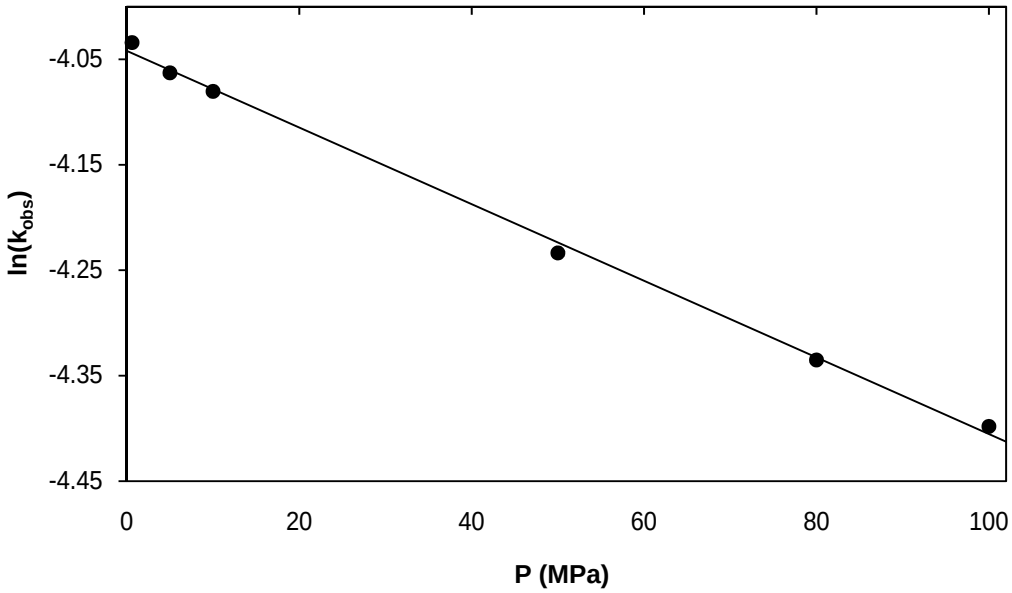


The reaction between *fac*-[Re(Trop)$(CO)_3$(MeOH)] and pyridine as entering ligand was studied next and was followed at 312 nm and at 25.9 °C. The data represented in Figure 6.3 were fitted to Equation 6.4 and the pressure parameter, $\Delta V^{\ddagger}$, was calculated from the slope of the plot of ln($k_{obs}$) *vs* pressure, as 10.1(2) $cm^3$ $mol^{-1}$.

**Figure 6.3: High pressure depencence study for the reaction between *fac*-[Re(Trop)(CO)$_3$(MeOH)] and pyridine. [Re] = 1 x 10$^{-4}$ M, [Py] = 4 x 10$^{-2}$ M, 25.9 °C, 312 nm, methanol.**

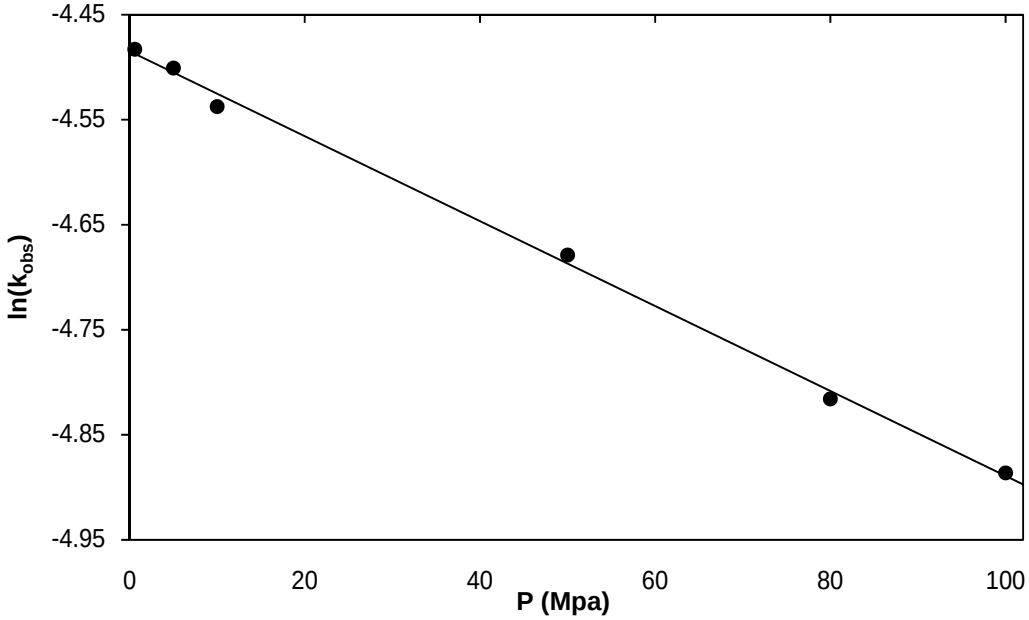


The pressure dependence of the reaction between *fac*-[Re(Trop)(CO)$_3$(MeOH)] and thiourea was also studied at a pressure ranging from 0.6 MPa to 100 MPa. The reaction was followed at 440 nm and at 25.6 °C. The data obtained is presented in Figure 6.4 and was fitted to Equation 6.4 to obtain a value of 10.0(3) cm$^3$ mol$^{-1}$ for the activation volume for the reaction.

**Figure 6.4: High pressure depencence study for the reaction between *fac*-[Re(Trop)(CO)$_3$(MeOH)] and thiourea. [Re] = 1 x 10$^{-4}$ M, [TU] = 5 x 10$^{-2}$ M, 25.6 °C, 440 nm, methanol.**

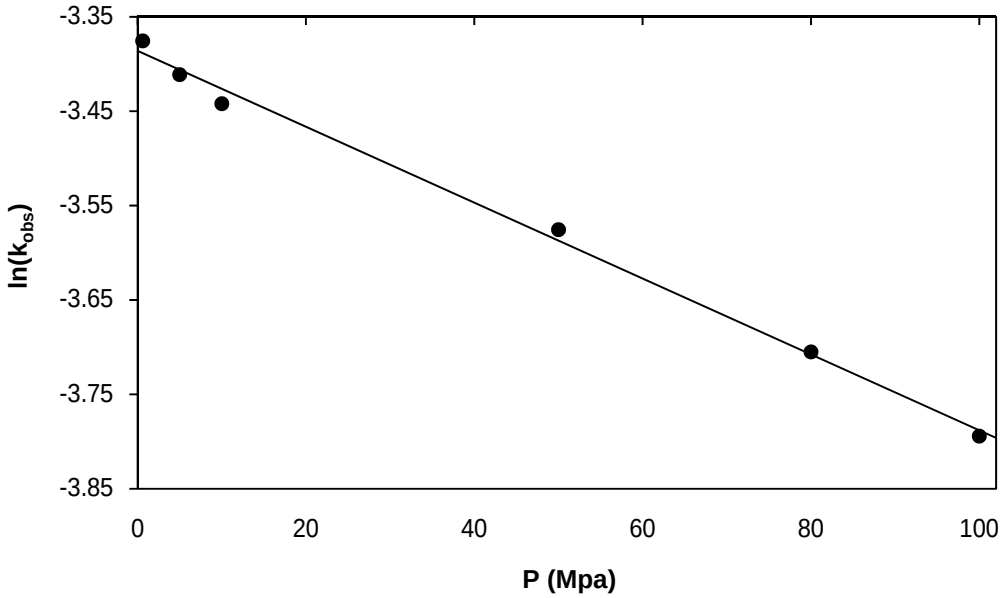


Finally, the methanol substitution reaction of the *fac*-[Re(Trop)(CO)$_3$(MeOH)] complex with 1-methyl-2-thiourea was monitored as different pressures. A plot of the $k_{obs}$ *vs* pressure is presented in Figure 6.5. Equation 6.4 was used to fit this data to determine the activation volume of the reaction. The value for $\Delta V^{\ddagger}$ was calculated as 14.5(3) cm$^3$ mol$^{-1}$.

**Figure 6.5: High pressure dependence study for the reaction between *fac*-[Re(Trop)(CO)$_3$(MeOH)] and MeTU. [Re] = 1 x 10$^{-4}$ M, [MeTU] = 5 x 10$^{-2}$ M, 25.9 °C, 435 nm, methanol.**

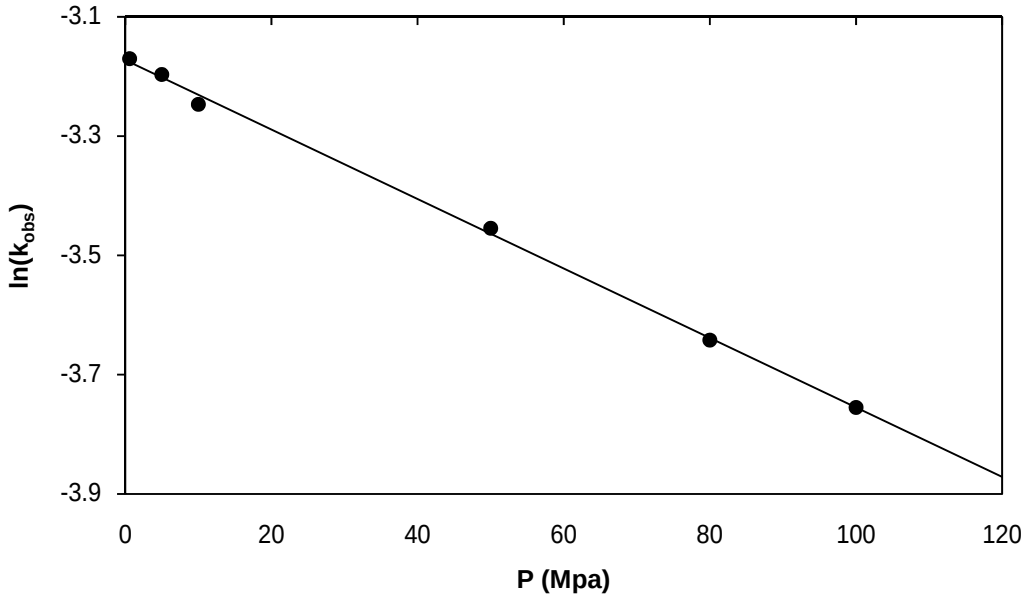


In Chapter 5, the methanol substitution kinetics between fac-[Re(Trop)(CO)$_3$(MeOH)] and various entering ligands were reported for a temperature range, to monitor the dependence of the $k_{obs}$ values toward the concentration of the entering ligand as well as the temperature. Also, the standard activation change of entropy was calculated for all of the reactions and was found to be medium to small negative for all of the reactions (included in the summary in Table 6.1), therefore indicating an associative mechanism type. However, the high pressure study reported here clearly indicates a positive volume of activation for all these reactions, pointing towards a dissociative interchange mechanism. This, together with the large $k_{-1}$ variation that indicates less dependence on the entering ligand, also points towards a dissociative type mechanism.

Once again the rate of the substitution reaction increases from the N-donor atom ligands to the S-donating ligands. The trend for the $k_{obs}$ values are imidazole < pyridine < thiourea < 1-methyl-2-thiourea, which is the same as for the reactions where no pressure was applied except for pyridine and imidazole that is switched around. The $\Delta V^{\ddagger}$ values for the four reactions are all in the same range with the 14.5(3) cm$^3$ mol$^{-1}$ value for the MeTU entering ligand a little bit higher than for the rest.

**Table 6.1: Summary of the kinetic data and activation parameters for the substitution reactions between *fac*-[Re(Trop)(CO)$_3$(MeOH)] and entering ligands.**

| | | Im | Py | TU | MeTU |
|---|---|---|---|---|---|
| $k_{obs}$ ($s^{-1}$) | **0.6 MPa** | 0.0177(3) | 0.0113(7) | 0.0342(3) | 0.042(1) |
| | **5 MPa** | 0.0172(4) | 0.0111(7) | 0.033(2) | 0.0409(7) |
| | **10 MPa** | 0.0169(8) | 0.0107(3) | 0.032(1) | 0.0389(6) |
| | **50 MPa** | 0.0145(9) | 0.00929(9) | 0.028(1) | 0.0316(6) |
| | **80 MPa** | 0.0131(7) | 0.0081(2) | 0.0246(7) | 0.0262(9) |
| | **100 MPa** | 0.0123(3) | 0.00755(7) | 0.0255(6) | 0.0234(3) |
| $k_1$[a] ($M^{-1}$ $s^{-1}$) | | 0.287(3) | 0.2632(1) | 0.556(3) | 0.626(2) |
| $k_{-1}$[a] ($s^{-1}$) | | 0.00046(9) | 0.00007(1) | 0.00095(10) | 0.00184(5) |
| $K_1$ ($M^{-1}$) | | 624(122) | 3760(537) | 585(62) | 340(9) |
| $\Delta H^{\ddagger,a}$ (kJ $mol^{-1}$) | | 61.8(7) | 64.7(9) | 58.0(7) | 59.0(4) |
| $\Delta S^{\ddagger,a}$ (J $K^{-1}$ $mol^{-1}$) | | -48(2) | -39(3) | -55(2) | -51(1) |
| $\Delta V^{\ddagger}$ ($cm^3$ $mol^{-1}$) | | 9.0(2) | 10.1(2) | 10.0(3) | 14.5(3) |

[a] calculated at 298 K and 0,101 MPa (see Chapter 5).

The values reported by Grundler *et al*.[7] on the *fac*-[Re(CO)$_3$(H$_2$O)$_3$]$^+$ complex, was $\Delta V^{\ddagger}$ = + 5.4 ± 1.5 $cm^3$ $mol^{-1}$ for pyrazine, $\Delta V^{\ddagger}$ = -6.6 ± 1 $cm^3$ $mol^{-1}$ for tetrahydro-thiophene and $\Delta V^{\ddagger}$ = -12 ± 1 $cm^3$ $mol^{-1}$ for dimethylsulphide. A gradual changeover for the mechanism was reported from an $I_d$ mechanism for the N-donors and an $I_a$ mechanism for the S-donor ligands. Overall they confirmed the ambivalent character of *fac*-[Re(CO)$_3$(H$_2$O)$_3$]$^+$ towards aqua substitution.

By comparing the results of Grundler to the results of *fac*-[Re(Trop)(CO)$_3$(MeOH)] reported here, it is clear that this O,O'-bidentate ligand influence the metal centre to such an extent that all the aqua substitution reactions point towards an $I_d$ type mechanism to even a pure dissociative type of activation, instead of observing the changeover effect where both $I_d$ and $I_a$ type mechanisms are reported. The more positive value for MeTU is difficult to explain when compared to the results by Grundler. According to that data, the softer S-donor ligands showed more negative $\Delta V^{\ddagger}$ values than the N-donor ligands. In this investigation it is reversed.

The data obtained from this study is just once again proof that the determination of the activation entropy is not always very accurate. For all four these reactions, negative $\Delta S^{\ddagger}$ values were obtained whereas the $\Delta V^{\ddagger}$ values indicates an $I_d$ mechanism. The final

proof of the mechanism determination was the fact that all four reaction rates decreased as the pressure was increased, clearly indicating a dissociative type mechanism.

More high-pressure studies need to be done to broaden the data available for complexes of the form *fac*-[Re(L,L'-bid)$(CO)_3(X)]^n$ to be able to compare the effect of the bidentate ligand (L,L'-bid) on the rate of the reaction with the variety of entering ligands.

For this study, only the entering ligands with $k_{-1} \sim 0$ were chosen. Part of the future research is to expand the *fac*-[Re(L,L'-bid)$(CO)_3(X)]^n$ type complexes with a variety of bidentate ligands as well as entering ligands, for instance halides with a large $k_{-1}$ value. In those cases, four or more concentrations of the incoming ligand will be used to accurately determine the activation volume.

It is interesting to note that the intimate reaction mechanism in these reactions are influenced in a subtle way by the L,L'-bidentate ligands employed. This is further discussed as $H_2O$ substitution in Chapter 7.

# 7 SUBSTITUTION KINETICS OF *fac*-[RE(TROP)(CO)$_3$(H$_2$O)] IN AQUEOUS MEDIUM

## 7.1 Introduction

The aqueous substitution kinetics of *fac*-Re(I) tricarbonyl complexes are virtually unexplored. In fact, the only kinetic data available in the literature is the water exchange studies by Salignac *et al*.[1] and the aqua substitution kinetics of the *fac*-$[Re(CO)_3(H_2O)_3]^+$ complex performed by Grundler *et al*.[2,3] The water exchange rate of *fac*-$[Re(CO)_3(H_2O)_3]^+$ was calculated as $k_{ex} = 6.3 \times 10^{-3}$ $s^{-1}$, which is relatively slow. A positive activation entropy $\Delta S^{\ddagger}_{ex}$ for the water exchange on *fac*-$[Re(CO)_3(H_2O)_3]^+$ of +14 ±10 J $K^{-1}$ $mol^{-1}$ was calculated. In the studies by Grundler, a small increase in the rate constant from the harder trifluoroacetate anion (TFA) – $2.9 \times 10^{-3}$ – to the softer thiourea (TU) – $41.5 \times 10^{-3}$ – was found for aqua substitution on the *fac*-$[Re(CO)_3(H_2O)_3]^+$ complex. The results obtained by Grundler *et al*. are consistent with the variety of ligands reported by Salignac *et al*. This is described in detail in Paragraph 2.7.1.

Until recently, there were no reports on the mono aqua substitution reactions on *fac*-$[Re(L,L'\text{-bid})(CO)_3(H_2O)]^n$ type complexes (L,L'-bid = bidentate ligands). The methanol substitution kinetics on a variety of *fac*-$[Re(L,L'\text{-bid})(CO)_3(MeOH)]^n$ type complexes[4] is the first of this kind.

Rhenium(I) tricarbonyl complexes easily form polymers in less acidic or neutral aqueous solutions and since most labeling kits on the market is in saline solution, it is imperative that the aqueous substitution kinetics of these types of complexes should be studied to

---

[1] Salignac, B., Grundler, P.V., Cayemittes, S., Frey, U., Scopelliti, R., Merbach, A.E., Hedinger, R., Hegetschweiler, K., Alberto, R., Prinz, U., Raabe, G., Kölle, U., Hall, S. *Inorg. Chem*. **2003**, *42*, 3516-3526.

[2] Grundler, P.V., Salignac, B., Cayemittes, S., Alberto, R., Merbach, A.E. *Inorg. Chem*. **2004**, *43*, 865-873.

[3] Grundler, P.V., Helm, L., Alberto, R., Merbach, A.E. *Inorg. Chem*. **2006**, *45*, 10378-10390.

[4] Schutte, M., Kemp, G., Visser, H.G., Roodt, A. *Inorg. Chem*. **2011**, *50(24)*, 12486-12498.

understand the fundamentals of these reactions. This is especially essential if the '2+1' approach should be adopted.

Another hindering factor is that most of the compounds of the form, *fac*-[Re(L,L'-bid)$(CO)_3(H_2O)]^n$, are insoluble in water. One of the aims of this study was to synthesize a complex that is soluble in water over a wide pH range. In this regard, *fac*-[Re(Trop)$(CO)_3(H_2O)$] was successfully synthesized.

## 7.2 Experimental procedure

All the chemicals and reagents used were of analytical reagent grade, purchased from Sigma-Aldrich, South Africa. Double-distilled water was used in all the experiments. All the pH measurements were performed on a Hanna pH 211 Microprocessor pH meter, with a HI 1131 probe using standard buffer solutions for calibrations. The kinetic measurements were performed on a Varian Cary 50 Conc UV-Visible spectrophotometer that is coupled to a personal computer capable of performing least-squares analyses on the absorption values *vs* time data obtained from the kinetic runs. The Scientist Micromath, Version 2.01[5] program and Microsoft Office Excel 2007[6] were used to fit the data to the specific functions. The temperature was controlled and maintained at ± 0.1 °C by circulating water bath systems.

The kinetic reactions were measured aerobically under *pseudo* first-order conditions with the ligand in excess in each case and a constant metal concentration of $5 \times 10^{-5}$ M. The ionic strength (μ) of all the solutions was maintained at 1 M by using $NaClO_4$. Each kinetic run was performed at least twice and an average of the values was taken. In the figures presented, the solid lines represent the computer least-squares fits of the data and the single points represent the experimental values, denoted by selected symbols. Reactions were fitted to Equation 5.1 which confirmed they were first order for at least 4 half lives.

In all the calculations, pH = -log $[H^+]$. *fac*-[Re(Trop)$(CO)_3(H_2O)$] was prepared as described in Chapter 3. All the detailed tables of the experimental values are given in Appendix B.

[5] MicroMath Scientist for Windows, Version 2.01, Copyright © 1986-1995, MicroMath, Inc.
[6] Microsoft Office 2007 Copyright © 2011 Microsoft Corporation.

# 7.3 Results and Discussion

This chapter deals with the influence of $H^+$ ions on the reactivity of *fac*-[Re(Trop)$(CO)_3(H_2O)$] towards aqua substitution with $NCS^-$ ions (Scheme 7.1). Throughout the rest of this chapter, there will be referred to Scheme 7.1 when the possible kinetic pathways and pH influences will be discussed.

**Scheme 7.1: Schematic representation of the possible reactions of *fac*-[Re(Trop)$(CO)_3(H_2O)$] with $NCS^-$ and $H^+$ in water.**

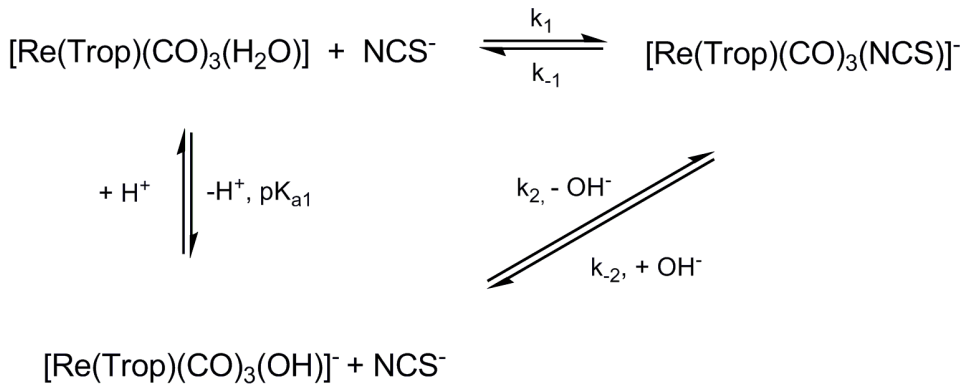


## 7.3.1 Influence of $H^+$ ions on *fac*-[Re(Trop)$(CO)_3(H_2O)$]

The pH dependence of *fac*-[Re(Trop)$(CO)_3(H_2O)$] was studied at 25.0 °C between pH 7 and 10.5. In general, the acid/base behaviour of a monoprotic species such as HA is given by Equation 7.1. For the determination of the acid dissociation constant, Equation 7.2 was used.

$$HA \overset{K_{a1}}{\rightleftharpoons} HA^- + H^+ \qquad \textbf{Equation 7.1}$$

$$A = \frac{A_h + A_0(K_{a1}/[H^+])}{1 + (K_{a1}/[H^+])} \qquad \textbf{Equation 7.2}$$

In Equation 7.2, A is the absorbance at a specific pH, $A_h$ is the absorbance of the protonated species, *fac*-[Re(Trop)$(CO)_3(H_2O)$], $A_0$ is the absorbance of the

deprotonated species, *fac*-[Re(Trop)$(CO)_3(OH)]^-$ and $K_{a1}$ is the acid dissociation constant.

The acid dissociation constant of *fac*-[Re(Trop)$(CO)_3(H_2O)$] was determined spectrophotometrically at 25.0 °C and at 275 nm by adjusting the pH of a 1 x $10^{-4}$ M Rhenium solution from pH 7 to 11 with NaOH and measuring the absorbance each time. From a non-linear fit of the data to Equation 7.2 the $pK_{a1}$ value was determined as 8.96(2) and is illustrated in Figure 7.1.

According to Egli *et al.*[7], who studied the hydrolysis of the *fac*-$[Re(CO)_3(H_2O)_3]^+$ aqua ion, the $pK_{a1}$ values of the mononuclear deprotonation products *fac*-$[Re(CO)_3(H_2O)_2(OH)]$ and *fac*-$[Re(CO)_3(H_2O)(OH)_2]^-$ are 7.5(2) and 9.3(3) respectively.

**Figure 7.1: A plot of Absorbance *vs* pH for the *fac*-[Re(Trop)$(CO)_3(H_2O)$] complex. [Re] = 1 x $10^{-4}$ M, 25.0 °C, 275 nm, μ = 1 M ($NaClO_4$).**

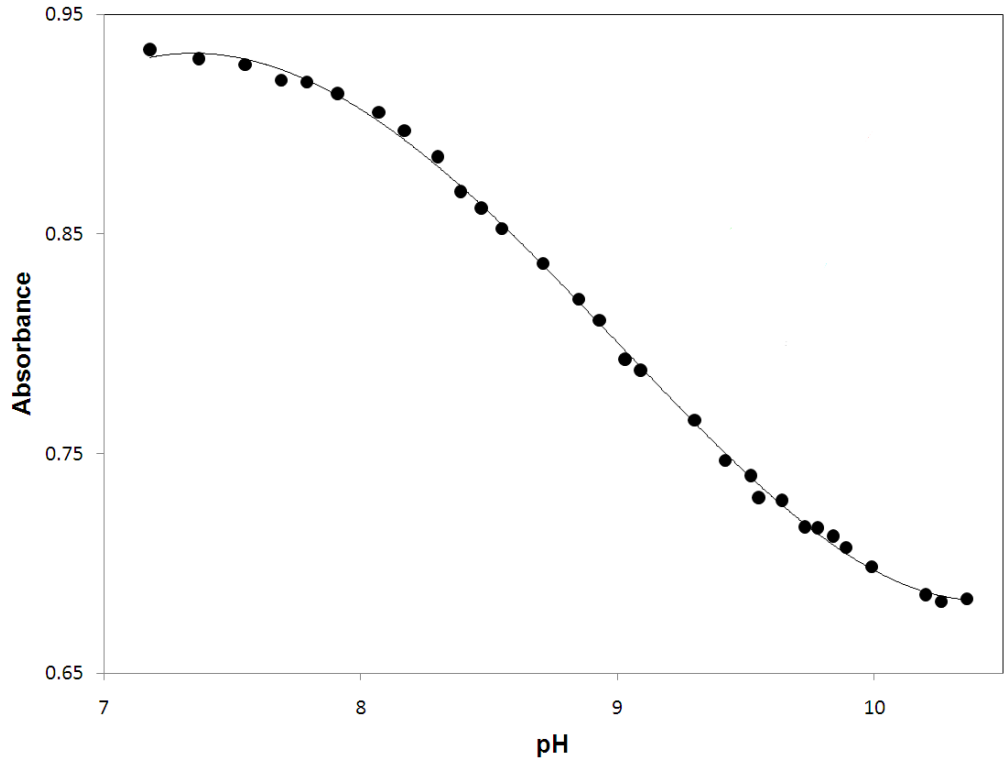


[7] Egli, A., Hegetschweiler, K., Alberto, R., Abram, U., Schibli, R., Hedinger, R., Gramlich, V., Kissner, R., Schubiger, P.A. *Organometallics* **1997**, *16*, 1833-1840.

## 7.3.2 Substitution reactions of *fac*-[Re(Trop)(CO)$_3$(H$_2$O)] with NCS$^-$ ions

The substitution reactions of *fac*-[Re(Trop)(CO)$_3$(H$_2$O)]/*fac*-[Re(Trop)(CO)$_3$(OH)$^-$] was studied between pH 7 and 10.5. At these pH values, considering the value of 8.96(2) obtained for p$K_{a1}$ in Paragraph 7.3.1, both Re(I) species can react with NCS$^-$. The overall rate law, according to Scheme 7.1, is given by Equation 7.3.

$$R = k_1[Re(Trop)(CO)_3(H_2O)][NCS^-] - k_{-1}[Re(Trop)(CO)_3(NCS)^-] + k_2[Re(Trop)(CO)_3(OH)^-][NCS^-] - k_{-2}[Re(Trop)(CO)_3(NCS)^-][OH^-]$$

**Equation 7.3**

The total concentration of the Re(I) aqua complex, $[Re]_{tot}$, is indicated in Equation 7.4 below.

$$[Re]_{tot} = [Re(Trop)(CO)_3(H_2O)] + [Re(Trop)(CO)_3(OH)^-]$$

**Equation 7.4**

The acid dissociation constant, $K_{a1}$, is given in Equation 7.5 and the relationship between the rate and the observed rate, $k_{obs}$ is given in Equation 7.6.

$$K_{a1} = \frac{[Re(Trop)(CO)_3(OH)^-][H^+]}{[Re(Trop)(CO)_3(H_2O)]}$$

**Equation 7.5**

$$R = k_{obs}[Re]_{tot}$$

**Equation 7.6**

By rearrangement of Equation 7.5, and substituting it into Equation 7.4, the following two equations are obtained (Equation 7.7 and Equation 7.8).

$$[Re(Trop)(CO)_3(OH)^-] = \frac{[Re]_{tot}}{\left(\frac{[H^+]}{K_{a1}} + 1\right)}$$

**Equation 7.7**

$$[Re(Trop)(CO)_3(H_2O)] = \frac{[Re]_{tot}}{\left(\frac{K_{a1}}{[H^+]} + 1\right)}$$

**Equation 7.8**

By substituting Equation 7.6, 7.7 and 7.8 into Equation 7.3, Equation 7.9 could be derived.

$$k_{obs} = \left(\frac{k_1[H^+] + k_2Ka_1}{Ka_1 + [H^+]}\right)[NCS^-] + k_{-1} + k_{-2}[OH^-]$$

**Equation 7.9**

Several preliminary experiments were performed to verify the proposed mechanism in Scheme 7.1. Firstly, the stability of *fac*-$[Re(Trop)(CO)_3(H_2O)]$/*fac*-$[Re(Trop)(CO)_3(OH)^-]$ with increasing pH was checked by slowly increasing the pH of a $1 \times 10^{-4}$ M solution of the complex and monitoring it on the UV/Vis spectrophotometer. At pH > 10.0, slow changes in the spectrum was observed. It was confirmed by UV/Vis spectroscopy to possibly be the formation of a polymeric Re(I) species (see Figure 7.2).

**Figure 7.2: UV/Vis spectrum of the proposed *fac*-[Re(Trop)(CO)$_3$(H$_2$O)] species at pH 6.4 and 6.1, *fac*-[Re(Trop)(CO)$_3$(OH)$^-$] at pH 9.5 and the Re(I) dimer species as pH 10.1.**

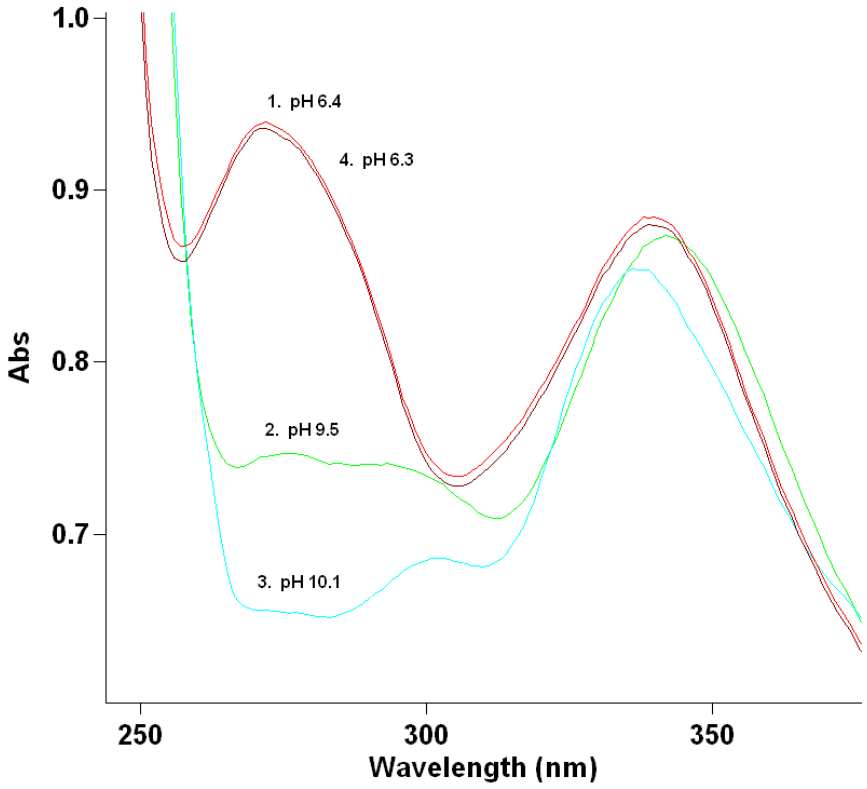


Figure 7.2 shows the change in UV/Vis spectrum for a 1 x $10^{-4}$ M solution of *fac*-[Re(Trop)(CO)$_3$(H$_2$O)] at pH 6.4 (**1** in Figure 7.2). The pH was increased to 9.5 (**2** in Figure 7.2) where the formation of *fac*-[Re(Trop)(CO)$_3$(OH)$^-$] is clear from the change in spectrum. The pH was then increased to 10.1 (**3** in Figure 7.2) where the formation of the Re(I) dimer is proposed, showing a definite peak at 297 nm. By lowering the pH of the same solution, the peak at 297 nm disappears and a spectrum almost similar to that obtained for the *fac*-[Re(Trop)(CO)$_3$(H$_2$O)] species is once again obtained (**4** in Figure 7.2), indicating that the reaction is reversible.

In terms of the substitution kinetics, preliminary experiments indicated that the observed rate, $k_{obs}$, decreases with an increase in pH. At pH ~ 10, the only reactions observed is the slow polymerisation reactions already mentioned; no substitution reactions were

observed. This confirms that *fac*-[Re(Trop)$(CO)_3(OH)]^-$ is not reacting with $NCS^-$ ions and that the $k_2/k_{-2}$ pathway can be ignored.

Figure 7.3 illustrates a typical spectrum change of absorbance over time for the substitution reactions of *fac*-[Re(Trop)$(CO)_3(H_2O)]$ with $NCS^-$ ions. Only one reaction step was observed between pH 6 and 10; more confirmation of the proposed rate law.

**Figure 7.3: Kinetic trace for the reaction between *fac*-[Re(Trop)$(CO)_3(H_2O)]$ and $NCS^-$ with the absorbance *vs* time plot indicating one reaction. [Re] = 5 x $10^{-5}$ M, [$NCS^-$] = 2.5 x $10^{-2}$ M, pH 6.4, 25.0 °C, 260 nm, Δt = 4 s.**

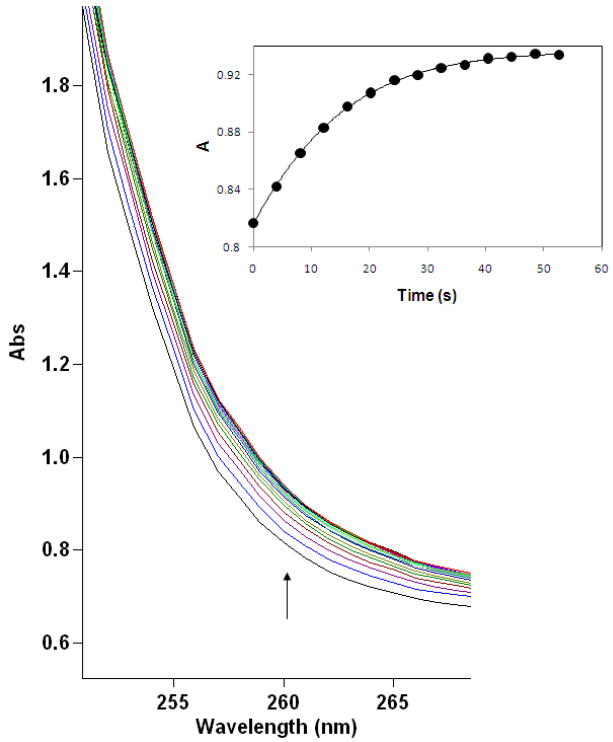


Even further confirmation of the proposed mechanism was obtained by isolating reaction products from the kinetic studies from solution and comparing the IR and NMR data with that obtained for *fac*-[$NEt_4$][Re(Trop)$(CO)_3$(NCS)] in Paragraph 3.6.6. In all cases, very good agreement was obtained, indicating that the final product at pH < 10 is in fact f*ac*-[$NEt_4$][Re(Trop)$(CO)_3$(NCS)].

From the above, and taking into consideration that the $k_2/k_{-2}$ pathways do not occur, under *pseudo* first-order conditions and the pH range studied, $[Re]_{tot} << [NCS^-]$, Equation 7.9 can be simplified to Equation 7.10.

$$k_{obs} = \frac{k_1[H^+][NCS^-]}{K_{a1} + [H^+]} + k_{-1}$$

**Equation 7.10**

At pH 6.4, $K_{a1} <<< [H^+]$, so that Equation 7.10 simplifies to:

$$k_{obs} = k_1[NCS^-] + k_{-1}$$

**Equation 7.11**

Equation 7.11 was used to calculate the rate constants for the substitution reactions between *fac*-[Re(Trop)$(CO)_3(H_2O)$] and $NCS^-$ ions (pH = 6.4, four temperatures μ = 1 M ($NaClO_4$)). According to Equation 7.11, plots of $k_{obs}$ *vs* $[NCS^-]$ should be straight lines (Figure 7.4).

From a least-squares fit of the data to Equation 7.11, at 15.0, 25.0, 35.0 and 45.0 °C, $k_1$ and $k_{-1}$ was obtained and is summarized in Table 7.1.

**Figure 7.4: Plot of $k_{obs}$ *vs* [$NCS^-$] for the reaction between *fac*-[Re(Trop)$(CO)_3(H_2O)$] and $NCS^-$ at different temperatures. [Re] = 5 x $10^{-5}$ M, [$NCS^-$] = 2.5 x $10^{-3}$ – 3 x $10^{-2}$ M, pH 6.4, 260 nm, μ = 1M ($NaClO_4$).**

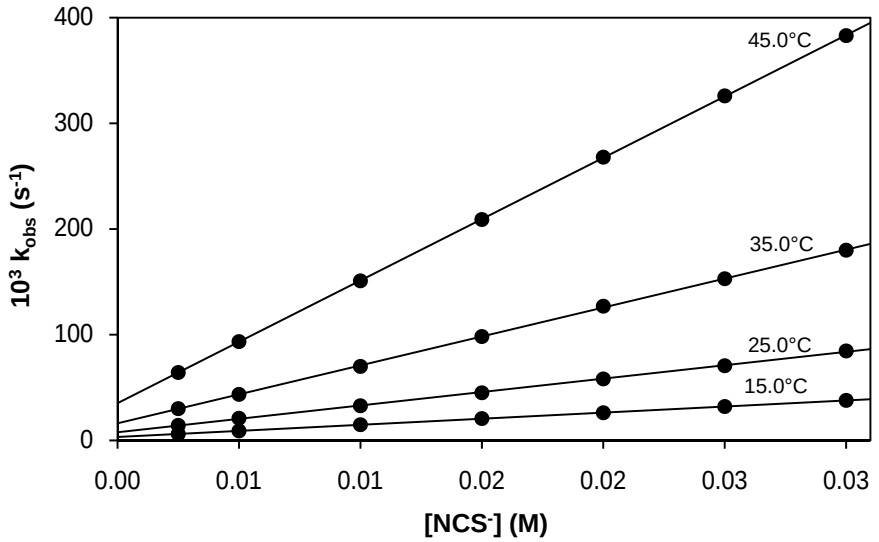


**Table 7.1: Summary of the kinetic data for the aqua substitution reaction between *fac*-[Re(Trop)$(CO)_3(H_2O)$] and $NCS^-$.**

| | 15.0 °C | 25.0 °C | 35.0 °C | 45.0 °C |
|---|---|---|---|---|
| $k_1$ ($M^{-1}s^{-1}$) | 1.152(4) | 2.54(3) | 5.48(3) | 11.61(2) |
| $k_{-1}$ ($s^{-1}$) | 0.00332(7) | 0.0077(5) | 0.0162(5) | 0.0353(3) |
| $K_1$ ($M^{-1}$) | 347(7) | 330(22) | 338(11) | 329(3) |

The activation parameters were calculated to provide more evidence of the type of mechanism for this reaction. Values for the standard activation enthalpy change ($\Delta H^{\ddagger}$) and the standard activation entropy change ($\Delta S^{\ddagger}$) were determined by using the logarithmic form of the Eyring equation (Equation 7.12).

$$\ln\left(\frac{k}{T}\right) = \ln\left(\frac{k_B}{h}\right) - \frac{\Delta H^{\ddagger}}{RT} + \frac{\Delta S^{\ddagger}}{R} \qquad \textbf{Equation 7.12}$$

By plotting $\ln\left(\frac{k}{T}\right)$ *vs* $\left(\frac{1}{T}\right)$, a straight line with slope $\left(-\frac{\Delta H^{\ddagger}}{RT}\right)$ and intercept $\left(\ln\left(\frac{k_B}{h}\right) + \frac{\Delta S^{\ddagger}}{R}\right)$ is obtained from which $\Delta H^{\ddagger}$ and $\Delta S^{\ddagger}$ could be obtained. In Equation 7.12, $K_B$ is the Boltzmann constant and h is Planck's constant.

The activation parameters for this aqua substitution reaction between *fac*-[Re(Trop)$(CO)_3(H_2O)$] and thiocyanate ions were calculated as 56.1(7) kJ $mol^{-1}$ and -49(2) J $K^{-1}$ $mol^{-1}$ for the standard change of enthalpy ($\Delta H^{\ddagger}$) and the standard change of entropy ($\Delta S^{\ddagger}$) respectively (Figure 7.5).

**Figure 7.5: Eyring plot for the reaction between *fac*-[Re(Trop)$(CO)_3(H_2O)$] and $NCS^-$ ions.**

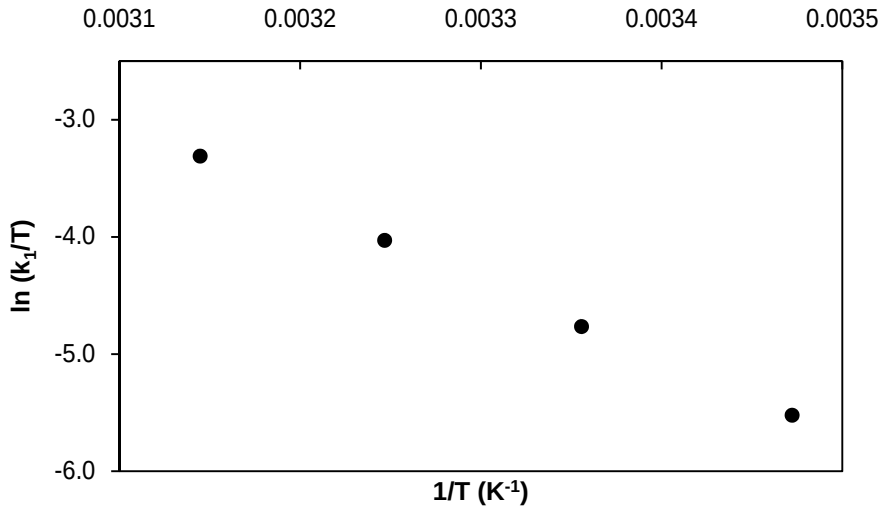


To further verify the proposed mechanism, the reaction of *fac*-[Re(Trop)$(CO)_3(H_2O)$] with $NCS^-$ ions were performed at various pH levels and at 25.0 °C and μ = 1 M ($NaClO_4$). The data obtained here was fitted simultaneously with the data obtained at pH 6.4 (T = 25.0 °C) and values for $k_1$, $k_{-1}$ and $pK_{a1}$ were obtained from least-squares linear fits to Equation 7.10 (Figure 7.6).

The $k_1$, $k_{-1}$ and $pK_{a1}$ values obtained, 2.64(4) $M^{-1}$ $s^{-1}$, 0.0063(9) $s^{-1}$ and 9.04(2) respectively, compare well to the data obtained before and we conclude that the $k_1/k_{-1}$ and $pK_{a1}$ pathway in Scheme 7.1 is a fair representation of the mechanism of the substitution reaction between *fac*-[Re(Trop)$(CO)_3(H_2O)$] and $NCS^-$ ions. A summary of the kinetic data is reported in Table 7.2.

**Figure 7.6: Plot of $k_{obs}$ *vs* pH for the reaction between *fac*-[Re(Trop)(CO)$_3$(H$_2$O)] and NCS$^-$ ions. [Re] = 5 x 10$^{-5}$ M, [NCS$^-$]= 3 x 10$^{-2}$ M, 260 nm, 25.0 °C, μ = 1.0 M (NaClO$_4$).**

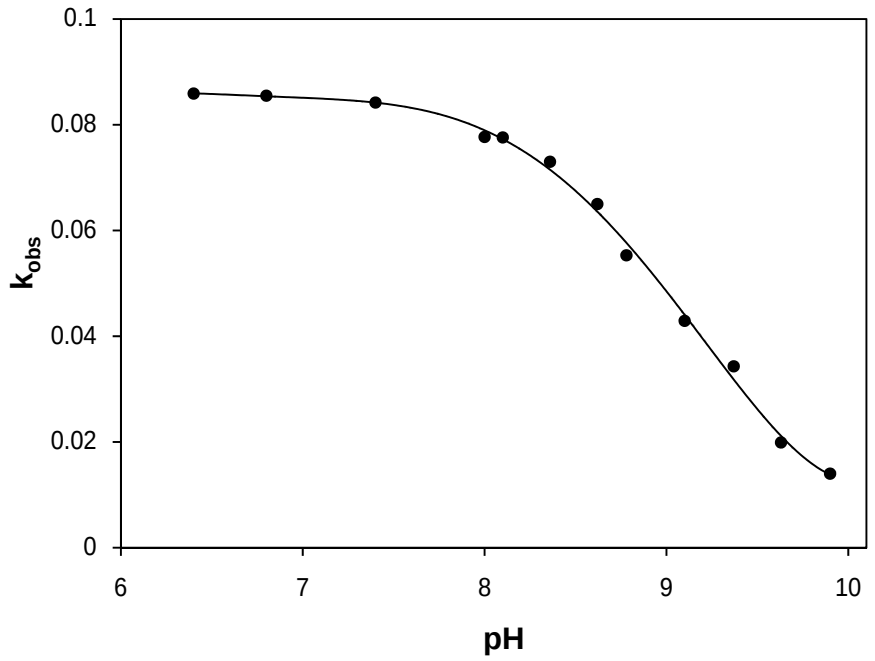


**Table 7.2: Rate constants and activation parameters for the reaction between *fac*-[Re(Trop)(CO)$_3$(H$_2$O)] and NCS$^-$ ions.**

| Constants | 15.0 °C | 25.0 °C[a] | 25.0 °C[b] | 35.0 °C | 45.0 °C |
|---|---|---|---|---|---|
| $k_1$ ($M^{-1}s^{-1}$) | 1.152(4) | 2.54(3) | 2.64(4) | 5.48(3) | 11.61(2) |
| $k_{-1}$ ($s^{-1}$) | 0.00332(7) | 0.0077(5) | 0.0063(9) | 0.0162(5) | 0.0353(3) |
| $K_1$ ($M^{-1}$) | 347(7) | 330(22) | | 338(11) | 329(3) |
| $\Delta H^{\ddagger}$ (kJ $mol^{-1}$) | | 56.1(7) | | | |
| $\Delta S^{\ddagger}$ (J $K^{-1}$ $mol^{-1}$) | | -49(2) | | | |
| $pK_{a1}$ | | 8.96(2) | 9.04(2) | | |

[a] calculated at pH 6.4 from Equation 7.11
[b] calculated from Equation 7.10

## 7.3.3 Discussion

One of the main aims for this project was to synthesize complexes that are water soluble and may be easily administered to patients if biolocially active and utilized as radiopharmaceuticals. Thus it was imperative that the water substitution reactions was performed and investigated.

*fac*-[Re(Trop)$(CO)_3(H_2O)$] is soluble and stable in water and in methanol. The substitution reactions between *fac*-[Re(Trop)$(CO)_3$(MeOH)] and $Br^-$, $I^-$. Py, Im, $NCS^-$, DMAP, TU and MeTU were performed in methanol, and are reported in Chapter 5.

To simplify the chemistry, thiocyanate ions ($NCS^-$) was chosen as the entering ligand since it does not form different species in solution in the pH range studied. This also affords the opportunity to compare the data obtained to the methanol substitution reaction. Thiocyanate is also found in blood plasma and is therefore a good representative biological ligand.

The summarized data in Table 7.3 show that the rate of the reaction in water is almost ten times faster than that of the reactions in methanol. Also, the stability constant is ~7 times larger for the reaction in aqueous medium. This is excellent results since this means that the aqua complex, *fac*-[Re(Trop)$(CO)_3(H_2O)$] is therefore more reactive and its product more stable than the methanol analogue. This might also indicate that the aqua complexes of this type will possibly have better potential during radiolabeling processes, expecially considering the '2+1' approach, with faster reactions and more stable products.

**Table 7.3: Summary of the kinetic data for the reaction between *fac*-[Re(Trop)$(CO)_3(H_2O)$] and *fac*-[Re(Trop)$(CO)_3$(MeOH)] and $NCS^-$ ions at 25.0 °C in different solvents.**

| | Solvent | $k_1$ ($M^{-1} s^{-1}$) | $k_{-1}$ ($s^{-1}$) | $K_1$ ($M^{-1}$) | $\Delta H^{\ddagger}_{(k1)}$ (kJ $mol^{-1}$) | $\Delta S^{\ddagger}_{(k1)}$ (J $K^{-1}$ $mol^{-1}$) |
|---|---|---|---|---|---|---|
| ***fac*-[Re(Trop)$(CO)_3$(MeOH)]** | MeOH | 0.268(2) | 0.0044(2) | 61(3) | 64(1) | -43(5) |
| ***fac*-[Re(Trop)$(CO)_3(H_2O)$]** | $H_2O$ | 2.54(3) | 0.0077(5) | 330(22) | 56.1(7) | -49(2) |

With the possibility for errors in the $\Delta S^{\ddagger}$ values, as discussed in Chapter 5 and 6, no real conclusion can be made regarding the mechanism. High pressure studies need to be

conducted to confirm or contradict the indication towards an associative type mechanism for the negative values found for this reaction.

A very good correlation is found between the thermodynamically determined $pK_{a1}$ value of 8.96(2) and the kinetically determined $pK_{a1}$ value of 9.04(2).

This was the first substitution kinetic study in aqueous medium reported on *fac*-[Re(L,L'-bid)$(CO)_3(H_2O)]^n$ type complexes. The incredible reactivity of *fac*-[Re(Trop)$(CO)_3(H_2O)$] and the high stability of the product, *fac*-[$NEt_4$][Re(Trop)$(CO)_3$(NCS)], definitely indicate good prospects for the '2+1' approach in compounds of this type. These novel results should fuel young scientists to further investigate the aqueous kinetics of these types of complexes for the application in nuclear medicine.

# 8 $^{99m}$Tc IN RADIOPHARMACY AND *IN VITRO* CANCER SCREENING REPORT

## 8.1 Background of $^{99m}$Tc radiopharmaceuticals

The availability of $^{99m}$Tc radiopharmaceuticals is one of the main reasons for the worldwide growth in nuclear medicine. The $^{99m}$Tc isotope is used in over 80% of imaging procedures and it is estimated that about 25 million procedures per year are carried out with $^{99m}$Tc radiopharmaceuticals. It is anticipated that this will increase with 15% every year.[1] The short lived isotope, $^{99m}$Tc with a half life of 6 hours, is readily available from a $^{99}$Mo/$^{99m}$Tc generator. The Brookhaven National Laboratory in the USA developed the generator in the early 1960's, and since then the search for potential $^{99m}$Tc radiopharmaceuticals as been a continuous research field.[2]

One of the major advantages of $^{99m}$Tc in radiopharmaceutical development is its multiple oxidation states. This ensures a versatile chemistry with the possibility to produce a wide variety of compounds with different characteristics, which can be tuned as required.

First generation $^{99m}$Tc radiopharmaceuticals was developed by considering only the absorption, distribution, metabolism and excretion properties of these simple $^{99m}$Tc complexes. Agents for the thyroid ($^{99m}TcO_4^-$), liver ($^{99m}$Tc colloids), bone ($^{99m}$Tc phosphonates) and kidney ($^{99m}$TcDTPA) were developed by these studies.[3,4] After that, the second generation $^{99m}$Tc radiopharmaceuticals, with more careful design of ligands and the complexes, led to the imaging agents for perfusion in the myocardium and the brain. $^{99m}$Tc-MIBI, $^{99m}$Tc-tetrofosmin, $^{99m}$Tc-HMPAO, $^{99m}$Tc-ECD, $^{99m}$Tc-MAG and $^{99m}$Tc-mebrofenin were developed by the above strategy and its *in vivo* behaviour is

[1] Cancer Research UK, http://info.cancerresearchuk.org
[2] Richards, P. Trans. 5th Nucl. Cong., 7th Int. Electr. Nucl. Symp., Rome, **1960**.
[3] Srivastava, S.C., Richards, P. *Radiotracers for Medical Applications* (Rayudu, G.V.S., Ed.), CRC Press Inc., Boca Raton, FL, **1983**, 107-185.
[4] Schwochau, K. *Angew. Chem. Int. Ed. Engl*. **1994**, *33*, 2258-2267.

driven by the agent's size, charge, lipophilicity etc.[5,6,7] Currently, the design of potential radiopharmaceuticals is based on suitable biomolecules that can function as effective vehicles for *in vivo* delivery of the radioactivity to receptors or transporters. It is imperative not to distort the part of the biomolecule responsible for its biologicial activity when introducing the radionuclide in the biomolecule. The bifunctional chelating agent strategy and mixed ligand approach are only two of the newest labeling processes. Two examples of this third generation $^{99m}$Tc radiopharmaceuticals are $^{99m}$Tc-HYNIC-TOC and $^{99m}$Tc-TRODAT-1.

## 8.2 Future of $^{99m}$Tc-radiopharmaceuticals

It is known that positron emission tomography/computed tomography (PET/CT) images are the superior choice for diagnostic use compared to the single photon emission computed tomography (SPECT) images, but it comes with a significant financial impact. With the current improvement in technology, the resolution of SPECT images is almost comparable to that of PET. The most desirable isotope for SPECT is $^{99m}$Tc, due to its favourable properties ($t_{1/2}$ = 6h, 100 % γ-rays, 142 keV) and availability form a $^{99}$Mo/$^{99m}$Tc generator. With the introduction of SPECT/CT, as well as the availability and price of $^{99m}$Tc and the SPECT/CT that can almost provide the same level of functional and anatomical information as PET/CT, there is a tremendous potential for $^{99m}$Tc radiopharmaceuticals.

Nowadays the kits for the formulation of $^{99m}$Tc radiopharmaceuticals are freeze-dried and only contains the ligand to which $^{99m}$Tc is to be complexed, the reducing agent, a buffer, stabilizing agents and the 'vehicles' to deliver the radioactivity. The $^{99m}$Tc pertechnetate can then be eluted from the generator and added to the kit.

The novel $^{99m}$Tc chemistry, many researchers are exploring currently involves the labeling of receptor ligands, metabolic agents, peptides, proteins, antibodies and antibiotics but to such an extent that these biomolecules retain their biochemical properties as well as physiological activities. This is mainly achieved by keeping the

[5] Deutsch, E.A., Libson, K., Jurisson, S. Progress in Inorganic Chemistry (Lippard, S.J., Ed.), John Wiley & Sons, New York, **1983**, 75-139.
[6] Nunn, A.D., Loberg, M.D., Conley, R.A. *J. Nucl. Med*. **1983**, *24*, 423-430.
[7] Bannerjee, S., Pillai, M.R.A., Ramamoorthy, N. *Semin. Nucl. Med*. **2001**, *31*, 260-277.

metal core as far away as possible from the biomolecule. According to researchers, the three most important methods to be considered for this labeling are Nitrido-, HYNIC- and tricarbonyl labeling.

## 8.2.1 Nitrido labeling

Research showed that by replacing the oxo-oxygen atom in technetium complexes by a nitrido group results in a core with higher stability as well as a core that is more compact.[8] One of the first nitrido technetium complexes reported was neutral lipophilic NOET (technetium-nitrido-N-ethyl-N-ethoxydithiocarbamate).[9] These type of complexes showed good promise with for example in myocardial uptake and brain studies.[10,11,12]

## 8.2.2 HYNIC labeling

The bifunctional chelating agent, hydrazinonicotinamide (HYNIC), was introduced by Callahan *et al*.[13] and it serves as 'bridge' between the biomolecule and the $^{99m}$Tc metal core. The HYNIC conjugated compounds react as monodentate ligands with coligands such as tricine or EDDA (ethylene-diaminediacetic aci) and there are many examples of this type of labeled compounds including the reported $^{99m}$Tc-EDDA-HYNIC-TOC[14,15] (expressing somatostatin receptors). HYNIC allows the labeling of specific proteins, and agents for imaging infection and inflammation.[16,17,18,19,20,21]

---

[8] Baldas, J., Bonnyman, J. *Int. J. App. Radiat. Isot*. **1985**, *36*, 919-923.
[9] Pasqualini, R., Duatti, A., Bellande, E., Comazzi, V., Brucato, V., Hoffschir, D., Fagret, D., Comet, M. *J. Nucl. Med*. **1994**, *35*, 334-341.
[10] Ghezzi, C., Fagret, D., Arvieux, C.C., Mathieu, J.-P., Bontron, R., Pasqualini, R., de Leiris, J., Comet, M. *J. Nucl. Med*. **1995**, *36*, 1069-1077.
[11] Johnson, G., Nguyen, K.N., Pasqualini, R., Okada, R.D. *J. Nucl. Med.* **1997**, *38*, 138-143.
[12] Bellande, E., Comazzi, V., Laine, J., Lecayon, M., Pasqualini, R., Duatti, A., Hoffschir, D. *Nucl. Med. Biol*. **1995**, *22*, 315-320.
[13] Callahan, R.J., Barrow, S.A., Abrams, M.J., Rubin, R.H., Fishman, A.J. *J. Nucl. Med*. **1996**, *37*, 843-846.
[14] Decristoforo, C., Mather, S.J., Cholewinski, W., Donnemiller, E., Riccabona, G., Moncayo, R. *Eur. J. Nucl. Med*. **2000**, *27*, 1318-1325.
[15] Plachcinska, A., Mikolajczak, R., Maecke, H.R., Mlodkowska, E., Kunert-Radek, J., Michalski, A., Rzeszutek, K., Kozak, J., Kusimierek, J. *Eur. J. Nucl. Mol. Imaging* **2003**, *30*, 1402-1406.
[16] Welling, M.M., Mongera, S., Lupetti, A., Balter, H.S., Bonetto, V., Mazzi, U., Pauwels, E.K.J., Nibbering, P.H. *Nucl. Med. Biol*. **2002**, *29*, 413-422.
[17] Rennen, H.J., Boerman, O.C., Oyen, W.J., Corstens, F.H. *J. Nucl. Med*. **2003**, *44*, 1502-1509.
[18] Liu, S., Harris, A.R., Williams, N.E., Edwards, D.S. *Bioconjug. Chem*. **2002**, *13*, 881-886.
[19] Edwards, D.S., Liu, S., Ziegler, M.C., Harris, A.R., Crocker, A.C., Heminqay, S.J., Barrett, J.A. *Bioconjug. Chem*. **1999**, *10*, 884-891.

### 8.2.3 Tricarbonyl labeling

In 1993, the use of organometallic carbonyl compounds was proposed in technetium chemistry and ever since 1998 when Alberto *et al*. unravelled the aqueous synthesis of the *fac*-$[Tc(CO)_3(H_2O)_3]^+$ precursor, the research towards tricarbonyl chemistry expanded.[22] Labeling with $^{99m}$Tc tricarbonyl has been accomplished with somatostatin- and bombesin derivatives, neurotensin pseudopeptides, isonitriles and even glucose, to name a few.[23,24,25,26,27]

## 8.3 Rhenium as analogue for $^{99m}$Tc

$^{99m}$Technetium is a chemical congener of Rhenium, and ever since the focus on $^{99m}$Tc in nuclear medicine increased, the chemistry on Rhenium gained a lot of importance in the nuclear medicine field. The chemistry of $^{99m}$Tc and $^{186/188}$Re are similar and sometimes even identical.[28,29] If the chemistry of a specific radiopharmaceutical are identical for the two elements, it can be used in combination with each other, with the $^{99m}$Tc compound used for the imaging and the $^{186/188}$Re compound used in the treatment of the site. There are a few methods known for the production of bioactive $^{188}$Re labeled monoclonal antibodies, which showed promising yields and stability and much faster clearance from the blood compared to $^{131}$I and $^{88}$Y labeled monoclonal antibodies.[29,30,31,32]

---

[20] Greenland, W.E., Howland, K., Hardy, J., Fogelman, I., Blower, P.J. *J. Med. Chem*. **2003**, *46*, 1751-1757.
[21] Zhang, Y.-M., Liu, C.-B., Liu, N., Flores, G.F., He, J., Ruschowski, M., Hnatowich, D.J. *Mol. Imaging Biol*. **2003**, *5*, 240-247.
[22] Alberto, R., Schibli, R., Egli, A., Schubiger, P.A. *J. Am. Chem. Soc*. **1998**, *120*, 7987-7988.
[23] Marmion, M.E., Bugaj, J.E., Schmidt, M.A., Srinivasan, A. *J. Nucl. Med*. **2000**, *41*, 40.
[24] La Bella, R., Garcia-Garayoa, E., Bähler, M., Bläuenstein, P., Schibli, R., Conrath, P., Tourwé, D., Schubiger, P.A. *Bioconjug. Chem*. **2002**, *13*, 599-604.
[25] Garcia-Garayoa, E., Bläuenstein, P., Bruehlmeier, M., Blanc, A., Iterbeke, K., Conrath, P., Tourwé, D., Schubiger, P.A. *J. Nucl. Med*. **2002**, *43*, 374-383.
[26] Marmion, M.E., MacDonald, J.R. *J. Nucl. Med.* **2000**, *41*, 124.
[27] Petrig, J., Schibli, R., Dumas, C., Alberto, R., Schubiger, P.A. *Chem*. **2001**, *7*, 1868-1873.
[28] Mausner, L.F., Srivastava, S.C. *Med. Phys*. **1993**, *20*, 503-509.
[29] Griffiths, G.L. *Cancer Therapy with Radiolabeled Antibodies* **1995**, 47.
[30] Breitz, H., Ratliff, B., Schroff, R., Vanderheyden, J.-L., Fritzberg, A.R., Appelbaum, J., Fisher, D.R., Abrams, P., Weiden, P. *J. Nucl. Med.* **1990**, *31*, 725-731.
[31] Griffiths, G.L. CRC Press, Inc.: Boca Raton, FL, **1995**, 77.
[32] Griffiths, G.L., Goldenberg, D.M., Knapp, F.F., Callahan, A.P., Chang, C.-H., Hansen, H.J. *Cancer Res*. **1991**, *51*, 4594-4602.

Having similar chemistry's but being non-radioactive, 'cold' Rhenium is a good model for Technetium and can be used to optimize the cold chemistry and perform the standard characterization techniques. It is used as a surrogate for the Technetium metal, that only exists as radioactive isotopes. Alberto *et al*. developed the facile method of labeling a variety of biomolecule conjugates with Re and $^{99m}$Tc from the *fac*-$[M(CO)_3(H_2O)_3]^+$ precursor.[33,34,35] These tricarbonyl complexes seem to be a promising approach to developing high specific activity and site-specific radiopharmaceuticals. The most promising characteristic of these carbonyl precursors is the high stability of the three facial carbonyl ligands, due to the M(I) metal ion's $d^6$ electronic configuration in the octahedral field, in conjunction with the high lability of the three coordinated aqua ligands towards substitution by entering ligands.[33,35]

# 8.4 *In vitro* cancer screening report for some Re(I) compounds

## 8.4.1 Assay background and method

A Sulforhodamine B (SRB) assay was used to test the growth inhibitory effects of several compounds in the 3-line panel consisting of renal (TK10), melanoma (UACC62) and breast (MCF7) cancer cells. The SRB assay was developed by Skehan *et al*.[36] in 1990 to essentially measure the drug-induced cytotoxicity and cell proliferation. The assay is based on the ability of sulforhodamine, the protein dye Acid Red 52, to bind electrostatically in a pH-dependent manner, to basic amino acid residues of trichloroacetic acid-fixed cells. It binds to the fixed cellular protein under mild acidic conditions and under mild basic conditions it can be extracted from the cells for measurement.

[33] Alberto, R., Schibli, R., Waibel, R., Abram, U., Schubiger, P.A. *Coord. Chem. Rev*. **1999**, *190*, 901-919.
[34] Alberto, R., Schibi, R., Schubiger, P.A., Abram, U., Hubener, R., Berke, H., Kaden, T.A. *Chem. Commun*. **1996**, 1291-1292.
[35] Egli, A., Hegetschweiler, K., Alberto, R., Abram, U., Schibli, R., Hedeinger, R., Gramlich, V., Kissner, R., Schubiger, P.A. *Organometallics* **1997**, *16*, 1833-1840.
[36] Skehan, P., Storeng, R., Scudiero, D., Monks, A., McMahon, J., Vistica, D., Warren, J.T., Bokesch, H., Kenney, S., Boyd, M.R. *J. Natl. Cancer. Inst*. **1990**, *82*, 1107-1112.

The SRB Assay performed on the compounds reported in this thesis is performed at CSIR in accordance with the protocol of the Drug Evaluation Branch, NCI (National Cancer Institute). The 3-cell line panel that were used is recommended by the NCI for preliminary screening.

The three human cell lines used in this study, TK10, UACC62 and MCF7 were obtained by the CSIR from NCI in the framework of a collaborative research program. The cell lines were routinely maintained as monoloyer cell cultures in RPMI, consisting of 5% heat activated fetal bovine serum, 2 mM L-glutamine and 50 µg/ml gentamicin at 37 °C in a humidified atmosphere containing 5% $CO_2$.

For the screening experiments, the cells were inoculated in 96-well microtiter plates at plating densities of 7-10 000 cells per well and were incubated for 24 hours. One of the plates was fixed with trichloroacetic cid after 24 hours to represent a measurement of the cell population for each cell line at the time of drug addition, $T_0$. The other plates were treated with the Rhenium(I) compounds as well as some ligand systems, reported in Paragraph 8.4.2 below.

The compounds were dissolved in DMSO as 10 mM stock solutions and diluted in medium to a final concentration of 10 µM. Blank wells contained complete medium without cells while cells without compounds served as controls. Emetine was used as a reference standard.

After addition of the compounds, the plates were incubated for 48 hours. The cells were fixed to the bottom of each well with cold 50% trichloroactic acid after 48 hours, washed, dried and dyed with SRB. The unbound dye was removed and the protein-bound dye was extracted with 10 mM Tris base for optical density determination at 540 nm using a multiwall spectrophotometer. The net percentage cell growth was calculated by optical density measurements. The percentage cell growth is calculated as follows:

$[(T_i - T_0)/(C - T_0)] \times 100$ – for concentrations where $T_i \geq T_0$

and

$[(T_i - T_0)/T_0] \times 100$ – for concentration where $T_i < T_0$

with $T_i$ = the optical density of the test wells after 48 hours of exposure to test compound, $T_0$ = the optical density at time zero and C = the optical density of the control (the untreated cells).

## 8.4.2 Results

The results are summarized in Table 8.1. The test compound concentration as well as the standard (Emetine) concentration, was 10 μM in every case. The percentage cell growth (% growth) is the net growth of the cells in the treated wells compared to the untreated controls over the 48 hour period. Therefore, 100% growth means there are the same amount of cells in the treated wells as in the untreated control wells, 0% growth means that the treated wells contain the same number of cells as was present at the start of the incubation, at time 0 meaning there was no increase in cell number. A -100% growth will mean there are no cells left in the after the 48 hour period.

**Table 8.1: Summary of SRB assay results.**

| Compound | % Growth TK10 | % Growth UACC62 | % Growth MCF7 |
|---|---|---|---|
| ***fac*-[$NEt_4$][Re(Isa)$(CO)_3$Br]** | 95.75(3) | 96.91(2) | 94.84(2) |
| ***fac*-[Re(Isa)$(CO)_3(H_2O)$]** | 100.09(2) | 97.86(7) | 94.83(0) |
| ***fac*-[$NEt_4$][Re(($F_3$CO)Isa)$(CO)_3$Br]** | 91.58(4) | 73.82(2) | 78.14(4) |
| ***fac*-[Re(($F_3$CO)Isa)$(CO)_3(H_2O)$]** | 98.15(4) | 83.28(0) | 96.40(6) |
| ***fac*-[Re(PMAPent)$(CO)_3$]** | 95.7(10 | 98.85(4) | 93.87(5) |
| ***fac*-[Re(2,4-PicoH)$(CO)_3(H_2O)$][a]** | 98.29(3) | 103.10(1) | 95.70(1) |
| ***fac*-[Re(2,5-PicoH)$(CO)_3(H_2O)$]** | 92.79(4) | 87.79(3) | 93.72(0) |
| ***fac*-[Re(Trop)$(CO)_3(H_2O)$]** | 50.46(9) | 38.01(7) | 43.52(7) |
| ***fac*-[Re(2,4-QuinH)$(CO)_3(H_2O)$]** | 98.87(3) | 94.51(8) | 93.49(0) |
| ***fac*-[Re(DMe-ox)$(CO)_3(H_2O)$]** | 66.34(8) | 52.02(3) | 69.06(3) |

[a] Schutte *et al*.[37]

Isa = isatin; ($F_3$CO)Isa = 5-(trifluoromethoxy)isatin; PMAPent = 2-(Bis-(2-pyridylmethyl)-amino)-pentanol; 2,4-PicoH = pyridine-2-carboxylato-4-carboxylic acid; 2,5-PicoH = pyridine-2-carboxylato-5-carboxylic acid; Trop = tropolonato; 2,4-QuinH = quinoline-2-carboxylato-4-carboxylic acid; DMe-ox = 5,7-dimethyl-8-hydroxyquinolinato.

[37] Schutte, M., Kemp, G., Visser, H.G., Roodt, A. *Inorg. Chem*. **2011**, *50(24)*, 12486-12498.

None of the samples resulted in a ≤ 0 cell growth percentage; not in any of the three cell lines. Therefore none of the compounds are regarded as biologically active. The $IC_{50}$ determinations and the compounds' toxicity against normal cell cultures were not tested in this assay and will be performed once a compound is regarded as active.

The $IC_{50}$ value, according the the FDA, represents the concentration of a drug that is required for 50% inhibition *in vitro*. $IC_{50}$ values for four compounds were determined, using HeLa cells, human adenocarcinoma of the cervix, with an incubation period of seven days. Four experiments per compound were done. The results are reported in Table 8.2. In a broad sence, $IC_{50}$ values can be used to classify a drug in a series with a high ($IC_{50}$ < 1μM), moderate (1 μM < $IC_{50}$ < 10 μM) and low ($IC_{50}$ > 10 μM) potential for drug-drug interaction. None of these compounds showed very good results with very high $IC_{50}$ values, with *fac*-[Re(Flav)$(CO)_3$$(H_2O)$] the most active between the four compounds.

**Table 8.2: $IC_{50}$ values for selected compounds on HeLa cells.**

| Compound | $IC_{50}$ (μM) | Standard error of mean |
|---|---|---|
| Benzohydroxamic acid | 31.132 | 7.628 |
| *fac*-[$NEt_4$][Re(BHA)$(CO)_3$(Br)] | > 50 | |
| *fac*-[Re(Flav)$(CO)_3$$(H_2O)$] | 11.186 | 0.918 |
| *fac*-[$NEt_4$][Re(Trop$Br_3$)$(CO)_3$(Br)] | > 50 | |

BHA = benzohydroxamato, Flav = 3-hydroxyflavonato, Trop$Br_3$ = tribromotropolonato

# 8.5 Conclusion

The results for these bidentate ligand backbones tested, as well as the organic ligand systems, do not look promising for potential therapeutic application since none of the compounds were found to biologically active. This is not necessarily bad news. It might seem disappointing if the compounds that were investigated were designed for therapy, but it was designed for imaging. For diagnostic purposes, toxic compounds are not very favourable since additional assessments must be performed prior to eventual application. Also, there is still the possibility to 'link' a radioactive nuclide to these compounds *via* a linker on the backbone, to essentially be used as a potential imaging agent.

## Chapter 8

Basically up until now, most clinical tests performed on Rhenium and Technetium compounds have been disappointing for newly developed potential radiopharmaceuticals. These radiopharmaceuticals have been tested on patients that mainly have a poor prognosis. For a better and much more realistic assessment of the application of these radioimmunoconjugates, it must be applied to patients with a better prognosis.

It is imperative for scientists to stay enthusiastic and to encourage young scientists about the potential and possibilities for Rhenium and Technetium in radioimmunoconjugates, with improvements on the design and modifications.[38,39]

There is no doubt as to the potential for Rhenium in the application of therapeutic agents and Technetium in imaging agents.[40,41,42,43] There is enough evidence of the possibilities for these radionuclides and the application thereof, the full potential of these metal centres still has to be realized.[30,44,45,46]

[38] Yang, D.J., Ford, R.J., Mendez, R., Zhang, Y.-H., Bryant, J., Oh, C.-S., Huang, J., Pham, L., Kohanim, S., Kim, E.E. *Cancer Res*. **2011**, *71*, Supl. 1, Abstract 306.
[39] Ghosh, D.B., O'Brien, A.R., Beck, D.J., Davidson, T., Keshtgar, M. *Cancer Res*. **2010**, *70*, Supl. 2, Abstract P1-01-25.
[40] Lyer, A.K., Lan, X., Zhu, X., Su, Y., Feng, J., Zhang, X., Gao, D., Seo, Y., VanBrocklin, H.F., Broaddus, V.C., Liu, B., He, J. *Cancer Res*. **2011**, *71*, 2428-2432.
[41] Zahnd, C., Kawe, M., Stumpp, M.T., de Pasquale, C., Tamaskovic, R., Nagy-Davidescu, G., Dreier, B., Schibli, R., Binz, H.K., Waibel, R., Plückthun, A. *Cancer Res*. **2010**, *70*, 1595-1605.
[42] Dwyer, R.M., Ryan, J., Havelin, R., Morris, J.C., O'Flatharta, C., Miller, B., Liu, Z., Foley, M., Barrett, H.H., Murphy, M., Barry, F.P., O'Brien, T., Kerin, M.J. *Cancer Res*. **2011**, *71*, Supl. 1, Abstract 5392.
[43] Cope, F.O., Metz, W.R., Blackburn, S., Abbruzzese, B., Orahood, R. *Cancer Res*. **2011**, *71*, Supl. 1, Abstract 5231.
[44] Visser, G.W.M., Gerretson, M., Herscheid, J.D.M., Snow, G.B., van Dongen, G. *J. Nucl. Med*. **1993**, *34*, 1953-1963.
[45] Breitz, H., Fisher, D.R., Wessels, B.W. *J. Nucl. Med.* **1998**, *39*, 1746-1751.
[46] Gerretsen, M., Visser, G.W.M., van Walsum, M., Meijer, C.J.L.M., Snow, G.B., van Dongen, G.A.M.S. *Cancer Res*. **1993**, *53*, 3524-3529.

# 9 CRITICAL EVALUATION OF THE STUDY

## 9.1 Results obtained

One of the main aims of the study was to investigate the substitution kinetics of *fac*-Re(I) tricarbonyl complexes. This study also expanded the current available knowledge of these systems.

Four novel ligand systems were synthesized successfully. Another five ligands were synthesized by 'linking' a biomolecule to a bidentate or tridentate ligand. All these ligands were fully characterized and were sent for *in vitro* screening. Some of the results are reported in Chapter 8, while the rest of the results were not yet known at the end of this study.

The synthesis of several Re(I) complexes of the type *fac*-[Re(L,L'-bid)$(CO)_3(H_2O)]^n$ and *fac*-[Re(L,L'-tri)$(CO)_3]^n$ (L,L'-bid = different bidentate ligands, L,L'-tri = different tridentate ligands, n = 0, +1) was successful and the complexes were fully characterized.

Some *fac*-[$^{99m}$Tc(L,L'-bid)$(CO)_3(H_2O)]^n$ type complexes were successfully synthesized, while the synthesis of both the *fac*-[$^{99m}$Tc(L,L'-tri)$(CO)_3]^n$ type complexes were unsuccessful). The synthesis of *fac*-[$^{99m}$Tc(2,5-PicoH)$(CO)_3(H_2O)]$, *fac*-[$^{99m}$Tc(Trop)$(CO)_3(H_2O)]$, *fac*-[$^{99m}$Tc(Cl-ox)$(CO)_3(H_2O)]$ and *fac*-[$^{99m}$Tc(DMe-ox)$(CO)_3(H_2O)]$ were successful (2,5-PicoH = pyridine-2-carboxylato-5-carboxylic acid, Trop = tropolonato, Cl-ox = 5-chloro-8-hydroxyquinolinato and DMe-ox = 5,7-dimethyl-8-hydroxyquinolinato). The $^{99m}$Tc complexes with isatin, 2,2'-bipyridine-3,3'-dicarboxylic acid, benzohydroxamic acid, bis(diphenylphosphino)-propylamine and N,N'-bis(2-pyridylmethyl)-2-aminoethanol used as ligand systems, was unsuccessful even though the Rhenium analogues were successfully synthesized. The crystal structures of three of these Rhenium analogues, of which the $^{99m}$Tc compounds could not be isolated, are reported in Paragraph 4.9, 4.11 and 4.12.

A few water soluble products were synthesized successfully, of which one complex was used in the aqueous kinetic study. Some of these water soluble complexes include *fac*-[Re(Trop)$(CO)_3(H_2O)$] (Trop = tropolonato), *fac*-[Re(Chrys)$(CO)_3(H_2O)$] (Chrys = chrysine), *fac*-[Re(Isa)$(CO)_3(H_2O)$] (Isa = isatin), *fac*-[Re($NO_2$Isa)$(CO)_3(H_2O)$] ($NO_2$Isa = 5-nitroisatin), *fac*-[Re($F_3$COIsa)$(CO)_3(H_2O)$] ($F_3$COIsa = 5-(trifluoromethoxy)isatin), *fac*-[Re(ox)$(CO)_3(H_2O)$] (ox = 8-hydroxyquinolinato), *fac*-[Re(Cl-ox)$(CO)_3(H_2O)$] (Cl-ox = 5-chloro-8-hydroyquinolinato) and *fac*-[Re(DMe-ox)$(CO)_3(H_2O)$] (DMe-ox = 5,7-dimethyl-8-hydroxyquinolinato).

One of the water soluble complexes, *fac*-[Re(Trop)$(CO)_3(H_2O)$] was used in the kinetic study in aqueous medium. The aqua substitution reaction between *fac*-[Re(Trop)$(CO)_3(H_2O)$] and thiocyanate ions were investigated and evaluated. The incredible reactivity of *fac*-[Re(Trop)$(CO)_3(H_2O)$] and the stability of the product *fac*-[$NEt_4$][Re(Trop)$(CO)_3$(NCS)], indicate good prospects for future studies, especially for the '2+1' approach of these type of complexes.

A range of complexes of the type *fac*-[Re(L,L'-bid)$(CO)_3(H_2O)$] was synthesized and after dissolution in methanol it was assumed to be the methanol complexes, *fac*-[Re(L,L'-bid)$(CO)_3$(MeOH)].[1,2] The methanol substitution reactions of *fac*-[Re(Trop)$(CO)_3$(MeOH)] (Trop = tropolonato), *fac*-[Re(2,5-PicoH)$(CO)_3$(MeOH)] (2,5-PicoH = pyridine-2-carboxylato-5-carboylic acid) and *fac*-[Re(Isa)$(CO)_3$(MeOH)] (Isa = isatin) with various incoming ligands were studied. The incoming ligands used were bromide ions ($Br^-$), iodide ions ($I^-$), pyridine (Py), imidazole (Im), 4-dimethylaminopyridine (DMAP), thiocyanate ions ($NCS^-$), thiourea (TU), 1-methyl-2-thiourea (MeTU). Excellent results were obtained and the available kinetic data for these type of complexes was significantly expanded. The available knowledge on the methanol and especially the aqua substitution kinetics of Re(I) complexes have been increased to a great extent and should be of good assistance in future studies

High pressure studies on *fac*-[Re(Trop)$(CO)_3$(MeOH)] was performed studying the methanol substitution with various incoming ligands, including imidazole, pyridine, thiourea and 1-methyl-2-thiourea. For all the reactions evaluated, negative $\Delta S^{\ddagger}$ values

[1] Schutte, M., Kemp, G., Visser, H.G., Roodt, A. *Inorg. Chem*. **2011**, *50(24)*, 12486-12498.
[2] Brink, A., Visser, H.G., Roodt, A. *J. Coord. Chem*. **2011**, *64*, 122-133.

were obtained whereas the $\Delta V^{\ddagger}$ values indicates an $I_d$ mechanism. The fact that all four reaction rates decreased as the pressure was increased, clearly indicated a dissociative type mechanism. More high-pressure studies need to be done to broaden the data available for complexes of the form *fac*-[Re(L,L'-bid)$(CO)_3(X)]^n$. Only then will it be possible to compare the effect of the bidentate ligand (L,L'-bid) on the rate of the reaction with the variety of entering ligands.

All the initial aims of this study have been met to a large extent. The fact that the final products in these kinetic studies could be isolated and characterized assisted in verifying the mechanism of the substitution and should be expanded in future. An interesting observation was made by comparing the IR data and the kinetic data of the complexes. A decrease in $\nu_{CO}$ stretching frequencies are observed in the order *fac*-[Re(2,5-PicoH)$(CO)_3(H_2O)$] > *fac*-[Re(Isa)$(CO)_3(H_2O)$] > *fac*-[Re(Trop)$(CO)_3(H_2O)$]. This can be explained by the increase in electron density on the Re(I) metal core from 2,5-PicoH to Trop, therefore increasing the C=O backbonding. This also gives an indication of the Re-$H_2O$/Re-MeOH bond strength. A good correlation is seen with an increase in $k_1$ values from *fac*-[Re(2,5-PicoH)$(CO)_3$(MeOH)] > *fac*-[Re(Isa)$(CO)_3$(MeOH)] > *fac*-[Re(Trop)$(CO)_3$(MeOH)]. This also indicates that the rates of the substitution are dependent on the entering ligand.

## 9.2 Future research

The kinetic evaluation of some more water soluble complexes is of future importance. Since most labeling kits are in saline solution, the aqueous kinetics of these type of complexes is imperative in order to truly understand the mechanism and chemistry of these complexes. Ideally, after some intensive studies, it will be possible to predict the reactivity of complexes as well as the time necessary to completely react as well as the stability. This will help to a great extent in the evaluation of these types of compounds in nuclear medicine. More high pressure studies should be attempted, because this is the only way to unambiguously determine the mechanism of a reaction.

Another aim for future studies is the synthesis and isolation of complexes of the form *fac*-[Re$(CO)_3(H_2O)_2$L] with L = various monodentate ligands. This might not be easy to accomplish, but it would provide very interesting scope for future studies.

## Chapter 9

A significant result from this study is considered to be the isolation and characterization of the *fac*-[Re(Trop)$(CO)_3(H_2O)$] complex, with the biologically active moiety, tropolone, introduced close to the metal centre. Also, a significant activation of the coordinated aqua ligand in the substitution kinetics as well as the methanol substitution is observed. The aqueous kinetics of *fac*-[Re(Trop)$(CO)_3(H_2O)$] is a first in this type of complexes and this gives scope for its application in the medical field and also for similar structures. More research towards the reactivity of *fac*-[Re(L,L'-bid)$(CO)_3(H_2O)$] type complexes in aqueous medium will be pursued since this is imperative for the use of these compounds in nuclear medicine.

# Appendix

# APPENDIX A

**Table A.1: Atomic coordinates (x $10^4$) and equivalent isotropic displacement parameters ($Å^2$ x $10^3$) for *fac*-[$NEt_4$][$Re(Trop)(CO)_3(Br)$] (1). U(eq) is defined as one third of the trace of the orthogonalized $U^{ij}$ tensor.**

| | x | y | z | U(eq) |
|---|---|---|---|---|
| C(1) | 8439(4) | 5302(5) | 5663(3) | 18(1) |
| C(2) | 9102(4) | 7076(5) | 4752(3) | 20(1) |
| C(11) | 5498(4) | 5523(4) | 3763(3) | 15(1) |
| C(12) | 5849(4) | 6462(4) | 3215(3) | 15(1) |
| C(13) | 5209(4) | 6930(5) | 2455(3) | 20(1) |
| C(14) | 4145(4) | 6621(6) | 2027(3) | 27(1) |
| C(15) | 3397(4) | 5777(6) | 2239(3) | 31(1) |
| C(16) | 3543(4) | 5036(6) | 2965(3) | 25(1) |
| C(17) | 4455(4) | 4958(5) | 3636(3) | 21(1) |
| C(21) | 5919(4) | 54(5) | 3394(3) | 21(1) |
| C(22) | 4687(4) | 6(6) | 3370(3) | 25(1) |
| C(23) | 7703(4) | 1180(5) | 3677(3) | 21(1) |
| C(24) | 8381(5) | 97(6) | 4099(4) | 29(1) |
| C(25) | 6461(4) | 1209(5) | 4744(3) | 21(1) |
| C(26) | 7123(5) | 2234(6) | 5273(3) | 30(1) |
| C(27) | 5946(4) | 2388(5) | 3406(3) | 22(1) |
| C(28) | 5810(5) | 2483(5) | 2445(3) | 26(1) |
| N(1) | 6509(3) | 1205(4) | 3806(3) | 18(1) |
| O(1) | 8829(3) | 4790(4) | 6285(2) | 30(1) |
| O(2) | 9905(3) | 7658(4) | 4826(2) | 28(1) |
| O(11) | 6230(3) | 5185(3) | 4416(2) | 16(1) |
| O(12) | 6850(3) | 6885(3) | 3472(2) | 16(1) |
| Re(1) | 7785(1) | 6112(1) | 4624(1) | 14(1) |
| Br(1A) | 6697(1) | 7775(1) | 5335(1) | 16(1) |
| C(3A) | 8454(5) | 4916(7) | 4061(4) | 19(1) |
| O(3A) | 8876(5) | 4139(5) | 3694(3) | 26(1) |
| Br(1B) | 8340(11) | 4525(12) | 3685(8) | 43(3) |
| C(3B) | 7180(50) | 7410(40) | 5220(30) | 19(1) |
| O(3B) | 6790(50) | 8160(40) | 5540(40) | 26(1) |

**Table A.2: Bond distances (Å) and angles (°) for *fac*-[$NEt_4$][$Re(Trop)(CO)_3(Br)$] (1).**

| Bond | Bond Distance | Bond Angle | Angle |
|---|---|---|---|
| C(1)-O(1) | 1.153(6) | O(1)-C(1)-Re(1) | 178.7(5) |
| C(1)-Re(1) | 1.906(5) | O(2)-C(2)-Re(1) | 179.5(5) |
| C(2)-O(2) | 1.156(6) | O(11)-C(11)-C(17) | 117.7(4) |
| C(2)-Re(1) | 1.903(5) | O(11)-C(11)-C(12) | 116.1(4) |
| C(11)-O(11) | 1.286(5) | C(17)-C(11)-C(12) | 126.2(4) |
| C(11)-C(17) | 1.398(7) | O(12)-C(12)-C(13) | 118.4(4) |
| C(11)-C(12) | 1.462(6) | O(12)-C(12)-C(11) | 115.6(4) |
| C(12)-O(12) | 1.300(5) | C(13)-C(12)-C(11) | 126.0(4) |
| C(12)-C(13) | 1.402(6) | C(14)-C(13)-C(12) | 130.4(5) |
| C(13)-C(14) | 1.389(7) | C(14)-C(13)-H(13) | 114.8 |
| C(13)-H(13) | 0.9300 | C(12)-C(13)-H(13) | 114.8 |
| C(14)-C(15) | 1.385(8) | C(15)-C(14)-C(13) | 130.1(5) |

| | |
|---|---|
| C(14)-H(14) | 0.9300 |
| C(15)-C(16) | 1.392(7) |
| C(15)-H(15) | 0.9300 |
| C(16)-C(17) | 1.390(7) |
| C(16)-H(16) | 0.9300 |
| C(17)-H(17) | 0.9300 |
| C(21)-C(22) | 1.513(7) |
| C(21)-N(1) | 1.517(6) |
| C(21)-H(21A) | 0.9700 |
| C(21)-H(21B) | 0.9700 |
| C(22)-H(22A) | 0.9600 |
| C(22)-H(22B) | 0.9600 |
| C(22)-H(22C) | 0.9600 |
| C(23)-C(24) | 1.510(7) |
| C(23)-N(1) | 1.529(6) |
| C(23)-H(23A) | 0.9700 |
| C(23)-H(23B) | 0.9700 |
| C(24)-H(24A) | 0.9600 |
| C(24)-H(24B) | 0.9600 |
| C(24)-H(24C) | 0.9600 |
| C(25)-N(1) | 1.520(6) |
| C(25)-C(26) | 1.521(7) |
| C(25)-H(25A) | 0.9700 |
| C(25)-H(25B) | 0.9700 |
| C(26)-H(26A) | 0.9600 |
| C(26)-H(26B) | 0.9600 |
| C(26)-H(26C) | 0.9600 |
| C(27)-C(28) | 1.520(6) |
| C(27)-N(1) | 1.525(6) |
| C(27)-H(27A) | 0.9700 |
| C(27)-H(27B) | 0.9700 |
| C(28)-H(28A) | 0.9600 |
| C(28)-H(28B) | 0.9600 |
| C(28)-H(28C) | 0.9600 |
| O(11)-Re(1) | 2.126(3) |
| O(12)-Re(1) | 2.135(3) |
| Re(1)-C(3A) | 1.861(7) |
| Re(1)-C(3B) | 1.923(18) |
| Re(1)-Br(1B) | 2.467(16) |
| Re(1)-Br(1A) | 2.6334(9) |
| C(3A)-O(3A) | 1.201(9) |
| C(3B)-O(3B) | 1.123(18) |

| | |
|---|---|
| C(15)-C(14)-H(14) | 114.9 |
| C(13)-C(14)-H(14) | 114.9 |
| C(14)-C(15)-C(16) | 127.1(5) |
| C(14)-C(15)-H(15) | 116.5 |
| C(16)-C(15)-H(15) | 116.5 |
| C(17)-C(16)-C(15) | 128.8(5) |
| C(17)-C(16)-H(16) | 115.6 |
| C(15)-C(16)-H(16) | 115.6 |
| C(16)-C(17)-C(11) | 131.3(5) |
| C(16)-C(17)-H(17) | 114.4 |
| C(11)-C(17)-H(17) | 114.4 |
| C(22)-C(21)-N(1) | 115.3(4) |
| C(22)-C(21)-H(21A) | 108.4 |
| N(1)-C(21)-H(21A) | 108.4 |
| C(22)-C(21)-H(21B) | 108.4 |
| N(1)-C(21)-H(21B) | 108.4 |
| H(21A)-C(21)-H(21B) | 107.5 |
| C(21)-C(22)-H(22A) | 109.5 |
| C(21)-C(22)-H(22B) | 109.5 |
| H(22A)-C(22)-H(22B) | 109.5 |
| C(21)-C(22)-H(22C) | 109.5 |
| H(22A)-C(22)-H(22C) | 109.5 |
| H(22B)-C(22)-H(22C) | 109.5 |
| C(24)-C(23)-N(1) | 114.4(4) |
| C(24)-C(23)-H(23A) | 108.7 |
| N(1)-C(23)-H(23A) | 108.7 |
| C(24)-C(23)-H(23B) | 108.7 |
| N(1)-C(23)-H(23B) | 108.7 |
| H(23A)-C(23)-H(23B) | 107.6 |
| C(23)-C(24)-H(24A) | 109.5 |
| C(23)-C(24)-H(24B) | 109.5 |
| H(24A)-C(24)-H(24B) | 109.5 |
| C(23)-C(24)-H(24C) | 109.5 |
| H(24A)-C(24)-H(24C) | 109.5 |
| H(24B)-C(24)-H(24C) | 109.5 |
| N(1)-C(25)-C(26) | 115.4(4) |
| N(1)-C(25)-H(25A) | 108.4 |
| C(26)-C(25)-H(25A) | 108.4 |
| N(1)-C(25)-H(25B) | 108.4 |
| C(26)-C(25)-H(25B) | 108.4 |
| H(25A)-C(25)-H(25B) | 107.5 |
| C(25)-C(26)-H(26A) | 109.5 |
| C(25)-C(26)-H(26B) | 109.5 |
| H(26A)-C(26)-H(26B) | 109.5 |
| C(25)-C(26)-H(26C) | 109.5 |
| H(26A)-C(26)-H(26C) | 109.5 |
| H(26B)-C(26)-H(26C) | 109.5 |
| C(28)-C(27)-N(1) | 115.3(4) |
| C(28)-C(27)-H(27A) | 108.4 |
| N(1)-C(27)-H(27A) | 108.4 |
| C(28)-C(27)-H(27B) | 108.4 |
| N(1)-C(27)-H(27B) | 108.4 |
| H(27A)-C(27)-H(27B) | 107.5 |
| C(27)-C(28)-H(28A) | 109.5 |
| C(27)-C(28)-H(28B) | 109.5 |

| | |
|---|---|
| H(28A)-C(28)-H(28B) | 109.5 |
| C(27)-C(28)-H(28C) | 109.5 |
| H(28A)-C(28)-H(28C) | 109.5 |
| H(28B)-C(28)-H(28C) | 109.5 |
| C(21)-N(1)-C(25) | 108.7(4) |
| C(21)-N(1)-C(27) | 111.2(4) |
| C(25)-N(1)-C(27) | 107.9(4) |
| C(21)-N(1)-C(23) | 108.3(4) |
| C(25)-N(1)-C(23) | 111.8(4) |
| C(27)-N(1)-C(23) | 109.0(4) |
| C(11)-O(11)-Re(1) | 116.9(3) |
| C(12)-O(12)-Re(1) | 116.4(3) |
| C(3A)-Re(1)-C(2) | 88.5(2) |
| C(3A)-Re(1)-C(1) | 87.7(2) |
| C(2)-Re(1)-C(1) | 87.6(2) |
| C(3A)-Re(1)-C(3B) | 176(2) |
| C(2)-Re(1)-C(3B) | 88(2) |
| C(1)-Re(1)-C(3B) | 92.1(19) |
| C(3A)-Re(1)-O(11) | 94.4(2) |
| C(2)-Re(1)-O(11) | 174.40(17) |
| C(1)-Re(1)-O(11) | 97.33(17) |
| C(3B)-Re(1)-O(11) | 89(2) |
| C(3A)-Re(1)-O(12) | 93.6(2) |
| C(2)-Re(1)-O(12) | 100.19(16) |
| C(1)-Re(1)-O(12) | 172.18(16) |
| C(3B)-Re(1)-O(12) | 87.1(18) |
| O(11)-Re(1)-O(12) | 74.88(12) |
| C(3A)-Re(1)-Br(1B) | 10.7(4) |
| C(2)-Re(1)-Br(1B) | 96.0(3) |
| C(1)-Re(1)-Br(1B) | 95.6(3) |
| C(3B)-Re(1)-Br(1B) | 171.5(19) |
| O(11)-Re(1)-Br(1B) | 86.3(3) |
| O(12)-Re(1)-Br(1B) | 84.8(3) |
| C(3A)-Re(1)-Br(1A) | 175.61(19) |
| C(2)-Re(1)-Br(1A) | 94.80(15) |
| C(1)-Re(1)-Br(1A) | 95.34(14) |
| C(3B)-Re(1)-Br(1A) | 7.5(19) |
| O(11)-Re(1)-Br(1A) | 82.07(9) |
| O(12)-Re(1)-Br(1A) | 83.01(9) |
| Br(1B)-Re(1)-Br(1A) | 165.0(3) |
| O(3A)-C(3A)-Re(1) | 179.3(6) |
| O(3B)-C(3B)-Re(1) | 177(6) |

**Table A.3: Anisotropic displacement parameters ($Å^2$ x $10^3$) for *fac*-[$NEt_4$][Re(Trop)$(CO)_3$(Br)] (1). The Anisotropic displacement factor exponent takes the form: $-2\pi^2(h2a^{*2}U^{11} + ... + 2hka^*b^*U^{12})$.**

| | U11 | U22 | U33 | U23 | U13 | U12 |
|---|---|---|---|---|---|---|
| C(1) | 19(2) | 20(3) | 17(2) | 2(2) | 6(2) | 2(2) |
| C(2) | 22(2) | 22(3) | 15(2) | 1(2) | 2(2) | 2(2) |
| C(11) | 19(2) | 15(2) | 11(2) | -1(2) | 4(2) | 1(2) |
| C(12) | 19(2) | 12(2) | 14(2) | 0(2) | 6(2) | 0(2) |
| C(13) | 20(2) | 25(3) | 15(2) | 4(2) | 7(2) | -1(2) |
| C(14) | 21(3) | 40(3) | 19(2) | 13(2) | 1(2) | 0(2) |
| C(15) | 14(2) | 50(4) | 26(3) | 13(2) | -4(2) | -3(2) |
| C(16) | 16(2) | 35(3) | 23(2) | 4(2) | 4(2) | -3(2) |

| | | | | | | |
|---|---|---|---|---|---|---|
| C(17) | 21(2) | 25(3) | 17(2) | 2(2) | 6(2) | -2(2) |
| C(21) | 27(2) | 16(2) | 21(2) | -3(2) | 8(2) | -1(2) |
| C(22) | 24(3) | 29(3) | 24(2) | -5(2) | 7(2) | -3(2) |
| C(23) | 19(2) | 19(3) | 29(2) | 1(2) | 12(2) | 1(2) |
| C(24) | 26(3) | 27(3) | 34(3) | 2(2) | 6(2) | 5(2) |
| C(25) | 24(3) | 22(3) | 18(2) | 3(2) | 8(2) | 0(2) |
| C(26) | 44(3) | 24(3) | 21(2) | -1(2) | 4(2) | -5(2) |
| C(27) | 29(3) | 18(3) | 20(2) | 4(2) | 9(2) | 4(2) |
| C(28) | 32(3) | 26(3) | 22(2) | 5(2) | 9(2) | 5(2) |
| N(1) | 20(2) | 14(2) | 20(2) | 2(2) | 9(2) | 3(2) |
| O(1) | 25(2) | 42(3) | 21(2) | 10(2) | 3(1) | 6(2) |
| O(2) | 22(2) | 29(2) | 31(2) | 2(2) | 3(1) | -5(2) |
| O(11) | 14(2) | 19(2) | 13(1) | 3(1) | 1(1) | -2(1) |
| O(12) | 15(2) | 18(2) | 15(1) | 2(1) | 4(1) | -2(1) |
| Re(1) | 15(1) | 16(1) | 11(1) | 0(1) | 2(1) | 0(1) |
| Br(1A) | 17(1) | 16(1) | 15(1) | -2(1) | 5(1) | 0(1) |
| C(3A) | 22(3) | 21(3) | 15(3) | -5(2) | 4(2) | -6(2) |
| O(3A) | 25(3) | 25(3) | 29(2) | -4(2) | 12(2) | 8(2) |
| Br(1B) | 48(7) | 39(7) | 45(6) | 10(5) | 17(6) | -14(5) |
| C(3B) | 22(3) | 21(3) | 15(3) | -5(2) | 4(2) | -6(2) |
| O(3B) | 25(3) | 25(3) | 29(2) | -4(2) | 12(2) | 8(2) |

**Table A.4: Hydrogen coordinates (x $10^4$) and isotropic displacement parameters (Å$^2$ x $10^3$) for *fac*-[$NEt_4$][Re(Trop)$(CO)_3$(Br)] (1).**

| | x | y | z | U(eq) |
|---|---|---|---|---|
| H(13) | 5552 | 7546 | 2196 | 24 |
| H(14) | 3896 | 7047 | 1520 | 33 |
| H(15) | 2724 | 5697 | 1854 | 37 |
| H(16) | 2949 | 4524 | 3006 | 30 |
| H(17) | 4355 | 4440 | 4077 | 25 |
| H(21A) | 6032 | -1 | 2814 | 25 |
| H(21B) | 6263 | -671 | 3698 | 25 |
| H(22A) | 4331 | 706 | 3056 | 38 |
| H(22B) | 4563 | 30 | 3940 | 38 |
| H(22C) | 4385 | -750 | 3098 | 38 |
| H(23A) | 7689 | 1153 | 3071 | 25 |
| H(23B) | 8066 | 1947 | 3898 | 25 |
| H(24A) | 8041 | -668 | 3872 | 44 |
| H(24B) | 8416 | 125 | 4702 | 44 |
| H(24C) | 9117 | 146 | 3991 | 44 |
| H(25A) | 6730 | 413 | 4987 | 25 |
| H(25B) | 5693 | 1285 | 4790 | 25 |
| H(26A) | 7890 | 2158 | 5247 | 45 |
| H(26B) | 7045 | 2161 | 5854 | 45 |
| H(26C) | 6850 | 3030 | 5052 | 45 |
| H(27A) | 5218 | 2442 | 3544 | 26 |
| H(27B) | 6373 | 3097 | 3664 | 26 |
| H(28A) | 5453 | 3254 | 2251 | 39 |
| H(28B) | 5366 | 1802 | 2178 | 39 |
| H(28C) | 6525 | 2452 | 2298 | 39 |

**Table A.5: Torsion angles (°) for *fac*-[$NEt_4$][Re(Trop)$(CO)_3$(Br)] (1).**

| Torsion Angle | Angle | Torsion Angle | Angle |
|---|---|---|---|
| C3A-Re1-O11-C11 | -94.6(4) | C21-N1-C23-C24 | -63.0(5) |
| Br1A-Re1-O12-C12 | -83.1(3) | C25-N1-C23-C24 | 56.8(5) |
| O11-Re1-O12-C12 | 0.5(3) | C27-N1-C23-C24 | 175.9(4) |
| C2-Re1-O12-C12 | -176.8(3) | C23-N1-C25-C26 | 54.3(6) |
| C3A-Re1-O12-C12 | 94.1(4) | C23-N1-C21-C22 | -173.0(4) |
| Br1A-Re1-O11-C11 | 82.8(3) | C21-N1-C25-C26 | 173.8(4) |
| O12-Re1-O11-C11 | -2.1(3) | O11-C11-C12-C13 | 177.3(5) |
| C1-Re1-O11-C11 | 177.2(3) | C17-C11-C12-O12 | 178.0(5) |
| Re1-O11-C11-C12 | 3.2(5) | O11-C11-C17-C16 | -173.4(5) |
| Re1-O11-C11-C17 | -177.5(3) | C12-C11-C17-C16 | 5.9(9) |
| Re1-O12-C12-C13 | -179.1(3) | C17-C11-C12-C13 | -2.0(8) |
| Re1-O12-C12-C11 | 0.9(5) | O11-C11-C12-O12 | -2.7(6) |
| C21-N1-C27-C28 | -54.9(5) | O12-C12-C13-C14 | 177.8(5) |
| C23-N1-C27-C28 | 64.5(5) | C11-C12-C13-C14 | -2.2(9) |
| C25-N1-C27-C28 | -174.1(4) | C12-C13-C14-C15 | 1.6(10) |
| C27-N1-C25-C26 | -65.5(5) | C13-C14-C15-C16 | 1.3(10) |
| C25-N1-C21-C22 | 65.4(5) | C14-C15-C16-C17 | -0.4(10) |
| C27-N1-C21-C22 | -53.3(5) | C15-C16-C17-C11 | -4.3(10) |

**Table A.6: Hydrogen bond distances (Å) and angles (°) for *fac*-[$NEt_4$][Re(Trop)$(CO)_3$(Br)] (1).**

| D-H…A | d (D-H) | d (H…A) | d (D…A) | D-H…A angle |
|---|---|---|---|---|
| C13-H13…O3A#1 | 0.93 | 2.43 | 3.344(7) | 169 |
| C25-H25A…Br1A#2 | 0.97 | 2.89 | 3.809(5) | 157.7 |
| C26-H26C…O11 | 0.96 | 2.58 | 3.542(7) | 176.2 |
| C27-H27B…O11 | 0.97 | 2.57 | 3.401(6) | 143.4 |

Symmetry codes, transformations used to generate equivalent atoms:
#1 -x+3/2,y+1/2,-z+½ #2 x,y-1,z

**Table A.7: Atomic coordinates (x $10^4$) and equivalent isotropic displacement parameters ($Å^2$ x $10^3$) for *fac*-[$NEt_4$][$Re(Trop)(CO)_3(H_2O)$].$NO_3$.$H_2O$ (2). U(eq) is defined as one third of the trace of the orthogonalized $U^{ij}$ tensor.**

| | x | y | z | U(eq) |
|---|---|---|---|---|
| C(3) | 8991(5) | 4291(7) | 9614(5) | 22(1) |
| C(2) | 7884(6) | 3910(8) | 7898(7) | 41(2) |
| C(1) | 7249(5) | 4207(8) | 9976(7) | 39(2) |
| C(11) | 8478(5) | 7958(7) | 9529(6) | 26(2) |
| C(17) | 8535(5) | 9103(8) | 10138(6) | 33(2) |
| C(16) | 8840(6) | 10303(8) | 9805(7) | 38(2) |
| C(15) | 9196(6) | 10736(9) | 8767(7) | 43(2) |
| C(14) | 9333(6) | 9971(8) | 7786(7) | 38(2) |
| C(13) | 9163(5) | 8678(7) | 7619(6) | 31(2) |
| C(12) | 8781(4) | 7751(7) | 8332(6) | 23(1) |
| C(21) | 5312(11) | 1024(16) | -828(13) | 36(4) |
| C(28) | 3532(16) | -590(30) | 1130(30) | 30(5) |
| C(26) | 4710(40) | -1660(50) | -1730(50) | 67(13) |
| C(22) | 6240(17) | 880(40) | -1300(30) | 52(9) |
| C(24) | 5450(40) | 1430(40) | 1590(40) | 46(9) |
| C(23) | 5563(12) | 150(18) | 1180(14) | 45(4) |
| C(25) | 5142(11) | -1279(17) | -347(14) | 43(4) |
| C(27) | 3997(10) | 329(16) | 320(14) | 39(4) |
| O(3) | 9568(4) | 3658(5) | 9991(4) | 35(1) |
| O(2) | 7851(5) | 3106(7) | 7202(5) | 67(2) |
| O(1) | 6784(4) | 3608(6) | 10582(5) | 55(2) |
| O(12) | 8675(3) | 6586(5) | 7948(4) | 26(1) |
| O(11) | 8136(3) | 6931(5) | 10026(4) | 30(1) |
| O(4) | 6797(4) | 6385(6) | 8388(5) | 54(2) |
| O(8) | 6765(4) | 7078(7) | 11625(5) | 53(2) |
| O(7) | 5534(7) | 5976(9) | 9980(10) | 38(3) |
| O(6) | 4758(8) | 4829(13) | 11045(7) | 46(3) |
| O(5) | 4799(9) | 4346(13) | 9276(11) | 47(3) |
| Re(1) | 7989(1) | 5241(1) | 9004(1) | 26(1) |
| N(2) | 5000 | 0 | 0 | 30(2) |
| N(1) | 5000 | 5000 | 10000 | 36(2) |

**Table A.8: Bond distances (Å) and angles (°) for *fac*-[$NEt_4$][$Re(Trop)(CO)_3(H_2O)$].$NO_3$.$H_2O$ (2).**

| Bond | Bond Distance | Bond Angle | Angle |
|---|---|---|---|
| C(3)-O(3) | 1.148(8) | O(3)-C(3)-Re(1) | 176.3(6) |
| C(3)-Re(1) | 1.890(7) | O(2)-C(2)-Re(1) | 177.5(8) |
| C(2)-O(2) | 1.160(9) | O(1)-C(1)-Re(1) | 178.0(8) |
| C(2)-Re(1) | 1.886(8) | O(11)-C(11)-C(17) | 119.3(6) |
| C(1)-O(1) | 1.157(9) | O(11)-C(11)-C(12) | 114.5(6) |
| C(1)-Re(1) | 1.894(8) | C(17)-C(11)-C(12) | 126.1(7) |
| C(11)-O(11) | 1.307(8) | C(16)-C(17)-C(11) | 130.3(7) |
| C(11)-C(17) | 1.379(10) | C(16)-C(17)-H(17) | 114.9 |
| C(11)-C(12) | 1.477(9) | C(11)-C(17)-H(17) | 114.9 |
| C(17)-C(16) | 1.373(11) | C(17)-C(16)-C(15) | 131.2(8) |
| C(17)-H(17) | 0.9500 | C(17)-C(16)-H(16) | 114.4 |
| C(16)-C(15) | 1.389(11) | C(15)-C(16)-H(16) | 114.4 |
| C(16)-H(16) | 0.9500 | C(16)-C(15)-C(14) | 125.5(8) |
| C(15)-C(14) | 1.402(11) | C(16)-C(15)-H(15) | 117.2 |
| C(15)-H(15) | 0.9500 | C(14)-C(15)-H(15) | 117.2 |

| | | | |
|---|---|---|---|
| C(14)-C(13) | 1.371(10) | C(13)-C(14)-C(15) | 129.5(8) |
| C(14)-H(14) | 0.9500 | C(13)-C(14)-H(14) | 115.2 |
| C(13)-C(12) | 1.384(9) | C(15)-C(14)-H(14) | 115.2 |
| C(13)-H(13) | 0.9500 | C(14)-C(13)-C(12) | 131.4(7) |
| C(12)-O(12) | 1.292(8) | C(14)-C(13)-H(13) | 114.3 |
| C(21)-C(22) | 1.47(3) | C(12)-C(13)-H(13) | 114.3 |
| C(21)-N(2) | 1.501(14) | O(12)-C(12)-C(13) | 118.9(6) |
| C(21)-H(21A) | 0.9900 | O(12)-C(12)-C(11) | 115.1(6) |
| C(21)-H(21B) | 0.9900 | C(13)-C(12)-C(11) | 126.0(7) |
| C(28)-C(27) | 1.50(3) | C(22)-C(21)-N(2) | 116.7(16) |
| C(28)-H(28B) | 0.9800 | C(22)-C(21)-H(21A) | 108.1 |
| C(28)-H(28C) | 0.9800 | N(2)-C(21)-H(21A) | 108.1 |
| C(28)-H(28A) | 0.9800 | C(22)-C(21)-H(21B) | 108.1 |
| C(26)-C(25) | 1.76(7) | N(2)-C(21)-H(21B) | 108.1 |
| C(26)-H(26B) | 0.9800 | H(21A)-C(21)-H(21B) | 107.3 |
| C(26)-H(26A) | 0.9800 | C(27)-C(28)-H(28B) | 109.5 |
| C(26)-H(26C) | 0.9800 | C(27)-C(28)-H(28C) | 109.5 |
| C(22)-H(22B) | 0.9800 | H(28B)-C(28)-H(28C) | 109.5 |
| C(22)-H(22A) | 0.9800 | C(27)-C(28)-H(28A) | 109.5 |
| C(22)-H(22C) | 0.9800 | H(28B)-C(28)-H(28A) | 109.5 |
| C(24)-C(23) | 1.41(5) | H(28C)-C(28)-H(28A) | 109.5 |
| C(24)-H(24A) | 0.9800 | C(25)-C(26)-H(26B) | 109.5 |
| C(24)-H(24C) | 0.9800 | C(25)-C(26)-H(26A) | 109.5 |
| C(24)-H(24B) | 0.9800 | H(26B)-C(26)-H(26A) | 109.5 |
| C(23)-N(2) | 1.600(16) | C(25)-C(26)-H(26C) | 109.5 |
| C(23)-H(23B) | 0.9900 | H(26B)-C(26)-H(26C) | 109.5 |
| C(23)-H(23A) | 0.9900 | H(26A)-C(26)-H(26C) | 109.5 |
| C(25)-N(2) | 1.396(18) | C(21)-C(22)-H(22B) | 109.5 |
| C(25)-H(25B) | 0.9900 | C(21)-C(22)-H(22A) | 109.5 |
| C(25)-H(25A) | 0.9900 | H(22B)-C(22)-H(22A) | 109.5 |
| C(27)-N(2) | 1.546(15) | C(21)-C(22)-H(22C) | 109.5 |
| C(27)-H(27B) | 0.9900 | H(22B)-C(22)-H(22C) | 109.5 |
| C(27)-H(27A) | 0.9900 | H(22A)-C(22)-H(22C) | 109.5 |
| O(12)-Re(1) | 2.108(4) | C(23)-C(24)-H(24A) | 109.5 |
| O(11)-Re(1) | 2.121(5) | C(23)-C(24)-H(24C) | 109.5 |
| O(4)-Re(1) | 2.213(5) | H(24A)-C(24)-H(24C) | 109.5 |
| O(8)-H(8B) | 0.85(2) | C(23)-C(24)-H(24B) | 109.5 |
| O(8)-H(8A) | 0.85(2) | H(24A)-C(24)-H(24B) | 109.5 |
| O(7)-O(5)#1 | 1.048(15) | H(24C)-C(24)-H(24B) | 109.5 |
| O(7)-N(1) | 1.273(7) | C(24)-C(23)-N(2) | 109(3) |
| O(7)-O(6)#1 | 1.511(15) | C(24)-C(23)-H(23B) | 110.0 |
| O(6)-O(5)#1 | 1.133(17) | N(2)-C(23)-H(23B) | 110.0 |
| O(6)-N(1) | 1.279(8) | C(24)-C(23)-H(23A) | 110.0 |
| O(6)-O(7)#1 | 1.511(15) | N(2)-C(23)-H(23A) | 110.0 |
| O(5)-O(7)#1 | 1.048(15) | H(23B)-C(23)-H(23A) | 108.4 |
| O(5)-N(1) | 1.116(11) | N(2)-C(25)-C(26) | 115(2) |
| O(5)-O(6)#1 | 1.133(17) | N(2)-C(25)-H(25B) | 108.5 |
| N(2)-C(25)#2 | 1.396(18) | C(26)-C(25)-H(25B) | 108.5 |
| N(2)-C(21)#2 | 1.501(14) | N(2)-C(25)-H(25A) | 108.5 |
| N(2)-C(27)#2 | 1.546(15) | C(26)-C(25)-H(25A) | 108.5 |
| N(2)-C(23)#2 | 1.600(16) | H(25B)-C(25)-H(25A) | 107.5 |
| N(1)-O(5)#1 | 1.116(11) | C(28)-C(27)-N(2) | 116.2(13) |
| N(1)-O(7)#1 | 1.273(8) | C(28)-C(27)-H(27B) | 108.2 |
| N(1)-O(6)#1 | 1.279(8) | N(2)-C(27)-H(27B) | 108.2 |
| | | C(28)-C(27)-H(27A) | 108.2 |

| | |
|---|---|
| N(2)-C(27)-H(27A) | 108.2 |
| H(27B)-C(27)-H(27A) | 107.4 |
| C(12)-O(12)-Re(1) | 117.8(4) |
| C(11)-O(11)-Re(1) | 117.2(4) |
| H(8B)-O(8)-H(8A) | 110(3) |
| O(5)#1-O(7)-N(1) | 56.5(8) |
| O(5)#1-O(7)-O(6)#1 | 110.3(10) |
| N(1)-O(7)-O(6)#1 | 53.9(5) |
| O(5)#1-O(6)-N(1) | 54.7(7) |
| O(5)#1-O(6)-O(7)#1 | 108.1(8) |
| N(1)-O(6)-O(7)#1 | 53.5(5) |
| O(7)#1-O(5)-N(1) | 72.0(9) |
| O(7)#1-O(5)-O(6)#1 | 141.0(14) |
| N(1)-O(5)-O(6)#1 | 69.3(9) |
| C(2)-Re(1)-C(3) | 86.4(3) |
| C(2)-Re(1)-C(1) | 87.3(4) |
| C(3)-Re(1)-C(1) | 85.6(3) |
| C(2)-Re(1)-O(12) | 96.8(3) |
| C(3)-Re(1)-O(12) | 101.1(2) |
| C(1)-Re(1)-O(12) | 172.2(3) |
| C(2)-Re(1)-O(11) | 171.1(3) |
| C(3)-Re(1)-O(11) | 98.2(2) |
| C(1)-Re(1)-O(11) | 100.7(3) |
| O(12)-Re(1)-O(11) | 74.82(17) |
| C(2)-Re(1)-O(4) | 96.2(3) |
| C(3)-Re(1)-O(4) | 176.8(2) |
| C(1)-Re(1)-O(4) | 92.7(3) |
| O(12)-Re(1)-O(4) | 80.38(19) |
| O(11)-Re(1)-O(4) | 79.5(2) |
| C(25)#2-N(2)-C(25) | 180(2) |
| C(25)#2-N(2)-C(21) | 64.2(9) |
| C(25)-N(2)-C(21) | 115.8(9) |
| C(25)#2-N(2)-C(21)#2 | 115.8(9) |
| C(25)-N(2)-C(21)#2 | 64.2(9) |
| C(21)-N(2)-C(21)#2 | 180.0(16) |
| C(25)#2-N(2)-C(27)#2 | 114.8(9) |
| C(25)-N(2)-C(27)#2 | 65.2(9) |
| C(21)-N(2)-C(27)#2 | 73.2(8) |
| C(21)#2-N(2)-C(27)#2 | 106.8(8) |
| C(25)#2-N(2)-C(27) | 65.2(9) |
| C(25)-N(2)-C(27) | 114.8(9) |
| C(21)-N(2)-C(27) | 106.8(8) |
| C(21)#2-N(2)-C(27) | 73.2(8) |
| C(27)#2-N(2)-C(27) | 180.0(18) |
| C(25)#2-N(2)-C(23) | 74.7(9) |
| C(25)-N(2)-C(23) | 105.3(9) |
| C(21)-N(2)-C(23) | 109.1(9) |
| C(21)#2-N(2)-C(23) | 70.9(9) |
| C(27)#2-N(2)-C(23) | 75.5(9) |
| C(27)-N(2)-C(23) | 104.5(9) |
| C(25)#2-N(2)-C(23)#2 | 105.3(9) |
| C(25)-N(2)-C(23)#2 | 74.7(9) |
| C(21)-N(2)-C(23)#2 | 70.9(9) |
| C(21)#2-N(2)-C(23)#2 | 109.1(9) |
| C(27)#2-N(2)-C(23)#2 | 104.5(9) |

| | | |
|---|---|---|
| | C(27)-N(2)-C(23)#2 | 75.5(9) |
| | C(23)-N(2)-C(23)#2 | 180.0(12) |
| | O(5)#1-N(1)-O(5) | 180.000(5) |
| | O(5)#1-N(1)-O(7)#1 | 128.5(8) |
| | O(5)-N(1)-O(7)#1 | 51.5(8) |
| | O(5)#1-N(1)-O(7) | 51.5(8) |
| | O(5)-N(1)-O(7) | 128.5(8) |
| | O(7)#1-N(1)-O(7) | 180.0(10) |
| | O(5)#1-N(1)-O(6) | 56.0(8) |
| | O(5)-N(1)-O(6) | 124.0(9) |
| | O(7)#1-N(1)-O(6) | 72.7(8) |
| | O(7)-N(1)-O(6) | 107.3(8) |
| | O(5)#1-N(1)-O(6)#1 | 124.0(9) |
| | O(5)-N(1)-O(6)#1 | 56.0(8) |
| | O(7)#1-N(1)-O(6)#1 | 107.3(8) |
| | O(7)-N(1)-O(6)#1 | 72.7(8) |
| | O(6)-N(1)-O(6)#1 | 180.000(4) |

Symmetry transformations used to generate equivalent atoms:
#1 -x+1,-y+1,-z+2 #2 -x+1,-y,-z

**Table A.9: Anisotropic displacement parameters ($Å^2$ x $10^3$) for *fac*-$[NEt_4][Re(Trop)(CO)_3(H_2O)].NO_3.H_2O$ (2). The Anisotropic displacement factor exponent takes the form: $-2\pi^2(h2a^{*2}U^{11} + \ldots + 2hka^*b^*U^{12})$.**

| | U11 | U22 | U33 | U23 | U13 | U12 |
|---|---|---|---|---|---|---|
| C(3) | 20(3) | 24(3) | 22(3) | -1(3) | 2(3) | -6(3) |
| C(2) | 48(5) | 37(5) | 38(5) | -1(4) | -1(4) | -21(4) |
| C(1) | 23(4) | 38(4) | 54(5) | 8(4) | 4(4) | 3(4) |
| C(11) | 25(4) | 30(4) | 25(4) | 0(3) | 2(3) | 2(3) |
| C(17) | 43(5) | 37(5) | 19(3) | 6(3) | 11(3) | -3(4) |
| C(16) | 54(5) | 30(4) | 30(4) | -8(4) | 3(4) | -1(4) |
| C(15) | 56(6) | 34(4) | 39(5) | 6(4) | -2(4) | -8(4) |
| C(14) | 44(5) | 39(5) | 32(4) | 3(3) | 8(3) | -14(4) |
| C(13) | 35(4) | 37(5) | 21(3) | -3(3) | 10(3) | -15(3) |
| C(12) | 19(3) | 26(4) | 24(3) | 0(3) | 3(3) | -5(3) |
| C(21) | 43(10) | 38(10) | 27(8) | 12(7) | 9(7) | 5(7) |
| C(28) | 15(11) | 36(11) | 38(13) | 9(9) | -10(9) | 7(8) |
| C(26) | 70(30) | 42(17) | 90(30) | -53(15) | 14(19) | 1(14) |
| C(22) | 16(12) | 120(30) | 23(10) | 28(13) | -6(9) | 10(12) |
| C(24) | 60(20) | 33(19) | 49(14) | -23(15) | 31(12) | -11(15) |
| C(23) | 37(9) | 65(12) | 33(9) | 16(8) | -1(7) | 3(9) |
| C(25) | 34(9) | 52(11) | 44(9) | 18(9) | 6(7) | 6(8) |
| C(27) | 28(8) | 47(10) | 44(9) | 11(8) | 3(7) | 9(8) |
| O(3) | 34(3) | 28(3) | 41(3) | -3(2) | 0(2) | 5(2) |
| O(2) | 98(6) | 65(5) | 39(4) | -12(3) | -5(4) | -37(4) |
| O(1) | 44(4) | 59(4) | 64(4) | 32(3) | 12(3) | -3(3) |
| O(12) | 30(3) | 31(3) | 19(2) | 2(2) | 11(2) | -4(2) |
| O(11) | 39(3) | 26(3) | 26(3) | 4(2) | 15(2) | -1(2) |
| O(4) | 29(3) | 80(5) | 53(4) | 44(3) | 7(3) | 7(3) |
| O(8) | 38(4) | 81(5) | 41(3) | -41(3) | 22(3) | -26(3) |
| O(7) | 32(6) | 39(7) | 42(7) | -12(5) | 9(5) | -9(5) |
| O(6) | 42(7) | 65(8) | 30(6) | -3(6) | 9(5) | -1(6) |
| O(5) | 53(8) | 50(8) | 37(7) | -28(7) | 4(6) | -10(7) |
| Re(1) | 24(1) | 32(1) | 23(1) | 6(1) | 4(1) | -4(1) |

| | | | | | | |
|---|---|---|---|---|---|---|
| N(2) | 42(5) | 12(5) | 36(5) | 5(3) | 9(4) | 3(3) |
| N(1) | 29(5) | 34(6) | 44(6) | 13(5) | 11(4) | 5(4) |

**Table A.10: Hydrogen coordinates (x $10^4$) and isotropic displacement parameters ($Å^2$ x $10^3$) for *fac*-[$NEt_4$][Re(Trop)$(CO)_3(H_2O)$].$NO_3$.$H_2O$ (2).**

| | x | y | z | U(eq) |
|---|---|---|---|---|
| H(17) | 8331 | 9052 | 10912 | 40 |
| H(16) | 8802 | 10950 | 10385 | 46 |
| H(15) | 9360 | 11625 | 8718 | 51 |
| H(14) | 9580 | 10414 | 7142 | 46 |
| H(13) | 9338 | 8362 | 6885 | 37 |
| H(21A) | 4871 | 1046 | -1481 | 43 |
| H(21B) | 5276 | 1874 | -435 | 43 |
| H(28B) | 2901 | -299 | 1269 | 45 |
| H(28C) | 3871 | -615 | 1862 | 45 |
| H(28A) | 3520 | -1461 | 792 | 45 |
| H(26B) | 4834 | -2574 | -1897 | 100 |
| H(26A) | 5005 | -1111 | -2301 | 100 |
| H(26C) | 4042 | -1513 | -1745 | 100 |
| H(22B) | 6369 | 1602 | -1818 | 78 |
| H(22A) | 6282 | 61 | -1718 | 78 |
| H(22C) | 6689 | 881 | -663 | 78 |
| H(24A) | 5796 | 1538 | 2309 | 69 |
| H(24C) | 4799 | 1602 | 1720 | 69 |
| H(24B) | 5687 | 2041 | 1013 | 69 |
| H(23B) | 5330 | -473 | 1757 | 54 |
| H(23A) | 6222 | -33 | 1051 | 54 |
| H(25B) | 4852 | -1862 | 221 | 52 |
| H(25A) | 5811 | -1456 | -335 | 52 |
| H(27B) | 3989 | 1204 | 669 | 47 |
| H(27A) | 3629 | 370 | -399 | 47 |
| H(8B) | 7220(30) | 7030(70) | 11180(50) | 40(30) |
| H(8A) | 6320(30) | 6640(80) | 11360(60) | 70(30) |

**Table A.11: Torsion angles (°) for *fac*-[$NEt_4$][Re(Trop)$(CO)_3(H_2O)$].$NO_3$.$H_2O$ (2).**

| Torsion Angle | Angle | Torsion Angle | Angle |
|---|---|---|---|
| O(11)-C(11)-C(17)-C(16) | -178.2(8) | C(26)-C(25)-N(2)-C(23)#2 | 7(2) |
| C(12)-C(11)-C(17)-C(16) | 2.5(13) | C(22)-C(21)-N(2)-C(25)#2 | 132(2) |
| C(11)-C(17)-C(16)-C(15) | -1.0(16) | C(22)-C(21)-N(2)-C(25) | -48(2) |
| C(17)-C(16)-C(15)-C(14) | -0.8(16) | C(22)-C(21)-N(2)-C(21)#2 | 0.0(10) |
| C(16)-C(15)-C(14)-C(13) | -0.3(15) | C(22)-C(21)-N(2)-C(27)#2 | 2.6(19) |
| C(15)-C(14)-C(13)-C(12) | 2.7(16) | C(22)-C(21)-N(2)-C(27) | -177.4(19) |
| C(14)-C(13)-C(12)-O(12) | 178.3(8) | C(22)-C(21)-N(2)-C(23) | 70(2) |
| C(14)-C(13)-C(12)-C(11) | -2.3(14) | C(22)-C(21)-N(2)-C(23)#2 | -110(2) |
| O(11)-C(11)-C(12)-O(12) | -0.6(9) | C(28)-C(27)-N(2)-C(25)#2 | -130.9(19) |
| C(17)-C(11)-C(12)-O(12) | 178.7(7) | C(28)-C(27)-N(2)-C(25) | 49.1(19) |
| O(11)-C(11)-C(12)-C(13) | 179.9(7) | C(28)-C(27)-N(2)-C(21) | 178.8(16) |
| C(17)-C(11)-C(12)-C(13) | -0.8(12) | C(28)-C(27)-N(2)-C(21)#2 | -1.2(16) |
| C(13)-C(12)-O(12)-Re(1) | -174.9(5) | C(28)-C(27)-N(2)-C(27)#2 | 0(100) |
| C(11)-C(12)-O(12)-Re(1) | 5.6(8) | C(28)-C(27)-N(2)-C(23) | -65.7(18) |
| C(17)-C(11)-O(11)-Re(1) | 176.1(5) | C(28)-C(27)-N(2)-C(23)#2 | 114.3(18) |
| C(12)-C(11)-O(11)-Re(1) | -4.5(8) | C(24)-C(23)-N(2)-C(25)#2 | 0(2) |
| O(2)-C(2)-Re(1)-C(3) | -67(19) | C(24)-C(23)-N(2)-C(25) | 180(2) |

| | | | |
|---|---|---|---|
| O(2)-C(2)-Re(1)-C(1) | -153(19) | C(24)-C(23)-N(2)-C(21) | 55(2) |
| O(2)-C(2)-Re(1)-O(12) | 33(19) | C(24)-C(23)-N(2)-C(21)#2 | -125(2) |
| O(2)-C(2)-Re(1)-O(11) | 53(20) | C(24)-C(23)-N(2)-C(27)#2 | 121(2) |
| O(2)-C(2)-Re(1)-O(4) | 114(19) | C(24)-C(23)-N(2)-C(27) | -59(2) |
| O(3)-C(3)-Re(1)-C(2) | -56(9) | C(24)-C(23)-N(2)-C(23)#2 | -70(100) |
| O(3)-C(3)-Re(1)-C(1) | 31(9) | O(7)#1-O(5)-N(1)-O(5)#1 | -53(100) |
| O(3)-C(3)-Re(1)-O(12) | -153(9) | O(6)#1-O(5)-N(1)-O(5)#1 | 122(100) |
| O(3)-C(3)-Re(1)-O(11) | 131(9) | O(6)#1-O(5)-N(1)-O(7)#1 | 175.5(14) |
| O(3)-C(3)-Re(1)-O(4) | 89(10) | O(7)#1-O(5)-N(1)-O(7) | 180.000(3) |
| O(1)-C(1)-Re(1)-C(2) | -143(22) | O(6)#1-O(5)-N(1)-O(7) | -4.5(14) |
| O(1)-C(1)-Re(1)-C(3) | 131(22) | O(7)#1-O(5)-N(1)-O(6) | 4.5(15) |
| O(1)-C(1)-Re(1)-O(12) | -21(23) | O(6)#1-O(5)-N(1)-O(6) | 180.000(3) |
| O(1)-C(1)-Re(1)-O(11) | 33(22) | O(7)#1-O(5)-N(1)-O(6)#1 | -175.5(14) |
| O(1)-C(1)-Re(1)-O(4) | -47(22) | O(6)#1-O(7)-N(1)-O(5)#1 | -176.1(13) |
| C(12)-O(12)-Re(1)-C(2) | 170.9(5) | O(5)#1-O(7)-N(1)-O(5) | 180.000(4) |
| C(12)-O(12)-Re(1)-C(3) | -101.5(5) | O(6)#1-O(7)-N(1)-O(5) | 3.9(13) |
| C(12)-O(12)-Re(1)-C(1) | 49(2) | O(5)#1-O(7)-N(1)-O(7)#1 | -103.6(11) |
| C(12)-O(12)-Re(1)-O(11) | -6.0(5) | O(6)#1-O(7)-N(1)-O(7)#1 | 80.3(8) |
| C(12)-O(12)-Re(1)-O(4) | 75.7(5) | O(5)#1-O(7)-N(1)-O(6) | -3.9(13) |
| C(11)-O(11)-Re(1)-C(2) | -15(2) | O(6)#1-O(7)-N(1)-O(6) | 180.000(3) |
| C(11)-O(11)-Re(1)-C(3) | 105.0(5) | O(5)#1-O(7)-N(1)-O(6)#1 | 176.1(13) |
| C(11)-O(11)-Re(1)-C(1) | -168.0(5) | O(7)#1-O(6)-N(1)-O(5)#1 | 176.3(12) |
| C(11)-O(11)-Re(1)-O(12) | 5.6(5) | O(5)#1-O(6)-N(1)-O(5) | 180.000(4) |
| C(11)-O(11)-Re(1)-O(4) | -77.2(5) | O(7)#1-O(6)-N(1)-O(5) | -3.7(12) |
| C(26)-C(25)-N(2)-C(25)#2 | 0.0(9) | O(5)#1-O(6)-N(1)-O(7)#1 | -176.3(12) |
| C(26)-C(25)-N(2)-C(21) | -52(2) | O(5)#1-O(6)-N(1)-O(7) | 3.7(12) |
| C(26)-C(25)-N(2)-C(21)#2 | 128(2) | O(7)#1-O(6)-N(1)-O(7) | 180.000(3) |
| C(26)-C(25)-N(2)-C(27)#2 | -107(2) | O(5)#1-O(6)-N(1)-O(6)#1 | 64(100) |
| C(26)-C(25)-N(2)-C(27) | 73(2) | O(7)#1-O(6)-N(1)-O(6)#1 | -120(100) |
| C(26)-C(25)-N(2)-C(23) | -173(2) | | |

Symmetry transformations used to generate equivalent atoms:
#1 -x+1,-y+1,-z+2 #2 -x+1,-y,-z

**Table A.12: Hydrogen bond distances (Å) and angles (°) for *fac*-[$NEt_4$][$Re(Trop)(CO)_3(H_2O)$] .$NO_3$.$H_2O$ (2).**

| D-H…A | d (D-H) | d (H…A) | d (D…A) | D-H…A angle |
|---|---|---|---|---|
| O8-H8A…O7 | 0.85(2) | 2.08(5) | 2.847(11) | 151(7) |
| O8-H8A…O5#1 | 0.85(2) | 2.05(2) | 2.898(14) | 178(9) |
| O8-H8B…O11 | 0.85(2) | 1.90(2) | 2.738(7) | 173(7) |
| C15-H15…O3#2 | 0.95 | 2.58 | 3.376(10) | 141.1 |
| C17-H17…O12#3 | 0.95 | 2.50 | 3.346(8) | 147.9 |
| C24-H24B…O1#4 | 0.98 | 2.33 | 3.19(5) | 146.5 |
| C25-H25B…O7#5 | 0.99 | 2.46 | 2.91(2) | 107.6 |
| C26-H26B…O6#6 | 0.98 | 2.60 | 3.45(5) | 145.7 |

Symmetry transformations used to generate equivalent atoms:
#1 1-x,1-y,2–z #2 x,1+y,z #3 x,1.5-y,0.5+z #4 x,y,-1+z #5 x,-1+y,-1+z #6 1-x,-y,1-z

# Appendix A

**Table A.13: Atomic coordinates (x $10^4$) and equivalent isotropic displacement parameters ($Å^2$ x $10^3$) for *fac*-[Re(Trop)$(CO)_3$(Py)] (3). U(eq) is defined as one third of the trace of the orthogonalized $U^{ij}$ tensor.**

| | x | y | z | U(eq) |
|---|---|---|---|---|
| Re(01) | 7187(1) | 2030(1) | 9874(1) | 15(1) |
| O(3) | 8049(3) | -733(6) | 8843(3) | 29(1) |
| O(12) | 8372(2) | 3583(6) | 10825(3) | 16(1) |
| C(11) | 8329(3) | 1449(8) | 12081(4) | 14(1) |
| C(13) | 9448(3) | 4225(8) | 12469(4) | 17(1) |
| C(1) | 6128(3) | 538(8) | 9202(4) | 19(1) |
| O(2) | 6510(3) | 4701(6) | 7989(3) | 25(1) |
| O(11) | 7682(2) | 592(5) | 11320(3) | 18(1) |
| N(1) | 6580(3) | 3928(7) | 10662(3) | 16(1) |
| C(15) | 9831(4) | 2824(8) | 14229(4) | 21(1) |
| O(1) | 5487(2) | -384(6) | 8803(3) | 23(1) |
| C(3) | 7750(3) | 323(9) | 9242(4) | 23(1) |
| C(2) | 6768(3) | 3657(9) | 8683(4) | 20(1) |
| C(14) | 9934(3) | 4079(9) | 13532(4) | 22(1) |
| C(17) | 8577(3) | 706(8) | 13077(4) | 18(1) |
| C(16) | 9208(3) | 1337(9) | 14014(4) | 21(1) |
| C(12) | 8720(3) | 3138(7) | 11794(4) | 15(1) |
| C(24) | 6427(4) | 7063(8) | 11309(4) | 19(1) |
| C(21) | 5969(4) | 3237(8) | 10984(4) | 19(1) |
| C(22) | 5577(4) | 4370(8) | 11479(4) | 21(1) |
| C(23) | 5803(4) | 6307(9) | 11647(4) | 22(1) |
| C(25) | 6788(3) | 5842(8) | 10819(4) | 21(1) |

**Table A.14: Bond distances (Å) and angles (°) for *fac*-[Re(Trop)$(CO)_3$(Py)] (3).**

| Bond | Bond Distance | Bond Angle | Angle |
|---|---|---|---|
| Re(01)-C(1) | 1.898(5) | C(1)-Re(01)-C(2) | 87.3(2) |
| Re(01)-C(2) | 1.909(6) | C(1)-Re(01)-C(3) | 86.9(2) |
| Re(01)-C(3) | 1.930(6) | C(2)-Re(01)-C(3) | 90.5(2) |
| Re(01)-O(11) | 2.121(4) | C(1)-Re(01)-O(11) | 98.01(18) |
| Re(01)-O(12) | 2.136(3) | C(2)-Re(01)-O(11) | 171.9(2) |
| Re(01)-N(1) | 2.208(4) | C(3)-Re(01)-O(11) | 95.96(19) |
| O(3)-C(3) | 1.148(7) | C(1)-Re(01)-O(12) | 172.05(18) |
| O(12)-C(12) | 1.293(6) | C(2)-Re(01)-O(12) | 99.7(2) |
| C(11)-O(11) | 1.302(6) | C(3)-Re(01)-O(12) | 96.85(19) |
| C(11)-C(17) | 1.400(7) | O(11)-Re(01)-O(12) | 74.68(14) |
| C(11)-C(12) | 1.465(7) | C(1)-Re(01)-N(1) | 93.9(2) |
| C(13)-C(14) | 1.392(7) | C(2)-Re(01)-N(1) | 91.8(2) |
| C(13)-C(12) | 1.399(7) | C(3)-Re(01)-N(1) | 177.55(18) |
| C(13)-H(17) | 0.9300 | O(11)-Re(01)-N(1) | 81.66(15) |
| C(1)-O(1) | 1.155(6) | O(12)-Re(01)-N(1) | 82.03(15) |
| O(2)-C(2) | 1.152(7) | C(12)-O(12)-Re(01) | 116.2(3) |
| N(1)-C(21) | 1.345(7) | O(11)-C(11)-C(17) | 118.3(5) |
| N(1)-C(25) | 1.358(7) | O(11)-C(11)-C(12) | 115.2(4) |
| C(15)-C(14) | 1.379(8) | C(17)-C(11)-C(12) | 126.5(5) |
| C(15)-C(16) | 1.387(8) | C(14)-C(13)-C(12) | 130.6(5) |
| C(15)-H(15) | 0.9300 | C(14)-C(13)-H(17) | 114.7 |
| C(14)-H(16) | 0.9300 | C(12)-C(13)-H(17) | 114.7 |
| C(17)-C(16) | 1.377(7) | O(1)-C(1)-Re(01) | 179.2(5) |
| C(17)-H(13) | 0.9300 | C(11)-O(11)-Re(01) | 116.7(3) |

| | | | |
|---|---|---|---|
| C(16)-H(14) | 0.9300 | C(21)-N(1)-C(25) | 117.3(5) |
| C(24)-C(25) | 1.372(8) | C(21)-N(1)-Re(01) | 121.1(4) |
| C(24)-C(23) | 1.396(8) | C(25)-N(1)-Re(01) | 121.6(4) |
| C(24)-H(24) | 0.9300 | C(14)-C(15)-C(16) | 127.0(5) |
| C(21)-C(22) | 1.375(8) | C(14)-C(15)-H(15) | 116.5 |
| C(21)-H(21) | 0.9300 | C(16)-C(15)-H(15) | 116.5 |
| C(22)-C(23) | 1.379(8) | O(3)-C(3)-Re(01) | 177.0(5) |
| C(22)-H(22) | 0.9300 | O(2)-C(2)-Re(01) | 177.1(5) |
| C(23)-H(23) | 0.9300 | C(15)-C(14)-C(13) | 130.0(5) |
| C(25)-H(25) | 0.9300 | C(15)-C(14)-H(16) | 115.0 |
| | | C(13)-C(14)-H(16) | 115.0 |
| | | C(16)-C(17)-C(11) | 130.9(5) |
| | | C(16)-C(17)-H(13) | 114.6 |
| | | C(11)-C(17)-H(13) | 114.6 |
| | | C(17)-C(16)-C(15) | 129.4(5) |
| | | C(17)-C(16)-H(14) | 115.3 |
| | | C(15)-C(16)-H(14) | 115.3 |
| | | O(12)-C(12)-C(13) | 118.7(5) |
| | | O(12)-C(12)-C(11) | 115.8(4) |
| | | C(13)-C(12)-C(11) | 125.4(5) |
| | | C(25)-C(24)-C(23) | 118.4(5) |
| | | C(25)-C(24)-H(24) | 120.8 |
| | | C(23)-C(24)-H(24) | 120.8 |
| | | N(1)-C(21)-C(22) | 122.8(5) |
| | | N(1)-C(21)-H(21) | 118.6 |
| | | C(22)-C(21)-H(21) | 118.6 |
| | | C(21)-C(22)-C(23) | 119.4(5) |
| | | C(21)-C(22)-H(22) | 120.3 |
| | | C(23)-C(22)-H(22) | 120.3 |
| | | C(22)-C(23)-C(24) | 118.9(5) |
| | | C(22)-C(23)-H(23) | 120.6 |
| | | C(24)-C(23)-H(23) | 120.6 |
| | | N(1)-C(25)-C(24) | 123.2(5) |
| | | N(1)-C(25)-H(25) | 118.4 |
| | | C(24)-C(25)-H(25) | 118.4 |

**Table A.15: Anisotropic displacement parameters ($Å^2$ x $10^3$) for *fac*-[Re(Trop)$(CO)_3$(Py)] (3). The Anisotropic displacement factor exponent takes the form: $-2\pi^2(h2a^{*2}U^{11} + \ldots + 2hka^*b^*U^{12})$.**

| | U11 | U22 | U33 | U23 | U13 | U12 |
|---|---|---|---|---|---|---|
| Re(01) | 12(1) | 16(1) | 14(1) | 0(1) | 4(1) | -3(1) |
| O(3) | 27(2) | 28(3) | 33(2) | -12(2) | 13(2) | -1(2) |
| O(12) | 12(2) | 22(2) | 12(2) | 1(2) | 3(1) | -4(2) |
| C(11) | 10(2) | 17(3) | 15(2) | 0(2) | 6(2) | 3(2) |
| C(13) | 14(2) | 19(3) | 20(2) | 1(2) | 8(2) | -4(2) |
| C(1) | 19(3) | 21(3) | 16(2) | 2(2) | 6(2) | 4(2) |
| O(2) | 25(2) | 26(2) | 20(2) | 7(2) | 5(2) | 1(2) |
| O(11) | 17(2) | 18(2) | 16(2) | 2(2) | 4(1) | -3(2) |
| N(1) | 14(2) | 18(2) | 16(2) | 1(2) | 6(2) | 2(2) |
| C(15) | 19(3) | 25(3) | 17(2) | -2(2) | 5(2) | 4(2) |
| O(1) | 17(2) | 25(2) | 24(2) | -3(2) | 4(2) | -7(2) |
| C(3) | 14(2) | 32(3) | 19(2) | 3(2) | 3(2) | -6(2) |
| C(2) | 15(2) | 26(3) | 20(3) | 1(2) | 9(2) | -2(2) |
| C(14) | 15(2) | 30(3) | 20(3) | -5(2) | 6(2) | -3(2) |
| C(17) | 16(2) | 19(3) | 22(2) | 2(2) | 10(2) | 3(2) |

| | | | | | | |
|---|---|---|---|---|---|---|
| C(16) | 16(3) | 28(3) | 19(2) | 5(2) | 9(2) | 8(2) |
| C(12) | 14(2) | 14(3) | 19(2) | -1(2) | 7(2) | 0(2) |
| C(24) | 23(3) | 13(3) | 20(3) | -2(2) | 8(2) | -3(2) |
| C(21) | 17(3) | 19(3) | 19(2) | -1(2) | 6(2) | -5(2) |
| C(22) | 22(3) | 21(3) | 22(3) | -1(2) | 10(2) | -3(2) |
| C(23) | 22(3) | 22(3) | 21(3) | -3(2) | 8(2) | 2(2) |
| C(25) | 19(3) | 22(3) | 21(2) | 5(2) | 7(2) | -5(2) |

**Table A.16: Hydrogen coordinates (x $10^4$) and isotropic displacement parameters (Å$^2$ x $10^3$) for *fac*-[Re(Trop)(CO)$_3$(Py)] (3).**

| | x | y | z | U(eq) |
|---|---|---|---|---|
| H(17) | 9638 | 5205 | 12157 | 21 |
| H(15) | 10220 | 2993 | 14918 | 25 |
| H(16) | 10402 | 4965 | 13815 | 27 |
| H(13) | 8264 | -399 | 13111 | 22 |
| H(14) | 9218 | 668 | 14586 | 25 |
| H(24) | 6594 | 8363 | 11414 | 23 |
| H(21) | 5806 | 1937 | 10866 | 22 |
| H(22) | 5163 | 3836 | 11698 | 25 |
| H(23) | 5545 | 7096 | 11981 | 26 |
| H(25) | 7195 | 6351 | 10583 | 25 |

**Table A.17: Torsion angles (°) for *fac*-[Re(Trop)(CO)$_3$(Py)] (3).**

| Torsion Angle | Angle | Torsion Angle | Angle |
|---|---|---|---|
| O12-Re01-O11-C11 | 10.1(4) | Re01-N1-C21-C22 | 179.8(4) |
| N1-Re01-O11-C11 | -73.9(4) | C25-N1-C21-C22 | -1.8(8) |
| C1-Re01-O11-C11 | -166.8(4) | O11-C11-C12-C13 | -176.7(5) |
| C3-Re01-O11-C11 | 105.5(4) | C17-C11-C12-O12 | -178.7(5) |
| O11-Re01-O12-C12 | -9.7(3) | O11-C11-C12-O12 | 0.6(7) |
| N1-Re01-O12-C12 | 73.8(4) | O11-C11-C17-C16 | -177.9(6) |
| C2 -Re01-O12-C12 | 164.3(4) | C17-C11-C12-C13 | 4.0(9) |
| C3-Re01-O12-C12 | -104.1(4) | C12-C11-C17-C16 | 1.4(10) |
| O11-Re01-N1-C21 | -63.3(4) | C11-C12-C13-C14 | -3.8(10) |
| O11-Re01-N1-C25 | 118.4(4) | O12-C12-C13-C14 | 179.0(6) |
| O12-Re01-N1-C21 | -138.9(4) | C12-C13-C14-C15 | -0.6(11) |
| O12-Re01-N1-C25 | 42.8(4) | C13-C14-C15-C16 | 1.7(11) |
| C1-Re01-N1-C21 | 34.2(4) | C14-C15-C16-C17 | 2.7(11) |
| C1-Re01-N1-C25 | -144.1(4) | C15-C16-C17-C11 | -5.5(11) |
| C2-Re01-N1-C21 | 121.6(4) | N1-C21-C22-C23 | 1.0(9) |
| C2-Re01-N1-C25 | -56.7(4) | C21-C22-C23-C24 | -0.1(8) |
| Re01-O11-C11-C12 | -9.2(6) | C22-C23-C24-C25 | 0.2(8) |
| Re01-O11-C11-C17 | 170.2(4) | C23-C24-C25-N1 | -1.2(8) |
| Re01-O12-C12-C11 | 8.2(6) | Re01-N1-C25-C24 | -179.7(4) |
| Re01-O12-C12-C13 | -174.4(4) | C21-N1-C25-C24 | 1.9(8) |

**Table A.18: Hydrogen bond distances (Å) and angles (°) for *fac*-[Re(Trop)(CO)$_3$(Py)] (3).**

| D-H…A | d (D-H) | d (H…A) | d (D…A) | D-H…A angle |
|---|---|---|---|---|
| C21-H21…O1#1 | 0.93 | 2.58 | 3.198(7) | 124.3 |
| C22-H22…O1#1 | 0.93 | 2.58 | 3.187(7) | 123.1 |
| C24-H24…O11#2 | 0.93 | 2.40 | 3.178(7) | 141.6 |

Symmetry codes, transformations used to generate equivalent atoms:
#1 1-x,-y,2-z #2 x,1+y,z

# Appendix A

**Table A.19: Atomic coordinates (x $10^4$) and equivalent isotropic displacement parameters ($Å^2$ x $10^3$) for *fac*-[Re(Trop)$(CO)_3$(DMAP)] (4). U(eq) is defined as one third of the trace of the orthogonalized $U^{ij}$ tensor.**

| | x | y | z | U(eq) |
|---|---|---|---|---|
| Re(01) | 432(1) | 2701(1) | 3479(1) | 22(1) |
| C(3) | -1608(8) | 2269(4) | 2768(5) | 33(1) |
| N(1) | 2735(5) | 3160(3) | 4371(3) | 22(1) |
| O(12) | 1707(6) | 1460(3) | 3632(3) | 36(1) |
| C(27) | 6773(8) | 4799(4) | 6817(4) | 33(1) |
| N(2) | 6974(6) | 4096(3) | 6140(3) | 25(1) |
| C(1) | -651(7) | 3815(4) | 3549(4) | 26(1) |
| C(2) | 1111(7) | 3110(4) | 2331(4) | 29(1) |
| O(11) | -64(5) | 2186(3) | 4791(3) | 30(1) |
| C(24) | 5719(8) | 3121(5) | 4870(5) | 37(1) |
| O(2) | 1530(6) | 3366(3) | 1644(3) | 40(1) |
| C(26) | 8599(8) | 3670(5) | 6227(6) | 43(2) |
| O(1) | -1319(5) | 4496(3) | 3619(3) | 37(1) |
| O(3) | -2855(6) | 2030(3) | 2346(4) | 50(1) |
| C(23) | 5625(8) | 3779(4) | 5568(5) | 40(1) |
| C(22) | 3996(8) | 4108(4) | 5626(6) | 43(1) |
| C(12) | 1742(8) | 1062(4) | 4439(5) | 38(2) |
| C(25) | 4288(7) | 2843(4) | 4308(5) | 32(1) |
| C(11) | 779(7) | 1486(4) | 5100(5) | 35(2) |
| C(14) | 2968(9) | -271(4) | 5395(6) | 43(1) |
| C(15) | 2502(8) | -158(4) | 6246(5) | 40(1) |
| C(17) | 692(7) | 1210(4) | 6021(5) | 32(1) |
| C(16) | 1476(7) | 508(5) | 6530(5) | 37(1) |
| C(13) | 2655(8) | 262(4) | 4584(5) | 38(1) |
| C(21) | 2643(8) | 3782(4) | 5038(5) | 38(1) |

**Table A.20: Bond distances (Å) and angles (°) for *fac*-[Re(Trop)$(CO)_3$(DMAP)] (4).**

| Bond | Bond Distance | Bond Angle | Angle |
|---|---|---|---|
| Re(01)-C(1) | 1.893(6) | C(1)-Re(01)-C(2) | 87.4(2) |
| Re(01)-C(2) | 1.915(7) | C(1)-Re(01)-C(3) | 87.8(3) |
| Re(01)-C(3) | 1.916(6) | C(2)-Re(01)-C(3) | 88.7(3) |
| Re(01)-O(12) | 2.121(4) | C(1)-Re(01)-O(12) | 171.1(2) |
| Re(01)-O(11) | 2.129(4) | C(2)-Re(01)-O(12) | 100.1(2) |
| Re(01)-N(1) | 2.205(4) | C(3)-Re(01)-O(12) | 97.0(2) |
| C(3)-O(3) | 1.152(7) | C(1)-Re(01)-O(11) | 97.3(2) |
| N(1)-C(21) | 1.348(8) | C(2)-Re(01)-O(11) | 173.9(2) |
| N(1)-C(25) | 1.352(7) | C(3)-Re(01)-O(11) | 95.5(2) |
| O(12)-C(12) | 1.302(8) | O(12)-Re(01)-O(11) | 74.90(18) |
| C(27)-N(2) | 1.460(7) | C(1)-Re(01)-N(1) | 92.7(2) |
| C(27)-H(27A) | 0.9600 | C(2)-Re(01)-N(1) | 94.7(2) |
| C(27)-H(27C) | 0.9600 | C(3)-Re(01)-N(1) | 176.6(2) |
| C(27)-H(27B) | 0.9600 | O(12)-Re(01)-N(1) | 82.01(16) |
| N(2)-C(23) | 1.349(7) | O(11)-Re(01)-N(1) | 81.20(17) |
| N(2)-C(26) | 1.444(8) | O(3)-C(3)-Re(01) | 178.2(6) |
| C(1)-O(1) | 1.165(7) | C(21)-N(1)-C(25) | 116.0(5) |
| C(2)-O(2) | 1.154(8) | C(21)-N(1)-Re(01) | 120.2(4) |
| O(11)-C(11) | 1.293(7) | C(25)-N(1)-Re(01) | 123.9(4) |
| C(24)-C(25) | 1.372(8) | C(12)-O(12)-Re(01) | 116.2(4) |
| C(24)-C(23) | 1.418(11) | N(2)-C(27)-H(27A) | 109.5 |

| | | | |
|---|---|---|---|
| C(24)-H(24) | 0.9300 | N(2)-C(27)-H(27C) | 109.5 |
| C(26)-H(26C) | 0.9600 | H(27A)-C(27)-H(27C) | 109.5 |
| C(26)-H(26B) | 0.9600 | N(2)-C(27)-H(27B) | 109.5 |
| C(26)-H(26A) | 0.9600 | H(27A)-C(27)-H(27B) | 109.5 |
| C(23)-C(22) | 1.413(10) | H(27C)-C(27)-H(27B) | 109.5 |
| C(22)-C(21) | 1.368(9) | C(23)-N(2)-C(26) | 122.3(6) |
| C(22)-H(22) | 0.9300 | C(23)-N(2)-C(27) | 120.3(5) |
| C(12)-C(13) | 1.406(8) | C(26)-N(2)-C(27) | 116.6(5) |
| C(12)-C(11) | 1.456(10) | O(1)-C(1)-Re(01) | 178.0(5) |
| C(25)-H(25) | 0.9300 | O(2)-C(2)-Re(01) | 179.1(5) |
| C(11)-C(17) | 1.399(9) | C(11)-O(11)-Re(01) | 116.3(4) |
| C(14)-C(15) | 1.342(11) | C(25)-C(24)-C(23) | 120.2(6) |
| C(14)-C(13) | 1.405(10) | C(25)-C(24)-H(24) | 119.9 |
| C(14)-H(14) | 0.9300 | C(23)-C(24)-H(24) | 119.9 |
| C(15)-C(16) | 1.394(10) | N(2)-C(26)-H(26C) | 109.5 |
| C(15)-H(15) | 0.9300 | N(2)-C(26)-H(26B) | 109.5 |
| C(17)-C(16) | 1.381(9) | H(26C)-C(26)-H(26B) | 109.5 |
| C(17)-H(17) | 0.9300 | N(2)-C(26)-H(26A) | 109.5 |
| C(16)-H(16) | 0.9300 | H(26C)-C(26)-H(26A) | 109.5 |
| C(13)-H(13) | 0.9300 | H(26B)-C(26)-H(26A) | 109.5 |
| C(21)-H(21) | 0.9300 | N(2)-C(23)-C(22) | 120.7(7) |
| | | N(2)-C(23)-C(24) | 123.8(6) |
| | | C(22)-C(23)-C(24) | 115.4(6) |
| | | C(21)-C(22)-C(23) | 120.0(7) |
| | | C(21)-C(22)-H(22) | 120.0 |
| | | C(23)-C(22)-H(22) | 120.0 |
| | | O(12)-C(12)-C(13) | 117.8(7) |
| | | O(12)-C(12)-C(11) | 115.9(5) |
| | | C(13)-C(12)-C(11) | 126.2(7) |
| | | N(1)-C(25)-C(24) | 123.9(6) |
| | | N(1)-C(25)-H(25) | 118.0 |
| | | C(24)-C(25)-H(25) | 118.0 |
| | | O(11)-C(11)-C(17) | 118.1(7) |
| | | O(11)-C(11)-C(12) | 115.6(6) |
| | | C(17)-C(11)-C(12) | 126.4(6) |
| | | C(15)-C(14)-C(13) | 130.2(7) |
| | | C(15)-C(14)-H(14) | 114.9 |
| | | C(13)-C(14)-H(14) | 114.9 |
| | | C(14)-C(15)-C(16) | 127.8(6) |
| | | C(14)-C(15)-H(15) | 116.1 |
| | | C(16)-C(15)-H(15) | 116.1 |
| | | C(16)-C(17)-C(11) | 130.2(7) |
| | | C(16)-C(17)-H(17) | 114.9 |
| | | C(11)-C(17)-H(17) | 114.9 |
| | | C(17)-C(16)-C(15) | 129.4(7) |
| | | C(17)-C(16)-H(16) | 115.3 |
| | | C(15)-C(16)-H(16) | 115.3 |
| | | C(14)-C(13)-C(12) | 129.4(7) |
| | | C(14)-C(13)-H(13) | 115.3 |
| | | C(12)-C(13)-H(13) | 115.3 |
| | | N(1)-C(21)-C(22) | 124.5(6) |
| | | N(1)-C(21)-H(21) | 117.7 |
| | | C(22)-C(21)-H(21) | 117.7 |

**Table A.21: Anisotropic displacement parameters ($Å^2$ x $10^3$) for *fac*-[Re(Trop)$(CO)_3$(DMAP)] (4). The Anisotropic displacement factor exponent takes the form: $-2\pi^2(h2a^{*2}U^{11} + \ldots + 2hka^*b^*U^{12})$.**

| | U11 | U22 | U33 | U23 | U13 | U12 |
|---|---|---|---|---|---|---|
| Re(01) | 16(1) | 14(1) | 34(1) | -1(1) | -5(1) | 0(1) |
| C(3) | 28(3) | 20(3) | 45(3) | 7(3) | -9(3) | -2(2) |
| N(1) | 15(2) | 20(2) | 30(2) | -7(2) | -2(2) | 0(2) |
| O(12) | 36(2) | 19(2) | 45(3) | -9(2) | -19(2) | 6(2) |
| C(27) | 34(3) | 44(4) | 22(3) | -11(3) | 7(2) | -16(3) |
| N(2) | 21(2) | 31(2) | 23(2) | -5(2) | 1(2) | -5(2) |
| C(1) | 17(2) | 27(3) | 34(3) | 4(2) | 2(2) | -2(2) |
| C(2) | 20(3) | 25(3) | 40(3) | -10(3) | -1(2) | 1(2) |
| O(11) | 24(2) | 26(2) | 37(2) | 8(2) | -5(2) | -6(2) |
| C(24) | 21(2) | 39(2) | 47(3) | 13(2) | -6(2) | -11(2) |
| O(2) | 41(3) | 44(3) | 38(3) | -6(2) | 11(2) | -5(2) |
| C(26) | 21(3) | 42(4) | 64(5) | -6(3) | -5(3) | -4(3) |
| O(1) | 28(2) | 28(2) | 55(3) | 3(2) | 5(2) | 10(2) |
| O(3) | 35(3) | 31(2) | 74(4) | 11(2) | -24(2) | -14(2) |
| C(23) | 29(2) | 33(2) | 52(3) | 15(2) | -14(2) | -13(2) |
| C(22) | 33(2) | 24(2) | 64(3) | -6(2) | -16(2) | -2(2) |
| C(12) | 29(3) | 19(3) | 56(4) | -1(3) | -25(3) | -7(2) |
| C(25) | 20(2) | 34(2) | 41(2) | 7(2) | -4(2) | -7(2) |
| C(11) | 22(3) | 25(3) | 51(4) | 8(3) | -16(3) | -11(2) |
| C(14) | 33(2) | 24(2) | 64(3) | -6(2) | -16(2) | -2(2) |
| C(15) | 29(2) | 33(2) | 52(3) | 15(2) | -14(2) | -13(2) |
| C(17) | 20(2) | 34(2) | 41(2) | 7(2) | -4(2) | -7(2) |
| C(16) | 21(2) | 39(2) | 47(3) | 13(2) | -6(2) | -11(2) |
| C(13) | 32(2) | 24(2) | 54(3) | -9(2) | -13(2) | 3(2) |
| C(21) | 32(2) | 24(2) | 54(3) | -9(2) | -13(2) | 3(2) |

**Table A.22: Hydrogen coordinates (x $10^4$) and isotropic displacement parameters ($Å^2$ x $10^3$) for *fac*-[Re(Trop)$(CO)_3$(DMAP)] (4).**

| | x | y | z | U(eq) |
|---|---|---|---|---|
| H(27A) | 7849 | 4944 | 7166 | 49 |
| H(27C) | 6035 | 4596 | 7241 | 49 |
| H(27B) | 6304 | 5319 | 6490 | 49 |
| H(24) | 6754 | 2877 | 4792 | 45 |
| H(26C) | 9385 | 3995 | 6667 | 65 |
| H(26B) | 8985 | 3662 | 5626 | 65 |
| H(26A) | 8509 | 3070 | 6446 | 65 |
| H(22) | 3844 | 4546 | 6064 | 51 |
| H(25) | 4392 | 2410 | 3857 | 39 |
| H(14) | 3596 | -782 | 5331 | 51 |
| H(15) | 2914 | -575 | 6701 | 48 |
| H(17) | -3 | 1554 | 6341 | 39 |
| H(16) | 1292 | 475 | 7153 | 45 |
| H(13) | 3120 | 56 | 4069 | 46 |
| H(21) | 1586 | 4005 | 5103 | 46 |

**Table A.23: Torsion angles (°) for *fac*-[Re(Trop)$(CO)_3$(DMAP)] (4).**

| Torsion Angle | Angle | Torsion Angle | Angle |
|---|---|---|---|
| O12-Re01-O11-C11 | -9.3(4) | Re01-O11-C11-C12 | 9.7(7) |
| N1-Re01-O11-C11 | 74.7(4) | Re01-O11-C11-C17 | -170.1(4) |

| | | | |
|---|---|---|---|
| C1-Re01-O11-C11 | 166.4(4) | Re01-O12-C12-C13 | 176.6(4) |
| C3-Re01-O11-C11 | -105.1(4) | Re01-O12-C12-C11 | -5.0(7) |
| O11-Re01-O12-C12 | 7.5(4) | Re01-N1-C25-C24 | 179.3(5) |
| N1-Re01-O12-C12 | -75.5(4) | C21-N1-C25-C24 | 0.4(9) |
| C2-Re01-O12-C12 | -168.9(5) | C25-N1-C21-C22 | -1.0(9) |
| C3-Re01-O12-C12 | 101.2(5) | Re01-N1-C21-C22 | -179.9(5) |
| O11-Re01-N1-C21 | 66.6(4) | C27-N2-C23-C22 | 1.2(9) |
| O11-Re01-N1-C25 | -112.2(5) | C27-N2-C23-C24 | -177.7(6) |
| O12-Re01-N1-C21 | 142.5(5) | C26-N2-C23-C22 | -168.2(6) |
| O12-Re01-N1-C25 | -36.3(5) | C26-N2-C23-C24 | 12.9(10) |
| C1-Re01-N1-C21 | -30.4(5) | C12-C11-C17-C16 | -1.2(11) |
| C1-Re01-N1-C25 | 150.9(5) | C17-C11-C12-O12 | 176.6(6) |
| C2-Re01-N1-C21 | -117.9(5) | C17-C11-C12-C13 | -5.1(11) |
| C2-Re01-N1-C25 | 63.3(5) | O11-C11-C17-C16 | 178.6(6) |
| O11-C11-C12-C13 | 175.1(6) | C15-C16-C17-C11 | 4.4(12) |
| O11-C11-C12-O12 | -3.2(8) | N1-C21-C22-C23 | 1.2(11) |
| O12-C12-C13-C14 | -176.3(7) | C21-C22-C23-N2 | -179.7(6) |
| C11-C12-C13-C14 | 5.5(11) | C21-C22-C23-C24 | -0.7(10) |
| C12-C13-C14-C15 | 0.8(13) | N2-C23-C24-C25 | 179.2(6) |
| C13-C14-C15-C16 | -4.3(13) | C22-C23-C24-C25 | 0.2(10) |
| C14-C15-C16-C17 | 0.1(12) | C23-C24-C25-N1 | -0.1(11) |

**Table A.24: Hydrogen bond distances (Å) and angles (°) for *fac*-[Re(Trop)(CO)$_3$(DMAP)] (4).**

| D-H…A | d (D-H) | d (H…A) | d (D…A) | D-H…A angle |
|---|---|---|---|---|
| C15-H15…O3#1 | 0.93 | 2.58 | 3.449(8) | 155.4 |
| C22-H22…O1#2 | 0.93 | 2.58 | 3.297(9) | 134.1 |
| C25-H25…O12 | 0.93 | 2.57 | 2.994(7) | 108.4 |
| C27-H27C…O12#3 | 0.96 | 2.55 | 3.229(8) | 128.0 |

Symmetry codes, transformations used to generate equivalent atoms:
#1 -x,-y,1-z #2 -x,1-y,1-z #3 0.5+x,0.5-y,0.5+z

# Appendix A

**Table A.25: Atomic coordinates (x $10^4$) and equivalent isotropic displacement parameters ($Å^2$ x $10^3$) for *fac*-[$NEt_4$][Re(2,5-PicoH)$(CO)_3$(Br)].$H_2O$ (5). U(eq) is defined as one third of the trace of the orthogonalized $U^{ij}$ tensor.**

| | x | y | z | U(eq) |
|---|---|---|---|---|
| Re(1) | 7431(1) | 3485(1) | 2299(1) | 13(1) |
| Br(1) | 6775(1) | 3910(1) | 4811(1) | 18(1) |
| N(1) | 6878(5) | 4094(2) | 411(8) | 13(1) |
| O(4) | 9144(4) | 3881(2) | 3790(7) | 16(1) |
| C(16) | 9095(6) | 4269(2) | 3107(10) | 14(1) |
| C(15) | 7805(6) | 4407(2) | 1170(10) | 15(1) |
| C(11) | 5692(6) | 4204(2) | -1205(10) | 14(1) |
| O(1) | 4828(5) | 3021(2) | -350(9) | 26(1) |
| C(1) | 5814(6) | 3191(2) | 710(11) | 17(1) |
| C(12) | 5354(6) | 4610(2) | -2124(10) | 15(1) |
| C(13) | 6315(6) | 4933(2) | -1353(11) | 16(1) |
| C(14) | 7568(6) | 4817(2) | 321(11) | 17(1) |
| O(5) | 9993(4) | 4528(2) | 3901(8) | 22(1) |
| C(2) | 8096(6) | 3009(2) | 4333(12) | 20(1) |
| O(3) | 8081(5) | 2970(2) | -658(9) | 24(1) |
| C(3) | 7866(6) | 3169(2) | 332(12) | 20(1) |
| O(2) | 8520(6) | 2721(2) | 5592(10) | 38(2) |
| C(17) | 3983(6) | 4701(2) | -3774(11) | 16(1) |
| O(7) | 3167(4) | 4413(2) | -4339(8) | 23(1) |
| O(6) | 3736(5) | 5103(2) | -4516(9) | 24(1) |
| N(2) | 2124(6) | 3431(2) | -8271(10) | 14(1) |
| C(23) | 1386(6) | 3848(2) | -8438(12) | 19(1) |
| C(24) | 50(6) | 3886(2) | -10494(12) | 20(1) |
| C(28) | 4312(6) | 3082(2) | -5664(12) | 22(1) |
| C(27) | 3422(8) | 3474(2) | -6243(13) | 19(2) |
| C(21) | 2217(7) | 3384(2) | -10353(12) | 20(1) |
| C(22) | 2774(8) | 3776(3) | -10874(13) | 28(2) |
| C(25) | 1422(6) | 3026(2) | -8177(11) | 19(1) |
| C(26) | 1275(8) | 2998(3) | -6136(14) | 28(2) |
| O(8) | 1303(5) | 5223(2) | -6761(9) | 26(1) |

**Table A.26: Bond distances (Å) and angles (°) for *fac*-[$NEt_4$][Re(2,5-PicoH)$(CO)_3$(Br)].$H_2O$ (5).**

| Bond | Bond Distance | Bond Angle | Angle |
|---|---|---|---|
| Re(1)-C(2) | 1.904(7) | C(2)-Re(1)-C(1) | 89.3(3) |
| Re(1)-C(1) | 1.906(7) | C(2)-Re(1)-C(3) | 89.2(3) |
| Re(1)-C(3) | 1.963(8) | C(1)-Re(1)-C(3) | 85.5(3) |
| Re(1)-O(4) | 2.152(5) | C(2)-Re(1)-O(4) | 97.9(2) |
| Re(1)-N(1) | 2.182(5) | C(1)-Re(1)-O(4) | 172.8(2) |
| Re(1)-Br(1) | 2.6188(13) | C(3)-Re(1)-O(4) | 94.6(2) |
| N(1)-C(11) | 1.335(8) | C(2)-Re(1)-N(1) | 171.0(2) |
| N(1)-C(15) | 1.358(8) | C(1)-Re(1)-N(1) | 98.4(2) |
| O(4)-C(16) | 1.268(8) | C(3)-Re(1)-N(1) | 96.0(2) |
| C(16)-O(5) | 1.223(8) | O(4)-Re(1)-N(1) | 74.38(18) |
| C(16)-C(15) | 1.509(8) | C(2)-Re(1)-Br(1) | 92.0(2) |
| C(15)-C(14) | 1.356(9) | C(1)-Re(1)-Br(1) | 93.1(2) |
| C(11)-C(12) | 1.363(9) | C(3)-Re(1)-Br(1) | 178.1(2) |
| C(11)-H(11) | 0.9300 | O(4)-Re(1)-Br(1) | 86.60(13) |
| O(1)-C(1) | 1.154(8) | N(1)-Re(1)-Br(1) | 82.99(14) |
| C(12)-C(13) | 1.403(9) | C(11)-N(1)-C(15) | 117.6(6) |

| | |
|---|---|
| C(12)-C(17) | 1.479(9) |
| C(13)-C(14) | 1.403(9) |
| C(13)-H(13) | 0.9300 |
| C(14)-H(14) | 0.9300 |
| C(2)-O(2) | 1.161(8) |
| O(3)-C(3) | 1.052(9) |
| C(17)-O(7) | 1.227(9) |
| C(17)-O(6) | 1.311(9) |
| O(7)-H(7) | 0.8200 |
| N(2)-C(27) | 1.485(12) |
| N(2)-C(25) | 1.522(8) |
| N(2)-C(21) | 1.525(9) |
| N(2)-C(23) | 1.529(9) |
| C(23)-C(24) | 1.517(9) |
| C(23)-H(23A) | 0.9700 |
| C(23)-H(23B) | 0.9700 |
| C(24)-H(24C) | 0.9600 |
| C(24)-H(24A) | 0.9600 |
| C(24)-H(24B) | 0.9600 |
| C(28)-C(27) | 1.522(10) |
| C(28)-H(28A) | 0.9600 |
| C(28)-H(28C) | 0.9600 |
| C(28)-H(28B) | 0.9600 |
| C(27)-H(27B) | 0.9700 |
| C(27)-H(27A) | 0.9700 |
| C(21)-C(22) | 1.509(11) |
| C(21)-H(21A) | 0.9700 |
| C(21)-H(21B) | 0.9700 |
| C(22)-H(22A) | 0.9600 |
| C(22)-H(22B) | 0.9600 |
| C(22)-H(22C) | 0.9600 |
| C(25)-C(26) | 0.9600 |
| C(25)-H(25A) | 0.9700 |
| C(25)-H(25B) | 0.9700 |
| C(26)-H(26A) | 0.9600 |
| C(26)-H(26B) | 0.9600 |
| C(26)-H(26C) | 0.9600 |
| O(8)-H(8A) | 0.85(6) |
| O(8)-H(8B) | 0.86(7) |

| | |
|---|---|
| C(11)-N(1)-Re(1) | 126.2(4) |
| C(15)-N(1)-Re(1) | 115.6(4) |
| C(16)-O(4)-Re(1) | 119.8(4) |
| O(5)-C(16)-O(4) | 125.2(6) |
| O(5)-C(16)-C(15) | 119.5(6) |
| O(4)-C(16)-C(15) | 115.3(5) |
| C(14)-C(15)-N(1) | 122.4(6) |
| C(14)-C(15)-C(16) | 122.8(6) |
| N(1)-C(15)-C(16) | 114.7(6) |
| N(1)-C(11)-C(12) | 124.2(6) |
| N(1)-C(11)-H(11) | 117.9 |
| C(12)-C(11)-H(11) | 117.9 |
| O(1)-C(1)-Re(1) | 176.5(6) |
| C(11)-C(12)-C(13) | 118.1(6) |
| C(11)-C(12)-C(17) | 118.9(6) |
| C(13)-C(12)-C(17) | 122.9(6) |
| C(12)-C(13)-C(14) | 118.0(6) |
| C(12)-C(13)-H(13) | 121.0 |
| C(14)-C(13)-H(13) | 121.0 |
| C(15)-C(14)-C(13) | 119.6(6) |
| C(15)-C(14)-H(14) | 120.2 |
| C(13)-C(14)-H(14) | 120.2 |
| O(2)-C(2)-Re(1) | 179.0(7) |
| O(3)-C(3)-Re(1) | 174.0(7) |
| O(7)-C(17)-O(6) | 124.5(6) |
| O(7)-C(17)-C(12) | 120.6(6) |
| O(6)-C(17)-C(12) | 114.9(6) |
| C(17)-O(7)-H(7) | 109.5 |
| C(27)-N(2)-C(25) | 111.7(5) |
| C(27)-N(2)-C(21) | 111.3(6) |
| C(25)-N(2)-C(21) | 106.4(5) |
| C(27)-N(2)-C(23) | 106.6(5) |
| C(25)-N(2)-C(23) | 111.5(5) |
| C(21)-N(2)-C(23) | 109.4(5) |
| C(24)-C(23)-N(2) | 115.5(6) |
| C(24)-C(23)-H(23A) | 115.5(6) |
| N(2)-C(23)-H(23A) | 108.4 |
| C(24)-C(23)-H(23B) | 108.4 |
| N(2)-C(23)-H(23B) | 108.4 |
| H(23A)-C(23)-H(23B) | 107.5 |
| C(23)-C(24)-H(24C) | 109.5 |
| C(23)-C(24)-H(24A) | 109.5 |
| H(24C)-C(24)-H(24A) | 109.5 |
| C(23)-C(24)-H(24B) | 109.5 |
| H(24C)-C(24)-H(24B) | 109.5 |
| H(24A)-C(24)-H(24B) | 109.5 |
| C(27)-C(28)-H(28A) | 109.5 |
| C(27)-C(28)-H(28C) | 109.5 |
| H(28A)-C(28)-H(28C) | 109.5 |
| C(27)-C(28)-H(28B) | 109.5 |
| H(28A)-C(28)-H(28B) | 109.5 |
| H(28C)-C(28)-H(28B) | 109.5 |
| N(2)-C(27)-C(28) | 116.0(6) |
| N(2)-C(27)-H(27B) | 108.3 |
| C(28)-C(27)-H(27B) | 108.3 |

| | |
|---|---|
| N(2)-C(27)-H(27A) | 108.3 |
| C(28)-C(27)-H(27A) | 108.3 |
| H(27B)-C(27)-H(27A) | 107.4 |
| C(22)-C(21)-N(2) | 114.7(6) |
| C(22)-C(21)-H(21A) | 108.6 |
| N(2)-C(21)-H(21A) | 108.6 |
| C(22)-C(21)-H(21B) | 108.6 |
| N(2)-C(21)-H(21B) | 108.6 |
| H(21A)-C(21)-H(21B) | 107.6 |
| C(21)-C(22)-H(22A) | 109.5 |
| C(21)-C(22)-H(22B) | 109.5 |
| H(22A)-C(22)-H(22B) | 109.5 |
| C(21)-C(22)-H(22C) | 109.5 |
| H(22A)-C(22)-H(22C) | 109.5 |
| H(22B)-C(22)-H(22C) | 109.5 |
| N(2)-C(25)-C(26) | 114.9(6) |
| N(2)-C(25)-H(25A) | 108.5 |
| C(26)-C(25)-H(25A) | 108.5 |
| N(2)-C(25)-H(25B) | 108.5 |
| C(26)-C(25)-H(25B) | 108.5 |
| H(25A)-C(25)-H(25B) | 107.5 |
| C(25)-C(26)-H(26A) | 109.5 |
| C(25)-C(26)-H(26B) | 109.5 |
| H(26A)-C(26)-H(26B) | 109.5 |
| C(25)-C(26)-H(26C) | 109.5 |
| H(26A)-C(26)-H(26C) | 109.5 |
| H(26B)-C(26)-H(26C) | 109.5 |
| H(8A)-O(8)-H(8B) | 108(2) |

**Table A.27: Anisotropic displacement parameters ($Å^2$ x $10^3$) for *fac*-[$NEt_4$][Re(2,5-PicoH)$(CO)_3$(Br)].$H_2O$ (5). The Anisotropic displacement factor exponent takes the form: $-2\pi^2(h2a^{*2}U^{11} + \ldots + 2hka^*b^*U^{12})$.**

| | U11 | U22 | U33 | U23 | U13 | U12 |
|---|---|---|---|---|---|---|
| Re(1) | 10(1) | 13(1) | 17(1) | 1(1) | 8(1) | 1(1) |
| Br(1) | 16(1) | 20(1) | 21(1) | -1(1) | 11(1) | 1(1) |
| N(1) | 10(2) | 13(2) | 17(3) | -2(2) | 9(2) | -2(2) |
| O(4) | 11(2) | 20(2) | 13(2) | 0(2) | 3(2) | 1(2) |
| C(16) | 9(3) | 21(3) | 15(3) | -3(3) | 7(2) | 0(2) |
| C(15) | 10(3) | 22(3) | 14(3) | -1(3) | 6(2) | 1(2) |
| C(11) | 10(3) | 17(3) | 16(3) | 1(2) | 6(2) | 1(2) |
| O(1) | 18(2) | 27(3) | 37(3) | -10(2) | 17(2) | -11(2) |
| C(1) | 21(3) | 15(3) | 21(3) | 1(3) | 15(3) | 6(3) |
| C(12) | 11(3) | 18(3) | 16(3) | -2(2) | 6(2) | 2(2) |
| C(13) | 15(3) | 15(3) | 18(3) | 5(3) | 9(3) | 4(2) |
| C(14) | 10(3) | 19(3) | 20(3) | -4(3) | 7(3) | -5(2) |
| O(5) | 11(2) | 26(3) | 22(2) | -5(2) | 4(2) | -7(2) |
| C(2) | 13(2) | 17(2) | 26(3) | 2(2) | 8(2) | 0(2) |
| O(3) | 12(2) | 35(3) | 25(3) | 7(2) | 9(2) | 0(2) |
| C(3) | 13(2) | 17(2) | 26(3) | 2(2) | 8(2) | 0(2) |
| O(2) | 62(4) | 26(3) | 38(3) | 16(3) | 35(3) | 20(3) |
| C(17) | 13(3) | 18(3) | 18(3) | 4(3) | 9(3) | 2(3) |
| O(7) | 13(2) | 20(3) | 23(2) | 2(2) | -1(2) | 2(2) |
| O(6) | 17(2) | 20(3) | 28(3) | 9(2) | 6(2) | 4(2) |

| | | | | | | |
|---|---|---|---|---|---|---|
| N(2) | 6(3) | 19(3) | 16(3) | -3(2) | 6(3) | -4(2) |
| C(23) | 16(3) | 21(4) | 22(3) | 1(3) | 11(3) | 2(3) |
| (24) | 13(3) | 24(4) | 22(3) | 0(3) | 7(3) | -1(2) |
| C(28) | 16(3) | 29(4) | 21(3) | -1(3) | 11(3) | -1(3) |
| C(27) | 17(4) | 20(4) | 19(4) | -4(3) | 10(3) | -4(2) |
| C(21) | 19(3) | 26(4) | 17(3) | -2(3) | 11(3) | 0(3) |
| C(22) | 32(4) | 30(4) | 29(4) | -1(3) | 22(3) | -1(3) |
| C(25) | 14(3) | 18(3) | 22(3) | -1(3) | 8(3) | -5(3) |
| C(26) | 26(4) | 33(4) | 37(4) | 6(3) | 25(3) | -2(3) |
| O(8) | 12(3) | 26(3) | 36(3) | 2(2) | 8(2) | -4(2) |

**Table A.28: Hydrogen coordinates (x $10^4$) and isotropic displacement parameters ($Å^2$ x $10^3$) for *fac*-[$NEt_4$][Re(2,5-PicoH)$(CO)_3$(Br)].$H_2O$ (5).**

| | x | y | z | U(eq) |
|---|---|---|---|---|
| H(11) | 5056 | 3990 | -1739 | 17 |
| H(13) | 6127 | 5214 | -1934 | 19 |
| H(14) | 8232 | 5021 | 844 | 20 |
| H(7) | 2458 | 4510 | -5265 | 35 |
| H(23A) | 1304 | 3867 | -7134 | 23 |
| H(23B) | 1894 | 4096 | -8403 | 23 |
| H(24C) | -338 | 4156 | -10447 | 31 |
| H(24A) | -474 | 3646 | -10533 | 31 |
| H(24B) | 117 | 3879 | -11801 | 31 |
| H(28A) | 5122 | 3143 | -4338 | 32 |
| H(28C) | 4454 | 3023 | -6868 | 32 |
| H(28B) | 3922 | 2831 | -5420 | 32 |
| H(27B) | 3311 | 3533 | -4990 | 22 |
| H(27A) | 3845 | 3726 | -6427 | 22 |
| H(21A) | 2745 | 3131 | -10176 | 23 |
| H(21B) | 1360 | 3329 | -11614 | 23 |
| H(22A) | 2798 | 3720 | -12201 | 41 |
| H(22B) | 3633 | 3829 | -9656 | 41 |
| H(22C) | 2246 | 4027 | -11095 | 41 |
| H(25A) | 1885 | 2769 | -8204 | 23 |
| H(25B) | 570 | 3018 | -9504 | 23 |
| H(26A) | 823 | 2735 | -6208 | 42 |
| H(26B) | 796 | 3246 | -6111 | 42 |
| H(26C) | 2112 | 2996 | -4810 | 42 |
| H(8A) | 760(50) | 5016(15) | -7130(140) | 20(20) |
| H(8B) | 1980(40) | 5120(20) | -6690(160) | 40(30) |

**Table A.29: Torsion angles (°) for *fac*-[$NEt_4$][Re(2,5-PicoH)$(CO)_3$(Br)].$H_2O$ (5).**

| Torsion Angle | Angle | Torsion Angle | Angle |
|---|---|---|---|
| C3-Re1-O4-C16 | -98.8(5) | C11-C12-C17-O7 | 1.5(11) |
| Br1-Re1-N1-C11 | 86.6(6) | C13-C12-C17-O6 | -1.9(11) |
| Br1-Re1-N1-C15 | -84.4(5) | Re1-N1-C15-C14 | 173.0(6) |
| O4-Re1-N1-C11 | 175.0(6) | Re1-N1-C15-C16 | -4.0(8) |
| O4-Re1-N1-C15 | 4.1(5) | C11-N1-C15-C14 | 1.2(10) |
| C1-Re1-N1-C11 | -5.5(6) | C11-N1-C15-C16 | -175.8(6) |
| C1-Re1-N1-C15 | -176.4(5) | N1-C11-C12-C13 | -1.1(11) |
| C3-Re1-N1-C11 | -91.9(6) | N1-C11-C12-C17 | 175.0(7) |
| C3-Re1-N1-C15 | 97.2(5) | C11-C12-C13-C14 | 0.0(10) |

| | | | |
|---|---|---|---|
| Br1-Re1-O4-C16 | 79.8(5) | C17-C12-C13-C14 | -175.8(7) |
| N1-Re1-O4-C16 | -3.8(5) | C11-C12-C17-O6 | -177.8(7) |
| C2-Re1-O4-C16 | 171.4(5) | C27-N2-C23-C24 | -176.2(7) |
| Re1-O4-C16-O5 | -176.5(5) | C21-N2-C25-C26 | -177.5(7) |
| Re1-O4-C16-C15 | 2.9(8) | C23-N2-C25-C26 | 63.3(8) |
| C25-N2-C27-C28 | -54.7(10) | C27-N2-C25-C26 | -56.0(9) |
| C23-N2-C21-C22 | -53.8(9) | C21-N2-C27-C28 | 64.1(9) |
| C25-N2-C21-C22 | -174.4(7) | C23-N2-C27-C28 | -176.8(7) |
| C27-N2-C21-C22 | 63.7(8) | Re1-N1-C11-C12 | -170.3(5) |
| C21-N2-C23-C24 | -55.9(9) | C15-N1-C11-C12 | 0.5(10) |
| C25-N2-C23-C24 | 61.6(8) | N1-C15-C16-O4 | 0.8(9) |
| C12-C13-C14-C15 | 1.5(11) | C13-C14-C15-C16 | 174.5(7) |
| C14-C15-C16-O5 | 3.4(11) | C13-C14-C15-N1 | -2.2(11) |
| C14-C15-C16-O4 | -176.1(7) | C13-C12-C17-O7 | 177.3(7) |
| N1-C15-C16-O5 | -179.7(6) | | |

**Table A.30: Hydrogen bond distances (Å) and angles (°) for *fac*-[$NEt_4$][Re(2,5-PicoH)$(CO)_3$(Br)].$H_2O$ (5).**

| D-H…A | d (D-H) | d (H…A) | d (D…A) | D-H…A angle |
|---|---|---|---|---|
| O7-H7…O8 | 0.82 | 2.51 | 3.192(7) | 141.0 |
| O8-H8B…O6 | 0.852(5) | 1.87(6) | 2.550(7) | 135(8) |
| C11-H11…O7 | 0.93 | 2.43 | 2.766(8) | 100.9 |
| C13-H13…Br1#1 | 0.93 | 2.88 | 3.613(7) | 136(4) |
| C22-H22C…O8#1 | 0.96 | 2.50 | 3.436(10) | 165.6 |
| O8-H8A…O5#2 | 0.851(5) | 2.08(5) | 2.830(8) | 148(8) |

Symmetry codes, transformations used to generate equivalent atoms:
#1 x,1-y,-0.5+z #2 -1+x,y,-1+z

# Appendix A

**Table A.31: Atomic coordinates (x $10^4$) and equivalent isotropic displacement parameters ($Å^2$ x $10^3$) for *fac*-[$NEt_4$][Re(2,5-PicoMe)$(CO)_3$(Br)] (6). U(eq) is defined as one third of the trace of the orthogonalized $U^{ij}$ tensor.**

| | x | y | z | U(eq) |
|---|---|---|---|---|
| Re(01) | 8015(1) | 6602(1) | 6072(1) | 16(1) |
| N(1) | 6791(3) | 5547(3) | 5728(1) | 16(1) |
| O(4) | 6778(2) | 6857(2) | 6465(1) | 21(1) |
| N(2) | 7495(3) | 884(3) | 6916(1) | 17(1) |
| C(3) | 7626(4) | 7817(4) | 5655(2) | 21(1) |
| C(13) | 5254(3) | 4028(4) | 5474(2) | 20(1) |
| C(14) | 5191(3) | 4754(4) | 5839(2) | 21(1) |
| C(21) | 8508(4) | -451(4) | 7506(2) | 25(1) |
| C(20) | 8384(4) | 93(4) | 7019(2) | 27(1) |
| C(25) | 6789(4) | 2240(4) | 6262(2) | 31(1) |
| C(15) | 5959(3) | 5494(3) | 5959(2) | 17(1) |
| C(11) | 6842(3) | 4859(3) | 5367(2) | 16(1) |
| C(12) | 6091(3) | 4085(3) | 5232(2) | 16(1) |
| C(23) | 8544(4) | 2358(4) | 7379(2) | 36(1) |
| C(24) | 7579(4) | 1394(4) | 6432(2) | 32(1) |
| C(22) | 7566(4) | 1702(4) | 7315(2) | 22(1) |
| O(3) | 7450(3) | 8502(3) | 5419(2) | 39(1) |
| O(2) | 9629(3) | 7949(3) | 6726(2) | 35(1) |
| C(2) | 9028(4) | 7444(4) | 6481(2) | 23(1) |
| O(1) | 9644(3) | 5964(3) | 5462(1) | 28(1) |
| C(1) | 9035(3) | 6222(3) | 5692(2) | 18(1) |
| O(5) | 5191(3) | 6342(3) | 6560(1) | 28(1) |
| C(16) | 5961(4) | 6286(3) | 6365(2) | 20(1) |
| C(26) | 6463(3) | 338(4) | 6898(2) | 21(1) |
| C(27) | 6206(5) | -527(4) | 6518(2) | 39(1) |
| O(6) | 6974(3) | 3397(3) | 4624(1) | 29(1) |
| O(7) | 5500(3) | 2629(2) | 4753(1) | 27(1) |
| C(17) | 6253(4) | 3346(3) | 4837(2) | 20(1) |
| Br(1) | 8461(1) | 4978(1) | 6648(1) | 23(1) |
| C(18) | 5611(5) | 1813(4) | 4398(2) | 40(1) |

**Table A.32: Bond distances (Å) and angles (°) for *fac*-[$NEt_4$][Re(2,5-PicoMe)$(CO)_3$(Br)] (6).**

| Bond | Bond Distance | Bond Angle | Angle |
|---|---|---|---|
| Re(01)-C(1) | 1.910(4) | C(1)-Re(01)-C(2) | 89.47(19) |
| Re(01)-C(2) | 1.918(5) | C(1)-Re(01)-C(3) | 90.02(18) |
| Re(01)-C(3) | 1.943(5) | C(2)-Re(01)-C(3) | 90.1(2) |
| Re(01)-O(4) | 2.136(3) | C(1)-Re(01)-O(4) | 173.09(15) |
| Re(01)-N(1) | 2.178(4) | C(2)-Re(01)-O(4) | 96.90(16) |
| Re(01)-Br(1) | 2.6129(8) | C(3)-Re(01)-O(4) | 92.63(15) |
| N(1)-C(11) | 1.343(6) | C(1)-Re(01)-N(1) | 97.68(17) |
| N(1)-C(15) | 1.363(5) | C(2)-Re(01)-N(1) | 169.91(17) |
| O(4)-C(16) | 1.282(6) | C(3)-Re(01)-N(1) | 96.99(17) |
| N(2)-C(26) | 1.511(6) | O(4)-Re(01)-N(1) | 75.67(13) |
| N(2)-C(22) | 1.512(6) | C(1)-Re(01)-Br(1) | 92.41(13) |
| N(2)-C(24) | 1.521(6) | C(2)-Re(01)-Br(1) | 90.64(15) |
| N(2)-C(20) | 1.526(5) | C(3)-Re(01)-Br(1) | 177.47(13) |
| C(3)-O(3) | 1.089(6) | O(4)-Re(01)-Br(1) | 84.88(8) |
| C(13)-C(14) | 1.384(7) | N(1)-Re(01)-Br(1) | 82.00(10) |
| C(13)-C(12) | 1.389(6) | C(11)-N(1)-C(15) | 118.2(4) |

| | |
|---|---|
| C(13)-H(13) | 0.9300 |
| C(14)-C(15) | 1.373(6) |
| C(14)-H(14) | 0.9300 |
| C(21)-C(20) | 1.508(7) |
| C(21)-H(21B) | 0.9600 |
| C(21)-H(21A) | 0.9600 |
| C(21)-H(21C) | 0.9600 |
| C(20)-H(20A) | 0.9700 |
| C(20)-H(20B) | 0.9700 |
| C(25)-C(24) | 1.508(7) |
| C(25)-H(25B) | 0.9600 |
| C(25)-H(25C) | 0.9600 |
| C(25)-H(25A) | 0.9600 |
| C(15)-C(16) | 1.512(6) |
| C(11)-C(12) | 1.393(6) |
| C(11)-H(11) | 0.9300 |
| C(12)-C(17) | 1.489(6) |
| C(23)-C(22) | 1.512(7) |
| C(23)-H(23B) | 0.9600 |
| C(23)-H(23C) | 0.9600 |
| C(23)-H(23A) | 0.9600 |
| C(24)-H(24B) | 0.9700 |
| C(24)-H(24A) | 0.9700 |
| C(22)-H(22A) | 0.9700 |
| C(22)-H(22B) | 0.9700 |
| O(2)-C(2) | 1.145(6) |
| O(1)-C(1) | 1.156(5) |
| O(5)-C(16) | 1.231(5) |
| C(26)-C(27) | 1.521(7) |
| C(26)-H(26A) | 0.9700 |
| C(26)-H(26B) | 0.9700 |
| C(27)-H(27B) | 0.9600 |
| C(27)-H(27C) | 0.9600 |
| C(27)-H(27A) | 0.9600 |
| O(6)-C(17) | 1.204(5) |
| O(7)-C(17) | 1.332(5) |
| O(7)-C(18) | 1.455(6) |
| C(18)-H(18A) | 0.9600 |
| C(18)-H(18B) | 0.9600 |
| C(18)-H(18C) | 0.9600 |

| | |
|---|---|
| C(11)-N(1)-Re(01) | 126.9(3) |
| C(15)-N(1)-Re(01) | 114.2(3) |
| C(16)-O(4)-Re(01) | 118.9(3) |
| C(26)-N(2)-C(22) | 106.1(3) |
| C(26)-N(2)-C(24) | 111.5(4) |
| C(22)-N(2)-C(24) | 111.2(4) |
| C(26)-N(2)-C(20) | 111.0(4) |
| C(22)-N(2)-C(20) | 111.2(4) |
| C(24)-N(2)-C(20) | 105.9(3) |
| O(3)-C(3)-Re(01) | 177.1(4) |
| C(14)-C(13)-C(12) | 118.6(4) |
| C(14)-C(13)-H(13) | 120.7 |
| C(12)-C(13)-H(13) | 120.7 |
| C(15)-C(14)-C(13) | 119.7(4) |
| C(15)-C(14)-H(14) | 120.1 |
| C(13)-C(14)-H(14) | 120.1 |
| C(20)-C(21)-H(21B) | 109.5 |
| C(20)-C(21)-H(21A) | 109.5 |
| H(21B)-C(21)-H(21A) | 109.5 |
| C(20)-C(21)-H(21C) | 109.5 |
| H(21B)-C(21)-H(21C) | 109.5 |
| H(21A)-C(21)-H(21C) | 109.5 |
| C(21)-C(20)-N(2) | 115.3(4) |
| C(21)-C(20)-H(20A) | 108.4 |
| N(2)-C(20)-H(20A) | 108.4 |
| C(21)-C(20)-H(20B) | 108.4 |
| N(2)-C(20)-H(20B) | 108.4 |
| H(20A)-C(20)-H(20B) | 107.5 |
| C(24)-C(25)-H(25B) | 109.5 |
| C(24)-C(25)-H(25C) | 109.5 |
| H(25B)-C(25)-H(25C) | 109.5 |
| C(24)-C(25)-H(25A) | 109.5 |
| H(25B)-C(25)-H(25A) | 109.5 |
| H(25C)-C(25)-H(25A) | 109.5 |
| N(1)-C(15)-C(14) | 122.1(4) |
| N(1)-C(15)-C(16) | 115.2(4) |
| C(14)-C(15)-C(16) | 122.7(4) |
| N(1)-C(11)-C(12) | 122.2(4) |
| N(1)-C(11)-H(11) | 118.9 |
| C(12)-C(11)-H(11) | 118.9 |
| C(13)-C(12)-C(11) | 119.1(4) |
| C(13)-C(12)-C(17) | 123.8(4) |
| C(11)-C(12)-C(17) | 117.1(4) |
| C(22)-C(23)-H(23B) | 109.5 |
| C(22)-C(23)-H(23C) | 109.5 |
| H(23B)-C(23)-H(23C) | 109.5 |
| C(22)-C(23)-H(23A) | 109.5 |
| H(23B)-C(23)-H(23A) | 109.5 |
| H(23C)-C(23)-H(23A) | 109.5 |
| C(25)-C(24)-N(2) | 115.4(4) |
| C(25)-C(24)-H(24B) | 108.4 |
| N(2)-C(24)-H(24B) | 108.4 |
| C(25)-C(24)-H(24A) | 108.4 |
| N(2)-C(24)-H(24A) | 108.4 |
| H(24B)-C(24)-H(24A) | 107.5 |

| | |
|---|---|
| N(2)-C(22)-C(23) | 114.0(4) |
| N(2)-C(22)-H(22A) | 108.8 |
| C(23)-C(22)-H(22A) | 108.8 |
| N(2)-C(22)-H(22B) | 108.8 |
| C(23)-C(22)-H(22B) | 108.8 |
| H(22A)-C(22)-H(22B) | 107.7 |
| O(2)-C(2)-Re(01) | 179.6(4) |
| O(1)-C(1)-Re(01) | 178.2(4) |
| O(5)-C(16)-O(4) | 126.1(4) |
| O(5)-C(16)-C(15) | 118.4(4) |
| O(4)-C(16)-C(15) | 115.5(4) |
| N(2)-C(26)-C(27) | 116.1(4) |
| N(2)-C(26)-H(26A) | 108.3 |
| C(27)-C(26)-H(26A) | 108.3 |
| N(2)-C(26)-H(26B) | 108.3 |
| C(27)-C(26)-H(26B) | 108.3 |
| H(26A)-C(26)-H(26B) | 107.4 |
| C(26)-C(27)-H(27B) | 109.5 |
| C(26)-C(27)-H(27C) | 109.5 |
| H(27B)-C(27)-H(27C) | 109.5 |
| C(26)-C(27)-H(27A) | 109.5 |
| H(27B)-C(27)-H(27A) | 109.5 |
| H(27C)-C(27)-H(27A) | 109.5 |
| C(17)-O(7)-C(18) | 116.3(4) |
| O(6)-C(17)-O(7) | 124.9(4) |
| O(6)-C(17)-C(12) | 124.0(4) |
| O(7)-C(17)-C(12) | 111.2(4) |
| O(7)-C(18)-H(18A) | 109.5 |
| O(7)-C(18)-H(18B) | 109.5 |
| H(18A)-C(18)-H(18B) | 109.5 |
| O(7)-C(18)-H(18C) | 109.5 |
| H(18A)-C(18)-H(18C) | 109.5 |
| H(18B)-C(18)-H(18C) | 109.5 |

**Table A.33: Anisotropic displacement parameters ($Å^2$ x $10^3$) for *fac*-[$NEt_4$][Re(2,5-PicoMe)$(CO)_3$(Br)] (6). The Anisotropic displacement factor exponent takes the form: $-2\pi^2(h2a^{*2}U^{11} + \ldots + 2hka^*b^*U^{12})$.**

| | U11 | U22 | U33 | U23 | U13 | U12 |
|---|---|---|---|---|---|---|
| Re(01) | 24(1) | 13(1) | 16(1) | 0(1) | 10(1) | -1(1) |
| N(1) | 19(2) | 16(2) | 14(2) | 4(2) | 6(2) | 2(2) |
| O(4) | 31(2) | 16(2) | 20(2) | 1(1) | 16(2) | 3(1) |
| N(2) | 16(2) | 28(2) | 9(2) | 2(2) | 5(2) | 9(2) |
| C(3) | 22(2) | 28(3) | 16(3) | -2(2) | 13(2) | -12(2) |
| C(13) | 20(2) | 23(2) | 15(3) | 8(2) | 1(2) | -3(2) |
| C(14) | 20(2) | 26(2) | 17(3) | 6(2) | 8(2) | 0(2) |
| C(21) | 28(3) | 29(3) | 20(3) | 7(2) | 8(2) | 9(2) |
| C(20) | 25(3) | 34(3) | 22(3) | 7(2) | 8(2) | 16(2) |
| C(25) | 34(3) | 39(3) | 22(3) | 11(2) | 5(2) | 16(2) |
| C(15) | 19(2) | 19(2) | 13(2) | 7(2) | 5(2) | 8(2) |
| C(11) | 21(2) | 17(2) | 10(2) | 5(2) | 4(2) | 3(2) |
| C(12) | 19(2) | 18(2) | 11(2) | 7(2) | 1(2) | 3(2) |
| C(23) | 29(3) | 31(3) | 45(4) | 16(3) | -2(3) | -5(2) |
| C(24) | 38(3) | 46(3) | 16(3) | 16(2) | 15(2) | 23(3) |

| | | | | | | |
|---|---|---|---|---|---|---|
| C(22) | 29(2) | 23(2) | 14(2) | 1(2) | 5(2) | 0(2) |
| O(3) | 41(2) | 32(2) | 45(3) | 6(2) | 15(2) | 4(2) |
| O(2) | 35(2) | 31(2) | 41(3) | -18(2) | 16(2) | -7(2) |
| C(2) | 29(3) | 19(2) | 25(3) | -3(2) | 14(2) | 2(2) |
| O(1) | 32(2) | 27(2) | 29(2) | -2(2) | 18(2) | -2(2) |
| C(1) | 25(2) | 13(2) | 17(3) | 1(2) | 8(2) | -2(2) |
| O(5) | 25(2) | 35(2) | 27(2) | 2(2) | 15(2) | 6(2) |
| C(16) | 25(2) | 19(2) | 17(3) | 7(2) | 8(2) | 7(2) |
| C(26) | 14(2) | 25(2) | 23(3) | -7(2) | 0(2) | 5(2) |
| C(27) | 49(4) | 34(3) | 30(3) | -10(3) | -3(3) | 8(3) |
| O(6) | 35(2) | 32(2) | 19(2) | -8(2) | 8(2) | -6(2) |
| O(7) | 29(2) | 20(2) | 30(2) | -3(2) | 3(2) | -5(1) |
| C(17) | 26(2) | 17(2) | 14(2) | 8(2) | 0(2) | 3(2) |
| Br(1) | 30(1) | 22(1) | 19(1) | 6(1) | 9(1) | 3(1) |
| C(18) | 54(4) | 22(3) | 42(4) | -10(3) | 1(3) | -4(3) |

**Table A.34: Hydrogen coordinates (x $10^4$) and isotropic displacement parameters ($Å^2$ x $10^3$) for *fac*-[$NEt_4$][Re(2,5-PicoMe)$(CO)_3$(Br)] (6).**

| | x | y | z | U(eq) |
|---|---|---|---|---|
| H(13) | 4747 | 3514 | 5394 | 24 |
| H(14) | 4631 | 4739 | 6002 | 25 |
| H(21B) | 9081 | -933 | 7538 | 38 |
| H(21A) | 7887 | -835 | 7530 | 38 |
| H(21C) | 8634 | 68 | 7760 | 38 |
| H(20A) | 8282 | -443 | 6767 | 32 |
| H(20B) | 9024 | 460 | 6997 | 32 |
| H(25B) | 6903 | 2515 | 5955 | 47 |
| H(25C) | 6854 | 2800 | 6497 | 47 |
| H(25A) | 6106 | 1942 | 6225 | 47 |
| H(11) | 7397 | 4901 | 5201 | 19 |
| H(23B) | 8537 | 2861 | 7636 | 54 |
| H(23C) | 8583 | 2726 | 7083 | 54 |
| H(23A) | 9135 | 1903 | 7460 | 54 |
| H(24B) | 8264 | 1701 | 6456 | 39 |
| H(24A) | 7516 | 844 | 6186 | 39 |
| H(22A) | 7528 | 1346 | 7619 | 26 |
| H(22B) | 6975 | 2172 | 7243 | 26 |
| H(26A) | 5923 | 870 | 6840 | 25 |
| H(26B) | 6447 | 32 | 7215 | 25 |
| H(27B) | 5538 | -818 | 6536 | 59 |
| H(27C) | 6720 | -1074 | 6578 | 59 |
| H(27A) | 6199 | -233 | 6201 | 59 |
| H(18A) | 5029 | 1342 | 4365 | 60 |
| H(18B) | 6237 | 1423 | 4505 | 60 |
| H(18C) | 5639 | 2137 | 4090 | 60 |

**Table A.35: Torsion angles (°) for *fac*-[$NEt_4$][Re(2,5-PicoMe)$(CO)_3$(Br)] (6).**

| Torsion Angle | Angle | Torsion Angle | Angle |
|---|---|---|---|
| Br1-Re01-N1-C11 | 90.2(4) | Re01-N1-C15-C14 | 169.7(3) |
| Br1-Re01-N1-C15 | -79.7(3) | Re01-N1-C15-C16 | -8.6(5) |
| O4-Re01-N1-C11 | 176.9(4) | C11-N1-C15-C14 | -1.1(6) |
| O4-Re01-N1-C15 | 7.0(3) | C11-N1-C15-C16 | -179.4(4) |
| C1-Re01-N1-C11 | -1.2(4) | N1-C11-C12-C13 | -0.7(6) |

| | | | |
|---|---|---|---|
| C1-Re01-N1-C15 | -171.1(3) | N1-C11-C12-C17 | 178.0(4) |
| C3-Re01-N1-C11 | -92.1(4) | C11-C12-C13-C14 | -0.8(6) |
| C3-Re01-N1-C15 | 98.0(3) | C17-C12-C13-C14 | -179.4(4) |
| Br1-Re01-O4-C16 | 78.4(3) | C11-C12-C17-O6 | 1.8(7) |
| N1-Re01-O4-C6 | -4.6(3) | C11-C12-C17-O7 | -178.2(4) |
| C3-Re01-O4-C16 | -101.2(3) | C13-C12-C17-O6 | -179.5(5) |
| Re01-O4-C16-O5 | -180.0(4) | C13-C12-C17-O7 | 0.5(6) |
| Re01-O4-C16-C15 | 1.5(5) | C12-C13-C14-C15 | 1.3(7) |
| C18-O7-C17-O6 | -4.3(7) | C13-C14-C15-N1 | -0.4(7) |
| C18-O7-C17-C12 | 175.7(4) | C13-C14-C15-C16 | 177.8(4) |
| C22-N2-C20-C21 | -54.3(5) | N1-C15-C16-O4 | 4.9(6) |
| C24-N2-C20-C21 | -175.3(4) | N1-C15-C16-O5 | -173.8(4) |
| C20-N2-C22-C23 | -60.8(5) | C14-C15-C16-O4 | -173.4(4) |
| C24-N2-C22-C23 | 57.0(5) | C14-C15-C16-O5 | 7.9(7) |
| C26-N2-C20-C21 | 63.6(5) | C22-N2-C26-C27 | -179.7(4) |
| C20-N2-C24-C25 | 178.1(4) | C24-N2-C26-C27 | -58.5(5) |
| C22-N2-C24-C25 | 57.1(5) | C26-N2-C22-C23 | 178.4(4) |
| C26-N2-C24-C25 | -61.1(5) | Re01-N1-C11-C12 | -167.9(3) |
| C20-N2-C26-C27 | 59.4(5) | C15-N1-C11-C12 | 1.7(6) |

**Table A.36: Hydrogen bond distances (Å) and angles (°) for *fac*-[$NEt_4$][Re(2,5-PicoMe)$(CO)_3$(Br)] (6).**

| D-H…A | d (D-H) | d (H…A) | d (D…A) | D-H…A angle |
|---|---|---|---|---|
| C11-H11…O6 | 0.93 | 2.49 | 2.808(5) | 100.0 |
| C20-H20B…O5#1 | 0.97 | 2.39 | 3.289(6) | 153.1 |
| C24-H24B…O5#1 | 0.97 | 2.54 | 3.384(6) | 146.0 |

Symmetry codes, transformations used to generate equivalent atoms:
#1 0.5+x,-0.5+y,z

**Table A.37: Atomic coordinates (x $10^4$) and equivalent isotropic displacement parameters ($Å^2$ x $10^3$) for *fac*-[$NEt_4$][Re(BHA)$(CO)_3$(Br)] (7). U(eq) is defined as one third of the trace of the orthogonalized $U^{ij}$ tensor.**

| | x | y | z | U(eq) |
|---|---|---|---|---|
| Br(1) | 7653(1) | 5127(1) | 9037(1) | 13(1) |
| O(1) | 4240(3) | 2364(2) | 5906(2) | 20(1) |
| C(1) | 4661(4) | 3553(3) | 6468(2) | 13(1) |
| O(2) | 7773(3) | 6839(3) | 6257(2) | 21(1) |
| C(2) | 6859(4) | 6314(3) | 6674(2) | 13(1) |
| O(3) | 2789(3) | 5988(3) | 5625(2) | 22(1) |
| C(3) | 3772(3) | 5806(3) | 6299(2) | 14(1) |
| O(4) | 4035(2) | 4851(2) | 8442(2) | 10(1) |
| O(5) | 6222(3) | 7588(2) | 8606(2) | 12(1) |
| N(1) | 4537(3) | 6077(3) | 9318(2) | 9(1) |
| C(4) | 5638(3) | 7421(3) | 9379(2) | 9(1) |
| C(5) | 6206(3) | 8742(3) | 10325(2) | 9(1) |
| C(6) | 6099(3) | 8587(3) | 11367(2) | 11(1) |
| C(10) | 6933(3) | 10190(3) | 10164(2) | 11(1) |
| C(7) | 6712(4) | 9878(3) | 12235(2) | 14(1) |
| C(9) | 7549(4) | 11473(3) | 11035(2) | 16(1) |
| C(8) | 7437(4) | 11319(3) | 12075(2) | 16(1) |
| C(16) | 6088(4) | -59(3) | 6577(3) | 17(1) |
| C(15) | 7574(3) | 324(3) | 6270(2) | 12(1) |
| C(13) | 10439(3) | 1949(3) | 6614(2) | 13(1) |
| C(17) | 9580(4) | 1916(3) | 8232(2) | 16(1) |
| C(18) | 9740(4) | 536(4) | 8562(3) | 22(1) |
| C(14) | 10146(4) | 2005(4) | 5388(3) | 21(1) |
| C(11) | 8593(4) | 3109(3) | 6757(3) | 14(1) |
| N(2) | 9040(3) | 1817(3) | 6969(2) | 9(1) |
| C(12) | 10012(4) | 4685(3) | 7285(3) | 22(1) |
| Re(1) | 5395(1) | 5504(1) | 7411(1) | 9(1) |

**Table A.38: Bond distances (Å) and angles (°) for *fac*-[$NEt_4$][Re(BHA)$(CO)_3$(Br)] (7).**

| Bond | Bond Distance | Bond Angle | Angle |
|---|---|---|---|
| Br(1)-Re(1) | 2.6690(5) | O(1)#1-O(1)-C(1) | 0(10) |
| O(1)-O(1) | 0.000(5) | O(1)#1-C(1)-O(1) | 0.00(14) |
| O(1)-C(1) | 1.156(3) | O(1)#1-C(1)-Re(1) | 178.8(3) |
| C(1)-O(1) | 1.156(3) | O(1)-C(1)-Re(1) | 178.8(3) |
| C(1)-Re(1) | 1.899(3) | O(2)-C(2)-Re(1) | 177.9(3) |
| O(2)-C(2) | 1.154(3) | O(3)-C(3)-Re(1) | 179.9(3) |
| C(2)-Re(1) | 1.910(3) | N(1)-O(4)-Re(1) | 109.74(15) |
| O(3)-C(3) | 1.149(3) | C(4)-O(5)-Re(1) | 113.20(17) |
| C(3)-Re(1) | 1.897(3) | C(4)-N(1)-O(4) | 120.3(2) |
| O(4)-N(1) | 1.373(3) | C(4)-N(1)-H(1) | 125(3) |
| O(4)-Re(1) | 2.1201(19) | O(4)-N(1)-H(1) | 115(3) |
| O(5)-C(4) | 1.281(3) | O(5)-C(4)-N(1) | 119.6(3) |
| O(5)-Re(1) | 2.128(2) | O(5)-C(4)-C(5) | 119.6(2) |
| N(1)-C(4) | 1.313(3) | N(1)-C(4)-C(5) | 120.7(2) |
| N(1)-H(1) | 0.90(4) | C(6)-C(5)-C(10) | 119.9(3) |
| C(4)-C(5) | 1.476(4) | C(6)-C(5)-C(4) | 122.4(2) |
| C(5)-C(6) | 1.391(4) | C(10)-C(5)-C(4) | 117.7(2) |
| C(5)-C(10) | 1.397(4) | C(7)-C(6)-C(5) | 119.5(3) |
| C(6)-C(7) | 1.387(4) | C(7)-C(6)-H(6) | 120.3 |

| | | | |
|---|---|---|---|
| C(6)-H(6) | 0.9300 | C(5)-C(6)-H(6) | 120.3 |
| C(10)-C(9) | 1.383(4) | C(9)-C(10)-C(5) | 120.4(3) |
| C(10)-H(10) | 0.9300 | C(9)-C(10)-H(10) | 119.8 |
| C(7)-C(8) | 1.390(4) | C(5)-C(10)-H(10) | 119.8 |
| C(7)-H(7) | 0.9300 | C(6)-C(7)-C(8) | 120.6(3) |
| C(9)-C(8) | 1.390(4) | C(6)-C(7)-H(7) | 119.7 |
| C(9)-H(9) | 0.9300 | C(8)-C(7)-H(7) | 119.7 |
| C(8)-H(8) | 0.9300 | C(10)-C(9)-C(8) | 119.8(3) |
| C(16)-C(15) | 1.521(4) | C(10)-C(9)-H(9) | 120.1 |
| C(16)-H(16C) | 0.9600 | C(8)-C(9)-H(9) | 120.1 |
| C(16)-H(16B) | 0.9600 | C(9)-C(8)-C(7) | 119.9(3) |
| C(16)-H(16A) | 0.9600 | C(9)-C(8)-H(8) | 120.1 |
| C(15)-N(2) | 1.510(3) | C(7)-C(8)-H(8) | 120.1 |
| C(15)-H(15A) | 0.9700 | C(15)-C(16)-H(16C) | 109.5 |
| C(15)-H(15B) | 0.9700 | C(15)-C(16)-H(16B) | 109.5 |
| C(13)-N(2) | 1.517(4) | H(16C)-C(16)-H(16B) | 109.5 |
| C(13)-C(14) | 1.518(4) | C(15)-C(16)-H(16A) | 109.5 |
| C(13)-H(13A) | 0.9700 | H(16C)-C(16)-H(16A) | 109.5 |
| C(13)-H(13B) | 0.9700 | H(16B)-C(16)-H(16A) | 109.5 |
| C(17)-C(18) | 1.516(4) | N(2)-C(15)-C(16) | 115.6(2) |
| C(17)-N(2) | 1.517(3) | N(2)-C(15)-H(15A) | 108.4 |
| C(17)-H(17A) | 0.9700 | C(16)-C(15)-H(15A) | 108.4 |
| C(17)-H(17B) | 0.9700 | N(2)-C(15)-H(15B) | 108.4 |
| C(18)-H(18C) | 0.9600 | C(16)-C(15)-H(15B) | 108.4 |
| C(18)-H(18B) | 0.9600 | H(15A)-C(15)-H(15B) | 107.5 |
| C(18)-H(18A) | 0.9600 | N(2)-C(13)-C(14) | 115.3(2) |
| C(14)-H(14A) | 0.9600 | N(2)-C(13)-H(13A) | 108.5 |
| C(14)-H(14B) | 0.9600 | C(14)-C(13)-H(13A) | 108.5 |
| C(14)-H(14C) | 0.9600 | N(2)-C(13)-H(13B) | 108.5 |
| C(11)-C(12) | 1.514(4) | C(14)-C(13)-H(13B) | 108.5 |
| C(11)-N(2) | 1.520(4) | H(13A)-C(13)-H(13B) | 107.5 |
| C(11)-H(11B) | 0.9700 | C(18)-C(17)-N(2) | 115.0(3) |
| C(11)-H(11A) | 0.9700 | C(18)-C(17)-H(17A) | 108.5 |
| C(12)-H(12B) | 0.9600 | N(2)-C(17)-H(17A) | 108.5 |
| C(12)-H(12C) | 0.9600 | C(18)-C(17)-H(17B) | 108.5 |
| C(12)-H(12A) | 0.9600 | N(2)-C(17)-H(17B) | 108.5 |
| | | H(17A)-C(17)-H(17B) | 107.5 |
| | | C(17)-C(18)-H(18C) | 109.5 |
| | | C(17)-C(18)-H(18B) | 109.5 |
| | | H(18C)-C(18)-H(18B) | 109.5 |
| | | C(17)-C(18)-H(18A) | 109.5 |
| | | H(18C)-C(18)-H(18A) | 109.5 |
| | | H(18B)-C(18)-H(18A) | 109.5 |
| | | C(13)-C(14)-H(14A) | 109.5 |
| | | C(13)-C(14)-H(14B) | 109.5 |
| | | H(14A)-C(14)-H(14B) | 109.5 |
| | | C(13)-C(14)-H(14C) | 109.5 |
| | | H(14A)-C(14)-H(14C) | 109.5 |
| | | H(14B)-C(14)-H(14C) | 109.5 |
| | | C(12)-C(11)-N(2) | 114.7(2) |
| | | C(12)-C(11)-H(11B) | 108.6 |
| | | N(2)-C(11)-H(11B) | 108.6 |
| | | C(12)-C(11)-H(11A) | 108.6 |
| | | N(2)-C(11)-H(11A) | 108.6 |
| | | H(11B)-C(11)-H(11A) | 107.6 |

| | |
|---|---|
| C(15)-N(2)-C(17) | 111.9(2) |
| C(15)-N(2)-C(13) | 108.3(2) |
| C(17)-N(2)-C(13) | 108.6(2) |
| C(15)-N(2)-C(11) | 109.0(2) |
| C(17)-N(2)-C(11) | 108.2(2) |
| C(13)-N(2)-C(11) | 110.9(2) |
| C(11)-C(12)-H(12B) | 109.5 |
| C(11)-C(12)-H(12C) | 109.5 |
| H(12B)-C(12)-H(12C) | 109.5 |
| C(11)-C(12)-H(12A) | 109.5 |
| H(12B)-C(12)-H(12A) | 109.5 |
| H(12C)-C(12)-H(12A) | 109.5 |
| C(3)-Re(1)-C(1) | 89.97(12) |
| C(3)-Re(1)-C(2) | 89.68(12) |
| C(1)-Re(1)-C(2) | 87.98(12) |
| C(3)-Re(1)-O(4) | 94.88(11) |
| C(1)-Re(1)-O(4) | 98.84(10) |
| C(2)-Re(1)-O(4) | 171.78(10) |
| C(3)-Re(1)-O(5) | 94.05(11) |
| C(1)-Re(1)-O(5) | 174.29(9) |
| C(2)-Re(1)-O(5) | 96.08(10) |
| O(4)-Re(1)-O(5) | 76.80(7) |
| C(3)-Re(1)-Br(1) | 177.86(9) |
| C(1)-Re(1)-Br(1) | 91.65(9) |
| C(2)-Re(1)-Br(1) | 91.78(9) |
| O(4)-Re(1)-Br(1) | 83.49(6) |
| O(5)-Re(1)-Br(1) | 84.24(6) |

**Table A.39: Anisotropic displacement parameters ($Å^2$ x $10^3$) for *fac*-[$NEt_4$][Re(BHA)$(CO)_3$(Br)] (7). The Anisotropic displacement factor exponent takes the form: $-2\pi^2(h2a^{*2}U^{11} + \ldots + 2hka^*b^*U^{12})$.**

| | U11 | U22 | U33 | U23 | U13 | U12 |
|---|---|---|---|---|---|---|
| Br(1) | 11(1) | 18(1) | 9(1) | 3(1) | 5(1) | 6(1) |
| O(1) | 26(1) | 14(1) | 16(1) | -1(1) | 3(1) | 9(1) |
| C(1) | 16(2) | 19(2) | 10(1) | 6(1) | 7(1) | 10(1) |
| O(2) | 27(1) | 25(1) | 21(1) | 12(1) | 18(1) | 14(1) |
| C(2) | 20(2) | 11(1) | 8(1) | 2(1) | 5(1) | 7(1) |
| O(3) | 24(1) | 26(1) | 18(1) | 10(1) | 4(1) | 14(1) |
| C(3) | 19(2) | 10(1) | 12(1) | 1(1) | 8(1) | 3(1) |
| O(4) | 11(1) | 7(1) | 9(1) | -2(1) | 5(1) | 0(1) |
| O(5) | 16(1) | 10(1) | 9(1) | 1(1) | 7(1) | 4(1) |
| N(1) | 11(1) | 10(1) | 6(1) | 0(1) | 5(1) | 4(1) |
| C(4) | 9(1) | 11(1) | 7(1) | 4(1) | 3(1) | 5(1) |
| C(5) | 8(1) | 9(1) | 9(1) | 0(1) | 3(1) | 4(1) |
| C(6) | 7(1) | 13(1) | 12(1) | 3(1) | 5(1) | 3(1) |
| C(10) | 10(1) | 14(1) | 11(1) | 4(1) | 5(1) | 5(1) |
| C(7) | 13(2) | 18(2) | 11(1) | 1(1) | 6(1) | 6(1) |
| C(9) | 16(2) | 12(1) | 18(2) | 2(1) | 7(1) | 5(1) |
| C(8) | 15(2) | 14(1) | 14(1) | -3(1) | 4(1) | 5(1) |
| C(16) | 11(2) | 17(2) | 20(2) | 6(1) | 7(1) | 3(1) |
| C(15) | 10(1) | 10(1) | 10(1) | -1(1) | 2(1) | 0(1) |
| C(13) | 8(1) | 17(1) | 15(1) | 3(1) | 7(1) | 5(1) |
| C(17) | 14(2) | 22(2) | 6(1) | 2(1) | 4(1) | 4(1) |
| C(18) | 16(2) | 31(2) | 20(2) | 17(1) | 7(1) | 11(1) |
| C(14) | 23(2) | 26(2) | 18(2) | 7(1) | 15(1) | 9(1) |

| | | | | | | |
|---|---|---|---|---|---|---|
| C(11) | 14(2) | 11(1) | 18(2) | 4(1) | 5(1) | 6(1) |
| N(2) | 8(1) | 10(1) | 7(1) | 1(1) | 3(1) | 3(1) |
| C(12) | 19(2) | 9(1) | 39(2) | 4(1) | 15(2) | 4(1) |
| Re(1) | 11(1) | 9(1) | 6(1) | 1(1) | 4(1) | 4(1) |

**Table A.40: Hydrogen coordinates (x $10^4$) and isotropic displacement parameters ($Å^2$ x $10^3$) for *fac*-[$NEt_4$][Re(BHA)$(CO)_3$(Br)] (7).**

| | x | y | z | U(eq) |
|---|---|---|---|---|
| H(6) | 5620 | 7626 | 11480 | 13 |
| H(10) | 7003 | 10293 | 9468 | 14 |
| H(7) | 6637 | 9779 | 12931 | 17 |
| H(9) | 8036 | 12435 | 10926 | 19 |
| H(8) | 7846 | 12178 | 12662 | 19 |
| H(16C) | 5224 | -1023 | 6090 | 25 |
| H(16B) | 5726 | 715 | 6480 | 25 |
| H(16A) | 6376 | -113 | 7355 | 25 |
| H(15A) | 7902 | -485 | 6349 | 15 |
| H(15B) | 7253 | 340 | 5475 | 15 |
| H(13A) | 10662 | 1089 | 6736 | 16 |
| H(13B) | 11409 | 2862 | 7108 | 16 |
| H(17A) | 10629 | 2802 | 8629 | 19 |
| H(17B) | 8799 | 2072 | 8493 | 19 |
| H(18C) | 10083 | 694 | 9372 | 32 |
| H(18B) | 10535 | 387 | 8330 | 32 |
| H(18A) | 8701 | -346 | 8192 | 32 |
| H(14A) | 11088 | 2084 | 5240 | 32 |
| H(14B) | 9959 | 2871 | 5260 | 32 |
| H(14C) | 9206 | 1093 | 4888 | 32 |
| H(11B) | 8113 | 2975 | 5942 | 17 |
| H(11A) | 7765 | 3040 | 7054 | 17 |
| H(12B) | 9628 | 5431 | 7115 | 33 |
| H(12C) | 10826 | 4780 | 6980 | 33 |
| H(12A) | 10482 | 4842 | 8095 | 33 |
| H(1) | 4050(50) | 5870(40) | 9810(30) | 33 |

**Table A.41: Torsion angles (°) for *fac*-[$NEt_4$][Re(BHA)$(CO)_3$(Br)] (7).**

| Torsion Angle | Angle | Torsion Angle | Angle |
|---|---|---|---|
| O(1)-O(1)-C(1)-Re(1) | 0(5) | C(18)-C(17)-N(2)-C(13) | -71.5(3) |
| Re(1)-O(4)-N(1)-C(4) | 3.7(3) | C(18)-C(17)-N(2)-C(11) | 168.1(3) |
| Re(1)-O(5)-C(4)-N(1) | -5.4(3) | C(14)-C(13)-N(2)-C(15) | 63.3(3) |
| Re(1)-O(5)-C(4)-C(5) | 174.83(19) | C(14)-C(13)-N(2)-C(17) | -175.1(2) |
| O(4)-N(1)-C(4)-O(5) | 1.2(4) | C(14)-C(13)-N(2)-C(11) | -56.2(3) |
| O(4)-N(1)-C(4)-C(5) | -179.1(2) | C(12)-C(11)-N(2)-C(15) | -172.5(3) |
| O(5)-C(4)-C(5)-C(6) | -157.0(3) | C(12)-C(11)-N(2)-C(17) | 65.7(3) |
| N(1)-C(4)-C(5)-C(6) | 23.3(4) | C(12)-C(11)-N(2)-C(13) | -53.4(3) |
| O(5)-C(4)-C(5)-C(10) | 20.4(4) | O(3)-C(3)-Re(1)-C(1) | 12(100) |
| N(1)-C(4)-C(5)-C(10) | -159.4(3) | O(3)-C(3)-Re(1)-C(2) | 100(100) |
| C(10)-C(5)-C(6)-C(7) | 0.2(4) | O(3)-C(3)-Re(1)-O(4) | -87(100) |
| C(4)-C(5)-C(6)-C(7) | 177.6(3) | O(3)-C(3)-Re(1)-O(5) | -164(100) |
| C(6)-C(5)-C(10)-C(9) | 0.1(4) | O(3)-C(3)-Re(1)-Br(1) | -127(100) |
| C(4)-C(5)-C(10)-C(9) | -177.4(3) | O(1)#1-C(1)-Re(1)-C(3) | 166(13) |
| C(5)-C(6)-C(7)-C(8) | -0.3(4) | O(1)-C(1)-Re(1)-C(3) | 166(13) |
| C(5)-C(10)-C(9)-C(8) | -0.3(5) | O(1)#1-C(1)-Re(1)-C(2) | 76(13) |

| | | | |
|---|---|---|---|
| C(10)-C(9)-C(8)-C(7) | 0.2(5) | O(1)-C(1)-Re(1)-C(2) | 76(13) |
| C(6)-C(7)-C(8)-C(9) | 0.1(5) | O(1)#1-C(1)-Re(1)-O(4) | -99(13) |
| C(16)-C(15)-N(2)-C(17) | 55.7(3) | O(1)-C(1)-Re(1)-O(4) | -99(13) |
| C(16)-C(15)-N(2)-C(13) | 175.4(2) | O(1)#1-C(1)-Re(1)-O(5) | -59(14) |
| C(16)-C(15)-N(2)-C(11) | -63.9(3) | O(1)-C(1)-Re(1)-O(5) | -59(14) |
| C(18)-C(17)-N(2)-C(15) | 48.0(3) | O(1)#1-C(1)-Re(1)-Br(1) | -15(13) |
| O(1)-C(1)-Re(1)-Br(1) | -15(13) | N(1)-O(4)-Re(1)-C(1) | 171.63(17) |
| O(2)-C(2)-Re(1)-C(3) | 114(7) | N(1)-O(4)-Re(1)-C(2) | 25.8(7) |
| O(2)-C(2)-Re(1)-C(1) | -156(7) | N(1)-O(4)-Re(1)-O(5) | -4.61(15) |
| O(2)-C(2)-Re(1)-O(4) | -9(8) | N(1)-O(4)-Re(1)-Br(1) | 80.97(15) |
| O(2)-C(2)-Re(1)-O(5) | 20(7) | C(4)-O(5)-Re(1)-C(3) | 99.5(2) |
| O(2)-C(2)-Re(1)-Br(1) | -64(7) | C(4)-O(5)-Re(1)-C(1) | -35.2(11) |
| N(1)-O(4)-Re(1)-C(3) | -97.64(18) | C(4)-O(5)-Re(1)-C(2) | -170.4(2) |
| C(4)-O(5)-Re(1)-Br(1) | -79.18(18) | C(4)-O(5)-Re(1)-O(4) | 5.46(18) |

**Table A.42: Hydrogen bond distances (Å) and angles (°) for *fac*-[$NEt_4$][Re(BHA)$(CO)_3$(Br)] (7).**

| D-H…A | d (D-H) | d (H…A) | d (D…A) | D-H…A angle |
|---|---|---|---|---|
| N1-H1…Br1#1 | 0.90(4) | 2.53(4) | 3.421(2) | 170(3) |
| C15-H15A…O2#2 | 0.97 | 2.59 | 3.520(4) | 161.6 |
| C13-H13B…O4#3 | 0.97 | 2.43 | 3.387(3) | 170.1 |
| C11-H11B…O3#4 | 0.97 | 2.42 | 3.285(4) | 148.7 |
| C16-H16B…O1 | 0.96 | 2.58 | 3.521(4) | 168.6 |

Symmetry codes, transformations used to generate equivalent atoms:
#1 1-x,1-y,2-z #2 x,-1+y,z #3 1+x,y,z #4 1-x,1-y,1–z

# Appendix A

**Table A.43: Atomic coordinates (x $10^4$) and equivalent isotropic displacement parameters ($Å^2$ x $10^3$) for *fac*-[Re(Flav)$(CO)_3(H_2O)$].Flav (8). U(eq) is defined as one third of the trace of the orthogonalized $U^{ij}$ tensor.**

| | x | y | z | U(eq) |
|---|---|---|---|---|
| Re(1) | 4694(1) | 6390(1) | 6888(1) | 15(1) |
| O(6) | 5969(3) | 5289(3) | 6284(2) | 21(1) |
| O(7) | 2206(3) | 1568(2) | 5614(2) | 20(1) |
| O(17) | 1491(3) | 5889(2) | 9236(2) | 19(1) |
| O(14) | 1029(3) | 2891(3) | 9495(3) | 25(1) |
| O(3) | 2810(3) | 7753(3) | 7816(3) | 31(1) |
| C(3) | 3503(4) | 7214(4) | 7452(3) | 20(1) |
| O(1) | 4974(3) | 7983(3) | 5390(3) | 27(1) |
| O(5) | 4488(3) | 5164(3) | 7816(2) | 21(1) |
| O(15) | 2209(3) | 4406(3) | 11724(2) | 24(1) |
| C(1) | 4861(4) | 7367(4) | 5944(3) | 20(1) |
| C(110) | 1514(4) | 1968(4) | 3905(3) | 19(1) |
| O(2) | 7080(3) | 8566(3) | 8926(3) | 29(1) |
| C(105) | 4309(4) | 3257(4) | 8775(3) | 19(1) |
| O(4) | 3151(3) | 4672(2) | 5557(2) | 19(1) |
| C(209) | 2153(4) | 6693(4) | 10408(3) | 19(1) |
| C(113) | -71(4) | 899(4) | 1483(4) | 23(1) |
| C(104) | 3638(4) | 3053(4) | 7589(3) | 20(1) |
| C(203) | 2050(4) | 4929(4) | 11006(3) | 20(1) |
| C(202) | 1389(4) | 4139(4) | 9755(3) | 19(1) |
| C(205) | 3140(4) | 7148(4) | 12504(3) | 23(1) |
| C(109) | 2855(4) | 1833(4) | 6794(3) | 21(1) |
| C(204) | 2449(4) | 6262(4) | 11320(3) | 19(1) |
| C(108) | 2691(4) | 835(4) | 7158(4) | 24(1) |
| C(211) | -29(4) | 4569(4) | 6911(4) | 25(1) |
| C(103) | 3752(4) | 4038(4) | 7155(3) | 20(1) |
| C(213) | -1112(4) | 2646(4) | 5174(4) | 24(1) |
| C(101) | 2280(4) | 2490(4) | 5189(3) | 19(1) |
| C(115) | 959(4) | 2678(4) | 3355(3) | 21(1) |
| C(206) | 3511(4) | 8395(4) | 12737(4) | 26(1) |
| C(207) | 3207(4) | 8813(4) | 11807(4) | 25(1) |
| C(107) | 3346(4) | 1062(4) | 8332(4) | 26(1) |
| C(111) | 1288(4) | 721(4) | 3205(3) | 21(1) |
| C(212) | -785(5) | 3925(4) | 5704(4) | 28(1) |
| C(210) | 386(4) | 3929(4) | 7613(3) | 18(1) |
| C(2) | 6191(4) | 7742(4) | 8139(3) | 21(1) |
| C(106) | 4171(4) | 2287(4) | 9148(3) | 23(1) |
| C(201) | 1114(4) | 4622(4) | 8905(3) | 18(1) |
| C(214) | -666(5) | 2011(4) | 5857(4) | 27(1) |
| C(102) | 3031(4) | 3726(4) | 5928(3) | 19(1) |
| C(112) | 510(4) | 200(4) | 2007(4) | 24(1) |
| C(215) | 72(4) | 2639(4) | 7063(4) | 23(1) |
| C(208) | 2529(4) | 7966(4) | 10638(4) | 23(1) |
| C(114) | 174(4) | 2132(4) | 2160(3) | 22(1) |

**Table A.44: Bond distances (Å) and angles (°) for *fac*-[Re(Flav)$(CO)_3(H_2O)$].Flav (8).**

| Bond | Bond Distance | Bond Angle | Angle |
|---|---|---|---|
| Re(1)-C(3) | 1.895(4) | C(3)-Re(1)-C(2) | 87.25(17) |
| Re(1)-C(2) | 1.897(4) | C(3)-Re(1)-C(1) | 87.25(17) |

| | | | |
|---|---|---|---|
| Re(1)-C(1) | 1.903(4) | C(2)-Re(1)-C(1) | 87.13(17) |
| Re(1)-O(5) | 2.130(3) | C(3)-Re(1)-O(5) | 96.24(14) |
| Re(1)-O(4) | 2.151(3) | C(2)-Re(1)-O(5) | 96.36(14) |
| Re(1)-O(6) | 2.188(3) | C(1)-Re(1)-O(5) | 175.16(13) |
| O(6)-H(6B) | 0.853(19) | C(3)-Re(1)-O(4) | 98.87(14) |
| O(6)-H(6A) | 0.842(19) | C(2)-Re(1)-O(4) | 171.08(13) |
| O(7)-C(101) | 1.356(5) | C(1)-Re(1)-O(4) | 99.58(14) |
| O(7)-C(109) | 1.372(5) | O(5)-Re(1)-O(4) | 76.61(11) |
| O(17)-C(201) | 1.363(5) | C(3)-Re(1)-O(6) | 174.38(14) |
| O(17)-C(209) | 1.370(4) | C(2)-Re(1)-O(6) | 95.22(14) |
| O(14)-C(202) | 1.354(5) | C(1)-Re(1)-O(6) | 97.90(14) |
| O(14)-H(14) | 0.85(2) | O(5)-Re(1)-O(6) | 78.49(11) |
| O(3)-C(3) | 1.160(5) | O(4)-Re(1)-O(6) | 78.13(11) |
| O(1)-C(1) | 1.159(5) | Re(1)-O(6)-H(6B) | 114(4) |
| O(5)-C(103) | 1.263(5) | Re(1)-O(6)-H(6A) | 114(3) |
| O(15)-C(203) | 1.245(5) | H(6B)-O(6)-H(6A) | 105(5) |
| C(110)-C(111) | 1.397(5) | C(101)-O(7)-C(109) | 121.3(3) |
| C(110)-C(115) | 1.400(5) | C(201)-O(17)-C(209) | 121.2(3) |
| C(110)-C(101) | 1.467(5) | C(202)-O(14)-H(14) | 107(4) |
| O(2)-C(2) | 1.157(5) | O(3)-C(3)-Re(1) | 177.8(4) |
| C(105)-C(106) | 1.364(5) | C(103)-O(5)-Re(1) | 114.1(2) |
| C(105)-C(104) | 1.403(5) | O(1)-C(1)-Re(1) | 178.6(3) |
| C(105)-H(105) | 0.9300 | C(111)-C(110)-C(115) | 118.3(3) |
| O(4)-C(102) | 1.337(5) | C(111)-C(110)-C(101) | 120.0(3) |
| C(209)-C(208) | 1.389(6) | C(115)-C(110)-C(101) | 121.7(3) |
| C(209)-C(204) | 1.392(5) | C(106)-C(105)-C(104) | 121.0(4) |
| C(113)-C(114) | 1.371(6) | C(106)-C(105)-H(105) | 119.5 |
| C(113)-C(112) | 1.383(6) | C(104)-C(105)-H(105) | 119.5 |
| C(113)-H(113) | 0.9300 | C(102)-O(4)-Re(1) | 111.8(2) |
| C(104)-C(109) | 1.387(6) | O(17)-C(209)-C(208) | 116.3(3) |
| C(104)-C(103) | 1.430(5) | O(17)-C(209)-C(204) | 122.1(3) |
| C(203)-C(204) | 1.439(6) | C(208)-C(209)-C(204) | 121.6(4) |
| C(203)-C(202) | 1.441(5) | C(114)-C(113)-C(112) | 119.0(4) |
| C(202)-C(201) | 1.365(5) | C(114)-C(113)-H(113) | 120.5 |
| C(205)-C(206) | 1.358(6) | C(112)-C(113)-H(113) | 120.5 |
| C(205)-C(204) | 1.411(5) | C(109)-C(104)-C(105) | 118.3(4) |
| C(205)-H(205) | 0.9300 | C(109)-C(104)-C(103) | 118.6(3) |
| C(109)-C(108) | 1.387(6) | C(105)-C(104)-C(103) | 123.1(4) |
| C(108)-C(107) | 1.378(6) | O(15)-C(203)-C(204) | 125.6(4) |
| C(108)-H(108) | 0.9300 | O(15)-C(203)-C(202) | 117.7(4) |
| C(211)-C(212) | 1.388(6) | C(204)-C(203)-C(202) | 116.7(3) |
| C(211)-C(210) | 1.398(5) | O(14)-C(202)-C(201) | 122.9(3) |
| C(211)-H(211) | 0.9300 | O(14)-C(202)-C(203) | 115.0(3) |
| C(103)-C(102) | 1.428(5) | C(201)-C(202)-C(203) | 122.0(4) |
| C(213)-C(212) | 1.376(6) | C(206)-C(205)-C(204) | 120.1(4) |
| C(213)-C(214) | 1.386(6) | C(206)-C(205)-H(205) | 120.0 |
| C(213)-H(213) | 0.9300 | C(204)-C(205)-H(205) | 120.0 |
| C(101)-C(102) | 1.379(5) | O(7)-C(109)-C(104) | 121.1(4) |
| C(115)-C(114) | 1.380(5) | O(7)-C(109)-C(108) | 117.4(4) |
| C(115)-H(115) | 0.9300 | C(104)-C(109)-C(108) | 121.6(4) |
| C(206)-C(207) | 1.402(6) | C(209)-C(204)-C(205) | 118.7(4) |
| C(206)-H(206) | 0.9300 | C(209)-C(204)-C(203) | 118.3(3) |
| C(207)-C(208) | 1.384(6) | C(205)-C(204)-C(203) | 123.0(4) |
| C(207)-H(207) | 0.9300 | C(107)-C(108)-C(109) | 119.0(4) |
| C(107)-C(106) | 1.406(6) | C(107)-C(108)-H(108) | 120.5 |

| | |
|---|---|
| C(107)-H(107) | 0.9300 |
| C(111)-C(112) | 1.382(5) |
| C(111)-H(111) | 0.9300 |
| C(212)-H(212) | 0.9300 |
| C(210)-C(215) | 1.391(5) |
| C(210)-C(201) | 1.472(5) |
| C(106)-H(106) | 0.9300 |
| C(214)-C(215) | 1.382(6) |
| C(214)-H(214) | 0.9300 |
| C(112)-H(112) | 0.9300 |
| C(215)-H(215) | 0.9300 |
| C(208)-H(208) | 0.9300 |
| C(114)-H(114) | 0.9300 |

| | |
|---|---|
| C(109)-C(108)-H(108) | 120.5 |
| C(212)-C(211)-C(210) | 120.7(4) |
| C(212)-C(211)-H(211) | 119.7 |
| C(210)-C(211)-H(211) | 119.7 |
| O(5)-C(103)-C(102) | 119.4(4) |
| O(5)-C(103)-C(104) | 122.1(3) |
| C(102)-C(103)-C(104) | 118.5(4) |
| C(212)-C(213)-C(214) | 119.2(4) |
| C(212)-C(213)-H(213) | 120.4 |
| C(214)-C(213)-H(213) | 120.4 |
| O(7)-C(101)-C(102) | 120.9(3) |
| O(7)-C(101)-C(110) | 110.9(3) |
| C(102)-C(101)-C(110) | 128.2(4) |
| C(114)-C(115)-C(110) | 120.0(4) |
| C(114)-C(115)-H(115) | 120.0 |
| C(110)-C(115)-H(115) | 120.0 |
| C(205)-C(206)-C(207) | 120.5(4) |
| C(205)-C(206)-H(206) | 119.8 |
| C(207)-C(206)-H(206) | 119.8 |
| C(208)-C(207)-C(206) | 120.8(4) |
| C(208)-C(207)-H(207) | 119.6 |
| C(206)-C(207)-H(207) | 119.6 |
| C(108)-C(107)-C(106) | 120.4(4) |
| C(108)-C(107)-H(107) | 119.8 |
| C(106)-C(107)-H(107) | 119.8 |
| C(112)-C(111)-C(110) | 120.6(4) |
| C(112)-C(111)-H(111) | 119.7 |
| C(110)-C(111)-H(111) | 119.7 |
| C(213)-C(212)-C(211) | 120.4(4) |
| C(213)-C(212)-H(212) | 119.8 |
| C(211)-C(212)-H(212) | 119.8 |
| C(215)-C(210)-C(211) | 118.4(4) |
| C(215)-C(210)-C(201) | 121.9(3) |
| C(211)-C(210)-C(201) | 119.7(3) |
| O(2)-C(2)-Re(1) | 177.9(3) |
| C(105)-C(106)-C(107) | 119.6(4) |
| C(105)-C(106)-H(106) | 120.2 |
| C(107)-C(106)-H(106) | 120.2 |
| O(17)-C(201)-C(202) | 119.6(3) |
| O(17)-C(201)-C(210) | 112.6(3) |
| C(202)-C(201)-C(210) | 127.7(4) |
| C(215)-C(214)-C(213) | 121.0(4) |
| C(215)-C(214)-H(214) | 119.5 |
| C(213)-C(214)-H(214) | 119.5 |
| O(4)-C(102)-C(101) | 123.5(3) |
| O(4)-C(102)-C(103) | 116.9(3) |
| C(101)-C(102)-C(103) | 119.6(4) |
| C(111)-C(112)-C(113) | 120.6(4) |
| C(111)-C(112)-H(112) | 119.7 |
| C(113)-C(112)-H(112) | 119.7 |
| C(214)-C(215)-C(210) | 120.3(4) |
| C(214)-C(215)-H(215) | 119.8 |
| C(210)-C(215)-H(215) | 119.8 |
| C(207)-C(208)-C(209) | 118.4(4) |
| C(207)-C(208)-H(208) | 120.8 |

| | |
|---|---|
| C(209)-C(208)-H(208) | 120.8 |
| C(113)-C(114)-C(115) | 121.5(4) |
| C(113)-C(114)-H(114) | 119.3 |
| C(115)-C(114)-H(114) | 119.3 |

**Table A.45: Anisotropic displacement parameters ($Å^2$ x $10^3$) for *fac*-[Re(Flav)$(CO)_3(H_2O)$].Flav (8). The Anisotropic displacement factor exponent takes the form: $-2\pi^2(h2a^{*2}U^{11} + ... + 2hka^*b^*U^{12})$.**

| | U11 | U22 | U33 | U23 | U13 | U12 |
|---|---|---|---|---|---|---|
| Re(1) | 17(1) | 13(1) | 12(1) | 4(1) | 2(1) | 5(1) |
| O(6) | 21(1) | 22(2) | 19(1) | 8(1) | 2(1) | 10(1) |
| O(7) | 24(1) | 14(1) | 18(1) | 6(1) | 1(1) | 4(1) |
| O(17) | 21(1) | 16(1) | 17(1) | 5(1) | 1(1) | 7(1) |
| O(14) | 31(2) | 19(2) | 21(1) | 9(1) | 0(1) | 7(1) |
| O(3) | 31(2) | 34(2) | 31(2) | 11(1) | 13(1) | 17(1) |
| C(3) | 21(2) | 16(2) | 16(2) | 4(2) | 2(2) | 3(2) |
| O(1) | 32(2) | 29(2) | 26(2) | 18(1) | 7(1) | 11(1) |
| O(5) | 25(1) | 19(1) | 18(1) | 7(1) | 5(1) | 8(1) |
| O(15) | 25(1) | 25(2) | 21(1) | 13(1) | 2(1) | 8(1) |
| C(1) | 20(2) | 17(2) | 18(2) | 3(2) | 2(2) | 5(2) |
| C(110) | 17(2) | 17(2) | 17(2) | 4(2) | 3(1) | 4(2) |
| O(2) | 26(2) | 26(2) | 21(2) | 4(1) | 3(1) | -6(1) |
| C(105) | 20(2) | 20(2) | 17(2) | 6(2) | 5(2) | 8(2) |
| O(4) | 21(1) | 17(1) | 14(1) | 4(1) | 1(1) | 5(1) |
| C(209) | 16(2) | 22(2) | 16(2) | 5(2) | 3(1) | 8(2) |
| C(113) | 18(2) | 27(2) | 20(2) | 8(2) | 5(2) | 5(2) |
| C(104) | 20(2) | 21(2) | 18(2) | 8(2) | 7(2) | 7(2) |
| C(203) | 15(2) | 26(2) | 20(2) | 9(2) | 4(2) | 9(2) |
| C(202) | 15(2) | 18(2) | 22(2) | 7(2) | 3(2) | 5(2) |
| C(205) | 19(2) | 29(2) | 18(2) | 8(2) | 3(2) | 7(2) |
| C(109) | 23(2) | 23(2) | 17(2) | 7(2) | 5(2) | 10(2) |
| C(204) | 14(2) | 22(2) | 20(2) | 7(2) | 4(1) | 7(2) |
| C(108) | 29(2) | 15(2) | 21(2) | 6(2) | 3(2) | 5(2) |
| C(211) | 32(2) | 18(2) | 22(2) | 6(2) | 5(2) | 11(2) |
| C(103) | 21(2) | 20(2) | 19(2) | 7(2) | 6(2) | 9(2) |
| C(213) | 29(2) | 23(2) | 15(2) | 5(2) | 2(2) | 7(2) |
| C(101) | 19(2) | 19(2) | 19(2) | 9(2) | 5(2) | 6(2) |
| C(115) | 20(2) | 17(2) | 20(2) | 3(2) | 2(2) | 8(2) |
| C(206) | 24(2) | 26(2) | 19(2) | 1(2) | 1(2) | 8(2) |
| C(207) | 24(2) | 20(2) | 26(2) | 5(2) | 4(2) | 7(2) |
| C(107) | 31(2) | 24(2) | 25(2) | 14(2) | 7(2) | 10(2) |
| C(111) | 26(2) | 15(2) | 19(2) | 6(2) | 5(2) | 7(2) |
| C(212) | 38(2) | 26(2) | 19(2) | 11(2) | 3(2) | 15(2) |
| C(210) | 16(2) | 22(2) | 18(2) | 9(2) | 5(1) | 8(2) |
| C(2) | 23(2) | 26(2) | 17(2) | 10(2) | 10(2) | 10(2) |
| C(106) | 25(2) | 29(2) | 17(2) | 11(2) | 7(2) | 11(2) |
| C(201) | 16(2) | 16(2) | 20(2) | 6(2) | 4(1) | 7(1) |
| C(214) | 37(2) | 18(2) | 20(2) | 6(2) | 5(2) | 8(2) |
| C(102) | 20(2) | 16(2) | 21(2) | 5(2) | 8(2) | 7(2) |
| C(112) | 28(2) | 15(2) | 22(2) | 6(2) | 6(2) | 1(2) |
| C(215) | 25(2) | 20(2) | 22(2) | 10(2) | 5(2) | 9(2) |
| C(208) | 23(2) | 20(2) | 21(2) | 5(2) | 2(2) | 9(2) |
| C(114) | 18(2) | 24(2) | 19(2) | 8(2) | 1(2) | 6(2) |

**Table A.46: Hydrogen coordinates (x $10^4$) and isotropic displacement parameters (Å$^2$ x $10^3$) for *fac*-[Re(Flav)$(CO)_3(H_2O)$].Flav (8).**

| | x | y | z | U(eq) |
|---|---|---|---|---|
| H(105) | 4857 | 4066 | 9316 | 23 |
| H(113) | -619 | 539 | 683 | 28 |
| H(205) | 3342 | 6879 | 13126 | 27 |
| H(108) | 2146 | 25 | 6617 | 28 |
| H(211) | 204 | 5436 | 7256 | 29 |
| H(213) | -1626 | 2213 | 4367 | 29 |
| H(115) | 1118 | 3517 | 3795 | 25 |
| H(206) | 3969 | 8976 | 13519 | 31 |
| H(207) | 3465 | 9669 | 11979 | 30 |
| H(107) | 3242 | 400 | 8585 | 31 |
| H(111) | 1665 | 238 | 3548 | 25 |
| H(212) | -1072 | 4361 | 5252 | 33 |
| H(106) | 4620 | 2435 | 9937 | 27 |
| H(214) | -865 | 1150 | 5499 | 32 |
| H(112) | 375 | -629 | 1549 | 29 |
| H(215) | 359 | 2198 | 7509 | 27 |
| H(208) | 2329 | 8242 | 10021 | 27 |
| H(114) | -197 | 2610 | 1806 | 26 |
| H(6B) | 6360(50) | 5510(50) | 5820(40) | 37(15) |
| H(6A) | 6620(40) | 5340(50) | 6840(30) | 29(13) |
| H(14) | 1310(60) | 2810(50) | 10150(30) | 49(17) |

**Table A.47: Torsion angles (°) for *fac*-[Re(Flav)$(CO)_3(H_2O)$].Flav (8).**

| Torsion Angle | Angle | Torsion Angle | Angle |
|---|---|---|---|
| O5-Re1-O4-C102 | -9.3(3) | C101-C110-C115-C114 | -176.1(4) |
| O6-Re1-O4-C102 | 71.5(3) | C111-C110-C115-C114 | 2.1(7) |
| C1-Re1-O4-C102 | 167.6(3) | C110-C111-C112-C113 | -0.7(7) |
| C3-Re1-O4-C102 | -103.7(3) | C111-C112-C113-C114 | 2.2(7) |
| O4-Re1-O5-C103 | 8.6(3) | C112-C113-C114-C115 | -1.5(7) |
| O6-Re1-O5-C103 | -71.8(3) | C113-C114-C115-C110 | -0.6(7) |
| C2-Re1-O5-C103 | -165.8(3) | O17-C201-C202-O14 | -179.1(4) |
| C3-Re1-O5-C103 | 106.3(3) | O17-C201-C202-C203 | -1.1(7) |
| Re1-O4-C102-C101 | -169.7(4) | C210-C201-C202-O14 | -1.4(7) |
| Re1-O4-C102-C103 | 9.3(5) | C210-C201-C202-C203 | 176.6(4) |
| Re1-O5-C103-C102 | -6.6(5) | O17-C201-C210-C211 | 9.7(6) |
| Re1-O5-C103-C104 | 172.0(3) | O17-C201-C210-C215 | -171.4(4) |
| C109-O7-C101-C102 | 1.1(6) | C202-C201-C210-C211 | -168.1(5) |
| C109-O7-C101-C110 | 179.5(4) | C202-C201-C210-C215 | 10.7(7) |
| C101-O7-C109-C104 | -1.5(6) | O14-C202-C203-O15 | 1.1(6) |
| C101-O7-C109-C108 | 178.2(4) | O14-C202-C203-C204 | -180.0(4) |
| C201-O17-C209-C208 | -178.0(4) | C201-C202-C203-O15 | -177.1(4) |
| C209-O17-C201-C202 | -0.5(6) | C201-C202-C203-C204 | 1.8(6) |
| C209-O17-C201-C210 | -178.5(4) | O15-C203-C204-C205 | -3.0(7) |
| C201-O17-C209-C204 | 1.3(6) | O15-C203-C204-C209 | 177.8(4) |
| O7-C101-C102-C103 | 0.5(6) | C202-C203-C204-C205 | 178.1(4) |
| C110-C101-C102-O4 | 1.3(7) | C202-C203-C204-C209 | -1.0(6) |
| C110-C101-C102-C103 | -177.6(4) | C203-C204-C205-C206 | -178.8(4) |
| O7-C101-C102-O4 | 179.4(4) | C209-C204-C205-C206 | 0.3(7) |
| C102-C101-C110-C115 | -27.7(7) | C203-C204-C209-O17 | -0.5(7) |
| C102-C101-C110-C111 | 154.2(5) | C203-C204-C209-C208 | 178.8(4) |

| | | | |
|---|---|---|---|
| O7-C101-C110-C111 | -24.1(6) | C205-C204-C209-O17 | -179.7(4) |
| O7-C101-C110-C115 | 154.0(4) | C205-C204-C209-C208 | -0.4(7) |
| O4-C102-C103-C104 | 179.3(4) | C204-C205-C206-C207 | -0.2(7) |
| C101-C102-C103-O5 | 177.0(4) | C205-C206-C207-C208 | 0.1(7) |
| C101-C102-C103-C104 | -1.7(6) | C206-C207-C208-C209 | -0.2(7) |
| O4-C102-C103-O5 | -2.0(6) | C207-C208-C209-C204 | 0.4(7) |
| O5-C103-C104-C105 | 1.0(7) | C201-C210-C211-C212 | 176.4(4) |
| O5-C103-C104-C109 | -177.3(4) | C215-C210-C211-C212 | -2.6(7) |
| C102-C103-C104-C105 | 179.6(4) | C201-C210-C215-C214 | -177.2(4) |
| C102-C103-C104-C109 | 1.3(6) | C211-C210-C215-C214 | 1.7(7) |
| C109-C104-C105-C106 | -1.6(7) | C210-C211-C212-C213 | 1.4(7) |
| C103-C104-C109-O7 | 0.3(6) | C211-C212-C213-C214 | 0.6(7) |
| C103-C104-C109-C108 | -179.4(4) | C212-C213-C214-C215 | -1.5(8) |
| C103-C104-C105-C106 | -179.9(4) | C213-C214-C215-C210 | 0.3(7) |
| C105-C104-C109-O7 | -178.1(4) | C107-C108-C109-C104 | -1.3(7) |
| C105-C104-C109-C108 | 2.2(7) | C107-C108-C109-O7 | 178.9(4) |
| C104-C105-C106-C107 | 0.1(7) | C101-C110-C111-C112 | 176.8(4) |
| C105-C106-C107-C108 | 0.7(7) | C115-C110-C111-C112 | -1.4(7) |
| C106-C107-C108-C109 | -0.2(7) | | |

**Table A.48: Hydrogen bond distances (Å) and angles (°) for *fac*-[Re(Flav)(CO)$_3$(H$_2$O)].Flav (8).**

| D-H…A | d (D-H) | d (H…A) | d (D…A) | D-H…A angle |
|---|---|---|---|---|
| O6-H6A…O15#1 | 0.842(19) | 1.81(2) | 2.636(4) | 166(5) |
| O6-H6B…O4#2 | 0.853(19) | 1.86(3) | 2.663(4) | 157(5) |
| O14-H14…O15 | 0.85(2) | 2.07(5) | 2.596(4) | 119(5) |
| C112-H112…O14#3 | 0.93 | 2.48 | 3.335(5) | 153.0 |
| C115-H115…O4 | 0.93 | 2.42 | 2.985(5) | 119.0 |
| C211-H211…O17 | 0.93 | 2.35 | 2.696(5) | 101.5 |
| C215-H215…O14 | 0.93 | 2.22 | 2.863(5) | 125.2 |

Symmetry codes, transformations used to generate equivalent atoms:
#1 1-x,1-y,2–z #2 1-x,1-y,1–z #3 -x,-y,1-z

**Table A.49: Atomic coordinates (x $10^4$) and equivalent isotropic displacement parameters ($Å^2$ x $10^3$) for μ-(*fac*-[Re(BipyDC)$(CO)_3$])$_2$.$4H_2O$ (9). U(eq) is defined as one third of the trace of the orthogonalized $U^{ij}$ tensor.**

| | x | y | z | U(eq) |
|---|---|---|---|---|
| Re(1) | 1964(1) | 890(1) | 1107(1) | 13(1) |
| C(11) | 1969(4) | 1781(2) | 2463(2) | 19(1) |
| C(45) | 5104(4) | 2948(2) | 901(2) | 15(1) |
| O(4A) | 3109(3) | 1820(2) | 808(1) | 17(1) |
| O(4B) | 3180(3) | 1654(2) | -305(2) | 24(1) |
| O(04A) | 6327(3) | 2208(2) | 2143(1) | 17(1) |
| C(16) | 5905(6) | 1237(4) | 3316(3) | 45(2) |
| O(3) | 343(3) | -339(2) | 1697(2) | 23(1) |
| O(2) | 1377(3) | 54(2) | -258(2) | 23(1) |
| C(22) | 5925(4) | -80(2) | 993(2) | 18(1) |
| O(06) | 824(3) | 3232(2) | 377(2) | 34(1) |
| C(12) | 2442(5) | 2038(3) | 3102(2) | 24(1) |
| N(1) | 2739(3) | 1417(2) | 2073(2) | 14(1) |
| C(25) | 4783(4) | 890(2) | 1829(2) | 14(1) |
| C(44) | 4800(4) | 2440(2) | 361(2) | 14(1) |
| C(3) | 1001(4) | 112(2) | 1479(2) | 16(1) |
| C(1) | 285(5) | 1413(2) | 896(2) | 21(1) |
| N(4) | 6381(3) | 3181(2) | 1092(2) | 16(1) |
| C(41) | 7305(4) | 3027(2) | 695(2) | 19(1) |
| C(14) | 4558(4) | 1486(3) | 2980(2) | 21(1) |
| C(43) | 5769(4) | 2288(2) | -43(2) | 18(1) |
| O(05) | 2650(3) | 3468(2) | -92(2) | 27(1) |
| C(34) | 2798(4) | 3442(2) | 1118(2) | 17(1) |
| C(32) | 2668(4) | 3919(3) | 2238(2) | 25(1) |
| C(26) | 7012(4) | 1603(2) | 2123(2) | 18(1) |
| N(3) | 4751(3) | 3478(2) | 1962(2) | 16(1) |
| C(21) | 4560(4) | -27(2) | 970(2) | 16(1) |
| C(42) | 7025(4) | 2610(3) | 107(2) | 19(1) |
| N(2) | 3990(3) | 447(2) | 1375(2) | 12(1) |
| C(46) | 3568(4) | 1944(2) | 256(2) | 16(1) |
| C(35) | 4156(4) | 3282(2) | 1331(2) | 15(1) |
| C(15) | 4034(4) | 1291(2) | 2315(2) | 14(1) |
| C(13) | 3745(5) | 1872(3) | 3370(2) | 24(1) |
| C(33) | 2071(4) | 3764(3) | 1589(2) | 23(1) |
| C(36) | 2108(4) | 3368(2) | 401(2) | 21(1) |
| C(24) | 6152(4) | 941(2) | 1813(2) | 16(1) |
| C(2) | 1575(4) | 381(2) | 245(2) | 18(1) |
| C(31) | 4022(4) | 3787(3) | 2405(2) | 21(1) |
| Re(2) | 6899(1) | 3378(1) | 2182(1) | 14(1) |
| O(01) | 7266(3) | 3550(2) | 3732(2) | 24(1) |
| O(04B) | 8222(3) | 1522(2) | 2284(2) | 30(1) |
| O(1) | -735(3) | 1699(2) | 787(2) | 34(1) |
| C(02) | 8792(4) | 3216(2) | 2279(2) | 19(1) |
| C(01) | 7132(4) | 3478(2) | 3147(2) | 18(1) |
| C(03) | 7235(4) | 4438(3) | 2094(2) | 18(1) |
| O(02) | 9925(3) | 3136(2) | 2342(2) | 25(1) |
| O(03) | 7486(3) | 5074(2) | 2020(2) | 28(1) |
| C(23) | 6727(4) | 433(2) | 1405(2) | 18(1) |
| O(7) | 628(4) | 1782(2) | -995(2) | 51(1) |
| O(8) | -559(4) | 3137(3) | -842(2) | 52(1) |

| | | | | |
|---|---|---|---|---|
| O(5B) | 6405(8) | 633(5) | 3250(3) | 38(2) |
| O(5A) | 6613(5) | 1826(4) | 3672(3) | 27(2) |
| O(6B) | 6244(16) | 1385(13) | 3908(8) | 45(7) |
| O(6A) | 6000(19) | 447(8) | 3186(10) | 27(2) |
| O(10) | 8140(14) | 311(8) | 4387(8) | 128(8) |
| O(9) | 9110(30) | 41(17) | 5695(11) | 315(19) |
| O(12) | 10322(7) | 5637(4) | 1723(4) | 72(2) |
| O(11) | 10480(30) | 5260(16) | 2043(15) | 72(2) |

**Table A.50: Bond distances (Å) and angles (°) for μ-(*fac*-[Re(BipyDC)(CO)$_3$])$_2$.4H$_2$O (9).**

| Bond | Bond Distance | Bond Angle | Angle |
|---|---|---|---|
| Re(1)-C(3) | 1.895(4) | C(3)-Re(1)-C(2) | 88.21(17) |
| Re(1)-C(2) | 1.922(4) | C(3)-Re(1)-C(1) | 86.31(18) |
| Re(1)-C(1) | 1.924(5) | C(2)-Re(1)-C(1) | 88.31(18) |
| Re(1)-O(4A) | 2.138(3) | C(3)-Re(1)-O(4A) | 173.12(14) |
| Re(1)-N(1) | 2.172(3) | C(2)-Re(1)-O(4A) | 98.64(15) |
| Re(1)-N(2) | 2.186(3) | C(1)-Re(1)-O(4A) | 94.41(15) |
| C(11)-N(1) | 1.344(5) | C(3)-Re(1)-N(1) | 95.55(15) |
| C(11)-C(12) | 1.367(6) | C(2)-Re(1)-N(1) | 170.72(15) |
| C(11)-H(11) | 0.9300 | C(1)-Re(1)-N(1) | 100.38(16) |
| C(45)-N(4) | 1.357(5) | O(4A)-Re(1)-N(1) | 77.59(11) |
| C(45)-C(44) | 1.394(6) | C(3)-Re(1)-N(2) | 99.86(15) |
| C(45)-C(35) | 1.502(6) | C(2)-Re(1)-N(2) | 96.41(15) |
| O(4A)-C(46) | 1.276(5) | C(1)-Re(1)-N(2) | 172.32(15) |
| O(4B)-C(46) | 1.238(5) | O(4A)-Re(1)-N(2) | 78.92(12) |
| O(04A)-C(26) | 1.272(5) | N(1)-Re(1)-N(2) | 74.60(12) |
| O(04A)-Re(2) | 2.128(3) | N(1)-C(11)-C(12) | 122.9(4) |
| C(16)-O(5B) | 1.189(9) | N(1)-C(11)-H(11) | 118.6 |
| C(16)-O(6B) | 1.207(12) | C(12)-C(11)-H(11) | 118.6 |
| C(16)-O(5A) | 1.389(8) | N(4)-C(45)-C(44) | 119.8(4) |
| C(16)-O(6A) | 1.414(14) | N(4)-C(45)-C(35) | 113.0(3) |
| C(16)-C(14) | 1.492(7) | C(44)-C(45)-C(35) | 127.2(4) |
| O(3)-C(3) | 1.160(5) | C(46)-O(4A)-Re(1) | 131.0(3) |
| O(2)-C(2) | 1.147(5) | C(26)-O(04A)-Re(2) | 131.0(3) |
| C(22)-C(21) | 1.382(6) | O(5B)-C(16)-O(6B) | 103.6(10) |
| C(22)-C(23) | 1.394(6) | O(5B)-C(16)-O(5A) | 121.4(6) |
| C(22)-H(22) | 0.9300 | O(6B)-C(16)-O(5A) | 45.0(11) |
| O(06)-C(36) | 1.318(5) | O(5B)-C(16)-O(6A) | 21.1(7) |
| O(06)-H(06) | 0.8200 | O(6B)-C(16)-O(6A) | 111.8(12) |
| C(12)-C(13) | 1.380(6) | O(5A)-C(16)-O(6A) | 140.9(9) |
| C(12)-H(12) | 0.9300 | O(5B)-C(16)-C(14) | 126.0(6) |
| N(1)-C(15) | 1.347(5) | O(6B)-C(16)-C(14) | 118.8(8) |
| C(25)-N(2) | 1.360(5) | O(5A)-C(16)-C(14) | 112.3(5) |
| C(25)-C(24) | 1.398(6) | O(6A)-C(16)-C(14) | 106.7(9) |
| C(25)-C(15) | 1.496(6) | C(21)-C(22)-C(23) | 117.9(4) |
| C(44)-C(43) | 1.389(6) | C(21)-C(22)-H(22) | 121.1 |
| C(44)-C(46) | 1.511(6) | C(23)-C(22)-H(22) | 121.1 |
| C(1)-O(1) | 1.141(5) | C(36)-O(06)-H(06) | 109.5 |
| N(4)-C(41) | 1.344(5) | C(11)-C(12)-C(13) | 118.1(4) |
| N(4)-Re(2) | 2.185(3) | C(11)-C(12)-H(12) | 120.9 |
| C(41)-C(42) | 1.373(6) | C(13)-C(12)-H(12) | 120.9 |
| C(41)-H(41) | 0.9300 | C(11)-N(1)-C(15) | 119.4(3) |
| C(14)-C(13) | 1.392(6) | C(11)-N(1)-Re(1) | 123.4(3) |
| C(14)-C(15) | 1.394(6) | C(15)-N(1)-Re(1) | 116.7(3) |

| | |
|---|---|
| C(43)-C(42) | 1.385(6) |
| C(43)-H(43) | 0.9300 |
| O(05)-C(36) | 1.210(5) |
| C(34)-C(33) | 1.397(6) |
| C(34)-C(35) | 1.407(6) |
| C(34)-C(36) | 1.500(6) |
| C(32)-C(33) | 1.371(6) |
| C(32)-C(31) | 1.383(6) |
| C(32)-H(32) | 0.9300 |
| C(26)-O(04B) | 1.229(5) |
| C(26)-C(24) | 1.523(6) |
| N(3)-C(31) | 1.349(5) |
| N(3)-C(35) | 1.354(5) |
| N(3)-Re(2) | 2.164(4) |
| C(21)-N(2) | 1.349(5) |
| C(21)-H(21) | 0.9300 |
| C(42)-H(42) | 0.9300 |
| C(13)-H(13) | 0.9300 |
| C(33)-H(33) | 0.9300 |
| C(24)-C(23) | 1.392(6) |
| C(31)-H(31) | 0.9300 |
| Re(2)-C(03) | 1.902(5) |
| Re(2)-C(01) | 1.912(4) |
| Re(2)-C(02) | 1.922(5) |
| O(01)-C(01) | 1.160(5) |
| C(02)-O(02) | 1.146(5) |
| C(03)-O(03) | 1.156(5) |
| C(23)-H(23) | 0.9300 |
| O(7)-H(7A) | 0.856(4) |
| O(7)-H(7B) | 0.853(4) |
| O(8)-H(8B) | 0.83(2) |
| O(8)-H(8A) | 0.84(2) |
| O(5A)-H(5A) | 0.8200 |
| O(6A)-H(6A) | 0.8200 |
| O(10)-H(10B) | 0.862(12) |
| O(10)-H(10A) | 0.89(2) |
| O(9)-H(9A) | 0.98(3) |
| O(9)-H(9B) | 0.88(3) |
| O(12)-H(12B) | 0.864(7) |
| O(12)-H(12A) | 0.862(7) |
| O(11)-H(11B) | 0.85(3) |
| O(11)-H(11A) | 0.86(3) |

| | |
|---|---|
| N(2)-C(25)-C(24) | 120.8(4) |
| N(2)-C(25)-C(15) | 113.1(3) |
| C(24)-C(25)-C(15) | 126.2(4) |
| C(43)-C(44)-C(45) | 118.6(4) |
| C(43)-C(44)-C(46) | 117.0(4) |
| C(45)-C(44)-C(46) | 123.6(4) |
| O(3)-C(3)-Re(1) | 175.9(4) |
| O(1)-C(1)-Re(1) | 176.9(4) |
| C(41)-N(4)-C(45) | 119.8(4) |
| C(41)-N(4)-Re(2) | 122.3(3) |
| C(45)-N(4)-Re(2) | 113.6(3) |
| N(4)-C(41)-C(42) | 122.5(4) |
| N(4)-C(41)-H(41) | 118.7 |
| C(42)-C(41)-H(41) | 118.7 |
| C(13)-C(14)-C(15) | 118.5(4) |
| C(13)-C(14)-C(16) | 118.2(4) |
| C(15)-C(14)-C(16) | 123.1(4) |
| C(42)-C(43)-C(44) | 120.4(4) |
| C(42)-C(43)-H(43) | 119.8 |
| C(44)-C(43)-H(43) | 119.8 |
| C(33)-C(34)-C(35) | 118.1(4) |
| C(33)-C(34)-C(36) | 117.2(4) |
| C(35)-C(34)-C(36) | 124.3(4) |
| C(33)-C(32)-C(31) | 118.3(4) |
| C(33)-C(32)-H(32) | 120.9 |
| C(31)-C(32)-H(32) | 120.9 |
| O(04B)-C(26)-O(04A) | 128.1(4) |
| O(04B)-C(26)-C(24) | 120.4(4) |
| O(04A)-C(26)-C(24) | 111.4(3) |
| C(31)-N(3)-C(35) | 119.9(4) |
| C(31)-N(3)-Re(2) | 122.4(3) |
| C(35)-N(3)-Re(2) | 117.4(3) |
| N(2)-C(21)-C(22) | 122.8(4) |
| N(2)-C(21)-H(21) | 118.6 |
| C(22)-C(21)-H(21) | 118.6 |
| C(41)-C(42)-C(43) | 117.7(4) |
| C(41)-C(42)-H(42) | 121.1 |
| C(43)-C(42)-H(42) | 121.1 |
| C(21)-N(2)-C(25) | 119.0(3) |
| C(21)-N(2)-Re(1) | 123.1(3) |
| C(25)-N(2)-Re(1) | 113.6(3) |
| O(4B)-C(46)-O(4A) | 126.9(4) |
| O(4B)-C(46)-C(44) | 120.2(4) |
| O(4A)-C(46)-C(44) | 112.5(3) |
| N(3)-C(35)-C(34) | 120.4(4) |
| N(3)-C(35)-C(45) | 113.3(3) |
| C(34)-C(35)-C(45) | 126.1(4) |
| N(1)-C(15)-C(14) | 120.7(4) |
| N(1)-C(15)-C(25) | 114.2(3) |
| C(14)-C(15)-C(25) | 125.0(4) |
| C(12)-C(13)-C(14) | 120.0(4) |
| C(12)-C(13)-H(13) | 120.0 |
| C(14)-C(13)-H(13) | 120.0 |
| C(32)-C(33)-C(34) | 120.8(4) |
| C(32)-C(33)-H(33) | 119.6 |

| | |
|---|---|
| C(34)-C(33)-H(33) | 119.6 |
| O(05)-C(36)-O(06) | 124.5(4) |
| O(05)-C(36)-C(34) | 123.9(4) |
| O(06)-C(36)-C(34) | 111.4(4) |
| C(23)-C(24)-C(25) | 118.6(4) |
| C(23)-C(24)-C(26) | 117.3(4) |
| C(25)-C(24)-C(26) | 123.3(4) |
| O(2)-C(2)-Re(1) | 177.2(4) |
| N(3)-C(31)-C(32) | 122.3(4) |
| N(3)-C(31)-H(31) | 118.9 |
| C(32)-C(31)-H(31) | 118.9 |
| C(03)-Re(2)-C(01) | 90.39(17) |
| C(03)-Re(2)-C(02) | 87.87(18) |
| C(01)-Re(2)-C(02) | 86.76(17) |
| C(03)-Re(2)-O(04A) | 171.56(14) |
| C(01)-Re(2)-O(04A) | 96.65(14) |
| C(02)-Re(2)-O(04A) | 97.13(15) |
| C(03)-Re(2)-N(3) | 95.26(15) |
| C(01)-Re(2)-N(3) | 99.34(15) |
| C(02)-Re(2)-N(3) | 173.10(15) |
| O(04A)-Re(2)-N(3) | 79.06(12) |
| C(03)-Re(2)-N(4) | 94.68(15) |
| C(01)-Re(2)-N(4) | 172.18(15) |
| C(02)-Re(2)-N(4) | 99.34(15) |
| O(04A)-Re(2)-N(4) | 77.84(12) |
| N(3)-Re(2)-N(4) | 74.31(13) |
| O(02)-C(02)-Re(2) | 178.5(4) |
| O(01)-C(01)-Re(2) | 179.0(4) |
| O(03)-C(03)-Re(2) | 176.7(4) |
| C(24)-C(23)-C(22) | 119.9(4) |
| C(24)-C(23)-H(23) | 120.0 |
| C(22)-C(23)-H(23) | 120.0 |
| H(7A)-O(7)-H(7B) | 106.8(5) |
| H(8B)-O(8)-H(8A) | 103(3) |
| C(16)-O(5A)-H(5A) | 109.5 |
| C(16)-O(6A)-H(6A) | 109.5 |
| H(10B)-O(10)-H(10A) | 103.5(17) |
| H(9A)-O(9)-H(9B) | 94(3) |
| H(12B)-O(12)-H(12A) | 105.4(8) |
| H(11B)-O(11)-H(11A) | 107(3) |

**Table A.51: Anisotropic displacement parameters ($Å^2$ x $10^3$) for μ-(*fac*-[Re(BipyDC)(CO)$_3$])$_2$.4H$_2$O (9). The Anisotropic displacement factor exponent takes the form: $-2\pi^2(h2a^{*2}U^{11} + \ldots + 2hka^*b^*U^{12})$.**

| | U11 | U22 | U33 | U23 | U13 | U12 |
|---|---|---|---|---|---|---|
| Re(1) | 13(1) | 12(1) | 14(1) | -1(1) | 1(1) | 0(1) |
| C(11) | 17(2) | 18(2) | 22(2) | -1(2) | 6(2) | 1(2) |
| C(45) | 16(2) | 14(2) | 14(2) | 1(2) | 2(2) | 2(2) |
| O(4A) | 21(2) | 15(2) | 14(1) | 0(1) | 2(1) | -2(1) |
| O(4B) | 29(2) | 24(2) | 19(2) | -7(1) | -1(1) | -5(1) |
| O(04A) | 16(2) | 14(2) | 21(2) | -4(1) | 1(1) | -1(1) |
| C(16) | 38(3) | 78(5) | 17(3) | -11(3) | -7(2) | 29(3) |
| O(3) | 21(2) | 23(2) | 23(2) | 8(1) | -1(1) | -5(1) |

| | | | | | | |
|---|---|---|---|---|---|---|
| O(2) | 21(2) | 30(2) | 18(2) | -7(1) | 3(1) | -6(1) |
| C(22) | 20(2) | 14(2) | 20(2) | -5(2) | 6(2) | 3(2) |
| O(06) | 20(2) | 58(2) | 22(2) | -5(2) | -2(1) | -11(2) |
| C(12) | 25(2) | 22(2) | 27(2) | -7(2) | 12(2) | -1(2) |
| N(1) | 17(2) | 11(2) | 14(2) | -2(1) | 4(1) | -2(1) |
| C(25) | 19(2) | 10(2) | 13(2) | 1(2) | 1(2) | 0(2) |
| C(44) | 19(2) | 13(2) | 11(2) | 3(2) | 2(2) | 3(2) |
| C(3) | 16(2) | 17(2) | 14(2) | -2(2) | -4(2) | 2(2) |
| C(1) | 24(2) | 18(2) | 21(2) | 2(2) | 0(2) | -2(2) |
| N(4) | 16(2) | 16(2) | 16(2) | -1(1) | 3(1) | 0(1) |
| C(41) | 15(2) | 21(2) | 22(2) | 2(2) | 4(2) | 2(2) |
| C(14) | 23(2) | 23(2) | 16(2) | -5(2) | 2(2) | 2(2) |
| C(43) | 23(2) | 17(2) | 12(2) | 2(2) | 2(2) | 5(2) |
| O(05) | 23(2) | 37(2) | 21(2) | 4(1) | 4(1) | 7(2) |
| C(34) | 17(2) | 15(2) | 21(2) | -1(2) | 7(2) | -2(2) |
| C(32) | 20(2) | 30(3) | 26(2) | -14(2) | 8(2) | -1(2) |
| C(26) | 16(2) | 21(2) | 17(2) | -4(2) | 0(2) | 1(2) |
| N(3) | 15(2) | 14(2) | 18(2) | -5(1) | 2(1) | -1(1) |
| C(21) | 22(2) | 12(2) | 15(2) | -2(2) | 2(2) | -1(2) |
| C(42) | 16(2) | 30(2) | 13(2) | 4(2) | 5(2) | 5(2) |
| N(2) | 14(2) | 11(2) | 13(2) | -1(1) | 3(1) | 1(1) |
| C(46) | 21(2) | 10(2) | 15(2) | -1(2) | 0(2) | 2(2) |
| C(35) | 14(2) | 12(2) | 17(2) | -1(2) | 1(2) | -4(2) |
| C(15) | 14(2) | 11(2) | 16(2) | -1(2) | 2(2) | -2(2) |
| C(13) | 27(2) | 27(2) | 20(2) | -5(2) | 4(2) | -2(2) |
| C(33) | 16(2) | 27(2) | 27(2) | -4(2) | 2(2) | -3(2) |
| C(36) | 19(2) | 16(2) | 26(2) | -2(2) | 2(2) | 3(2) |
| C(24) | 18(2) | 15(2) | 15(2) | 1(2) | -2(2) | 1(2) |
| C(2) | 13(2) | 19(2) | 21(2) | 0(2) | 3(2) | 1(2) |
| C(31) | 21(2) | 23(2) | 19(2) | -7(2) | 5(2) | -2(2) |
| Re(2) | 13(1) | 14(1) | 15(1) | -4(1) | 1(1) | -1(1) |
| O(01) | 31(2) | 23(2) | 17(2) | -4(1) | 4(1) | 0(1) |
| O(04B) | 17(2) | 24(2) | 47(2) | -11(2) | -6(2) | 2(1) |
| O(1) | 21(2) | 32(2) | 48(2) | 5(2) | 1(2) | 11(2) |
| C(02) | 23(2) | 17(2) | 17(2) | -5(2) | 3(2) | -2(2) |
| C(01) | 13(2) | 12(2) | 28(2) | -1(2) | 4(2) | 1(2) |
| C(03) | 16(2) | 21(2) | 16(2) | -5(2) | -2(2) | 1(2) |
| O(02) | 16(2) | 29(2) | 31(2) | -5(1) | 3(1) | 1(1) |
| O(03) | 33(2) | 19(2) | 31(2) | -1(1) | 0(2) | -3(1) |
| C(23) | 17(2) | 16(2) | 22(2) | -1(2) | 6(2) | 2(2) |
| O(7) | 58(3) | 47(2) | 41(2) | 12(2) | -20(2) | -19(2) |
| O(8) | 41(2) | 78(3) | 38(2) | -18(2) | 10(2) | -25(3) |
| O(5B) | 32(4) | 36(4) | 38(3) | -10(3) | -19(3) | 10(3) |
| O(5A) | 21(3) | 35(4) | 22(3) | -9(2) | -8(2) | 0(2) |
| O(6B) | 31(8) | 61(14) | 37(10) | -27(9) | -13(7) | -1(8) |
| O(6A) | 21(3) | 35(4) | 22(3) | -9(2) | -8(2) | 0(2) |
| O(10) | 93(11) | 97(11) | 167(15) | 83(10) | -72(10) | -32(8) |
| O(9) | 410(40) | 350(40) | 141(19) | -90(20) | -110(20) | 50(30) |
| O(12) | 98(5) | 42(4) | 68(5) | 3(3) | -15(4) | -4(4) |
| O(11) | 98(5) | 42(4) | 68(5) | 3(3) | -15(4) | -4(4) |

**Table A.52: Hydrogen coordinates (x $10^4$) and isotropic displacement parameters ($Å^2$ x $10^3$) for μ-(*fac*-[Re(BipyDC)$(CO)_3$])$_2$.4$H_2O$ (9).**

| | x | y | z | U(eq) |
|---|---|---|---|---|
| H(11) | 1076 | 1862 | 2291 | 23 |
| H(22) | 6297 | -446 | 741 | 21 |
| H(06) | 437 | 3309 | -9 | 51 |
| H(12) | 1900 | 2316 | 3348 | 29 |
| H(41) | 8168 | 3208 | 823 | 23 |
| H(43) | 5573 | 1967 | -416 | 21 |
| H(32) | 2176 | 4108 | 2558 | 30 |
| H(21) | 4012 | -331 | 662 | 19 |
| H(42) | 7657 | 2547 | -181 | 23 |
| H(13) | 4081 | 2019 | 3811 | 29 |
| H(33) | 1172 | 3873 | 1460 | 28 |
| H(31) | 4444 | 3914 | 2837 | 25 |
| H(23) | 7644 | 437 | 1408 | 21 |
| H(5A) | 7317 | 1660 | 3876 | 41 |
| H(6A) | 5821 | 370 | 2776 | 41 |
| H(10B) | 7443 | 209 | 4097 | 109 |
| H(10A) | 7809 | 535 | 4723 | 109 |
| H(9A) | 8989 | -110 | 6158 | 109 |
| H(9B) | 9409 | -409 | 5590 | 109 |
| H(11B) | 11088 | 4941 | 2010 | 109 |
| H(11A) | 10186 | 5165 | 2419 | 109 |
| H(12B) | 10471 | 5589 | 1310 | 109 |
| H(12A) | 9792 | 6022 | 1718 | 109 |
| H(8B) | -220(70) | 2730(20) | -950(40) | 70(30) |
| H(8A) | -170(110) | 3460(30) | -1050(60) | 200(60) |
| H(7A) | 1403 | 1595 | -862 | 293 |
| H(7B) | 373 | 1612 | -1395 | 293 |

**Table A.53: Torsion angles (°) for μ-(*fac*-[Re(BipyDC)$(CO)_3$])$_2$.4$H_2O$ (9).**

| Torsion Angle | Angle | Torsion Angle | Angle |
|---|---|---|---|
| N1-Re1-O4A-C46 | 162.2(4) | O04A-Re2-N4-C41 | -97.6(4) |
| N2-Re1-O4A-C46 | 85.7(4) | O04A-Re2-N4-C45 | 59.2(3) |
| C1-Re1-O4A-C46 | -98.2(4) | N3-Re2-N4-C41 | -179.5(4) |
| C2-Re1-O4A-C46 | -9.2(4) | N3-Re2-N4-C45 | -22.7(3) |
| O4A-Re1-N1-C11 | 112.2(3) | C02-Re2-N4-C41 | -2.2(4) |
| O4A-Re1-N1-C15 | -75.3(3) | C02-Re2-N4-C45 | 154.5(3) |
| N2-Re1-N1-C11 | -166.1(3) | C03-Re2-N4-C41 | 86.4(4) |
| N2-Re1-N1-C15 | 6.4(3) | C03-Re2-N4-C45 | -116.9(3) |
| C1-Re1-N1-C11 | 19.9(3) | Re2-O04A-C26-C24 | -156.4(3) |
| C1-Re1-N1-C15 | -167.6(3) | Re1-O4A-C46-O4B | 20.1(6) |
| C3-Re1-N1-C11 | -67.4(3) | Re1-O4A-C46-C44 | -153.1(3) |
| C3-Re1-N1-C15 | 105.2(3) | Re1-N1-C11-C12 | 172.7(3) |
| O4A-Re1-N2-C21 | -97.4(3) | C15-N1-C11-C12 | 0.4(6) |
| O4A-Re1-N2-C25 | 59.0(3) | C11-N1-C15-C25 | -179.4(3) |
| N1-Re1-N2-C21 | -177.5(3) | Re1-N1-C15-C14 | -168.2(3) |
| N1-Re1-N2-C25 | -21.1(3) | C11-N1-C15-C14 | 4.6(6) |
| C2-Re1-N2-C21 | 0.2(3) | Re1-N1-C15-C25 | 7.8(4) |
| C2-Re1-N2-C25 | 156.6(3) | C21-N2-C25-C15 | -170.9(3) |
| C3-Re1-N2-C21 | 89.4(3) | Re1-N2-C25-C24 | -148.1(3) |
| C3-Re1-N2-C25 | -114.2(3) | C21-N2-C25-C24 | 9.4(5) |

| | | | |
|---|---|---|---|
| N3-Re2-O04A-C26 | 168.0(4) | Re1-N2-C25-C15 | 31.7(4) |
| N4-Re2-O04A-C26 | 91.9(3) | C25-N2-C21-C22 | -0.5(6) |
| C02-Re2-O04A-C26 | -6.1(4) | Re1-N2-C21-C22 | 154.7(3) |
| C01-Re2-O04A-C26 | -93.7(4) | C01-Re2-N3-C31 | 19.0(4) |
| O04A-Re2-N3-C31 | 114.0(4) | C01-Re2-N3-C35 | -166.9(3) |
| O04A-Re2-N3-C35 | -71.9(3) | C03-Re2-N3-C31 | -72.2(4) |
| N4-Re2-N3-C31 | -165.7(4) | C03-Re2-N3-C35 | 101.9(3) |
| N4-Re2-N3-C35 | 8.4(3) | C45-C44-C46-O4A | -24.3(5) |
| C35-N3-C31-C32 | -0.4(7) | C23-C24-C26-O04A | 143.3(4) |
| Re2-N3-C31-C32 | 173.5(4) | C26-C24-C25-N2 | 158.4(4) |
| Re2-N3-C35-C34 | -170.2(3) | C23-C24-C26-O04B | -33.0(6) |
| C31-N3-C35-C34 | 4.1(6) | C23-C24-C25-C15 | 169.3(4) |
| C31-N3-C35-C45 | 179.9(4) | C25-C24-C26-O04B | 157.5(4) |
| Re2-N3-C35-C45 | 5.7(4) | C25-C24-C26-O04A | -26.2(5) |
| C41-N4-C45-C44 | 11.1(6) | N3-C31-C32-C33 | -3.3(8) |
| C45-N4-C41-C42 | -2.7(7) | C31-C32-C33-C34 | 3.4(7) |
| C41-N4-C45-C35 | -169.8(4) | C32-C33-C34-C36 | -173.7(4) |
| Re2-N4-C41-C42 | 152.7(4) | C32-C33-C34-C35 | 0.1(7) |
| Re2-N4-C45-C44 | -146.3(3) | C35-C34-C36-O06 | 153.2(4) |
| Re2-N4-C45-C35 | 32.8(4) | C35-C34-C36-O05 | -31.0(6) |
| N1-C11-C12-C13 | -4.2(7) | C33-C34-C36-O05 | 142.3(4) |
| C11-C12-C13-C14 | 3.1(7) | C36-C34-C35-C45 | -5.9(6) |
| C12-C13-C14-C16 | -172.9(5) | C33-C34-C36-O06 | -33.5(5) |
| C12-C13-C14-C15 | 1.6(7) | C36-C34-C35-N3 | 169.4(3) |
| C16-C14-C15-N1 | 168.6(5) | C33-C34-C35-C45 | -179.1(4) |
| C13-C14-C15-N1 | -5.6(7) | C33-C34-C35-N3 | -3.9(6) |
| C13-C14-C15-C25 | 178.9(4) | C34-C35-C45-N4 | 150.0(4) |
| C15-C14-C16-O5A | 135.5(5) | N3-C35-C45-C44 | 153.5(4) |
| C13-C14-C16-O5B | 136.3(7) | N3-C35-C45-N4 | -25.5(5) |
| C16-C14-C15-C25 | -6.9(7) | C34-C35-C45-C44 | -31.0(6) |
| C15-C14-C16-O5B | -37.9(9) | N4-C41-C42-C43 | -5.5(7) |
| C13-C14-C16-O5A | -50.3(7) | C41-C42-C43-C44 | 5.4(6) |
| N1-C15-C25-C24 | 153.5(4) | C42-C43-C44-C45 | 2.7(6) |
| C14-C15-C25-N2 | 149.5(4) | C42-C43-C44-C46 | -167.5(4) |
| C14-C15-C25-C24 | -30.8(6) | C43-C44-C45-N4 | -11.0(5) |
| N1-C15-C25-N2 | -26.3(5) | C45-C44-C46-O4B | 162.0(4) |
| N2-C21-C22-C23 | -6.5(6) | C43-C44-C45-C35 | 170.0(4) |
| C21-C22-C23-C24 | 4.6(6) | C46-C44-C45-N4 | 158.4(4) |
| C22-C23-C24-C25 | 3.8(6) | C46-C44-C45-C35 | -20.6(6) |
| C22-C23-C24-C26 | -166.2(4) | C43-C44-C46-O4A | 145.3(4) |
| C26-C24-C25-C15 | -21.3(6) | C43-C44-C46-O4B | -28.4(5) |
| C23-C24-C25-N2 | -11.0(6) | | |

**Table A.54: Hydrogen bond distances (Å) and angles (°) for μ-(*fac*-[Re(BipyDC)(CO)$_3$])$_2$.4H$_2$O (9).**

| D-H…A | d (D-H) | d (H…A) | d (D…A) | D-H…A angle |
|---|---|---|---|---|
| O06-H06…O8 | 0.82 | 1.83 | 2.620(5) | 160.5 |
| O5A-H5A…O8#1 | 0.82 | 2.17 | 2.886(7) | 145.6 |
| O7-H7A…O4B | 0.856(4) | 1.972(3) | 2.751(5) | 150.8(3) |
| O7-H7B…O02#2 | 0.853(4) | 2.530(3) | 3.288(5) | 148.5(3) |
| O7-H7B…O3#3 | 0.853(4) | 2.394(3) | 2.983(5) | 126.6(3) |
| O8-H8A…O12#4 | 0.84(2) | 2.06(6) | 2.808(9) | 148(11) |
| O8-H8B…O7 | 0.83(2) | 1.88(2) | 2.702(7) | 169(8) |
| C9-H9A…O03#5 | 0.98(3) | 2.468(3) | 3.33(3) | 145.3(18) |
| C12-H12A…O8#4 | 0.864(7) | 2.425(6) | 2.808(10) | 107.5(5) |

| | | | | |
|---|---|---|---|---|
| C12-H12B…O8#4 | 0.864(7) | 2.425(6) | 2.808(10) | 107.5(5) |
| C11-H11…O02#6 | 0.93 | 2.53 | 3.137(5) | 123.4 |
| C12-H12…O7#5 | 0.93 | 2.53 | 3.453(6) | 172.5 |
| C22-H22…O4B#7 | 0.93 | 2.38 | 3.269(5) | 160.6 |

Symmetry codes, transformations used to generate equivalent atoms:
#1 1+x,0.5-y,0.5+z #2 -1+x,0.5-y,-0.5+z #3 -x,-y,-z #4 1-x,1-y,-z #5 x,0.5-y,0.5+z #6 -1+x,y,z #7 1-x,-y,-z.

**Table A.55: Atomic coordinates (x $10^4$) and equivalent isotropic displacement parameters ($Å^2$ x $10^3$) for *fac*-[Re(PNP)(CO)$_3$(Br)] (10). U(eq) is defined as one third of the trace of the orthogonalized $U^{ij}$ tensor.**

| | x | y | z | U(eq) |
|---|---|---|---|---|
| Re(1) | 6867(1) | 1066(1) | 2022(1) | 21(1) |
| P(2) | 7319(1) | 2013(1) | 3209(1) | 24(1) |
| P(1) | 8556(1) | 1950(1) | 1787(1) | 24(1) |
| C(2) | 5544(5) | 550(3) | 2545(3) | 29(1) |
| O(2) | 4813(4) | 257(2) | 2910(3) | 41(1) |
| C(34) | 8309(8) | 726(4) | 5839(4) | 54(2) |
| C(35) | 9231(8) | 940(3) | 5363(5) | 59(2) |
| O(1) | 6682(4) | -50(2) | 405(2) | 44(1) |
| C(1) | 6767(5) | 356(3) | 1004(3) | 30(1) |
| C(32) | 6848(6) | 1351(3) | 4772(3) | 33(1) |
| C(44) | 4952(6) | 4065(3) | 3942(4) | 44(2) |
| C(46) | 5320(6) | 3030(3) | 2950(4) | 37(1) |
| C(31) | 7784(5) | 1570(3) | 4284(3) | 27(1) |
| C(11) | 10162(5) | 1714(3) | 1741(3) | 24(1) |
| C(26) | 7771(5) | 3402(3) | 1033(4) | 37(1) |
| C(22) | 8530(5) | 2458(3) | 66(4) | 33(1) |
| C(21) | 8280(5) | 2662(3) | 914(3) | 27(1) |
| C(13) | 11832(5) | 804(4) | 1978(4) | 38(1) |
| C(16) | 10980(5) | 2284(3) | 1531(3) | 26(1) |
| C(41) | 6376(5) | 2829(3) | 3499(3) | 28(1) |
| C(36) | 8976(6) | 1362(3) | 4586(4) | 41(2) |
| C(15) | 12208(5) | 2119(3) | 1548(3) | 31(1) |
| C(14) | 12640(5) | 1374(4) | 1773(4) | 40(1) |
| N(1) | 8534(5) | 2416(3) | 2781(3) | 36(1) |
| C(45) | 4618(6) | 3653(4) | 3180(4) | 45(2) |
| C(24) | 7837(6) | 3709(4) | -495(4) | 44(2) |
| C(12) | 10608(5) | 967(3) | 1967(3) | 29(1) |
| C(25) | 7571(6) | 3918(3) | 334(4) | 45(2) |
| C(23) | 8290(5) | 2972(4) | -641(4) | 41(1) |
| C(42) | 6723(5) | 3252(3) | 4263(4) | 32(1) |
| C(43) | 6020(6) | 3875(3) | 4491(4) | 41(2) |
| C(33) | 7131(8) | 925(3) | 5559(4) | 49(2) |
| Br(2) | 8260(2) | 30(2) | 2910(2) | 27(1) |
| C(3A) | 5759(17) | 1762(8) | 1278(10) | 28(2) |
| O(3A) | 5099(18) | 2120(12) | 825(14) | 41(6) |
| Br(1) | 5387(2) | 1954(1) | 986(2) | 25(1) |
| C(3B) | 7961(12) | 396(7) | 2678(8) | 28(2) |
| O(3B) | 8632(15) | -78(12) | 3052(13) | 55(6) |
| C(4B) | 9665(16) | 2791(10) | 3419(10) | 26(4) |
| C(5B) | 9803(16) | 3628(10) | 3113(11) | 34(2) |
| C(6B) | 10900(40) | 3978(18) | 3650(30) | 36(7) |
| C(4A) | 9177(8) | 3159(5) | 2997(5) | 25(2) |
| C(5A) | 10330(10) | 3019(5) | 3604(6) | 34(2) |
| C(6A) | 11120(20) | 3748(10) | 3713(19) | 47(4) |

**Table A.56: Bond distances (Å) and angles (°) for *fac*-[Re(PNP)(CO)$_3$(Br)] (10).**

| Bond | Bond Distance | Bond Angle | Angle |
|---|---|---|---|
| Re(1)-C(3B) | 1.866(15) | C(3B)-Re(1)-C(2) | 88.2(3) |
| Re(1)-C(2) | 1.952(5) | C(3B)-Re(1)-C(1) | 90.8(3) |

| | | | |
|---|---|---|---|
| Re(1)-C(1) | 1.962(6) | C(2)-Re(1)-C(1) | 93.7(2) |
| Re(1)-C(3A) | 1.969(18) | C(3B)-Re(1)-C(3A) | 177.1(5) |
| Re(1)-P(2) | 2.4375(14) | C(2)-Re(1)-C(3A) | 93.9(5) |
| Re(1)-P(1) | 2.4583(15) | C(1)-Re(1)-C(3A) | 87.1(4) |
| Re(1)-Br(2) | 2.617(3) | C(3B)-Re(1)-P(2) | 87.2(3) |
| Re(1)-Br(1) | 2.619(2) | C(2)-Re(1)-P(2) | 95.62(16) |
| P(2)-N(1) | 1.702(5) | C(1)-Re(1)-P(2) | 170.40(16) |
| P(2)-C(31) | 1.820(5) | C(3A)-Re(1)-P(2) | 94.6(4) |
| P(2)-C(41) | 1.828(5) | C(3B)-Re(1)-P(1) | 90.3(3) |
| P(2)-P(1) | 2.6897(18) | C(2)-Re(1)-P(1) | 162.26(16) |
| P(1)-N(1) | 1.713(4) | C(1)-Re(1)-P(1) | 104.00(16) |
| P(1)-C(21) | 1.804(5) | C(3A)-Re(1)-P(1) | 88.3(4) |
| P(1)-C(11) | 1.824(5) | P(2)-Re(1)-P(1) | 66.65(4) |
| C(2)-O(2) | 1.146(6) | C(3B)-Re(1)-Br(2) | 5.0(3) |
| C(34)-C(33) | 1.361(10) | C(2)-Re(1)-Br(2) | 84.41(16) |
| C(34)-C(35) | 1.364(10) | C(1)-Re(1)-Br(2) | 87.79(16) |
| C(34)-H(34) | 0.9300 | C(3A)-Re(1)-Br(2) | 174.5(4) |
| C(35)-C(36) | 1.386(9) | P(2)-Re(1)-Br(2) | 90.82(7) |
| C(35)-H(35) | 0.9300 | P(1)-Re(1)-Br(2) | 94.96(7) |
| O(1)-C(1) | 1.142(6) | C(3B)-Re(1)-Br(1) | 175.4(3) |
| C(32)-C(31) | 1.392(7) | C(2)-Re(1)-Br(1) | 93.85(16) |
| C(32)-C(33) | 1.405(8) | C(1)-Re(1)-Br(1) | 85.02(16) |
| C(32)-H(32) | 0.9300 | C(3A)-Re(1)-Br(1) | 2.1(4) |
| C(44)-C(45) | 1.370(9) | P(2)-Re(1)-Br(1) | 96.64(7) |
| C(44)-C(43) | 1.399(9) | P(1)-Re(1)-Br(1) | 88.92(7) |
| C(44)-H(44) | 0.9300 | Br(2)-Re(1)-Br(1) | 172.48(9) |
| C(46)-C(45) | 1.388(8) | N(1)-P(2)-C(31) | 111.2(3) |
| C(46)-C(41) | 1.392(8) | N(1)-P(2)-C(41) | 106.0(2) |
| C(46)-H(46) | 0.9300 | C(31)-P(2)-C(41) | 102.2(2) |
| C(31)-C(36) | 1.385(8) | N(1)-P(2)-Re(1) | 95.10(15) |
| C(11)-C(16) | 1.392(7) | C(31)-P(2)-Re(1) | 113.44(16) |
| C(11)-C(12) | 1.402(7) | C(41)-P(2)-Re(1) | 128.11(19) |
| C(26)-C(25) | 1.381(8) | N(1)-P(2)-P(1) | 38.18(15) |
| C(26)-C(21) | 1.407(7) | C(31)-P(2)-P(1) | 126.09(18) |
| C(26)-H(26) | 0.9300 | C(41)-P(2)-P(1) | 125.45(16) |
| C(22)-C(23) | 1.393(8) | Re(1)-P(2)-P(1) | 57.05(4) |
| C(22)-C(21) | 1.395(7) | N(1)-P(1)-C(21) | 108.3(2) |
| C(22)-H(22) | 0.9300 | N(1)-P(1)-C(11) | 104.6(2) |
| C(13)-C(12) | 1.374(7) | C(21)-P(1)-C(11) | 101.6(2) |
| C(13)-C(14) | 1.382(8) | N(1)-P(1)-Re(1) | 94.08(16) |
| C(13)-H(13) | 0.9300 | C(21)-P(1)-Re(1) | 117.41(18) |
| C(16)-C(15) | 1.379(7) | C(11)-P(1)-Re(1) | 128.48(18) |
| C(16)-H(16) | 0.9300 | N(1)-P(1)-P(2) | 37.89(16) |
| C(41)-C(42) | 1.385(8) | C(21)-P(1)-P(2) | 120.47(17) |
| C(36)-H(36) | 0.9300 | C(11)-P(1)-P(2) | 128.68(17) |
| C(15)-C(14) | 1.393(8) | Re(1)-P(1)-P(2) | 56.30(4) |
| C(15)-H(15) | 0.9300 | O(2)-C(2)-Re(1) | 175.1(5) |
| C(14)-H(14) | 0.9300 | C(33)-C(34)-C(35) | 120.5(6) |
| N(1)-C(4A) | 1.477(9) | C(33)-C(34)-H(34) | 119.8 |
| N(1)-C(4B) | 1.619(18) | C(35)-C(34)-H(34) | 119.8 |
| C(45)-H(45) | 0.9300 | C(34)-C(35)-C(36) | 120.2(7) |
| C(24)-C(25) | 1.376(9) | C(34)-C(35)-H(35) | 119.9 |
| C(24)-C(23) | 1.386(8) | C(36)-C(35)-H(35) | 119.9 |
| C(24)-H(24) | 0.9300 | O(1)-C(1)-Re(1) | 178.4(5) |
| C(12)-H(12) | 0.9300 | C(31)-C(32)-C(33) | 119.3(6) |

| | |
|---|---|
| C(25)-H(25) | 0.9300 |
| C(23)-H(23) | 0.9300 |
| C(42)-C(43) | 1.388(8) |
| C(42)-H(42) | 0.9300 |
| C(43)-H(43) | 0.9300 |
| C(33)-H(33) | 0.9300 |
| C(3A)-O(3A) | 1.12(2) |
| C(3B)-O(3B) | 1.20(2) |
| C(4B)-C(5B) | 1.52(2) |
| C(4B)-H(4B1) | 0.9700 |
| C(4B)-H(4B2) | 0.9700 |
| C(5B)-C(6B) | 1.50(5) |
| C(5B)-H(5B1) | 0.9700 |
| C(5B)-H(5B2) | 0.9700 |
| C(6B)-H(6B1) | 0.9600 |
| C(6B)-H(6B2) | 0.9600 |
| C(6B)-H(6B3) | 0.9600 |
| C(4A)-C(5A) | 1.500(13) |
| C(4A)-H(4A1) | 0.9700 |
| C(4A)-H(4A2) | 0.9700 |
| C(5A)-C(6A) | 1.52(3) |
| C(5A)-H(5A1) | 0.9700 |
| C(5A)-H(5A2) | 0.9700 |
| C(6A)-H(6A1) | 0.9600 |
| C(6A)-H(6A2) | 0.9600 |
| C(6A)-H(6A3) | 0.9600 |

| | |
|---|---|
| C(31)-C(32)-H(32) | 120.3 |
| C(33)-C(32)-H(32) | 120.3 |
| C(45)-C(44)-C(43) | 120.6(6) |
| C(45)-C(44)-H(44) | 119.7 |
| C(43)-C(44)-H(44) | 119.7 |
| C(45)-C(46)-C(41) | 119.4(6) |
| C(45)-C(46)-H(46) | 120.3 |
| C(41)-C(46)-H(46) | 120.3 |
| C(36)-C(31)-C(32) | 119.0(5) |
| C(36)-C(31)-P(2) | 124.2(4) |
| C(32)-C(31)-P(2) | 116.4(4) |
| C(16)-C(11)-C(12) | 118.8(5) |
| C(16)-C(11)-P(1) | 120.7(4) |
| C(12)-C(11)-P(1) | 120.4(4) |
| C(25)-C(26)-C(21) | 120.7(5) |
| C(25)-C(26)-H(26) | 119.6 |
| C(21)-C(26)-H(26) | 119.6 |
| C(23)-C(22)-C(21) | 120.9(5) |
| C(23)-C(22)-H(22) | 119.5 |
| C(21)-C(22)-H(22) | 119.5 |
| C(22)-C(21)-C(26) | 118.0(5) |
| C(22)-C(21)-P(1) | 118.4(4) |
| C(26)-C(21)-P(1) | 123.5(4) |
| C(12)-C(13)-C(14) | 120.6(6) |
| C(12)-C(13)-H(13) | 119.7 |
| C(14)-C(13)-H(13) | 119.7 |
| C(15)-C(16)-C(11) | 120.8(5) |
| C(15)-C(16)-H(16) | 119.6 |
| C(11)-C(16)-H(16) | 119.6 |
| C(42)-C(41)-C(46) | 120.1(5) |
| C(42)-C(41)-P(2) | 119.6(4) |
| C(46)-C(41)-P(2) | 120.2(4) |
| C(31)-C(36)-C(35) | 120.5(7) |
| C(31)-C(36)-H(36) | 119.8 |
| C(35)-C(36)-H(36) | 119.8 |
| C(16)-C(15)-C(14) | 119.9(5) |
| C(16)-C(15)-H(15) | 120.0 |
| C(14)-C(15)-H(15) | 120.0 |
| C(13)-C(14)-C(15) | 119.7(5) |
| C(13)-C(14)-H(14) | 120.2 |
| C(15)-C(14)-H(14) | 120.2 |
| C(4A)-N(1)-C(4B) | 37.7(6) |
| C(4A)-N(1)-P(2) | 130.1(4) |
| C(4B)-N(1)-P(2) | 121.1(6) |
| C(4A)-N(1)-P(1) | 122.9(4) |
| C(4B)-N(1)-P(1) | 128.7(6) |
| P(2)-N(1)-P(1) | 103.9(2) |
| C(44)-C(45)-C(46) | 120.5(6) |
| C(44)-C(45)-H(45) | 119.7 |
| C(46)-C(45)-H(45) | 119.7 |
| C(25)-C(24)-C(23) | 120.3(6) |
| C(25)-C(24)-H(24) | 119.9 |
| C(23)-C(24)-H(24) | 119.9 |
| C(13)-C(12)-C(11) | 120.2(5) |
| C(13)-C(12)-H(12) | 119.9 |

| | | |
|---|---|---|
| | C(11)-C(12)-H(12) | 119.9 |
| | C(24)-C(25)-C(26) | 120.3(5) |
| | C(24)-C(25)-H(25) | 119.8 |
| | C(26)-C(25)-H(25) | 119.8 |
| | C(24)-C(23)-C(22) | 119.6(6) |
| | C(24)-C(23)-H(23) | 120.2 |
| | C(22)-C(23)-H(23) | 120.2 |
| | C(41)-C(42)-C(43) | 120.4(6) |
| | C(41)-C(42)-H(42) | 119.8 |
| | C(43)-C(42)-H(42) | 119.8 |
| | C(42)-C(43)-C(44) | 119.0(6) |
| | C(42)-C(43)-H(43) | 120.5 |
| | C(44)-C(43)-H(43) | 120.5 |
| | C(34)-C(33)-C(32) | 120.4(7) |
| | C(34)-C(33)-H(33) | 119.8 |
| | C(32)-C(33)-H(33) | 119.8 |
| | O(3A)-C(3A)-Re(1) | 176(2) |
| | O(3B)-C(3B)-Re(1) | 174.9(14) |
| | C(5B)-C(4B)-N(1) | 106.8(12) |
| | C(5B)-C(4B)-H(4B1) | 110.4 |
| | N(1)-C(4B)-H(4B1) | 110.4 |
| | C(5B)-C(4B)-H(4B2) | 110.4 |
| | N(1)-C(4B)-H(4B2) | 110.4 |
| | H(4B1)-C(4B)-H(4B2) | 108.6 |
| | C(6B)-C(5B)-C(4B) | 108.4(17) |
| | C(6B)-C(5B)-H(5B1) | 110.0 |
| | C(4B)-C(5B)-H(5B1) | 110.0 |
| | C(6B)-C(5B)-H(5B2) | 110.0 |
| | C(4B)-C(5B)-H(5B2) | 110.0 |
| | H(5B1)-C(5B)-H(5B2) | 108.4 |
| | C(5B)-C(6B)-H(6B1) | 109.5 |
| | C(5B)-C(6B)-H(6B2) | 109.5 |
| | H(6B1)-C(6B)-H(6B2) | 109.5 |
| | C(5B)-C(6B)-H(6B3) | 109.5 |
| | H(6B1)-C(6B)-H(6B3) | 109.5 |
| | H(6B2)-C(6B)-H(6B3) | 109.5 |
| | N(1)-C(4A)-C(5A) | 110.3(7) |
| | N(1)-C(4A)-H(4A1) | 109.6 |
| | C(5A)-C(4A)-H(4A1) | 109.6 |
| | N(1)-C(4A)-H(4A2) | 109.6 |
| | C(5A)-C(4A)-H(4A2) | 109.6 |
| | H(4A1)-C(4A)-H(4A2) | 108.1 |
| | C(4A)-C(5A)-C(6A) | 111.6(9) |
| | C(4A)-C(5A)-H(5A1) | 109.3 |
| | C(6A)-C(5A)-H(5A1) | 109.3 |
| | C(4A)-C(5A)-H(5A2) | 109.3 |
| | C(6A)-C(5A)-H(5A2) | 109.3 |
| | H(5A1)-C(5A)-H(5A2) | 108.0 |
| | C(5A)-C(6A)-H(6A1) | 109.5 |
| | C(5A)-C(6A)-H(6A2) | 109.5 |
| | H(6A1)-C(6A)-H(6A2) | 109.5 |
| | C(5A)-C(6A)-H(6A3) | 109.5 |
| | H(6A1)-C(6A)-H(6A3) | 109.5 |
| | H(6A2)-C(6A)-H(6A3) | 109.5 |

**Table A.57: Anisotropic displacement parameters ($Å^2$ x $10^3$) for *fac*-[Re(PNP)$(CO)_3$(Br)] (10). The Anisotropic displacement factor exponent takes the form: $-2\pi^2(h2a^{*2}U^{11} + \ldots + 2hka^*b^*U^{12})$.**

| | U11 | U22 | U33 | U23 | U13 | U12 |
|---|---|---|---|---|---|---|
| Re(1) | 23(1) | 18(1) | 22(1) | 4(1) | 4(1) | 3(1) |
| P(2) | 25(1) | 25(1) | 23(1) | 0(1) | 8(1) | 2(1) |
| P(1) | 28(1) | 19(1) | 28(1) | -2(1) | 11(1) | -1(1) |
| C(2) | 32(3) | 21(3) | 33(3) | 9(2) | 1(2) | 4(2) |
| O(2) | 32(2) | 45(3) | 47(2) | 17(2) | 9(2) | -4(2) |
| C(34) | 100(6) | 21(3) | 32(3) | -6(3) | -25(4) | 7(4) |
| C(35) | 72(5) | 25(4) | 68(5) | -1(3) | -43(4) | 0(3) |
| O(1) | 65(3) | 35(2) | 30(2) | -4(2) | -4(2) | 11(2) |
| C(1) | 31(3) | 29(3) | 29(3) | 9(2) | 4(2) | 4(2) |
| C(32) | 51(4) | 23(3) | 26(3) | 4(2) | 10(3) | 9(3) |
| C(44) | 63(4) | 28(3) | 47(4) | 13(3) | 31(3) | 16(3) |
| C(46) | 46(4) | 39(3) | 28(3) | 8(2) | 16(3) | 13(3) |
| C(31) | 37(3) | 19(3) | 26(3) | -7(2) | 4(2) | 5(2) |
| C(11) | 25(3) | 26(3) | 23(2) | -4(2) | 6(2) | 0(2) |
| C(26) | 44(4) | 21(3) | 49(4) | 2(2) | 20(3) | 7(3) |
| C(22) | 35(3) | 27(3) | 38(3) | -2(2) | 8(3) | 7(2) |
| C(21) | 26(3) | 20(3) | 38(3) | 3(2) | 14(2) | 2(2) |
| C(13) | 30(3) | 31(3) | 53(4) | 11(3) | 2(3) | 6(3) |
| C(16) | 34(3) | 18(2) | 26(3) | -1(2) | 7(2) | -1(2) |
| C(41) | 38(3) | 21(3) | 28(3) | 4(2) | 15(2) | 2(2) |
| C(36) | 46(4) | 28(3) | 48(4) | -7(3) | -4(3) | -2(3) |
| C(15) | 28(3) | 32(3) | 33(3) | 4(2) | 1(2) | -10(2) |
| C(14) | 25(3) | 43(3) | 49(4) | 14(3) | -3(3) | -1(3) |
| N(1) | 41(3) | 30(3) | 39(3) | -17(2) | 20(2) | -12(2) |
| C(45) | 58(4) | 39(3) | 39(3) | 18(3) | 17(3) | 25(3) |
| C(24) | 46(4) | 37(3) | 50(4) | 16(3) | 8(3) | 6(3) |
| C(12) | 32(3) | 23(3) | 33(3) | 0(2) | 10(2) | -5(2) |
| C(25) | 56(4) | 24(3) | 59(4) | 14(3) | 19(3) | 13(3) |
| C(23) | 38(3) | 47(4) | 39(3) | 8(3) | 9(3) | 7(3) |
| C(42) | 42(3) | 23(3) | 36(3) | 3(2) | 20(3) | 2(3) |
| C(43) | 64(4) | 26(3) | 38(3) | 6(3) | 29(3) | 2(3) |
| C(33) | 99(6) | 18(3) | 33(3) | -4(2) | 16(4) | 6(3) |
| Br(2) | 31(1) | 21(1) | 30(1) | 5(1) | 8(1) | 1(1) |
| C(3A) | 49(6) | 9(4) | 28(5) | 0(4) | 21(4) | -7(4) |
| O(3A) | 48(12) | 32(10) | 44(10) | 7(6) | 6(7) | 11(7) |
| Br(1) | 23(1) | 29(1) | 25(1) | 9(1) | 5(1) | 6(1) |
| C(3B) | 49(6) | 9(4) | 28(5) | 0(4) | 21(4) | -7(4) |
| O(3B) | 64(13) | 42(8) | 63(10) | 5(6) | 25(8) | 6(8) |
| C(4B) | 29(10) | 25(9) | 23(8) | -1(7) | -1(7) | 3(8) |
| C(5B) | 38(5) | 29(4) | 34(4) | -4(3) | -4(4) | -6(4) |
| C(6B) | 47(19) | 16(16) | 40(12) | 9(12) | -14(12) | -5(11) |
| C(4A) | 27(5) | 22(4) | 26(4) | -1(4) | 9(4) | 0(4) |
| C(5A) | 38(5) | 29(4) | 34(4) | -4(3) | -4(4) | -6(4) |
| C(6A) | 50(9) | 25(10) | 58(9) | 4(8) | -20(6) | 5(8) |

**Table A.58: Hydrogen coordinates (x $10^4$) and isotropic displacement parameters ($Å^2$ x $10^3$) for *fac*-[Re(PNP)$(CO)_3$(Br)] (10).**

| | x | y | z | U(eq) |
|---|---|---|---|---|
| H(34) | 8487 | 442 | 6359 | 64 |
| H(35) | 10033 | 801 | 5560 | 71 |

| | | | | |
|---|---|---|---|---|
| H(32) | 6042 | 1485 | 4580 | 40 |
| H(44) | 4465 | 4474 | 4094 | 53 |
| H(46) | 5087 | 2749 | 2435 | 44 |
| H(26) | 7567 | 3544 | 1587 | 44 |
| H(22) | 8862 | 1971 | -28 | 40 |
| H(13) | 12120 | 306 | 2126 | 46 |
| H(16) | 10695 | 2781 | 1377 | 31 |
| H(36) | 9609 | 1507 | 4266 | 50 |
| H(15) | 12748 | 2505 | 1410 | 38 |
| H(14) | 13467 | 1260 | 1784 | 48 |
| H(45) | 3914 | 3791 | 2815 | 54 |
| H(24) | 7713 | 4063 | -960 | 53 |
| H(12) | 10074 | 579 | 2110 | 34 |
| H(25) | 7254 | 4410 | 425 | 55 |
| H(23) | 8432 | 2823 | -1207 | 49 |
| H(42) | 7432 | 3118 | 4624 | 39 |
| H(43) | 6254 | 4161 | 5002 | 49 |
| H(33) | 6510 | 779 | 5890 | 59 |
| H(4B1) | 9497 | 2780 | 4031 | 31 |
| H(4B2) | 10409 | 2500 | 3371 | 31 |
| H(5B1) | 9907 | 3637 | 2489 | 41 |
| H(5B2) | 9076 | 3925 | 3197 | 41 |
| H(6B1) | 11003 | 4505 | 3458 | 54 |
| H(6B2) | 11613 | 3680 | 3561 | 54 |
| H(6B3) | 10782 | 3973 | 4262 | 54 |
| H(4A1) | 8648 | 3509 | 3279 | 30 |
| H(4A2) | 9372 | 3405 | 2456 | 30 |
| H(5A1) | 10789 | 2602 | 3367 | 41 |
| H(5A2) | 10124 | 2856 | 4179 | 41 |
| H(6A1) | 11849 | 3639 | 4105 | 70 |
| H(6A2) | 10673 | 4159 | 3956 | 70 |
| H(6A3) | 11339 | 3905 | 3147 | 70 |

**Table A.59: Torsion angles (°) for *fac*-[Re(PNP)(CO)$_3$(Br)] (10).**

| Torsion Angle | Angle | Torsion Angle | Angle |
|---|---|---|---|
| Br1-Re1-P1-N1 | 100.85(19) | P2-Re1-P1-C11 | 115.4(2) |
| Br1-Re1-P1-C11 | -146.9(2) | P2-Re1-P1-C21 | -109.91(19) |
| Br1-Re1-P1-C21 | -12.20(19) | C2-Re1-P2-C31 | 60.5(3) |
| P2-Re1-P1-N1 | 3.14(18) | C2-Re1-P2-C41 | -68.8(3) |
| C3B-Re1-P1-C21 | 163.3(4) | C3B-Re1-P2-N1 | 88.4(4) |
| Br1-Re1-P2-N1 | -89.10(19) | C3B-Re1-P2-C31 | -27.4(4) |
| Br1-Re1-P2-C31 | 155.1(2) | C3B-Re1-P2-C41 | -156.7(4) |
| Br1-Re1-P2-C41 | 25.8(2) | Re1-P1-N1-P2 | -4.3(2) |
| P1-Re1-P2-N1 | -3.17(18) | Re1-P1-N1-C4A | -166.3(5) |
| P1-Re1-P2-C31 | -119.0(2) | C11-P1-N1-P2 | -135.8(3) |
| P1-Re1-P2-C41 | 111.7(2) | C11-P1-N1-C4A | 62.2(6) |
| C2-Re1-P2-N1 | 176.3(2) | C21-P1-N1-P2 | 116.4(3) |
| C3B-Re1-P1-C11 | 28.6(4) | C21-P1-N1-C4A | -45.6(6) |
| C3B-Re1-P1-N1 | -83.7(4) | Re1-P1-C11-C12 | -9.0(5) |
| C1-Re1-P1-C21 | 72.4(2) | N1-P2-C41-C46 | 101.8(5) |
| C1-Re1-P1-C11 | -62.3(3) | C31-P2-C41-C42 | 39.0(5) |
| C1-Re1-P1-N1 | -174.6(2) | C41-P2-C31-C36 | -132.0(5) |
| Re1-P1-C11-C16 | 174.8(3) | C41-P2-C31-C32 | 55.8(4) |
| N1-P1-C11-C12 | 98.6(4) | N1-P2-C31-C36 | -19.3(5) |

| | | | |
|---|---|---|---|
| N1-P2-C41-C42 | -77.6(5) | N1-P2-C31-C32 | 168.5(4) |
| Re1-P2-C41-C46 | -8.1(5) | Re1-P2-C31-C36 | 86.5(5) |
| Re1-P2-C41-C42 | 172.5(3) | Re1-P2-C31-C32 | -85.7(4) |
| N1-P1-C11-C16 | -77.7(4) | C41-P2-N1-C4A | 32.4(6) |
| C21-P1-C11-C12 | -148.8(4) | C41-P2-N1-P1 | -127.8(3) |
| C21-P1-C11-C16 | 35.0(4) | N1-P1-C21-C26 | -17.6(6) |
| Re1-P1-C21-C22 | -89.6(5) | C11-P1-C21-C22 | 55.7(5) |
| Re1-P1-C21-C26 | 87.3(5) | C11-P1-C21-C26 | -127.4(5) |
| N1-P1-C21-C22 | 165.5(4) | Re1-P2-N1-P1 | 4.3(2) |
| Re1-P2-N1-C4A | 164.5(6) | C31-P2-C41-C46 | -141.6(4) |
| C31-P2-N1-P1 | 121.9(3) | P1-N1-C4A-C5A | 103.3(7) |
| C31-P2-N1-C4A | -77.9(6) | P2-N1-C4A-C5A | 99.8(8) |
| N1-C4A-C5A-C6A | 170.3(12) | C14-C15-C16-C11 | 0.3(7) |
| P1-C11-C12-C13 | -176.4(4) | P1-C21-C22-C23 | 177.4(4) |
| C16-C11-C12-C13 | -0.1(7) | C26-C21-C22-C23 | 0.4(8) |
| P1-C11-C16-C15 | 176.0(4) | P1-C21-C26-C25 | -179.3(5) |
| C12-C11-C16-C15 | -0.3(7) | C22-C21-C26-C25 | -2.4(8) |
| C11-C12-C13-C14 | 0.5(8) | C21-C22-C23-C24 | 2.4(9) |
| C12-C13-C14-C15 | -0.4(9) | C22-C23-C24-C25 | -3.1(9) |
| C13-C14-C15-C16 | 0.0(8) | C23-C24-C25-C26 | 1.1(10) |
| C24-C25-C26-C21 | 1.7(9) | C32-C33-C34-C35 | 0.3(9) |
| P2-C31-C32-C33 | 172.7(4) | C33-C34-C35-C36 | -0.2(9) |
| C36-C31-C32-C33 | 0.0(7) | C34-C35-C36-C31 | -0.1(9) |
| P2-C31-C36-C35 | -171.9(4) | P2-C41-C42-C43 | 179.8(4) |
| C32-C31-C36-C35 | 0.1(8) | C46-C41-C42-C43 | 0.4(8) |
| C31-C32-C33-C34 | -0.3(8) | P2-C41-C46-C45 | -179.8(5) |
| C42-C41-C46-C45 | -0.4(8) | C43-C44-C45-C46 | 1.4(9) |
| C41-C42-C43-C44 | 0.5(9) | C44-C45-C46-C41 | -0.5(9) |
| C42-C43-C44-C45 | -1.4(9) | | |

**Table A.60: Hydrogen bond distances (Å) and angles (°) for *fac*-[Re(PNP)(CO)$_3$(Br)] (10).**

| D-H…A | d (D-H) | d (H…A) | d (D…A) | D-H…A angle |
|---|---|---|---|---|
| C12-H12…O3B | 0.95 | 2.51 | 3.39(2) | 155.1 |
| C14-H14…Br1#1 | 0.95 | 2.81 | 3.524(6) | 133 |
| C46-H46…Br1 | 0.95 | 2.63 | 3.519(6) | 156.8 |

#1 1+x,y,z

# APPENDIX B

The methanol substitution reactions between *fac*-[Re(2,5-PicoH)$(CO)_3$(MeOH)] and bromide ions ($Br^-$), iodide ions ($I^-$), pyridine (Py), imidazole (Im), thiocyanate ions ($NCS^-$), thiourea (TU) and 1-methyl-2-thiourea as entering ligands were followed. Each reaction was performed at four temperatures (15.0, 25.0, 35.0 and 45.0 °C) and the Rhenium concentration was kept constant at 1 x $10^{-4}$ M throughout.

**Table B.1: Temperature and [$Br^-$] dependence of the *pseudo* first-order reaction between *fac*-[Re(2,5-PicoH)$(CO)_3$(MeOH)] and bromide ions. [Re] = 1 x $10^{-4}$ M, λ = 250 nm, MeOH.**

| | $10^3$ $k_{obs}$ ($s^{-1}$) | | | |
|---|---|---|---|---|
| **[$Br^-$] (M)** | **15.0 °C** | **25.0 °C** | **35.0 °C** | **45.0 °C** |
| 0.005 | 0.224(3) | 0.965(3) | 2.55(4) | 6.05(3) |
| 0.01 | 0.240(2) | 1.016(9) | 2.71(9) | 6.4(1) |
| 0.02 | 0.273(4) | 1.12(7) | 3.02(2) | 7.30(8) |
| 0.03 | 0.307(5) | 1.22(8) | 3.34(5) | 8.1(2) |
| 0.04 | 0.341(2) | 1.33(9) | 3.65(5) | 8.98(4) |
| 0.05 | 0.374(4) | 1.44(7) | 3.98(5) | 9.84(2) |

**Table B.2: Temperature and [$I^-$] dependence of the *pseudo* first-order reaction between *fac*-[Re(2,5-PicoH)$(CO)_3$(MeOH)] and iodide ions. [Re] = 1 x $10^{-4}$ M, λ = 275 nm, MeOH.**

| | $10^3$ $k_{obs}$ ($s^{-1}$) | | | |
|---|---|---|---|---|
| **[$I^-$] (M)** | **15.0 °C** | **25.0 °C** | **35.0 °C** | **45.0 °C** |
| 0.005 | 0.113(4) | 0.491(2) | 1.04(2) | 1.56(3) |
| 0.01 | 0.130(2) | 0.552(3) | 1.20(4) | 1.98(2) |
| 0.02 | 0.1662(8) | 0.670(7) | 1.53(6) | 2.80(1) |
| 0.03 | 0.202(4) | 0.787(4) | 1.86(3) | 3.65(2) |
| 0.04 | 0.236(4) | 0.898(3) | 2.174(3) | 4.49(3) |
| 0.05 | 0.2741(7) | 1.01(6) | 2.496(6) | 5.32(4) |

**Table B.3: Temperature and [Py] dependence of the *pseudo* first-order reaction between *fac*-[Re(2,5-PicoH)$(CO)_3$(MeOH)] and pyridine. [Re] = 1 x $10^{-4}$ M, λ = 300 nm, MeOH.**

| | $10^3$ $k_{obs}$ ($s^{-1}$) | | | |
|---|---|---|---|---|
| **[Py] (M)** | **15.0 °C** | **25.0 °C** | **35.0 °C** | **45.0 °C** |
| 0.05 | 0.0359(2) | 0.0989(7) | 0.255(2) | 0.8031(9) |
| 0.1 | 0.05576(3) | 0.16(1) | 0.434(8) | 1.31(5) |
| 0.2 | 0.0954(2) | 0.287(3) | 0.814(7) | 2.43(3) |
| 0.3 | 0.135(2) | 0.416(3) | 1.19(2) | 3.57(8) |
| 0.4 | 0.1745(9) | 0.542(2) | 1.56(2) | 4.71(3) |
| 0.5 | 0.2145(3) | 0.6761(4) | 1.93(4) | 5.86(2) |

# Appendix B

**Table B.4: Temperature and [Im] dependence of the *pseudo* first-order reaction between *fac*-[Re(2,5-PicoH)(CO)$_3$(MeOH)] and imidazole. [Re] = 1 x 10$^{-4}$ M, λ = 264 nm, MeOH.**

| | $10^3$ $k_{obs}$ ($s^{-1}$) | | | |
|---|---|---|---|---|
| **[Im] (M)** | **15.0 °C** | **25.0 °C** | **35.0 °C** | **45.0 °C** |
| 0.05 | 0.0256(3) | 0.0894(6) | 0.267(4) | 0.798(9) |
| 0.1 | 0.0414(6) | 0.148(4) | 0.430(3) | 1.31(4) |
| 0.2 | 0.0739(2) | 0.268(3) | 0.765(8) | 2.31(6) |
| 0.3 | 0.106(8) | 0.387(4) | 1.12(4) | 3.34(3) |
| 0.4 | 0.139(4) | 0.505(6) | 1.45(9) | 4.35(2) |
| 0.5 | 0.172(5) | 0.626(7) | 1.8(3) | 5.36(7) |

**Table B.5: Temperature and [NCS$^-$] dependence of the *pseudo* first-order reaction between *fac*-[Re(2,5-PicoH)(CO)$_3$(MeOH)] and thiocyanate ions. [Re] = 1 x 10$^{-4}$ M, λ = 270 nm, MeOH.**

| | $10^3$ $k_{obs}$ ($s^{-1}$) | | | |
|---|---|---|---|---|
| **[NCS$^-$] (M)** | **15.0 °C** | **25.0 °C** | **35.0 °C** | **45.0 °C** |
| 0.02 | 0.0278(3) | 0.134(1) | 0.275(1) | 0.677(1) |
| 0.03 | 0.0345(3) | 0.155(4) | 0.341(2) | 0.888(2) |
| 0.04 | 0.0414(8) | 0.176(7) | 0.397(4) | 1.06(3) |
| 0.05 | 0.0481(2) | 0.198(7) | 0.463(6) | 1.242(8) |
| 0.1 | 0.0801(4) | 0.3028(7) | 0.7785(9) | 2.16(9) |
| 0.2 | 1.447(8) | 0.5128(6) | 1.418(6) | 4.03(1) |

**Table B.6: Temperature and [TU] dependence of the *pseudo* first-order reaction between *fac*-[Re(2,5-PicoH)(CO)$_3$(MeOH)] and thiourea. [Re] = 1 x 10$^{-4}$ M, λ = 326 nm, MeOH.**

| | $10^3$ $k_{obs}$ ($s^{-1}$) | | | |
|---|---|---|---|---|
| **[TU] (M)** | **15.0 °C** | **25.0 °C** | **35.0 °C** | **45.0 °C** |
| 0.005 | 0.0796(2) | 0.211(1) | 0.447(3) | 1.03(4) |
| 0.01 | 0.111(3) | 0.307(1) | 0.687(2) | 1.57(9) |
| 0.02 | 0.175(4) | 0.5035(8) | 1.18(2) | 2.69(2) |
| 0.03 | 0.2441(3) | 0.693(8) | 1.68(4) | 3.83(4) |
| 0.04 | 0.311(5) | 0.880(7) | 2.139(7) | 4.97(6) |
| 0.05 | 0.377(2) | 1.077(3) | 2.65(4) | 6.18(1) |

**Table B.7: Temperature and [MeTU] dependence of the *pseudo* first-order reaction between *fac*-[Re(2,5-PicoH)(CO)$_3$(MeOH)] and 1-methyl-2-thiourea. [Re] = 1 x 10$^{-4}$ M, λ = 380 nm, MeOH.**

| | $10^3$ $k_{obs}$ ($s^{-1}$) | | | |
|---|---|---|---|---|
| **[MeTU] (M)** | **15.0 °C** | **25.0 °C** | **35.0 °C** | **45.0 °C** |
| 0.005 | 0.0577(3) | 0.165(2) | 0.398(2) | 0.990(3) |
| 0.01 | 0.0969(2) | 0.275(5) | 0.655(2) | 1.71(7) |
| 0.02 | 0.175(1) | 0.497(1) | 1.18(3) | 2.96(1) |
| 0.03 | 0.251(3) | 0.719(2) | 1.67(9) | 4.13(4) |
| 0.04 | 0.328(4) | 0.934(3) | 2.19(7) | 5.43(3) |
| 0.05 | 0.41(1) | 1.153(4) | 2.71(3) | 6.85(8) |

## Appendix B

The methanol substitution reactions between *fac*-[Re(Isa)$(CO)_3$(MeOH)] and pyridine (Py), thiocyanate ions ($NCS^-$), thiourea (TU) and 1-methyl-2-thiourea as entering ligands were followed. Each reaction was performed at four temperatures (15.0, 25.0, 35.0 and 45.0 °C) and the Rhenium concentration was kept constant at 1.25 x $10^{-3}$ M throughout.

**Table B.8: Temperature and [Py] dependence of the *pseudo* first-order reaction between *fac*-[Re(Isa)$(CO)_3$(MeOH)] and pyridine. [Re] = 1.25 x $10^{-3}$ M, λ = 370 nm, MeOH.**

| | $10^3$ $k_{obs}$ ($s^{-1}$) | | | |
|---|---|---|---|---|
| **[Py] (M)** | **15.0 °C** | **25.0 °C** | **35.0 °C** | **45.0 °C** |
| 0.05 | 1.11(3) | 3.28(4) | 11.33(7) | 24.76(3) |
| 0.1 | 1.41(6) | 4.21(3) | 14.0(3) | 31.8(4) |
| 0.2 | 1.985(8) | 5.99(2) | 19.4(6) | 46.0(2) |
| 0.3 | 2.55(6) | 7.80(2) | 24.4(3) | 59.7(5) |
| 0.4 | 3.12(4) | 9.56(4) | 29.8(3) | 74.0(2) |
| 0.5 | 3.675(4) | 11.2(8) | 35.2(1) | 87.8(3) |

**Table B.9: Temperature and [$NCS^-$] dependence of the *pseudo* first-order reaction between *fac*-[Re(Isa)$(CO)_3$(MeOH)] and thiocyanate ions. [Re] = 1.25 x $10^{-3}$ M, λ = 378 nm, MeOH.**

| | $10^3$ $k_{obs}$ ($s^{-1}$) | | | |
|---|---|---|---|---|
| **[$NCS^-$] (M)** | **15.0 °C** | **25.0 °C** | **35.0 °C** | **45.0 °C** |
| 0.05 | 0.431(2) | 1.45(2) | 3.91(4) | 10.7(3) |
| 0.1 | 0.741(3) | 2.38(6) | 6.74(3) | 18.0(5) |
| 0.2 | 1.34(6) | 4.17(2) | 12.3(4) | 32.5(4) |
| 0.3 | 1.92(2) | 6.06(3) | 17.9(2) | 46.2(1) |
| 0.4 | 2.53(1) | 8.01(3) | 23.4(1) | 61.0(2) |
| 0.5 | 3.12(4) | 9.86(7) | 28.9(7) | 76.5(2) |

**Table B.10: Temperature and [TU] dependence of the *pseudo* first-order reaction between *fac*-[Re(Isa)$(CO)_3$(MeOH)] and thiourea. [Re] = 1.25 x $10^{-3}$ M, λ = 320 nm, MeOH.**

| | $10^3$ $k_{obs}$ ($s^{-1}$) | | | |
|---|---|---|---|---|
| **[TU] (M)** | **15.0 °C** | **25.0 °C** | **35.0 °C** | **45.0 °C** |
| 0.005 | 0.627(4) | 1.89(2) | 6.303(9) | 12.0(2) |
| 0.01 | 0.688(2) | 2.07(4) | 6.82(6) | 13.5(6) |
| 0.02 | 0.810(1) | 2.44(3) | 7.88(1) | 16.4(5) |
| 0.03 | 0.925(4) | 2.82(1) | 8.94(3) | 19.4(2) |
| 0.04 | 1.046(8) | 3.17(8) | 9.99(2) | 22.3(2) |
| 0.05 | 1.16(7) | 3.53(9) | 11.04(7) | 25.2(3) |

# Appendix B

**Table B.11: Temperature and [MeTU] dependence of the *pseudo* first-order reaction between *fac*-[Re(Isa)(CO)$_3$(MeOH)] and 1-methyl-2-thiourea. [Re] = 1.25 x 10$^{-3}$ M, λ = 360 nm, MeOH.**

| | $10^3$ $k_{obs}$ ($s^{-1}$) | | | |
|---|---|---|---|---|
| **[MeTU] (M)** | **15.0 °C** | **25.0 °C** | **35.0 °C** | **45.0 °C** |
| 0.005 | 0.658(2) | 2.44(2) | 9.62(3) | 16.9(3) |
| 0.01 | 0.7458(7) | 2.70(2) | 10.4(2) | 18.9(2) |
| 0.02 | 0.907(3) | 3.21(4) | 11.9(4) | 22.8(4) |
| 0.03 | 1.09(2) | 3.72(3) | 13.4(4) | 27.0(3) |
| 0.04 | 1.255(6) | 4.23(4) | 14.8(2) | 30.9(4) |
| 0.05 | 1.429(9) | 4.73(1) | 16.2(3) | 35.0(2) |

## Appendix B

The methanol substitution reactions between *fac*-[Re(Trop)$(CO)_3$(MeOH)] and bromide ions ($Br^-$), iodide ions ($I^-$), pyridine (Py), imidazole (Im), thiocyanate ions ($NCS^-$), thiourea (TU) and 1-methyl-2-thiourea as entering ligands were followed. Each reaction was performed at four temperatures (15.0, 25.0, 35.0 and 45.0 °C) and the Rhenium concentration was kept constant at 1 x $10^{-4}$ M throughout.

**Table B.12: Temperature and [$Br^-$] dependence of the *pseudo* first-order reaction between *fac*-[Re(Trop)$(CO)_3$(MeOH)] and bromide ions. [Re] = 1 x $10^{-4}$ M, λ = 430 nm, MeOH.**

| | $k_{obs}$ ($s^{-1}$) | | | |
|---|---|---|---|---|
| **[$Br^-$] (M)** | **15.7 °C** | **25.1 °C** | **34.9 °C** | **44.9 °C** |
| 0.2 | 0.204(6) | 0.578(3) | 1.6810(7) | 3.9610(7) |
| 0.3 | 0.223(8) | 0.628(2) | 1.826(3) | 4.335(2) |
| 0.4 | 0.241(3) | 0.6799(6) | 1.968(3) | 4.700(2) |
| 0.5 | 0.2601(2) | 0.729(1) | 2.1084(8) | 5.085(3) |

**Table B.13: Temperature and [$I^-$] dependence of the *pseudo* first-order reaction between *fac*-[Re(Trop)$(CO)_3$(MeOH)] and iodide ions. [Re] = 1 x $10^{-4}$ M, λ = 430 nm, MeOH.**

| | $k_{obs}$ ($s^{-1}$) | | | |
|---|---|---|---|---|
| **[$I^-$] (M)** | **15.8 °C** | **24.3 °C** | **34.4 °C** | **44.2 °C** |
| 0.2 | 0.306(3) | 0.827(4) | 2.51(1) | 6.146(4) |
| 0.3 | 0.338(4) | 0.902(3) | 2.748(7) | 6.733(2) |
| 0.4 | 0.370(2) | 0.980(4) | 2.969(6) | 7.313(3) |
| 0.5 | 0.402(1) | 1.057(4) | 3.191(4) | 7.879(2) |
| 0.6 | 0.433(2) | 1.133(6) | 3.411(5) | 8.45(3) |
| 0.7 | 0.4648(8) | 1.2085(8) | 3.624(5) | 9.00(4) |

**Table B.14: Temperature and [Py] dependence of the *pseudo* first-order reaction between *fac*-[Re(Trop)$(CO)_3$(MeOH)] and pyridine. [Re] = 1 x $10^{-4}$ M, λ = 312 nm, MeOH.**

| | $10^3$ $k_{obs}$ ($s^{-1}$) | | | |
|---|---|---|---|---|
| **[Py] (M)** | **15.0 °C** | **25.0 °C** | **35.0 °C** | **45.0 °C** |
| 0.02 | 2.31(2) | 5.34(2) | 13.38(9) | 36.1(2) |
| 0.03 | 3.4(1) | 7.97(1) | 19.8(2) | 52.7(4) |
| 0.04 | 4.51(3) | 10.6(3) | 26.2(4) | 67.4(1) |
| 0.05 | 5.57(2) | 13.2(6) | 32.9(2) | 82.5(4) |
| 0.1 | 11.0(8) | 26.4(8) | 65.6(1) | 157(8) |
| 0.2 | 21.7(6) | 52.7(3) | 131.1(7) | 308.5(9) |

# Appendix B

**Table B.15: Temperature and [Im] dependence of the *pseudo* first-order reaction between *fac*-[Re(Trop)(CO)$_3$(MeOH)] and imidazole. [Re] = 1 x 10$^{-4}$ M, λ = 255 nm, MeOH.**

| | $10^3$ $k_{obs}$ ($s^{-1}$) | | | |
|---|---|---|---|---|
| **[Im] (M)** | **15.0 °C** | **25.0 °C** | **35.0 °C** | **45.0 °C** |
| 0.005 | 0.87(2) | 1.826(9) | 4.63(2) | 10.65(4) |
| 0.01 | 1.47(1) | 3.45(4) | 8.05(2) | 18.6(3) |
| 0.02 | 2.69(4) | 6.22(3) | 14.8(2) | 32.8(6) |
| 0.03 | 3.9(1) | 8.91(2) | 21.4(7) | 49.0(8) |
| 0.04 | 5.10(6) | 12.0(4) | 28.3(4) | 63.9(2) |
| 0.05 | 6.31(2) | 14.80(9) | 35.1(2) | 79(1) |

**Table B.16: Temperature and [NCS$^-$] dependence of the *pseudo* first-order reaction between *fac*-[Re(Trop)(CO)$_3$(MeOH)] and thiocyanate ions. [Re] = 1 x 10$^{-4}$ M, λ = 265 nm, MeOH.**

| | $10^3$ $k_{obs}$ ($s^{-1}$) | | | |
|---|---|---|---|---|
| **[NCS$^-$] (M)** | **15.0 °C** | **25.0 °C** | **35.0 °C** | **45.0 °C** |
| 0.02 | 3.80(2) | 9.2(1) | 24.2(7) | 48.6(9) |
| 0.03 | 4.93(1) | 12.5(3) | 29.6(4) | 59.9(3) |
| 0.04 | 6.13(4) | 15.2(3) | 35.1(9) | 72.0(7) |
| 0.05 | 7.193(6) | 18.12(9) | 41(2) | 83.33(8) |
| 0.1 | 12.2(4) | 31.51(6) | 72.1(3) | 149(3) |
| 0.2 | 22.16(6) | 57.87(9) | 136(2) | 279(1) |

**Table B.17: Temperature and [DMAP] dependence of the *pseudo* first-order reaction between *fac*-[Re(Trop)(CO)$_3$(MeOH)] and 4-dimethylaminopyridine. [Re] = 1 x 10$^{-4}$ M, λ = 318 nm, MeOH.**

| | $10^3$ $k_{obs}$ ($s^{-1}$) | | | |
|---|---|---|---|---|
| **[DMAP] (M)** | **15.0 °C** | **25.0 °C** | **35.0 °C** | **45.0 °C** |
| 0.005 | 1.37(4) | 3.31(4) | 6.75(3) | 13.1(3) |
| 0.01 | 2.14(3) | 5.17(6) | 11.09(8) | 22.9(6) |
| 0.02 | 3.7(1) | 8.56(9) | 18.9(6) | 41.1(8) |
| 0.03 | 5.27(8) | 11.8(3) | 26.9(4) | 59.9(7) |
| 0.04 | 6.83(2) | 15.4(3) | 35.7(7) | 79.9(6) |
| 0.05 | 8.4(1) | 18.7(2) | 44(1) | 99(8) |

**Table B.18: Temperature and [TU] dependence of the *pseudo* first-order reaction between *fac*-[Re(Trop)(CO)$_3$(MeOH)] and thiourea. [Re] = 1 x 10$^{-4}$ M, λ = 440 nm, MeOH.**

| | $10^3$ $k_{obs}$ ($s^{-1}$) | | | |
|---|---|---|---|---|
| **[TU] (M)** | **15.0 °C** | **25.0 °C** | **35.0 °C** | **45.0 °C** |
| 0.005 | 1.61(4) | 3.710(8) | 10.0(8) | 27.31(9) |
| 0.01 | 2.74(2) | 6.62(4) | 15.7(2) | 40.8(4) |
| 0.02 | 5.28(4) | 12.1(8) | 27.6(2) | 66.7(2) |
| 0.03 | 7.79(9) | 17.5(2) | 41.1(4) | 95(1) |
| 0.04 | 10.2(2) | 23.14(8) | 53.10(8) | 120.9(6) |
| 0.05 | 12.7(1) | 28.91(9) | 66(1) | 147(2) |

# Appendix B

**Table B.19: Temperature and [MeTU] dependence of the *pseudo* first-order reaction between *fac*-[Re(Trop)(CO)$_3$(MeOH)] and 1-methyl-2-thiourea. [Re] = 1 x 10$^{-4}$ M, λ = 435 nm, MeOH.**

| | $10^3$ $k_{obs}$ ($s^{-1}$) | | | |
|---|---|---|---|---|
| **[MeTU] (M)** | **15.0 °C** | **25.0 °C** | **35.0 °C** | **45.0 °C** |
| 0.005 | 2.1(1) | 5.00(3) | 12.7(6) | 33.6(3) |
| 0.01 | 3.31(4) | 8.12(4) | 19.6(2) | 49.1(2) |
| 0.02 | 6.05(2) | 14.3(2) | 33.4(7) | 79.2(4) |
| 0.03 | 8.68(7) | 20.6(3) | 47.1(8) | 109(3) |
| 0.04 | 11.3(2) | 26.8(4) | 61.0(9) | 139(7) |
| 0.05 | 14.0(6) | 33.2(3) | 74.6(2) | 169(8) |

## Appendix B

The methanol substitution reactions between *fac*-[Re(Trop)$(CO)_3$(MeOH)] and pyridine (Py), imidazole (Im), thiourea (TU) and 1-methyl-2-thiourea as entering ligands were followed. Each reaction was performed at six pressures (0.6, 5, 10, 50, 80 and 100 MPa) and the Rhenium concentration was kept constant at 1 x $10^{-4}$ M throughout.

**Table B.20: Pressure dependence of the *pseudo* first-order reaction between *fac*-[Re(Trop)$(CO)_3$(MeOH)] and pyridine. [Re] = 1 x $10^{-4}$ M, [Py] = 5 x $10^{-2}$ M, λ = 312 nm, 25.9 °C, MeOH.**

| Pressure (MPa) | $k_{obs}$ |
|---|---|
| 0.6 | 0.0113(7) |
| 5 | 0.0111(7) |
| 10 | 0.0107(3) |
| 50 | 0.00929(9) |
| 80 | 0.0081(2) |
| 100 | 0.00755(7) |

**Table B.21: Pressure dependence of the *pseudo* first-order reaction between *fac*-[Re(Trop)$(CO)_3$(MeOH)] and imidazole. [Re] = 1 x $10^{-4}$ M, [Im] = 5 x $10^{-2}$ M, λ = 450 nm, 25.8 °C, MeOH.**

| Pressure (MPa) | $k_{obs}$ |
|---|---|
| 0.6 | 0.0177(2) |
| 5 | 0.0172(4) |
| 10 | 0.0169(8) |
| 50 | 0.0145(9) |
| 80 | 0.0131(7) |
| 100 | 0.0123(3) |

**Table B.22: Pressure dependence of the *pseudo* first-order reaction between *fac*-[Re(Trop)$(CO)_3$(MeOH)] and thiourea. [Re] = 1 x $10^{-4}$ M, [TU] = 5 x $10^{-2}$ M, λ = 440 nm, 25.6 °C, MeOH.**

| Pressure (MPa) | $k_{obs}$ |
|---|---|
| 0.6 | 0.0342(3) |
| 5 | 0.033(2) |
| 10 | 0.032(1) |
| 50 | 0.028(1) |
| 80 | 0.0246(7) |
| 100 | 0.0225(6) |

# Appendix B

**Table B.23: Pressure dependence of the *pseudo* first-order reaction between *fac*-[Re(Trop)(CO)$_3$(MeOH)] and 1-methyl-2-thiourea. [Re] = 1 x 10$^{-4}$ M, [MeTU] = 5 x 10$^{-2}$ M, λ = 435 nm, 25.9 °C, MeOH.**

| Pressure (MPa) | $k_{obs}$ |
|---|---|
| 0.6 | 0.042(1) |
| 5 | 0.0409(7) |
| 10 | 0.0389(6) |
| 50 | 0.0316(6) |
| 80 | 0.0262(9) |
| 100 | 0.0234(3) |

## Appendix B

The aqua substitution reaction between *fac*-[Re(Trop)$(CO)_3(H_2O)$] thiocyanate ions ($NCS^-$) as entering ligand was followed. The reaction was performed at four temperatures (15.0, 25.0, 35.0 and 45.0 °C) and the Rhenium concentration was kept constant at 5 x $10^{-5}$ M.

**Table B.24: Temperature and [$NCS^-$] dependence of the *pseudo* first-order reaction between *fac*-[Re(Trop)$(CO)_3(H_2O)$] and thiocyanate ions. [Re] = 5 x $10^{-5}$ M, λ = 260 nm, $H_2O$.**

| | $10^3$ $k_{obs}$ ($s^{-1}$) | | | |
|---|---|---|---|---|
| [$NCS^-$] (M) | 15.0 °C | 25.0 °C | 35.0 °C | 45.0 °C |
| 0.0025 | 6.18(2) | 14.3(7) | 30.1(4) | 64.3(1) |
| 0.005 | 9.03(2) | 21.0(6) | 43.6(2) | 93.5(4) |
| 0.01 | 14.9(7) | 32.8(4) | 70(1) | 151(3) |
| 0.015 | 20.7(3) | 45.1(3) | 98.3(4) | 209(3) |
| 0.02 | 26.2(1) | 58.2(4) | 127(3) | 268(5) |
| 0.025 | 32.1(4) | 70.7(3) | 153(2) | 326(2) |

**Table B.25: Data for the global fit of pH, [$NCS^-$] and $k_{obs}$ for the aqua substitution reaction between *fac*-[Re(Trop)$(CO)_3(H_2O)$] and thiocyanate ions. [Re] = 5 x $10^{-5}$ M, λ = 260 nm, $H_2O$.**

| pH | [$NCS^-$] | $k_{obs}$ |
|---|---|---|
| 6.4 | 0.03 | 0.0859 |
| 6.8 | 0.03 | 0.08548 |
| 7.4 | 0.03 | 0.08421 |
| 8.0 | 0.03 | 0.0777 |
| 8.1 | 0.03 | 0.0776 |
| 8.36 | 0.03 | 0.0730 |
| 8.62 | 0.03 | 0.0650 |
| 8.78 | 0.03 | 0.0553 |
| 9.1 | 0.03 | 0.0429 |
| 9.37 | 0.03 | 0.03428 |
| 9.63 | 0.03 | 0.0199 |
| 9.9 | 0.03 | 0.014 |
| 6.4 | 0.03 | 0.0847 |
| 6.4 | 0.025 | 0.0707 |
| 6.4 | 0.02 | 0.0582 |
| 6.4 | 0.015 | 0.0451 |
| 6.4 | 0.01 | 0.0328 |
| 6.4 | 0.005 | 0.0210 |
| 6.4 | 0.0025 | 0.0143 |